Studies Related to the Charleston, South Carolina, Earthquake of 1886— A Preliminary Report

GEOLOGICAL SURVEY PROFESSIONAL PAPER 1028

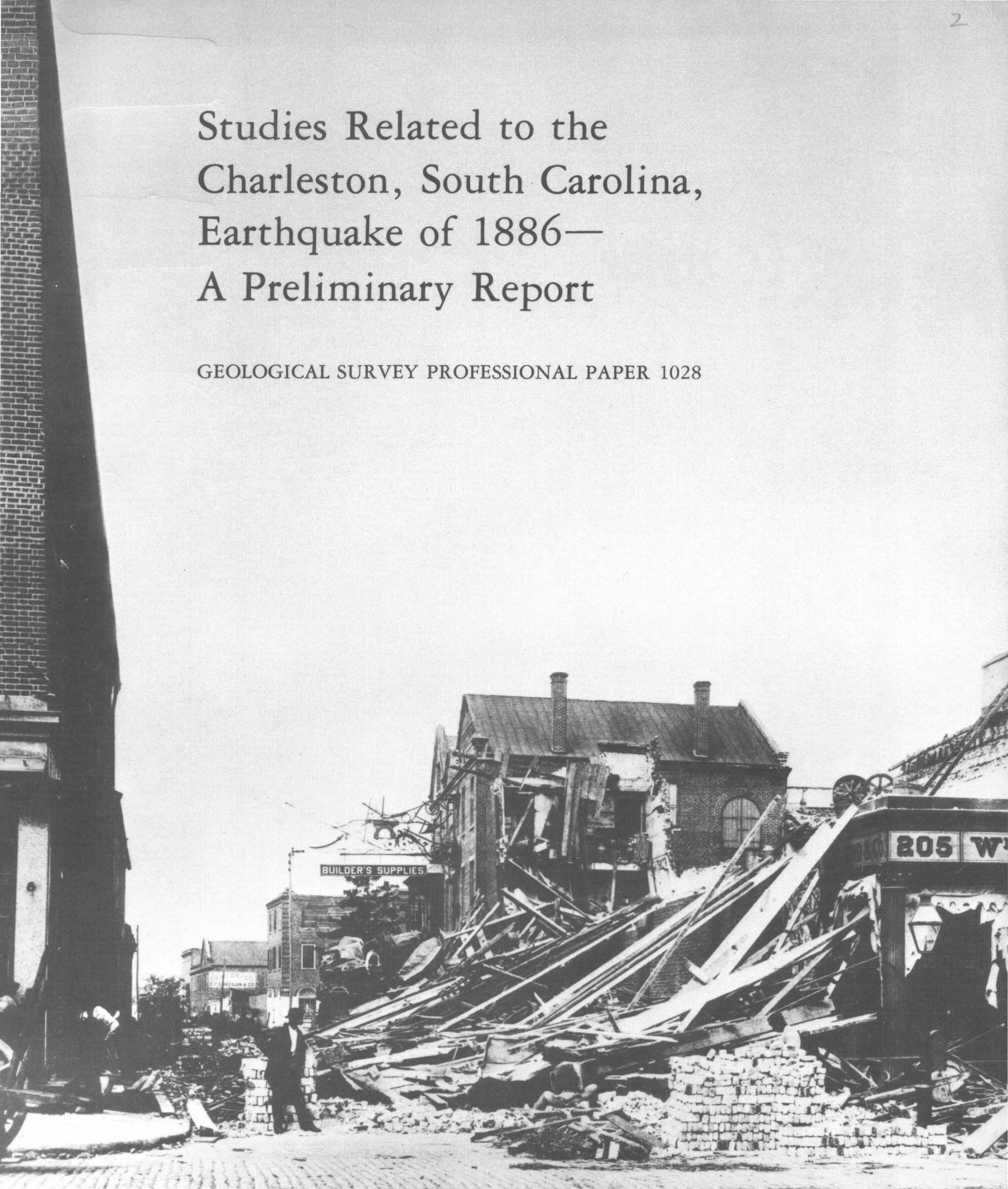

STUDIES RELATED TO THE CHARLESTON, SOUTH CAROLINA, EARTHQUAKE OF 1886—A PRELIMINARY REPORT

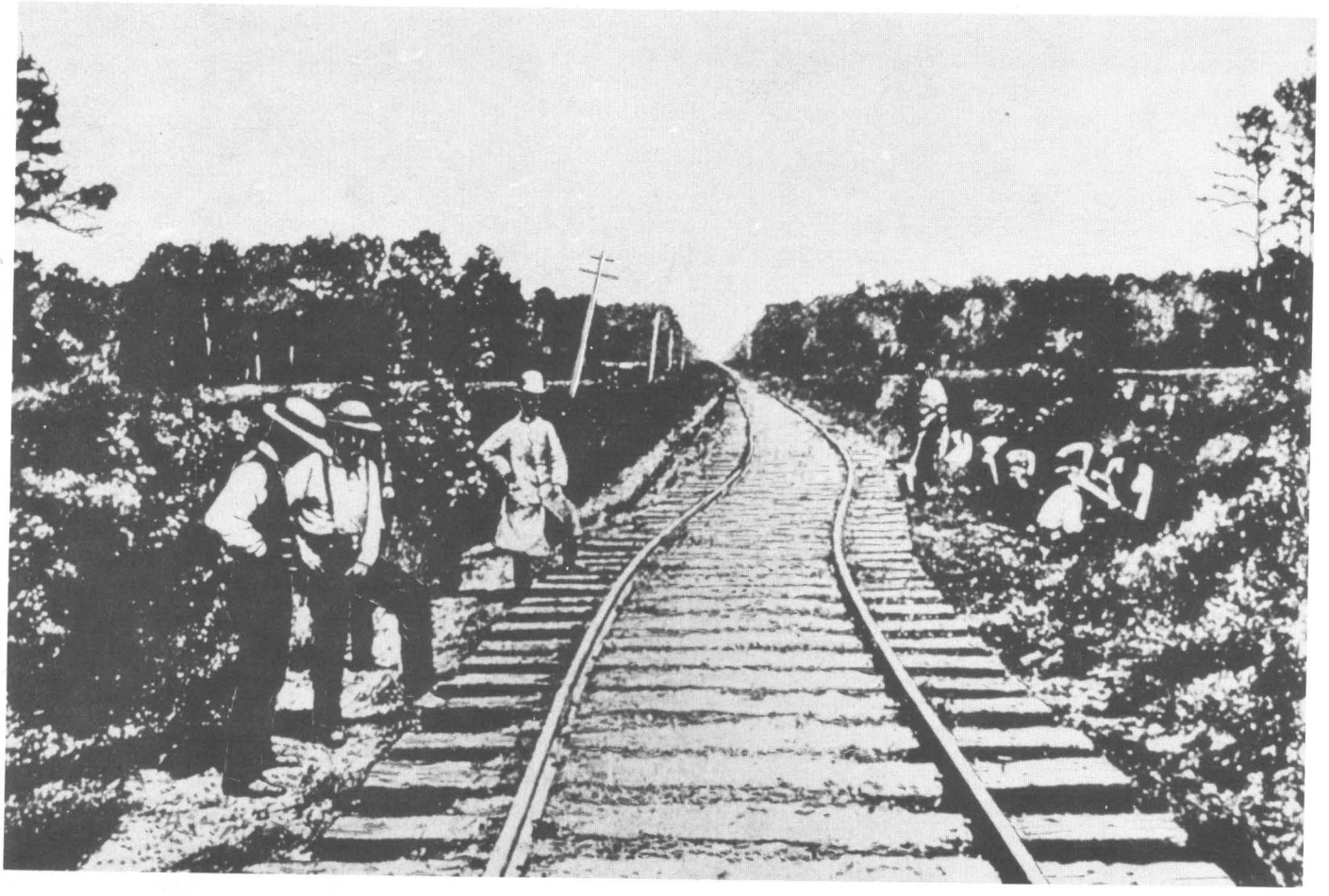

Studies Related to the Charleston, South Carolina, Earthquake of 1886—A Preliminary Report

Edited by Douglas W. Rankin

GEOLOGICAL SURVEY PROFESSIONAL PAPER 1028

UNITED STATES GOVERNMENT PRINTING OFFICE, WASHINGTON : 1977

UNITED STATES DEPARTMENT OF THE INTERIOR

CECIL D. ANDRUS, ***Secretary***

GEOLOGICAL SURVEY

V. E. McKelvey, ***Director***

Library of Congress catalog-card No. 78—600007

For sale by the Superintendent of Documents, U.S. Government Printing Office
Washington, D.C. 20402
Stock Number 024-001-03047-1

CONTENTS

Studies Related to the Charleston, South Carolina, Earthquake of 1886—Introduction and Discussion

By DOUGLAS W. RANKIN

GEOLOGICAL SURVEY PROFESSIONAL PAPER 1028-A

CONTENTS

ILLUSTRATIONS

STUDIES RELATED TO THE CHARLESTON, SOUTH CAROLINA, EARTHQUAKE OF 1886—INTRODUCTION AND DISCUSSION

By DOUGLAS W. RANKIN

"One [Cordilleran earthquake], in 1812, destroyed a church in Los Angeles, California, killing a score or more people. Together with the Charleston earthquake [of 1886] this shock is entitled to a peculiar place in our history; these two shocks being the only earthquakes which have caused any loss of life in the country."

N. S. Shaler (1899)

"The absence of large-magnitude earthquakes in eastern North America since the Charleston, S.C., earthquake of 1886 has resulted in complacency, or perhaps unawareness on the part of the general populace of the existence of any earthquake threat to them."

Otto Nuttli (1973)

ABSTRACT

The seismic history of the southeastern United States is dominated by the 1886 earthquake near Charleston, S.C. An understanding of the specific source and the uniqueness of the neotectonic setting of this large earthquake is essential in order to properly assess seismic hazards in the southeastern United States. Such knowledge will also contribute to the fundamental understanding of intraplate earthquakes and will aid indirectly in deciphering the evolution of Atlantic-type continental margins. The 15 chapters in this volume report on the first stage of an ongoing multidisciplinary study of the Charleston earthquake of 1886.

The Modified Mercalli intensity for the 1886 earthquake was X in the meizoseismal area, an elliptical area 35 by 50 km, the center of which was Middleton Place. Seismic activity is continuing today in the Middleton Place–Summerville area at a higher level than prior to 1886. The present seismicity is originating at depths of 1 to 8 km, mostly in the crystalline basement beneath sedimentary rocks of the Coastal Plain.

The crystalline basement beneath the Charleston-Summerville area is not simply a seaward extension of crystalline rocks of the Appalachian orogen that are exposed in the Piedmont to the northwest, but has a distinctive magnetic signature that does not reflect Appalachian orogenic trends. The area underlain by this distinctive geophysical basement, the Charleston block, may represent a broad zone of Triassic and (or) Jurassic crustal extension formed during the early stages of the opening of the Atlantic Ocean. The Charleston block is characterized in part by prominent, roughly circular magnetic and gravity highs that are thought to reflect mafic or ultramafic plutons.

A continuously cored borehole put down over the shallowest (about 1.5 km deep) of these magnetic anomalies on the edge of the meizoseismal area bottomed at 792 m in amygdaloidal basalt. Although the K-Ar ages of about 100 m.y. for the basalt are consistent with the Late Cretaceous (Cenomanian) age of the overlying Cape Fear Formation, this must be a minimum age as a result of chemical alteration. The interpreted magmatic composition of the basalt most closely resembles the high-Ti quartz-normative tholeiites of Late Triassic and Early Jurassic age from eastern North America; age of the basalt is probably similar. Various geophysical surveys suggest that Coastal Plain sedimentary rocks do not simply dip homoclinally to the southeast on a gently dipping basement surface but are disturbed by structures not yet clearly deciphered.

The present stress regime of the Charleston-Summerville area appears to be one of NE.-SW. compression rather than of extension as it presumably was in the Mesozoic. The present stress regime seems similar to that of much of the eastern United States. Comparison of several seismic source areas in eastern North America shows that epicenters are typically near the periphery of positive gravity features interpreted to represent mafic or ultramafic bodies. Earthquakes may be caused by the concentration of regional stress around the peripheries of these inhomogeneities in an otherwise more homogeneous plate. Whether the inhomogeneities are more or less rigid than the surrounding material is uncertain.

INTRODUCTION

One of the largest historic earthquakes in eastern North America, and by far the largest earthquake in southeastern United States took place about 9:50 p.m. on August 31, 1886, near Charleston, S.C. The major shock lasted less than 1 minute, but resulted in about 60 deaths and extensive damage to the city of Charleston. Because the event took place before seismological instrumentation, estimates of its location and size must come from observations of the damage and effects caused by the earthquake. Most of what we know of the event and the resulting damage comes from a comprehensive report by C. E. Dutton published in 1889. A review of Dutton's (1889) intensity data by Bollinger (this volume) confirms a Modified Mercalli intensity of X for the meizoseismal area (area of maximum damage) and of intensity IX for the city of Charleston.

Dutton's report shows the location of craterlets formed of sand, but does not report any surface faulting. No fault, in fact, is known to be exposed at the surface within 100 km of the meizoseismal area. The cause of the Charleston earthquake has not been adequately explained in the 90 years since the event. An understanding of this large earthquake is essential in order to properly assess seismic hazards in the southeastern United States. The specific source of the earthquake and its tectonic setting must be established, both to permit evaluation of expectable future seismicity in the Charleston region and to determine whether that region differs in any tectonically significant fashion from other parts of the Eastern United States.

With a few notable exceptions, the earth's seismicity is largely associated with plate boundaries or active volcanic areas within the plates such as Hawaii (see Tarr, 1974). Plate boundaries, in fact, were originally defined on the basis of seismicity. Oceanic crust is created at divergent plate boundaries and consumed at convergent plate boundaries. Where plate motion is parallel to the plate boundary, crust is neither created nor consumed. Continents are envisaged as being carried passively within moving oceanic crust. Because of its lower density, continental crust is probably not consumed (is not subducted) at convergent margins but becomes progressively deformed and crumpled, causing orogenic belts.

A divergent plate boundary may originate within a continental mass through rifting and the subsequent formation of an oceanic ridge within the growing rift. Such a history is hypothesized for the growth of the Atlantic Ocean during the Mesozoic. Rifting within the large continental mass that included North America and Africa began in the Triassic as evidenced by the cratonal Triassic basins preserved in eastern North America. By the Cretaceous, a significant ocean basin had formed between the United States and Africa (Pitman and Talwani, 1972). As spreading from the Mid-Atlantic Ridge continued, the eastern margin of the North American continent was carried passively farther from the active spreading center. This continental margin is now commonly referred to as the type example of the seismically quiet Atlantic-type continental margin (Dewey and Bird, 1970).

The meizoseismal area of the Charleston earthquake, although close to the Atlantic coastline, is well within the North American continental mass if one accepts the East Coast magnetic anomaly more than 200 km to the southeast as the continental margin (Taylor and others, 1968). The active plate boundary, the Mid-Atlantic Ridge, is about 3,000 km east-southeast of Charleston. An in-depth study of the Charleston area offers an opportunity to advance the fundamental understanding of Atlantic-type continental margins. Earthquakes along boundaries of plates, such as the San Francisco 1906 and Alaska 1964 earthquakes, are readily understood in terms of relative plate motions and plate tectonics. No similar understanding yet exists for deformation and earthquakes such as Charleston which occur within plates.

The Charleston earthquake shares its intraplate setting with the other largest historical earthquakes in eastern and central United States. Those took place in 1755 near Cape Ann, Mass., and in the winter of 1811–12 in the Mississippi Valley near New Madrid, Mo., as a series of three widely felt shocks. All of these large intraplate earthquakes occurred before instrumentation. An adequate explanation of any of them should aid in explaining the others (see Kane, this volume).

The epicenter of the Cape Ann earthquake appears to have been offshore. It is, thus, not well located and not easy to study. The available data for the Mississippi Valley series, however, have been extensively analyzed by several seismologists (see particularly Nuttli, 1973 and 1976; and Evernden, 1975 and 1976) and the epicentral area is under investigation today.

The Mississippi Valley series included three major shocks: one on Dec. 16, 1811, one on Jan. 23, 1812, and one on Feb. 7, 1812. The February shock is considered the largest. Gupta and Nuttli (1976) recently revised upward the maximum intensity for each

of these events, and Nuttli is quoted by Mosaic magazine (1976) as rating the surface-wave magnitude (M_S) of these events in chronologic order as 8.0, 7.7, and 8.2, respectively. Nuttli (oral commun. 1977) states that this revision assumes that the surface-wave behavior of the Mississippi Valley earthquakes is similar to that of interplate earthquakes, such as those which have occurred in California. He would not necessarily change his published (Nuttli, 1976) estimates of the body-wave magnitude (m_b) for these events of 7.2, 7.1, and 7.4, respectively.

Bollinger (this volume) arrived at a body-wave magnitude (m_b) estimate for the Charleston earthquake of 6.8 using the attenuation of intensity as a function of distance from the epicenter and Nuttli's (1976) intensity-particle velocity data for the central United States. As noted by Bollinger (this volume), the number of significant earthquakes in the central United States for which both intensity and particle velocity data are available is quite small because of the short period of instrumented record relative to the low rate of earthquake occurrence. Using the more abundant western United States intensity-particle velocity data, he estimates the m_b for the Charleston earthquake at 7.1.

Seismologists disagree as to what is the most appropriate measure of earthquake size, particularly when comparing earthquakes in different geologic terranes, for example, in the eastern United States and the western United States (Nuttli, 1976; Evernden, 1976; and Bollinger, this volume). In a general way, however, the Mississippi Valley earthquakes of 1811–12 have been equated with the San Francisco earthquake of 1906 (these are probably the largest historic earthquakes in the conterminous United States), and the Charleston earthquake has been equated with the San Fernando earthquake of 1971 which had an instrumentally determined magnitude $M_L = 6.4$ (Allen and others, 1973) and a $m_b = 6.0$ estimated from intensity data (Nuttli, 1976).

The hazards which must be considered in any discussion of South Carolina seismicity include not only ground breakage and ground motion in the epicentral area, but significant ground motion at considerable distance from the epicenter as is common with all larger earthquakes. Because of the low attenuation of seismic energy in the East, the area of equivalent damage for earthquakes of the same magnitude is far larger for eastern and central United States earthquakes than for those taking place on the west coast (fig. 1). The Charleston earthquake, for example, produced intensity V effects in Chicago (Bollinger, this volume), 1,200 km from the earthquake epicenter.

Important recent work related to the seismicity of the Charleston earthquake includes the monitoring of microearthquakes in the summer of 1971 in the Summerville area by Bollinger, a review of seismic activity in South Carolina by Bollinger (1972), and the establishment of a 5-station reconnaissance seismographic network in March 1973 by the Seismological Investigations Group of NOAA under the auspices of the AEC. The Geological Survey assumed responsibility for the operation of this network and began some geophysical surveys of the area in 1973. In the spring of 1974, these efforts were expanded into a large multidisciplinary study of the Charleston earthquake by the Geological Survey funded largely by the NRC, Office of Nuclear Regulatory Research under Agreement No. AT(49–25)–1000. The studies include the operation of an enlarged seismographic network, a wide variety of geophysical studies, a geological program of mapping surface and near surface features, a deep-drilling program, a geochemical and paleontologic study of appropriate samples, and detailed and regional synthesis of the results. This research is continuing today.

This volume is a preliminary report of these and some related studies. Most of the papers reflect data gathered before June 1976. Work in progress and future work undoubtedly will modify some of the conclusions, but should not change the data presented.

In this introductory chapter, I have tried to provide a framework into which the individual studies fit and to summarize the more significant findings of the studies. Some promising directions of continued research are suggested by what these studies have shown. I am indebted to Carl Wentworth as well as the members of the various Charleston projects for numerous lengthy discussions concerning the cause of the seismicity of the Charleston area.

SEISMICITY

A commonly held view is that the 1886 event took place in an area that had been essentially aseismic for nearly two centuries. An archival study by Bollinger and Visvanathan (this volume) reports 18 probable earthquakes in South Carolina between 1698 and 1886. Of these, 13 appear to have been in the Charleston area. The maximum intensity of the pre-1886 events appears to be V or possibly VI. Bollinger and Visvanathan (this volume) conclude that although South Carolina was not aseismic in the

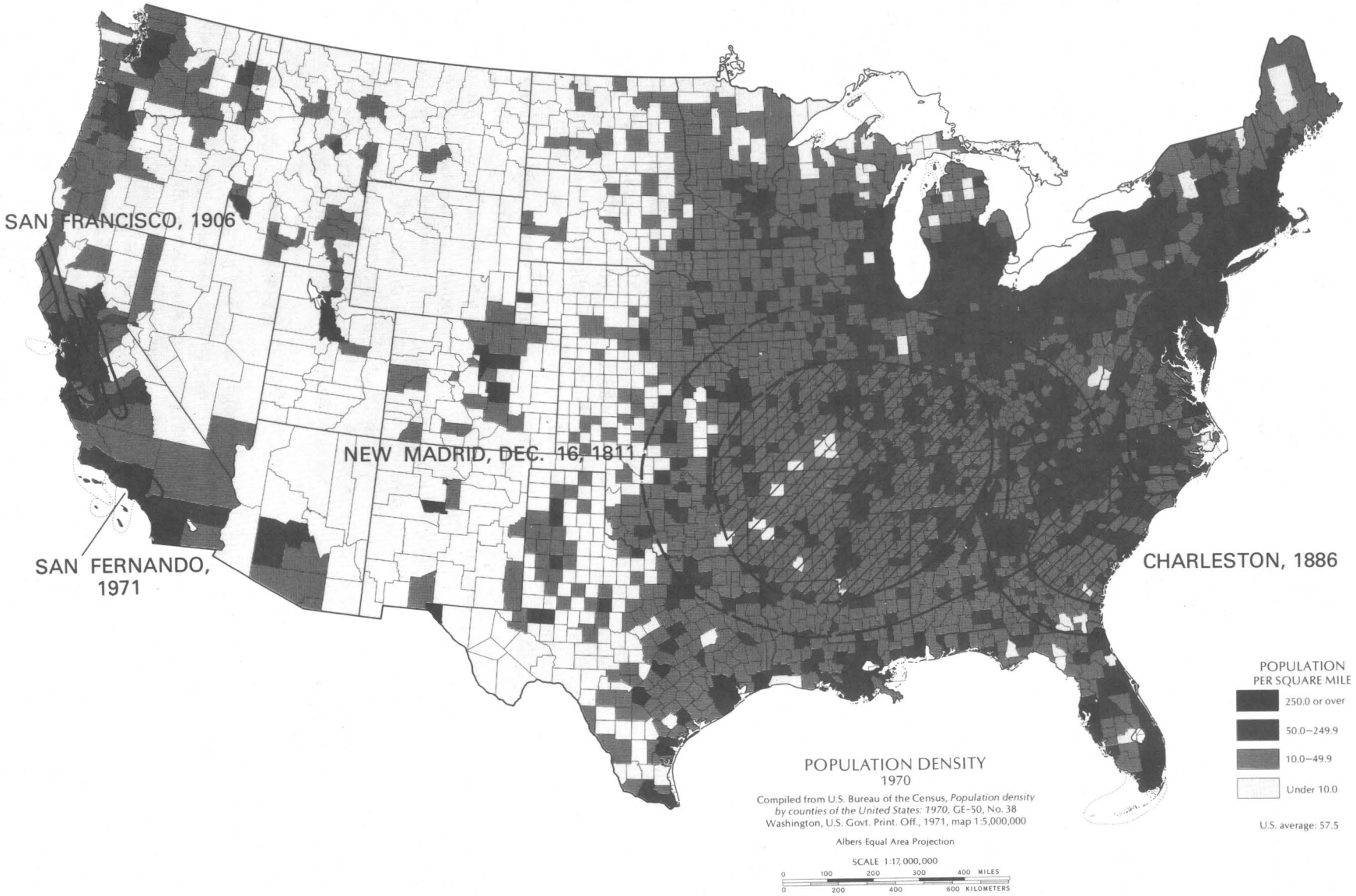

FIGURE 1.—Comparison of areas of observed Modified Mercalli (MM) intensities for four major United States earthquakes. For each earthquake, the outer ring encloses intensities of VI to VII and the patterned inner area represents intensities of VII and greater. Damage areas correspond to intensity VII and greater. Modified from Mosaic (1976). Sources of intensity contours are as follows: Charleston, 1886, Bollinger (this volume); New Madrid, Dec. 16, 1811, Nuttli (1973) (the closure of the intensity contours to the west is arbitrary because of the absence of information); San Fernando, 1971, Scott (1973); and San Francisco, 1906, Mosaic (1976). The base map showing population density for 1970 is from Sheet No. 418 of the U.S. Geological Survey National Atlas of the United States of America, Separate Sales Edition, 1974.

50-year period prior to 1886, the seismic activity does not appear to have been anomalously high relative to the surrounding States either in number of events or in energy levels. It should be pointed out, however, that their catalog lists nine events in South Carolina during this 50-year period, eight of which are approximately located in the vicinity of a specific town. Four of these were in the Charleston area.

The 1886 earthquake was followed by a series of aftershocks which may still be underway today. Of 435 or more earthquakes reported to have taken place in South Carolina between 1754 and 1975, more than 300 were aftershocks in the first 35 years following 1886 (Tarr, this volume).

The 1886 earthquake and its aftershocks dominate the seismic record of the southeast. The seismotectonic map of Hadley and Devine (1974) based upon the record from 1800 to 1972 depicts the Charleston area as having the highest concentration of epicenters and the largest single event in the southeastern United States. Several seismic frequency contours close around Charleston, yet these authors show the area to have no known geologic control for the seismicity. On the other hand, on the basis of a 225-year record (1754–1970) of felt earthquakes in the southern Appalachians, Bollinger (1972) suggests a diffuse zone of seismicity trending NW. across South Carolina roughly perpendicular to the structural grain of the Appalachians. Whether the Charleston seismicity is part of a broad NW.-trending zone (Bollinger, 1972) or whether the seismicity originates in an isolated source area (Hadley and Devine, 1974) is a question that has not been resolved. Most of the historical seismicity in the East, however, is associated spatially with the Appalachian orogen. As we shall see, Charleston is outside the Appalachian orogenic belt and is the locus of the only significant seismic energy release in the Coastal Plain province.

The meizoseismal area of the 1886 earthquake has been variously drawn by several investigators, but has been most recently reinterpreted by Bollinger (this volume) as an elliptical area roughly 35 by 50 km trending northeast between Charleston and Jedburg and including Summerville (fig. 2). This interpretation contrasts considerably with the dual epicentrums of Dutton (1889). Middleton Place is approximately in the center of Bollinger's ellipse, about midway between the two epicenters shown by Dutton.

The South Carolina seismographic network has recorded about 30 events in the South Carolina area between its inception in March 1973 and December 1975 (Carver and others, 1977). It should be noted that the 8-month period from March through December 1973 was a reconnaissance study with 5 stations operating in the Charleston area. No stations operated during the period from January to May 1974, and 10 stations operated over a larger area in South Carolina between May 1974 and December 1975. Thirteen of the 30 events recorded are in the Charleston-Summerville area, mostly between Summerville and Middleton Place. Tarr (this volume) now refers to this area specifically as the Middleton Place-Summerville seismic zone, defined by a cluster of epicenters trending roughly NW. The hypocenters are at approximate depths of 1 to 8 km. Tarr notes that the coordinates of the epicenters are well determined, but that because none of the seismograph stations of the 10-station network were close to the seismic activity, the depths of the hypocenters are not well determined. The largest event thus far recorded by the South Carolina seismographic network is a magnitude (m_{bLg}) 3.8 event on Nov. 22, 1974 very close to Middleton Place at a depth of 4.1 km (Tarr, this volume). Analysis of first-motion of this event indicates NE.-SW. compression acting on planes striking N. 42°W. and dipping either 12° NE. or 78° SW. Tarr (this volume, fig. 7) favors the plane dipping steeply to the SW. because the hypocenters of other events in the Middleton Place-Summerville seismic zone are closer to this plane.

The historic record suggests that the Charleston-Summerville area had a continuum of low-level seismicity prior to 1886 and that a low-level of strain energy release continues in the same area today. More specifically, Middleton Place is roughly in the center of the meizoseismal area of the 1886 event and at the SE. end of a zone, perhaps 15 km long, of continuing microearthquake activity. These recent events, in the depth range of 1 to 8 km, are thought to be either the continuation of the aftershock series or events located along closely related structural features as the result of the modification of the stress environment by the 1886 earthquake. For lack of contrary evidence here or elsewhere, we assume that the 1886 earthquake originated at similar depths.

GEOLOGIC SETTING: THE ATLANTIC COASTAL PLAIN

The Middleton Place–Summerville seismic zone is near the shoreline of the emerged part of the Atlantic Coastal Plain, which consists of an essentially eastward-thickening wedge of very gently seaward-

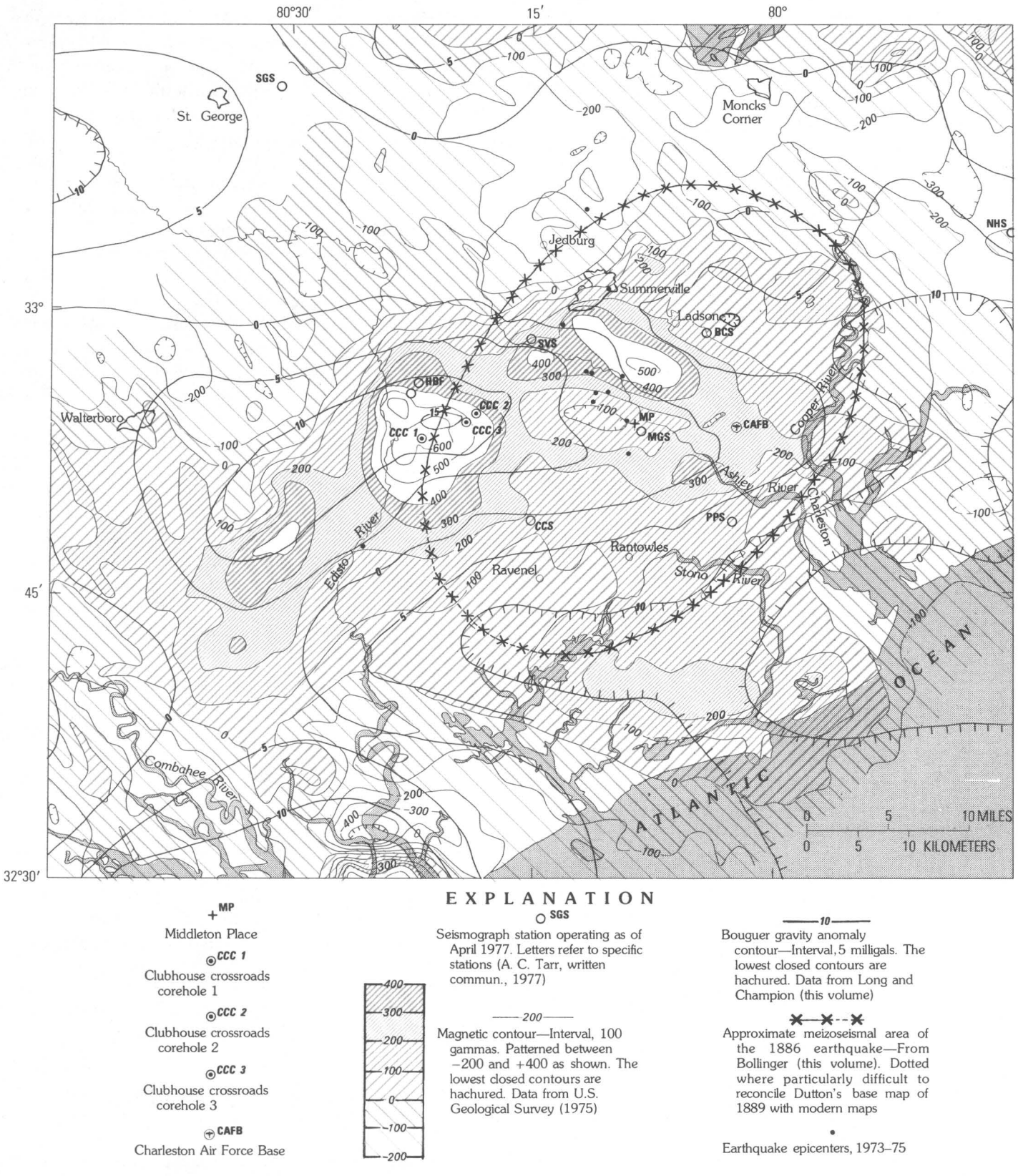

FIGURE 2.—Map of the vicinity of Charleston, S.C., showing the approximate location of the meizoseismal area of the 1886 earthquake in reference to the locations of coreholes, seismograph stations, magnetic contours, Bouguer gravity anomalies, earthquake epicenters (1973–75), and geographic features.

dipping unconsolidated and semiconsolidated sedimentary rocks. The wedge thickens from a feather edge against the crystalline rocks of the Appalachian orogenic belt along the Fall Line to thicknesses of more than 1 km near the coast in southeastern South Carolina (fig. 3). The rocks range in age from

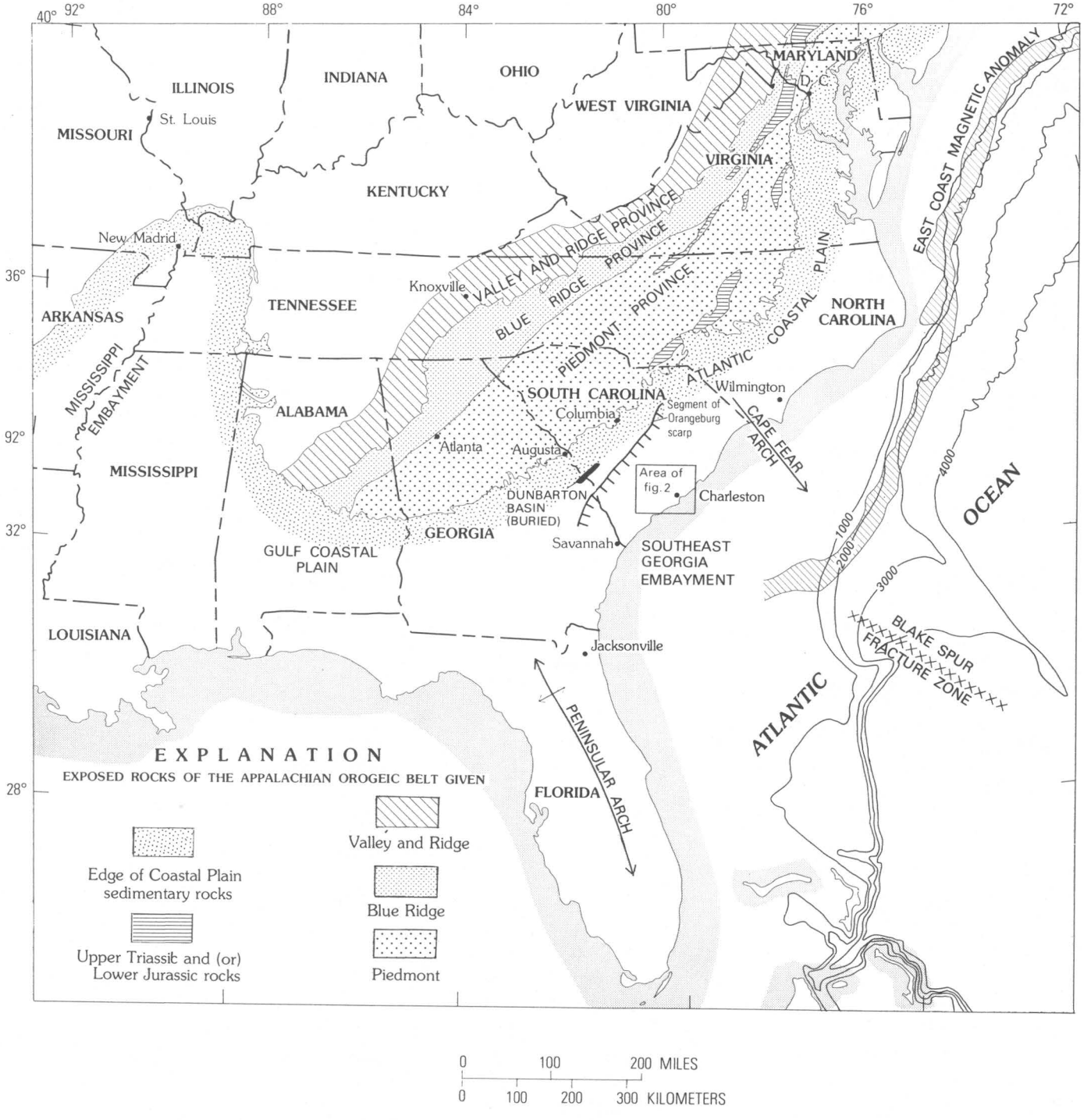

FIGURE 3.—Map of the southeastern United States showing location of Charleston, S.C., relative to regional features. The Fall Line represents the downstream extent of crystalline rock outcrops of the Piedmont and is roughly the same as the mapped edge of Coastal Plain rocks. Contour interval for submarine topography is 1,000 m. The east coast magnetic anomaly shown is from Schouten and Klitgord (1977) and Taylor and others (1968). The Blake Spur fracture zone is from Schouten and Klitgord (1977).

Mesozoic to Holocene; the oldest rocks exposed at the surface decrease in age toward the coast.

Most of the following description of the physiography of the Coastal Plain comes from Colquhoun and Johnson (1968). The Coastal Plain in South Carolina consists of three physiographic belts roughly parallel to the Atlantic coast. These are referred to from northwest to southeast as the Upper, Middle, and Lower Coastal Plains. The Upper Coastal Plain is a surface of fluvial or more rarely eolian erosion, which slopes irregularly from a maximum elevation of 150 to 180 m along the Fall Line to about 75 m on its southeastern side. It is separated from the Middle Coastal Plain by the Orangeburg scarp which has a relief of about 30 m across a distance of a few kilometers (fig. 3). The scarp is the locus of upper Miocene and Pliocene(?) shoreline deposits and coincides roughly with earlier Eocene shorelines as well (Colquhoun and Johnson, 1968). The Middle Coastal Plain consists of a surface on which fluvial erosion has proceeded to the point where the primary depositional topography, although present, is generally not obvious.

The Charleston-Summerville area is within the Lower Coastal Plain. The surface of the Lower Coastal Plain consists mainly of primary depositional topography formed during the Pleistocene and Holocene. Larger landforms, such as barrier island chains and marsh surfaces, can be seen, particularly close to the present shoreline. As Colquhoun and Johnson (1968) point out, individual storm-beach ridges can be seen on aerial photographs and topographic maps. Six barrier-beach systems (old shorelines) have been recognized on the Lower Coastal Plain; their landward surfaces rise to approximately 33, 21, 12, 8, 5, and 3 m. They have been named the Wicomico, Penholoway, Talbot, Pamlico, Princess Anne, and "Silver Bluff," respectively.

The oldest rocks known to date for which there is paleontologic control in the Coastal Plain of South Carolina are of Late Cretaceous (Cenomanian) age (Hazel and others, this volume), although at least one tectonic basin containing red terrigenous sedimentary rocks (Dunbarton basin, see below) is buried beneath the Upper Cretaceous rocks. Most of our detailed knowledge of the subsurface stratigraphy in the Charleston-Summerville area comes from the continuously cored drill hole (Clubhouse Crossroads corehole 1, hereafter called CCC 1) put down in 1974 and 1975 about 40 km west-northwest of Charleston as part of the Charleston studies (fig. 2). Results from this corehole not only provide detailed information on the stratigraphy of the Charleston-Summerville area but modify considerably the previously held interpretations of the geologic history of the Coastal Plain. (see papers in this volume by Gohn and others, Hazel and others, and Gottfried and others).

CCC 1 penetrated 750 m of Tertiary and Upper Cretaceous clastic and calcareous sedimentary rocks with good core recovery. The hole bottomed in 42 m of amygdaloidal basalt with excellent core recovery; the total depth was 792 m (Gohn and others, this volume). A general change in paleoenvironments is indicated from continental and marginal marine in the lower part of the Upper Cretaceous section to mostly marine in the upper Upper Cretaceous and younger section (Gohn and others, this volume, and Hazel and others, this volume). The change is not a simple transgression, however, but involves several transgressive-regressive cycles and four large time gaps. The most recent hiatus is within the Cooper Formation (the uppermost of the Tertiary units penetrated by CCC 1) composed of monotonous, bioturbated marine deposits (Gohn and others, this volume). The Cooper was deposited in an outer sublittoral (outer shelf) or deeper environment, and the hiatus which spans the Eocene-Oligocene boundary represents approximately the early Oligocene (Hazel and others, this volume). Work in progress suggests that this hiatus is useful in mapping nearsurface geology (L. M. Force, G. S. Gohn, B. B. Higgins, and Laurel Bybell, written and oral commun., 1976).

One of the most significant results from the deep-drilling program has been the recovery and analysis of samples of lava flows of amygdaloidal basalt from the bottom of the corehole (CCC 1). Two flows have been identified. The interpretation by Gottfried and others (this volume) of the geochemistry of the basalt considerably constrains the various models proposed for the Mesozoic tectonic setting of Charleston. Analyses show that the basalt has undergone slight to extreme oxidation, hydration, and hydrothermal alteration. The effects of alteration are greatest near the margins of the flows, and the least altered rocks can be identified. Gottfried and others (this volume) report that the light rare earth element (REE) enriched pattern and low K/Rb indicate an origin for the basalt from an undepleted source area in the upper mantle. The abundances of the REE, Ti, Zr and Nb, and the pattern of light REE enrichment are most similar to those obtained by other workers from the high-Ti quartz-normative tholeiites of Mesozoic age from eastern North America (ENA).

These continental basalts were erupted during rifting and crustal extension in the early stages of continental breakup when North America separated from Africa. In eastern North America these basalts are of Late Triassic or Early Jurassic age (Johnson and McLaughlin, 1957, and Cornet and others, 1973). This age is consistent with the evidence from magnetic anomaly patterns and deep-sea drilling for the initiation of the opening of the North Atlantic Ocean 180 m.y. ago (Pitman and Talwani, 1972; Vogt, 1973). K-Ar ages of 94.8 ± 4.2 m.y. and 109 ± 4 m.y. were obtained for the CCC 1 basalt by Richard Marvin, U.S. Geological Survey. Although the K-Ar ages are consistent with a Late Cretaceous (Cenomanian) age of the overlying Cape Fear Formation (Hazel and others, this volume), such a young age for the corehole basalt poses problems. By the beginning of Late Cretaceous time, the North Atlantic Ocean was already a significant feature and Charleston would have been on the order of 1,600 km from the Mid-Atlantic spreading center (see Pitman and Talwani, 1972). Gottfried and others (this volume) note that a magma-generating regime in the Charleston area 100 m.y. ago would almost certainly have been different from that of 180 m.y. ago which produced spacially related ENA tholeiitic basalts. Because of the close geochemical similarities of the corehole basalt to the ENA tholeiitic basalts, they conclude that these basalts are related in time as well as space. If that is true, a buried Triassic and (or) Jurassic basin may be present in the Charleston-Summerville area.

Because of the documented chemical alteration of the corehole basalt, the K-Ar ages must be considered minimum ages and permissive of an original Triassic or Jurassic age of the basalt (Gottfried and others, this volume). The alteration and minimum ages may reflect postmagmatic processes associated with Cretaceous(?) tectonic activity.

Sass and Ziagos (this volume) report on temperature measurements made in CCC 1 at 3-m intervals from the surface to the lowest depth of the hole. They obtain an average heat flow value of 1.3 ± 0.12 HFU (1 Heat-Flow-Unit (HFU) $= 10^{-6}$ cal cm^{-2} sec^{-1}). They note that this value is within the range of other values measured in eastern United States and that no thermal anomaly is associated with the Charleston-Summerville area.

In the Upper Coastal Plain in the area of the Savannah River, a buried graben containing terrestrial redbeds has been documented in the subsurface by extensive drilling and geophysical surveys, and has been named the Dunbarton basin by Marine and Siple (1974) (fig. 3). The basin is about 10 km wide and 50 km long and is wholly overlain by the Tuscaloosa Formation of Late Cretaceous age. As much as 903 m of maroon mudstone, sandstone of fluvial origin and fanglomerate fill the basin; no basalt flows were penetrated in the drilling. No fossils have been recovered from the basin drill holes, but by comparison with graben containing dated redbeds that are exposed elsewhere in the east, Marine and Siple (1974) suggest that the redbeds of the Dunbarton basin are of Triassic age.

GEOLOGY BENEATH COASTAL PLAIN ROCKS AND TECTONIC SETTING

The basement surface upon which the Coastal Plain sediments were deposited now dips gently seaward, on the average, but it is deformed by several transverse structures and contains at least one Mesozoic graben (the Dunbarton basin). The most important of these transverse structures in the southeast are the Cape Fear arch near the North Carolina-South Carolina border and the Peninsular arch (also called the Ocala arch or uplift) of Florida (fig. 3). These two arches are separated by the Southeast Georgia embayment. As summarized by Owens (1970), the Cape Fear arch divides the Atlantic Coastal Plain into two large poorly-defined sedimentary basins. Whereas glauconite-rich clastic rocks are dominant in the emerged Coastal Plain north of the arch, carbonate rocks are increasingly important southward and culminate in the Florida carbonate platform. The carbonate section is relatively thin over the Peninsula arch. A further difference in the basins is that Lower Cretaceous rocks are abundant in the Coastal Plain north of the Cape Fear arch, but, as noted in the previous section, have not been identified in South Carolina.

Over the Cape Fear arch, rocks as old as Cretaceous have been planed off by marine erosion which took place as early as late Miocene and which continued into the Pliocene and Pleistocene (Colquhoun and Johnson, 1968). Recent work by Winker and Howard (1977) has shown that the conventional wisdom of correlating barrier-beach systems (old shorelines) by elevation above present sea level (for example, Colquhoun and Johnson, 1968) is not valid. The old shorelines have been deformed into the Pliocene and Pleistocene by persistent Cenozoic structural features such as the Cape Fear arch and the Peninsular arch. A study of the deformation of these old shorelines offers one of the most promising ap-

proaches to the elucidation of Quaternary deformation in the Charleston-Summerville area.

The basement rocks in which the present seismicity takes place and in which the 1886 earthquake is presumed to have originated are not directly accessible for observation because of the Coastal Plain sedimentary cover. These basement rocks traditionally have been considered to be an extension of the metamorphic rocks of the Piedmont province exposed northwest of the feather edge of the Coastal Plain section (Rodgers, 1970). Aeromagnetic data suggest that this is not true. The basement beneath the Coastal Plain in the Charleston-Summerville area differs from the metamorphic terrane of the Piedmont in having a relatively smooth and continuous low-amplitude magnetic field which Popenoe and Zietz (this volume) suggest represents undeformed tuffaceous clastic rocks intermixed with basaltic and rhyolitic flows and ash-fall deposits. High-amplitude, steep-gradient, generally circular magnetic and gravity positive anomalies (fig. 2) within and adjacent to this basement block are interpreted to reflect mafic or ultramafic plutons in the basement (see papers by Popenoe and Zietz, Phillips, Long and Champion, and Kane, this volume). For convenience, this distinctive basement terrane is hereafter called the Charleston block. All of the area shown on figure 2 is thought to be within the Charleston block.

The extent and boundaries of the Charleston block are not well known, but it does appear to underlie a sizeable area of the emerged and submerged Coastal Plain. The Orangeburg scarp (fig. 3) appears to coincide with the northwestern boundary of the Charleston block and may be structurally controlled (Popenoe and Zietz, this volume; Higgins and others, 1976). A possible delineation of the other boundaries of the Charleston block is presented in the paper by Popenoe and Zietz (this volume).

Why did the 1886 earthquake occur in the Charleston-Summerville area rather than elsewhere in the Charleston block? Is it reasonable, in fact, to restrict the probability of a recurrence of an 1886 earthquake to the Charleston block at all? Clearly, we need to know more about the Charleston block and about the nature and location of the boundaries of this block.

In southwesternmost Georgia and northern Florida the mainly carbonate rocks of the Coastal Plain are underlain by nonfolded and nonmetamorphosed clastic rocks containing fossils ranging in age from Early Ordovician to probably Middle Devonian (Rodgers, 1970, and references therein). These fossiliferous Paleozoic rocks are clearly not part of the Appalachian orogenic belt. They have not been deformed by Appalachian orogenic events and they contain a pelecypod fauna that is closest to that of central Bohemia and Poland but that also has similarities to that of Nova Scotia, North Africa, and South America (Pojeta and others, 1976). Florida may thus represent a fragment of Africa (Rodgers, 1970) that was attached to North America during the closing of the late Precambrian and early Paleozoic Iapetus Ocean (Odom and Brown, 1976) and was then left behind during the opening of the present Atlantic Ocean basin (Rodgers, 1970). The Charleston block separates Florida from the Appalachian orogenic belt. As suggested by Popenoe and Zietz (this volume) and Long and Lowell (1973), the Charleston block basement may have formed as a zone of Mesozoic crutsal extension similar to the exposed Triassic and (or) Jurassic basins but much larger. This zone of extension is quite broad, perhaps as wide as 100 to 200 km, and is presumably related to the initial stages of the Mesozoic opening of the present Atlantic. The extension was apparently accompanied by the extrusion of continental tholeiitic lava such as that penetrated in CCC 1, and probably by the intrusion of large mafic plutons.

Charleston probably shared this general Mesozoic extensional setting with New Madrid. The zone of extension at New Mardrid can reasonably be called an aulocogen or failed-arm trough (Burke and Dewey, 1973), the location of which may have been controlled by an even earlier failed-arm trough (Ervin and McGinnis, 1975). The zone of extension, if that is what it is, occupied by the Charleston block, is more analogous to, but much larger than, the exposed Triassic and (or) Jurassic basins in eastern North America.

THE SOURCE AREA: METHOD OF APPROACH

An adequate explanation of the Charleston earthquake of 1886 must include detailed studies of the source area. Earthquakes in the area are presumably caused by the sudden release of gradually accumulated strain by faulting as no active volcanoes are present in the Coastal Plain. A first step in the study of the source area is, therefore, to identify and analyse faults. The history of fault movement through time, as well as the recency of movement must be determined, and this can be done only through study of the Coastal Plain section which records younger geologic events. From an understanding of the patterns of behavior of the fault through time as well as of changes in these patterns

it may be possible to place limits on the likely future behavior of the faults. It may be possible to establish a crude recurrence interval of movement for a given fault. It may be possible to establish the probability of the length of a fault that would break in a single event and to predict the geometry of that movement.

The modern regional stress field should be established from an analysis of the most recently formed structures and from in situ stress measurements. In unraveling these complex relations, a thorough understanding of the geologic history is necessary; the structure, structural history, and stress field must make sense in terms of the geologic history of the area.

A next step in understanding the source area is to characterize the modern seismicity including earthquake distribution and focal mechanisms. Only then, but not necessarily then, can one hope to relate the seismicity to a given fault or fault system.

A reevaluation of the historical record shows that Middleton Place is roughly in the center of the meizoseismal area of the 1886 earthquake (Bollinger, this volume). Seismicity continues in the same area today (the Middleton Place-Summerville seismic zone), and is either a continuation of the aftershock series or strain-energy release along structural features closely related to the origins of the 1886 event (Tarr, this volume). Most, if not all, of this recent seismicity originates in the basement beneath the Coastal Plain sedimentary rocks.

Observations of the basement may be made only by drilling and by various geophysical measurements. Drilling is extremely expensive but the information obtained is indispensible for calibrating the geophysical measurements as well as for the obvious direct geologic returns discussed earlier. Interpretation of the basement geology involves the construction of geologically reasonable models from the synthesis of the geophysical measurements, from drill-hole data (including extrapolation from the petrology of the cores) and from an understanding of the geology of the eastern seaboard.

Structures identified in the basement must be traced upward into the youngest rocks possible in order to determine as much as possible about the history and recurrence of movement and the geometry of movement. The interpretation of the deeper Coastal Plain geology involves the same process of constructing geologically reasonable models from drill-hole data and geophysics as in the interpretation of the basement geology. In addition, information on the biostratigraphy and lithostratigraphy is provided from the drill holes. For the shallow subsurface, a wealth of information can be obtained from shallow drilling. Given a mappable geophysical horizon and the control from shallow drilling, a definitive map of the shallow structure should be obtainable. These studies are underway. Geologic mapping of surface exposures will provide data on the Quaternary history and information to guide shallow drilling and shallow geophysical exploration and interpretation. Study of the raised and deformed barrier-beach systems are underway, and should contribute to the understanding of the Quaternary structural history. Along with this, a review of available geodetic leveling may provide information on any modern crustal movement.

The seismicity monitored by the South Carolina Seismographic Network must be related to basement structures as constrained by structures in Coastal Plain rocks. In the long run, this may be the most difficult as well as the most relevant task. Finally, the stress axes measured in drill holes by hydrofracturing must be related to stress axes inferred from focal mechanisms.

STUDIES OF THE MEIZOSEISMAL AREA

Clubhouse Crossroads corehole 1 was drilled over the center of the largest of the positive magnetic anomalies in the meizoseismal area (fig. 2). This magnetic anomaly coincides with a positive Bouguer gravity anomaly described by Long and Champion (this volume). Some of the numerous findings resulting from this drilling have already been cited and reported in this volume in articles by Gohn and others, Hazel and others, and Gottfried and others. Unfortunately, the corehole drilling had to be abandoned in the basalt and did not reach the body causing the anomaly and (or) crystalline basement. Additional deep drilling is in progress, in part to sample the source of that geophysical anomaly.[1] Figure 2

[1] Additional information has been received since this report was written. Clubhouse Crossroads corehole 3 (CCC 3), the deepest of the drill holes, reached a total depth of 1,152 m (3,780 ft) before a broken drill rod on May 19, 1977, forced abandonment of the drilling operation (see fig. 2). The drill penetrated basalt at 774 m (2,540 ft), passed through a thick section of it that contained one or two thin sedimentary rock interlayers, and entered red sandstone and shale at 1,031 m (3,384 ft) (Gohn, oral commun., 1977). No fossils have yet been recovered from these sedimentary rocks, but they do resemble rocks from exposed Triassic and (or) Jurassic basins. Thus, at CCC 3, 257 m of basalt are underlain by at least 121 m of red, probably terrestrial, clastic rocks.

The vertical electrical sounding (VES) data which suggest that the basalt near CCC 1 and CCC 3 is less than 75 m thick (Campbell, this volume) is in obvious conflict with the drill-hole findings. The cause of this discrepancy is under investigation. Ackermann's (this volume) calculations of basement depths were made assuming a thin basalt layer. These depth estimates must now also be increased, at least in the vicinity of CCC 3.

shows in a simplified way the geographic relationship between many of the features discussed in the meizoseismal area in this and other articles.

Phillips (this volume) presents the results of automated depth analysis performed on the aeromagnetic data. His work suggests that tops of most of the mafic plutons presumed to cause the pronounced magnetic anomalies are at a depth of 2.5 to 3.5 km and probably extend to depths of 4.5 km. His analysis also suggests that the crystalline basement is at a depth of 0.6 to 1.5 km. Hence, the mafic plutons are within the crystalline basement. The mafic body causing the large anomaly at CCC 1 appears to extend up to the top of the crystalline basement and is probably the only mafic pluton in the area which does so. The east-west magnetic low under Middleton Place is modeled as a nonmagnetic zone within the crystalline basement. Phillips suggests that this could be an altered zone along a fault, but also discusses the possibility that the magnetic pattern could be caused by reversed polarity of basalt lavas. The presence of reversely polarized basalts would also modify some other interpretations, and these complications are recognized by Phillips.

Ackermann (this volume) reports on the results of seismic refraction studies in the meizoseismal area, designed for full reverse coverage from a basement horizon 600 to 1,000 m deep, and partial reverse coverage from shallower horizons. Of three refracting horizons discovered, the shallowest corresponds to a thin well-indurated calcarenite at the base of the Santee Limestone. This horizon, which is about 100 m deep in CCC 1, may prove useful for mapping structures in the shallow subsurface. The intermediate refracting horizon corresponds to the top of the basalt at a depth of 750 m in the corehole. Ackermann determined this horizon had seismic velocities which range from 5.8 km/s at the corehole to 4.3 km/s at Middleton Place. He suggests that the velocity decrease could be caused either by increased fracture porosity or by a termination of the basalt layer and notes that the lowest velocity coincides with the epicentral area of the Nov. 22, 1974, earthquake. The surface of the intermediate refracting layer shows a broad trough-like depression trending N. or NNW. (Ackermann, this volume, fig. 4). The trough could be more than 50 m deep and is several kilometers west of Middleton Place.

Arrivals from the basalt layer, the intermediate refracting layer (assumed to be basalt), are shingled suggesting that this relatively high-velocity layer is interlayered in a lower velocity sequence. One interpretation of this is that the basalt is underlain by sedimentary rock. Ackermann calculates the depth to the lowest refracting horizon, which he interprets as high-velocity crystalline basement (6.3 to 6.5 km/s) using as a model a zone of constant velocity (4.2 km/s) between the basalt and the basement. Under this assumption, the basalt and basement horizons appear to diverge toward the southeast, with crystalline basement at a depth of about 900 m at CCC 1 but at a depth of 2,000 m some 25 km to the ESE. (Ackermann, this volume, fig. 5). The basement surface, so calculated, appears to slope more steeply in the southeast part of the surveyed area and Ackermann suggests that this may be a flexure or a fault.

Talwani (this volume) reports on the results of monitoring quarry blasts by portable seismographs in the area between Columbia and Georgetown, S.C.

By combining data from monitoring blasts in the Berkeley quarry (about 35 km north of Summerville), data from seismic-refraction lines of Ackermann (this volume and unpub. data, 1977), regional Bouguer gravity, and densities of samples from CCC 1, Talwani (this volume) has calculated three possible crustal models between the Berkeley quarry and the vicinity of Middleton Place. Two of the seismic-refraction lines used by Talwani in constraining his model were run by Ackermann after he had submitted his manuscript for this volume.

Campbell (this volume) reports on the results of 18 audio-frequency magnetotelluric (AMT) soundings and 9 Schlumberger d.c. resistivity soundings (vertical electrical soundings=VES) in the meizoseismal area. The most significant results to date are from the latter. In analysing the data, the resistivity of the electrical basement is assumed to be high with respect to that of the overlying sedimentary rocks; a value of 200 ohm-m is arbitrarily chosen. None of the VES showed a high-resistivity layer near the 750 m depth analogous to the basalt in CCC 1. Campbell argues that the basalt is, therefore, less than 75 m thick and is underlain by low-resistivity material. These data suggests that near the corehole the electrical basement is at 1,300 m and that the basalt is underlain by about half a kilometer of sedimentary rock.

Three VES soundings in the triangle between CCC 1, Summerville, and Middleton Place show an electrical basement at 900 m, significantly shallower than the 1,100- to 1,300-m-deep electrical basement elsewhere. These are soundings VES 2, 4, and 7 shown as Campbell's figure 2. Campbell suggests

that this shallower highly resistive horizon (the deepest observed at those locations) may reflect thickened basalt rather than crystalline basement. If true, the basalt is not only thicker, but also deeper (down-faulted or down-bent) on the southeast side of a line trending northeast between CCC 1 and Summerville. Long and Champion (this volume) speculate a similar down-dropped basin (Triassic?) on the basis of the gravity data.

EARTHQUAKE ORIGINS

The present seismicity which takes place along a NW.-SE. zone between Summerville and Middleton Place, is either part of the aftershock series of the 1886 earthquake or strain release along structures related to that earthquake. This seismicity is originating in the basement at depths significantly deeper than the basalt in CCC 1.

The largest event so far recorded (Nov. 22, 1974) was at the SE. end of this zone under Middleton Place, also essentially the center of the meizoseismal area of the 1886 event. The focal mechanism for this event suggests compression along a NE.-SW. axis. One of the nodal planes determined for this event is consistent with nearly vertical (perhaps reverse) faulting on a plane striking N. 42° W. (Tarr, this volume). The suggested NE.-SW. compression is consistent with the pattern of compressive stress found by Sbar and Sykes (1973) for eastern North America. On the basis of this, the stress environment of Charleston appears to have changed from the Mesozoic stress environment which involved extension on a NE.-SW. axis. Sbar and Sykes (1973) further speculate that the Charleston-Summerville seismicity may be localized at the continental margin along the landward projection of the Blake Spur fracture zone (fig. 3). This hypothesis should certainly be pursued. As yet, no geologic feature has been recognized in the exposed crystalline rocks of the Piedmont that can be related to the fracture zone such as the train of alkalic plutons of the White Mountain Plutonic Series in New England which has been suggested as the continental projection of the Kelvin Sea Mount chain (Diment and others, 1972, and Sbar and Sykes, 1973).

Kane (this volume) notes a correlation between Bouguer gravity highs and seven well-defined eastern North American earthquake regions including Charleston, New Madrid, and Cape Ann. The gravity highs are interpreted as being caused by mafic or ultramafic plutons. He notes that the major seismic activity in each region does not coincide with the position of the gravity anomalies but is peripheral to them. He suggests that the plutons may act to concentrate regional stress around their peripheries —perhaps through plastic deformation of serpentinized rocks, a concept derived from the hole-in-plate problem of mechanics. A somewhat similar hypothesis of stress amplification has been proposed by Long (1976) for the observed relationship between mafic plutons (as deduced from the gravity field) and seismicity. His concept differs from Kane's in that the inhomogeneities in the plate (the mafic plutons) are interpreted to be more rigid than the enclosing plate.

CONCLUSIONS

The more important concepts that are emerging from the work underway are as follows:

1. Seismic activity is continuing today in the center of the meizoseismal area of the 1886 earthquake at a higher level than prior to 1886.
2. The present seismic activity probably originates in the crystalline basement beneath the Coastal Plain sedimentary rocks.
3. The crystalline basement beneath the Charleston-Summerville area is not simply a seaward extension of crystalline rocks exposed in the Piedmont.
4. The Charleston block may represent a broad zone of Triassic and Jurassic crustal extension formed during the early stages of the opening of the Atlantic Ocean.
5. The present stress regime appears to be one of NE.-SW. compression rather than extension, and is similar to the stress regime of a large part of the eastern United States.
6. The structure in the Charleston-Summerville area is not a simple homocline of Coastal Plain sedimentary rocks dipping toward the sea on a gently dipping basement surface.
7. Various geophysical surveys yield interpretations that are not yet consistent.
8. Geologic mapping is incomplete but should yield valuable results.
9. Studies of one large eastern earthquake area may yield results that are useful to studies of others; for example, the association of seismicity with the margins of positive gravity anomalies.

The cause of the Charleston-Summerville seismicity is still not determined. We certainly know a great deal more about the area than we did a few years ago and can begin to draw some constraints around some of the possibilities. The papers in this volume

report on the first stage of an ongoing study. If the seismicity is to be understood, the answer will come from the multidisciplinary approach we are trying to pursue. Such detailed geologic and geophysical studies seeking to understand the geologic history and current tectonic regime of a seismic source area are very few and for intraplate sources areas, represent a new dimension in seismic analysis.

REFERENCES CITED

Allen, C. R., Hanks, T. C., and Whitcomb, J. H., 1973, San Fernando Earthquake: seismological studies and their tectonic implications, *in* U.S. Natl. Oceanic and Atmospheric Admin., San Fernando, California, earthquake of February 9, 1971: Washington, D.C., U.S. Govt. Printing Office, v. 3, p. 13–21.

Bollinger, G. A., 1972, Historical and recent seismic activity in South Carolina: Seismol. Soc. America Bull., v. 62, no. 3, p. 851–864.

Burke, Kevin, and Dewey, J. F., 1973, Plume-generated triple junctions: key indicators in applying plate tectonics to old rocks: Jour. Geology, v. 81, no. 4, p. 406–433.

Carver, David, Turner, L. M., and Tarr, A. C., 1977, South Carolina seismological data report May 1974–June 1975: U.S. Geol. Survey open-file rept. 77–429, 66 p.

Colquhoun, D. J., and Johnson, H. S., Jr., 1968, Tertiary sea-level fluctuation in South Carolina: Palaeogeography, Palaeoclimatology, Palaeoecology, v. 5, no. 1, p. 105–126.

Cornet, Bruce, Traverse, Alfred, and McDonald, N. G., 1973, Fossil spores, pollen, and fishes from Connecticut indicate Early Jurassic age for part of the Newark Group: Science, v. 186, p. 1243–1247.

Dewey, J. F., and Bird, J. M., 1970, Mountain belts and the new global tectonics: Jour. Geophys. Research, v. 75, no. 14, p. 2625–2647.

Diment, W. H., Urban, T. C., and Revetta, F. A., 1972, Some geophysical anomalies in the eastern United States, *in* Robertson, E. C., ed., The nature of the solid earth: New York, McGraw-Hill Book Co., p. 544–572.

Dutton, C. E., 1889, The Charleston earthquake of August 31, 1886: U.S. Geol. Survey, Ninth Ann. Rept. 1887–88, p. 203–528.

Ervin, C. P., and McGinnis, L. D., 1975, Reelfoot Rift; reactivated precursor to the Mississippi Embayment: Geol. Soc. America Bull., v. 86, no. 9, p. 1287–1295.

Evernden, J. F., 1975, Seismic intensities, "size" of earthquakes and related parameters: Seismol. Soc. America Bull., v. 65, no. 5, p. 1287–1313.

——— 1976, A reply to "Comments on 'Seismic intensities, "size" of earthquakes and related parameters' by Otto W. Nuttli": Seismol. Soc. America Bull., v. 66, p. 339–340.

Gupta, I. N., and Nuttli, O. W., 1976, Spatial attenuation of intensities for central U. S. earthquakes: Seismol. Soc. America Bull., v. 66, no. 3, p. 743–751.

Hadley, J. B., and Devine, J. F., 1974, Seismotectonic map of the eastern United States: U.S. Geol. Survey Misc. Field Studies Map MF–620.

Higgins, B. B., Owens, J. P., Popenoe, Peter, and Gohn, G. S., 1976, Structures in the Coastal Plain of South Carolina: Geol. Soc. America Abstracts with Programs, v. 8, no. 2, p. 195–196.

Johnson, M. E., and McLaughlin, D. B., 1957, Triassic formations in the Delaware Valley: Geol. Soc. America Guidebook for field trips, Atlantic City 1957, Field Trip No. 2, p. 31–56.

Long, L. T., 1976, Speculations concerning southeastern earthquakes, mafic intrusions, gravity anomalies, and stress amplification: Earthquake Notes, v. 47, p. 29–35.

Long, L. T., and Lowell, R. P., 1973, Thermal model for some continental margin sedimentary basins and uplift zones: Geology, v. 1, no. 2, p. 87–88.

Marine, I. W., and Siple, G. E., 1974, Buried Triassic basin in the central Savannah River area, South Carolina and Georgia: Geol. Soc. America Bull., v. 85, no. 2, p. 311–320.

Mosaic, 1976, Quakes in search of a theory: Mosaic, v. 7, no. 4, p. 2–11.

Nuttli, O. W., 1973, The Mississippi Valley earthquakes of 1811 and 1812; intensities, ground motion and magnitudes: Seismol. Soc. America Bull., v. 63, no. 1, p. 227–248.

——— 1976, Comments on "Seismic intensities, 'size' of earthquakes and related parameters" by Jack F. Evernden: Seismol. Soc. America Bull., v. 66, no. 1, p. 331–340.

Odom, A. L., and Brown, J. F., 1976, Was Florida a part of North America in the lower Paleozoic?: Geol. Soc. America Abs. with Programs, v. 8, no. 2, p. 237–238.

Owens, J. P., 1970, Post-Triassic tectonic movements in the central and southern Appalachians as recorded by sediments of the Atlantic Coastal Plain, *in* Fisher, G. W., and others, eds., Studies of Appalachian geology, central and southern: New York, Intersci. Publishers, p. 417–427.

Pitman, W. C., III, and Talwani, Manik, 1972, Sea-floor spreading in the North Atlantic: Geol. Soc. America Bull., v. 83, no. 3, p. 619–646.

Pojeta, John, Jr., Kříž, Jiří, and Berdan, J. M., 1976, Silurian-Devonian pelocypods and Paleozoic stratigraphy of subsurface rocks in Florida and Georgia and related Silurian pelecypods from Bolivia and Turkey: U.S. Geol. Survey Prof. Paper 879, 32 p.

Rodgers, John, 1970, The tectonics of the Appalachians: New York, Intersci. Publishers, 271 p.

Sbar, M. L., and Sykes, L. R., 1973, Contemporary compressive stress and seismicity in eastern North America: An example of intraplate tectonics: Geol. Soc. America Bull., v. 84, no. 6, p. 1861–1881.

Schouten, Hans, and Klitgord, K. D., 1977, Mesozoic magnetic anomalies, western North Atlantic: U.S. Geol. Survey Misc. Field Studies Map MF–915.

Scott, N. H., 1973, Felt area and intensity of San Fernando earthquake, *in* U.S. Natl. Oceanic and Atmospheric Admin., San Fernando, California, earthquake of February 9, 1971: Washington, D.C., U.S. Govt. Printing Office, v. 3, p. 23–48.

Shaler, N. S., 1899, Aspects of the Earth: New York, Charles Scribner's Sons, 344 p.

Tarr, A. C., comp., 1974, World seismicity map: Reston, Va., U. S. Geol. Survey.

Taylor, P. T., Zietz, Isidore, and Dennis, L. S., 1968, Geologic implications of aeromagnetic data for the eastern continental margin of the United States: Geophysics, v. 33, no. 5, p. 755–780.

U.S. Geological Survey, 1975, Aeromagnetic map of Charleston and vicinity, South Carolina: U.S. Geol. Survey open-file map 75–590.

Vogt, P. R., 1973, Early events in the opening of the North Atlantic, *in* Tarling, D. H., and Runcorn, S. K., eds., Implications of continental drift to the earth sciences, NATO Advance Study Institute, Newcastle-upon-Tyne, England (1972), v. 2, p. 693–712.

Winker, C. D., and Howard, J. D., 1977, Correlation of tectonically deformed shorelines on the southern Atlantic Coastal Plain: Geology, v. 5, p. 123–127.

Reinterpretation of the Intensity Data for the 1886 Charleston, South Carolina, Earthquake

By G. A. BOLLINGER

STUDIES RELATED TO THE CHARLESTON, SOUTH CAROLINA, EARTHQUAKE OF 1886—A PRELIMINARY REPORT

GEOLOGICAL SURVEY PROFESSIONAL PAPER 1028-B

CONTENTS

ILLUSTRATIONS

TABLES

STUDIES RELATED TO THE CHARLESTON, SOUTH CAROLINA, EARTHQUAKE OF 1886—
A PRELIMINARY REPORT

REINTERPRETATION OF THE INTENSITY DATA FOR THE 1886 CHARLESTON, SOUTH CAROLINA, EARTHQUAKE

By G. A. BOLLINGER [1]

ABSTRACT

In 1889, C. E. Dutton published all his basic intensity data for the 1886 Charleston, S.C., shock but did not list what intensity values he assigned to each report, nor did he show the distribution of the locations of these data reports on his isoseismal map. The writer and two other seismologists have each independently evaluated Dutton's 1,300 intensity reports (at least two of the three interpreters agreed on intensity values for 90 percent of the reports), and the consensus values were plotted and contoured. One map was prepared on which contours emphasized the broad regional pattern of effects (with results similar to Dutton's); another map was contoured to depict the more localized variations of intensity. As expected, the latter map shows considerable detail in the epicentral region as well as in the far-field. In particular, intensity VI (Modified Mercalli (MM)) effects are noted as far away as central Alabama and the Illinois-Kentucky-Tennessee border area. Dutton's "low intensity zone" in West Virginia appears on both isoseismal maps.

A maximum MM intensity of X for the epicentral region and IX for Charleston appears to be appropriate. Epicentral effects included at least 80 km of railroad track seriously damaged and more than 1,300 km^2 of extensive cratering and fissuring. In Charleston, the railroad-track damage and cratering were virtually absent, whereas many, but not most, buildings on both good and poor ground were destroyed.

The epicentral distances to some 800 intensity-observation localities were measured, and the resulting data set was analyzed by least-square regression procedures. The attenuation equation derived is similar to others published for different parts of the eastern half of the United States. The technique of using intensity-distance pairs rather than isoseismal maps has the advantages, however, of completely bypassing the subjective contouring step in the data handling and of being able to specify the particular fractile of the intensity data to be considered.

When one uses intensities in the VI to X range, and their associated epicentral distances for this earthquake, body-wave magnitude estimates of 6.8 (Central United States intensity-velocity data published by Nuttli in 1976) and 7.1 (Western United States intensity-velocity data published by Trifunac and Brady in 1975) are obtained.

[1] Virginia Polytechnic Institute and State University, Blacksburg, Va.

INTRODUCTION

The problems associated with the description of seismic ground motion in a minor seismicity area such as the Southeastern United States are well known. In that region, the largest events took place before instruments were available to record them, so that only qualitative descriptions of their effects exist. During the past few decades, when instruments began to be used, no event having $m_b>5$ has taken place. Thus we have quantitative data only for small events, and we need to analyze the qualitative data, which are all that is available for larger events.

The purpose of this study is to review thoroughly the data that do exist and to derive as much information as possible concerning regional seismic ground motions. Fortunately, the largest earthquake known to have occurred in the region, the 1886 Charleston, S.C., earthquake, was well studied by Dutton (1889) and his coworkers. An excellent suite of intensity information is thus available for that important earthquake. Secondly, the Worldwide Standard Seismograph Network (WWSSN) stations in the Eastern United States provide data on the radiation from the regional earthquakes that have occurred since installation of the stations. Finally, intensity-particle-velocity relationships as well as attenuation values for various seismic phases have been proposed that can be utilized in an attempt to synthesize the above data types.

The initial part of this paper is concerned with a reevaluation of the intensity data for the 1886 Charleston earthquake, and the second part, with a consideration of the attenuation of intensity as distance from the epicenter increases. (The distance

from the epicenter is hereafter called epicentral distance.) The concluding section presents a magnitude estimate for the 1886 shock.

This research was conducted while the author was on study-research leave with the U.S. Geological Survey (U.S.G.S.) in Golden, Colo. Thanks are extended to the members of the Survey, particularly Robin McGuire and David Perkins, for their many helpful discussions. Robin McGuire did the regression analysis presented in this paper, and Carl Stover provided a plot program for the intensity data. Thanks are also due to Rutlage Brazee (National Oceanographic and Atmospheric Administration, N.O.A.A.) and Ruth Simon (U.S.G.S.) for interpreting the sizable amount of intensity data involved in this study.

This research was sponsored in part by the National Science Foundation under grant No. DES 75–14691.

INTENSITY EFFECTS IN THE EPICENTRAL REGION

Dutton assigned an intensity X as the maximum epicentral intensity for the 1886 shock. He used the Rossi-Forel scale; conversion to the Modified Mercalli (MM) scale results in a X–XII value. However, the revised edition (through 1970) of the "Earthquake History of the United States" (U.S. Environmental Data Service, 1973) downgraded Dutton's value to a IX–X (MM). Because of this revision, it is appropriate to compare the scale differences between these two intensity levels (IX and X) with the meizoseismal effects as presented by Dutton.

Ground effects, such as cracks and fissures, and damage to structures increase from the intensity IX to the intensity X level, whereas damage to rails is first listed in the MM scale at the X level. Taken literally, rail damage is indicative of at least intensity-X-level shaking. Richter (1958, p. 138) also listed "Rails bent slightly" for the first time at intensity X. However, he instructed (p. 136) that, "Each effect is named at that level of intensity at which it first appears frequently and characteristically. Each effect may be found less strongly, or in fewer instances, at the next lower grade of intensity; more strongly or more often at the next higher grade." Thus, widespread damage to rails is a firm indicator of intensity-X shaking.

In discussing building damage, it is convenient to use Richter's (1958, p. 136–137) masonry A, B, C, D classification:

> Masonry A. Good workmanship, mortar, and design; reinforced, especially laterally, and bound together by using steel, concrete, etc.; designed to resist lateral forces.
>
> Masonry B. Good workmanship and mortar; reinforced, but not designed in detail to resist lateral forces.
>
> Masonry C. Ordinary workmanship and mortar; no extreme weaknesses like failing to tie in at corners, but neither reinforced nor designed against horizontal forces.
>
> Masonry D. Weak materials, such as adobe; poor mortar; low standards of workmanship; weak horizontally.

At the IX level, masonry D structures are destroyed, masonry C structures are heavily damaged, sometimes completely collapsed, and masonry B structures are seriously damaged. Frame structures, if not bolted, are shifted off their foundations and have their frames racked at IX-level shaking, whereas at intensity X most such structures are destroyed. Nearly complete destruction of buildings up to and including those in the masonry B class is a characteristic of the intensity-X level.

Only in Charleston do we have a valid sample of the range of structural damage caused by the 1886 earthquake. It was the only nearby large city, and it contained structural classes up to the range between masonry C and masonry B. Many of the important public buildings, as well as mansions and churches, had thick walls of rough handmade bricks joined with an especially strong oyster-shell-lime mortar. The workmanship was described as excellent, but nowhere in Dutton's (1889) account is reference made to special reinforcement or design to resist lateral forces. Structures outside the Charleston area (as in Summerville, see p. 21) were built on piers, some 1–2 m (3–6 ft) high, thereby making the structures inverted pendulums. Dutton's report for Charleston indicates that although the damage was indeed extensive (see below), most masonry buildings and frame structures were not destroyed. This fact plus Dutton's report on the absence of rail damage and extensive ground effects in the Charleston area indicates an intensity level of IX.

The following quotations from Dutton's report (1889, p. 248–249, 253) contain detailed descriptions of the structural damage in Charleston caused by the earthquake of 1886:

> There was not a building in the city which had wholly escaped injury, and very few had escaped serious injury. The extent of the damage varied greatly, ranging from total demolition down to the loss of chimney tops and the dislodgment of more or less plastering. The number of buildings which were completely demolished and leveled to the ground was not great. But there were several hundred which lost a large portion of their walls. There were very many also which remained standing, but so badly shattered

that public safety required that they should be pulled down altogether. There was not, so far as at present known, a brick or stone building which was not more or less cracked, and in most of them the cracks were a permanent disfigurement and a source of danger or inconvenience. A majority of them however were susceptible of repair by means of long bolts and tie-rods. But though the buildings might be made habitable and safe against any stresses that houses are liable to except fire and earthquake, the cracked walls, warped floors, distorted foundations, and patched plaster and stucco must remain as long as the buildings stand permanent eye-sores and sources of inconveniences. As soon as measures were taken to repair damages the amount of injury disclosed was greater than had at first appeared. Innumerable cracks which had before been unnoticed made their appearance. The bricks had "worked" in the embedding mortar and the mortar was disintegrated. The foundations were found to be badly shaken and their solidity was greatly impaired. Many buildings had suffered horizontal displacement; vertical supports were out of plumb; floors out of level; joints parted in the wood work; beams and joists badly wrenched and in some cases dislodged from their sockets. The wooden buildings in the northern part of the city usually exhibited externally few signs of the shaking they received except the loss of chimney tops. Some of them had been horizontally moved upon their brick foundations, but none were overthrown. Within these houses the injuries were of the same general nature as within those of brick, though upon the whole not quite so severe.

The amount of injury varied much in different sections of the city from causes which seem to be attributable to the varying nature of the ground. The peninsula included between the Cooper and Ashley Rivers, upon which Charleston is built, was originally an irregular tract of comparatively high and dry land, invaded at many points of its boundary by inlets of low swampy ground or salt marsh. These inlets, as the city grew, were gradually filled up so as to be on about the same level as the higher ground. * * * As a general rule, though not without a considerable number of exceptions, the destruction was greater upon made ground than upon the original higher land. [p. 248–249] * * *

In truth, there was no street in Charleston which did not receive injuries more or less similar to those just described. To mention them in detail would be wearisome and to no purpose. The general nature of the destruction may be summed up in comparatively few words. The destruction was not of that sweeping and unmitigated order which has befallen other cities, and in which every structure built of material other than wood has been either leveled completely to the earth in a chaos of broken rubble, beams, tiles, and planking, or left in a condition practically no better. On the contrary, a great majority of houses were left in a condition shattered indeed, but still susceptible of being repaired. Undoubtedly there were very many which, if they alone had suffered, would never have been repaired at all, but would have been torn down and new structures built in their places; for no man likes to occupy a place of business which suffers by contrast with those of his equals. But when a common calamity falls upon all, and by its very magnitude and universality renders it difficult to procure the means of reconstruction, and where thousands suffer much alike, his action will be different. Thus a very large number of buildings were repaired which, if the injuries to them had been exceptional misfortunes instead of part of a common disaster, would have been replaced by new structures. Instances of total demolition were not common.

This is probably due, in some measure, to the stronger and more enduring character of the buildings in comparison with the rubble and adobe work of those cities and villages which are famous chiefly for the calamities which have befallen them. Still the fact remains that the violence of the quaking at Charleston, as indicated by the havoc wrought, was decidely less than that which has brought ruin to other localities. The number of houses which escaped very serious injuries to their walls was rather large; but few are known to have escaped minor damages, such as small cracks, the loss of plastering, and broken chimney tops. [p. 253]

Damage to the three railroad tracks that extend north, northwest, and southwest from Charleston began about 6 km (3.7 mi) northwest of the city and was extensive (fig. 1*A*). More than 80 km (62 mi) of these tracks was affected. The effects listed were: lateral and vertical displacement, formation of S-shaped curves, and the longitudinal movement of hundreds of meters of track. A detailed listing of the effects along the South Carolina Railroad tracks, which run northwest from Charleston directly through the epicentral region, is given in table 1.

Ground cracks from which mud or sand are ejected and in which earthquake fountains or sand craters are formed begin on a small scale at intensity VIII, become notable at IX, and are large and spectacular phenomena at X (Richter, 1958, p. 139). The formation of sand craterlets and the ejection of sand were certainly widespread in the epicentral area of the 1886 earthquake. Many acres of ground were overflowed with sand, and craterlets as much as 6.4 m (21 ft) across were formed. Dutton (1889, p. 281) wrote: "Indeed, the fissuring of the ground within certain limits may be stated to have been universal, while the extravasation of water was confined to certain belts. The area within which these fissures may be said to have been a conspicuous and almost universal phenomenon may be roughly estimated at nearly 600 square miles [1,550 sq. km]." By comparison, the elliptical intensity-X contour suggested by the present study encloses an area of approximately 1,300 km^2.

The distribution of craterlets taken from Dutton (1889, pl. 28) is also shown in figure 1*A*. In a few localities, the water from the craters probably spouted to heights of 4.5–6 m (15–20 ft), as indicated by sand and mud on the limbs and foliage of trees overhanging the craters.

Other ground effects indicating the intensity-X level are fissures as much as a meter wide running parallel to canal and streambanks, and changes of

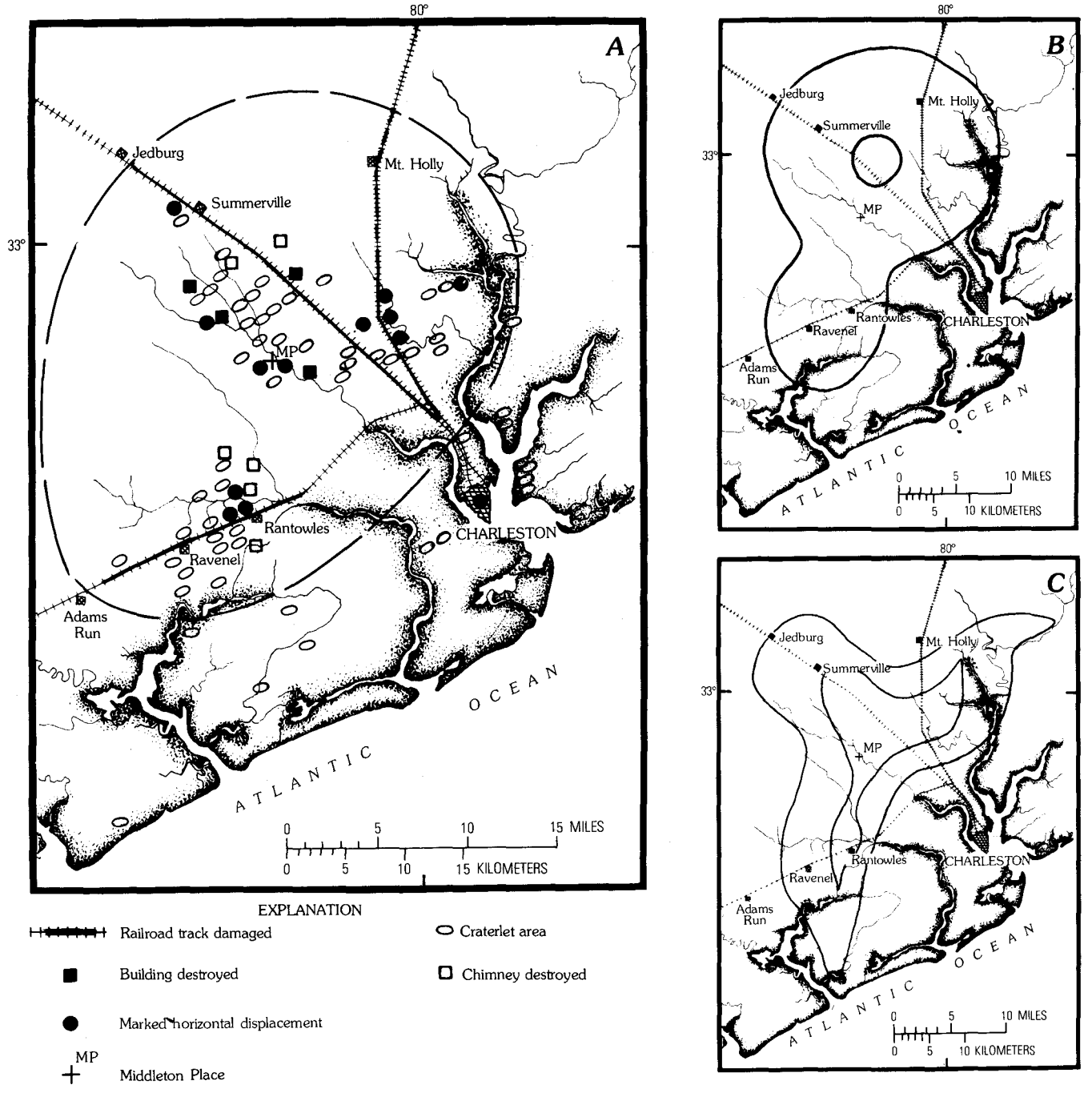

FIGURE 1.—Epicentral area maps for the 1886 Charleston, S.C., earthquake. *A*, This study. Dashed contour encloses intensity-X effects. *B*, Dutton's map and *C*, Sloan's map (modified from Dutton, 1889, pls. 26 and 27, respectively) show contours enclosing the highest intensity zone, although neither Dutton nor Sloan labeled his contours. Base map modified from Dutton (1889). Rivers flowing past the Charleston peninsula are the Ashley River flowing from the northwest and the Cooper River flowing from the north.

the water level in wells (Wood and Neuman, 1931). Dutton (1889, p. 298) reported that a series of wide cracks opened parallel to the Ashley River (see caption, fig. 1) and that the sliding of the bank riverward uprooted several large trees, which fell over into the water. His plate 23 shows a crack along the bank of the Ashley River about a meter wide and some tens of meters long across the field of view of the photograph.

In a belt of craterlets (trend N. 80° E., length ~5 km) about 10 km (6.2 mi) southeast of Summerville, Sloan reported (Dutton, 1889, p. 297) that

TABLE 1.—*Variation of intensity effects along the South Carolina Railroad*

[Based on Dutton, 1889, p. 282–287. Refer to fig. 1 for locations mentioned]

Distance from Charleston (km)	Distance from Charleston (mi)	Effects
<5.8	<3.66	Occasional cracks in ground; no marked disturbance of track or roadbed.
5.8	3.66	Rails notably bent and joints between rail opened.
5.8–8	3.66–5	Ground cracks and small craterlets.
8	5	Fishplates torn from fastenings by shearing of the bolts; joints between rails opened to 17.5 cm (7 in.).
9.6	6	Joints opened, roadbed permanently depressed 15 cm (6 in.).
14.4	9	Lateral displacements of the track more frequent and greater in amount; serious flexure in the track that caused a train to derail; more and larger craterlets.
16	10	Craterlets seemed to be greater in size (as much as 6.4 m (21 ft) across) and number; many acres overflowed with sand.
16–17.6	10–11	Maximum distortions and dislocations of the track; often displaced laterally and sometimes alternately depressed and elevated; occasional severe lateral flexures of double curvature and great amount; many hundreds of meters of track shoved bodily to the southeast; track parted longitudinally, leaving gaps of 17.5 cm (7 in.) between rail ends; 46 cm (18 in.) depression or sink in roadbed over a 18-m (60-ft) length.
17.6–24	11–15	Many lateral deflections of the rails.
24–25.6	15–16	Epicentral area—a few wooden sheds with brick chimneys completely collapsed; railroad alinement distorted by flexures; elevations and depressions, some of considerable amount, also produced.
29–30.6	18.5–19	Flexures in track, one in an 8.8-m (29-ft) section of single rails had an S-shape and more than 30 cm (12 in.) of distortion.
32	≈20	"... a still more complex flexure was found. Beneath it was a culvert which had been strained to the northwest and broken" (p. 286); a long stretch of the roadbed and track distorted by many sinuous flexures of small amplitude.
33.9	21	Tracks distorted laterally and vertically for a considerable distance.
34.9	21.66	At Summerville—many flexures, one of which was a sharp S-shape; broken culvert under tracks in a sharp double curvature.
35.4–44.3	22–27.5	Disturbance to track and roadbed diminishes rapidly.
44.3	27.5	At Jedburg—a severe buckling of the track.

wells had been cracked in vertical planes from top to bottom, and that the wells had been almost universally disturbed, many overflowing and subsequently subsiding, others filling with sand or becoming muddy.

In Summerville, whose population at that time was about 2,000, the structures were supported on wood posts or brick piers 1–2 m high and, though especially susceptible to horizontal motions, the great majority did not fall. Rather, the posts and piers were driven into the soil so that many houses settled in an inclined position or were displaced as much as 5 cm. Chimneys, which were constructed to be independent of the houses, generally had the part above the roofline dislodged and thrown to the ground. Below the roofs, many chimneys were crushed at their bases, both bricks and mortar being disintegrated and shattered, allowing the whole column to sink down through the floors. This absence of overturning in piered structures plus the nature of the damage to chimneys was interpreted by Dutton as evidence for predominantly vertical ground motions.

The preceding discussion indicates an intensity-X level of shaking in the epicentral area. Figure 1*A* depicts the approximate extent of this region along with the locations of rail damage, craterlet areas, building damage, and areas of marked horizontal displacements. Dutton and his coworkers did not map the regions of pronounced vertical-motion effects, but they did emphasize the importance of these effects in the epicentral region. Also shown in figure 1 (*B* and *C*) is the extent of the highest intensity zone, as given by Dutton and by Sloan. Because of the sparsely settled and swampy nature of the region, the meizoseismal area cannot be defined accurately.

INTENSITY EFFECTS THROUGHOUT THE COUNTRY

Dutton (1889) published all his intensity reports, some 1,337, but he did not list the intensity values that he assigned to each report, nor did he show the location of the data points on his isoseismal map. By using the basic data at hand, a reevaluation was attempted to present another interpretation of the data (in the MM scale) and to determine whether additional information could be extracted concerning this important earthquake. The writer and two other seismologists (Rutlage Brazee, N.O.A.A., and Ruth Simon, U.S.G.S.) each independently evaluated Dutton's intensity data listing according to the MM scale. For the resulting 1,047 usable reports, ranging from MM level I to X, at least two of the three interpreters agreed on intensity values for 90 percent of the reports. As would be expected, most of the disagreement was found at the lower intensity levels (II–V). A full listing of the three independent intensity assignments for each location was made by Bollinger and Stover (1976).

The consensus values, or the average intensity values, in the 10 percent of the reports where all three interpreters disagreed were plotted at two different map scales and contoured (figs. 2–5). When multiple reports were involved, for example, those from cities, the highest of the intensity values obtained was assigned as the value for that location.

The greatest number of reports (178) for an individual State was from South Carolina. Figure 2 presents the writer's interpretation of these data. Even

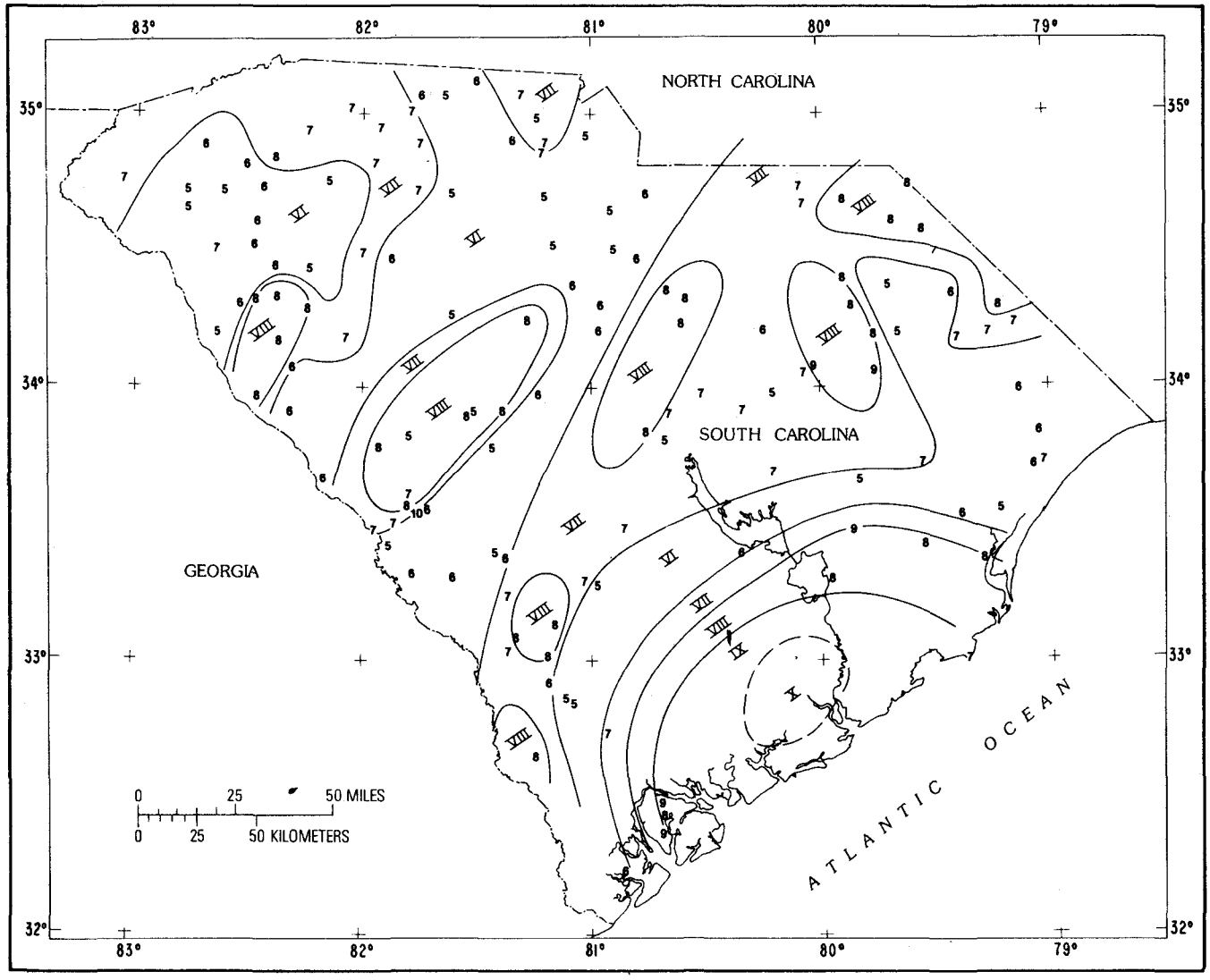

FIGURE 2.—Isoseismal map showing the State of South Carolina for the 1886 Charleston earthquake. Intensity observations are indicated by Arabic numerals, and the contoured levels are shown by Roman numerals.

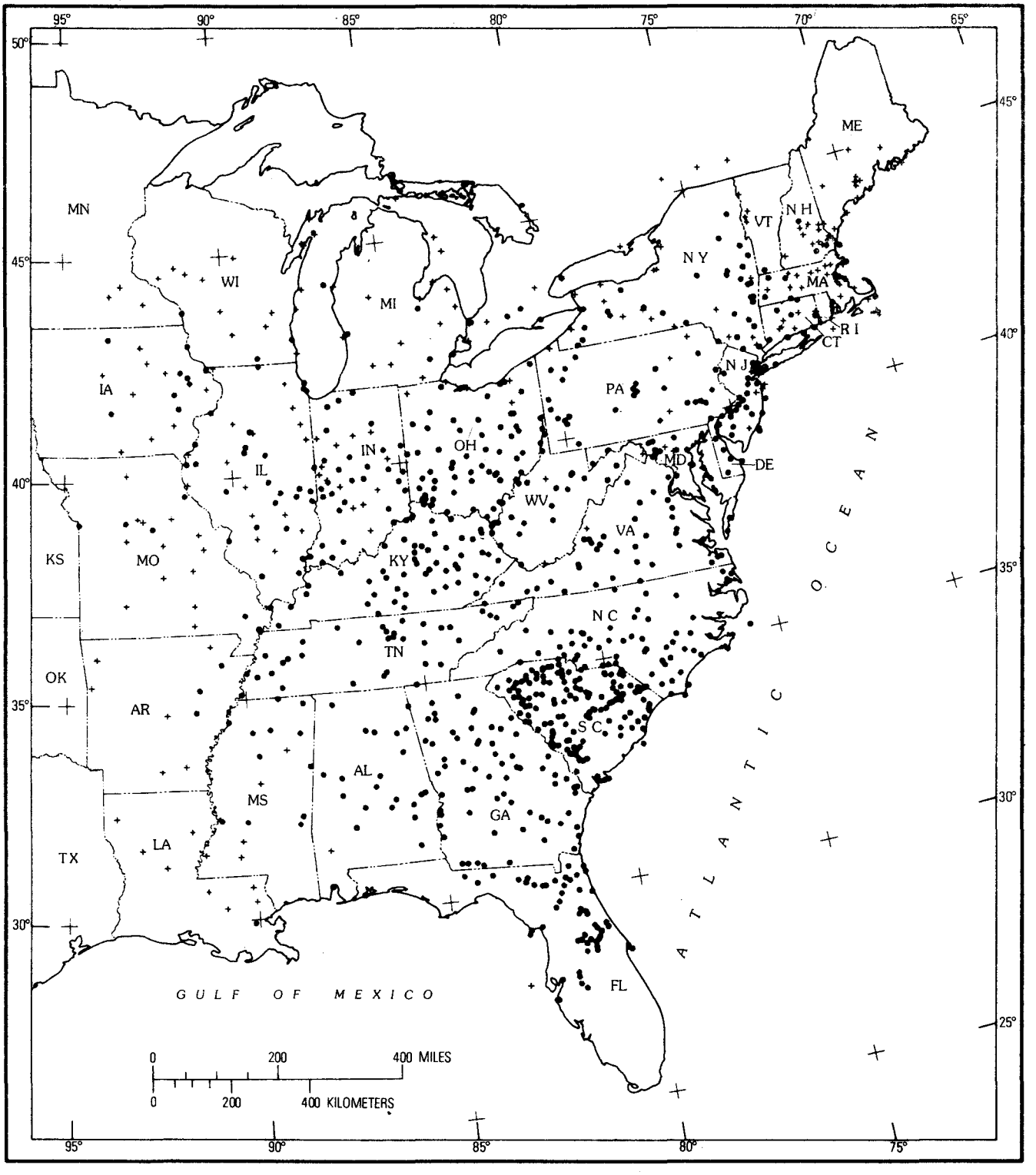

FIGURE 3.—Eastern United States showing the distribution of intensity observations for the 1886 Charleston earthquake. Solid circles indicate felt reports; small crosses indicate not-felt reports.

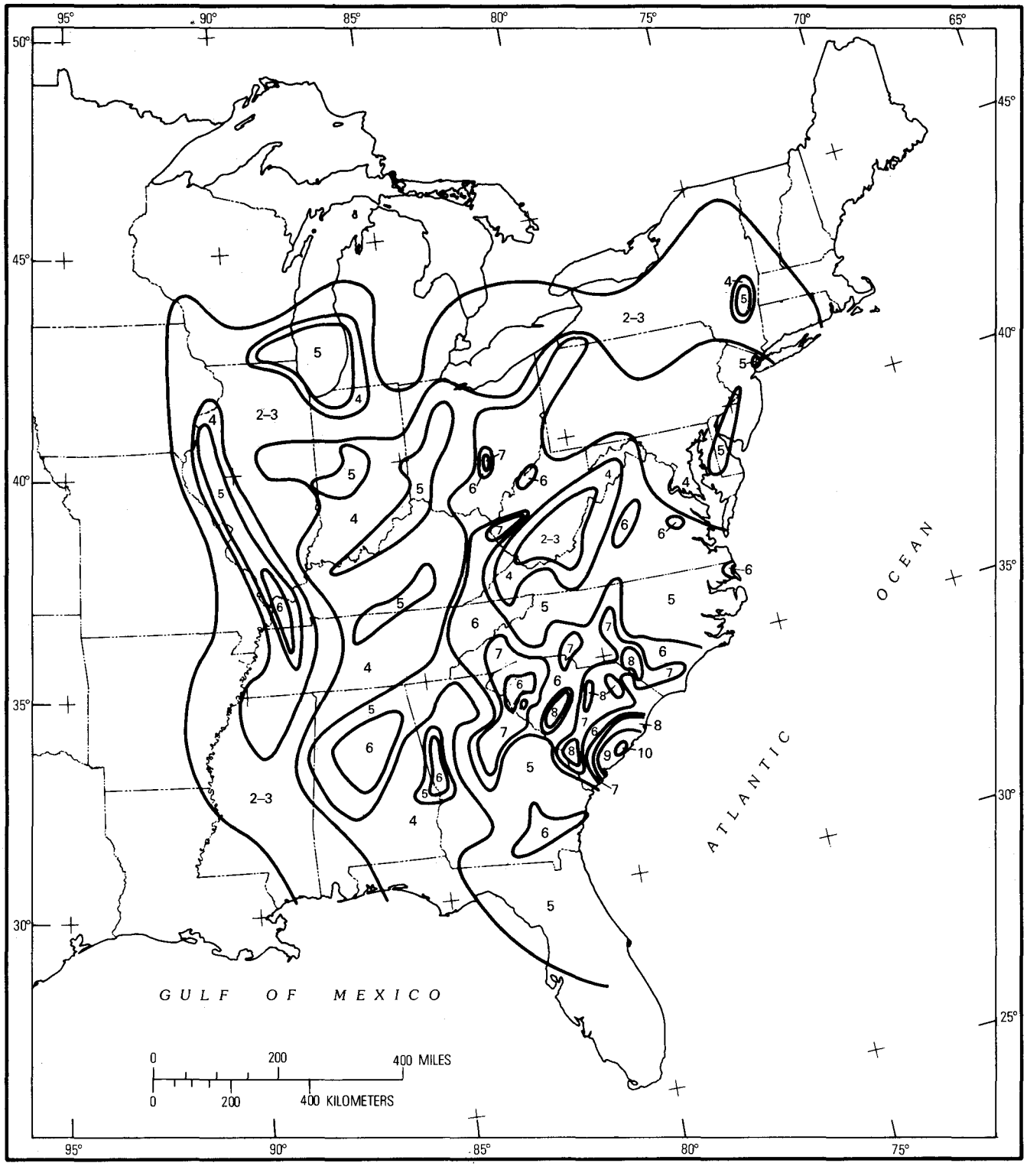

FIGURE 4.—Isoseismal map of the Eastern United States contoured to show the more localized variations in the reported intensities for the 1886 Charleston earthquake. Contoured intensity levels are shown by Arabic numerals.

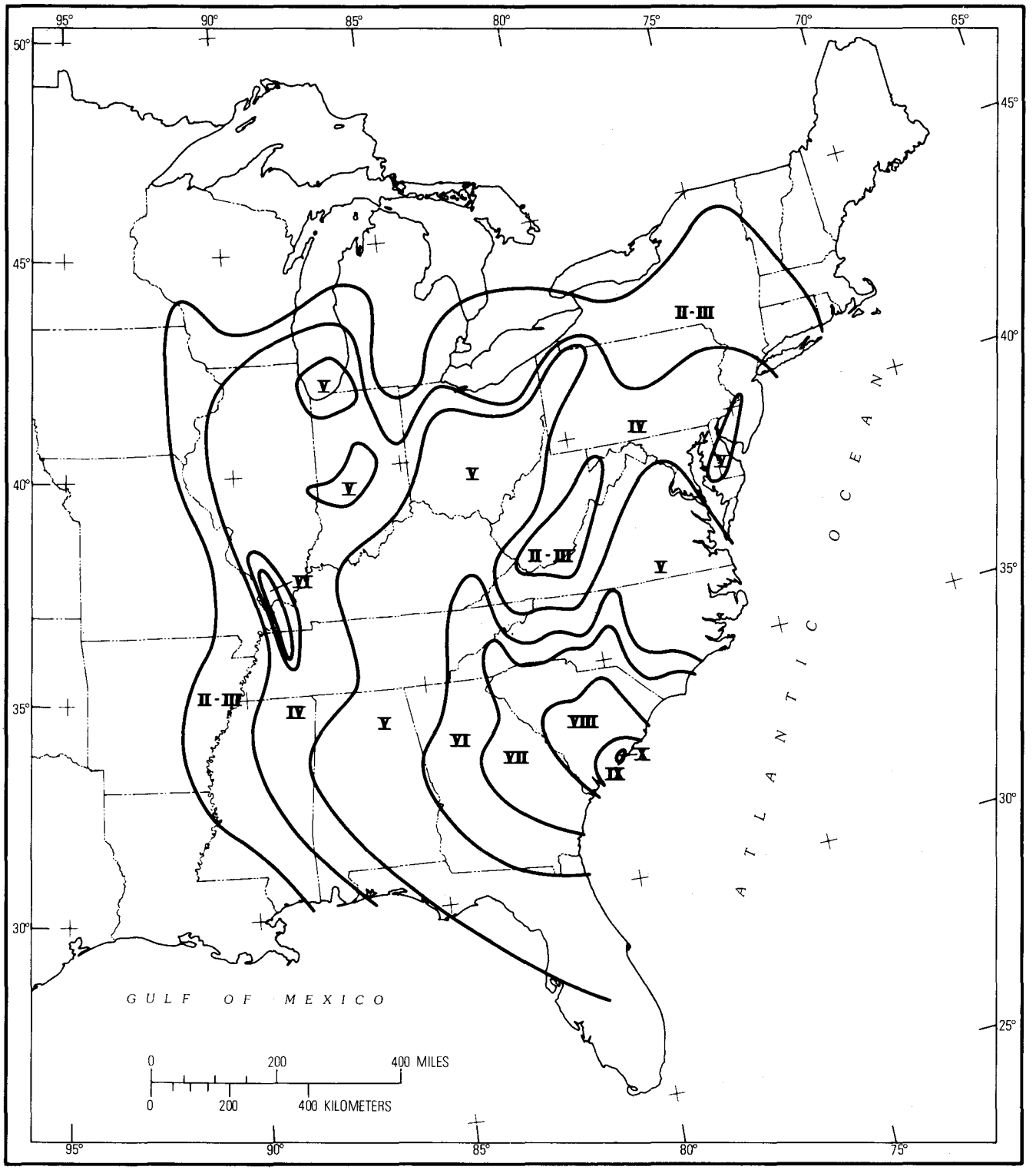

FIGURE 5.—Isoseismal map of the Eastern United States contoured to show the broad regional patterns of the reported intensities for the 1886 Charleston earthquake. Contoured intensity levels are shown in Roman numerals.

in contouring the mode of the intensity values, as was done here, intensity effects vary considerably with epicentral distance within the State. In particular, two intensity-VI zones are shown that trend northeastward across the State and separate areas of intensity-VIII effects. Although some of this variation may be due to incomplete reporting and (or) population density, it seems more likely that the local effects of surficial geology, soils, and water-table level are being seen. Interpreted literally, a very complex behavior of intensity is seen in the epicentral region.

The intensity data base and interpretive, isoseismal lines throughout the Eastern United States are shown in figures 3–5. In figure 4, the data are contoured to emphasize local variations, whereas figure 5 depicts the broad regional pattern of effects. Richter (1958, p. 142–145), in discussing the problem of how to allow for or represent the effect of ground in drawing isoseismal lines, suggested that two isoseismal maps might be prepared. One map would show the actual observed intensities; the other map would show intensities inferred for typical or average ground. The procedure followed here was to contour the mode of the intensity values (figs. 2 and 4) so as to portray the observed intensities in a manner that emphasizes local variations. Those isoseismal lines were then subjectively smoothed to produce a second isoseismal map showing the regional pattern of effects (fig. 5). The two maps that result from this procedure seem to the writer to represent reasonable extremes in the interpretation of intensity data. The subjectivity always involved in the contouring of intensity data is well known to workers concerned with such efforts. The purpose of the dual presentation here is to emphasize this subjectivity and to point out that, depending on the application, one form may be more useful than the other. Both local and regional contouring interpretations are to be found in the literature for U.S. earthquakes.

Figures 4 and 5 show that a rather complex isoseismal pattern, including Dutton's low-intensity zone (epicentral distance = $\Delta \cong 550$ km (341 mi)) in West Virginia, was present outside South Carolina. Intensity-VIII effects were observed at distances of 250 km (150 mi) and intensity-VI effects were observed 1,000 km (620 mi) from Charleston. Individual reports, given below, are all paraphrased from Dutton (1889). They note what took place in areas affected by intensity VI (MM) or higher at epicentral distances greater than about 600 km (372 mi). Some of these reports were ignored in the contouring shown in figure 4.

Intensity VI–VIII in Virginia ($\Delta \cong 600$ km (372 mi)):

Richmond (VIII)—Western part of the city: bricks shaken from houses, plaster and chimneys thrown down, entire population in streets, people thrown from their feet; in other parts of the city, earthquake not generally felt on ground floors, but upper floors considerably shaken.

Charlottesville (VII)—Report that several chimneys were overthrown.

Ashcake (VI)—Piano and beds moved 15 cm (6 in.); everything loose moved.

Danville (VI)—Bricks fell from chimneys, walls cracked, loose objects thrown down, a chandelier swung for 8 minutes after shocks.

Lynchburg (VI)—Bricks thrown from chimneys, walls cracked in several houses.

Intensity VII in eastern Kentucky and western West Virginia ($\Delta \cong 650$ km (404 mi)):

Ashland, Ky. (VIII)—Town fearfully shaken, several houses thrown down, three or four persons injured.

Charleston, W. Va.—"A number of chimneys toppled over" (p. 522).

Mouth of Pigeon, W. Va.—Chimneys toppled off to level of roofs, lamps broken, a house swayed violently.

Intensity VI in central Alabama ($\Delta \cong 700$ km (434 mi)):

Clanton (VII)—Water level rose in wells, some went dry and others flowed freely; plastering ruined.

Cullman—House wall cracked, lamp on table thrown over.

Gadsden—People ran from houses.

Tuscaloosa—Walls cracked, chimneys rocked, blinds shaken off, screaming women and children left houses.

Intensity VII in central Ohio ($\Delta \cong 800$ km (496 mi)):

Lancaster—Several chimneys toppled over, decorations shaken down, hundreds rushed to the streets.

Logan—Bricks knocked from chimney tops, houses shaken and rocked.

Intensity VI in southeastern Indiana and northern Kentucky ($\Delta \cong 800$ km (496 mi)):

Rising Sun, Ind.—Plaster dislodged, ornaments thrown down, glass broken.

Stanford, Ky.—Some plaster thrown down, hanging lamps swung 15 cm (6 in.).

Intensity VI in southern Illinois, eastern Tennessee, and Kentucky (Δ≅950 km (590 mi)):

Cairo, Ill.—Broken windows, "houses settled considerably" (p. 430) in one section, ceiling cracked in post office.

Murphysboro, Ill.—Brick walls shook, firebell rang for a minute, suspended objects swung.

Milan, Tenn.—Cracked plaster, people sitting in chairs knocked over.

Clinton, Ky.—Some bricks fell from chimneys.

Intensity VI in central and western Indiana (Δ≅1,000 km (620 mi)):

Indianapolis—Earthquake not felt on ground floors; part of a cornice displaced on one hotel, people prevented from writing at desks, clock in court house tower stopped, a lamp thrown from a mantle.

Terre Haute—Plaster dislodged, sleepers awakened; in Opera House, earthquake felt by a few on the ground floor, but swaying caused a panic in the upper galleries.

Madison—Several walls cracked, chandeliers swung.

Intensity VI in northern Illinois and Indiana (Δ≅1,200 km (744 mi)):

Chicago, Ill.—Plaster shaken from walls and ceilings in one building above the fourth floor; barometer at Signal Office "stood 0.01 inches higher than before the shock for eight minutes" (p. 432); earthquake not felt in some parts of City Hall, especially noticeable in upper stories of tall buildings, not felt on streets and lower floors.

Valparaiso, Ind.—Plaster thrown down in hotel, chandeliers swung, windows cracked, pictures thrown from walls.

The preceding reports indicate that structural damage extended to epicentral distances of several hundred kilometers and that apparent long-period effects were present at distances exceeding 1,000 km (620 mi). Persons also frequently reported nausea at these greater distances.

Dutton apparently contoured his isoseismal map in a generalized manner, which is an entirely valid procedure. The rationale in that approach is to depict not the more local variations, as was presented in the above discussion, but rather the regional pattern of effects from the event. Figure 5 is the writer's attempt at that type of interpretation, and the resulting map is very similar to Dutton's.

ATTENUATION OF INTENSITY WITH EPICENTRAL DISTANCE

The decrease of intensity with epicentral distance is influenced by such a multiplicity of factors that it is particularly difficult to measure. The initial task in any attenuation study is to specify the distance (or distance range) associated with a given intensity level. Common selections are: minimum, maximum, or average isoseismal contour distances or the radius of an equivalent area circle. In all these approaches, the original individual intensities are not considered; rather, isoseismal maps are used. Perhaps a better, but more laborious, procedure has been suggested by Perkins (oral commun., 1975), wherein the intensity distribution of observations is plotted for specific distance intervals. In this manner, all the basic data are presented to the reader without interpretation by contouring. He is then in a position to know exactly how the data base is handled and thereby to judge more effectively the results that follow. Once the intensity-distance data are cast in this format, they are then also available for use in different applications.

The epicentral distances to some 800 different locations affected by the 1886 shock were measured and are listed in table 2. For these measurements, the center of the intensity X (fig. 1) area was assumed to be the epicenter. Figure 6 presents the resulting intensity distributions as functions of epicentral distance. The complexity present in the isoseismal maps (figs. 4 and 5) is now transformed to specific distances, and the difficulty of assigning a single distance or distance interval to a given intensity level is clearly shown. The approach followed here was to perform a regression analysis on the intensity-distance data set, using an equation of the form,

TABLE 2.—*Number of intensity observations as a function of epicentral distance intervals for the 1886 Charleston, S. C., earthquake*

Epicentral distance (km)	IX	VIII	VII	VI	V	IV	II–III	Number of observations
50– 99	3	4	3	3	3	---	---	16
100– 199	2	18	18	17	18	1	---	74
200– 299	-	9	22	25	30	5	---	91
300– 399	-	3	16	12	31	8	---	70
400– 499	-	2	3	10	26	19	12	72
500– 599	-	1	3	11	13	19	7	54
600– 699	-	1	3	3	14	33	11	65
700– 799	-	--	3	4	22	16	22	67
800– 899	-	--	1	2	29	20	20	72
900– 999	-	--	--	3	18	17	30	68
1,000–1,249	-	--	--	4	24	19	48	95
1,250–1,499	-	--	--	--	6	6	20	32
1,500–1,749	-	--	--	--	---	1	3	4
Totals	5	38	72	94	234	164	173	780

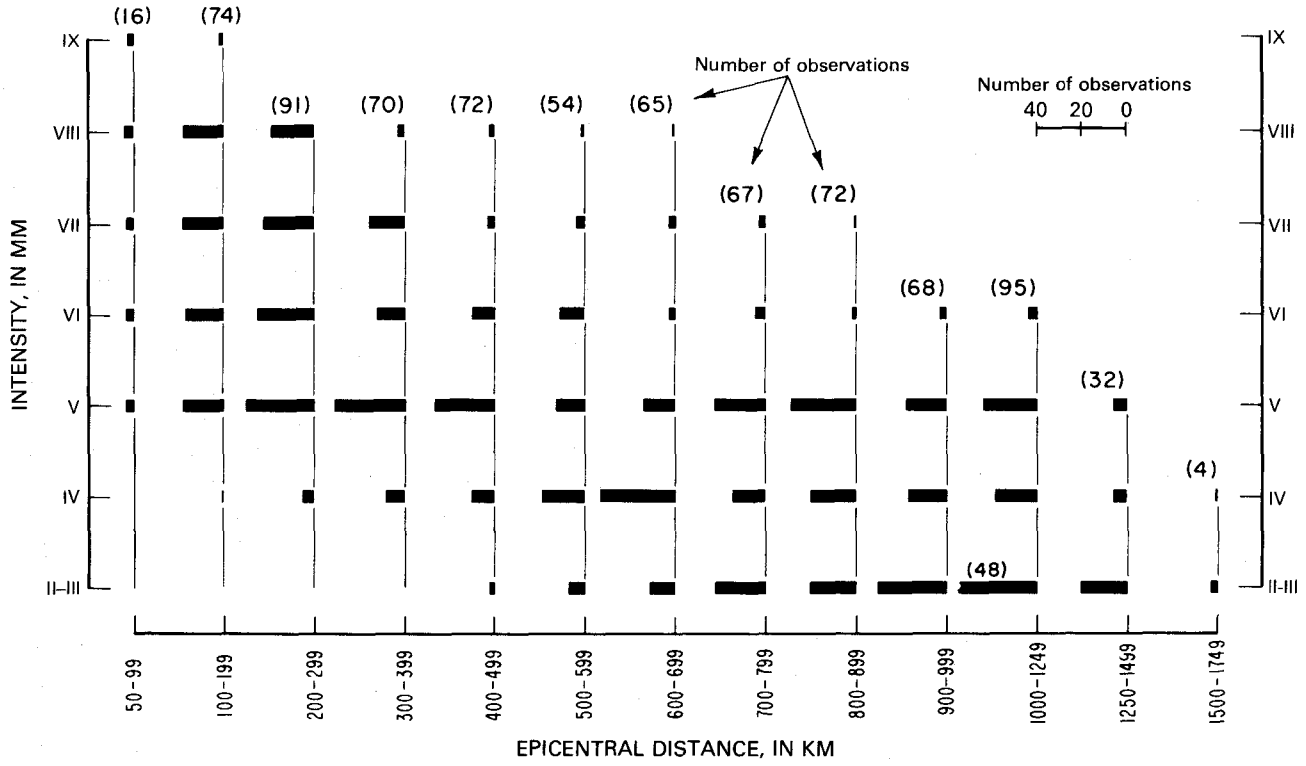

FIGURE 6.—Distribution of intensity (Modified Mercalli, MM) as a function of epicentral distance (km) for the 1886 Charleston earthquake. Intensity distribution is shown for specific distance intervals.

$$I = I_0 + a + b\Delta + c \log \Delta,$$

where a, b, c are constants, Δ is the epicentral distance in kilometers, I_0 is the epicentral intensity, and I is the intensity at distance Δ. This equation form was selected because it has been found useful by other investigators (for example, Gupta and Nuttli, 1976). The resulting fit for the median, or 50-percent fractile, was,

$$I = I_0 + 2.87 - 0.00052\Delta - 2.88 \log \Delta.$$

The standard deviation, σ_I, between the observed and predicted intensities, is 1.2 intensity units for these data. For the 75-percent fractile, the a constant is 3.68; for the 90-percent fractile, the a constant is 4.39. The b term is very small and could perhaps be deleted, as it results in only half an intensity unit at 1,000 km. The minimum epicentral distance at which the equation is valid is probably 10–20 km. The intensity-distance pairs extend to within only 50 km of the center of the epicentral region, but that region (fig. 1) has a diameter of approximately 20 km.

The curves for the 50-, 75-, and 90-percent fractiles are shown in figures 7 and 8 along with other published intensity attenuation curves for the Central and Eastern United States. Isoseismal maps

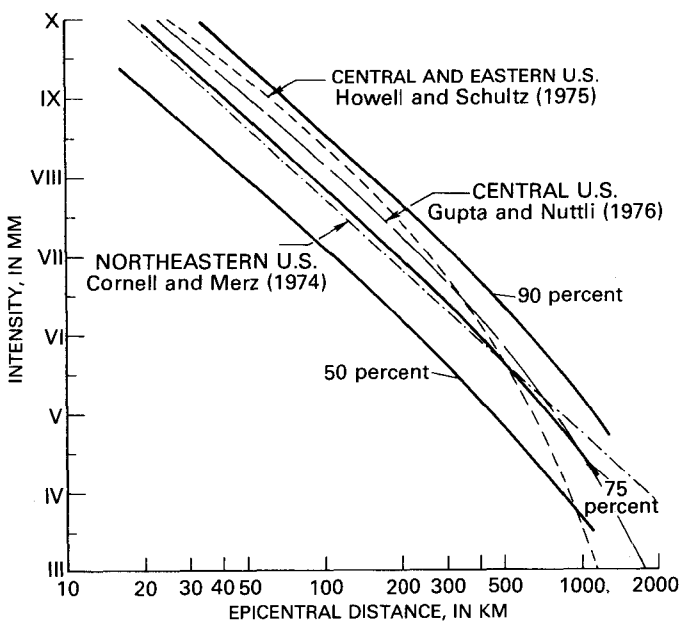

FIGURE 7.—Attenuation of intensity (MM) with epicentral distance (km) for various fractiles of intensity at given distance intervals for the 1886 Charleston earthquake (heavy solid curves). Attenuation functions by Howell and Schultz (1975), Gupta and Nuttli (1976), and Cornell and Merz (1974) are shown by light dashed curves.

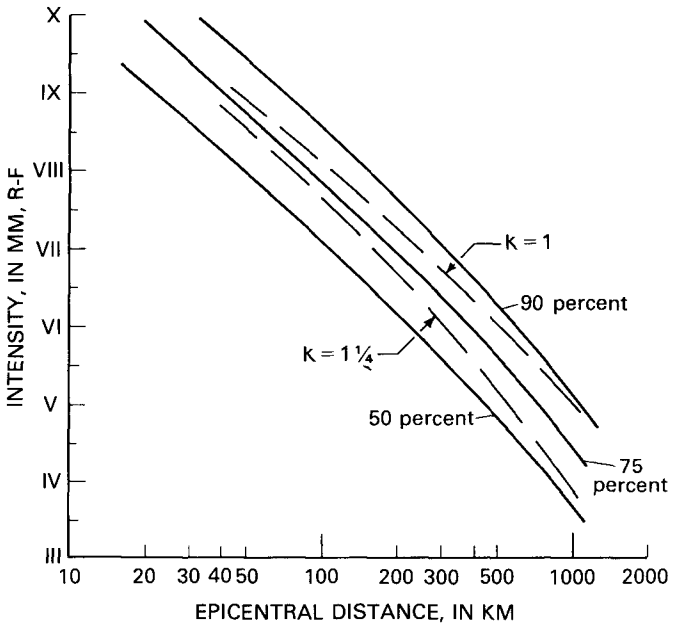

FIGURE 8.—Attenuation of intensity (MM) with epicentral distance (km) for various fractiles of intensity at given distance intervals for the Charleston earthquake (solid curves). Evernden's attenuation curves (1975) (Rossi-Forel intensity scale; L=10 km, C=25 km, k=1 and 1¼) are shown by dashed curves for I_0=X.

were utilized to develop these latter curves, and the general agreement between the entire suite of curves is remarkable. A direct comparison between curves, which may not be valid because of different data sets and different regions, would suggest that the Howell and Schultz (1975) curve is at about the 85-percent fractile, the Gupta and Nuttli (1976) curve is at the 80-percent fractile, and the Cornell and Merz (1974) curve is at the 70-percent fractile. At the intensity-VI level and higher, note that there is less than one intensity-unit difference among the Central United States, Central and Eastern United States, and Northeastern United States curves and the 75- and 90-percent fractile curves of this study.

Evernden's (1975) curves (fig. 8) for his k=1 and k=1¼ factors lie between the 50- and 90-percent fractile curves of this study. Evernden used k factors to describe the different patterns of intensity decay with distance in the United States. A value of k=1¼ was found for the Gulf and Atlantic Coastal Plains and the Mississippi Embayment and a k=1 for the remainder of the Eastern United States. Evernden prefers to work with the Rossi-Forel (R–F) intensity scale. The difference between the R–F and MM scales is generally about half an intensity unit, and conversion to R–F values would essentially result in translating the fractile curves of this study upward by that amount. This would put the 75-percent fractile curve in near superposition with Evernden's k=1 curve. Such a result is perhaps not surprising because approximately two-thirds of the felt area from the 1886 shock is in Evernden's k=1 region, and isoseismal lines are often drawn to enclose most of the values at a given intensity level. Although differences in intensity attenuation may exist between various parts of the Eastern United States, it would appear from this study that the dispersion of the data (σ_I=1.2) could preclude its precise definition. If, indeed, significant differences do exist between the various regions, then the curves given here would apply to large shocks in the Coastal Plain province of the Southeastern United States.

The advantages of the method presented herein are that it allows a prior selection of the fractile of the intensity observations to be considered and that it eliminates one subjective step, the contouring inerpretation of the intensity data. Furthermore, the dispersion of the intensity values can be calculated.

Neumann (1954) also presented intensity-versus-distance data in a manner similar to that described above. However, Neumann did not consider the intensity distribution for specific distance intervals as was done herein, but rather plotted the distance distribution for each intensity level. To illustrate the difference in the two approaches, the 1886 earthquake data were cast in Neumann's format (fig. 9).

MAGNITUDE ESTIMATE

Nuttli (1973), in arriving at magnitude estimates for the major shocks in the 1811–1812 Mississippi Valley earthquake sequence, developed a technique for correlating isoseismal maps and instrumental ground-motion data. Later, he (1976) presented specific amplitude-period $(A/T)_z$ values for MM intensities IV through X for the 3-second Rayleigh wave. Basically, Nuttli's technique consists of:

(1) Determination of a relation between $(A/T)_z$ and intensity from instrumental data and isoseismal maps,

(2) Use of the $(A/T)_z$ level at 10-km epicentral distance derived from the m_b value for the largest well-recorded earthquake in the region. That level will serve as a reference level from which to scale other m_b magnitudes,

(3) For the historical event of interest, assign epicentral distances (Δ) to each intensity level from the isoseismal map for the event. Convert from intensity to $(A/T)_z$, according to the relationship of (1) above, then

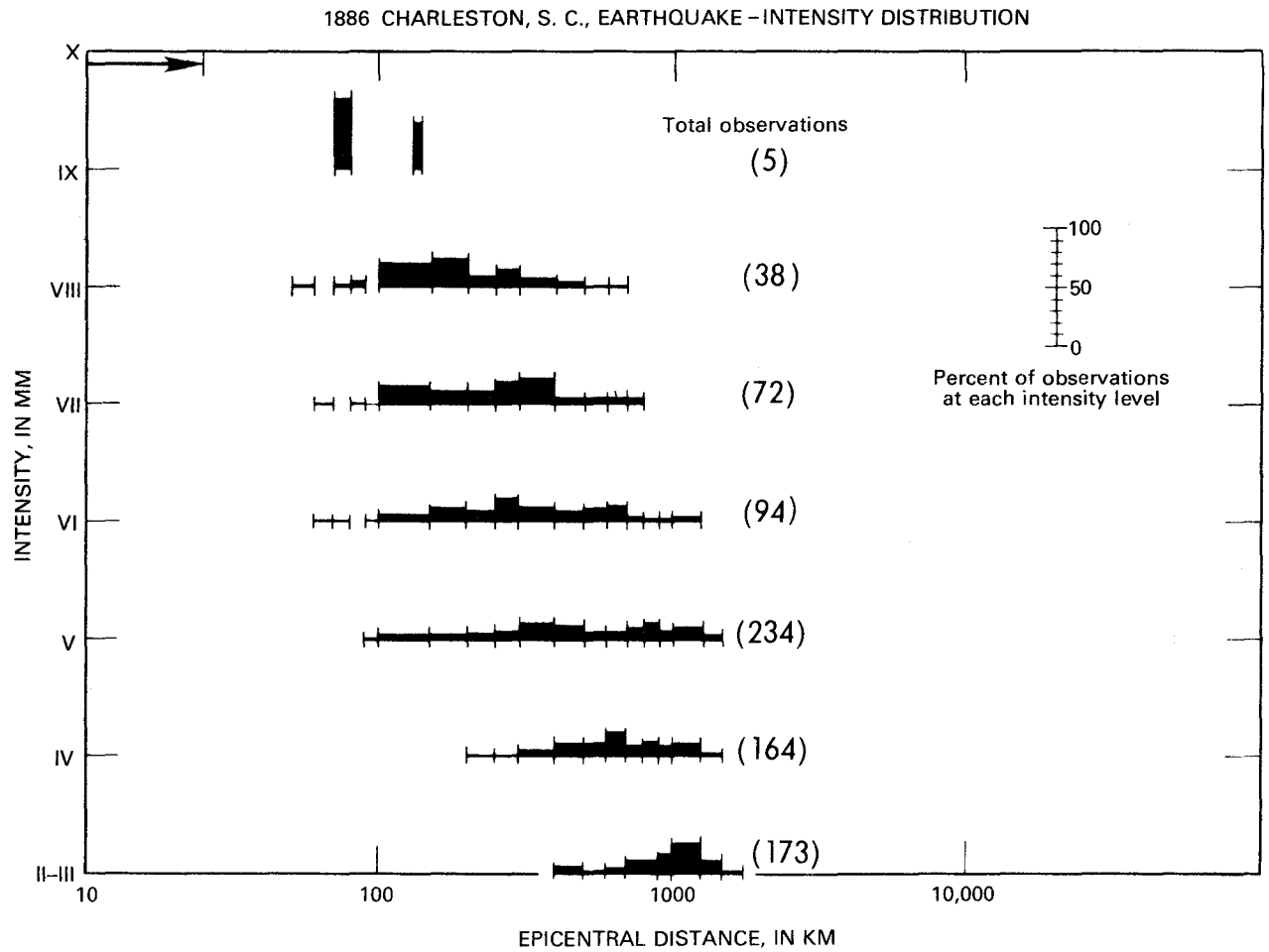

FIGURE 9.—Distribution of epicentral distances (km) for given intensity (MM) levels of the 1886 Charleston earthquake.

(4) Plot $(A/T)_z$ versus Δ and fit with a theoretical attenuation curve. Next, scale from (2) above to determine the Δm_b between the historical shock and the reference earthquake.

In the $(A/T)_z$ versus intensity of (1) and the curve fitting of (4), Nuttli found that surface waves having periods of about 3 seconds (s) were implied. He justified the use of m_b (determined from waves having periods of about 1 s) by assuming that the corner periods of the source spectra of the earthquakes involved are no less than 3 s. This implies a constant proportion between the 1- and 3-s energy in the source spectra. Nuttli used m_b rather than M_s because he felt that, for his reference earthquake, the former parameter was the more accurately determined.

If we apply Nuttli's technique to the 1886 earthquake and use the distances associated with the 90-percent fractile intensity-distance relationship, the resulting m_b estimate is 6.8 (fig. 10) Nuttli (1976) obtained a value of 6.5 when he used Dutton's isoseismal map and converted from the Rossi-Forel scale to the MM scale. If the Trifunac and Brady (1975) peak velocity versus MM intensity relationship, derived from Western United States data, is taken with the 90-percent fractile distances, then the m_b estimate is 7.1 (fig. 10). Because the 90-percent fractile curve is the most conservative, it results in the largest intensity estimate at a given distance. The magnitude estimates in this study would be upper-bound values.

My magnitude estimates, as well as those of Nuttli, are based primarily on three previously mentioned factors: intensity-distance relations, intensity-particle velocity relations, and reference magnitude level (or, equivalently, the reference earthquake, which in this instance is the November 9, 1968, Illinois earthquake with $m_b = 5.5$). In the Central and Eastern United States, the data base for the later two factors is very small. It is in this context that the magnitude estimates should be considered.

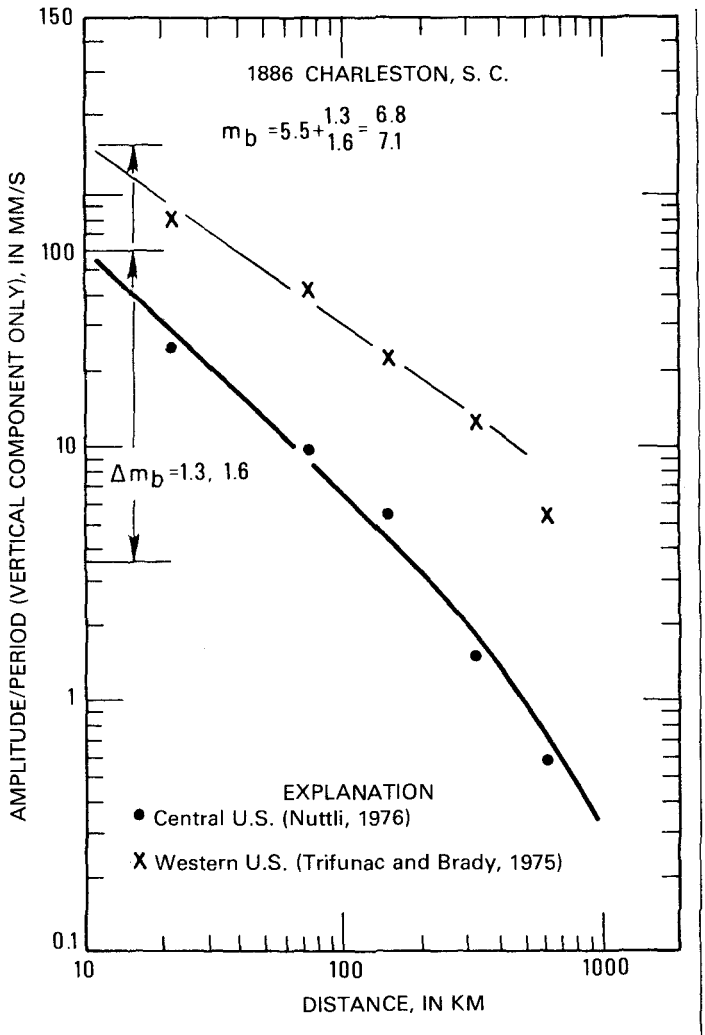

FIGURE 10.—Body wave magnitude (m_b) estimates for the 1886 Charleston earthquake based on Nuttli's (1973, 1976) technique. Nuttli's Central United States particle velocity-intensity data are indicated by solid circles. Trifunac and Brady's (1975) Western United States particle velocity-intensity data are indicated by X's. Distances are from the 90-percent fractile curve of this study. Heavy curve is Nuttli's (1973) theoretical attenuation for the 3-s Rayleigh wave. Western United States data fit with a straight line (light curve).

CONCLUSIONS

The intensity data base published by Dutton (1889) has been studied, and the principal results of that effort are as follows:

1. The maximum epicentral intensity was X (MM), and the intensity in the city of Charleston was IX (MM).
2. The writer verified that Dutton's isoseismal map was contoured so as to depict the broad regional pattern of the effects from ground shaking.
3. When contoured to show more localized variations, the intensity patterns show considerable complexity at all distances.
4. The epicentral distance was measured to each intensity observation point and the resulting data set (780 pairs) was subjected to regression analysis. For the 50-percent fractile of that data set, the equation developed was

$$I = I_0 + 2.87 - 0.00052\Delta - 2.88 \log \Delta$$

with a standard deviation (σ_I) of 1.2. For the 90- and 75-percent fractiles, the 2.87 constant is replaced by 4.39 and 3.68, respectively. This variation of intensity with distance agrees rather closely with relationships obtained by other workers for the central, eastern, and northeastern parts of the United States. It thus appears that the broad overall attenuation of intensities may be very similar throughout the entire Central and Eastern United States.
5. Using intensity-particle velocity data derived from Central United States earthquakes, the writer estimates a body-wave magnitude (m_b) of 6.8 for the main shock of August 31, 1886. However, the data base upon which this estimate is made is very small; therefore, the estimated m_b should be considered provisional until more data are forthcoming. Use of Western United States intensity-particle velocity data produces an m_b estimate of 7.1.

REFERENCES CITED

Bollinger, G. A., and Stover, C. W., 1976, List of intensities for the 1886 Charleston, South Carolina, earthquake: U.S. Geol. Survey open-file rept. 76–66, 31 p.

Cornell, C. A., and Merz, H. A., 1974, A seismic risk analysis of Boston: Am. Soc. Civil Engineers Proc., Structural Div. Jour., v. 110, no. ST 10 (Paper 11617), p. 2027–2043.

Dutton, C. E., 1889, The Charleston earthquake of August 31, 1886: U.S. Geol. Survey, Ninth Ann. Rept. 1887–88, p. 203–528.

Evernden, J. F., 1975, Seismic intensities, "size" of earthquakes and related parameters: Seismol. Soc. America Bull., v. 65, no. 5, p. 1287–1313.

Gupta, I. N., and Nuttli, O. W., 1976, Spatial attenuation of intensities for Central United States earthquake: Seismol. Soc. America Bull., v. 66, no. 3, p. 743–751.

Howell, B. F., Jr., and Schultz, T. R., 1975, Attenuation of Modified Mercalli intensity with distance from the epicenter: Seismol. Soc. America Bull., v. 65, no. 3, p. 651–665.

Neumann, Frank, 1954, Earthquake intensity and related ground motion: Seattle, Wash., Univ. Washington Press, 77 p.

Nuttli, O. W., 1973, The Mississippi Valley earthquakes of 1811 and 1812—Intensities, ground motion and magnitudes: Seismol. Soc. America Bull., v. 63, no. 1, p. 227–248.

——— 1976, Comments on "Seismic intensities, 'size' of earthquakes and related parameters," by Jack F. Evernden: Seismol. Soc. America Bull., v. 66, no. 1, p. 331–338.

Richter, C. F., 1958, Elementary seismology: San Francisco, Calif., W. H. Freeman Co., 768 p.

Trifunac, M. D., and Brady, A. G., 1975, On the correlation of seismic intensity scales with the peaks of recorded strong ground motion: Seismol. Soc. America Bull., v. 65, no. 1, p. 139–162.

U.S. Environmental Data Service, 1973, Earthquake history of the United States: U.S. Environmental Data Service Pub. 41–1, rev. ed. (through 1970), 208 p.

Wood, H. O., and Neumann, Frank, 1931, Modified Mercalli intensity scale of 1931: Seismol. Soc. America Bull., v. 21, no. 4, p. 277–283.

The Seismicity of South Carolina Prior to 1886

By G. A. BOLLINGER and T. R. VISVANATHAN

STUDIES RELATED TO THE CHARLESTON, SOUTH CAROLINA, EARTHQUAKE OF 1886—A PRELIMINARY REPORT

GEOLOGICAL SURVEY PROFESSIONAL PAPER 1028-C

CONTENTS

ILLUSTRATIONS

TABLES

STUDIES RELATED TO THE CHARLESTON, SOUTH CAROLINA, EARTHQUAKE OF 1886—
A PRELIMINARY REPORT

THE SEISMICITY OF SOUTH CAROLINA PRIOR TO 1886

By G. A. BOLLINGER [1] and T. R. VISVANATHAN [2]

ABSTRACT

Archival material on the seismicity of South Carolina prior to the great 1886 Charleston earthquake has been studied. Data sources consisted of 34 different newspapers, meteorological reports from 41 localities in South Carolina, 4 historical treatises, and 6 previously published earthquake catalogs. Study of these data resulted in a list of 18 probable earthquakes between 1698 and 1886, and intensity maps for shocks in 1799, 1817, 1857, and 1860. The maximum Modified Mercalli intensity (MM) for the pre-1886 events appears to be V.

A comparison of seismic activity in South Carolina with that in three neighboring States for the 50 years preceding 1886 shows 9 events in South Carolina, 5 in Georgia, 7 in Tennessee, and 21 in North Carolina. For the five decades before the 1886 earthquake, South Carolina's seismic activity does not appear as anomalously high, either in the number or energy levels of seismic events.

INTRODUCTION

The August 31, 1886, Charleston, S.C., earthquake was the single large seismic event in the southeastern United States during the past three centuries. Its maximum intensity of X (MM, Modified Mercalli) is a full two levels higher than that of the next largest event. Because no comparable shocks had been reported since the region was settled by the English about 200 years prior to the event, it has been stated that the 1886 earthquake took place in an aseismic region.

The purpose of this study is to investigate the seismicity of the State of South Carolina prior to 1886. Because seismological instruments were not in use then, this study is necessarily archival. However, copies of newspapers and reports published during the rapid development that followed the very early settlement of Charleston may contain adequate information to specify, at least partially, the pre-1886 seismicity. By analysing such data, perhaps we can gain some insight into the nature of the Charleston area's seismic regime.

This study was supported by State Geology, State Development Board of South Carolina, and by the National Science Foundation (Grant DES75-14691).

DATA SET FOR THE PRE-1886 PERIOD IN SOUTH CAROLINA

The English derived their first knowledge of South Carolina from Sebastian Cabot who visited the coast in 1497, shortly after the discovery of America. D'Ayllon landed on St. Helena Island (about 40 km southwest of Charleston) in 1520, gave it its name, and claimed the country for Spain. In 1562, a settlement by 26 French Huguenots was attempted in Port Royal (presumably at the site of the modern community having the same name which is located about 80 km southwest of Charleston), but they returned to France the following year, leaving the area its name, "Caroline," after their King Charles IX. Charles I of England in 1629 granted Sir Robert Heath the area under the name, "Carolina." However, the first permanent white settlement in South Carolina began in Beaufort (about 75 km southwest of Charleston) in 1670 under a grant from Charles II of England. That colony moved the next year to the west bank of the Ashley River, and a few years later (about 1680) to the east bank to occupy the present site of Charleston (South Carolina State Board of Agriculture, 1883).

Microfilm files of early newspapers constituted an important data source for this study. The first newspaper in South Carolina, *The South Carolina Gazette,* was published in January 1732. It was the fifth newspaper in America and flourished for a long

[1] Virginia Polytechnic Institute and State University, Blacksburg, Va.
[2] University of South Carolina, Union, S. C.

time without a rival in South Carolina (South Caroline State Board of Agriculture, 1883). Thirty-four newspaper sources were found that contained information concerning earthquake activity. Eleven of these gave thorough coverage to the Charleston area for the entire pre-1886 period (fig. 1, table 1). The other 23 newspapers (table 2) were supplemental in that they provided data for shorter, discrete time frames or for individual events.

Other important data sources were meteorological reports. These reports, some of which were made as early as 1820, were derived from voluntary observers, the hospital staff of the Surgeon General's Office, and the Army Signal Corps. During the earlier periods, earthquake reports were not necessarily made by every observer, but from 1870 onwards, the Signal Corps urged that particular efforts be made to report earthquakes. The coverage, therefore, is more complete after 1870. Table 1 lists the names of the 41 reporting localities within South Carolina.

Lastly, four historical treatises and six previously published earthquake catalogs or lists were found that contributed data pertinent to the pre-1886 period (see "References Cited").

A possible relevant factor here is population density. Figure 2 presents the pre-1900 population levels

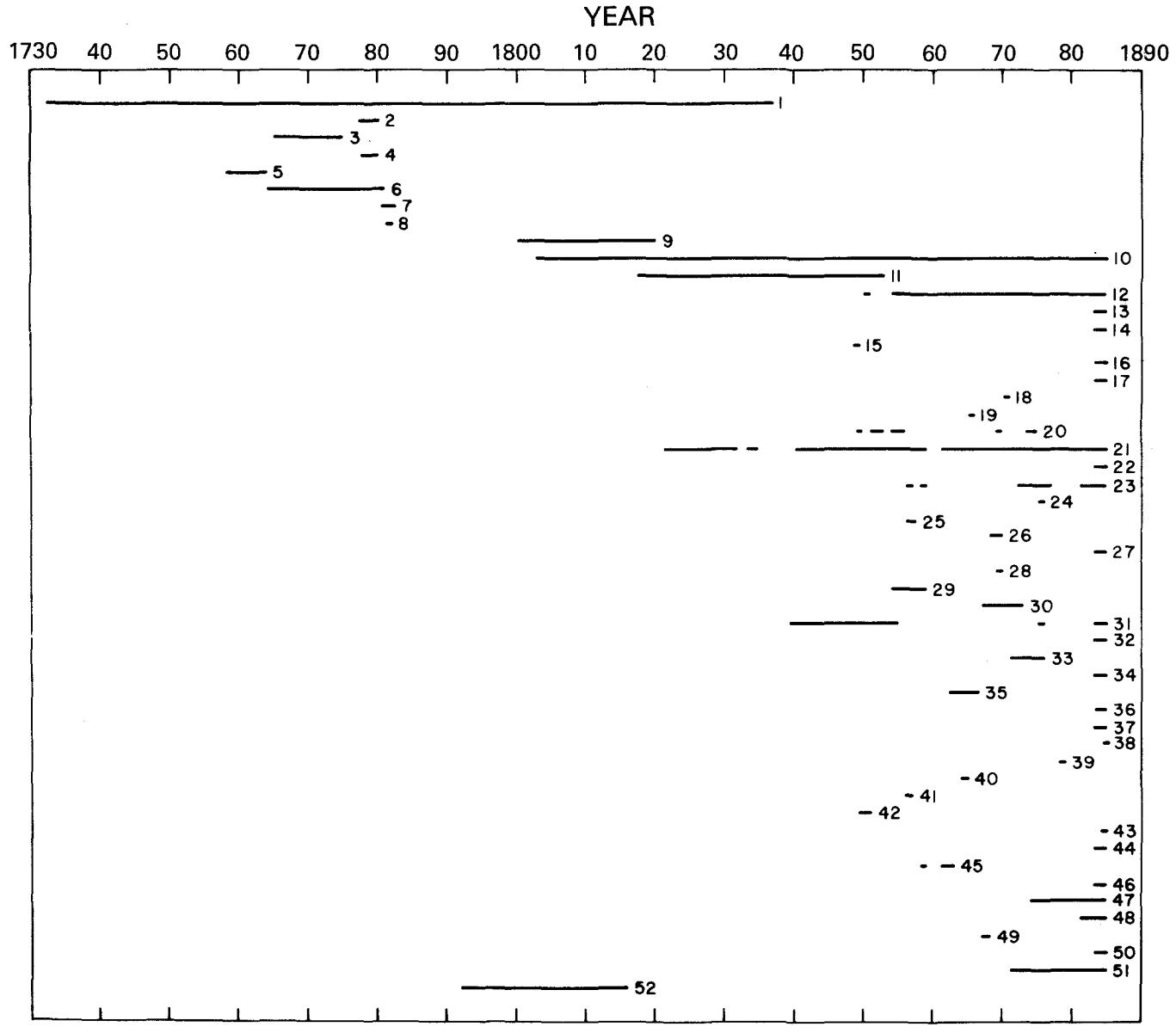

FIGURE 1.—Newspaper and meteorological report coverage for the time period 1730–1886. Length of bars indicates the time intervals investigated. Numbers at the right end of each bar are keyed to the list of references given in table 1.

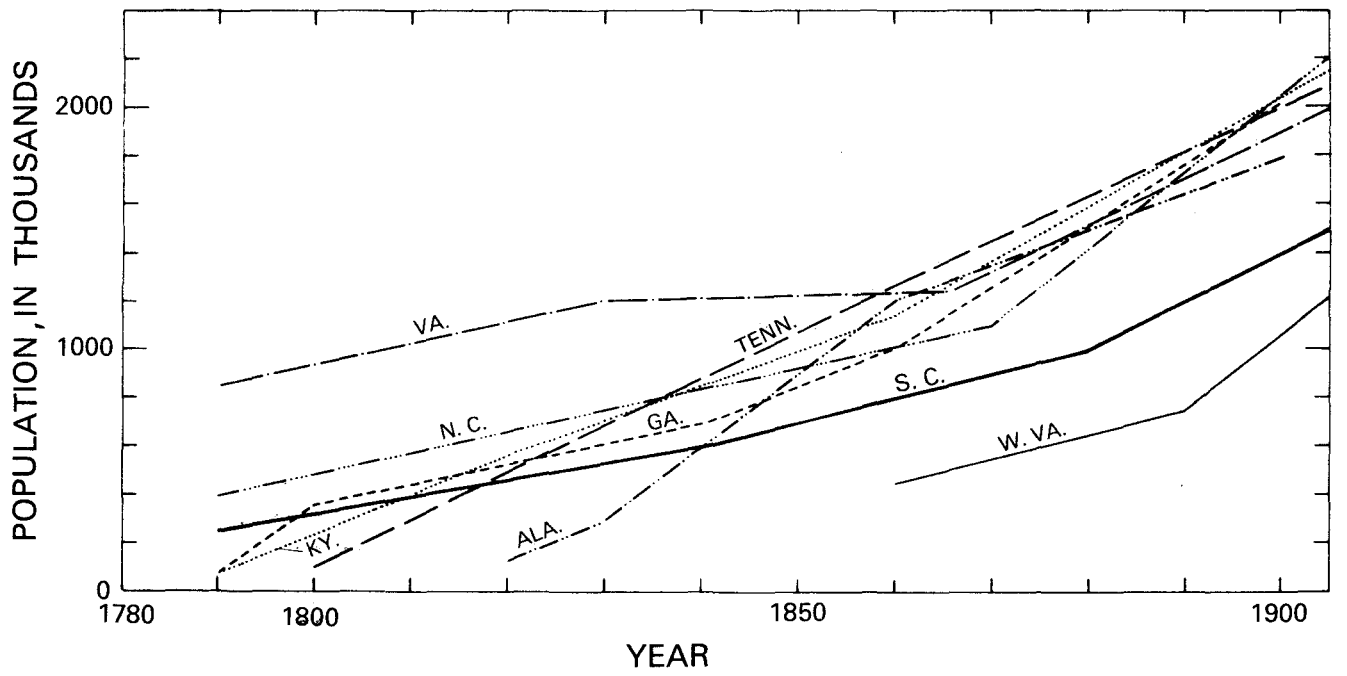

FIGURE 2.—Population levels in the southeastern States, 1790–1900. Data compiled from the Encyclopedia Britannica (1970, 14th edition).

TABLE 1.—*Newspapers and meteorological stations whose reports were used in this study*

[Newspapers 1–10 were published in Charleston, S. C.]

Newspaper references
1. The South Carolina Gazette 1732–1837
2. Gazette of the State of South Carolina
3. South Carolina Gazette and Country Journal
4. Charleston Gazette
5. South Carolina Weekly Gazette
6. South Carolina and American General Gazette
7. Royal South Carolina Gazette 1
8. Royal Gazette
9. Charleston Times
10. Charleston Courier/Charleston News and Courier/ Charleston Daily Courier/News and Courier
11. Camden Gazette/Camden Journal/Camden Weekly Journal (Camden, S. C.)
Meteorological stations in South Carolina
12. Aiken
13. Allendale
14. Anderson
15. Barratsville (Abbeville County)
16. Batesburg
17. Blackville
18. Bluffton
19. Braddock's Point (Beaufort County)
20. Camden
21. Charleston (and nearby points)
22. Chester
23. Columbia
24. Edgefield
25. Edisto Island
26. Evergreen (Anderson County)
27. Florence
28. Fort Mill (York County)
29. Georgetown
30. Gowdysville (Union County)
31. Greenville
32. Greenwood
33. Hacienda Saluda (Greenville County)
34. Hardeesville
35. Hilton Head

TABLE 1.—*Newspapers and metrological stations whose reports were used in this study*—Continued.

Meteorological stations in South Carolina—Continued
36. Jacksonboro
37. Kingstree
38. Kirkwood (Kershaw County)
39. Limestone Springs (Spartanburg County)
40. Morris Island (Berkeley County)
41. Mount Pleasant
42. Orangeburg
43. Pacolet
44. St. George
45. St. Johns
46. St. Mathews
47. Spartanburg
48. Stateburg
49. Summerville
50. Yemassee
51. Charleston: Abstract of Daily Weather Report
52. James Kershaw's Diary (Camden)

for eight of the southeastern States. The population in South Carolina, for the most part, lagged somewhat behind that of the seven other States of the region. By 1900, the difference was about 30 percent. Even so, that disparity was probably not so great as to bias the historical data base for South Carolina seriously with respect to that for the neighboring States.

RESULTS

Examination of the above-mentioned data sources resulted in a list of 18 probable earthquakes that took place between 1698 and 1886 (table 3) and four

TABLE 2.—*Auxiliary newspaper references*

Augusta Chronicle & Gazette of the State (Augusta, Ga.)
Augusta Herald (Augusta, Ga.)
Carolina Spartan (Spartanburg, S. C.)
Charleston Mercury (Charleston, S. C.)
Charleston Tri-Weekly Courier/Triweekly Courier (Charleston, S. C.)
Charlotte Bulletin (Charlotte, N. C.)
City Gazette & Daily Advertiser/City Gazette & Commercial Advertiser (Charleston, S. C.)
Daily Constitutionalist (August, Ga.)
Edgefield Advertiser (Edgefield, S. C.)
Georgetown Gazette (Georgetown, S. C.)
Laurensville Herald (Laurens, S. C.)
National Intelligencer (Washington, D. C.)
Providence Gazette (Providence, R. I.)
Savannah Georgian (Savannah, Ga.)
Savannah Republican (Savannah, Ga.)
South Carolina State Gazette & Timothy's Daily Advertiser
Spartanburg Express (Spartanburg, S. C.)
Sumter Watchman (Sumter, S. C.)
The Journal (Milledgeville, Ga.)
Wilmington Journal (Wilmington, S. C.)
Winnsboro News & Herald (Winnsboro, S. C.)
Winnsboro Register (Winnsboro, S. C.)
Yorkville Enquirer (York, S. C.)

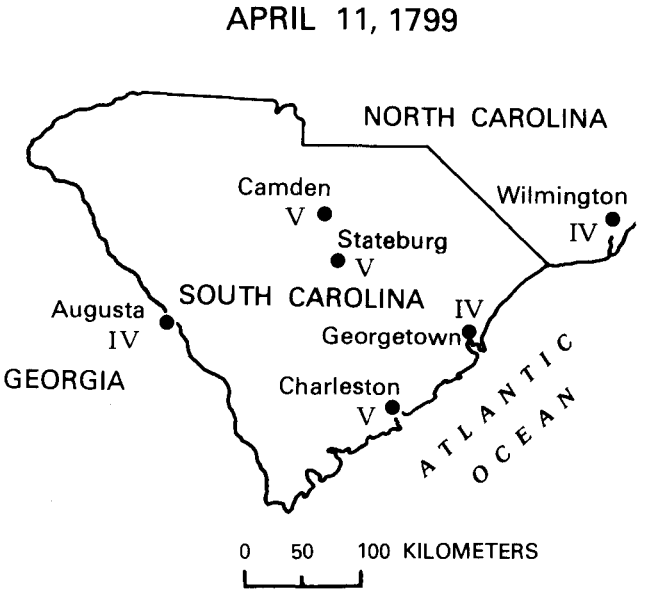

FIGURE 3.—Intensity data for the Charleston, S.C., earthquake of April 11, 1799. Intensities in this figure and the following figures are Modified Mercalli intensities.

new intensity maps (figs. 3–6). In table 4 are excerpts from published felt reports for pre-1886 South Carolina earthquakes. None of the data (except one report on the earthquake of May 20, 1853; see table 4) indicates a level of intensity greater than V (MM) for the pre-1886 time period. Because so much information has been reported for events of intensity V and lower levels, we think that larger events are unlikely to have been missed. Thus, the

TABLE 3.—*Pre-1886 South Carolina earthquakes*

Year	Date	Locality	Time of occurrence [1]	Maximum Intensity (MM scale)	References
1698	February	Charleston		Felt	McCrady (1897), Wallace (1961).
1754	May 19	Charleston	11:00	Felt	*South Carolina Gazette*, 1754, Taber (1914)
1757	Feb. 07	Charleston		Felt	Wallace (1934).
1766	Nov. 23	Charleston		(Meteor?)	R. B. Whorton and R. Clary (unpub. data, 1972).
1776	November	Charleston			R. B. Whorton and R. Clary (unpub. data, 1972).
1799	April 11	Charleston, Camden.	03:20 & 14:55.	V	Taber (1914), this study, R. B. Whorton and R. Clary (unpub. data 1972).
1816	Dec. 30	Charleston, Camden(?).		Felt	*Providence Gazette*, January 25 1817.
1817	Jan. 08	Charleston(?)	04:00	V	MacCarthy (1957, 1961), this study.
1820	Sept. 03	Georgetown	03:00–04:00.	Felt	*Camden Gazette*, September 24, 1820.
1843	April 11	Camden			Wallace (1934).
1853	May 20	Lexington	AM	VI	*Camden Journal*, May 31, 1853.
1857	Dec. 19	Charleston	09:04	V	Coffman and von Hake (1973), Taber (1914), this study, R. B. Whorton and R. Clary (unpub. data, 1972), Woollard (1968).
1860	Jan. 19	Charleston	18:–19:	V	MacCarthy (1961), this study.
	Oct. 22	Abbeville(?)		Felt	Taber (1914), R. B. Whorton and R. Clary (unpub. data, 1972).
	Dec. 19	Charleston		Felt	Wallace (1934).
1869	Summer			Felt	R. B. Whorton and R. Clary (unpub. data, 1972).
1876	Dec. 12	Charleston(?)	PM	Felt	Taber (1914), Woollard (1968).
1879	Oct. 26	Winnsboro	20:00	Felt	Woollard (1968), Winnsboro News & Herald, October 29, 1879.

[1] All times are in hours and minutes according to a 24-hour clock; for example, 2:55 p.m. is 14:55. For two shocks, the exact time is not reported, but we do give the hours between which each took place.

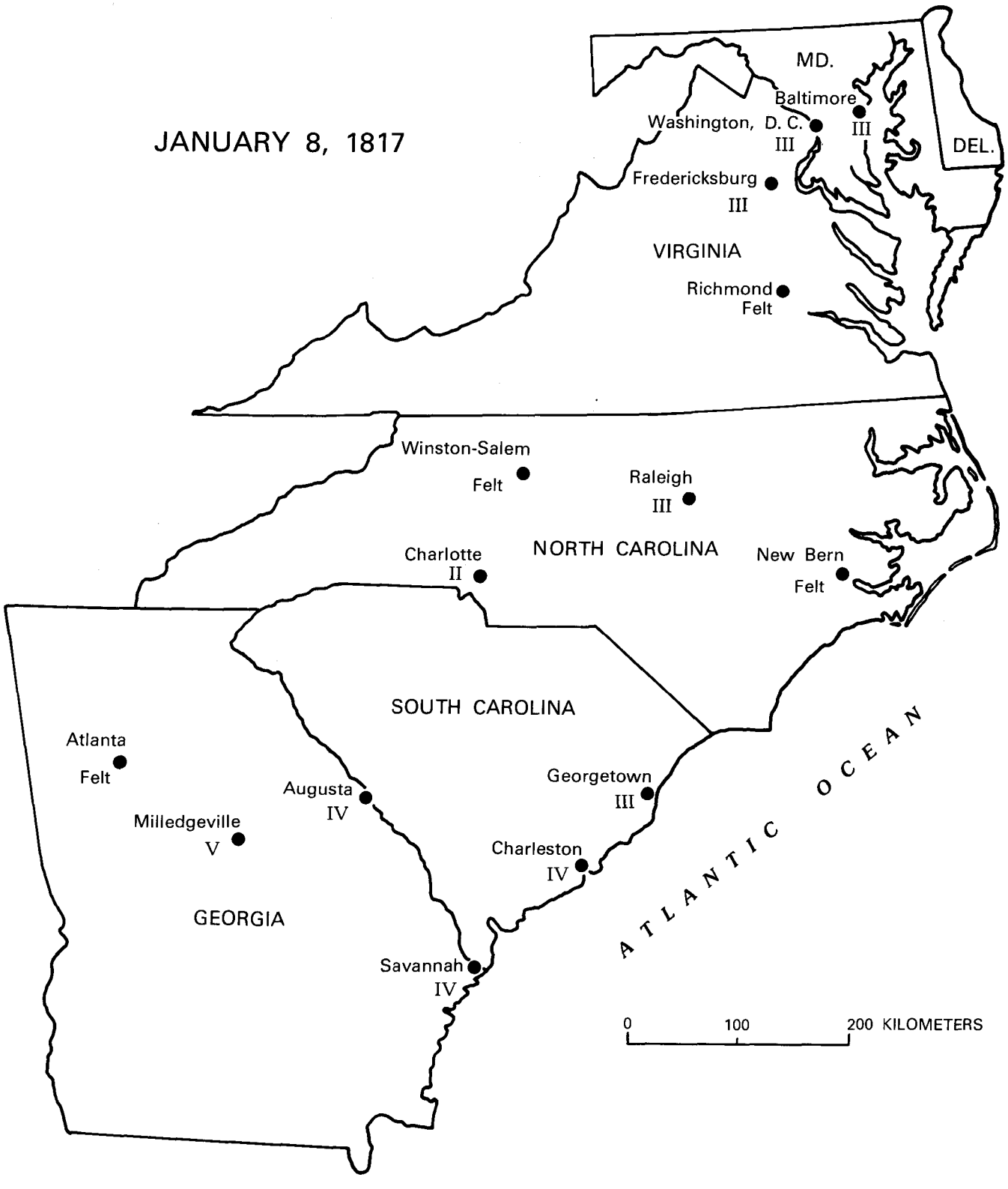

FIGURE 4.—Intensity data for the Charleston, S.C.(?), earthquake of January 8, 1817.

TABLE 4.—*Felt reports for pre-1886 South Carolina earthquakes*

Locality	Reports and source	Intensity (MM)
	Earthquake of April 11, 1799	
Augusta, Ga	Everyone in the house awakened and alarmed (*Augusta Chronicle and Gazette of the State*, Apr. 27, 1799).	IV
Camden, S. C	Windows and furniture rattled; some people left their homes; animals frightened; loud rattling noise (*South Carolina State Gazette & Timothy's Daily Advertiser*, Apr. 18, 1799).	V
Charleston, S. C	Houses shook, furniture and windows rattled, several people left bed (*City Gazette & Daily Advertiser*, Apr. 12, 1799).	V
Georgetown, S. C	Very generally felt. Duration about 4 s. (*City Gazette & Daily Advertiser*, Apr. 17, 1799).	IV
Stateburg, S. C	Awoke and alarmed every person in the house; felt throughout neighborhood (*City Gazette & Daily Advertiser*, Apr. 17, 1799).	V
Wilmington, N. C	"* * * a great trembling of the earth"; rumbling noise; felt by boats in the river; duration about 30 s. (*City Gazette & Daily Advertiser*, Apr. 27, 1799).	IV
	Earthquake of December 30, 1816	
Charleston and Camden, S. C	"Two [earthquakes] are reported to have been felt in Camden, two in Charleston both on 30th December 1816 * * *" (*Providence Gazette*, Jan. 25, 1817).	Felt
	Earthquake of January 8, 1817	
Atlanta, Ga	Felt (MacCarthy, 1961)	Felt
Augusta, Ga	"A smart shock of an earthquake * * *"; some people awakened (*Augusta Herald*, Jan. 10, 1817).	IV
Baltimore, Md	Three distinct shocks, each of about 10-s duration, separated by about 6 or 8 s (*City Gazette & Commercial Advertiser*, Jan. 16, 1817).	III
Charleston, S. C	"A pretty severe shock (some say two) * * *"; rumbling noise; duration about 30 s (*Charleston Courier*, Jan. 9, 1817; *City Gazette & Commercial Advertiser*, Jan. 9, 1817).	IV
Charlotte, N. C	Felt by some (*Charlotte Bulletin*, no date)	II
Fredericksburg, Va	Sensibly felt; rumbling noise (*City Gazette & Commercial Advertiser*, Jan. 23, 1817).	III
Georgetown, S. C	Duration about 4 s (*Georgetown Gazette*, Jan. 11, 1817).	III
Milledgeville, Ga	Felt; bell in state capital building struck several times (*The Journal*, Jan. 14, 1817).	V
Raleigh, N. C	Slight shock, short duration (*City Gazette & Commercial Advertiser*, Jan. 14, 1817).	III
Richmond, Va	Felt (*Providence Gazette*, Jan. 25, 1817).	Felt
Salem and New Bern, N. C	Felt. "The epicenter appears to be quite close to Charleston, S. C." (MacCarthy, 1961).	Felt
Savannah, Ga	"A severe shock * * *"; duration about 30 s (*Savannah Republican*, Jan. 9, 1817).	IV
Washington, D. C	Slight but sensible earthquake felt (*City Gazette & Commercial Advertiser*, Jan. 20, 1817).	III
Winstom-Salem area, N. C	Felt (MacCarthy, 1957)	Felt
	Earthquake of September 3, 1820	
Georgetown, S. C	"Between the hours of 3 and 4 on the morning of 3rd instance the shock of an earthquake was sensibly felt by several person in Georgetown, S. C. The shock was accompanied by a rumbling noise which was distinctly heard." (*Camden Gazette*, Sept. 24, 1820).	Felt
	Earthquake of May 20, 1853	
Lexington, S. C	"*An Earthquake:* On Friday morning last (20th), just before sunrise the citizens of Lexington and all the surrounding country were visited with a severe shock, the effects of an earthquake, no doubt followed by a rumbling distant thunder. Some persons in the vicinity had window glass broken and others had crockery shaken from its lodging and destroyed. The shock was so sensibly felt that many were awakened from sleep." (The above report was abstracted from the *Lexington Telegraph* and published by the *Camden Weekly Journal*, May 31, 1853).	VI

TABLE 4.—*Felt Reports for pre-1886 South Carolina earthquakes*—Continued

Locality	Reports and source	Intensity (MM)
	Earthquake of December 19, 1857	
Augusta, Ga	Felt by a few people (*Daily Constitutionalist*, Dec. 20, 1857)	II
Charleston, S. C	Hanging objects swung, doors rattled, felt by everyone in house; rumbling noise; duration 6-8 s (Gibbes, 1859).	V
	Considerable alarm in some localities where occupants left building; dishes rattled; chandeliers swung; pictures moved; duration about 5 s (*Charleston Mercury*, Dec. 21, 1857).	V
	A very decided rocking or shaking of the earth (*Charleston Daily Courier*, Dec. 21, 1857).	Felt
Columbia, S. C	Felt (*Carolina Spartan*, Dec. 24, 1857)	Felt
Georgetown, S. C	Felt (L. R. Gibbes, paper read in July 1887, pub. in Elliot Soc. Science and Art Charleston Proc., 1890, v. 2, p. 153).	Felt
Moultrieville, S. C. (near Charleston)	Deep rumbling noise; windows, doors, shutters rattled (*News and Courier*, Aug. 29, 1886).	IV
Savannah, Ga	Most severe north bay; buildings so shaken that all occupants rushed into streets (*Savannah Republican*, Dec. 21, 1857).	V
	Earthquake of January 19, 1860	
Augusta, Ga	"A slight shock of an earthquake was felt * * *"; rumbling sound (*Daily Constitutionalist*, Jan. 20, 1860).	III
Camden, S. C	Windows and dishes rattled; duration about a minute; roaring noise (*Charleston Tri-weekly Courier*, Jan. 24, 1860).	IV
	"The shock was hard and of considerable duration." Crockery rattled (*Camden Weekly Journal*, Jan. 21, 1860).	IV
Charleston, S. C	"* * * more violence than any felt or recorded for fifty years."; furniture shaken with papers, letters, etc. thrown out; many people alarmed and frightened; more strongly felt in upper floors of buildings; in some cases not felt on ground floors or out-of-doors. Duration 20 or 30 s. (*Charleston Daily Courier*, Jan. 20, 1860).	V
	James Island correspondent report: House shook for a minute as if struck by a locomotive going at full speed; negroes alarmed and ran from cabins. (*Tri-Weekly Courier*, Jan. 24, 1860).	V
	"* * * no section of the city seems to have been exempted * * * rumbling noises were heard."; alarm in some families; duration about 15 s; "No shock of equal severity was experienced since the shock of the earthquake in 1843 or 44." (*Charleston Mercury*, Jan. 21, 1860).	V
Columbia, S. C	Windows and dishes rattled; some people frightened (*Spartanburg Express*, Jan. 25, 1860).	IV
Edgefield, S. C	Felt by several people; rattled doors and windows (*Edgefield Advertiser*, Jan. 25, 1860).	III
Georgetown, S. C	Duration 10 s or longer (*Charleston Tri-Weekly Courier*, Jan. 24, 1860).	Felt
Laurens, S. C	Rocking motions, more pronounced in brick houses; two distinct vibrations separated by a short interval; oscillations east to west (*Laurensville Herald*, Jan. 27, 1860).	III
Macon, Ga	Felt by some (*National Intelligencer*, Jan. 21, 1860).	II
Savannah, Ga	Felt by a number of persons (*Savannah Georgian*, Jan. 20, 1860).	III
Spartanburg, S. C	Felt by some; perceptible shaking of houses (*Spartanburg Express*, Jan. 25, 1860).	III
Sumter, S. C	Buildings shook; glasses rattled; "The timbers of wooden buildings cracked from roof to base in a similar manner as caused by moving."; roaring sounds some 5 or 6 s, then vibrations for about 10 s,; some people "* * * became momentarily somewhat alarmed." (*Sumter Watchmen*, Jan. 24, 1860).	IV
Wilmington, N. C	Felt by many and most distinctly on upper floors; windows rattled (*Wilmington Journal*, Jan. 21, 1860).	IV
Winnsboro, S. C	Felt by many (*Winnsboro Register*, no date).	III
York, S. C	"A slight earthquake was felt" (*Yorkville Enquirer*, Jan. 26, 1860).	III
	Earthquake of October 26, 1879	
Winnsboro, S. C	"*An Earthquake*: A definite shock of earthquake was felt in Winnsboro and its vicinity about eight o'clock on Sunday evening (26th). In some localities it sounded like a mere thump or thud. In others, there was a rattling sound lasting several seconds." (*Winnsboro News & Herald*, Oct. 29, 1879).	Felt

FIGURE 5.—Intensity data for the Charleston, S.C., earthquake of December 19, 1857.

TABLE 5.—*1886 Charleston-Summerville area earthquakes prior to August 31*

Date	Time of occurrence [1]	Effects	Reference
Spring	(PM)	Knocked books off shelves at the College Library in Charleston; felt by a few people.	R. B. Whorton and R. Clary (unpub. data, 1972).
August 27	01:30	"Slight"; felt at Summerville	Taber (1914).
	08:30	"V ?"; felt at Summerville	Taber (1914).
		Explosive sound; a single jolt or heavy jar; some ran from houses.	Dutton (1889).
		A "decided" shock at Summerville; felt by a few people in Charleston.	R. B. Whorton and R. Clary (unpub. data, 1972).
August 28	05:30	Felt at Summerville and by a few in Charleston.	Taber (1914), R. B. Whorton and R. Clary (unpub. data, 1972).
		Sleepers awakened and alarmed in Summerville.	Dutton (1889).
August 29		Light tremors, some with sounds at Summerville.	Taber (1914), Dutton (1889).

[1] All times are in hours and minutes according to a 24-hour clock; for example, 5:30 a.m. is 05:30.

data do not indicate any type of gradual or long-term increase in the numbers and energy levels of "precursory" shocks.

TABLE 6.—*Maximum intensities of events in South Carolina and neighboring States from 1836 to August 31, 1886*

[Events having no maximum intensity reported are assumed to be IV(MM) shocks. IV(2) indicates that two shocks of intensity IV occurred in the time interval. Dash leaders, no events reported.]

Year	South Carolina	North Carolina	Georgia	Tennessee (East of 88°W)
1836–37				
1938–39				
1840–41				
1842–43	IV			IV
1844–45		IV		VI
1846–47				
1848–49				
1850–51		IV(2)		
1852–53	VI			
1854–55				
1856–57	V			
1858–59				
1860–61	V, IV(2)	IV		IV
1862–63				
1864–65				
1866–67				
1868–69	IV			
1870–71		IV(2)		
1872–73			V	
1874–75		VI	III, VI	IV
1876–77	IV	IV		IV, V
1878–79	IV	IV, V		
1880–81		IV(2)		
1882–83		IV(4)		
1884–85		V, IV(4)	III, IV	IV
1886	IV(5)	IV		

The total number (18) of pre-1886 events is small. As was typical of the region, no earthquake reports were made during the Civil War period (1861–1865). However, a comparison can be made between the seismic activity in South Carolina and that in the three nearest States during the 50 years preceding 1886. Such a comparison shows 9 events in South Carolina, 5 in Georgia, 7 in Tennessee, and 21 in North Carolina (Bollinger, 1975). Thus, the seismicity of South Carolina, even when the 1886 period prior to August 31 is considered, was not anomalously high with respect to that of its neighbors, as can be seen in figure 7 and tables 5 and 6.

In summary, an extensive archival search effort has failed to reveal any indication of the forthcoming large event. However, inadequate knowledge of historic earthquakes prior to 1886 has led to the notion that the event of 1886 took place in a region that was seismically quiet for centuries. South Carolina was not aseismic but experienced earthquakes on the average of one every 3 years during the 1836–86 period. Certainly, there were additional felt shocks that we failed to uncover at this late date. However, the probability is very low that an event of intensity VI or higher has been missed.

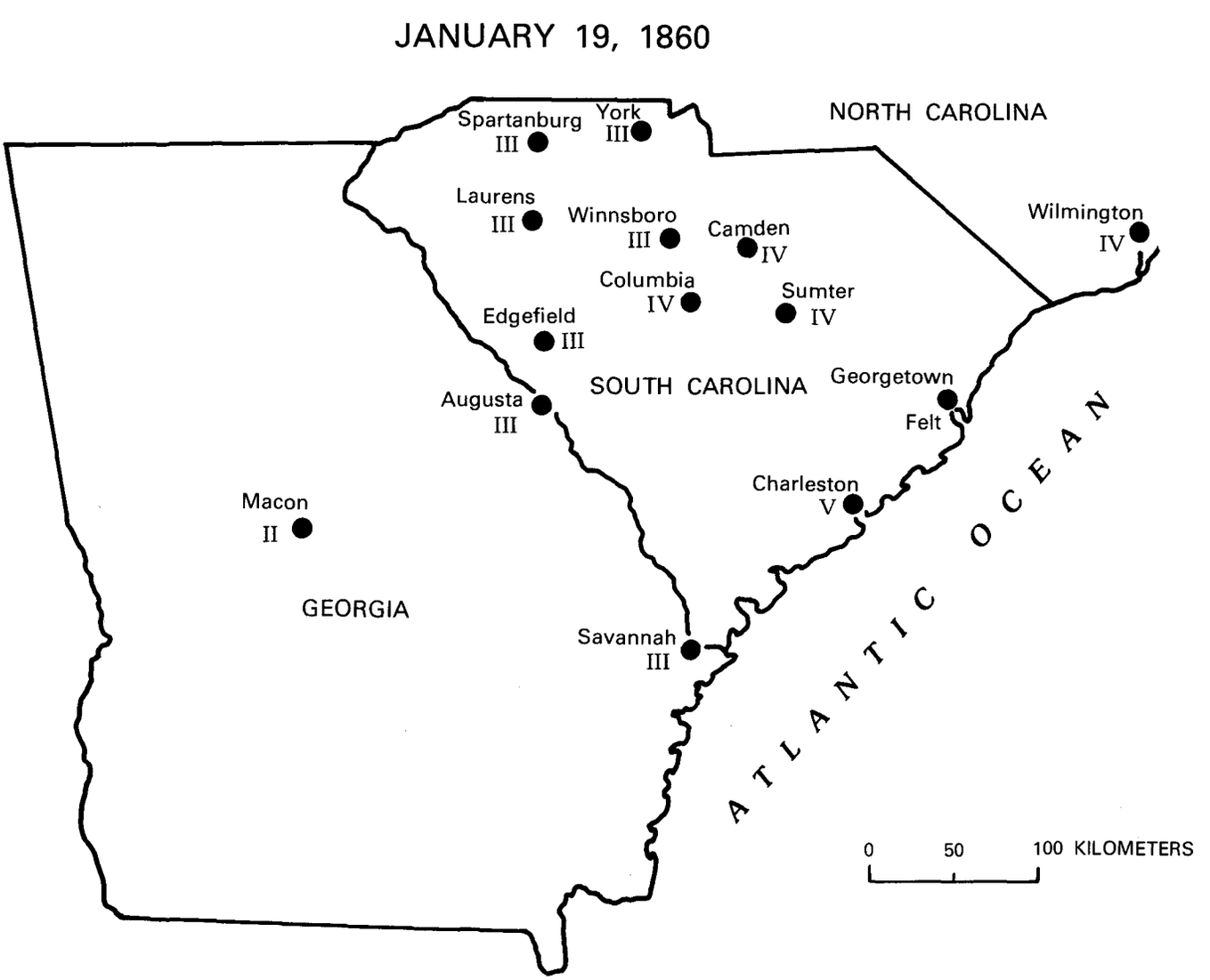

FIGURE 6.—Intensity data for the Charleston, S.C., earthquake of January 19, 1860.

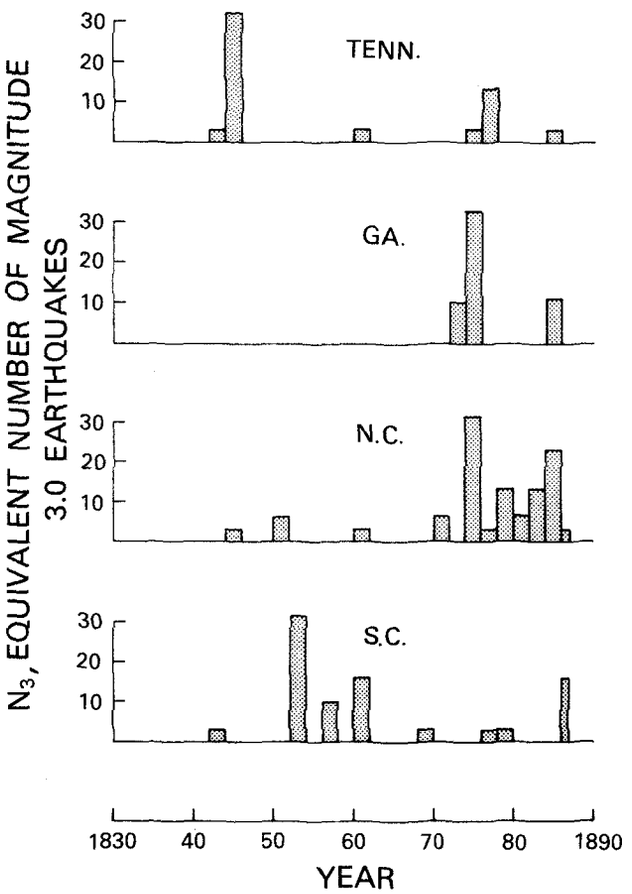

FIGURE 7.—Equivalent number of magnitude 3.0 earthquakes (N_3) versus time (1836 to August 31, 1886) for South Carolina and nearest States. Two-year increments were plotted (wide bars), except for the year 1886 (narrow bar); data tabulated in table 6. Conversion of intensity (I_0, maximum epicentral intensity) to magnitude (M) according to $M=1+(2/3)\ I_0$ (Gutenberg and Richter, 1956). Conversion of M to N_3 according to $N_3=10^{0.75\ (M-3.0)}$ (Allen and others, 1965).

REFERENCES CITED

Allen, C. R., St. Amand, P., Richter, C. F., and Nordquist, J. M., 1965, Relationship between seismicity and geologic structure in the southern California region: Seismol. Soc. America Bull., v. 55, no. 4, p. 753–797.

Bollinger, G. A., 1975, A catalog of Southern United States earthquakes—1754 through 1974: Virginia Polytech. Inst. and State Univ. Research Div. Bull. 101, 68 p.

Coffman, J. L., and von Hake, C. A., eds., 1973, Earthquake history of the United States: U.S. Dept. Commerce, Pub. 41–1, (Revised ed., through 1970), 208 p.

Dutton, C. E., 1889, The Charleston earthquake of August 31, 1886: U.S. Geol. Survey Ann. Rept. 9, 1887–88, p. 203–528.

Gibbes, L. R., 1859, Notice of the phenomena attending the shock of the earthquake of Dec. 19, 1857 [Charleston, S.C.]: Elliott Soc. Nat. History Charleston Proc., v. 1, p. 288–289 (paper read Sept. 1, 1858).

Gutenberg, B., and Richter, C. F., 1956, Earthquake magnitude, intensity, energy, and acceleration: Seismol. Soc. America Bull., v. 46, no. 2, p. 105–145.

MacCarthy, G. R., 1957, An annotated list of North Carolina earthquakes: Elisha Mitchell Sci. Soc. Jour., v. 73, no. 1, p. 84–100.

———1961, North Carolina earthquakes, 1958 and 1959, with additions and corrections to previous lists: Elisha Mitchell Sci. Soc. Jour., v. 77, no. 1, p. 62–64.

McCrady, Edward, 1897, The history of South Carolina under the proprietary government, 1670–1719: New York, Macmillan Co., 762 p. (see especially p. 307–308).

South Carolina State Board of Agriculture, 1883, South Carolina. Resources and Population. Institutions and Industries: Charleston, S.C., Walker, Evans & Cogswell, 724 p. (see especially p. 381–83, 529–534). [Reproduced in 1972 by The Reprint Co., Spartanburg, S.C.]

Taber, Stephen, 1914, Seismic activity in the Atlantic Coastal Plain near Charleston, South Carolina: Seismol. Soc. Bull., v. 4, no. 3, p. 108–160.

Wallace, D. D., 1934, The history of South Carolina: New York, Am. Hist. Soc., 3 v. (see especially v. 3, p. 333–334).

———1961, South Carolina, a short history, 1520–1948: Columbia, S.C., Univ. South Carolina Press, 753 p. (see especially p. 56).

Woollard, G. P., 1968, A catalogue of the earthquakes in the United States prior to 1925; based on unpublished data compiled by Harry Fielding Reid and published sources prior to 1930: Hawaii Inst. Geophysics Data Rept. 10 (HIG–68–9). [approx. 156 p.].

Recent Seismicity Near Charleston, South Carolina, and its Relationship to the August 31, 1886, Earthquake

By ARTHUR C. TARR

STUDIES RELATED TO THE CHARLESTON, SOUTH CAROLINA, EARTHQUAKE OF 1886—A PRELIMINARY REPORT

GEOLOGICAL SURVEY PROFESSIONAL PAPER 1028-D

CONTENTS

ILLUSTRATIONS

TABLES

STUDIES RELATED TO THE CHARLESTON, SOUTH CAROLINA, EARTHQUAKE OF 1886—
A PRELIMINARY REPORT

RECENT SEISMICITY NEAR CHARLESTON, SOUTH CAROLINA, AND ITS RELATIONSHIP TO THE AUGUST 31, 1886, EARTHQUAKE

By ARTHUR C. TARR

ABSTRACT

The hypocenters of recent earthquakes located in the epicentral area of the intensity-X August 31, 1886, Charleston, S.C., earthquake are inferred in this study to be associated with the probable source volume of the main shock. The hypocenters were determined from data recorded by a 5-station temporary seismic network which operated near Summerville for 8 months in 1973 and by a 10-station permanent seismic network which began operating in May 1974.

The temporary network revealed an ill-defined cluster of activity northwest of Charleston and south of Summerville. Earthquakes recorded from May 1974 through December 1975 by the larger, permanent network defined a linear trend of hypocenters which extended northwest from Middleton Place to Summerville and to depths as great as 8 km. A well-constrained focal mechanism was determined for the largest earthquake in the zone. The strike (N. 42° W.) and dip (78°) of one nodal plane are similar to the strike and dip of the seismicity.

The historical catalog of Charleston-Summerville earthquakes shows that the area has experienced declining earthquake activity since the 1886 main shock; however, the seismic activity has not yet reached pre-1886 levels. The persistence of seismic activity during nine decades and the observation that the nearly vertical zone of recent seismicity is located near the center of the zone of highest epicentral intensities of the 1886 shock, suggest that the Middleton Place-Summerville zone is closely associated with the rupture surface of the 1886 shock. The results of this study do not support a hypothetical connection, along a continuous northwest-trending seismic zone, of the Middleton Place-Summerville seismic activity with activity offshore to the southeast or with a persistent cluster of earthquakes near Bowman to the northwest.

INTRODUCTION

The most destructive earthquake in the history of the southeastern United States took place at 9:51 p.m. (local time) on August 31, 1886. The shaking destroyed much of Charleston, S. C., killed approximately 60 persons, and caused injury to many others (Dutton, 1889). Intensity-IX (Modified Mercalli scale) effects were observed in Charleston, and a maximum intensity of X was reported in the epicentral area, inferred to be near the town of Summerville, 25 km northwest of Charleston (Dutton, 1889; Bollinger, this volume). The magnitude (m_{bLg}) has been estimated at 6.8-7.1 (Bollinger, this volume).

The main shock was preceded by several foreshocks (Dutton, 1889; Taber, 1914) and followed by an extensive aftershock series (Dutton, 1889; Taber, 1914; Bollinger, 1975). The largest aftershock occurred about 8 minutes after the main shock and was of sufficiently high intensity that reference is made (U.S. Environmental Data Service, 1973, p. 25) to the "earthquakes of August 31, 1886." The catalog of earthquakes of South Carolina (Bollinger, 1975) shows that the Charleston-Summerville area was quite active for at least three decades after the main shock.

Most of the details contained in Dutton's (1889) report of the Charleston earthquake do not need to be reviewed. For the purposes of this study, however, several facts in the Dutton (1889) report are significant:

1. Personal observations and distribution of damage indicate that the epicenter was nearer to Summerville than to Charleston. This fact is significant for interpretation of the recent seismicity instrumentally located near Summerville and Middleton Place.
2. The extensive survey of earthquake effects showed an elongate, NNE-trending zone of highest intensities which, to Dutton, indicated the presence of two epicenters. Later, Taber (1914) reinterpreted the elongate zone as indicating the presence of a buried NNE-trending fault passing under Woodstock, a railroad stop 10 km southeast of Summerville.

3. Dutton's (1889) survey of intensities (reevaluated by Bollinger, this volume) throughout the Eastern United States showed that the area in which the earthquake was felt was very large and that major geological features (for example, the Appalachian Mountains) strongly affected the intensity pattern.

The 1886 shock is very important for earthquake hazards studies (see, for example, Algermissen and Perkins, 1976) because it took place within an intraplate region characterized by infrequent earthquakes of relatively small and moderate magnitudes. In terms of damage and the size of the area in which it was felt, the shock ranks with the 1663 St. Lawrence Valley, 1755 Cape Ann, and 1811-1812 Mississippi Valley shocks as the most significant in the Eastern and Central United States. The characterization of recent earthquake activity near Charleston and the relationship of the activity to the South Carolina-Georgia seismic zone are the principal topics of this chapter. Incorporated herein are the results of seismological studies conducted in the Charleston area by the U.S. Geological Survey during the period 1973 through 1975.

Support for this study was provided by the Atomic Energy Commission and the Nuclear Regulatory Commission, Office of Nuclear Research, under Agreement No. AT(49-25)-1000.

The efforts of Kenneth W. King in the design, installation, and operation of the South Carolina seismograph network and of David L. Carver in seismogram analysis and data processing activities were particularly important contributions to this study. The critical review of the manuscript in its early stages by Margaret Hopper, Charley Langer, and Frank McKeown and the continually fruitful collaboration and support of G. A. Bollinger and Pradeep Talwani are gratefully acknowledged.

SOUTH CAROLINA-GEORGIA SEISMIC ZONE

SPATIAL DISTRIBUTION OF EARTHQUAKES

The South Carolina-Georgia seismic zone is a broad band of seismicity that extends southeastward from the southern Appalachian seismic zone across most of South Carolina and northeastern Georgia (fig. 1). The zone is mapped on the basis of information from Bollinger's (1975) earthquake catalog, which is a listing of hypocenter coordinates, intensities, and (or) magnitudes (if determined) of earthquakes that took place in the time period 1754–1974. The catalog has been supplemented by new information on several pre-1886 shocks (Bollinger and Visvanathan, this volume) and by instrumentally recorded information on earthquakes which took place in 1975 (Carver and others, 1977).

The Bollinger (1975) catalog lists both *macroseismic epicenters* and *instrumental hypocenters* for the southeastern United States. Macroseismic epicenters are qualitative estimates of earthquake locations inferred from one or more subjective intensity observations. Instrumental hypocenters are quantitatively determined from precisely timed arrivals of *P*- and *S*-waves of earthquakes recorded by at least four seismograph stations.

A rectangle approximately 500 km long and 350 km wide defines the South Carolina-Georgia seismic zone in this study. Its long axis (*A*–*A*′) is oriented northwest-southeast, perpendicular to the southern Appalachian seismic zone (fig. 1), and the rectangle is similar in shape and orientation to Bollinger's (1975) definition of the zone.

The largest South Carolina and northeast Georgia earthquakes, in addition to several clusters of significant seismic activity, are enclosed by the rectangle. These clusters are located in the Charleston-Summerville area, in the Orangeburg-Bowman area, and in the vicinity of Clark Hill Reservoir (figs. 1 and 2).

Previously, several workers (Woollard, 1969; Bollinger, 1973; Sbar and Sykes, 1973) noted that the South Carolina-Georgia seismic zone appears to trend northwest, perpendicular to the trend of the southern Appalachians in eastern Tennessee and western North Carolina (fig. 1). The axis (*A*–*A*′) of the seismic zone, inferred from an alinement of well-determined epicenters of earthquakes which took place in the period 1961–1975, is a northwest-trending line that passes near Greenville, Columbia, Orangeburg, and Charleston (fig. 1). The axis *A*–*A*′ is the approximate center line of the rectangle defining the seismic zone (fig. 1); extension of the axis to the southeast and northwest connects several epicenters on the Continental Shelf and the epicenter of the eastern Tennessee earthquake of November 30, 1973 (Bollinger and others, 1976).

Figure 3 is a map showing epicenters of earthquakes that took place in the Charleston area prior to the initiation of U.S. Geological Survey seismological studies there in 1973. The distribution of epicenters of the 1886 earthquake, of its aftershocks, and of subsequent activity is mapped in figure 3 and suggests the presence of a source area northwest of Charleston and near Summerville. However,

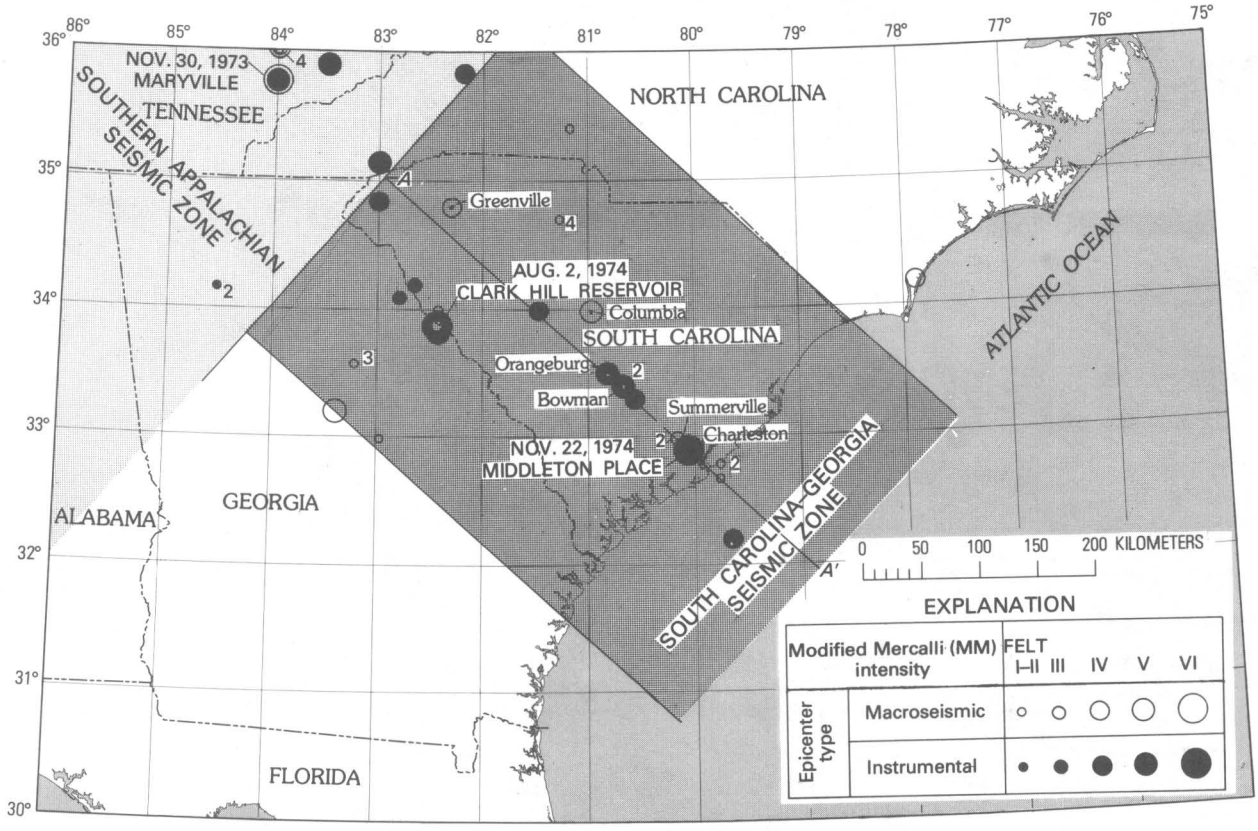

FIGURE 1.—Seismicity of the southeastern United States, 1961–75. Figure shows the relationship of the South Carolina-Georgia seismic zone to other seismicity in the southeastern United States. The axis A–A' is the approximate center line of the rectangle defining the South Carolina-Georgia seismic zone. Numbers beside the epicenter symbols show the number of events recorded. The macroseismic epicenters were determined from accounts of damage and felt reports, whereas instrumental epicenters were determined from seismographic data.

a more precise location of the source area is virtually impossible because of the inherent inaccuracies in the macroseismic observations used to locate the historical epicenters.

TEMPORAL DISTRIBUTION OF EARTHQUAKES

The temporal aspects of earthquake statistics are conventionally represented by the Gutenberg and Richter (1944) relationship

$$\log N = \mathrm{a} + \mathrm{b}M \qquad (1)$$

where N is the number of earthquakes recorded during time interval T, M is a magnitude (such as M_L, m_b, M_S, or m_{bLg}), and a and b are constants. The number N may be either *incremental number* $N_I(M)$ where N_I is the number of earthquakes having magnitude in the interval

$$M - \frac{\delta M}{2} \leq M < M + \frac{\delta M}{2} \qquad (2)$$

or *cumulative number* $N_c(M)$ where N_c is the number of earthquakes having magnitude greater than or equal to M. The functional relationship (1) is identical for either N_I or N_c; only the constants a and b are different in the equivalent representations.

The fit of equation (1) to a plot of log N versus M is a straight line and yields a value for the slope b, a negative number that varies with the source region (Utsu, 1961; Kárník, 1969), the type of earthquake process (swarm, aftershock, or ambient (secular) activity) (Utsu, 1961; Page, 1968), and possibly, even with time itself. A relationship

$$\log N = \mathrm{A} + \mathrm{B}I_o \qquad (3)$$

analogous to (1) is used when magnitudes are not available but maximum intensities I_o are (Kárník, 1969; Bollinger, 1973).

Many difficulties exist in the use of the historical South Carolina earthquake catalog as a sample for

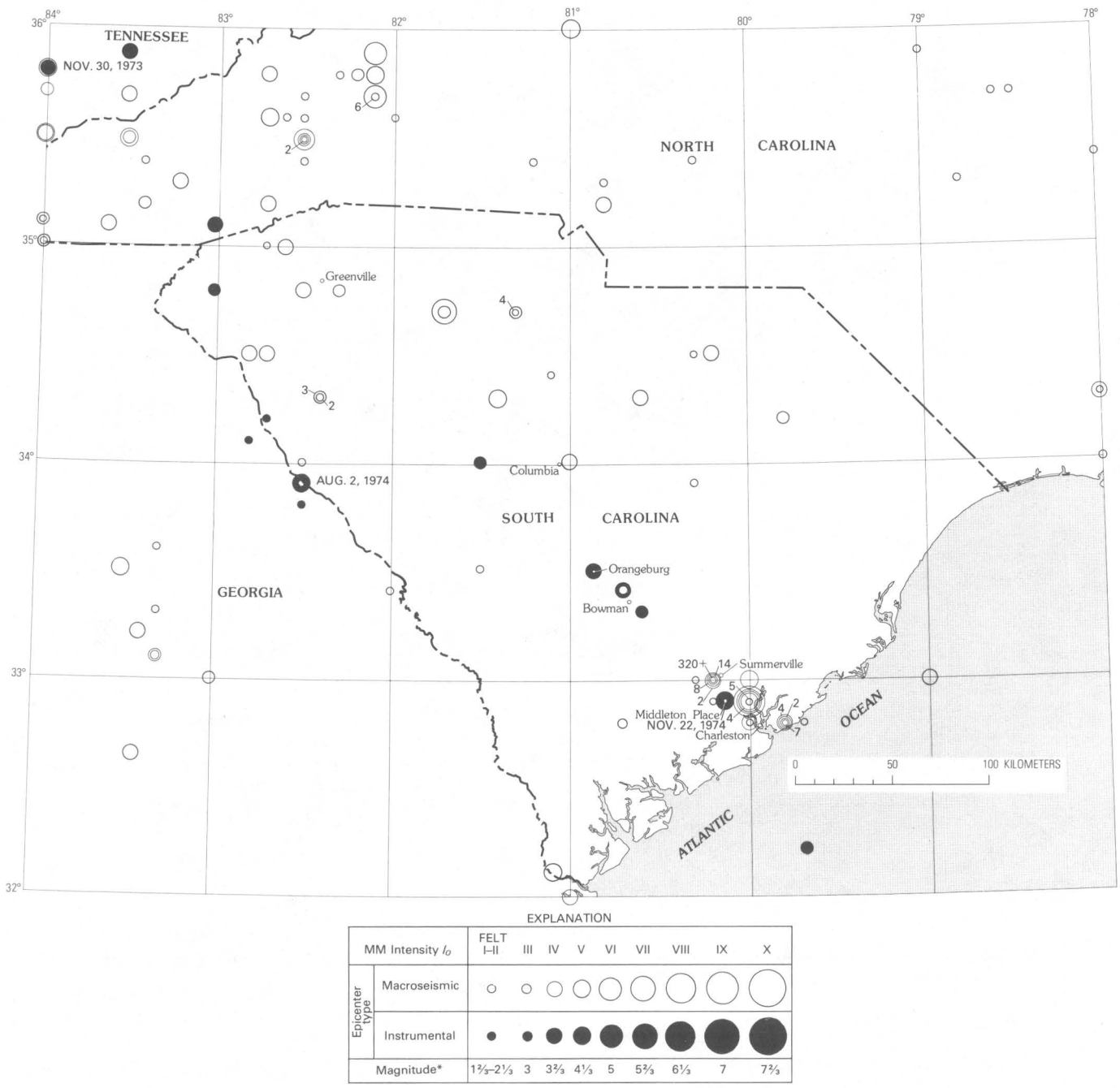

FIGURE 2.—Seismicity in South Carolina and adjoining States, 1754–1975. Earthquakes are indicated by circles of varying sizes, which represent the maximum Modified Mercalli intensities shown in the explanation. Numbers beside the epicenter symbols show the number of events recorded. Earthquakes are from the catalog of Bollinger (1975), supplemented by earthquakes reported by Carver and others (1977) and Bollinger and Visvanathan (this volume).

statistical treatment. Questions exist regarding (1) the accuracy of the values of maximum intensity I_o for the historical shocks (Were maximum intensity effects always reported to newspapers and other data sources if population densities were low in the epicentral area?), (2) the completeness of the catalog (Could significant numbers of seismic events, especially of lower I_o events, have been missed because of low population densities or inadequate reporting?), and (3) the size of the data sample (Is it sufficiently free from fluctuation to be characterized by equations (1) or (3)?).

In order to determine the constants in a frequency-maximum intensity relationship of the form

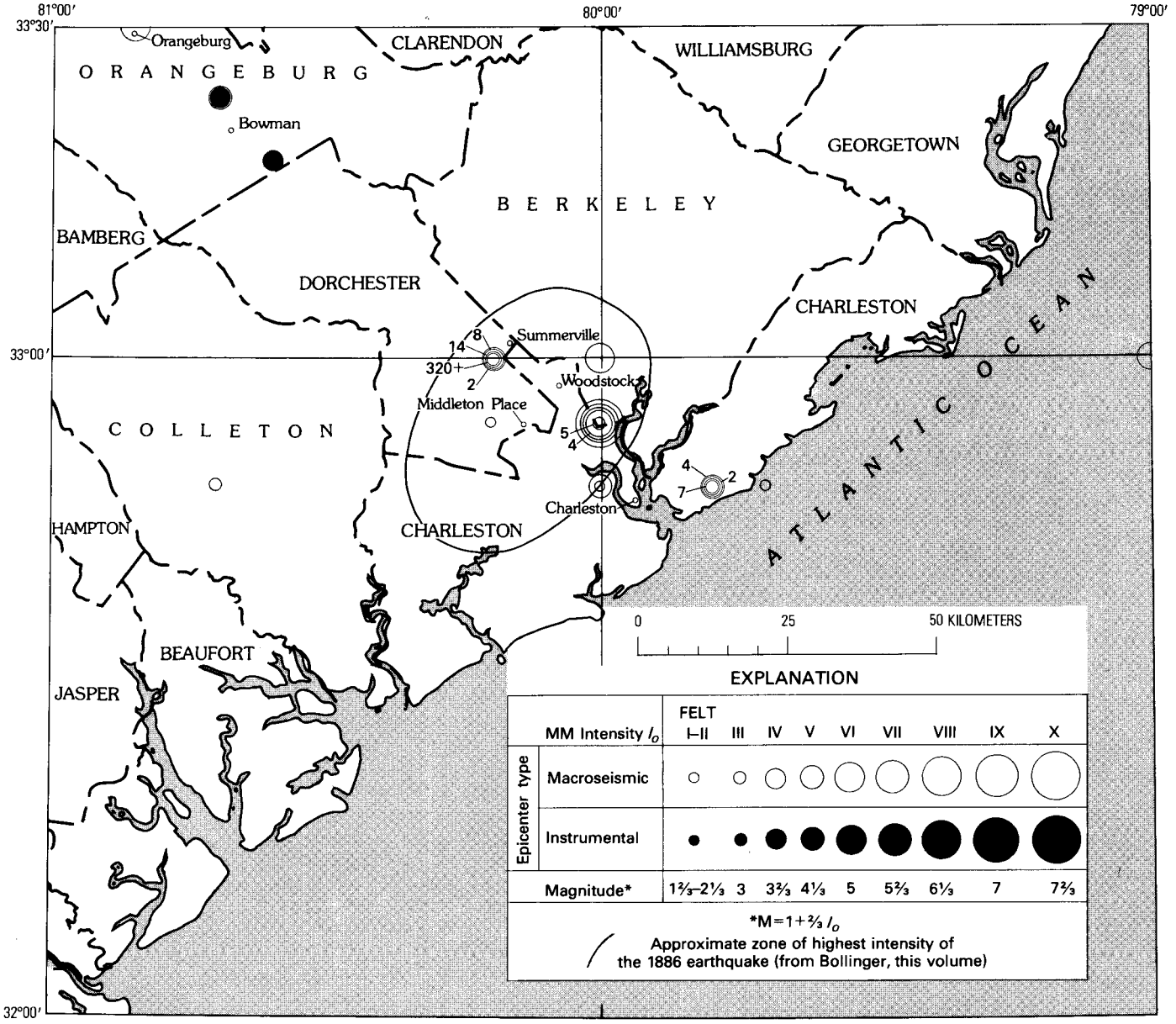

FIGURE 3.—Seismicity in the Charleston, S. C., area, 1754–1972. Data are from the same catalogs as in figure 2. The earthquakes shown are principally, but not exclusively, macroseismic epicenters. Numbers beside the epicenter symbols show the number of events recorded.

of equation (3), several assumptions have been made: (1) the information in table 1 is complete in listing earthquakes of the highest intensities down to those of an intensity level where the cumulative number departs from the straight-line relationship by 10 percent or more; (2) searches of data sources, such as those by Bollinger (1975) and Bollinger and Visvanathan (this volume), have been exhaustive; (3) all large and moderately large events were reported to newspapers and other data sources; and (4) population densities in South Carolina were sufficiently high that reports were made on all events having intensities stronger or equal to the intensity where the cumulative number departs from the straight-line relationship by 10 percent or more.

The Bollinger (1975) catalog is used and is supplemented by information on pre-1886 events (Bollinger and Visvanathan, this volume) and on several events in the instrumental catalog of Carver and others (1977) which were felt. The catalog entries have been separated according to incremental maximum intensity class and decade of occurrence for

TABLE 1.—*South Carolina earthquakes, 1754–1975*

[C.–S., Charleston-Summerville area; S.C., South Carolina exclusive of Charleston-Summerville area. Leaders (---) indicate no earthquake reported. Data from Bollinger (1975), Carver and others (1977), and Bollinger and Visvanathan (this volume).]

	Maximum Modified Mercalli intensity																						
	Felt	I	I-II	II	II-III	III	III-IV	IV	IV-V	V	V-VI	VI	VI-VII	VII	VII-VIII	VIII	VIII-IX	IX	IX-X	X	Total	Grand Total
1750–60:																						
C.–S.	2	---	---	---	---	---	---	---	---	---	---	---	---	---	---	---	---	---	---	---	2	2
S.C.	---	---	---	---	---	---	---	---	---	---	---	---	---	---	---	---	---	---	---	---	---	
1760–70:																						
C.–S.	---	---	---	---	---	---	---	---	---	---	---	---	---	---	---	---	---	---	---	---	---	---
S.C.	---	---	---	---	---	---	---	---	---	---	---	---	---	---	---	---	---	---	---	---	---	---
1770–80:																						
C.–S.	1	---	---	---	---	---	---	---	---	---	---	---	---	---	---	---	---	---	---	---	1	1
S.C.	---	---	---	---	---	---	---	---	---	---	---	---	---	---	---	---	---	---	---	---	---	
1780–90:																						
C.–S.	---	---	---	---	---	---	---	---	---	---	---	---	---	---	---	---	---	---	---	---	---	---
S.C.	---	---	---	---	---	---	---	---	---	---	---	---	---	---	---	---	---	---	---	---	---	---
1790–1800:																						
C.–S.	1	---	---	---	---	---	---	---	---	---	---	---	---	---	---	---	---	---	---	---	1	4
S.C.	2	---	---	---	---	---	---	---	---	1	---	---	---	---	---	---	---	---	---	---	3	
1800–10:																						
C.–S.	---	---	---	---	---	---	---	---	---	---	---	---	---	---	---	---	---	---	---	---	---	---
S.C.	---	---	---	---	---	---	---	---	---	---	---	---	---	---	---	---	---	---	---	---	---	---
1810–20:																						
C.–S.	1	---	---	---	---	---	---	---	---	1	---	---	---	---	---	---	---	---	---	---	2	3
S.C.	1	---	---	---	---	---	---	---	---	---	---	---	---	---	---	---	---	---	---	---	1	
1820–30:																						
C.–S.	---	---	---	---	---	---	---	---	---	---	---	---	---	---	---	---	---	---	---	---	---	1
S.C.	1	---	---	---	---	---	---	---	---	---	---	---	---	---	---	---	---	---	---	---	1	
1830–40:																						
C.–S.	---	---	---	---	---	---	---	---	---	---	---	---	---	---	---	---	---	---	---	---	---	---
S.C.	---	---	---	---	---	---	---	---	---	---	---	---	---	---	---	---	---	---	---	---	---	---
1840–50:																						
C.–S.	1	---	---	---	---	---	---	---	---	---	---	---	---	---	---	---	---	---	---	---	1	2
S.C.	1	---	---	---	---	---	---	---	---	---	---	---	---	---	---	---	---	---	---	---	1	
1850–60:																						
C.–S.	---	---	---	---	---	---	---	---	---	1	---	---	---	---	---	---	---	---	---	---	1	2
S.C.	---	---	---	---	---	---	---	---	---	---	---	1	---	---	---	---	---	---	---	---	1	
1860–70:																						
C.–S.	3	---	---	---	---	---	---	---	---	1	---	---	---	---	---	---	---	---	---	---	4	5
S.C.	1	---	---	---	---	---	---	---	---	---	---	---	---	---	---	---	---	---	---	---	1	
1870–80:																						
C.–S.	1	---	---	---	---	---	---	---	---	---	---	---	---	---	---	---	---	---	---	---	1	2
S.C.	1	---	---	---	---	---	---	---	---	---	---	---	---	---	---	---	---	---	---	---	1	
1880–90:																						
C.–S.	155+	---	---	---	---	---	---	---	---	1	---	2	---	1	---	[1]1	---	---	---	1	161+	161+
S.C.	---	---	---	---	---	---	---	---	---	---	---	---	---	---	---	---	---	---	---	---	---	
1890–1900:																						
C.–S.	72+	---	---	---	---	---	---	---	---	---	---	---	---	---	---	---	---	---	---	---	72+	72+
S.C.	---	---	---	---	---	---	---	---	---	---	---	---	---	---	---	---	---	---	---	---	---	
1900–10:																						
C.–S.	51	---	---	---	---	1	5	---	1	---	---	---	---	---	---	---	---	---	---	---	58	58
S.C.	---	---	---	---	---	---	---	---	---	---	---	---	---	---	---	---	---	---	---	---	---	
1910–20:																						
C.–S.	16	---	1	5	---	2	1	1	---	1	---	---	---	1	---	---	---	---	---	---	28	40
S.C.	---	---	---	---	---	2	2	---	6	1	---	---	---	---	1	---	---	---	---	---	12	
1920–30:																						
C.–S.	1	---	---	---	2	6	---	---	---	---	---	---	---	---	---	---	---	---	---	---	9	14
S.C.	2	---	---	---	---	---	---	---	1	2	---	---	---	---	---	---	---	---	---	---	5	
1930–40:																						
C.–S.	10	---	---	---	---	1	---	1	1	---	---	---	---	---	---	---	---	---	---	---	13	16
S.C.	3	---	---	---	---	---	---	---	---	---	---	---	---	---	---	---	---	---	---	---	3	
1940–50:																						
C.–S.	12	---	---	---	---	---	---	1	---	---	---	---	---	---	---	---	---	---	---	---	13	15
S.C.	1	---	---	---	---	---	---	---	---	---	1	---	---	---	---	---	---	---	---	---	2	
1950–60:																						
C.–S.	4	---	---	---	---	---	---	---	---	1	---	1	---	---	---	---	---	---	---	---	6	12
S.C.	---	---	---	---	---	---	---	4	---	1	---	1	---	---	---	---	---	---	---	---	6	
1960–70:																						
C.–S.	3	---	---	---	---	2	---	---	---	1	---	---	---	---	---	---	---	---	---	---	6	16
S.C.	4	---	---	---	---	---	---	3	---	3	---	---	---	---	---	---	---	---	---	---	10	
1970–75:																						
C.–S.	1	---	---	---	---	---	---	1	---	---	---	1	---	---	---	---	---	---	---	---	3	10
S.C.	---	---	---	---	---	2	---	3	---	1	---	1	---	---	---	---	---	---	---	---	7	
Total:																						
C.S.	335+	---	1	5	2	12	6	4	2	7	---	4	---	2	---	1	---	---	---	1	382+	436+
S.C.	17	---	---	---	---	4	2	10	7	9	1	3	---	---	1	---	---	---	---	---	54	

[1] The principal aftershock of the August 31, 1886, main event is assumed to have been intensity VIII.

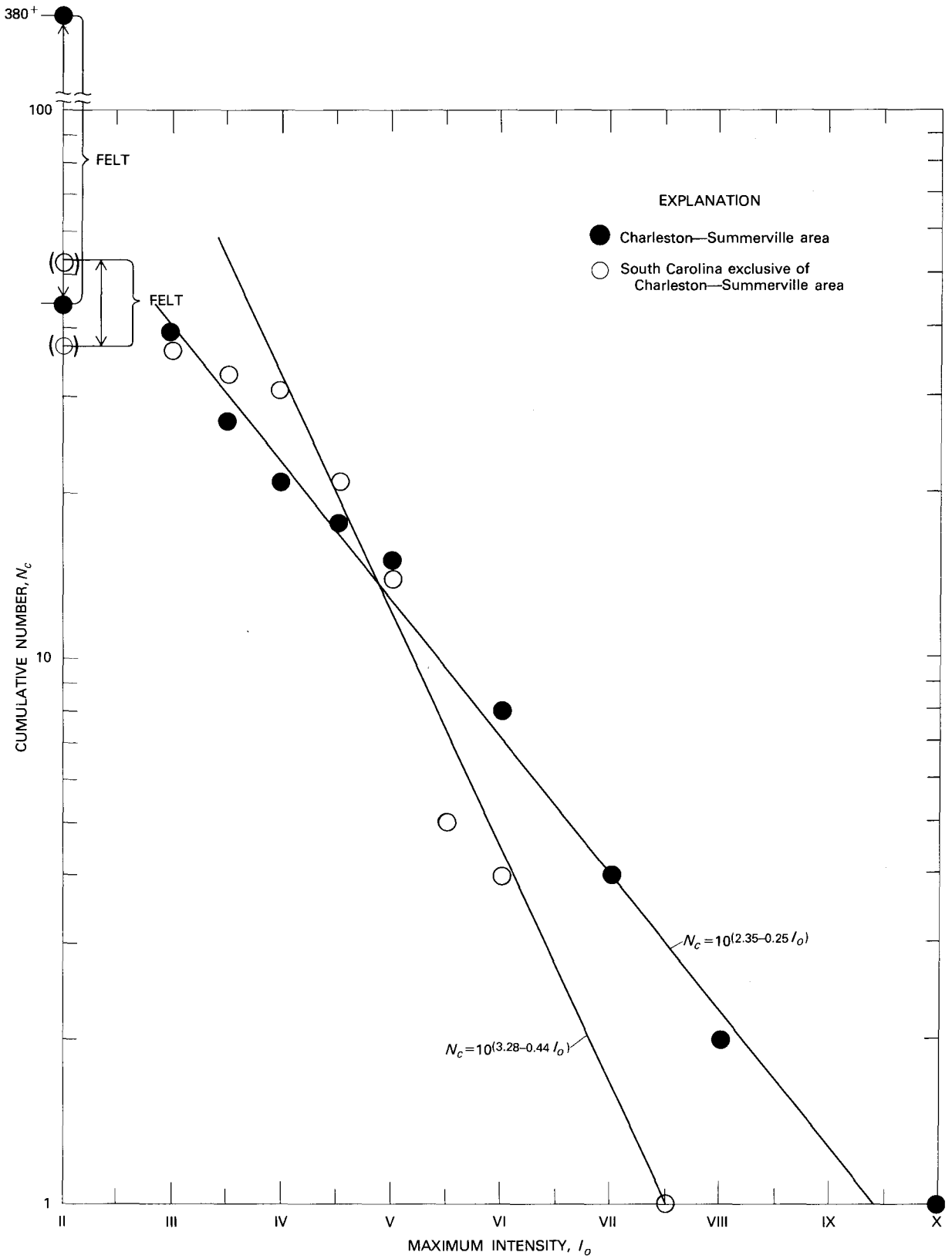

FIGURE 4.—Graph showing the cumulative number (N_c) of earthquakes in South Carolina versus maximum Modified Mercalli intensity (I_o), 1754–1975. The data, taken from table 1, are separated into two regional sets. Felt earthquakes are added at the intensity-II level. Symbols in parentheses are interpolated points. The Charleston-Summerville data set appears to be complete down to I_o=III, and the South Carolina data set appears to be complete down to I_o=IV, if the anomalous value of N_c at I_o=V–VI is ignored.

two groups, Charleston-Summerville area events and South Carolina exclusive of Charleston-Summerville events (table 1). Table 1 gives the incremental numbers for the two groups and for the combined South Carolina total group. Events for which no intensity was assigned in the Bollinger (1975) catalog are classified as "Felt" in table 1.

The N_c vs. I_o graph (fig. 4), constructed from the incremental numbers of earthquakes having assigned intensities in table 1, shows relatively linear behavior to about intensity III for Charleston-Summerville events and to about intensity IV for other South Carolina shocks. These intensity values are assumed to be the levels at which the information in table 1 is complete. The paucity of events at lower intensities is probably caused by reduced potential for perception. According to figure 4, the perceptibility threshold in the more populated Charleston-Summerville area is apparently at least one intensity degree smaller than that in the more rural areas of South Carolina.

The catalog may be complete to intensity levels slightly lower than the values cited above. For example, if it is assumed that all events in the "Felt" class of the South Carolina exclusive of Charleston-Summerville group were intensity-IV shocks, then that group is complete to no lower than intensity IV because the cumulative number of "Felt" events is less than the number expected from the straight-line fit at higher intensities. Conversely, if it is assumed that the "Felt" events of the Charleston-Summerville group were intensity-II shocks or stronger, the cumulative number greatly exceeds the number expected from the straight-line fit at higher intensities. Clearly, the hundreds of aftershocks following the August 31, 1886, earthquake cause the slope of the N_c vs I_o graph of the aftershock series to be steeper than that of the graph of ambient seismicity.

Bollinger (1972) found a B value of -0.3 for South Carolina earthquakes, exclusive of Charleston-Summerville events, that took place in the period 1886–1971. This B value is low compared to B values of earthquakes in other seismic zones in the East, and it implies a paucity of small events relative to large events during that 86-year period. Figure 4 suggests that a B value of -0.44 is appropriate for the data set of earthquakes in South Carolina exclusive of Charleston-Summerville during 1754–1975.

RECENT SEISMICITY NEAR CHARLESTON

PRIOR INSTRUMENTAL STUDIES

Only two instrumental studies of seismicity of the lower Coastal Plain were conducted prior to the beginning of the seismological program described in this chapter. Bollinger (1972) monitored microearthquakes in the Summerville area during the summer of 1971 and recorded 61 events, about half of which were clustered in swarmlike groups. Although no epicenter locations were possible from these single-station recordings, a b value of -1.8 ± 0.5 was determined from his microearthquake data set.

McKee (1973) monitored microearthquakes in the Bowman area in 1972 and 1973 and obtained a b value of -0.5 for seven events. McKee (1973) noted that this b value compares favorably with $b = -0.5$ determined by Bollinger (1972) for all South Carolina earthquakes, exclusive of the 1886 aftershock series.

Although these two studies demonstrated that small earthquakes were taking place in the Summerville and Bowman areas, they were severely limited in their scope. The need for additional seismological studies in South Carolina, and more specifically, the need for a seismic monitoring capability to locate local earthquakes provided the initial justification for a seismic program that included the design, installation, and operation of a 10-station seismograph network in South Carolina.

RECONNAISSANCE STUDY MARCH 1973–DECEMBER 1973

A reconnaissance seismicity study was conducted during 1973 for 8 months in the Charleston-Summerville area for the purpose of gaining experience in the problems of operating seismograph stations in the environment of the lower Coastal Plain while procurement and fabrication of the permanent South Carolina network stations were underway.

The field instruments, which included both vertical and horizontal seismometers, were deployed at five sites near Charleston. The data were transmitted by short radio-telemetry links to a recording site near Charleston where the seismic signals from different stations were recorded simultaneously with a time signal on magnetic tape and visual drum-type recorders. Operating magnifications were relatively low because of poor site conditions. Nevertheless, a loose cluster of eight earthquakes was located northwest of Charleston (fig. 5).

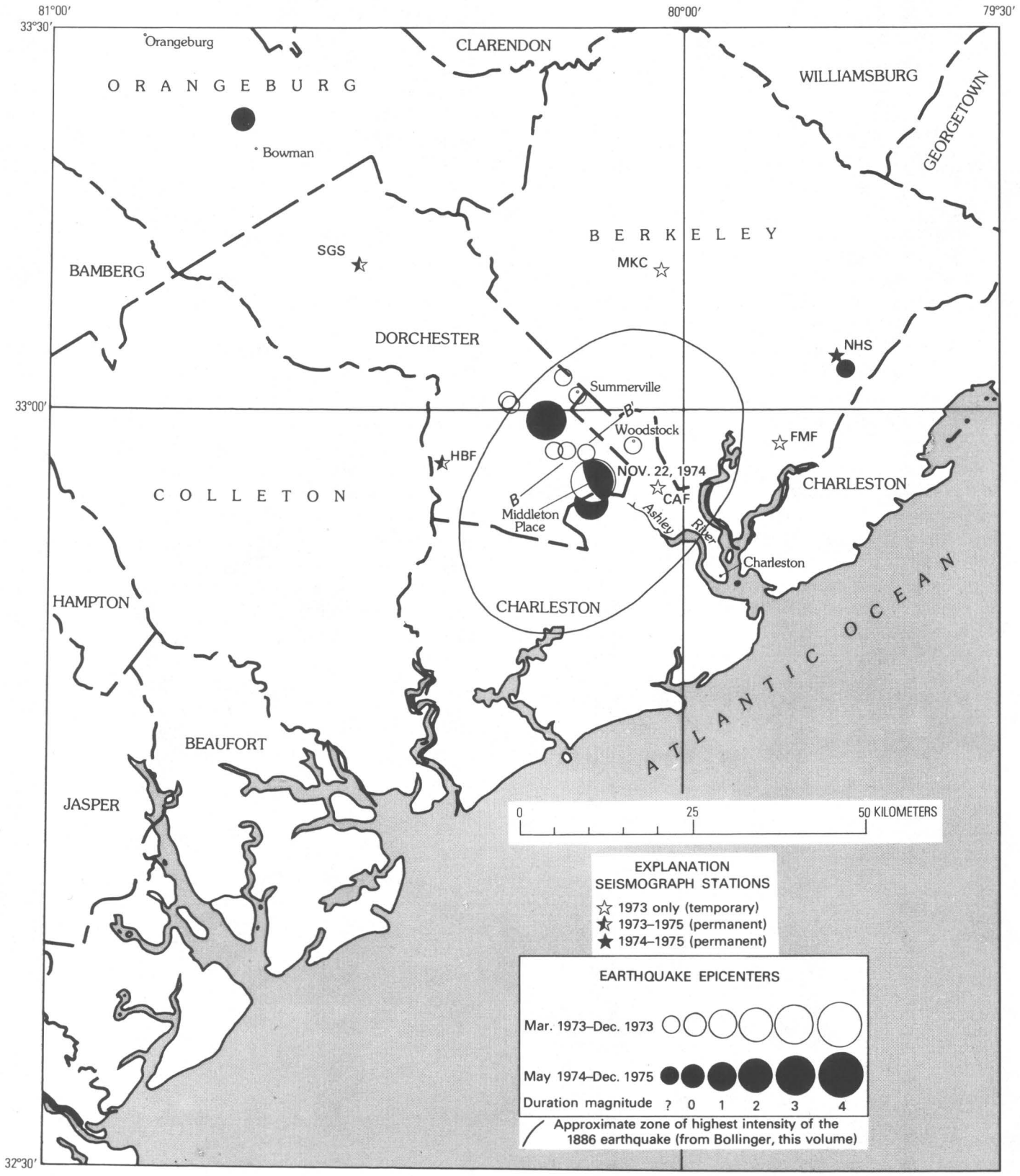

FIGURE 5.—Charleston area seismicity and seismograph stations, March 1973-December 1975. The earthquake at Middleton Place is represented by its focal mechanism. Profile *B–B′* is shown on figure 7. Seismograph station abbreviations, coordinates, and instrumentation are discussed by Carver and others (1977).

TABLE 2.—*A representative South Carolina crustal model*

Layer	Depth to top of layer (km)	Thickness (km)	Compressional velocity (V_P) (km/sec)	Shear velocity (V_S) (km/sec)
1	0.0	1.2	2.5	1.4
2	1.2	2.3	5.8	3.3
3	3.5	28.5	6.2	3.5
Half space	32.0	---	8.2	4.6

Program HYPO71 (Lee and Lahr, 1975) was used for hypocenter computations. A representative crustal model assumed three layers on a half space (table 2). A summary of hypocenter locations, depths, and times is given in table 3.

The reconnaissance survey demonstrated, as had Bollinger's (1972) survey, that low-level seismic activity was indeed taking place near Summerville and furthermore, that the activity was located near the inferred location of the 1886 earthquake and aftershocks. However, it was not possible to discern whether the cluster represented a small source area or was only a segment of a longer zone of activity that extended beyond the network perimeter. This difficulty is due to the tendency for more smaller earthquakes to be detected and located near the center of a network (where the detection threshold is lowest) than in the area outside the network (where the detection threshold increases).

SOUTH CAROLINA SEISMOGRAPHIC NETWORK

The design of the South Carolina network and the objectives of the seismological program have been discussed by Tarr and King (1974). One of the principal objectives of the program was to monitor the South Carolina-Georgia seismic zone and provide, for the first time, an instrumental data base for earthquakes in the zone. Ten stations were installed in the Coastal Plain astride the hypothetical northwest-trending axis of the seismic zone. Stations were spaced 50–100 km apart at the northwestern end of the network to insure wide areal coverage and 30–60 km apart at the southeastern end where a lower detection threshold was desirable. A nominal three-station detection threshold of $M_L=2.5$ or better was estimated for the area bounded roughly by the cities of Columbia, Sumter, Georgetown, Charleston, Beaufort, and Aiken.

The 10-station network became operational in May 1974. All data channels were radio-telemetered to a central site at Columbia where all the signals were recorded on 16-mm film and magnetic tape, and where three channels were recorded on visual drum-type recorders for monitoring purposes. The network configuration was altered slightly in 1975 to locate more accurately aftershocks of the August 2, 1974, earthquake at Clark Hill Reservoir; however, the network that was operative during the occurrence of most of the earthquakes discussed in the next section is shown in figure 6.

SEISMICITY MAY 1974–DECEMBER 1975

Between May 1974 and December 1975, earthquakes in the South Carolina-Georgia seismic zone were recorded and located by the use of data from

TABLE 3.—*Hypocenter summary*

[Leaders (----), insufficient data for computation]

Date		Origin time (Universal Coordinated Time)	RMS [1] (sec)	Latitude (degrees)	ERY [2] (km)	Longitude (degrees)	ERX [3] (km)	Depth (km)	ERZ [4] (km)	Duration [5] magnitude	Number of observations
1973											
March	25	04 29 31.6	0.11	32.953N.	--	80.080W.	--	0.9	----	--	4
April	18	10 06 10.7	.56	33.044N.	--	80.190W.	--	2.5	----	--	4
	23	21 32 38.2	.38	33.012N.	--	80.280W.	--	3.3	----	--	4
June	9	19 24 52.7	.29	32.942N.	0.7	80.153W.	1.5	3.5	395.6	--	9
	12	20 45 25.0	.29	33.018N.	1.2	80.168W.	1.8	3.7	496.8	--	6
August	25	09 17 30.1	.27	32.944N.	.5	80.186W.	.9	5.7	4.3	--	7
November	13	15 10 03.0	.05	32.945N.	--	80.205W.	--	1.3	----	--	4
December	19	10 16 18.3	---	33.008N.	--	80.275W.	--	8.3	----	--	4
1974											
May	28	05 01 36.1	0.22	33.388N.	1.0	80.697W.	0.9	3.6	268.7	1.6	12
September	2	08 54 47.0	.33	33.053N.	--	79.742W.	--	2.6	----	--	4
November	22	05 25 55.8	.15	32.902N.	.9	80.147W.	2.0	4.1	261.0	3.8	6
	22	06 22 43.9	.35	32.874N.	1.7	80.145W.	4.4	2.2	541.8	2.6	7
1975											
April	28	05 46 52.3	0.04	32.986N.	0.2	80.215W.	0.3	3.7	63.9	3.0	7

[1] RMS: Root-mean-square of travel time residuals
[2] ERY: Standard error in latitude
[3] ERX: Standard error in longitude
[4] ERZ: Standard error in depth
[5] Duration magnitude is an estimation of Richter magnitude M found by $M=0.87+2.00 \log(\tau)+0.0035\ \Delta$ where τ is signal duration in seconds and Δ is epicentral distance in kilometers (see Lee, Bennett, and Meagher, 1972)

FIGURE 6.—South Carolina seismographic network, May 1974–December 1975. Seismograph station abbreviations, coordinates, and instrumentation are discussed by Carver and others (1977).

the 10-station network. Although the region of uniform detection threshold is quite large, most of the earthquakes detected and located were concentrated near Summerville (table 3). The most important of the shocks outside the Charleston-Summerville area was the August 2, 1974, Clark Hill Reservoir earthquake (fig. 1). This event and its aftershock sequence have been described by Talwani and others (1975) and need not be discussed further. Another significant event took place on May 28, 1974, and was located near Bowman (fig. 1).

Epicenters of earthquakes taking place in the Charleston-Summerville area tend to cluster about 20–25 km northwest of Charleston and about 0–10 km south of Summerville, near Middleton Place and near the cluster of small earthquakes recorded by the five-station network in the reconnaissance study of 1973 (fig. 5).

Figure 5 shows that the seismic activity of the 3-year period is confined principally to a zone between Middleton Place and Summerville. The zone of epicenters seems to trend northwest, and the depth section shows that the activity is in the depth interval 1–8 km (fig. 7). Although the epicenter co-

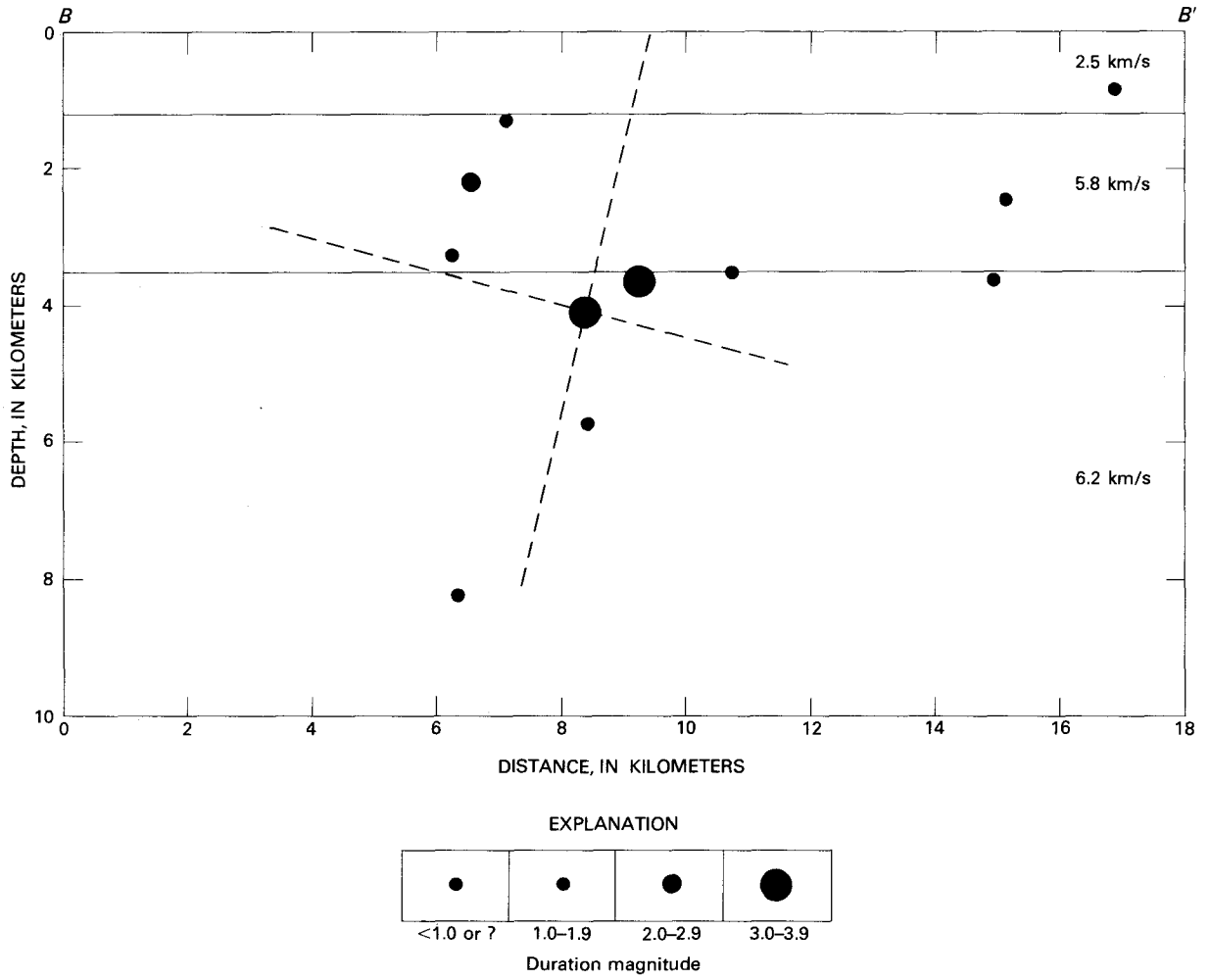

FIGURE 7.—Profile of the Middleton Place-Summerville seismic zone. Hypocenters are projected onto a vertical plane passing through *B–B'*, which is shown in figure 5. The plane *B–B'* is perpendicular to the strike of the two nodal planes (dashed lines) determined for the November 22, 1974, earthquake (fig. 8). The upper layers of the crustal model, used in the hypocenter computations, are shown by horizontal interfaces and compressional (*P*) velocities.

ordinates are well determined, the vertical extent of the zone cannot be known with comparable certainty because of large errors in the estimates of depth (table 3). The absence of seismograph stations close to the seismic activity is the principal reason for the lack of depth control. The largest earthquake of the period had a magnitude (m_{bLg}) of 3.8 and took place on November 22, 1974; its focus was very near Middleton Place at a depth of about 4.1 km. Despite the relatively small magnitude of this earthquake, it was widely felt in South Carolina (fig. 8*A*).

A focal-mechanism solution was determined from 13 short-period *P*-wave first-motion observations of the November 22, 1974, event (fig. 8*B*). Eight of the first-motions of the aftershock recorded by 10 network stations are consistent with the first motions of the main shock. One of the permissible focal-mechanism solutions, in which all observations are consistent, is shown in figure 8*B*. The B- (null-) axis in this solution is horizontal and parallel to the strike of the two planes. The strike (N. 42° W.) of the preferred (A) nodal plane is well-constrained by observations from stations both within and outside the seismic network. The dip (78°) is controlled by the position of the auxiliary (C) nodal plane. The profile B–B′ in figure 7 is oriented perpendicularly to the B-axis and, hence, the two nodal planes are viewed end-on in the figure. Uncertainties in hypocenter coordinates and permissible variations of the crustal velocity model allow for slightly different nodal plane orientations than the ones shown in figure 8*B*.

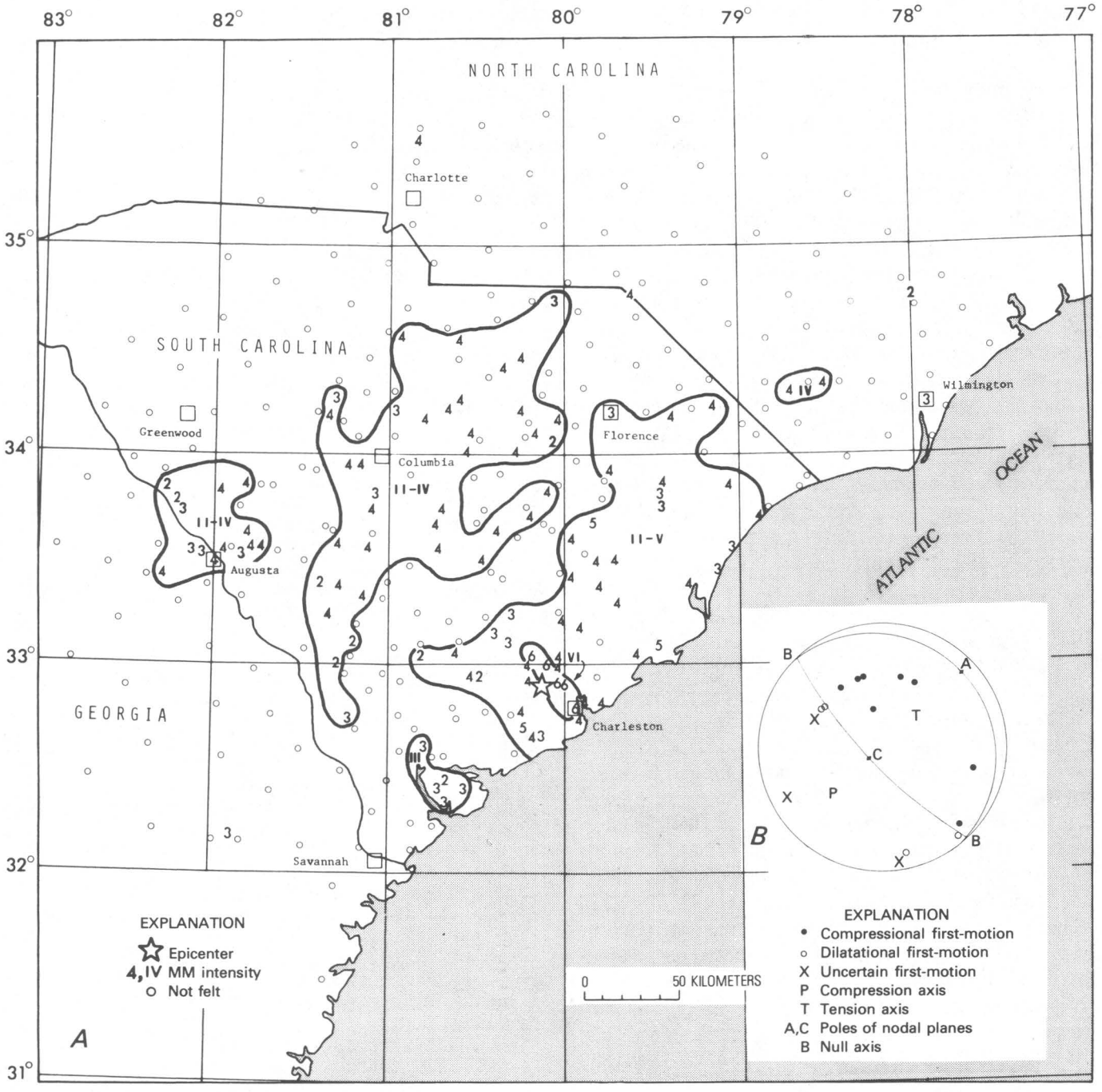

FIGURE 8.—Isoseismal map (*A*) and focal mechanism (*B*) of the November 22, 1974, earthquake. Figure (modified from fig. 11 of Stover and others, 1976) depicts interpretations of Modified Mercalli intensities from questionnaire canvass of postmasters in the area. Maximum intensity was VI.

INTERPRETATION OF RESULTS

The seismological studies conducted from 1973 through 1975 have provided new information about the South Carolina-Georgia seismic zone near Charleston. Our data suggest that the small but persistent zone of seismic activity between Middleton Place and Summerville may be associated with the source volume of the 1886 Charleston earthquake. In addition, the Middleton Place-Summerville zone appears to coincide with anomalous seismic velocities of shallow-layered structures under Middleton Place (Ackermann, this volume) and large local gravity (Long and Champion, this volume), electrical and electromagnetic (Campbell, this

volume), and aeromagnetic (Popenoe and Zietz, this volume; Phillips, this volume) anomaly patterns.

The seismological data presented in this chapter suggest that current seismic activity in the Middleton Place-Summerville area is taking place along a nearly vertical plane striking northwest and passing near Middleton Place (fig. 5). The largest recent event took place (November 22, 1974) at the southeastern end of the zone. The Middleton Place-Summerville seismic activity takes place within the zone of highest intensities of the 1886 shock as contoured by Sloan in the Dutton (1889) report and by Bollinger (this volume). Furthermore, the epicenter of the November 22, 1974, shock was located midway between the two epicenters in Dutton's (1889) contouring of the maximum intensity zone. The preferred nodal plane determined from the focal mechanisms of the November 22, 1974, event is nearly vertical and suggests reverse faulting on a plane striking N. 42° W.; the trace of this plane at the surface is along the course of the Ashley River (fig. 5).

In prior studies, Taber (1914) and Bollinger (1972) suggested that the earthquakes felt in the Charleston-Summerville area since August 31, 1886, are related to, if they are not actually aftershocks of, the main shock. Certainly the frequency of occurrence statistics of felt earthquakes in the Charleston-Summerville area (table 1) shows a decline of activity typical of aftershock sequences (Richter, 1958) and, even in the last two decades, the frequency has not decreased to pre-1886 levels. Therefore, it may be that the current Middleton Place-Summerville activity is taking place within the rupture zone of the main shock. The current seismic data cannot discriminate between the alternative hypotheses that the earthquake activity represents either true seismic afterslip in the rupture zone or a response to the regional stress field in locally weak geologic structures near the 1886 rupture zone.

Determination of the dimensions of the Middleton Place-Summerville zone must await detection and location of further seismic activity and will require more precisely determined hypocenters than were possible for this study. Five new local seismic stations currently provide the seismographic network with this capability. In addition, several new coastal stations northeast and southwest of Charleston will expand the monitoring capability necessary to detect and locate the possible extension of the seismic zone onto the Continental Shelf. Because of the current configuration of the network, the detection and location capability fall off rapidly to the southeast. The seismic data from this study do not indicate that a seismic relationship exists between the Middleton Place-Summerville and Bowman source areas.

The identification of the subsurface structure responsible for the current seismicity in the Middleton Place-Summerville zone and by inference, for the 1886 Charleston earthquake, cannot be made at this time. Only one focal mechanism has been determined thus far, and many more will be required to determine the nature of faulting throughout the entire zone and to establish the relationship of the relatively deeper seismicity to shallow structures under Middleton Place.

REFERENCES CITED

Algermissen, S. T., and Perkins, D. M., 1976, A probabilistic estimate of maximum acceleration in rock in the contiguous United States: U.S. Geol. Survey open-file rept. 76–416, 45 p., 2 pls., 1 table.

Bollinger, G. A., 1972, Historical and recent seismic activity in South Carolina: Seismol. Soc. America Bull., v. 62, p. p. 851–864.

——— 1973, Seismicity of the southeastern United States: Seismol. Soc. America Bull., v. 63, p. 1785–1808.

——— 1975, A catalog of southeastern United States earthquakes 1754 through 1974: Virginia Polytech. Inst. and State Univ., Research Div. Bull. 101, 68 p.

Bollinger, G. A., Langer, C. J., and Harding, S. T., 1976, The eastern Tennessee earthquake sequence of October through December, 1973: Seismol. Soc. America Bull., v. 66, no. 2, p. 525–547.

Carver, David, Turner, L. M., and Tarr, A. C., 1977, South Carolina seismological data report May 1974–June 1975: U.S. Geol. Survey open-file rept. 77–429, 66 p.

Dutton, C. E., 1889, The Charleston earthquake of August 31, 1886: U.S. Geol. Survey 9th Ann. Rept., 1887–88, p. 203–528.

Gutenberg, Beno, and Richter, C. F., 1942, Earthquake magnitude, intensity, energy, and acceleration: Seismol. Soc. America Bull., v. 32, p. 163–191.

——— 1944, Frequency of earthquakes in California: Seismol. Soc. America Bull., v. 34, p. 185–188.

Kárník, Vít, 1969, Seismicity of the European area, Part I: Dordrecht, Holland, D. Reidel Pub. Co., 364 p.

Lee, W. H. K., Bennett, R. E., and Meagher, K. L., 1972, A method of estimating magnitude of local earthquakes from signal duration: U.S. Geol. Survey open-file rept., 28 p., 5 figs., 1 table.

Lee, W. H. K., and Lahr, J. C., 1975, HYPO71 (revised), A computer program for determining hypocenter, magnitude, and first motion pattern of local earthquakes: U.S. Geol. Survey open-file rept. 75–311, 59 p., 5 figs., 48 tables.

McKee, J. H., 1973, A geophysical study of microearthquake activity near Bowman, South Carolina: Atlanta, Ga., Georgia Inst. of Tech., unpub. Masters thesis, 75 p.

Page, Robert, 1968, Aftershocks and microaftershocks of the great Alaska earthquake of 1964: Seismol. Soc. America Bull., v. 58, p. 1131–1168.

Richter, C. F., 1958, Elementary seismology: San Francisco, Calif., W. H. Freeman, 768 p.

Sbar, M. L., and Sykes, L. R., 1973, Contemporary compressive stress and seismicity in eastern North America; an example of intra-plate tectonics: Geol. Soc. America Bull., v. 84, no. 6, p. 1861–1881.

Stover, C. W., Simon, R. B., and Person, W. J., 1976, Earthquakes in the United States, October-December 1974: U.S. Geol. Survey Circ. 723–D, p. D1–D27.

Taber, Stephen, 1914, Seismic activity in the Atlantic Coastal Plain near Charleston, South Carolina: Seismol. Soc. America Bull., v. 4, p. 108–160.

Talwani, Pradeep, Secor, D. T., and Scheffler, P., 1975, Preliminary results of aftershock studies following the 2 August 1974 South Carolina earthquake: Earthquake Notes, v. 46, no. 4, p. 21–28.

Tarr, A. C., and King, K. W., 1974, South Carolina seismic program: U.S. Geol. Survey open-file rept. 74–58, 15 p., 4 figs., 2 tables.

U.S. Environmental Data Service, 1973, Earthquake history of the United States: U.S. Environmental Data Service Pub. 41–1, rev. ed. (through 1970), 208 p.

Utsu, T., 1961, A statistical study on the occurrence of aftershocks: Geophys. Magazine, v. 30, p. 521–605.

Woollard, G. P., 1969, Tectonic activity in North America as indicated by earthquakes, *in* Hart, P. J., ed., The earth's crust and upper mantle: Am. Geophys. Union Geophys. Mon. 13, p. 125–133.

Lithostratigraphy of the Deep Corehole (Clubhouse Crossroads Corehole 1) Near Charleston, South Carolina,

By GREGORY S. GOHN, BRENDA B. HIGGINS, CHARLES C. SMITH, and JAMES P. OWENS

STUDIES RELATED TO THE CHARLESTON, SOUTH CAROLINA, EARTHQUAKE OF 1886—A PRELIMINARY REPORT

GEOLOGICAL SURVEY PROFESSIONAL PAPER 1028-E

CONTENTS

ILLUSTRATIONS

STUDIES RELATED TO THE CHARLESTON, SOUTH CAROLINA, EARTHQUAKE OF 1886—
A PRELIMINARY REPORT

LITHOSTRATIGRAPHY OF THE DEEP COREHOLE (CLUBHOUSE CROSSROADS COREHOLE 1) NEAR CHARLESTON, SOUTH CAROLINA

By GREGORY S. GOHN, BRENDA B. HIGGINS, CHARLES C. SMITH, and JAMES P. OWENS

ABSTRACT

The continuously cored Clubhouse Crossroads test hole is in the Cottageville 15-minute quadrangle, 40 km (25 mi) west-northwest of Charleston, S.C. Total depth of the hole is 792 m (2,599 ft). Seven hundred and fifty meters (2,462 ft) of Cenozoic and Upper Cretaceous sediments was penetrated, and 70 percent of the core was recovered. Below that, 42 m (137 ft) of amygdaloidal basalt was penetrated, and 100 percent of this part of the core was recovered.

The formations recognized in the core, their ages, and approximate thicknesses are: amygdaloidal basalt (K/Ar minimum ages: 94.8±4.2 m.y. and 109±4 m.y.), greater than 42 m (137 ft); Cape Fear Formation, Upper Cretaceous, 59 m (194 ft); Middendorf Formation, Upper Cretaceous, 124 m (408 ft); Black Creek Formation, Upper Cretaceous, 159 m (520 ft); Peedee Formation, Upper Cretaceous, 164 m (540 ft); Beaufort(?) Formation, Paleocene, 52 m (170 ft); Black Mingo Formation, Paleocene and Eocene, 67 m (220 ft); Santee Limestone, Eocene, 56 m (183 ft); Cooper Formation, Eocene and Oligocene, 64 m (211 ft); unconsolidated sediments, Pleistocene(?), 5 m (16 ft).

The Cape Fear Formation contains feldspathic sand and interbedded clay similar to those in the overlying Middendorf Formation, but it also contains marginal marine deposits of thinly interbedded fine sand and dark clay. The Middendorf Formation contains fining-upward cycles of conglomeratic to fine-grained quartzose, feldspathic sand, and mottled clay deposited in continental environments. The Black Creek Formation is a heterogeneous sequence of sandy mud, well-sorted sand, shelly sand, and dark clay deposited in marine and marginal marine environments. The Peedee and Beaufort(?) Formations are homogeneous marine sequences of dark-gray silty clay and muddy sand. The Black Mingo Formation contains silty clay, muddy sand, thinly interbedded sand and clay, and shelly limestone deposited in marine and marginal marine environments. The Santee Limestone and Cooper Formation are dominantly impure glauconitic marine limestone containing varying amounts of silt- and sand-sized quartz.

INTRODUCTION

In January, February, and March 1975, a 792-m (2,599-ft) continuously cored test hole, the Clubhouse Crossroads corehole 1, was drilled near Charleston, S.C. (fig. 1). The hole was drilled in support of the Charleston Project, a multidisciplinary investigation by the U.S. Geological Survey, to determine the cause of seismicity in the Coastal Plain near Charleston, S.C. Prior to the analysis of the core, the lithologic character and three-dimensional stratigraphy of the Coastal Plain sediments in this area were poorly understood. Analysis of the core has established the stratigraphic column necessary for the construction of a regional stratigraphic framework.

The corehole is at lat 32°53.25′ N., long 80°21.41′ W., near the center of the Cottageville 15-minute quadrangle, 3.5 km (2.2 mi) southwest of Clubhouse Crossroads and approximately 40 km (25 mi) west-northwest of Charleston. The Clubhouse Crossroads hole was drilled to a total depth of 792 m (2,599 ft) below a surface elevation of 6 m (20 ft). Of that total, 244 m (800 ft) of Cenozoic and 506 m (1,662 ft) of Cretaceous sediments were penetrated, and 70 percent of the core was recovered. The basal 42 m (137 ft) is composed of weathered and fresh basalt; 100 percent of this part of the core was recovered. Mechanical problems prevented further drilling. The diameter of most of the upper 225 m (738 ft) of the core is 15 cm (6 in.); that of the lower 567 m (1,861 ft) is 7 cm (2.75 in.). The drilling was done by a U.S. Army Corps of Engineers team using hydraulic rotary drilling equipment. Eight geophysical logs were made by the Schlumberger Corp. (Rhodehamel, 1975). Descriptive logs of the core were made at the drill site before more detailed laboratory investigations.

The preliminary biostratigraphic and lithostratigraphic analyses of the core sediments and fossils have been completed, and the basic stratigraphic

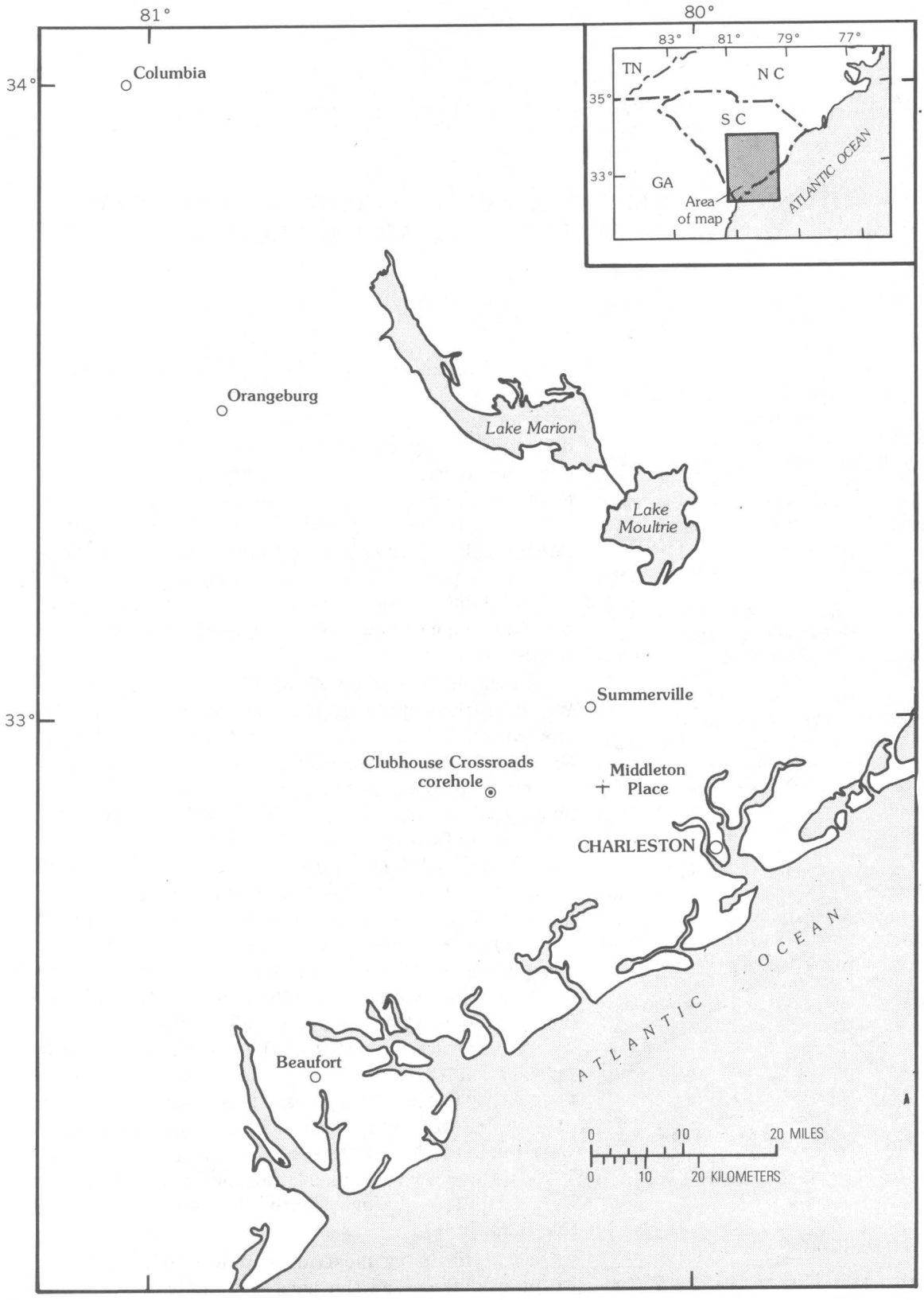

FIGURE 1.—Location of Clubhouse Crossroads corehole 1, Charleston, S.C.

framework and sediment composition are described herein. The purpose of this report is to describe the mineralogy, texture, sedimentary structures, and general appearance of the core sediments and the nomenclature and contact relationships of the formations that have been identified. The biostratigraphic framework for the core sediments has been described by Hazel and others (this volume).

This work was supported by the U.S. Nuclear Regulatory Commission, Office of Nuclear Research, Agreement No. AT (49–25)–1000. Melodie Hess, Ray Schneider, and Steve Perlman performed the many laboratory analyses of the core sediments. The potassium-argon radiometric age analyses were done by R. F. Marvin, U.S. Geological Survey.

We wish to express particular appreciation to the Westvaco Corporation for allowing us to locate the drilling site on their land and for their interest and cooperation throughout this project.

CORE STRATIGRAPHY

BASALT

The Clubhouse Crossroads corehole bottomed in 42 m (137 ft) of basalt of Cretaceous(?) age. K/Ar age determinations on two basalt samples gave ages of 109±4 m.y. (latest Early Cretaceous) and 94.8±4.2 m.y. (earliest Late Cretaceous). These ages are considered to be minimum ages, however, because of observed geochemical alteration of the basalt (Gottfried and others, this volume). Both ages are consistent with the Woodbinian (Cenomanian) age, as determined by microfossils from sediments immediately overlying the basalt (see Hazel and others, this volume).

The distribution of weathered, amygdaloidal, and massive basalts within the core indicates at least two distinct flow units. Seven meters (23 ft) of the lower flow were recovered. This flow displays distinct vertical changes in lithology. The lower 1.8 m (6 ft) contains a network of fine fractures along which considerable alteration of the basalt has occurred. Above the fractured basalt the remaining 5.2 m (17 ft) shows an upward increase in the size and abundance of amygdules. The upper flow (34.7 m, 114 ft) contains a similar sequence of lithologies with 3 m (10 ft) of fractured basalt below 22.9 m (75 ft) of fresh, dark-gray amygdaloidal basalt. Amygdules increase in size and abundance upward in the fresh basalt. The dark-gray basalt grades upward into dark-red weathered basalt (4.2 m, 14 ft), which grades into red-, yellow-, and white-mottled clay (4.6 m, 15 ft) displaying a relict amygdaloidal texture.

UPPER CRETACEOUS SERIES

Upper Cretaceous sediments (fig. 2) are present from the 750-m (2,462-ft) level to the 244-m (800-ft) level in the core, a thickness of 507 m (1,662 ft). The section is provisionally divided into four formations that have been recognized previously as outcrop and subsurface units in the Carolina Coastal Plain (Swift and Heron, 1969). From the base to the top, the formations are the Cape Fear (59 m, 194 ft), Middendorf (124 m, 408 ft), Black Creek (159 m, 520 ft), and Peedee (164 m, 540 ft). Unlike the Tertiary formations, contacts between the four Cretaceous units are difficult to identify precisely because of poor core recovery in some intervals and similar sediment types in more than one interval.

The base of the Cape Fear Formation (750 m, 2,462 ft) is drawn between an upper conglomeratic muddy sand and the top of the basalt. The Cape Fear–Middendorf boundary (691 m, 2,268 ft) is placed at the base of the lowest 0.3 m (1 ft) or thicker feldspathic sand in an interbedded sand-clay sequence.

Recognition of the Middendorf–Black Creek boundary is hampered by a lack of core recovery for several intervals. Core recovery between 575 m (1,787 ft) and 567 m (1,860 ft) is poor, and the small amount of sediment that was recovered consists of friable sand and dark clay lithologically similar to overlying thinly interbedded sand and clay. The section between 567 m (1,860 ft) and 750 m (2,462 ft) consists mostly of interbedded 1- to 5-m-thick (3–15–ft) yellowish-gray-, greenish-gray-, and red-mottled clay and coarse feldspathic sand. On the basis of the most pronounced lithologic change, the Middendorf–Black Creek contact is placed at 567 m (1,860 ft). Rock resistivity also decreases significantly at this point (fig. 2).

Despite the fact that the Middendorf–Black Creek contact is not sharply defined, the paleontologic data (Hazel and others, this volume) suggest that an unconformity of considerable temporal magnitude is present. Fossils at about 560 m (1,837 ft) indicate a late Austinian age; at 586 m (1,923 ft), early Eaglefordian (late Cenomanian) fossils are present. The 26-m (85-ft) interval between these two points is barren of diagnostic fossils. The data suggest that either the lower Austinian and middle and upper Eaglefordian (that is, approximately Coniacian and Turonian) deposits are absent, or they are represented by only 26 m (85 ft) of section. Data from

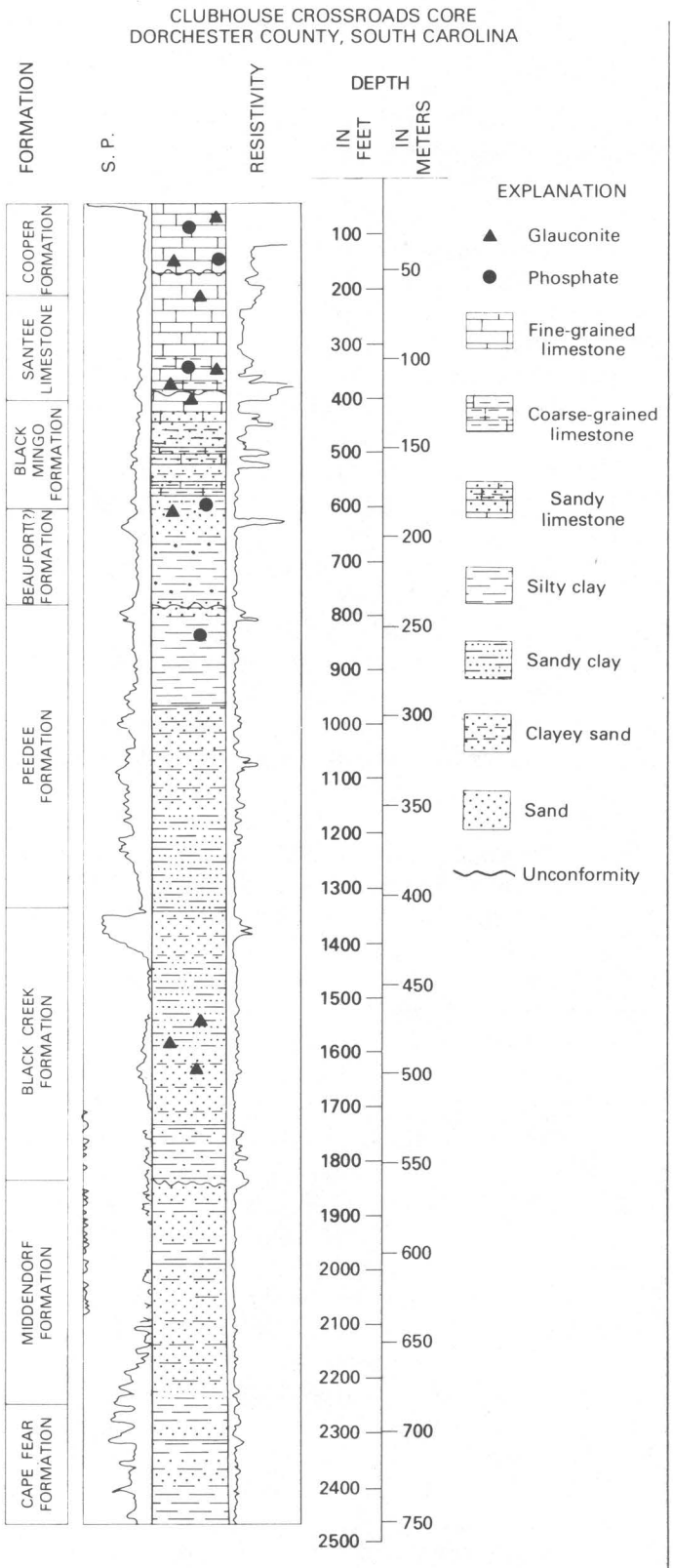

FIGURE 2.—Stratigraphic column for the Clubhouse Crossroads core. Spontaneous potential (S.P.) log and resistivity log are shown next to the lithologic log.

heavy minerals, discussed below, suggest a different sediment provenance for the deposits above and below this barren zone.

The Black Creek–Peedee boundary is placed at the contact (408 m, 1,340 ft) between an upper gray-green silty clay that has a basal phosphate pebble bed, and a lower calcareous, light-colored, relatively well-sorted quartz sand. Deposition of the sediments now found between 244 m (800 ft) and 567 m (1,860 ft) was nearly continuous (see Hazel and others, this volume), and similar gray-green silty and sandy clays are common sediment types in both formations. Placement of the boundary at 408 m (1,340 ft) confines shell-rich limestone, dark carbonaceous clay, and clean light-colored sand to the Black Creek Formation. In addition, the major change in the spontaneous potential log between 244 m (800 ft) and 567 m (1,860 ft) takes place at 408 m (1,340 ft).

As defined, the Black Creek and Peedee Formations are identifiable lithologic units. Some evidence exists, however, for the cyclical occurrence of coarser and finer grained units in these formations. Such cycles would be more fundamental depositional and lithologic units than the two formations as presently defined. As a result of further study, refinement of changes in the lithostratigraphy of these units may be required.

TERTIARY SYSTEM

The Tertiary section (fig. 2) recovered from the corehole has been divided into four named formations: (1) a basal Paleocene unit tentatively identified as the Beaufort(?) Formation (52 m, 170 ft); (2) the Black Mingo Formation, Paleocene and Eocene (67 m, 220 ft); (3) the Santee Limestone, Eocene (56 m, 183 ft); and (4) the Cooper Formation, Eocene and Oligocene (64 m, 211 ft). The surficial Pleistocene(?) sand and clay (5 m, 16 ft) overlying the Cooper were not named.

The name Beaufort(?) has been tentatively applied to the sequence of calcareous mud and muddy sand of Paleocene age that is lithologically similar and stratigraphically equivalent to the Beaufort Formation in North Carolina (Brown, 1958, 1959). This unit may also be equivalent to the "unnamed beds of Midway age" described by Siple (1975) from nearby Orangeburg County, S.C. The Black Mingo and the Santee have been recognized previously in the South Carolina Coastal Plain (Malde, 1959; Pooser, 1965; Colquhoun and Johnson, 1968; and many others). Most authors have referred to the Cooper as the Cooper Marl. However, as noted by Pooser

(1965) and Malde (1959), the Cooper sediments contain too much quartz sand to be true marl. In this paper, the lithologic designation is dropped in favor of the name Cooper Formation.

From their physical appearance, boundaries of three of the four Tertiary formations have been interpreted as unconformities, disconformities, or diastems. Irregular, burrowed and bored carbonate-cemented mud or shelly limestone overlain and infiltrated by glauconite- and phosphate-rich sediments are formed at the Cretaceous–Tertiary boundary (244 m, 800 ft) at the base of the Beaufort(?) Formation, the Beaufort(?)–Black Mingo boundary (192 m, 630 ft), and the Santee–Cooper boundary (69 m, 227 ft). Similar surfaces are present at the Paleocene–Eocene boundary (132 m, 433 ft), within the Eocene part of the Cooper Formation (57 m, 186 ft), and at the Eocene–Oligocene boundary (55 m, 180 ft). The Black Mingo–Santee contact (125 m, 410 ft) is sharp and is between an upper (Santee) skeletal limestone and a lower (Black Mingo) fine-grained limestone (see also Hazel and others, this volume).

TEXTURE AND MINERALOGY

Sixty samples selected from representative sediment types throughout the core were subjected to textural and mineralogical examination. Textural variation, percentage of acid-soluble fraction (mostly calcium carbonate), and mineralogy of the sand- and clay-sized fractions are shown in figures 3–6.

CALCIUM CARBONATE CONTENT AND TEXTURAL ANALYSIS

On the basis of the distribution of calcium carbonate (acid-soluble fraction) in the core sediments (fig. 3), two fundamental sequences may be recognized: an Upper Cretaceous to lower Eocene siliciclastic sequence, and a middle Eocene to Oligocene carbonate sequence. Within the siliciclastic sequence, calcium carbonate is present primarily (from 5 to 40 percent) as shell debris and less commonly as calcite-cemented nodules and layers in the Cape Fear, Black Creek, Peedee, Beaufort(?), and Black Mingo Formations. The Middendorf Formation is noncalcareous and is the least fossiliferous of the formations. The amount of soluble material in the Middendorf averages less than 5 percent and is probably iron carbonate. In the carbonate sequence (Santee Limestone and Cooper Formation), the amount of carbonate averages 50–70 percent and is present primarily as macrofossil and microfossil shell debris.

The relative percentages of clay, silt, and sand, including the acid-soluble fraction, are shown in figure 3. The low density of analyzed samples throughout the core has resulted in limited detail; however, general trends in the sediment size distribution are the bimodal size distribution of sediments below 567 m (1,860 ft) (Cape Fear, Middendorf), the heterogeneous nature of the sediments between 408 and 567 m (1,340 to 1,860 ft) (Black Creek) and between 125 and 192 m (410 to 630 ft) (Black Mingo), and the homogeneous size distribution between 244 and 408 m (800 to 1,340 ft) (Peedee) and between 192 m and 244 m (630 to 800 ft) (Beaufort(?)). The abundant sand fraction of the calcareous sediments above 125 m (410 ft) is composed primarily of macrofossil and microfossil shells.

SAND-FRACTION MINERALOGY

Several trends in the distribution of sand-sized minerals are recognizable in figure 4. Cristobalite is abundant in most of the Beaufort(?) and the lower part of the Black Mingo sediments, common in most of the upper part of the Black Mingo sediments, rare in the lower part of the Santee sediments, abundant in most of the upper part of the Santee and lower part of the Cooper sediments, and rare in the upper part of the Cooper sediments. This pattern matches the distribution of cristobalite in the clay-sized fraction of the Tertiary samples (fig. 4). Potassium feldspar is common throughout the core but is more abundant below 458 m (1,500 ft) and very abundant below 533 m (1,750 ft). Plagioclase is common only below about 396 m (1,300 ft).

On the basis of the heavy minerals in the sand fraction (fig. 5), the sedimentary sequence of the core may be divided into two parts. The transition zone separating the two parts is from 540 m (1,770 ft) to 567 m (1,860 ft). Below 567 m (1,860 ft), the heavy-mineral suite contains abundant zircon, tourmaline, staurolite, and monazite, and common apatite, epidote, rutile, and garnet. This suite suggests a source area dominated by granitic plutons or pegmatites intruded into regionally metamorphosed pelitic rocks. Above 540 m (1,770 ft), apatite and monazite are rare, and rutile is much less abundant. Above 567 m (1,860 ft), the amount of zircon and epidote is much decreased. Instead, chloritoid is abundant, and the amount of kyanite increases above 540 m (1,770 ft). This change suggests that regionally metamorphosed pelitic rocks became the important sediment contributors and that granitic intrusions were rare or absent in the source area.

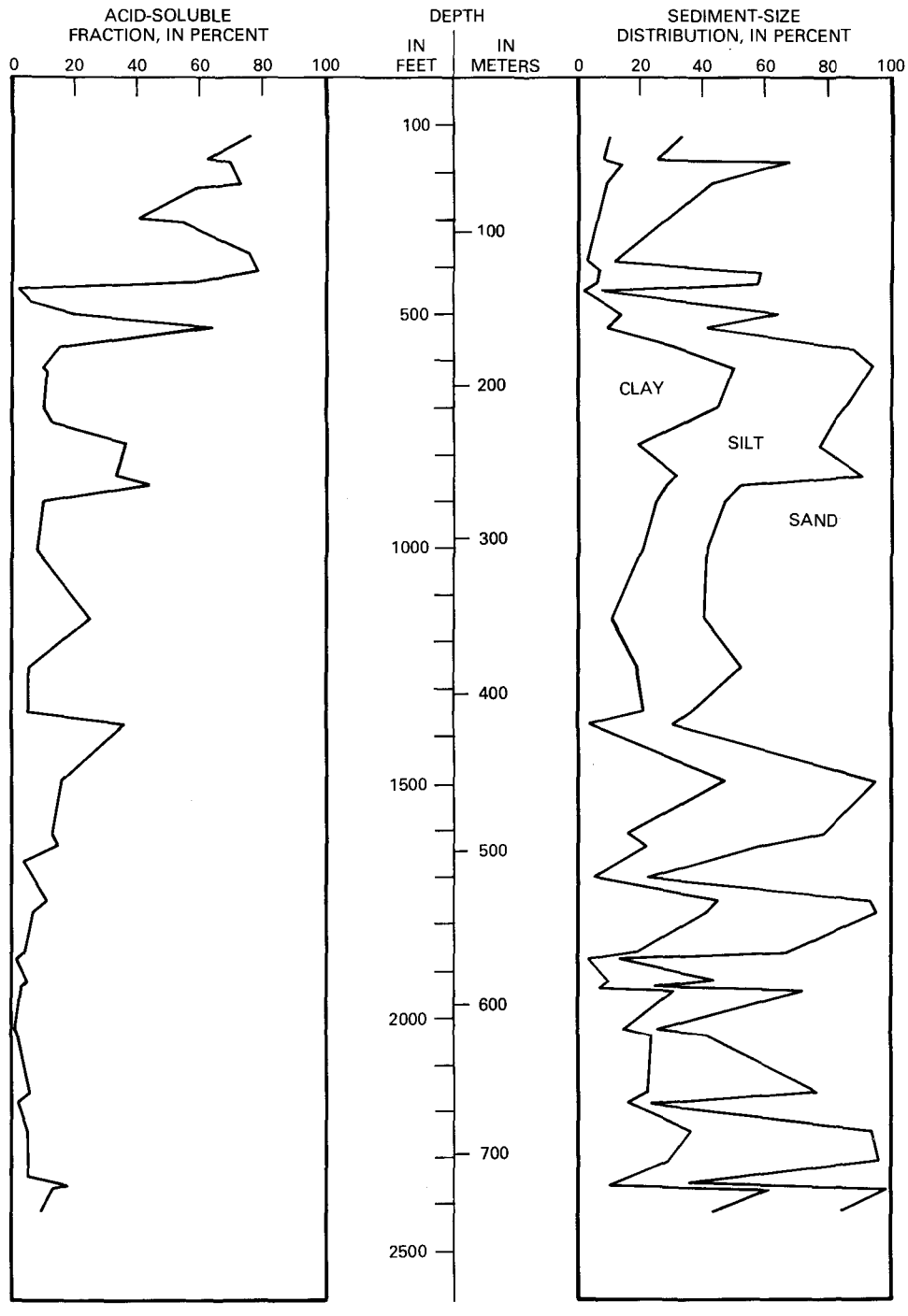

FIGURE 3.—Distribution of the acid-soluble fraction and the textural composition of the core sediments. The acid-soluble fraction is included in the textural analysis.

This fundamental change in sediment provenance is shown in figure 6. With two exceptions, heavy-mineral suites from above and below 540 m (1,770 ft) plot in separate fields on the diagram. The transition zone, 540–567 m (1,770–1,860 ft), separating the two heavy-mineral suites in part overlaps the section of unfossiliferous sediments (560–586 m, 1,837–1,923 ft) that separates fossiliferous lower Eaglefordian and Austinian sediments (Hazel and others, this volume). This overlap supports the concept, derived from the fossil evidence, that a major unconformity exists between 560 m (1,837 ft) and 586 m (1,923 ft), and probably between 560 m (1,837 ft) and 567 m (1,860 ft).

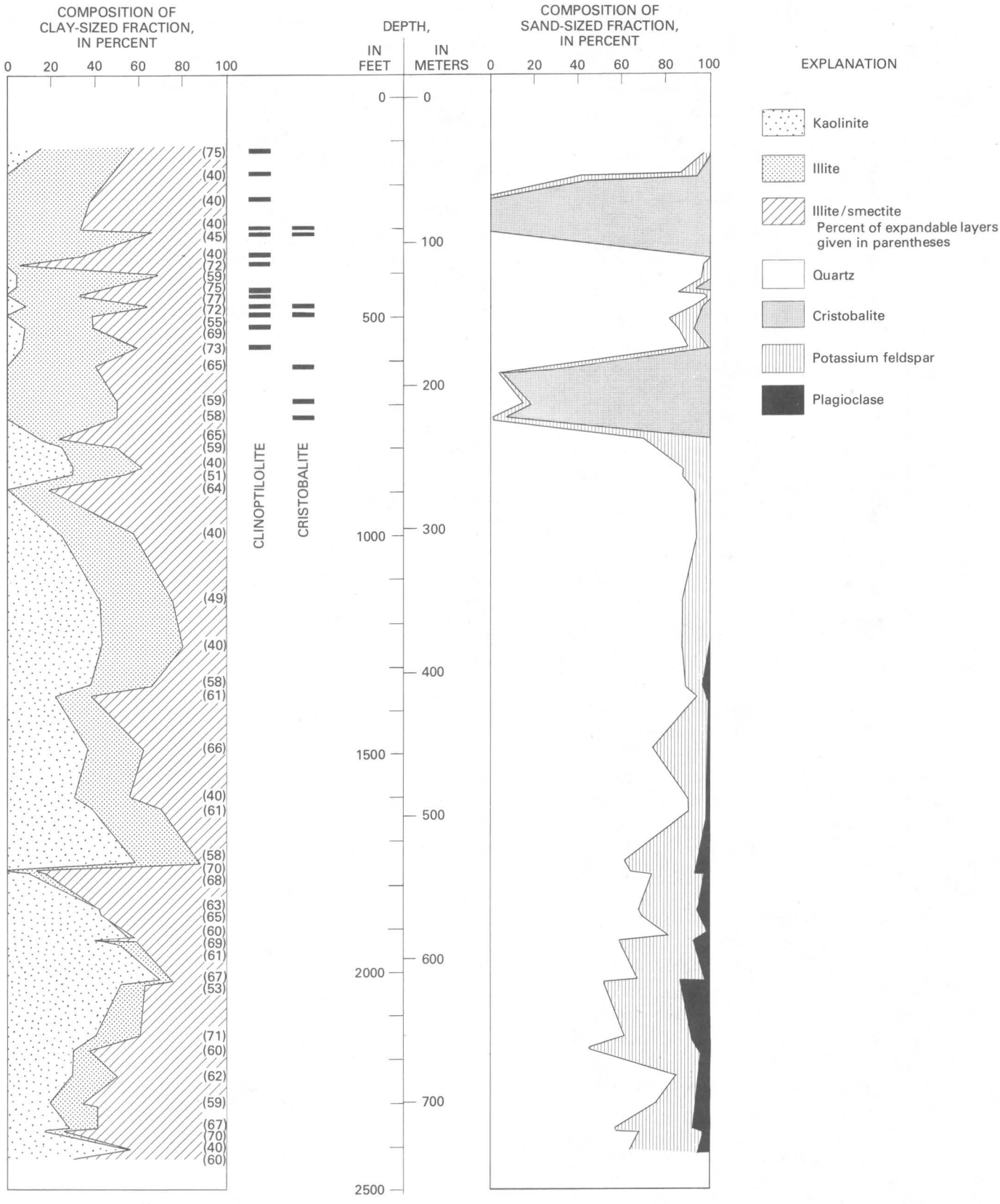

FIGURE 4.—Mineralogy of the clay-sized fraction and the light-mineral split of the sand-sized fraction. The feldspars are divided into potassium feldspar and plagioclase only below 244 m (800 ft). Plagioclase is rare above 244 m.

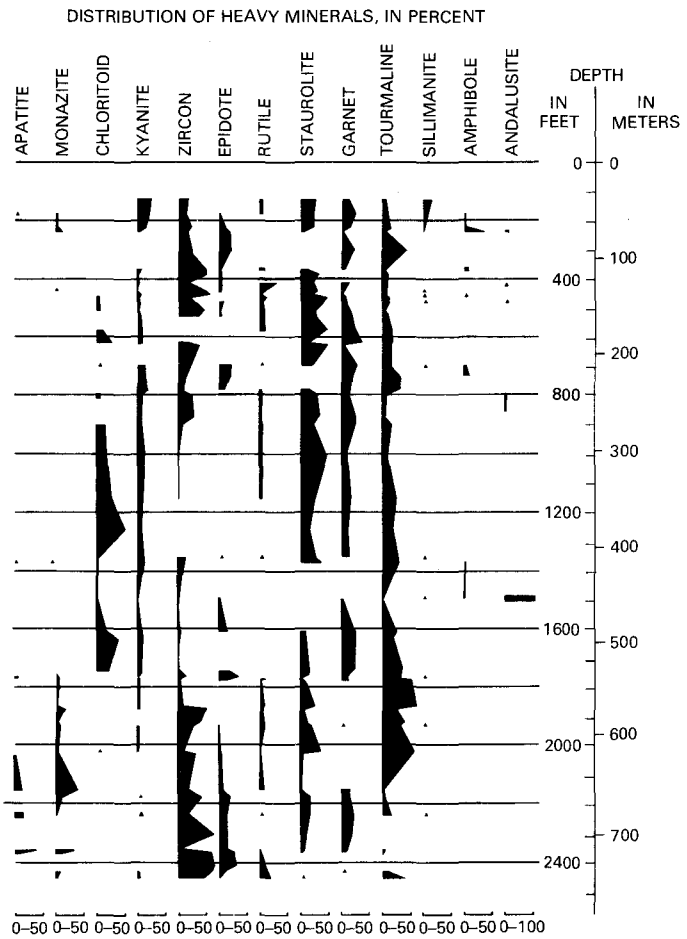

FIGURE 5.—Stratigraphic distribution of heavy minerals in the sand-sized fraction of the core sediments.

An interesting and significant heavy-mineral suite, perhaps related to the tectonic history of the Charleston area, is present in the upper half of the Black Creek Formation at 455 m (1,492 ft). This suite contains 95 percent andalusite. The remaining 5 percent consists of biotite, minor cordierite, and trace amounts of zircon, tourmaline, garnet, amphibole, kyanite, epidote, chloritoid, and sillimanite. The dominant association of andalusite, biotite, and cordierite suggests that the source of the assemblage was the contact aureole of a magma body intruded into pelitic rocks. The unusually high concentration of one mineral, in this case andalusite, suggests that this heavy-mineral suite was deposited very close to its source area.

Some credence is given to this idea by the presence of Cretaceous(?) basalt in the Clubhouse Crossroads core and the presence of diabase in the nearby Summerville test well (Cooke, 1936). The unroofing of Cretaceous or older Mesozoic shallow intrusive rocks and their contact zones could have provided a local source for the andalusite and associated minerals found in the younger Cretaceous sediments.

CLAY-FRACTION MINERALOGY

Variations in the mineralogy of the clay-sized fraction primarily involve small changes in the relative percentages of kaolinite, illite, and mixed-layer illite-smectite (fig. 4). In Cape Fear, Middendorf, and basal Black Creek sediments below 541 m (1,775 ft), kaolinite and mixed-layer clay are most abundant. In Black Creek, Peedee, and basal Beaufort(?) sediments between 541 m (1,775 ft) and 238 m (780 ft), kaolinite, illite, and illite-smectite are present in nearly equal proportions. Siliciclastic and carbonate sediments above 238 m (780 ft) contain little kaolinite and abundant illite and mixed-layer clay.

In addition to the three clay minerals, cristobalite and clinoptilolite are abundant within parts of the Tertiary section (fig. 4). The abundance of these two minerals in the Tertiary sediments and their absence in the Cretaceous sediments represent a fundamental change in the origin of some of the sediments deposited in the South Carolina Coastal Plain. Specifically, many authors have used clinoptilolite and cristobalite as indicators of diagenetically altered volcanic and volcaniclastic materials in the Atlantic and Gulf Coastal Plains (Heron, 1969; Reynolds, 1970; and others).

FORMATION DESCRIPTIONS

Cape Fear Formation

The Cape Fear Formation overlies the basalt and contains unconsolidated interbedded clay and sand. The lower 13 m (42 ft) is composed primarily of red or brown clay and less common feldspathic sand and has a basal unit of muddy conglomeratic sand. The clay is typically silty, noncalcareous, and unfossiliferous, and contains a trace of mica and pyrite. The clay has a knobby appearance and lacks primary sedimentary structures. Rare muddy feldspathic sand is interbedded with the nodular clay. The sand is massive, noncalcareous, and typically contains 10 to 20 percent feldspar.

The middle part (24 m, 80 ft) of the formation consists of thinly interbedded gray-olive silty clay and light-greenish-gray fine-grained sand. The sand contains abundant mica, and sparse shell fragments are found in both the sand and clay. The upper 22 m (72 ft) of the Cape Fear Formation is composed of knobby clay similar to that in the lower part of the formation. The upper clay is reddish-brown to yellowish-gray, noncalcareous, and micaceous.

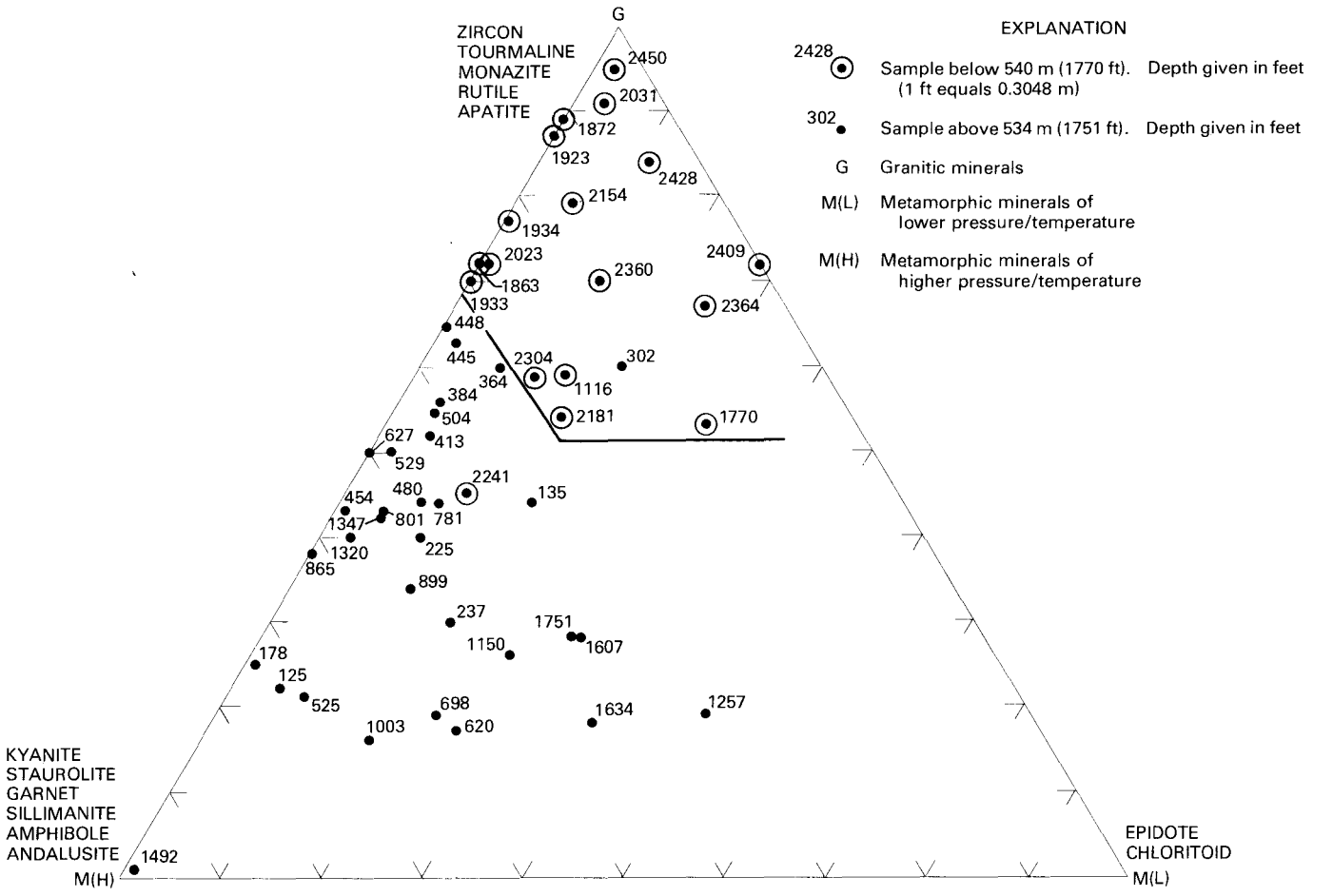

FIGURE 6.—Distribution of granitic, low-rank metamorphic, and high-rank metamorphic minerals in heavy-mineral suites of 57 core samples. Samples from above and below 540 m (1,770 ft) fall into two separate distinct fields.

Middendorf Formation

The Middendorf Formation is a thick sequence of feldspathic sand, clayey silt, and sandy and silty clay. The clay is typically pale red or reddish brown, or it may be red and gray green mottled. The fine-grained deposits are noncalcareous, micaceous, and lack primary sedimentary structures. The sand is poorly sorted, feldspathic, and noncalcareous. Typical colors for the sand are mottled combinations of red, reddish brown, and gray green. The sand is fine to coarse grained, and thin quartz-pebble-rich conglomeratic sand is common. Horizontal and inclined bedding are common in the sand. The clay, silt, sand, and conglomeratic sand are arranged in 1- to 5-m-thick (3–15–ft) fining-upward cycles. The cycles tend to be better defined and more complete in the upper half of the formation than in the lower half.

Black Creek Formation

The Black Creek Formation is the most heterogeneous of the Upper Cretaceous formations in the core. Abundant fossiliferous silty clay, muddy sand, and clean sand alternate in 15- to 46-m-thick (50–150 ft) sequences with thinly interbedded sand and clay and less common shelly limestone.

The silty clay and muddy sand are typically medium-gray or gray-green, calcareous, fossiliferous sediments that resemble similar sediment types in the overlying Peedee Formation. Quartz sand and silt constitute as much as 50 to 60 percent of the coarser grained beds, and calcium carbonate content reaches a maximum of 40 percent. Macrofossil shells and shell fragments and microfossil tests vary from sparse to very abundant. Unusually heavy concentrations of shells are preserved in impure, shelly limestone. Minor constituents of the mud and muddy sand are glauconite, phosphate, mica, and pyrite. Physical sedimentary structures are rare in the muddy sediments, probably because of extensive bioturbation.

Light-colored, feldspathic, quartz silt and fine sand are interbedded with dark-gray clay near the base

of the Black Creek. Bedding in this basal unit is planar, wavy, or discontinuous on a 1–10-mm scale. The clay contains as much as 20 percent black carbonaceous debris.

Well-sorted, calcareous quartz sand is found at the top of the Black Creek. Core recovery is poor in this interval, but relatively clean, poorly consolidated, very fine to fine-grained quartz sand was collected throughout the interval.

Peedee Formation

The Peedee Formation is a thick sequence of calcareous muddy sand and calcareous mud. The lower half of the formation is dominantly medium-gray to olive-gray fossiliferous muddy sand. The sand typically contains 50 to 60 percent fine- to medium-grained quartz sand, 30 to 40 percent clay and silt, and 10 to 20 percent whole macrofossils, shell fragments, and microfossils. Trace amounts to a few percent of sand-sized glauconite, phosphate, and mica are also present. The acid-soluble fraction consists almost entirely of fossils, although calcite-cemented nodules and layers do exist. The upper half of the formation is composed of medium-gray to olive-gray, silty or sandy calcareous clay. These beds are dominantly silty clay but may contain as much as 20 to 25 percent quartz sand and abundant macrofossils and microfossils. Glauconite, pyrite, phosphate, and mica are accessory constituents. Calcium carbonate content varies from 10 to 40 percent and represents both fossils and calcite cement.

Physical sedimentary structures are rare in the Peedee and are restricted to thin intervals of wavy or disrupted laminations or thin beds. Biogenic sedimentary structures, including distinct burrows and bioturbated fabric, typify the poorly sorted Peedee sediments.

Beaufort(?) Formation

The Beaufort(?) Formation is primarily composed of medium-gray-green silty clay above a basal unit of nodular muddy sand. The dominant sediment type is a yellowish-gray to greenish-gray, moderately calcareous silty clay or locally sandy clay. Calcium carbonate averages 10 to 20 percent and is contained almost exclusively in microfossil tests. Accessory constituents include sand-sized glauconite, carbonized woody material, and pyrite. Physical sedimentary structures include planar, wavy, and disrupted laminae and thin bedding, and micrograded silt and fine sand. The bedding is typically disrupted or obliterated by burrows.

The basal 11 m (37 ft) of the formation consists of gray-green to light-gray glauconitic muddy sand containing an abundant microfauna. If physical sedimentary structures were originally present in this interval, they have been obliterated by intense bioturbation. Calcite-cemented nodules averaging 60 to 80 percent calcium carbonate are common throughout; sediment between the nodules averages 15 to 25 percent calcium carbonate.

Black Mingo Formation

The Black Mingo is the most heterogeneous of the Tertiary formations recovered in the core. Much of the middle and lower part of the formation is gray-green bioturbated silty clay and muddy sand similar to those of the underlying Beaufort(?) and Peedee Formations. The uppermost 7 m (22 ft) of the formation is light-colored, fine-grained, impure limestone similar to the limestone in the upper part of the overlying Santee Limestone.

Other sediment types in the Black Mingo are thinly interbedded sand and clay and less common quartzose shelly limestone. The interbedded sand and clay form a regularly alternating sequence of olive-gray silty clay that often contains abundant wood fragments, and light-colored, fine-grained, slightly calcareous quartz sand or shelly limestone. Stratification is typically in the form of flaser and lenticular beds that are disrupted by vertical and horizontal burrows. The shelly limestone is 0.3–1 m (1–3 ft) thick, and is typically composed of oyster and other pelecypod valves and fine- to medium-grained quartz sand.

Santee Limestone

The Santee Limestone is herein divided into three informal lithologic units: a lower bryozoan-pelecypod sand, 11 m (35 ft) thick; a middle shelly limestone, 7 m (23 ft) thick; and an upper fine-grained limestone, 38 m (125 ft) thick. The basal part of the Santee consists of porous bryozoan-pelecypod sand. Calcium carbonate averages 60 to 80 percent; the remainder of the unit is composed of quartz and sand-sized glauconite and phosphate. Sedimentary structures are restricted to inclined bedding, probably representing crossbedding, and to local concentrations of the noncarbonate fraction that may represent burrows.

The middle part of the formation is composed of yellowish-gray glauconitic, quartzose fossiliferous limestone. These rocks average 60 to 70 percent calcium carbonate. Whole shells and valves of pelecy-

pods plus foraminifers and ostracode shells dominate the fauna.

The upper unit resembles similar sediments in the overlying Cooper Formation but is a pale yellowish gray rather than the more greenish gray of the Cooper sediments. This unit is composed primarily of microfossil tests and fine quartz sand, with minor glauconite and clay minerals. Calcium carbonate averages 40 to 60 percent. Hard cemented nodules and occasional burrows are present in the fine-grained limestone.

Cooper Formation

The Cooper Formation is a monotonous sequence of impure limestone. The amount of calcium carbonate ranges from 60 to 75 percent. Minor lithologic components include quartz sand (5–25 percent), glauconite (1–10 percent), phosphatic sand and pebbles (1–5 percent), bone material (1–5 percent), pelecypod shell hash (1–5 percent), mica (1 percent), and clay minerals (10–30 percent). Subtle differences in the abundance of these components result in the variability observed in the Cooper sediments. Colors of the sediment vary from moderate or pale greenish or yellowish gray to olive brown and pale olive. Grain-size analysis indicates that most of the Cooper is made up of sand-sized foraminiferal tests (40–70 percent).

Physical sedimentary structures are rare in the Cooper and are restricted to thin wavy laminae. The Cooper sediments are either thoroughly bioturbated or contain distinct burrows.

DEPOSITIONAL HISTORY

From the preliminary study of the core sediments, generalized depositional paleoenvironments may be assigned to the formations in the core (fig. 7). In figure 7, the terms "continental," "marginal marine," "inner shelf," and "middle to outer shelf" are each used to represent a spectrum of specific related paleoenvironments. The term "continental" potentially represents both fluvial sediments and residual materials. Marginal marine sediments accumulated in estuarine, lagoonal, tidal-flat, or barrier-system environments. Inner- and middle- to outer-shelf sediments were deposited on the marine shelf at various distances from the shoreline and under various energy regimes.

Unfossiliferous reddish clay and coarse-grained feldspathic sand in the Cape Fear and Middendorf Formations are assigned to the continental environment. Rare fossiliferous clay in the Middendorf and

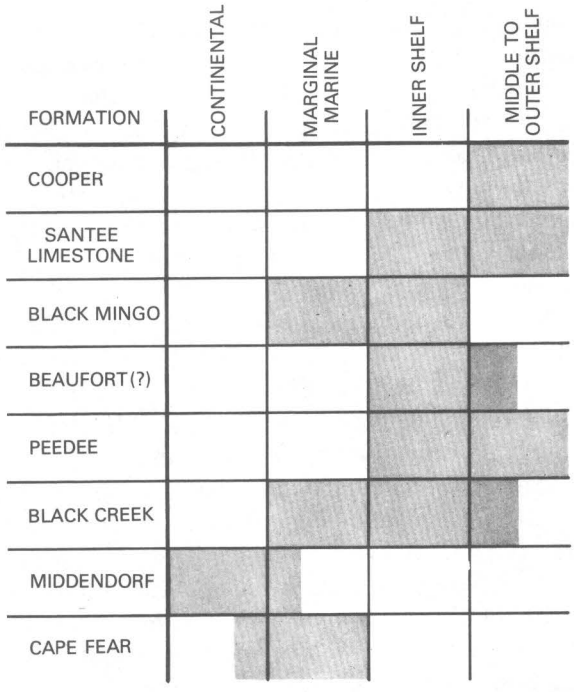

FIGURE 7.—Generalized paleoenvironments represented by Cretaceous and Tertiary sediments of the Clubhouse Crossroads core.

fossiliferous thinly interbedded sand and dark clay in the Cape Fear indicate a marginal marine setting for those specific beds. The heterogeneous Black Creek Formation represents a cyclic alternation of poorly sorted marine deposits and marginal marine beds including shelly or well-sorted sand and dark clay. The more homogeneous Peedee Formation contains sandy and silty marine clay that may also be present in cyclic units.

The large-scale sequence of paleoenvironments found in the Upper Cretaceous sediments of the Clubhouse Crossroads core is superficially similar to that described by Swift, Heron, and Dill (Swift and Heron, 1969; Swift, Heron, and Dill, 1969) for sediments in the Cretaceous outcrop belt of North and South Carolina. These authors described a vertical sequence composed of thin basal estuarine? sediments (Cape Fear), then fluvial sediments (Middendorf), estuarine sediments (Black Creek), and neritic sediments (Peedee). In general, a large-scale transgressive sequence (Middendorf, Black Creek, Peedee) is indicated.

The temporal distribution of sediments in the Clubhouse Crossroads core does not readily support the model of Swift, Heron, and Dill (1969). In the Clubhouse Crossroads core, most or all of the fluvial facies (Middendorf) is restricted to the Woodbinian

and lower Eaglefordian and is separated by a considerable period of time from the upper Austinian and younger estuarine and neritic facies (Black Creek and Peedee). Time transgression of facies is implicit in a transgressive sedimentary sequence. However, large time gaps should not exist in a vertical sedimentary sequence produced by transgressing lithosomes of a single horizontal facies sequence.

The repetition of coarse- and fine-grained units in the Black Creek and Peedee Formations on a scale of 15–46 m (50–150 ft) is similar to that shown by cyclic units in the Cretaceous section of New Jersey described by Owens and Sohl (1969). Such transgressive-regressive cycles are on a smaller scale than the single transgression described by Swift, Heron, and Dill (1969) and would require more frequent shifts of the shoreline and of paleoenvironments. These two concepts may possibly be reconciled, at least for the Black Creek and Peedee, if the smaller cycles are considered second-order features superimposed on a generally transgressive upper Austinian to Navarroan sequence. In such a setting, environmental shifts within each of the smaller cycles may have been only of limited magnitude. Environmental shifts within Black Creek cycles would have involved marginal marine and marine lithotopes, whereas Peedee cycles would have involved only marine deposits of the outer, middle, and inner shelf.

The fine-grained microfossiliferous Beaufort(?) Formation represents an open marine environment, whereas cyclic deposits in the Black Mingo Formation include marine and marginal marine beds and represent a large-scale Tertiary regressive sequence. Fine-grained limestones of the Santee Limestone and Cooper Formation are monotonous bioturbated marine deposits. Skeletal limestone in the Santee does not appear to be a part of a peritidal facies mosaic and is also assigned a marine (subtidal) origin.

Pooser (1965), Colquhoun and Johnson (1968), Inden and Zupan (1976), and others have assigned Tertiary sediments in South Carolina to a wide range of marine and nonmarine environments. Their studies are based primarily upon surface and subsurface data from the updip outcrop belt. Predictably, the more downdip location of the Clubhouse Crossroads core is reflected in the dominantly marine nature of the Tertiary sediments in the core.

REFERENCES CITED

Brown, P. M., 1958, Well logs from the Coastal Plain of North Carolina: North Carolina Div. Mineral Resources Bull. 72, 68 p.

——— 1959, Geology and ground-water resources in the Greenville area, North Carolina: North Carolina Div. Mineral Resources Bull. 73, 87 p.

Colquhoun, D. J., and Johnson, H. S., Jr., 1968, Tertiary sea-level fluctuations in South Carolina, *in* Tanner, W. F., ed., Tertiary sea-level fluctuations: Paleogeography, Paleoclimatology, Paleoecology, v. 5, no. 1, p. 105–126.

Cooke, C. W., 1936, Geology of the Coastal Plain of South Carolina: U.S. Geol. Survey Bull. 867, 196 p.

Heron, S. D., Jr., 1969, Mineralogy of the Black Mingo mudrocks: South Carolina Div. Geology, Geol. Notes, v. 13, no. 1, p. 27–41.

Inden, R. F., and Zupan, Alan-Jon W., 1976, Facies and facies equivalents of the Santee Limestone (Lower Tertiary) in South Carolina: Geol. Soc. America Abs. with Programs, v. 8, no. 2, p. 204–205.

Malde, H. E., 1959, Geology of the Charleston phosphate area, South Carolina: U.S. Geol. Survey Bull. 1079, 105 p.

Owens, J. P., and Sohl, N. F., 1969, Shelf and deltaic paleoenvironments in the Cretaceous-Tertiary formations of the New Jersey Coastal Plain, *in* Subitzky, Seymour, ed., Geology of selected areas in New Jersey and eastern Pennsylvania and guidebook of excursions: New Brunswick, N.J., Rutgers Univ. Press, p. 235–278.

Pooser, W. K., 1965, Biostratigraphy of Cenozoic ostracoda from South Carolina: Kansas Univ. Paleont. Contr., Arthropoda, art. 8, p. 1–80.

Reynolds, W. R., 1970, Mineralogy and stratigraphy of Lower Tertiary clays and claystones of Alabama, *in* Symposium on environmental aspects of clay minerals: Jour. Sed. Petrology, v. 40, no. 3, p. 829–838.

Rhodehamel, E. C., 1975, Geophysical logs from a geologic test hole near Charleston, South Carolina: U.S. Geol. Survey open-file report 75–247, 1 p.

Siple, G. E., 1975, Ground-water resources of Orangeburg County, South Carolina: South Carolina Div. Geology Bull. 36, 59 p.

Swift, D. J. P., and Heron, S. D., Jr., 1969, Stratigraphy of the Carolina Cretaceous: Southeastern Geology, v. 10, no. 4, p. 201–245.

Swift, D. J. P., Heron, S. D., Jr., and Dill, C. E., Jr., 1969, The Carolina Cretaceous—Petrographic reconnaissance of a graded shelf: Jour. Sed. Petrology, v. 39, no. 1, p. 18–33.

Biostratigraphy of the Deep Corehole (Clubhouse Crossroads Corehole 1) Near Charleston, South Carolina,

By J. E. HAZEL, L. M. BYBELL, R. A. CHRISTOPHER, N. O. FREDERIKSEN, F. E. MAY, D. M. McLEAN, R. Z. POORE, C. C. SMITH, N. F. SOHL, P. C. VALENTINE, and R. J. WITMER

STUDIES RELATED TO THE CHARLESTON, SOUTH CAROLINA, EARTHQUAKE OF 1886–A PRELIMINARY REPORT

GEOLOGICAL SURVEY PROFESSIONAL PAPER 1028-F

CONTENTS

ILLUSTRATIONS

TABLES

STUDIES RELATED TO THE CHARLESTON, SOUTH CAROLINA, EARTHQUAKE OF 1886—
A PRELIMINARY REPORT

BIOSTRATIGRAPHY OF THE DEEP COREHOLE (CLUBHOUSE CROSSROADS COREHOLE 1) NEAR CHARLESTON, SOUTH CAROLINA

By J. E. HAZEL, L. M. BYBELL, R. A. CHRISTOPHER, N. O. FREDERICKSEN, F. E. MAY, D. M. MCLEAN, R. Z. POORE, C. C. SMITH, N. F. SOHL, P. C. VALENTINE, and R. J. WITMER

ABSTRACT

Microfossils (calcareous nannoplankton, dinoflagellates, foraminifers, ostracodes, and sporomorphs) and mollusks have been used to date the sedimentary part of a 792–m (2,599–ft) core from a test hole (Clubhouse Crossroads corehole 1) drilled 40 km (25 mi) west-northwest of Charleston, S.C. The sedimentary section is 750 m (2,462 ft) thick and is of Late Cretaceous and (except for a few meters of probable Pleistocene) early Tertiary age. The drillhole bottomed in amygdaloidal basalt of Cretaceous(?) age.

The Cretaceous section is composed almost entirely of clastic sediments. The oldest Cretaceous sedimentary unit is the Cape Fear Formation which contains Cenomanian (Woodbinian) fossils. The Middendorf Formation overlies the Cape Fear. Rare fossils in the Middendorf indicate a Cenomanian (lower Eaglefordian) placement. No fossils suggestive of a Turonian or Coniacian Age (middle Eaglefordian to early Austinian) were found. The overlying Black Creek Formation is of probable late Santonian and early Campanian Age (late Austinian and early Tayloran). The youngest Cretaceous unit is the Peedee Formation. The Peedee contains assemblages indicative of a late Campanian to middle Maestrichtian Age (late Tayloran and Navarroan). The Cretaceous-Tertiary boundary is at 244 m (800 ft).

The oldest Tertiary unit is the Beaufort(?) Formation, the clays and sands of which contain early Paleocene assemblages (Danian; early and middle Midwayan). Overlying the Beaufort(?) are clayey sands and sandy clays assigned to the Black Mingo Formation. This unit is of Paleocene and early Eocene age (Thanetian and Ypresian; late Midwayan and Sabinian). The overlying Santee Limestone is of middle and late Eocene age (late Lutetian and Bartonian; late Claibornian and Jacksonian). The youngest Tertiary formation present is the Cooper Formation. The lower part of the Cooper is late Eocene (Bartonian; Jacksonian). The upper part, however, is of late Oligocene age (Chattian; Chickasawhayan). Both the Cooper and the Santee are dominantly carbonate.

The biostratigraphy is summarized as follows:

Formation	*Thickness* (m)	*Age*
	5	Pleistocene(?).
Cooper	64	Chattian and Bartonian.
Santee	56	Bartonian and Lutetian.
Black Mingo	67	Ypresian and Thanetian.
Beaufort(?)	52	Danian.
Peedee	164	Maestrichtian and Campanian.
Black Creek	159	Campanian and Santonian(?).
Middendorf	124	Cenomanian.
Cape Fear	59	Cenomanian.

Palynomorphs, foraminifers, and ostracodes were studied from both the Cretaceous and Tertiary parts of the core. Mollusks have been examined from only the Cretaceous part, and calcareous nannofossils from only the Tertiary.

INTRODUCTION

The sedimentary rocks of a 792-m (2,599-ft) core from the Clubhouse Crossroads corehole 1 (CCC 1) in Dorchester County, S.C., (fig. 1) have been examined for micro- and macrofossils. Most of the core is 15 cm (6 in.) in diameter for approximately the upper 225 m (738 ft) and 7 cm (2.75 in.) in diameter for the remaining 567 m (1,861 ft). The following groups have been studied in some detail: calcareous nannofossils (by Bybell), dinoflagellates (by May, McLean, and Witmer), mollusks (by Sohl), ostracodes (by Hazel and Valentine), planktic foraminifers (by Poore and Smith), and sporomorphs (by Christopher and Frederiksen). Other calcareous forms are rare or absent, and no siliceous microfossils were observed.

In this paper, the lithostratigraphic units delineated in the core are dated paleontologically, assigned to commonly used provincial and international stages, and correlated with other lithostratigraphic units in the Atlantic and Gulf Coastal Province. In-

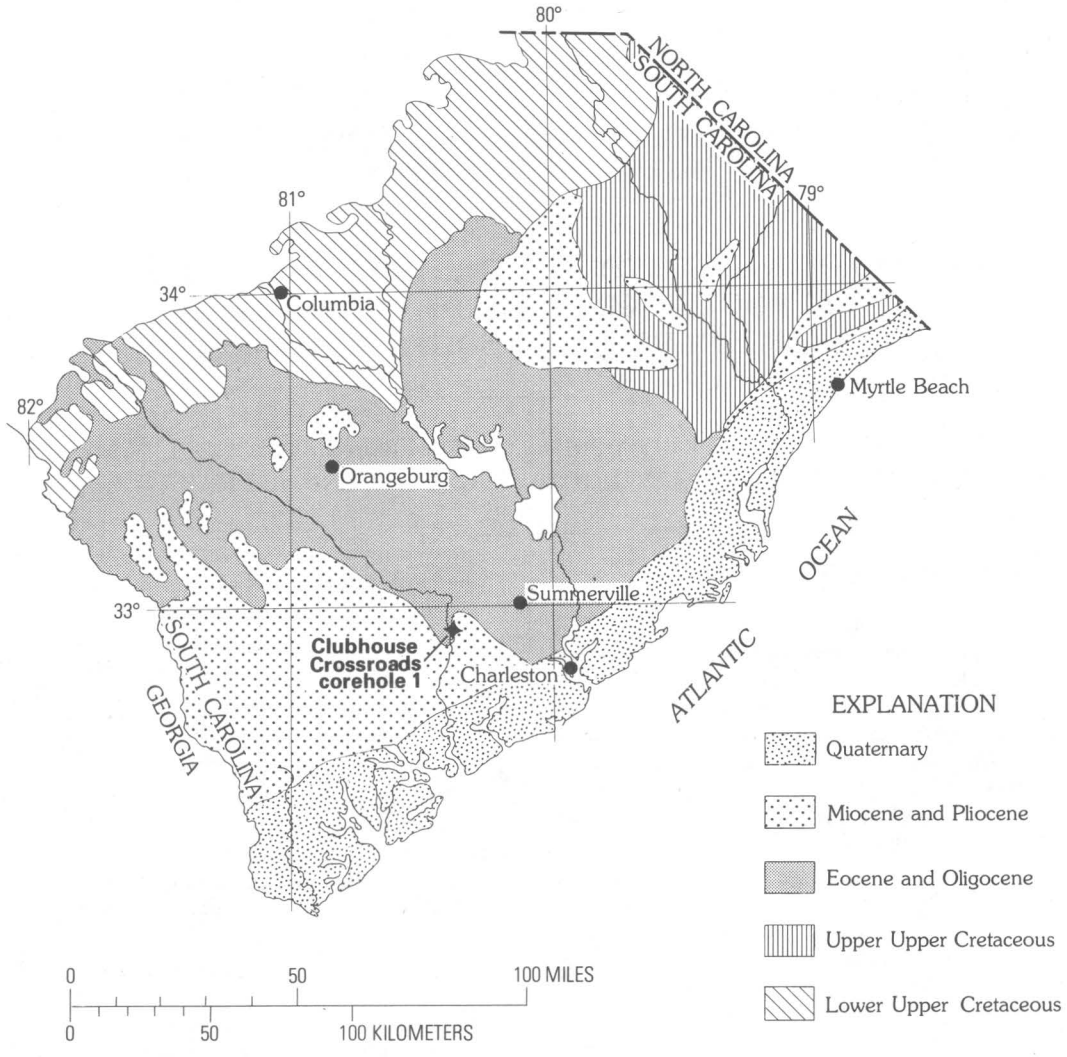

FIGURE 1.—Generalized geologic map of South Carolina showing location of the Clubhouse Crossroads corehole 1. The exact site is in the Cottageville, 1943, 15′ quadrangle, at lat 32°53.25′ N., long 80°21.4′ W., 3.5 km (2.2 mi) southwest of Clubhouse Crossroads and 40 km (25 mi) west-northwest of Charleston, S.C. Geology modified from Cooke (1936).

terpretations as to environment of deposition are also presented. Most of the studies are still incomplete at this writing, and investigations are continuing. We are confident of the age assignments of most of the beds seen in the core, but some assignments are tentative, and examination of additional samples in some intervals will be needed to document more precisely both zone and stage boundaries. At present, paleoenvironmental conclusions are very generalized and quite tentative.

This paper is divided into two parts—in the first part, our interpretations are presented on biostratigraphy and paleoenvironment of the core; in the second part are short discussions on the occurrence, value, and degree of study of the six biologic groups used.

Without the excellent technical support of many persons, this report could not have been prepared in the time allotted. Ellen E. Compton, Diane V. McNeave, W. A. Bryant, and Patricia B. Swain of the U.S. Geological Survey deserve special mention for their efforts.

This study was funded in part by the U.S. Nuclear Regulatory Commission, Office of Nuclear Regulatory Research, under agreement number AT (49–25)–1000.

BIOSTRATIGRAPHY

STAGE PLACEMENT

Figure 2 is a generalized lithologic log of the core showing the spontaneous potential and resistivity curves and the formations recognized. The lithologies present are discussed in some detail by Gohn and others in this volume. Except for the upper 5 m (16 ft) of unconsolidated Pleistocene(?) sediments, the core is entirely of Paleogene and Late Cretaceous age. Below the Pleistocene(?) to a depth of 137 m (449 ft), the deposits are dominantly carbonate.

The lowermost sedimentary rocks, present in the core above 13 m (43 ft) of mottled red clay which perhaps represents weathering of the underlying basalt, extend from 750 m (2,462 ft) to about 691 m (2,268 ft) and are assigned to the Cape Fear Formation. Rare late Cenomanian planktic foraminifers are present in the Cape Fear, and pollen in the unit suggests a Woodbinian assignment. The Woodbinian is placed in the middle Cenomanian by Pessagno (1969).

Beds assigned to the Middendorf Formation are present between about 691 m (2,268 ft) and 567 m (1,860 ft). These beds are largely unfossiliferous; however, planktic foraminifers of the *Rotalipora cushmani–R. greenhornensis* Subzone of late Cenomanian Age (early Eaglefordian) are present at 586 m (1,923 ft). This indicates that the unfossiliferous interval between 586 and 560 m (1,923–1,837 ft), including whatever disconformities that may be present, represents the Turonian and Coniacian Stages, or in provincial terms, the middle and upper Eaglefordian and most, if not all, of the lower Austinian. According to the time scale of van Hinte (1976), this interval would approximate 11 million years. An erosional disconformity probably is present in this 26-m (85-ft) interval, although the paleontological data do not indicate definitely whether this presumed disconformity is between the Middendorf and Black Creek Formations or within the Middendorf. Heavy-mineral data (Gohn and others, this volume) suggest that it is at the base of the Black Creek Formation.

The sands and clays between 567 and 408 m (1,860–1,340 ft) are assigned to the Black Creek Formation. The fauna and flora of the Black Creek in the core indicate that the unit is of questionable Santonian to Campanian Age and is referable to the upper part of the Austinian and lower part of the Tayloran Provincial Stages. No diagnostic fossils have been found in the lower 7 m (23 ft) of the Black Creek. The interval from about 560 to 533 m

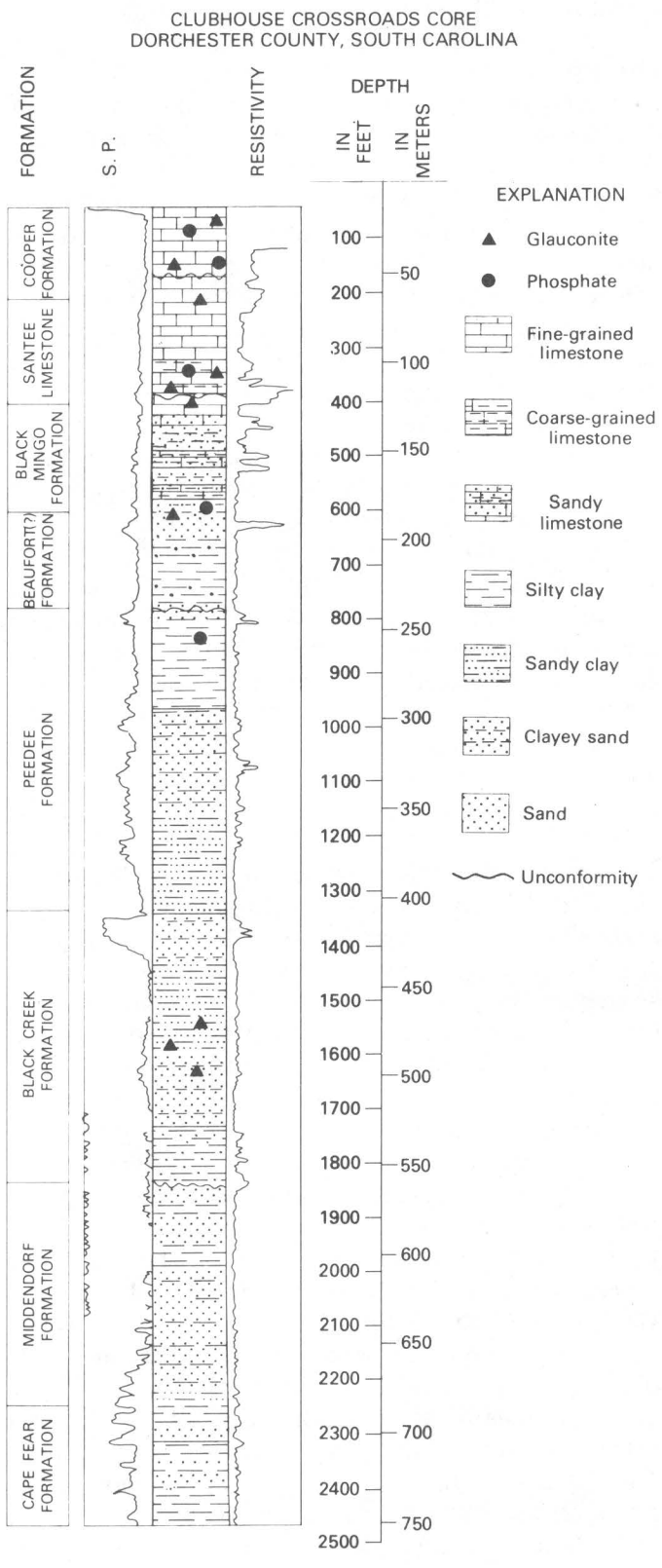

FIGURE 2.—Stratigraphic column for the Clubhouse Crossroads core. Spontaneous potential (S.P.) and resistivity logs are also shown.

(1,837–1,749 ft) contains mollusks, ostracodes, and pollen of early late Austinian Age, which may be Santonian (Pessagno, 1969) or early Campanian (Young, 1963) in age. The Austinian–Tayloran boundary in the core is between 522 and 473 m (1,713–1,552 ft). Foraminifer data suggest that this provincial stage boundary should be placed in the lower part of this interval, between 522 and 487 m (1,713–1,598 ft). Ostracode data, on the other hand, suggest that the stage boundary is at about 480 m (1,575 ft). For the purposes of this paper, the last depth is tentatively accepted, with the realization that the Austinian–Tayloran boundary may ultimately be revised downward in the core (but almost certainly not upward).

The uppermost Cretaceous lithostratigraphic unit recognized in the core is the Peedee Formation; it is represented by sandy clays and clayey sands within the interval between 408 and 244 m (1,340–800 ft). The lower beds of the Peedee from between 408 and 335 m (1,340–1,100 ft) are Tayloran on the basis of both benthic macrofaunas and benthic and planktic microfaunas. The mollusks, foraminifers, ostracodes, dinoflagellates, and sporomorphs of the 335- to 244-m (1,100- to 800-ft) interval indicate that these beds are Navarroan. The Campanian-Maestrichtian boundary is at about 335 m (1,100 ft). According to Pessagno (1969), the Campanian–Maestrichtian and provincial Tayloran–Navarroan Stage boundaries are coincident. This assignment is followed herein, although this practice is not accepted by many workers, and more research on the problem is called for. The more argillaceous upper part of the formation from between 296 and 281 m (971–922 ft) to 244 m (800 ft) is of middle Maestrichtian age as determined by planktic foraminifers, and is assignable to the *Globotruncana gansseri* Subzone of Pessagno (1969).

Overlying the Peedee is a silty- to sandy-claystone unit not known from outcrops in the area of the Clubhouse Crossroads core. Beds of the same age do crop out to the northeast on the Black River near Georgetown, S.C. The unit is at least biostratigraphically equivalent in part to and is here questionably referred to the Beaufort Formation of North Carolina (see Gohn and others, this volume). The stratigraphic interval between 244 and 192 m (800–630 ft) is of Danian Age. The upper part, from about 213 m (700 ft) to 192 m (630 ft), is in the P 2 planktic foraminifer zone, and the lower part is in the P 1 zone.

The Black Mingo Formation overlies the Beaufort(?) Formation and is present from 192 to 125 m (630–410 ft). The unit consists mostly of clayey sands and sandy clays; sandy limestone beds are in the middle and at the top of the formation. The base of the Sabinian Stage is at 180 m (590 ft); thus, the lower 12 m (40 ft) of the Black Mingo, as identified in the core, is of Midwayan Age. Above this, from 180 m to about 132 m (590–433 ft), the Black Mingo is late Paleocene in age (Thanetian). The upper beds of the Black Mingo, at least from 132 to 125 m (433–410 ft), are lower Eocene (Ypresian and upper Sabinian). The upper bed of the Black Mingo can be placed in the NP 12 nannoplankton zone, which is the middle zone of the Ypresian (Berggren, 1972). An unconformity between the Black Mingo and the Santee Limestone seems to represent the upper Ypresian and the lower Lutetian.

The Santee Limestone is present from 125 to 69 m (410–227 ft) in the core. The lower part of the Santee, from 125 to 102 m (410–336 ft), is of late Lutetian Age (NP 16–17) and is correlative with upper Claibornian formations in the Gulf Coast (Bybell, 1975). Nannofossils suggest that the middle Eocene–late Eocene boundary (Lutetian–Bartonian) is between 104 and 101 m (341–331 ft) in the core. This age assignment is consistent with ostracode data that suggest that the Claibornian–Jacksonian boundary is between 110 and 95 m (361–312 ft). The boundary is placed at 102 m (336 ft) in the core, at a point where the resistivity increases markedly. The interval between 104 and 82 m (341–269 ft) can be placed in the upper Eocene nannofossil zones NP 18 or NP 19, which are approximately equivalent to P 15 and P 16 in the planktic foraminifer zonation of Blow (1969) (see Berggren, 1972, p. 203).

The contact between the lower part of the Cooper Formation and the underlying Santee Limestone is quite sharp. The upper beds of the Santee are extensively bored, and the borings are filled by glauconitic calcareous sediment of the lower part of the Cooper. Phosphate pebbles are concentrated near the boundary; some pebbles are as much as 3 cm (1.2 in) in diameter. The beds above and below this contact are upper Eocene (Bartonian and Jacksonian), however, and both are placed in nannofossil zone NP 20.

The Cooper Formation, as that term has been used in South Carolina (for example, Pooser, 1965; Sanders, 1974), is present from 69 to 5 m (227–16 ft) and contains beds of late Eocene and Oligocene age. At least in the area of the Clubhouse Crossroads core, the contact between the Eocene and Oligocene

parts of the Cooper is an unconformity representing the lower Oligocene (Lattorfian and Rupelian Stages), a duration of approximately 5 million to 6 million years (Berggren, 1972). This indicates that the lower part of the Cooper is part of a separate depositional cycle, even though the lithologies of the upper and lower parts perhaps cannot be consistently differentiated in the field without fossil control.

The Cooper Formation present between 69 and 55 m (227–180 ft) is of late Eocene age on the basis of its planktic flora and fauna. Ostracodes suggest assignment to the Jacksonian Provincial Stage. The upper 50 m (164 ft) of the Cooper from a depth of 55 to 5 m (180–16 ft) is of Oligocene age. Ostracodes, particularly, suggest the presence of at least upper Vicksburgian sediments, and the Vicksburgian–Chickasawhayan boundary is placed at about 35 m (115 ft) depth. However, calcareous nannoplankton zones NP 21, 22, and 23 (see Martini, 1971) are seemingly absent; all of the Cooper above 55 m (180 ft) is referable to NP 24, therefore, suggesting that the entire upper part of the Cooper is Chickasawhayan and upper Chattian. However, foraminifers questionably indicating planktic foraminifer zone P 20 are present at 52 m (171 ft), and P 20 is considered indicative of the lower Chattian and equates with the upper part of nannoplankton zone NP 23 according to Berggren (1972). Thus, the nannoplankton, ostracode, and planktic foraminifer data are not compatible, although the apparent age disagreement is comparatively slight. The problem probably is in the correlation of the ostracode range zones with the nannoplankton (NP) and planktic foraminifer (P) zones. Data from all three groups do indicate that most, if not all, of the lower Oligocene is missing.

For the purposes of this paper, the upper part of the Cooper Formation (above 55 m; 180 ft) is considered to be late Vicksburgian and Chickasawhayan in age, and foraminifer zone P 20 is placed in the lower Chattian (and upper Vicksburgian), which was suggested as a possibility by Berggren (1972, fig. 3). Thus, the entire Oligocene part of the Cooper is considered to be Chattian.

CORRELATION

Figure 3 is a generalized chart showing our conclusions as to correlation of the units of the Clubhouse Crossroads core with outcropping lithostratigraphic units in the Atlantic and Gulf Coastal Plains. The figure is self-explanatory, but some comments are appropriate. Note that several of the lithostratigraphic units of the Carolinas approach stage magnitude in temporal extent. Note also the significant segments of time that are not represented by sediments in the core or in the North Carolina outcrop.

PALEOENVIRONMENT

Incomplete studies of the fauna and flora of the Clubhouse Crossroads core lead to the following conclusions. The Cape Fear Formation represents inner sublittoral to brackish-water conditions of deposition (also see Swift and Heron, 1969). The Middendorf Formation was deposited under fluvial to marginal marine conditions. The lower part (Santonian?) of the Black Creek contains a nearshore possibly brackish-water assemblage, whereas the upper part was deposited at inner to middle sublittoral depths. The Peedee Formation was generally deposited in middle to outer sublittoral environments.

The lower part of the Beaufort(?) Formation was deposited at middle to outer sublittoral depths; the upper part was deposited in the inner to middle sublittoral zone. The lower part of the Black Mingo was deposited in the middle to inner sublittoral zone with considerable oscillation in the depth of deposition, but the upper part of the formation seems to represent outer sublittoral deposition. The lower part of the Santee Limestone probably represents middle to outer sublittoral depths. The upper part of the Santee and both the lower and upper parts of the Cooper Formation were deposited at outer sublittoral (outer shelf) or even greater depths.

TRANSGRESSIONS AND REGRESSIONS

Figure 4 is a generalized comparison of transgressive and regressive cycles in the northeast Texas and Mississippi embayments with those in the core and with those in other areas in the Atlantic Coastal Plain. The Clubhouse Crossroads core contains more major hiatuses, which represent regressions or periods of nondeposition. Otherwise, the curves for the Gulf Coast are generally similar to the curve for the core, except (1) in late Eaglefordian time, when there was regression in the eastern Gulf Coastal region and Atlantic Coastal region and transgression in the western Gulf Coastal region; and (2) in late Oligocene time, when apparently there was major transgression in the southern Atlantic Coastal region but minor regression in the Gulf Coastal region.

The Jacksonian and Chickasawhayan transgressions of the core did not take place in the Salisbury embayment of the Virginia–Maryland–Delaware re-

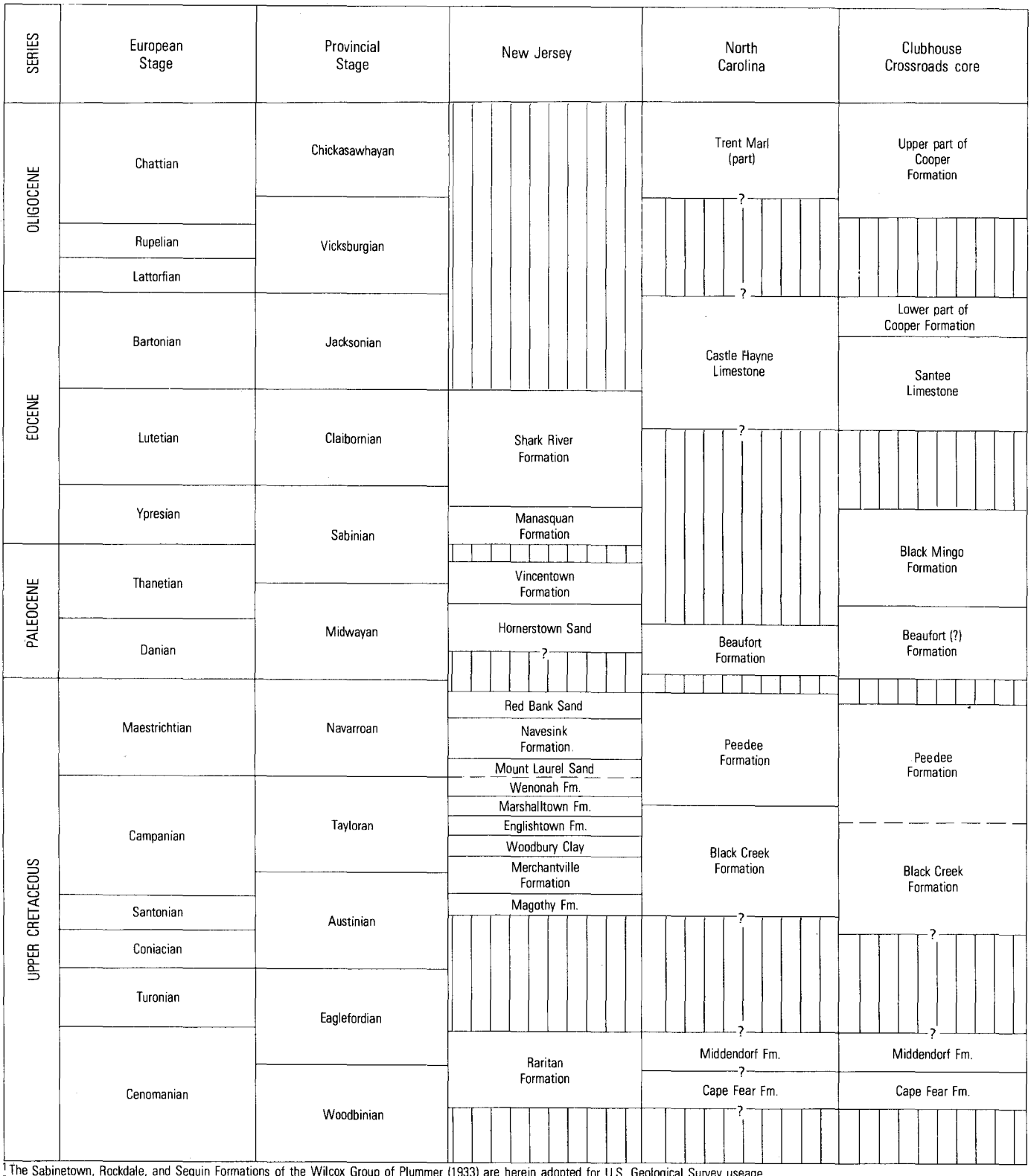

[1] The Sabinetown, Rockdale, and Seguin Formations of the Wilcox Group of Plummer (1933) are herein adopted for U.S. Geological Survey useage.
[2] The Bergstrom and Sprinkle Formations of Young (1965) are herein adopted for U.S. Geological Survey useage.

FIGURE 3.—Generalized correlation chart for the Upper Cretaceous and lower Tertiary of the Atlantic and Gulf Coastal Plains. The interpreted stratigraphic position of the formations of the Clubhouse Crossroads core is shown. The Cape Fear Formation at Clubhouse Crossroads is underlain by basalt which has yielded K–Ar whole-rock ages of 94.8 m.y. and 109 m.y. Gottfried and others (this volume) present arguments that these are probably minimum ages and that the basalt is most likely of Late Triassic or Early Jurassic age.

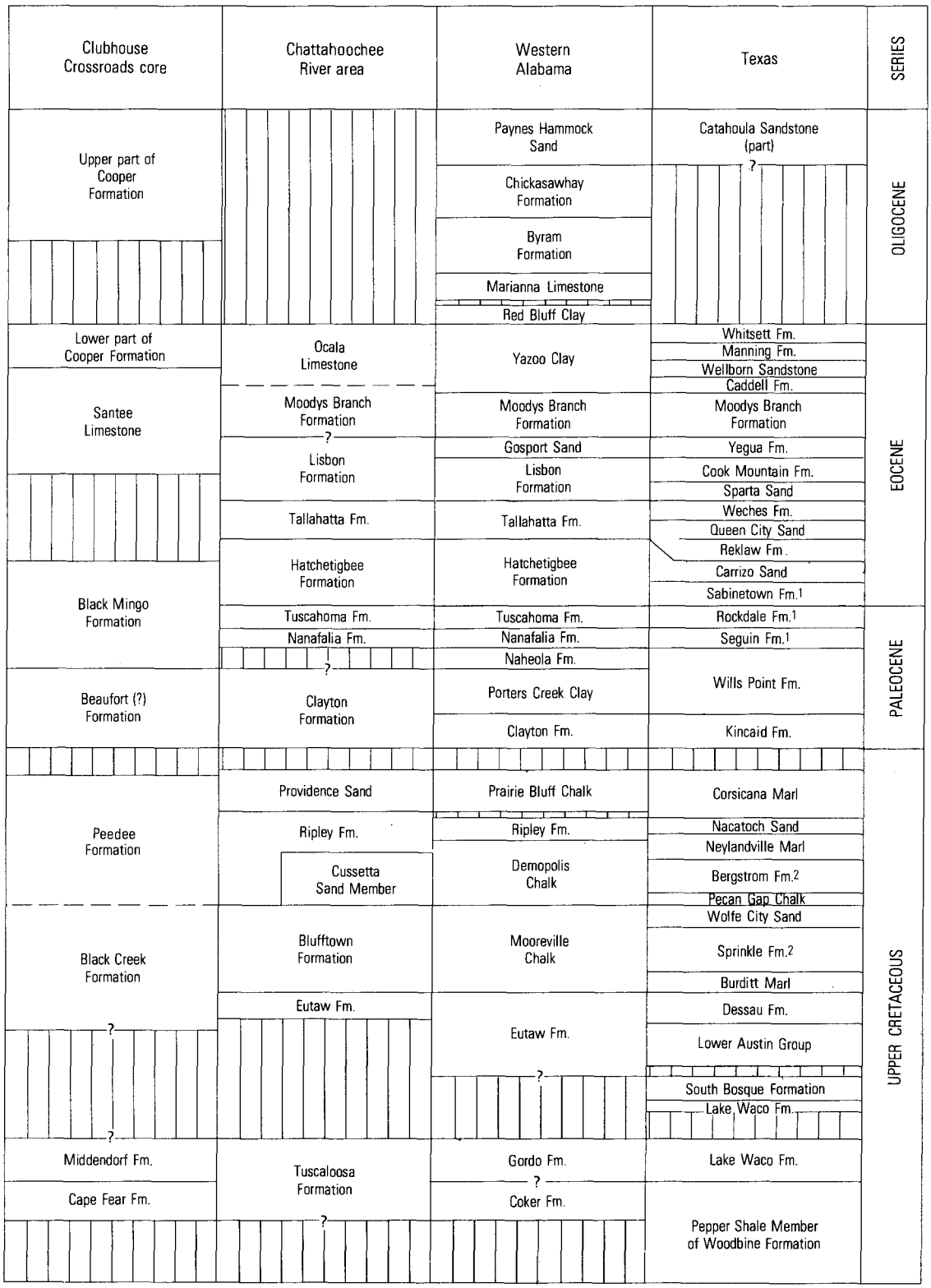

FIGURE 3.—Continued.

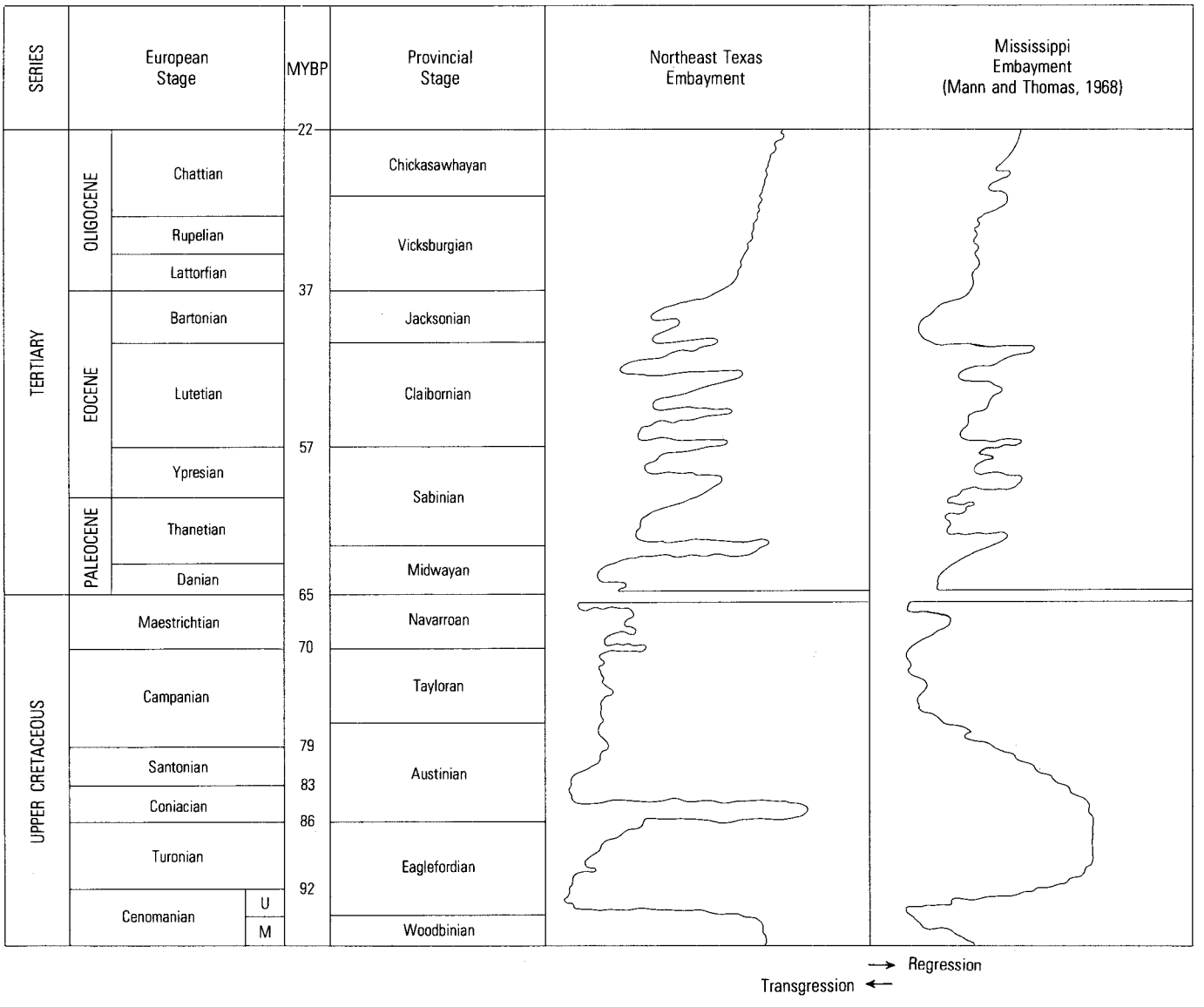

FIGURE 4.—Generalized transgressive and regressive cycles in the Gulf and Atlantic Coastal Plains.

gion or in the Raritan embayment of New Jersey. Published (Brown and others, 1972, plates 24, 27) and unpublished data indicate, however, that sediments deposited during the Chickasawhayan transgression are present as far north as the Richmond, Va., area.

RATES OF SEDIMENTATION

By use of the time scales recently published by Berggren (1972), Obradovich and Cobban (1975), and van Hinte (1976), the duration in millions of years (m.y.) for the provincial and European stages recognized in the study of the Clubhouse Crossroads core has been calculated. From these data, the rate of sedimentation per million years for each stage also can be calculated. However, because differences in compaction rates of the lithologies present have not been taken into consideration, the values can only be considered rough approximations. Table 1 lists the thickness, duration, and calculated sedimentation rate for each provincial stage, and table 2 gives the same data for each European stage. Missing section is taken into consideration. For example, the fossils suggest that only the upper Claibornian (upper Lutetian) is present; thus the sedimentation rate given, 7.7 m/m.y. (25 ft/m.y.), is based on 3.0 m.y. rather than on the 6.0-m.y. estimated duration of the Claibornian Stage (Berggren, 1972). Where significant parts of stages are represented by disconformities, the stages are divided into parts

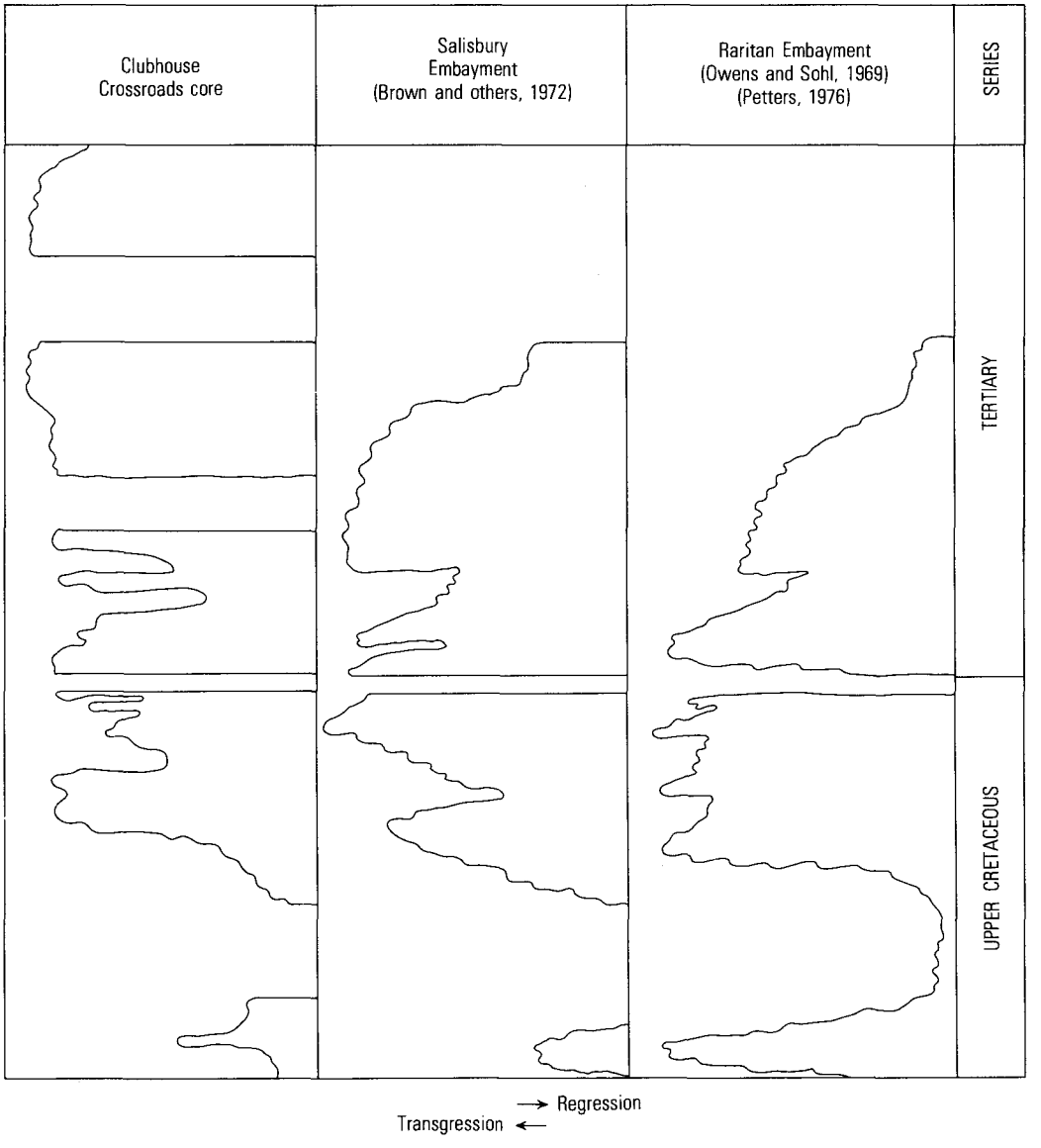

FIGURE 4.—Continued.

TABLE 1.—*The thickness, duration, and calculated sedimentation rate for each provincial stage represented in the Clubhouse Crossroads core*

Stage	Time represented (m.y.)	Thickness (m)	Rate (m/m.y.)
Chickasawhayan	6.0	30	5.0
Upper Vicksburgian	2.0	20	10.0
Lower Vicksburgian	0	0	---
Jacksonian	5.5	47	8.5
Upper Claibornian	3.0	23	7.7
Lower Claibornian	0	0	---
Sabinian	7.0	55	7.9
Midwayan	6.0	64	10.7
Navarroan	3.0	91	30.3
Tayloran	6.0	145	24.2
Upper Austinian	7.0	87	12.4
Lower Austinian	0	0	---
Middle and Upper Eaglefordian	0	0	---
Lower Eaglefordian	2.7	124	45.9
Woodbinian	2.7	59	21.9

TABLE 2.—*The thickness, duration, and calculated sedimentation rate for each European stage represented in the Clubhouse Crossroads core*

Stage	Time represented (m.y.)	Thickness (m)	Rate (m/m.y.)
Chattian	8.0	50	6.3
Rupelian	0	0	---
Lattorfian	0	0	---
Bartonian	5.5	47	8.5
Upper Lutetian	3.0	23	7.7
Lower Lutetian	0	0	---
Ypresian	2.5	12	4.8
Thanetian	6.5	55	8.5
Danian	4.0	52	13.0
Upper Maestrichtian	0	0	---
Lower and Middle Maestrichtian	3.0	91	30.3
Campanian	8.0	198	24.8
Santonian(?)	5.0	34	6.8
Coniacian	0	0	---
Turonian	0	0	---
Middle and Upper Cenomanian	5.4	183	33.9

(lower, middle, or upper) to reflect this in the tables.

The biostratigraphic assignment of the lithostratigraphic units of the core suggests that a rapid rate of clastic sedimentation during the Woodbinian and early Eaglefordian (middle and late Cenomanian) was followed by a regression resulting in the absence of middle and upper Eaglefordian and lower Austinian deposits (Turonian and Coniacian). After this event, the rate of clastic deposition increased throughout the remainder of the Cretaceous. The end of this period of marine deposition is marked by the unconformity at the Cretaceous–Tertiary boundary.

Rates of sedimentation were generally lower in the Tertiary. The sedimentation rate decreased during the Paleocene and early Eocene, culminating in an unconformity seemingly equivalent to the upper part of the Sabinian and the lower part of the Claibornian. The Paleocene and lower Eocene sediments, like the Cretaceous, are dominantly clastic. The remainder of the Tertiary was characterized by two episodes of carbonate deposition apparently separated by a regressive phase as evidenced by an unconformity representing the lower Oligocene.

FAUNA AND FLORA

As stated in the "Introduction," six fossil groups were studied—calcareous nannofossils, dinoflagellates, mollusks, ostracodes, planktic foraminifers, and sporomorphs. However, not all groups were found or studied throughout the core. To date, mollusks have been studied only in the Cretaceous, and calcareous nannofossils only in the Tertiary.

OSTRACODES

Ostracodes are absent below 538 m (1,765 ft) except for a small assemblage in the Cape Fear Formation at 721 m (2,365 ft). The presence of *Fossocytheridea lenoirensis* Swain and Brown, 1964, at 721 m (2,365 ft) suggests placement in the brackish water facies of Unit F of Brown and others (1972).

At 538 m (1,765 ft) *Asciocythere macropunctata* (Swain, 1952) occurs with *"Cythereis" canteriolata* Crane, 1965, and other species. This sample is probably correlative in part with Unit C of Brown and others (1972). Assemblages of probable late Austinian Age are present from a depth of about 538 m (1,765 ft) to about 481 m (1,578 ft). An assemblage at 481 m (1,578 ft) includes *Haplocytheridea? nanifaba* Crane, 1965, *Cythereis dallasensis* Alexander, 1929, *Brachycythere pyriforma* Hazel and Paulson, 1964, and *"Phacorhabdotus" pokornyi* Hazel and Paulson, 1964 (late form). This assemblage suggests correlation with the Burditt Marl or lowermost beds of the Sprinkle Formation of Texas. Assemblages suggesting uppermost Austinian to, perhaps, lower Tayloran are present from between 481 and 473 m (1,578–1,552 ft) up to 408 m (1,340 ft).

The early to middle Tayloran species *"Cythereis" plummeri* Alexander, 1929, is present at 408 m (1,340 ft) and at 398 m (1,306 ft). *Haplocytheridea insolita* (Alexander and Alexander, 1933), *"Veenia" gapensis* (Alexander, 1929), and *Brachycythere porosa* Crane, 1965, also occur in the deeper sample. At 385 m (1,263 ft), the Tayloran markers *Haplocytheridea insolita* and *"Veenia" gapensis* again occur. From between 385 and 366 m (1,263–1,201 ft) to just below 322 m (1,056 ft), the ostracode assemblage consists of species that occur in both the Navarroan and the Tayloran. The Peedee Formation above 322 m (1,056 ft) contains a typical Navarroan assemblage including such species as *Haplocytheridea renfroensis* Crane, 1965, *"Cythereis" pidgeoni* Berry, 1925, *Brachycythere ovata* Berry, 1925, *"Cythereis" huntensis* (Alexander, 1929), and *Haplocytheridea everetti* (Berry, 1925).

A diverse assemblage indicative of an early Midwayan Age is present in the lower part of the Beaufort(?) Formation. Occurring in the lower part of the Beaufort(?), among others, are *Phractocytheridea ruginosa* Alexander, 1934, *Loxoconcha atlantica* (Alexander, 1934), *Hermanites gibsoni* Hazel, 1968, *H. midwayensis* (Alexander, 1934), *Phacorhabdotus sculptilis* (Alexander, 1934), *Acanthocythereis washingtonensis* Hazel, 1968, *Brachycythere plena* Alexander, 1934, and *Opimocythere browni* Hazel, 1968. Ostracode assemblages of late Midwayan Age are not well known in the Gulf and Atlantic Coastal Plains. Therefore, although ostracodes occur in the lower part of the Black Mingo Formation and upper part of the Beaufort(?) Formation in the core, they have not been as biostratigraphically definitive as the other fossil groups studied in this interval.

Ostracode assemblages suggesting a Sabinian Age are present in the core from about 150 m (492 ft) to at least 125 m (410 ft). *Ouachitaia broussardi* (Howe and Garrett, 1934), *Haplocytheridea leei* (Howe and Garrett, 1934), *Acanthocythereis hilgardi* (Howe and Garrett, 1934), *Buntonia alabamensis* (Howe and Garrett, 1934), *Phractocytheridea moodyi* (Howe and Garrett, 1934), *"Cythereis" dictyolobus* of Pooser (1965), *Hermanites bassleri*

(Ulrich, 1901), and *Opimocythere* cf. *O. nanafaliana* (Howe and Garrett, 1934), occur in this interval.

The Claibornian indicators *Opimocythere martini* (Murray and Hussey, 1942) and *Actinocythereis gosportensis* (Blake, 1950) occur at about 110 m (361 ft). Ostracodes are fairly common in that part of the Cooper assigned to the Jacksonian, 69–55 m (227–180 ft). *Cytheretta jacksonensis* (Meyer, 1887), *Acanthocythereis spinomuralis* Howe and Howe, 1973, *Echinocythereis jacksonensis* (Howe and Chambers, 1935), *Acanthocythereis florienensis* (Howe and Chambers, 1935), and several others are typical Jacksonian species that are present in this interval.

Several Vicksburgian guide species occur in the core between 55 and 35 m (180–115 ft). These include *Actinocythereis dacyi* (Howe and Law, 1936), *A. thomsoni* (Howe and Law, 1936), *Buntonia sulcata* Butler, 1963, and *Buntonia huneri* Howe and Law, 1936. The Chickasawhayan upper part of the Cooper Formation contains a diverse ostracode assemblage of about 40 species. *Actinocythereis waynensis* Butler, 1963, and *Leguminocythereis scarabaeus* of Brown (1958) and Pooser (1965), are two of the diagnostic species that occur in this interval. In the uppermost part of the Cooper, above about the 10-m (33-ft) depth in the core, species common in lower Miocene sediments, for example *Echinocythereis clarkana* (Ulrich and Bassler, 1904), make their first appearance.

CRETACEOUS LARGER INVERTEBRATES

Macrofossils are common at many Upper Cretaceous levels in the core between 537 and 245 m (1,763–804 ft). Although the shelled larger invertebrate groups of worms, sponges, bryozoans, scaphopods, and cephalopods are all represented, the assemblages are dominated by bivalves and gastropods. No single sample contains more than 20 species of mollusks, but this is only because of the limited nature of the core samples. Samples equivalent in volume to outcrop collections would undoubtedly yield greater diversity, including many of the larger forms not recoverable in cores.

Below 537 m (1,763 ft) only one sample, at 721 m (2,365 ft), contained fossil mollusks; these are poorly preserved and nondiagnostic.

The species *Ostrea cretacea* Morton, 1834, was found from 537 to 535 m (1,763–1,754 ft). This species is common to the upper part of the Eutaw Formation of the Chattahoochee River region of Alabama and Georgia, and to the Tombigbee Sand Member of the Eutaw of central and western Alabama; it has been reported from the uppermost part of the Magothy Formation at Cliffwood, N.J. In addition, it has been encountered in wells in North and South Carolina at a similar stratigraphic level. In outcrop, the Tombigbee Sand Member contains ammonites of the upper Austinian which Young (1963) has assigned to the early Campanian.

Up to 444 m (1,456 ft) the association of abundant *Lucina glebula* Conrad, 1875, *Veniella mullenensis* Stephenson, 1923, *Camptonectes perlamellosa* Whitfield, 1885, and others is similar to assemblages that occur through the middle and lower parts of the Blufftown Formation of the Chattahoochee River region and in the Woodbury Clay of New Jersey. The occurrence of a large *Trigonarca* and *Aphrodina* of the *A. regia* Conrad, 1875, type and several other mollusks in the assemblages at 411 and 410 m (1,347 and 1,345 ft) suggests a correlation with the type section of the Snow Hill Member of the Black Creek Formation of North Carolina and the basal part of the Cusseta Sand Member of the Ripley Formation of Georgia and eastern Alabama. The lowest depth in the core at which *Exogyra ponderosa* Roemer, 1849, is found is 354 m (1,162 ft). This species ranges through the upper Austinian into the Tayloran and forms the basis for a stratigraphically broad but well-recognized zone throughout the Gulf and Atlantic Coastal Plains.

Navarroan molluscan assemblages are present from a depth of at least 332 m (1,090 ft) to 245 m (804 ft). Specimens of *Exogyra* assignable to *E. costata* Say, 1820, occur sporadically throughout this interval; the varietal form *spinifera* is common. In outcrop, the *Exogyra costata* zone has been considered coordinate in range with the Navarroan. *Flemingostrea subspatulata* (Forbes, 1845), occurs commonly in samples at depths between 325 and 314 m (1,066–1,030 ft). This species ranges through the lower and middle Navarroan, but the specimens from the core material represent the form common to the lower part of the range zone that on the outcrop is associated with *Exogyra cancellata* Stephenson, 1914. The *Exogyra cancellata* zone is considered lower Navarroan. Thus, the interval from about 335 to about 314 m (1,100–1,030 ft) appears to be assignable to the *E. cancellata* zone. This early form of *Flemingostrea subspatulata* occurs in the uppermost part of the Wenonah Formation of New Jersey, the basal part of the Peedee Formation in North Carolina, and in the upper part of the Cusseta Sand Member of the Ripley Formation of Georgia and eastern Alabama.

TERTIARY CALCAREOUS NANNOFOSSILS

Calcareous nannofossils are present throughout the Paleogene part of the core except for a 6-m (20-ft) interval at the Paleocene–Eocene boundary. Coccolith abundance and diversity are less than normally observed in Gulf Coast Paleogene material, but coccoliths are present in sufficient numbers to be one of the more biostratigraphically useful groups in the Clubhouse Crossroads core.

Martini's (1971) standard calcareous nannoplankton zonation contains 25 NP zones in the Paleocene through Oligocene. Because many calcareous nannofossil marker species are absent from the core, and because several unconformities are present, only eight of these zones can be confidently recognized.

The Beaufort(?) Formation from 244 to 192 m (800–630 ft) is entirely within the lower Paleocene NP 3 zone (Danian). Some of the lowest nannofossil diversities are in the Paleocene part of the core; however, the first appearances of *Chiasmolithus danicus* (Brotzen, 1959) and *Coccolithus pelagicus* (Wallich, 1877) within this interval indicate zone NP 3. Other typical Paleocene species are *Coccolithus cribellum* (Bramlette and Sullivan, 1961), *Cruciplacolithus tenuis* (Stradner, 1961), *Neococcolithes protenus* (Bramlette and Sullivan, 1961), and *Zygolithus sigmoides* (Bramlette and Sullivan, 1961).

The Black Mingo Formation from 192 to 125 m (630–410 ft) is divided among three zones—NP 4, NP 5–9, and NP 12. The first late Paleocene (Thanetian) species appear within this formation. *Chiasmolithus bidens* (Bramlette and Sullivan, 1961) and *Toweius craticulus* Hay and Mohler, 1967, occur in the assemblage and indicate the presence of zone NP 4.

From 177 to 138 m (581–454 ft), the Black Mingo Formation covers zones NP 5 through NP 9 (upper Paleocene). Because of low species diversity, individual zones within this interval could not be recognized. *Ellipsolithus distichus* (Bramlette and Sullivan, 1961) and *Fasciculithus typmpaniformis* Hay and Mohler, 1967, have their first occurrences within the NP 5 zone, and *Discoaster multiradiatus* Bramlette and Riedel, 1954, has its extinction at the top of zone NP 9.

Between 138 and 136 m (451 and 445 ft), the Black Mingo Formation is barren of calcareous nannofossils, and this interval may include an unconformity encompassing zones NP 10–11. From 131 to 125 m (431 to 410 ft), the Black Mingo Formation is within the lower Eocene (Ypresian) NP 12 zone. Here the first *Discoaster barbadiensis* (Tan Sin Hok, 1927) *Sphenolithus moriformis* Brönnimann and Stradner, 1960), and several discolith species, among them *Pontosphaera duocava* (Bramlette and Sullivan, 1961), *P. pulchra* (Deflandre, 1954), *P. ocellata* (Bramlette and Sullivan, 1961), and *P. vesca* (Sullivan, 1965), are found. Some late Paleocene species have been reworked into these sediments.

The contact of the Black Mingo Formation with the overlying Santee Limestone represents an unconformity covering zones NP 13–16. The lower part of the Santee Limestone from 125 to 104 m (410–341 ft) is in zones NP 16–17 (middle Eocene, Lutetian). Typical middle Eocene species first occurring within this interval include *Blackites spinosus* (Deflandre and Fert, 1954), *Cyclococcolithus formosus* Kamptner, 1963, *Cyclococcolithus reticulatus* Gartner and Smith, 1967, *Helicopontosphaera compacta* (Bramlette and Wilcoxon, 1967), *Pontosphaera pulcheroides* (Sullivan, 1956), *Reticulofenestra umbilica* (Levin, 1965), and *Zygrhablithus bijugatus* (Deflandre, 1954).

The calcareous nannofossil species diversity increases from 16 species in the Paleocene part of the core to 54 species in the upper Eocene. Part of this increase is due to a normally increasing diversity of calcareous nannofossils in the Paleocene and Eocene, but in the Clubhouse Crossroads core, it is also due to either more favorable living conditions in the water column or better preservation of upper Eocene sediments. Several species, normally common throughout the middle and upper Eocene, are present only in upper Eocene sediments in the core.

The Santee Limestone interval between 101 and 83 m (331–271 ft) represents zones NP 18–19 (upper Eocene, Bartonian). *Helicopontosphaera bramletti* Müller, 1970, *H. euphratis* (Haq, 1966), and *Sphenolithus obtusus* Bukry, 1971, first appear here, and many other typical middle and late Eocene species are also found. Pentaliths are especially abundant within this interval.

The uppermost part of the Santee Limestone and lowermost part of the Cooper Formation, 81–55 m (266–180 ft) can be placed in the upper Eocene NP 20 zone. *Sphenolithus pseudoradians* Bramlette and Wilcoxon, 1967, and *Helicopontosphaera intermedia* (Martini, 1965) first occur in this zone, whereas species with their last occurrences here include *Discoaster barbadiensis* (Tan Sin Hok, 1927), *D. saipanensis* Bramlette and Riedel, 1954, and *Micrantholithus procerus* Bukry and Bramlette, 1969.

An unconformity occurs within the Cooper Formation at 55 m (180 ft) and represents zones NP

21–23. From 55 to 5 m (180–16 ft) the Cooper Formation is in zone NP 24 (upper Oligocene, Chattian), which is marked by the first occurrence of *Helicopontosphaera recta* (Haq, 1966) and *Pontosphaera clathrata* (Roth and Hay, 1967). *Heliocopontosphaera compacta* Bramlette and Wilcoxon, 1967, and *Sphenolithus predistentus* Bramlette and Wilcoxon, 1967, which become extinct within zone NP 24, are found throughout this interval. Considerable reworking of late Eocene species into the lower half of this zone has taken place.

FORAMINIFERS

Late Cretaceous planktic foraminifers are common to abundant throughout much of the Cretaceous strata penetrated in the Clubhouse Crossroads core; they are particularly abundant in the Campanian and Maestrichtian parts of the Peedee and Black Creek Formations. Samples from these units have yielded superbly preserved faunas, many having a species diversity nearly identical to the rich faunas documented from the Upper Cretaceous of the western Gulf Coastal Plain area (Pessagno, 1967; Smith and Pessagno, 1973). Within the Campanian–Maestrichtian interval, however, is strong faunal and floral evidence, supported by lithologic data, of rapid and in some instances rather extensive changes in paleoenvironmental depositional settings. Within these more shallow neritic intervals, diversity of the planktic foraminifers is quite low (although preservation remains excellent) and is accompanied by the appearance of or increase in abundance of typical shallow-water benthic foraminifers. The more shallow neritic parts of the Campanian and Maestrichtian sections, as well as the majority of pre-Campanian samples that were studied, are characterized by low species diversity and the absence of many key species normally present in more open marine paleoenvironments. This has resulted in questionable biostratigraphic assignments for several samples. In instances such as these, the zonal assignment of the sample is questioned or, where practicable, referred to an interval of two or more biostratigraphic zones. The biostratigraphic zonal assignment and chronostratigraphic correlation of these samples closely follows that utilized by Pessagno (1967, 1969) in his studies of the western Gulf Coast.

Both the Middendorf and the Cape Fear Formations, from the total depth of available samples, 741–579 m (2,430–1,900 ft), contain a restricted shallow-water foraminiferal fauna, many samples being barren of planktic foraminifers. However, this interval contains rare individuals of *Heterohelix moremani* (Cushman), *Hedbergella brittonensis* Loeblich and Tappan, *Globigerinelloides* cf. *G. caseyi* (Bolli, Loeblich, and Tappan), and very abundant and excellently preserved *Guembelitria harrisi* Tappan, which are referable to the *Rotalipora cushmani-greenhornensis* Subzone of late Cenomanian Age. This subzone is also present within the upper parts of the Woodbine Formation and about the lower half of the Eagle Ford Group of Texas (Pessagno, 1967; 1969).

In the interval from 579 to 522 m (1,900–1,713 ft), all samples that were studied were barren or contained no biostratigraphically important planktic foraminiferal faunas. In the lower part of the Black Creek Formation, a sample at 522 m (1,713 ft) contained *Marginotruncana angusticarenata* (Gandolfi), as well as several species of the genus *Archaeoglobigerina*. The concurrent range of these species is indicative of the *Marginotruncana concavata* Subzone of Santonian Age.

The Black Creek section between 518 and about 494 m (1,700–1,620 ft) contains a sparse and poorly preserved foraminiferal fauna lacking the key species that would permit a precise biostratigraphic zonal assignment. Tentatively these faunas can be referred to the lower and middle Campanian *Globotruncana fornicata* and *Archaeoglobigerina blowi* Subzones. According to Pessagno (1969), these subzones are representative of the upper part of the Austinian and the lower part of the Tayloran Provincial Stages. A sample at 487 m (1,599 ft), in the middle part of the Black Creek Formation, contains a moderately diverse planktic foraminiferal fauna that can be assigned to the *Archaeoglobigerina blowi* Subzone of middle Campanian Age.

Samples from the upper part of the Black Creek Formation and the lower part of the Peedee Formation, from about 480 to 375 m (1,575–1,230 ft), are assignable to the Campanian *Globotruncana elevata* Subzone. Planktic foraminifers within this interval are very abundant, moderately diverse, and generally well preserved. Characteristic of this interval is the overlap between the ranges of *Globigerinelloides multispina* (Lalicker) and *Globotruncana linneiana* (d'Orbigny) and those of *Ventilabrella glabrata* (Cushman), *Rugoglobigerina tradinghousensis* Pessagno, and *Globotruncana elevata* (Brotzen). Units normally placed in the middle and upper parts of the Tayloran Provincial Stage contain an assemblage characteristic of this subzone (see Pessagno, 1967, 1969; Olsson, 1975; Petters, 1976). Lower and middle parts of the Peedee strata

within the interval between about 375 and 312 m (1,230–1,025 ft) are predominantly shallow marine; they contain nondiagnostic planktic foraminifers but probably are equivalent to either the upper Campanian *Globotruncana elevata* Subzone or to the lower Maestrichtian *Rugotruncana subcircumnodifer* Subzone.

Samples from the Peedee within the interval between about 312 and 290 m (1,025–950 ft) are assignable to the lower Maestrichtian *Rugotruncana subcircumnodifer* Subzone. Although the planktic foraminiferal faunas within this interval are less diverse than those from overlying strata, the presence of *Globigerinelloides yaucoensis* (Pessagno), *Archaeoglobigerina blowi* Pessagno, *Globotruncana bulloides* (Vogler), and *G. fornicata* Plummer, is indicative of an early Maestrichtian Age and indicates placement of the interval in the lower part of the Navarroan Provincial Stage.

The upper part of the Peedee Formation, within the interval between 290 and 244 m (950–800 ft), is assignable to the middle Maestrichtian *Globotruncana gansseri* Subzone. Samples within this section have yielded an excellently preserved and diverse planktic formaminiferal assemblage including abundant individuals of *Guembelitria cretacea* Cushman, *Heterohelix glabrans* (Cushman), *Planoglobulina carseyae* (Plummer), *Pseudotextularia deformis* (Kikoine), *Globotruncana aegyptiaca* Nakkady, *G. duwi* Nakkady, *G. gansseri* Bolli, *G. trinidadensis* Gandolfi, *Rugoglobigerina hexacamerata* Brönnimann, *R. reicheli* Brönnimann, and *Globotruncanella monmouthensis* (Olsson). None of these species have been documented from strata older than middle Maestrichtian in age (Smith and Pessagno, 1973).

Planktic foraminiferal faunas assignable to the uppermost Maestrichtian *Abathomplalus mayaroensis* Subzone were not found during this investigation. Because an obvious erosional unconformity exists between the Maestrichtian Peedee Formation and the overlying Danian Beaufort(?) Formation, and because both lithologic units are richly microfossiliferous, it seems reasonable to presume that strata assignable to the *A. mayaroensis* Subzone were removed (rather than never deposited) during latest Maestrichtian and (or) Danian time.

Examination of the rather poorly preserved planktic foraminifers from the Cenozoic parts of the Clubhouse Crossroads core has resulted in the following biostratigraphic zonal assignments and age determinations. The lower part of the Beaufort(?) strata from its unconformable contact with the underlying Peedee Formation at 244 m (800 ft) to approximately 215 m (705 ft) contains *Globoconusa daubjergensis* (Brönnimann) and other species diagnostic of the *G. daubjergensis* Zone (zone P 1) of early Paleocene (early Danian) age. Beaufort(?) strata in the interval from between about 215 and 201 m (705 and 659 ft) are questionably assigned to the *Morozovella uncinata–M. angulata* Zone (P 2) of late early Paleocene (late Danian) age.

The uppermost 8–15 m (25–50 ft) of the Beaufort(?) Formation and the basal few feet of the Black Mingo Formation contain *Morozovella angulata* (Bolli), *Subbotina triloculinoides* (Plummer), *S. pseudobulloides* Plummer, *Planorotalites compressa* (Plummer), and *P. ehrenbergi* (Bolli). This assemblage is typical of the early part of the late Paleocene (early Thanetian) and is assignable to the *Morozovella pusilla pusilla–M. angulata* Zone (P 3).

A sample at 170 m (557 ft) from the middle of the Black Mingo Formation contains a fauna that includes *Morozovella angulata* (Bolli), *M. pusilla* (Bolli), *Planorotalites imitata* (Subbotina), *P. ehrenbergi* (Bolli), *P.* cf. *P. pseudomenardii* (Bolli), *P. compressa* (Plummer), and *Truncorotaloides esnaensis* (Le Roy). This assemblage is referable to the *Planorotaloides pseudomenardii* Zone (zone P 4) of late (although not latest) Paleocene age. The upper part of the Black Mingo Formation contains a distinctive early Eocene planktic foraminiferal assemblage, although because of the lack of diagnostic species, the Paleocene–Eocene boundary (between zones P 6a and P 6b, Berggren, 1972) can be defined no more precisely than somewhere within the interval between 169 to 133 m (555–435 ft).

Most of the Santee Limestone strata within the interval between about 120 and 77 m (393–254 ft), contain poorly preserved and generally nondiagnostic planktic foraminiferal assemblages assignable to zones P 11 through P 14 of middle Eocene (Claibornian) age.

The lower part of the Cooper Formation contains a rare and generally poorly preserved fauna, although species such as *Cassigerinella eocaena* Cordey, *Chiloguembelina cubensis* (Palmer), *C. martini* (Pijpers), *Pseudohastigerina barbadoensis* Blow, *Globigerina ouachitaensis* Howe and Wallace, *G. angiporoides* Hornibrook, *G. praebulloides* Blow, *Hantkenina primitiva* Cushman and Jarvis, *Globigerinatheka mexicana* (Cushman), and *Globorotalia cerroazulensis* (Cole) are present and indicate a late Eocene age assignment (zones P 15–17 of Blow, 1969).

A sample from the Cooper Formation at 57 m (188 ft) is questionably referred to the *Globigerina tapuriensis* Zone (P 18) of early Oligocene age; however, a late Eocene age assignment is also quite possible. If the sample at 57 m (188 ft) is Oligocene, then the Eocene–Oligocene boundary is between 59 m (193 ft) and 57 m (188 ft). If the sample at 57 m (188 ft) is of late Eocene age, then the Eocene–Oligocene boundary is somewhat higher, between 57 and 55 m (188–179 ft). From about 55 to 25 m (179–83 ft), the presence of forms related to *Globigerina angulisuturalis* Bolli suggests assignment to the upper part of the *Globigerina ampliapertura* Zone (zone P 20 of Blow). Foraminifers recovered between about 25 and 10 m (83–32 ft) are referable to zone P 21.

Samples from the upper part of the Cooper Formation, from a depth of 10–5 m (32–16 ft), contain *Cassigerinella chipolensis* (Cushman and Ponton), *Globigerina angulisuturalis* Bolli, *G. angulioffícinalis* Blow, G. *angustiumbilicata* Bolli, *G. ciperoensis* Bolli, and *Globoquadrina* cf. *G. globularis* Bermudez, among others, which suggest correlation with the *Globigerina angulisuturalis—Globorotalia opima* Zone or the *Globigerina angulisuturalis* Zone (zones P 21–22 of Blow, 1969) of late Oligocene age.

SPORES AND POLLEN

Very little has been published on spores and pollen from the Tertiary of the Atlantic Coast; therefore, study of the Clubhouse Crossroads core has provided an opportunity to gather the first detailed information on the stratigraphic distribution of spores and pollen in the Paleogene rocks of the southern Atlantic Coastal Plain. No spore-pollen zonation of the Paleogene rocks of the Gulf Coast has been proposed in the literature, but the ranges of many Gulf Coast species are fairly well known from the Midwayan to the lower Vicksburgian and can be compared with the ranges of the species determined in the South Carolina material.

All samples below 733 m (2,404 ft) were barren of palynomorphs. Spore-pollen assemblages from the Cretaceous System of the core were correlated with the informal palynological zones established by Brenner (1963), Doyle (1969), Sirkin (1974), and Wolfe (1976) for the Middle Atlantic States.

From 733 to 714 m (2,404–2,342 ft), the assemblage is considered equivalent to Doyle's (1969) Zone IV, on the basis of samples from the Woodbridge Clay Member of the Raritan Formation of New Jersey. At 714 m (2,342 ft), this assemblage includes only the Normapolles genera *Atlantopollis* and *Complexiopollis*, along with *Tricolpites crassimurus* (Groot and Penny, 1960) Singh, 1971, *"Retitricolpites" georgensis* Brenner, 1963, and *"R." geranioides* (Couper, 1958) Brenner, 1963.

All samples examined between 714 and 580 m (2,342–1,902 ft) in the core were barren of palynomorphs. Between the 580- and 550-m (1,902- and 1,804-ft) depths in the core, units equivalent to the South Amboy Fire Clay Member of the Raritan Formation were identified on the basis of the presence of *Porocolpopollenites* spp., *Labrapollis* sp., *Triatriopollenites* spp., *Complexiopollis* spp., *Santalacites* spp., and *Pseudoplicapollis* spp.

A comparison of samples from the Clubhouse Crossroads core with outcropping units from New Jersey indicates that the biostratigraphic equivalents of the Magothy Formation extend from 550 to 520 m (1,804–1,706 ft) in the core. Within this interval occur the Normapolles *Praecursipollis* sp., *Santalacites* spp., *Complexiopollis funiculus* Tschudy, 1973, *C. abditus* Tschudy, 1973, *Pseudoplicapollis* spp., *Plicapollis rusticus* Tschudy, 1975, and *Trudopollis* spp., along with an abundance of oblate triangular foveoreticulate tricolporates.

In the Middle Atlantic States, Wolfe's (1976) Zone CA–2 encompasses the entire Merchantville Formation of the Raritan embayment and the lower part of the Merchantville Formation of the Salisbury embayment. In the core this zone is recognized between 520 and 490 m (1,706–1,607 ft); it is characterized by an assemblage that includes *Holkopollenites* sp. A (CP3D–1), *Plicapollis rusticus* Tschudy, 1975 (NE–1), *Propylipollis* sp. B (PR–1), *Complexiopollis abditus* Tschudy, 1973 (NB–1), *Santalacites* sp. (NB–2), and *Osculapollis* cf. *O. perspectus* Tschudy, 1975 (NO–4). (Note: the alphanumeric code following each binomen refers to Wolfe's, 1976, species designation.)

Zone CA–3 of Wolfe (1976), established for the Woodbury Clay of the Raritan embayment and the upper part of the Merchantville Formation of the Salisbury embayment, extends from 490 to 430 m (1,607–1,410 ft) in the core. Within this interval the following species occur: *Brevicolporites* sp. A (CP3F–1), *Tricolporites* sp. C (C3C–2), and *Holkopollenites* sp. B (CP3D–2).

In the core, the biostratigraphic equivalent of the Englishtown Formation of the Middle Atlantic States (Wolfe's, 1976, Zone CA–4) was difficult to delineate. However, the assemblage that characterizes this unit in both the Salisbury and Raritan embayments and in what is interpreted to be Englishtown equivalent in the core includes *Santalacites* sp.

(NB–2), *?Plicapollis* sp. A (ND–1), *Plicapollis rusticus* Tschudy, 1975 (NE–1), and *Holkopollenites* sp. B (CP3D–2). The unit extends from the 430- to 420-m (1,410- to 1,378-ft) depths in the core.

Wolfe's (1976) Subzone CA–5, characteristic of the Marshalltown Formation of the Raritan and Salisbury embayments, is between 420 and 360 m (1,378–1,181 ft) in the core. The concurrent ranges of *Complexiopollis abditus* Tschudy, 1973 (NB–1), *Pseudoculapollis admirabilis* Tschudy, 1975 (NR–1), *?Plicapollis* sp. B (ND–2), *Holkopollenites* cf. *H. chemardensis* Fairchild in Stover, Elsik, and Fairchild, 1966 (CP3D–3), and *Plicapollis retusus* Tschudy, 1975 (NE–3), among others, were used to identify this biostratigraphic unit.

Beds correlative with the Mt. Laurel Sand and Wenonah Formation of the Middle Atlantic States (Subzone CA–5 B of Wolfe, 1976) exist between the 360- and 290-m (1,181- and 951-ft) depths in the core. The occurrence of *Pseudoplicapollis endocuspis* Tschudy, 1975 (NC–2), *Osculapollis aequalis* Tschudy, 1975 (NO–1), *Triatriopollenites* sp. (NP–2), *Labrapollis* sp. (NV–1), and *Pseudovacuopollis involutus* Tschudy, 1975 (NT–1), help to correlate this interval.

Biostratigraphic equivalents of the Navesink Formation and Red Bank Sand of the Raritan embayment and of the Monmouth Group of the Salisbury embayment (Wolfe's, 1976, Zone CA–6/MA–1) were identified between the 290- and 244-m (951- and 800-ft) depths in the core. The lower boundary of this interval is marked by the last occurrence of *Pseudoplicapollis endocuspis* Tschudy, 1975 (NC–2), and *?Plicapollis* sp. C (ND–3) and by the first appearance of *Plicatopollis* sp. (NN–2) and *Momipites* sp. (NK–3).

The Cretaceous–Tertiary boundary in the Clubhouse Crossroads core is marked by the first appearances of *Momipites coryloides* Wodehouse, 1933, *Momipites* cf. *M. inaequalis* Anderson, 1960, and *Favitricolporites baculoferus* (Pflug in Thomson and Pflug, 1953) Srivastava, 1972. Whether these three species also have first occurrences at this horizon in the Gulf Coast is not known.

The middle Midwayan is characterized by the first occurrences of *Trudopollis plena* Tschudy, 1975, and probably also *Triporopollenites* n. sp. A (thin-walled) of Tschudy, 1973. The last occurrence of *Pseudoplicapollis serena* Tschudy, 1975, is within the upper Midwayan in both the Gulf Coast and the core and is one of the most important spore-pollen extinction events of the Paleogene. The first occurrence of *Aesculiidites circumstriatus* (Fairchild in Stover and others, 1966) Elsik, 1968, is at about the Midwayan–Sabinian boundary in both regions. In the middle Sabinian of the Gulf Coast and in the core, the best datum is provided by the last occurrences of *Momipites dilatus* (Fairchild in Stover and others, 1966) Nichols, 1973, and *Momipites* spp. of the Tenuipolus Group. The upper Sabinian (lower Eocene) both of the Gulf Coast and of the core from 137 to about 125 m (450–410 ft) is distinguished by the concurrence of *Thomsonipollis magnifica* (Pflug in Thomson and Pflug, 1953) Krutzsch, 1960, and *Nuxpollenites* spp. and especially by the rather high relative abundance of *Platycarya* spp. and *Platycaryapollenites* spp.

In the Gulf Coastal Plain and in the Clubhouse Crossroads core, the Jacksonian and the uppermost Claibornian contain similar spore-pollen assemblages. Important marker species present for this part of the Paleogene are *Quercoidites microhenricii* (Potonié, 1931) Potonié, 1960, and *Pollenites ventosus* Potonié, 1931. *Nuxpollenites* spp. is regularly present in the Claibornian but is extremely rare in the Jacksonian. The Chickasawhayan and late Vicksburgian, 55- to 5-m (180- to 16-ft), spore-pollen assemblages of the Clubhouse Crossroads core are dominated by *Cupressacites* spp., *Quercus* spp., and a new species of *Momipites* that is most similar morphologically and stratigraphically to *Triatriopollenites coryphaeus* s. str. (Potonié, 1931) Thomson and Pflug, 1953. Many species found in the lower Vicksburgian of the Gulf Coast are lacking from the upper Vicksburgian and Chickasawhayan of South Carolina, including *Momipites coryloides* Wodehouse, 1933, and *M. microfoveolatus* (Stanley, 1965) Nichols, 1973.

DINOFLAGELLATES

Phytoplankton, primarily dinoflagellates, are present in many of the stratigraphic intervals of the Clubhouse Crossroads core. Dinoflagellates are rare in the deepest interval sampled, 734–714 m (2,404–2,342 ft). No phytoplankton were observed in samples from an interval between 704 and 580 m (2,309–1,902 ft), and diversity is very low between 559 and 543 m (1,835–1,781 ft). Dinoflagellates are present in moderate abundance and diversity from between 543 and 518 m (1,781–1,700 ft) to 244 m (800 ft). From 244 to 198 m (800–649 ft), dinoflagellates are abundant, but diversity is generally low. In the interval from 190 to 124 m (623–407 ft), dinoflagellates are virtually absent. Between 120 and 5 m

(394–16 ft) dinoflagellates are generally abundant and diversity is variable.

Only three species of dinoflagellates were observed in the core below 559 m (1,835 ft). *Odontochitina costata* Alberti, 1961, *Florentinia lasciniata* Davey and Verdier, 1975, and *Oligosphaeridium pulcherrimum* (Deflandre and Cookson) Davey and Williams, 1966, occur between 733 and 714 m (2,404–2,342 ft). The concurrent ranges of these species suggest a Cenomanian Age for the interval.

Because of low species diversity, the sampled interval between 559 and 543 m (1,835–1,781 ft) could not be dated precisely. The concurrence of the ranges of *Deflandrea granulifera* Manum, 1963, and *Palaeohystrichophora infusorioides* Deflandre, 1935, suggests an age not older than Santonian.

On the basis of the concurrent ranges of *Horologinella apiculata* Cookson and Eisenack, 1962, *Deflandrea sverdrupiana* Manum, 1963, and *Palaeostomacystis laevigata* Drugg, 1967, it is suggested that the 518- to 383-m (1,700- to 1,257-ft) interval is of Campanian Age. Other species present in this interval are *Dinogymnium undulosum* Cookson and Eisenack, 1970, *Dinogymnium euclaensis* Cookson and Eisenack, 1970, *Dinogymnium digitus* (Deflandre) Evitt and others, 1967, *Dinogymnium denticulatum* (Alberti) Evitt and others, 1967, and *Deflandrea echinoidea* Cookson and Eisenack, 1960.

The assemblages in the 366- to 305-m (1200- to 1000-ft interval of the core are distinctly different from those of the Maestrichtian units above. The most characteristic feature is the presence of species that appear to be restricted to the Marshalltown and Wenonah Formations of New Jersey. Included in the flora are *Deflandrea victoriensis* Cookson and Manum, 1964, *Deflandrea* cf. *D. armata* Cookson and Eisenack, 1970, *Palaeocystodinium* sp., *Dinogymnium* sp., and *Amphidinium mitratum* Vozzhennikova, 1967. The apparent correlation of this interval with the Marshalltown and Wenonah Formations of New Jersey is also supported by the occurrence of the following species: *Odontochitina costata* Alberti, 1961, *Deflandrea* n. sp., and *Trigonopyxidia ginella* (Cookson and Eisenack) Downie and Sarjeant, 1964, *Palaeohystrichophora infusorioides* Deflandre, 1935, and *Phoberocysta ceratioides* Deflandre, 1937. The age of this interval is late Campanian.

The interval from 296 to 270 m (970–885 ft) contains an assemblage that, in terms of the outcrop section, is a mixture of species restricted to either the Mount Laurel Sand and older units of the northern Atlantic Plain or to the Navesink and Red Bank interval. These forms are *Deflandrea pannucea* Stanley, 1965, *Gonyaulacysta* sp., *Achomosphaera ramulifera* (Deflandre) Evitt, 1963, *Ophiobolus lapidaris* Wetzel, 1933, *Samlandia angustivela* (Deflandre and Cookson) Eisenack, 1963, *Palaeohystrichophora infusorioides* Deflandre, 1935, *Systematophora* n. sp., and *Phoberocysta ceratioides* Deflandre, 1937. This assemblage is what one might expect in rocks equivalent to the disconformity between the Mount Laurel Sand and the Navesink Formation of northern New Jersey. The suggested age is late Campanian or early Maestrichtian.

Between 267 and 244 m (875–800 ft), dinoflagellate-acritarch assemblages are similar to those of the Navesink Formation–Red Bank Sand sequence of northern New Jersey. Species restricted to both this interval in the core and the Navesink–Red Bank interval are *Palaeocystodinium australinum* (Cookson) Lentin and Williams, 1976, *Gonyaulacysta* sp., *Deflandrea speciosa* Alberti, 1961, Drugg, 1967, and *Dinogymnium westralium* (Cookson and Eisenack) Evitt and others, 1967. Between 267 and 259 m (875 and 850 ft), the assemblage also contains three undescribed species that are known to occur elsewhere only in the Navesink Formation of New Jersey. These are new species of *Dinogymnium, Hystrichokolpoma,* and *Trithyrodinium.* The above occurrences suggest that the 267- to 244-m (875- to 800-ft) interval is Navesink equivalent (lower Maestrichtian).

The presence of at least three species of the Cretaceous genus *Dinogymnium* at 245 m (804 ft) and 244 m (800 ft) suggests that the Cretaceous–Tertiary boundary is at about 244 m (800 ft).

Between 244 and 198 m (800–649 ft) an assemblage is present that suggests an early Paleocene age and correlation, at least in part, with the Brightseat Formation of Maryland. Present in this interval are *Deflandrea* n. sp., which is known only from the Brightseat Formation; *Deflandrea magnifica* Stanley, 1965; *Deflandrea obscura* Drugg, 1967; *Deflandrea dilwynensis* Cookson and Eisenack, 1965; *Spiniferites buccina* (Davey and Williams) Sarjeant, 1970; *Spiniferites septatus* (Cookson and Eisenack) McLean, 1971; and *Spinidinium densipinatum* Stanley, 1965.

In the interval from 190 to 124 m (623–407 ft), dinoflagellates are too rarely represented to be of biostratigraphic value. The interval from 120 to 55 m (394–179 ft) is tentatively considered to be of middle and late Eocene age. The difficulty of separating the middle from the late Eocene in this core by means of dinoflagellates was also experienced by Gradstein and Williams (1976) on the Labrador

Shelf. Species that characterize the middle and late Eocene assemblages in both areas include *Cyclonophelium ordinatum* Williams and Downie, 1966, *Wetzeliella articulata* Eisenack, 1938, *W. coleothrypta* Williams and Downie, 1966, *W. tenuivirgula* Williams and Downie, 1966, and *Diphyes colligerum* (Deflandre and Cookson) Cookson, 1965. The first appearance of *Pentadinium laticinctum* Gerlach, 1961, and *Achilleodinium biformoides* (Eisenack) Eaton, 1976, at 69 m (225 ft) suggests a late Eocene age because *P. laticinctum* Gerlach, 1961, was found in the upper Eocene of wells on the Grand Banks, Newfoundland (Gradstein and Williams, 1976). Also, *Achilleodinium biformoides* (Eisenack) Eaton, 1976, has been found only in upper Eocene sediments from other areas. Some of the other more common species recovered from this interval include *Deflandrea heterophlycta* Deflandre and Cookson, 1955, *Hystrichokolpoma rigaudae* Deflandre and Cookson, 1955, *Homotryblium* (=*Cordosphaeridium*) *floripes* Eisenack, 1963, *Pentadinium laticinctum* subsp. *granulatum* Gocht, 1969, *Spiniferites pseudofurcatus* (Klumpp) Sarjeant, 1970, *Tectadodinium* spp., *Systematophora placacantha* (Deflandre and Cookson) Davey and others, 1969, *Gonyaulacysta giuseppei* (Morgenroth) Sarjeant, 1969, and a new species of *Leptodinium*.

The assemblage of the interval 53–12 m (175–41 ft) contains *Chiropteridium lobospinosum* Gocht, 1960, and suggests an Oligocene age. Other species present in this interval include *Hystrichokolpoma rigaudae* Deflandre and Cookson, 1955, *Pentadinium laticinctum* subsp. *granulatum* Gocht, 1969, *Wetzeliella articulata* Eisenack, 1938, *Homotryblium* (=*Cordosphaeridium*) *floripes* Eisenack, 1963, *Cordosphaeridium funiculatum Morgenroth*, 1966, *Gonyaulacysta cantharellum* (Brosius) Gocht, 1969, *Lingulodinium machaerophorum* (Deflandre and Cookson) Wall, 1967, *Deflandrea heterophlycta* Deflandre and Cookson, 1955, *Thalassiphora pelagica* Eisenack and Gocht, 1960, *Gonyaulacysta giuseppei* (Morgenroth) Sarjeant, 1969, *Chiropeteridium aspinatum* (Gerlach) Brosius, 1963, and *Spiniferites* spp. The interval from 11 to 5 m (37–16 ft) in the upper part of the Cooper Formation contains, among other forms, *Tuberculodinium vancampoae* (Rossignol) Wall, 1967, which in other areas is used as a marker for the Miocene.

REFERENCES CITED

Berggren, W. A., 1972, A Cenozoic time-scale—some implications for regional geology and paleobiogeography: Lethaia, v. 5, no. 2, p. 195–215.

Blow, W. H., 1969, Late middle Eocene to Recent planktonic foraminiferal biostratigraphy, *in* Brönnimann, P., and Renz, H. H., *eds.*, International Conference on Planktonic Microfossils, 1st, Geneva, 1967, Proceedings: Leiden, Netherlands, E. J. Brill, v. 1, p. 199–422, 54 pls.

Brenner, G. J., 1963, The spores and pollen of the Potomac Group of Maryland: Maryland Dept. Geology, Mines and Water Resources Bull. 27, 215 p.

Brown, P. M., 1958, Well logs from the Coastal Plain of North Carolina: North Carolina Div. Mineral Resources Bull. 72, 68 p.

Brown, P. M., Miller, J. A., and Swain, F. M., 1972, Structural and stratigraphic framework, and spatial distribution of permeability of the Atlantic Coastal Plain, North Carolina to New York: U.S. Geol. Survey Prof. Paper 796, 79 p.

Bybell, L. M., 1975, Middle Eocene calcareous nannofossils at Little Stave Creek, Alabama: Tulane Studies Geology and Paleontology, v. 11, no. 4, p. 178–252.

Cooke, C. W., 1936, Geology of the Coastal Plain of South Carolina: U.S. Geol. Survey Bull. 867, 196 p.

Doyle, J. A., 1969, Angiosperm pollen evolution and biostratigraphy of the basal Cretaceous formations of Maryland, Delaware, and New Jersey [abs.]: Geol. Soc. America Abs. with Programs, [v. 1], pt. 7, p. 51.

Gradstein, F. M., and Williams, G. L., 1976, Biostratigraphy of the Labrador Shelf, Part I: Canada Geol. Survey, open file 349, 39 p.

Mann, C. J., and Thomas, W. A., 1968, The ancient Mississippi River: Gulf Coast Assoc. Geol. Socs. Trans., v. 18, p. 187–204.

Martini, Erlend, 1971, Standard Tertiary and Quaternary calcareous nannoplankton zonation, *in* Farinacci, Anna, and Matteucci, R., *eds.*, Proceedings of the II Planktonic Conference, Roma, 1970: Rome, Edizioni Tecnoscienza, v. 2, p. 739–785.

Obradovich, J. D., and Cobban, W. A., 1975, A time-scale for the late Cretaceous of the Western Interior of North America: Geol. Assoc. Canada Spec. Paper 13, p. 31–54.

Olsson, R. K., 1975, Upper Cretaceous and lower Tertiary stratigraphy of New Jersey coastal plain: Petroleum Exploration Soc. New York, Second Ann. Field Trip Guidebook, May 3, 1975, 49 p.

Owens, J. P., and Sohl, N. F., 1969, Shelf and deltaic paleoenvironments in the Cretaceous–Tertiary formations of the New Jersey Coastal Plain, *in* Subitzky, Seymour, *ed.*, Geology of selected areas in New Jersey and eastern Pennsylvania and guidebook of excursions: New Brunswick, N. J., Rutgers Univ. Press, p. 235–278.

Pessagno, E. A., Jr., 1967, Upper Cretaceous planktonic Foraminifera from the western Gulf Coastal Plain: Paleontographica Americana, v. 5, no. 37, p. 245–445, pl. 48–101, fig. 1–63.

——— 1969, Upper Cretaceous stratigraphy of the western Gulf Coast area of México, Texas, and Arkansas: Geol. Soc. America Mem. 111, 139 p., 60 pls.

Petters, S. W., 1976, Upper Cretaceous subsurface stratigraphy of Atlantic Coastal Plain of New Jersey: Am. Assoc. Petroleum Geologists Bull., v. 60, no. 1, p. 87–107, fig. 1–7.

Plummer, F. B., 1933, The geology of Texas, part 3, Cenozoic systems in Texas: Texas Univ. Bull. 3232, p. 519–818.

Pooser, W. K., 1965, Biostratigraphy of Cenozoic Ostracoda from South Carolina: Kansas Univ. Paleont. Contr. [38], Arthropoda, art. 8, 80 p.

Sanders, A. E., 1974, A paleontological survey of the Cooper Marl and Santee Limestone near Harleyville, South Carolina—preliminary report: Columbia, South Carolina Div. Geology Geol. Notes, v. 18, no. 1, p. 4–12.

Sirkin, L. A., 1974, Palynology and stratigraphy of Cretaceous strata in Long Island, New York, and Block Island, Rhode Island: U.S. Geol. Survey Jour. Research, v. 2, no. 4, p. 431–440.

Smith, C. C., and Pessagno, E. A., Jr., 1973, Planktonic foraminifera and stratigraphy of the Corsicana Formation (Maestrichtian) north-central Texas: Cushman Found. Foram. Research Spec. Pub. 12, p. 1–68, pl. 1–27, fig. 1–24.

Swift, D. J. P., and Heron, S. D., Jr., 1969, Stratigraphy of the Carolina Cretaceous: Southeastern Geology, v. 10, no. 4, p. 201–245.

Tschudy, R. H., 1973, Stratigraphic distribution of significant Eocene palynomorphs of the Mississippi embayment: U.S. Geol. Survey Prof. Paper 743–B, p. B1–B24.

van Hinte, J. E., 1976, A Cretaceous time scale: Am. Assoc. Petroleum Geologists Bull., v. 60, no. 4, p. 498–516.

Wolfe, J. A., 1976, Stratigraphic distribution of some pollen types from the Campanian and lower Maestrichtian rocks (Upper Cretaceous) of the Middle Atlantic States: U.S. Geol. Survey Prof. Paper 977, 18 p.

Young, Keith, 1963, Upper Cretaceous ammonites from the Gulf Coast of the United States: Texas Univ. Pub. 6304, 373 p.

——— 1965, A revision of Taylor nomenclature, Upper Cretaceous, central Texas: Texas Univ. Bur. Econ. Geology Geol. Circ. 65–3, 10 p.

Geochemistry of Subsurface Basalt From the Deep Corehole (Clubhouse Crossroads Corehole 1) Near Charleston, South Carolina—Magma Type and Tectonic Implications

By DAVID GOTTFRIED, C. S. ANNELL, and L. J. SCHWARZ

STUDIES RELATED TO THE CHARLESTON, SOUTH CAROLINA, EARTHQUAKE OF 1886—A PRELIMINARY REPORT

GEOLOGICAL SURVEY PROFESSIONAL PAPER 1028-G

CONTENTS

ILLUSTRATIONS

TABLES

STUDIES RELATED TO THE CHARLESTON, SOUTH CAROLINA, EARTHQUAKE OF 1886—A PRELIMINARY REPORT

GEOCHEMISTRY OF SUBSURFACE BASALT FROM THE DEEP COREHOLE (CLUBHOUSE CROSSROADS COREHOLE 1) NEAR CHARLESTON, SOUTH CAROLINA—MAGMA TYPE AND TECTONIC IMPLICATIONS

By DAVID GOTTFRIED, C. S. ANNELL, and L. J. SCHWARZ

ABSTRACT

Geophysical studies indicate that mafic volcanic and associated plutonic rocks may be important components of the basement beneath the Coastal Plain of the southeastern United States. A drill hole, 40 km northwest of Charleston, S.C., over a magnetic and gravity high penetrated 750 m of Coastal Plain sediments and bottomed in 42 m of basalt. Petrographic and major element data on 11 samples of basalt selected from the drill core, representing at least 2 lava flows, indicate that the basalts have undergone slight to extreme oxidation, hydration, and hydrothermal alteration. Effects of alteration are greatest in the marginal zones and least in the interior parts of the flows. The upper parts of the flows have abundant amygdules which contain laumontite, calcite, and chlorite. Petrochemical data on the least altered samples indicate that the basalts are of the quartz-normative tholeiitic magma type and closely resemble the Mesozoic high-Ti quartz-normative chilled diabase of eastern North America.

Eight samples were analyzed for 27 trace elements, including rare-earth elements (REE), Rb, Ba, Sr, Th, Zr, Hf, Nb, Ta, Ni, Co, Cr, and Cu, by neutron activation, emission spectrography, and spectrophotometry. Concentrations of K, Rb, Ba, and Sr are highly variable in the marginal zones and reflect the mobility of these elements during postmagmatic processes. K/Rb ratios of the least altered samples are in the range 300–400. The abundances of REE, P, Ti, Zr, Nb, and Th show little (<20 percent) or no variation regardless of the degree of alteration and indicate that the two flows were originally of the same chemical composition.

The contents of minor and trace elements of the corehole basalts are compared with those of rocks of tholeiitic composition which occur on Atlantic-type passive continental margins (eastern North America, Tasmania, Antarctica, South Africa: all of Mesozoic age) and with basalts from island arc and oceanic-ridge settings. The low abundances of REE, Ti, Zr, and Nb in the corehole basalt and in quartz-normative tholeiites from eastern North America and Tasmania are more similar to those of island arc and oceanic-ridge basalts than to those of "average" continental basalts. However, the pattern of enrichment in light REE and the low ratio, K/Rb, for the corehole basalt indicate that it originated from an undepleted source area in the upper mantle. The abundances of REE, Ti, Zr, and Nb and the light-REE enrichment patterns are strikingly similar to those of the high-Ti quartz-normative tholeiitic diabases of eastern North America. K-Ar analyses of a relatively fresh sample and an altered sample yield ages of 94.8 m.y. and 109 m.y., respectively. These are considered minimum ages and may be significantly younger than the time of volcanism. The characteristic geochemical features of the corehole basalts suggest that they have a temporal as well as spatial relationship with the Late Triassic and Early Jurassic tholeiitic province of eastern North America which formed during an extensional tectonic regime. The subsurface basalts may be associated with structural features produced by tensional faulting and suggest the possible presence of a buried Triassic basin beneath the Charleston area.

INTRODUCTION

Recent geophysical surveys of the Charleston area show pronounced positive magnetic and gravity anomalies which are interpreted as mafic or ultramafic plutons associated with mafic volcanic rocks (Popenoe and Zietz, this volume; Long and Champion, this volume; Kane, this volume; Phillips, this volume). Contrasting models based largely on the magnetic and gravity patterns have been proposed for the tectonic setting of the crust beneath the Coastal Plain: Zietz and others (1976) proposed an ocean-floor or island arc tectonic setting, and Popenoe and Zietz (this volume) propose a zone of continental extension. A deep hole was drilled over a magnetic and gravity high about 40 km west-northwest of Charleston as part of the program to investigate the seismicity of the Charleston-Summerville area (see fig. 3 of Rankin, this volume). The drill hole, called Clubhouse Crossroads corehole 1 (CCC 1), penetrated 750 m of Coastal Plain sediments and bottomed in 42 m of basaltic lavas which may be genetically related to the bodies causing the magnetic and gravity highs. The basalt is overlain by fossiliferous sediments of early Late Cretaceous (Cenomanian) age (Hazel and others, this volume; Gohn and others, this volume). A geochemical study of the basaltic rocks recovered from the corehole should provide direct evidence for constraining mod-

els of the regional tectonic setting that have been inferred from the geophysical and geological data.

The purpose of the present study is to present new data on major elements and trace elements for the corehole basalts and to discuss the implications of the data with regard to tectonic setting. The first stage of the study is to determine the composition of the parental magma of the basalts. This, by necessity, includes an assessment of the degree of alteration of the basalts. The second stage is to infer the tectonic setting of the basalts from a comparison of geochemical features of the corehole basalts with those of basalts of known tectonic setting. The third stage is to apply this information to an interpretation of the tectonic setting of the Charleston area at the time of extrusion of the basalts; therefore, knowledge of the age of the basalts is essential. In reading the detailed discussion that follows, the reader should keep in mind that one of our major conclusions is that no single group or pair of geochemically associated elements can be used alone for distinguishing magma type and tectonic setting.

We have benefited greatly from many helpful discussions with D. W. Rankin, Peter Popenoe, J. P. Owens, B. B. Higgins, R. L. Smith, and S. L. Russell. J. D. Fletcher provided preliminary semiquantitative spectrographic analyses which later expedited quantitative spectrographic determinations. M. E. Mrose and E. J. Dwornik provided important mineralogical data by X-ray diffraction and scanning electron microscopy. We are grateful to Michael Fleischer, G. T. Faust, L. P. Greenland, and J. G. Arth for critical reviews of this paper and for their suggestions for its improvement. Part of the work was supported by the U.S. Nuclear Regulatory Commission, Office of Nuclear Regulatory Research, Agreement No. AT (49–25)–1000.

DESCRIPTION OF BASALT

The basalt can be divided into two flows on the basis of criteria described by Nichols (1936) for distinguishing successive flows. The following criteria have been used in the present study: distribution of vesicles (now amygdules), grain size, and petrography. The upper flow is 35 m thick. The top of the flow (5 m) is highly oxidized, is reddish brown, and contains abundant amygdules. This zone grades downward into relatively fresh dark gray basalt containing fewer amygdules. The basal zone of the flow (3 m) is essentially aphyric and greenish; fractures are greenish black. Only 7 m of the lower flow were penetrated before drilling was terminated. The top of the lower flow is amygdaloidal, but less oxidized than the top of the upper flow, and grades downward into less altered gray fractured basalt.

Limited mineralogical studies have been carried out to date because the basalts are altered and the matrix is fine grained. Petrographic data obtained on least altered samples from the upper flow show that the basalt is composed mainly of clinopyroxene, plagioclase (An_{60}), and Fe-Ti oxides. Preliminary studies by scanning electron microscope and X-ray diffraction techniques have thus far identified the following secondary minerals: laumontite, calcite, chlorite (all in large amygdules), and stilbite.

ANALYTICAL METHODS

Major-element oxide, water, and CO_2 contents were determined by the rapid rock-analysis methods described by Shapiro (1975). Abundances of 10 major constituents were determined from a single solution obtained by a nitric acid dissolution of a sample fused with lithium metaborate-lithium tetraborate. CaO, MgO, Na_2O, and K_2O contents were determined by atomic absorption spectrometry; SiO_2, Al_2O_3, Fe_2O_3, TiO_2, P_2O_5, and MnO contents were determined spectrophotometrically. Separate sample portions were used to determine FeO, H_2O (+ and −), and CO_2 contents.

Minor- and trace-element abundances were determined by means of chemical, emission spectrographic, and instrumental neutron-activation analyses. Niobium content was determined by a spectrophotometric method (Greenland and Campbell, 1974). After decomposition by hydrofluoric acid and evaporation to volatilize silica, the samples were fused with pyrosulfate and dissolved in hydrochloric acid-tartaric acid. After separation by a thiocyanate extraction with amyl alcohol and back-extraction with dilute hydrofluoric acid, the niobium was reacted with 4-(2-pyridylazo)-resorcinol. Analytical error, calculated on the basis of replicate analyses of eight U.S.G.S. (U.S. Geological Survey) standard rocks, ranges from 2.9 to 6.4 percent in the concentration range from 10 to 27 ppm (parts per million).

Three modifications of d.c. (direct-current) arc emission spectroscopy were used to determine the concentrations of 17 minor and trace elements.

1. A 15-ampere arc in air was used to determine Ba, Co, Cr, Cu, Ga, Mn, Ni, Sc, Sn, Sr, V, Y, and Zr concentrations; this method has a co-

efficient of variation of approximately 15 percent (Bastron and others, 1960).

2. A 25-ampere arc in an argon atmosphere was used to determine Pb and Zn concentrations by fractional volatilization of a sample buffered by a Na_2CO_3 admixture. This method has a coefficient of variation of approximately 10 percent at the concentrations reported by Annell (1967).
3. A 15-ampere arc in air and a sample buffered with K_2CO_3 were used to determine Rb and Li concentrations. A coefficient of variation of 10 percent is realized by this technique (Annell, 1964).

Synthetic standards and U.S.G.S. standards, BCR–1, W–1, and AGV–1 (Flanagan, 1973), were used to establish analytical curves for the element concentrations determined spectrographically.

Instrumental neutron activation was used to determine La, Ce, Sm, Eu, Tb, Yb, Lu, Hf, Ta, and Th concentrations. Three 0.15-g replicate samples packed in polyethylene vials were irradiated for 2 hours at a flux of 5×10^{13} neutrons cm^{-2} sec^{-1} at the National Bureau of Standards reactor, Gaithersburg, Md. A standard was synthesized from an analyzed obsidian doped with solutions of selected trace elements, dried, reground, and calibrated relative to seven U.S.G.S. standard rocks: BCR–1, G–2, AGV–1, GSP–1, PCC–1, DTS–1, and W–1 (Flanagan, 1973). The samples and standards were counted on a Ge(Li) detector 1 week and 6 weeks after irradiation. The tantalum content was determined by counting on a low-energy photon detector 5 months following irradiation. The spectral data were processed on an IBM 370 [1] computer by means of the program SPECTRA (Baedecker, 1976).

ANALYTICAL RESULTS

MAJOR ELEMENTS

Major-element analyses were made on 11 corehole samples that represent the different zones of the two flow units as characterized by texture and grain size and that show to varying degrees the effect of posteruptive processes. The major-oxide compositions and the normative mineral compositions of the basalts are presented in table 1, where the data are arranged in order of increasing depth of the samples in the corehole. The contact between the upper and lower flow units is between samples B–5A and B–6. Chemical evidence of variable alteration in the suite of samples is clearly indicated by the relatively high and variable contents of H_2O and CO_2. As expected from megascopic observation, sample B–1, which is reddish brown, amygdaloidal, and extensively zeolitized, and which is taken from the top of the upper flow, has the highest H_2O content and Fe_2O_3/FeO ratio; it also has the lowest MgO content. Some important petrogenetic elements have been remobilized, and possibly others have been introduced along the contact between the upper and lower flow units. The lowest K_2O and Na_2O contents (0.02 and 0.48 percent, respectively) are in the top of the lower flow (sample B–6), which resembles the top of the upper flow (B–1) in texture and zeolite content and has the third highest content of H_2O, second highest content of Fe_2O_3, and next lowest MgO content. This sample also has an exceptionally high SiO_2 content and is strongly depleted in Al_2O_3. The highest contents of K_2O (1.3–1.4 percent) and Na_2O (3.4 percent) are found in samples (B–5, B–5A) of massive aphanitic rock in which amygdules are virtually absent. The basal zone showing potassium enrichment extends approximately 1 m above the contact between the flows. The presence of an analogous zone of potassium enrichment extending downward for approximately 3 m from the contact is indicated by the relatively high potassium content in B–7. The approximate symmetry of alteration indicates that in addition to weathering, oxidation, and hydration processes, which have affected the tops of the two flows to a greater degree than the interior parts, hydrothermal activity has affected the contact zone between the two flows.

An important feature of the chemistry of the samples is the uniformity of concentrations of two minor constituents, phosphorus and titanium. P_2O_5 concentrations are virtually the same (range, 0.12 to 0.15 percent) within the limits of error of the analytical method; titanium is nearly as uniform in its distribution except for the two most altered samples, B–1 and B–6, which show a depletion of about 15 percent in TiO_2 content (range, 0.82–0.87 percent) relative to that of the other samples (range, 0.95–1.1 percent). Although the introduction of water has strongly influenced the variations in the oxidation state of the rocks, the total iron concentrations are relatively unaffected. The distribution pattern for the values of total iron is approximately parallel to the pattern for the values of titanium. Prior studies (Cann, 1970; Pearce and Cann, 1971, 1973; Pearce and others, 1975; Floyd and Winchester, 1975; Winchester and Floyd, 1976) have shown that Ti and P concentrations have remained stable in

[1] Any trade names in this publication are used for descriptive purposes only and do not constitute endorsement by the U.S. Geological Survey.

TABLE 1.—*Major oxide and normative mineral compositions, in weight percent, of basalt from Clubhouse Crossroads corehole 1, near Charleston, S.C.*

[Analyses by F. W. Brown, S. D. Botts, and Leonard Shapiro, using methods described by Shapiro (1975)]

Sample No.	B-1	B-2	B-3	B-3A	B-4	B-4A	B-5	B-5A	B-6	B-7	B-8
Depth below surface (meters)	756	764	771	774	779	782	784.6	785	785.4	789	791
Major-oxide composition											
SiO_2	49.5	51.3	52.6	54.4	52.8	53.5	50.5	52.1	64.2	50.7	51.1
Al_2O_3	14.4	13.3	13.4	14.0	13.5	14.2	13.4	14.4	6.8	12.8	13.6
Fe_2O_3	8.2	2.9	2.7	3.6	2.4	3.0	3.1	3.2	4.1	3.9	3.2
FeO	.68	7.5	8.4	8.0	8.7	8.5	8.2	8.1	5.5	7.4	8.0
MgO	2.2	5.6	5.7	5.7	5.9	6.0	6.0	6.2	4.5	6.4	5.9
CaO	6.7	7.7	9.2	9.0	9.0	9.0	7.8	7.5	7.0	6.6	8.7
Na_2O	2.7	3.1	2.4	2.3	2.4	2.2	3.4	3.4	.48	3.3	2.7
K_2O	.70	.73	.50	.53	.62	.48	1.3	1.4	.02	.98	.48
H_2O+	8.6	4.4	1.7	1.4	2.0	2.0	2.6	2.1	4.3	3.6	3.4
H_2O-	4.0	1.2	.66	1.1	.61	.93	1.2	1.5	1.2	1.6	.88
TiO_2	.75	.89	.96	.98	.96	1.1	.99	1.0	.77	.93	.91
P_2O_5	.13	.12	.14	.12	.14	.13	.14	.13	.12	.13	.13
MnO	.12	.19	.21	.24	.22	.26	.24	.26	.18	.22	.21
CO_2	.08	.03	.04	.05	.02	.07	.01	.03	.62	.07	.01
Total	99	99	99	101	99	101	99	101	100	99	99
Major-oxide composition recalculated volatile-free											
SiO_2	57.5	55.0	54.7	55.0	54.6	54.4	53.1	53.3	68.5	54.3	53.8
Al_2O_3	16.7	14.3	13.9	14.2	14.0	14.4	14.1	14.7	7.3	13.7	14.3
Fe_2O_3	9.5	3.1	2.8	3.6	2.5	3.1	3.3	3.3	4.4	4.2	3.4
FeO	.79	8.0	8.7	8.1	9.0	8.6	8.6	8.3	5.9	7.9	8.4
MgO	2.6	6.0	5.9	5.8	6.1	6.1	6.3	6.4	4.8	6.9	6.2
CaO	7.8	8.3	9.6	9.1	9.3	9.2	8.2	7.7	7.5	7.1	9.2
Na_2O	3.1	3.3	2.5	2.3	2.5	2.2	3.6	3.5	.51	3.5	2.8
K_2O	.81	.78	.52	.54	.64	.49	1.4	1.4	.02	1.1	.51
TiO_2	.87	.95	1.0	.99	.99	1.1	1.0	1.0	.82	1.0	.96
P_2O_5	.15	.13	.15	.12	.14	.13	.15	.13	.13	.14	.14
MnO	.14	.20	.22	.24	.23	.26	.25	.27	.19	.24	.22
Total	100	100	100	100	100	100	100	100	100	100	100
Normative mineral composition [1]											
Q	12.49	3.86	7.08	8.80	6.68	8.16	----	----	41.51	1.14	4.14
OR	4.84	4.63	3.08	3.17	3.80	2.88	8.09	8.48	.13	6.22	2.99
AB	26.75	28.15	21.13	19.71	21.03	18.93	30.31	29.47	4.32	29.97	24.12
AN	29.40	21.70	25.30	26.64	25.10	27.91	18.40	20.38	17.39	18.48	24.88
WO	3.45	7.80	8.96	7.23	8.52	6.67	9.03	6.88	6.22	6.55	8.40
EN	6.42	14.97	14.77	14.37	15.22	15.19	12.19	13.97	11.93	17.11	15.51
FS	12.24	14.24	14.80	15.01	14.79	14.85	11.79	13.08	12.92	15.46	15.17
FO	----	----	----	----	----	----	2.49	1.30	----	----	----
FA	----	----	----	----	----	----	2.65	1.34	----	----	----
MT	2.28	2.62	2.72	2.75	2.72	2.75	2.80	2.72	2.36	2.83	2.78
IL	1.67	1.81	1.90	1.88	1.89	2.12	1.98	1.95	1.56	1.90	1.82
AP	.31	.28	.34	.28	.34	.31	.34	.31	.28	.31	.28
CC	.21	.07	.10	.12	.05	.16	.02	.07	1.50	.17	.02
Total	100	100	100	100	100	100	100	100	100	100	100

[1] Based on analyses recalculated to 100 percent water-free oxides; $Fe_2O_3/FeO+Fe_2O_3$ ratio assumed to be 0.15.

mafic rocks that have undergone weathering, deuteric alteration, and greenschist facies metamorphism; these studies have used concentrations of Ti and P in various combinations with concentrations of other stable trace elements, such as Zr, Y, and Nb, to characterize magma types and tectonic environments.

These stable elements are indicators of the stage of fractional crystallization during the early and middle stages of differentiation of tholeiitic magmas (Anderson and Greenland, 1969). Their contrasting patterns of variation, such as progressive enrichment in tholeiitic differentiates and depletion as contents of K_2O and SiO_2 increase in calc-alkaline lavas, are also useful as indicators of petrologic province and hence geologic setting (Anderson and Gottfried, 1971; Miyashiro, 1974; Miyashiro and Shido, 1975; Martin and Piwinskii, 1972).

The results of the present study provide further confirmation that P and Ti are relatively insensitive to processes of chemical alteration. Thus, we interpret the uniform distribution of these elements plus that of total iron (1) as a primary feature of the flows, (2) as an indication that the random variations of the other petrogenetic elements within and between the flows are a reflection of secondary alter-

ation processes, and (3) as evidence that all the rocks were originally of the same chemical composition.

NORMATIVE COMPOSITION

Plots of the normative compositions of the corehole samples in the normative diopside-hypersthene-olivine-nepheline-quartz diagram are shown in figure 1. Because hydration and attendant oxidation affect the position of the points in the diagram, the normative calculations were made on water-free oxides, and the $Fe_2O_3/(FeO+Fe_2O_3)$ ratio was assumed to be 0.15. On the basis of their normative mineralogy, two of the basalt samples are olivine-normative tholeiites, but the other nine are quartz-normative tholeiites according to the classification scheme of Yoder and Tilley (1962). The olivine-normative tholeiites (samples B–5, B–5A) and the strongly quartz-normative tholeiite (sample B–6), which together represent the opposite extremes in composition of the compositions plotted on the diagram, reflect the introduction of potassium and silica, respectively, during alteration of the marginal zones of the flows. The next most altered samples (B–7, B–1) plot on the diagram in positions intermediate between the extremely altered and the least altered samples. Inasmuch as the effects of secondary processes appear to be gradational, any distinction based on the degree of alteration is arbitrary. Analyses representing the interior parts of the flows, (samples B–2, B–3, B–4, B–8) cluster closely together in the quartz-tholeiite field. Petrographic and chemical evidence indicate that these are the least altered samples. This suggests that their composition best approximates the composition of the liquids from which they were formed. The average major-element composition of these samples is also assumed to be close to the original composition of the two lava flows. This will be discussed further when comparisons are made between basalts from CCC1 and mafic rocks representative of a variety of magma types and tectonic settings.

TRACE ELEMENTS

The results of analyses for 27 trace elements in individual samples are given in table 2. The data are subdivided according to the scheme recommended by Taylor (1965) and Taylor and White (1966) wherein elements are grouped mainly on the basis of their geochemical associations and within each group are listed according to their ionic radius and charge. As noted above, the nature of the variations of the major elements indicates a complicated history of

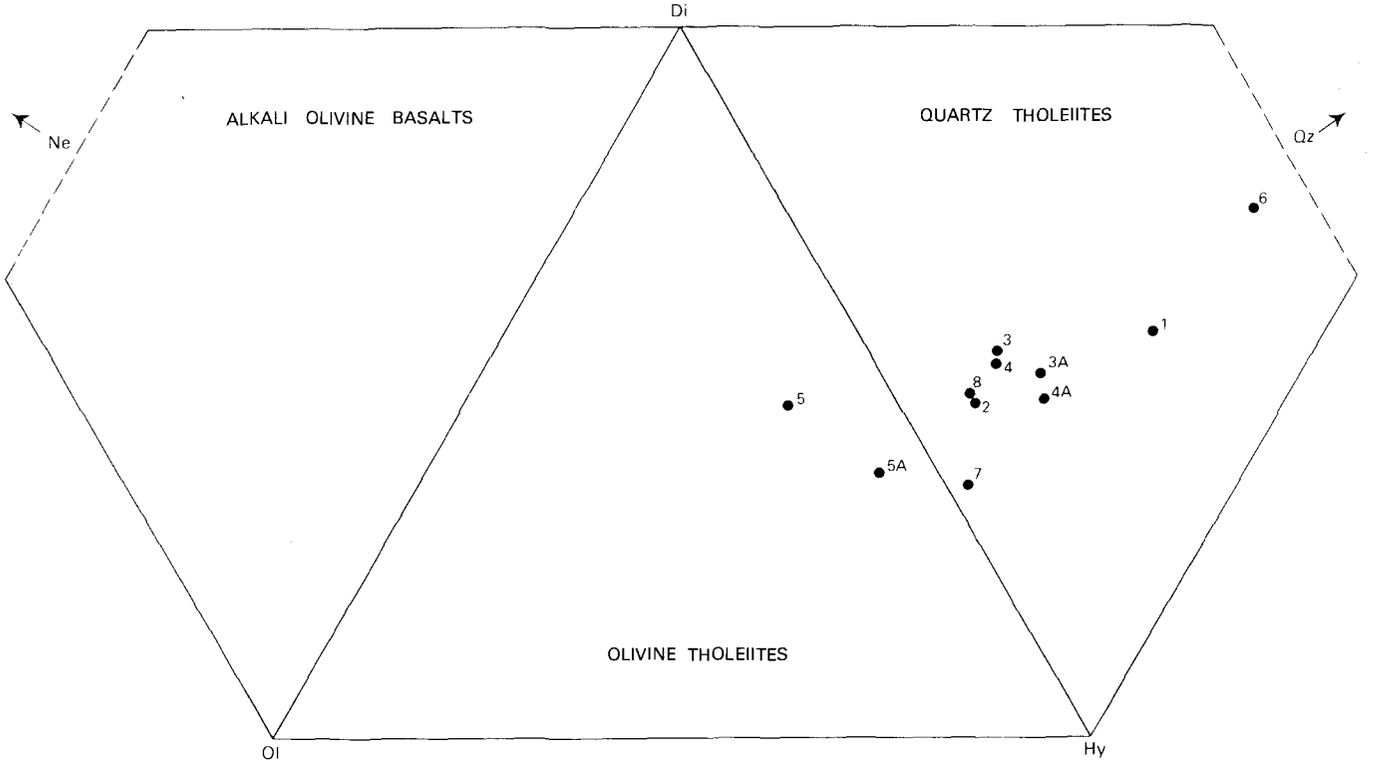

FIGURE 1.—Normative mineralogy of Clubhouse Crossroads corehole 1 basalts from table 1 (prefix B is omitted here) plotted on a diopside (Di)-hypersthene (Hy)-olivine (Ol)-nepheline (Ne)-quartz (Qz) diagram.

TABLE 2.—*Trace-element abundances, in parts per million, in basalt from Clubhouse Crossroads corehole 1 near Charleston, S.C.*

Sample No.	B-1	B-2	B-3	B-3A	B-4	B-4A	B-5	B-5A	B-6	B-7	B-8
Large cations											
Rb^{+}	2	26	14	16	19	10	43	52	0.7	34	19
Ba^{2+}	155	230	120	140	135	140	360	330	20	235	110
K^{+}	6,700	6,500	4,300	4,500	5,300	4,100	11,600	11,600	200	9,100	4,200
Sr^{2+}	140	190	200	160	200	220	160	160	40	250	160
Ca^{2+}	56,000	59,000	69,000	65,000	66,000	66,000	59,000	55,000	54,000	51,000	66,000
Pb^{2+}	5.4	5.0	5.0	3.9	4.6	4.6	4.5	4.6	4.7	3.9	4.2
K/Rb	3,400	250	310	280	280	410	270	230	285	270	220
Ba/Rb	78	8.8	8.6	8.8	7.1	14	8.4	6.3	29	6.9	5.8
K/Ba	43	28	36	32	39	29	32	35	10	39	38
High-valence cations											
Th^{4+}	1.7	1.9	2.0		2.2		2.1		1.7	2.0	2.0
Zr^{4+}	65	74	82		77		70		71	71	73
Hf^{4+}	1.6	1.8	2.1		2.1		2.0		1.7	1.7	2.0
Nb^{5+}	7.0	7.0	7.4		6.8		7.4		7.5	7.2	7.7
Ta^{5+}	.33	.28	.32		.26		.33		.18	.32	.30
$\frac{Zr}{Hf}$	41	41	39		37		35		42	42	37
$\frac{Nb \times 100}{Ti}$	.13	.13	.13		.12		.13		.16	.13	.14
$\frac{Nb}{Ta}$	21	25	23		26		22		42	22	26
Ferromagnesian elements											
Co^{2+}	35	49	47	40	46	52	42	44	42	45	43
Cu^{2+}	8	28	34	25	20	28	26	24	38	19	16
Li^{+}	16	6	7	5	14	10	16	16	36	25	11
Ni^{2+}	24	19	20	19	17	16	16	14	15	11	14
Zn^{2+}	55	80	90	84	82	96	80	82	95	78	88
Cr^{3+}	39	38	36	35	34	28	32	31	30	37	32
Ga^{3+}	26	14	15	15	15	18	14	12	16	16	15
Sc^{3+}	40	54	50	52	56	52	54	52	48	48	46
V^{3+}	210	310	310	310	320	400	400	330	310	280	250
Ni/Co	.69	.39	.43	.48	.37	.31	.38	.32	.36	.24	.33
Rare earth elements											
La	10	10	11		11		11		10	11	9
Ce	17	18	19		19		19		17	18	18
Nd	<28	<36	<36		10		10		<36	<37	<37
Sm	2.9	2.7	3.1		3.0		3.0		2.6	3.5	3.0
Eu	.99	.90	1.02		.95		.96		.75	.99	.99
Tb	.62	.61	.73		.68		.70		.59	.66	.68
Yb	1.9	1.8	2.1		2.3		2.4		1.8	2.1	2.1
Lu	.38	.42	.47		.44		.44		.38	.47	.44
Y	28	34	33		34		32		34	31	28

alteration for the lava flows; therefore it is important to evaluate the effects of alteration on the suites of trace elements before they can be used for characterization of magmatic and tectonic affinities.

LARGE CATIONS

The elements in the group of large cations that have the largest ionic radii, Rb, Ba, and K, cannot conveniently fit into the crystal structures of the major minerals (pyroxenes, plagioclase, olivine) of basaltic rocks. These elements are probably highly concentrated in interstitial material, and thus, they may be more susceptible to leaching and remobilization by geologic processes during and after crystallization. The concentrations of these elements vary the most in the altered zone (extending from sample B–5 to B–7) that straddles the contact between the upper and low flows. The patterns of abundance variations for Rb and Ba are similar to those for K. In samples from the altered zone in which the K content is relatively high, the contents of Rb (34–52 ppm) and Ba (235–360 ppm) are relatively high; in sample B–6, in which the K content is low, Rb (0.7 ppm) and Ba (20 ppm) contents are also low. An extreme depletion of Rb relative to Ba and K is found in the strongly hydrated and oxidized sample (B–1) from the top of the upper flow, although K, and to a lesser extent Ba, are somewhat enriched in this sample with respect to the least altered samples of the suite. Sample B–2, which in figure 1 is shown to be similar in normative composition to the least altered basalts, has distinctly higher Rb (26 ppm)

and Ba (230 ppm) contents than B–1 (2 ppm Rb and 155 ppm Ba), though both have essentially the same K contents. Rubidium appears to be the most sensitive indicator of alteration and is particularly useful for subdividing the heterogeneously altered flows into alteration domains. The wide variations for Rb, between adjacent samples (B–1 and B–2) from the top of the upper flow (thirteenfold) and between the top of the lower flow and adjacent samples (approximately fiftyfold), outline the extent of the alteration zones developed at the margins of the flows. In the least altered zone, the Rb variation is less than twofold (10–19 ppm). Except for the anomalously high value for the K/Rb ratio (3,400) in sample B–1, the K/Rb ratios range from 220 to 410. Because of the lack of any appreciable difference between the K/Rb ratios of the relatively unaltered samples and those of the strongly altered samples, it might be argued that the K/Rb ratio of the least altered samples does not reflect the original K/Rb ratio of the rocks. However, the original K/Rb ratio may have been modified to a limited extent because of the close geochemical coherence of these two elements in hydrothermal as well as magmatic processes. Inasmuch as the magnitude of the change is unknown, the K/Rb ratio would have to be used with caution in distinguishing between magma types.

The range of variation of Sr concentration is less than that of Rb, Ba, and K concentrations. The maximum change (fivefold) is in the lower alteration zone where Sr is strongly depleted in B–6 (40 ppm) relative to adjacent samples B–5A and B–7 (160 and 250 ppm, respectively). In this zone, the variation of Sr concentration is similar to that of the alkali metals. However, in the least altered zone and in the upper alteration zone (upper flow) the concentration pattern for Sr is nearly the same as that observed for Ca. Possible explanations for the diverse behavior of Sr are (1) Sr is in part located in sites similar to those occupied by the alkali metals; (2) Sr is incorporated to some extent in plagioclase, pyroxene, and zeolites; and (3) the nature and (or) degree of the alteration may vary in different parts of the basalt flows.

The uniformity in Pb contents (3.9 to 5.4 ppm) in the suite of samples is somewhat surprising. Lead is generally considered a K-related element in igneous rocks, and we would have expected somewhat analogous variations.

RARE-EARTH ELEMENTS

The rare-earth elements (REE) are probably the most important single group of geochemically coherent trace elements that have been used in studies on modes of origin, petrologic evolution, and tectonic setting of basaltic rocks (Frey and others, 1968; Kay and others, 1970; Schilling and Winchester, 1967; Jakeš and Gill, 1970). Moreover, prior studies have shown that the processes of weathering, low-grade metamorphism (greenschist facies), and spilitization do not change or alter the primary REE pattern (Frey and others, 1968; Kay and Senechal, 1976; Herrmann and others, 1974). It is, therefore, important to extend such studies to include the corehole basalts. The abundances of eight REE and Y were determined (by neutron-activation analysis and emission spectrography, respectively) in eight samples. The data given in table 2 indicate that the abundances are virtually the same in each of the samples, regardless of the degree of alteration. The REE data also support our previous interpretation based on the uniformity of Ti and P concentrations, that all samples were of the same composition prior to alteration. The normalized REE pattern of the basalts is shown in figure 2, in which the ratios of the average concentration for each REE in the eight samples to the average concentration of the same REE in chondrites are plotted on a logarithmic ordinate against a linear scale of the REE atomic number along the abscissa. For normalization purposes, the average concentrations of the individual REE in 20 ordinary chondritic meteorites (table 8 in Haskin and others, 1966) were used. The REE pattern of the corehole basalts shows enrichment of the light REE (La-Sm) relative to the heavy REE (Gd-Lu). A comparison of this REE pattern with those of basalts of known tectonic setting and magma type is made in a later section.

HIGH-VALENCE CATIONS

The contents of Th, Zr, Hf, Nb, and Ta are remarkably uniform in this suite of samples, except for Ta depletion in highly altered sample B–6. Their uniformity leaves little doubt about the immobility of these elements during alteration. These elements generally show threefold to fivefold increases in abundances in the course of differentiation of continental tholeiitic magmas (Gottfried and others, 1968; Eales and Robey, 1976). The constancy of these elements in the two flows again suggests the absence of any differentiation trends in the two flows. The stability of the high-valence cations is an important feature because in this study we use Zr

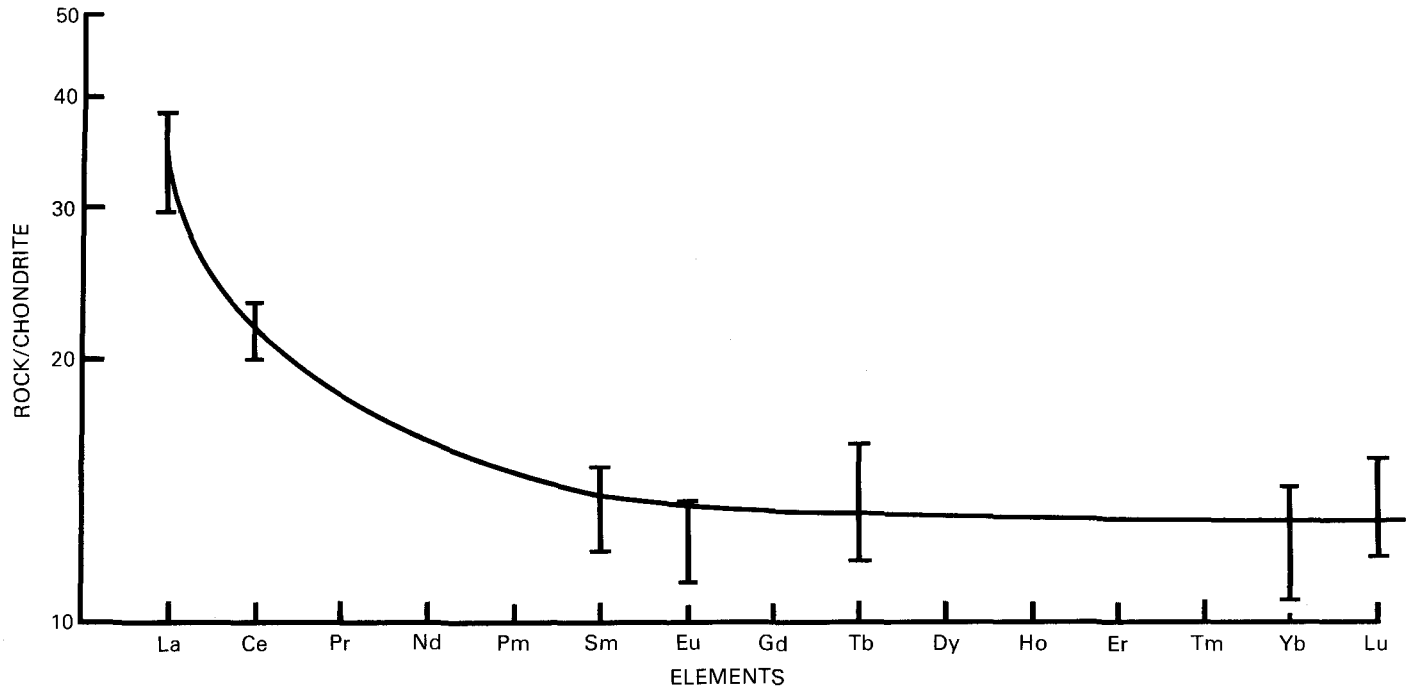

FIGURE 2.—Average abundances of rare-earth elements (REE) in basalts from the Clubhouse Crossroads corehole 1 near Charleston, S.C., normalized to average REE abundances in 20 chondrites (Haskin and others, 1966). Each vertical bar indicates the range of normalized values of eight samples.

in conjunction with other immobile minor and trace elements, in particular Ti, Y, and Nb, in our attempt to identify the tectonic setting of the volcanic rocks according to the classification scheme of Pearce and Cann (1973). Discrimination diagrams, such as Ti-Zr, Ti-Zr-Y, and Ti-Zr-Sr, have been widely utilized by many workers to investigate past environments of a wide variety of mafic rocks (Pearce, 1975; Seidel, 1974; Bickle and Nisbet, 1972; Pearce and Cann, 1971; Smewing, Simonian, and Gass, 1975; Kay and Senechal, 1976; Perfit, 1977).

FERROMAGNESIAN ELEMENTS

Features of petrologic interest in the group of ferromagnesian elements are the low abundance levels of Ni, Co, Cr, and especially Cu as compared to the average abundances given by Prinz (1967) of these elements in quartz-normative tholeiites. Although Cu is a chalcophile element, it is included here for convenience. Variations in the abundances of these elements between the least altered and strongly altered samples of the corehole basalts are generally less than twofold to threefold. The effect of alteration is readily apparent for Cu which is depleted (8 ppm) in the strongly oxidized sample (B–1) from the top of the upper flow and somewhat enriched (38 ppm) in the intensely altered sample (B–6) from the top of the lower flow relative to the least altered samples (16–34 ppm). Mobility of Cu during weathering and alteration of tholeiitic diabase from Pennsylvania has been noted by Smith and others (1975).

Copper is generally enriched in the residual liquids during tholeiitic differentiation until a copper-rich sulfide appears. This is clearly shown in the well-studied Palisades sill (Walker, 1969) and in differentiated diabase intrusions of the Tasmanian tholeiitic province (Greenland and Lovering, 1966). In the latter province, crystallization of chalcopyrite during the middle stage of differentiation resulted in strong depletion of Cu in the later differentiates (McDougall and Lovering, 1963; and McDougall, 1964). The low copper contents of the corehole basalt might reflect prior crystallization of sulfides. Sample B–1 is also depleted in cobalt, zinc, scandium, and vanadium. Chromium and scandium contents are uniform and do not appear to have been affected by alteration. Bloxam and Lewis (1972) previously noted that chromium is fairly stable during alteration. The Ni/Co ratios of the corehole basalts (0.24–0.48) are significantly lower than the Ni/Co ratios commonly found in nonorogenic tholeiitic basalts (2–3). Variation of this ratio in several tholeiitic diabase-granophyre suites has been reviewed by Fleischer (1968) who showed that the Ni/Co ratio decreases systematically during differentiation (~3

to <1) and is useful as an index of fractionation. Thus the low Ni/Co ratios and also the low Cr contents (28–39 ppm) could be accounted for if the corehole basalts represent residual liquids derived from a more primitive magma that has undergone extensive fractionation prior to eruption. However, low Ni and Co contents and low Ni/Co ratios are considered characteristic features of some calc-alkalic basalts and andesites of island arcs and active continental margins. The petrogenetic significance of these elements has been extensively discussed by Taylor (1969), Taylor and others (1969, 1971), Hedge (1971), and Marsh (1976). Taylor and others (1969, 1971) suggested that neither fractional crystallization of basalt nor partial melting of undifferentiated mantle can account for the relative abundances of these elements in orogenic magmas; they postulated a two-stage model to explain the low Ni, Co, and Cr contents and low Ni/Co ratios. Therefore, caution is required in using contents of these elements by themselves to identify magma type and tectonic setting because similar abundance relations may occur in mafic volcanic rocks of contrasting magma types (calc-alkalic and tholeiitic) and, hence, tectonic settings (orogenic and non-orogenic).

ALTERATION EFFECTS

In this study, our efforts were directed mainly at "seeing through" the effects of alteration by an empirical approach. Detailed studies of the zeolites and other secondary minerals dispersed through parts of the flow are clearly needed before we can achieve an adequate understanding of the mechanism or the nature of the alteration processes. Petrographic, mineralogic, and chemical data indicate that alteration is greatest in the marginal zones and least in the interior parts of the flows. A gross correlation exists among the degrees of alteration indicated by (1) trace-element composition, (2) megascopic examination, for example, of color variation (Gohn and others, this volume), and (3) H_2O and Fe_2O_3 contents. By analogy with alteration studies of sea-floor basalts, in which altered rims are compared with less altered interior parts of pillow fragments (Hart, 1969, 1971; Hart and others, 1974; Philpotts and others, 1969), we have compared chemical variations between margin and interior samples.

Various aspects of the effects of alteration of the major and minor elements have been discussed in preceding sections. Some of the results are summarized in figure 3, where selected major-, minor-, and trace-element concentrations in six samples from altered marginal zones are compared with the average concentration of the least altered samples from the interiors of the flows. The elements selected are those that have been used for identification of magma type or tectonic setting. They are plotted in figure 3 in order of decreasing ionic radii. In a general way, this also is their order of relative susceptibility of alteration; the larger ions are most easily altered (Rb>K≧Ba>Sr>Ca), and the REE and highly charged cations (Zr, Nb, Ti, and P) are the least easily altered. The large alkali trace elements are the most sensitive indicators of alteration, and they enhance the recognition of the existence and extent of subtle alteration effects in the flows.

Figures 3 and 4 show that the magnitude and direction of the chemical changes resulting from alteration in B–1 and B–2 (top of upper flow) are different from those of the chemical changes in B–6 (top of lower flow). The two contrasting alteration trends may be the effects of different degrees or types of alteration. The trends for B–1 and B–2 suggest a stage of alteration during which the alkali metals were added to these samples. However, continued alteration, or some later process, resulted in preferential loss of Rb relative to K and hence the anomalously high K/Rb ratio (3,400). Except for Rb loss in B–1, this alteration trend for the large-sized ions is similar to those observed in slightly weathered margins of submarine basalt fragments (Hart, 1971). The alteration trend for B–6 suggests that the top of the lower flow may have undergone alteration of a different type. Alkali metals in this sample are depleted by more than an order of magnitude relative to the least altered samples. The fractionation of Ta from Nb, as indicated by the high Nb/Ta ratio (42), is also an important feature of this sample. Samples immediately above (B–5, B–5A) and below (B–7) have alteration patterns showing relatively strong enrichment of the alkali elements and seem qualitatively to have a complementary relationship to that of sample B–6. These abrupt chemical changes along the contact zone may reflect the effects of a hydrothermal event which took place after extrusion of the upper flow. Weathering (hydration and oxidation), hydrothermal activity, and possibly low-grade metamorphism (zeolite facies) have contributed in varying degrees to the complex chemical and mineralogical changes that much of the lava flows have undergone. However it is extremely difficult, if at all possible, in some samples from the lava flows, to determine the sequence in which some of these processes occurred or to assign them correctly.

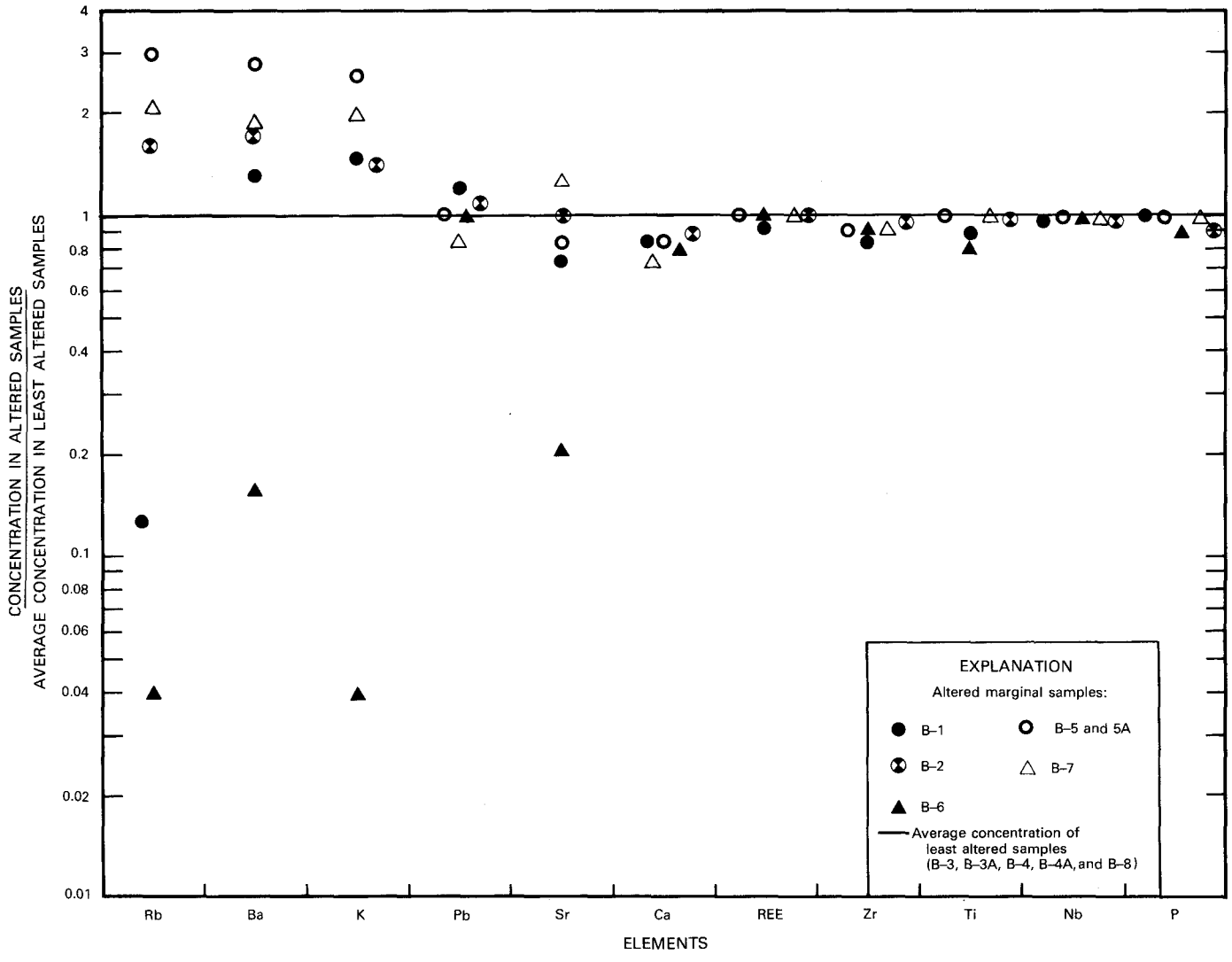

FIGURE 3.—Comparison of alteration effects on concentrations of selected elements in altered marginal samples relative to the average concentration of the less altered interior samples of the basalt flows penetrated in the Clubhouse Crossroads corehole 1 near Charleston, S.C.

AGE

Knowledge of the time of volcanism and associated tectonic activity is essential to understanding the pre-Late Cretaceous structural evolution of the Charleston area. Potassium-argon (K-Ar) whole-rock ages were determined on a fine-grained sample (B–3) from the least altered zone and an altered aphyric sample (B–5A) from the base of the upper flow. The K-Ar ages and analytical data are given in table 3. The similarity in age between the least altered sample (94.8 m.y.) and a more altered K-rich sample (109 m.y.) indicates that these are minimum ages, probably dating some posteruptive processes that have affected the volcanic rocks. These apparent ages are not in stratigraphic conflict with the Cenomanian Age (Hazel and others, this volume) of the overlying sedimentary rocks. Currently assigned estimates of the time interval of the Cenomanian Stage are 90 m.y. to 94 m.y. (Obradovich and Cobban, 1975). Prior to the detailed analysis of the geochemistry of the basalts and because of the similarity in ages of the basalts and the overlying rocks there was little reason to question the K-Ar ages. However, the possibility cannot be precluded that this similarity is fortuitous and that the basalts are significantly older than the K-Ar ages indicate.

Several investigators have evaluated the effects of alteration on K-Ar ages of basaltic rocks whose ages were well established by geologic evidence or by in-

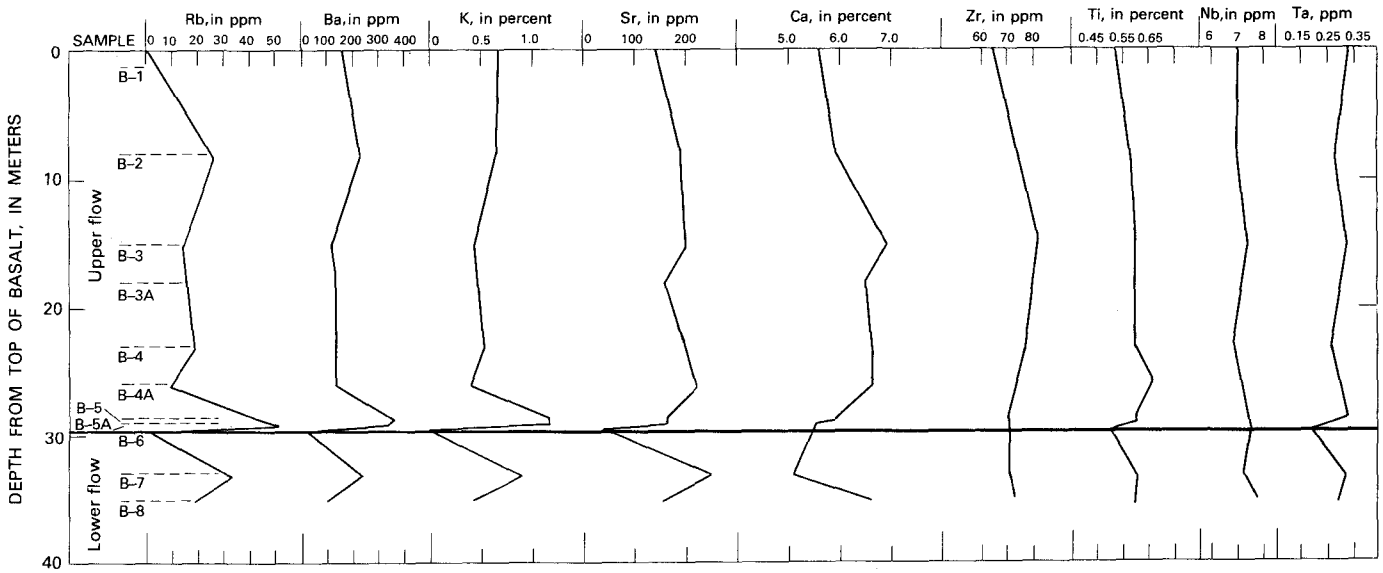

FIGURE 4.—Variations of large cations and smaller high-valence cations in samples from different depths in the two basalt flows penetrated in the Clubhouse Crossroads corehole 1 near Charleston, S.C.

TABLE 3.—*K-Ar ages and analytical data of basalts from Clubhouse Crossroads corehole 1, 32° 53.2′ N., 80° 21.5′ W., Dorchester County, S.C.*

[Analysts: R. F. Marvin, H. H. Mehnert, and Violet Merritt, U.S. Geological Survey]

Sample No.	Depth below surface (meters)	K_2O (wt. percent)	$^{1}Ar^{40}$ (10^{-10} moles/g)	$^{1}Ar^{40}$ (wt. percent)	Calculated age (m.y.)[2] ±2σ
B–3	770	0.63, 0.62 .625 avg.	0.8968	83	94.8±4.2
B–5A	785	1.37, 1.43 1.40 avg.	2.309	85	109±4

[1] Radiogenic argon.
[2] Constants: $K^{40}\lambda_\epsilon = 0.585 \times 10^{-10}$/yr.
$\lambda_\beta = 4.72 \times ^{-10}$/yr.
$K^{40} = 1.19 \times 10^{-4}$ atomic abundance.

dependent radiometric methods. Kaneoka (1972) found that rocks containing more than 1 percent $H_2O(+)$ generally show much younger ages than fresh rocks as a result of radiogenic ^{40}Ar loss due to hydration. Mankinen and Dalrymple (1972) showed that significant amounts of radiogenic ^{40}Ar have been lost from basaltic rocks in which K is concentrated in interstitial glass and which show no evidence of chemical alteration. They suggested that only holocrystalline rocks, in which K is bound in primary minerals, are suitable for age work. Low and variable K-Ar ages of Mesozoic tholeiitic basalts from Antarctica were ascribed to significant loss of radiogenic ^{40}Ar which varies inversely with amount of devitrified matrix in the samples (Fleck and others, 1977). Fleck and others (1977) found no chemical or petrographic evidence for loss or gain of K in the samples and postulated that argon loss occurred only during the devitrification process. Armstrong and Besancon (1970) discussed in some detail the problems encountered in interpreting the geologic significance of K-Ar ages for the Upper Triassic tholeiitic hypabyssal and extrusive rocks of eastern North America. They believed that, regardless of the close grouping of most of the ages between 180 m.y. and 200 m.y., the ages do not record the time of igneous activity but are probably the result of zeolite facies regional metamorphism which has affected all of the sedimentary and volcanic rocks. Taking into consideration the alteration history of the corehole basalts and the chemical and (or) petrographic criteria suggested by various geochronologists for selection of samples for age determination, we think that all of the corehole basalts and, for that matter, most of the older basalts are unsuitable for yielding reliable K-Ar ages. The age of the lavas can only be considered as pre-Late Cretaceous until additional detailed geochronological studies, such as, $^{40}Ar/^{39}Ar$ experiments, are carried out.

COMPARISON WITH BASALTS OF OTHER PROVINCES

A comparison of the major-element and selected trace-element abundances in the corehole basalts, with mean compositions of several types of basalts representative of diverse magma types and tectonic settings is shown in table 4. The composition given for the corehole basalts is the average of five samples (B–3, B–3A, B–4, B–4A, and B–8), which on the basis of petrographic and chemical criteria are the least altered. Data for basalts chosen for comparative study are taken from compilations by other authors. (See references in table 4.) Because of their proximity to the study area, compositions of the main tholeiitic magma types represented by eastern North America (ENA) chilled diabases were selected to represent continental tholeiites. Data from the well-studied continental tholeiitic province from Tasmania are also given for comparison.

MAJOR ELEMENTS

Misleading comparisons can be made using the major-element chemistry of the corehole basalts especially with regard to the alkali elements. However, some important petrochemical features appear to have been retained that are important for characterization of magma type. For example, except for the

TABLE 4.—*Geochemical comparison of basalt from the Clubhouse Crossroads corehole 1 (CCC 1) near Charleston, S.C., with basaltic rocks from other provinces*

	CCC 1 basalt	Eastern North America tholeiitic diabases				Tasmania Mesozoic tholeiitic diabase	Island arc series		Oceanic-ridge tholeiitic basalt
		High-Ti Qtz.-Norm.	High-Fe Qtz.-Norm.	Low-Ti Qtz.-Norm.	Olivine-Norm.		High-Al Calc-Alk. basalt	Tholeiitic basalt	
Major oxides (weight percent)									
SiO_2	54.0	52.1	52.7	51.7	47.9	53.4	50.59	51.57	49.9
Al_2O_3	14.0	14.2	14.2	15.0	15.3	16.4	16.29	15.91	17.3
Fe_2O_3	3.08	[1]11.6	[1]13.9	[1]11.8	[1]12.1	.52	3.66	2.74	2.01
FeO	8.56					8.32	5.08	7.04	6.9
MgO	6.01	7.41	5.53	7.44	10.5	6.72	8.96	6.73	7.3
CaO	8.99	10.66	9.86	10.8	10.7	11.49	9.50	11.74	11.9
Na_2O	2.75	2.12	2.51	2.23	2.0	1.60	2.89	2.41	2.8
K_2O	.54	.66	.64	.48	.29	.91	1.07	.44	.16
TiO_2	.97	1.12	1.14	.76	.59	.59	1.05	.80	1.5
Trace elements (parts per million)									
Rb	16	21	22	15	8	33	10	5	1
Ba	130	160	--	115	100	--	115	75	10
Sr	190	186	180	186	115	130	375	200	135
Zr	77	92	90	60	44	55	100	52	95
Hf	2.0	2.5	--	1.5	1.1	.8	2.6	1.0	2.9
Nb	7.2	9.5	8.0	5	3	5	2.5	2	5
Th	2.0	--	2.4	--	.4	3.2	1.1	.5	.18
Ni	18	81	34	48	308	67	25	12	97
Co	46	49	52	53	65	42	40	34	32
K/Rb	310	280	240	285	300	200	340	900	1,060
Nb×100/Ti	.12	.13	.12	.11	.14	.13	.05	.03	.06
Zr/Hf	39	37	--	40	40	69	38	52	33
Ni/Co	.39	1.7	.65	.91	4.7	1.3	.63	.4	3.0

Sources of data

Major elements	CCC 1 basalt	this paper, table 1, average of least altered samples (B–3, B–3A, B–4, B–4A, and B–8).
	Eastern North America tholeiitic diabases	Weigand and Ragland, 1970.
	Tasmania Mesozoic tholeiitic diabase	Edwards, 1942.
	Island arc series	Jakeš and White, 1972a, b.
	Ocean-ridge tholeiitic basalt	Engel and others, 1965.
Trace elements	CCC 1 basalt	this paper, table 2, average of least altered samples (B-3, B–3A, B–4, B–4A, and B–8).
	Eastern North America tholeiitic diabases	Weigand and Ragland, 1970; Ragland and others, 1968; Smith and others, 1975; David Gottfried, unpub. data.
	Tasmania Mesozoic tholeiitic diabase	Heier and others, 1965; Compston and others, 1968; Gottfried and others, 1968.
	Island arc series	Jakeš and White, 1970, 1972a, b; Pearce and Cann, 1973; Taylor, 1969; Gill, 1970.
	Oceanic-ridge tholeiitic basalt	Engel and others, 1965; Tatsumoto and others, 1965; Hart, 1971; Pearce and Cann, 1973; David Gottfried, unpub. data.

[1] Total Fe as Fe_2O_3.

most altered samples, the magnitude of the effects of alteration for total Fe, Mg, and Al is small compared with the variations of these elements between the corehole basalts and some other groups of basalt. The contents of Fe, Mg, and Al, thus, are still useful for comparative purposes.

To explore the relationship between magma type and tectonic setting a rank ordering of chemical similarities between the corehole basalts and the comparison basalts was obtained, following the procedure of Ragland and others (1968). The following statistics were calculated:

1. The sum, for all oxides of the quantity

$$\frac{|\%x - \%Ch|}{\%Ch}$$

2. The sum, for all oxides of the quantity

$$\frac{(\%x - \%Ch)^2}{\%Ch}$$

where $\%x$ is the oxide abundance in the comparison basalt and $\%Ch$ is the oxide abundance in the corehole basalt. The two comparison numbers obtained permit a rank ordering of the comparison basalts compared to the corehole basalts; the smaller values indicate closer similarity between the comparison basalts and the corehole basalts. Results of the comparison are given in table 5 in which the comparison basalts are listed according to this rank-ordering. This rank-ordering shows that the corehole basalts are most similar to the Mesozoic continental high-Fe-Ti quartz-normative tholeiitic diabases from eastern North America.

TABLE 5.—*Rank ordering of chemical similarities between basalts from the Clubhouse Crossroads corehole 1 near Charleston, S.C., and selected comparison basaltic rocks*

Comparison basalts [1]	$\sum \frac{\lvert \%x - \%Ch \rvert}{\%Ch}$		$\sum \frac{(\%x - \%Ch)^2}{\%Ch}$	
	Value	Rank	Value	Rank
ENA[2] High-Fe, quartz-normative tholeiitic diabase	0.76	1	0.58	1
ENA[2] High-Ti, quartz-normative tholeiitic diabase	1.15	2	.97	2
ENA[2] Low-Ti, quartz-normative tholeiitic diabase	1.15	2	1.19	3
Island arc, tholeiitic basalt	1.26	3	1.68	4
Island arc, high-Al, calc-alk. basalt	2.13	4	3.41	6
Tasmania Mesozoic tholeiitic diabase	2.26	5	2.59	5
ENA[2] olivine-normative tholeiitic diabase	2.32	6	5.14	8
Oceanic-ridge tholeiitic basalts	2.32	6	3.46	7

[1] Data from table 4, Fe as FeO, and analyses recalculated water-free.
[2] ENA = Eastern North America.

TRACE ELEMENTS

For the most part, variations in trace elements in these basaltic provinces can be related to (1) the composition and mineralogy of the source region and (2) the degree of partial melting and subsequent fractional crystallization during ascent of magma in the mantle and in the crust. Other factors that may play a role are "wall rock reaction," which is discussed in detail by Green and Ringwood (1967), and contamination resulting from interaction of basaltic magma with rocks of the continental crust (Faure and others, 1974). Although these processes affect the major-element chemistry to some extent, the trace-element concentrations are affected much more and, more importantly, can provide clues to the history and origin of basalts that are not readily observed from the relations among the major elements.

Comparison of the trace-element data in table 4 indicates that the corehole basalts show the greatest similarity to the ENA quartz-normative diabases, in particular to the high-Fe and high-Ti types. Wiegand and Ragland (1970) and Ragland, Brunfelt, and Weigand (1971) regarded the ENA high-Fe type as a subgroup of the ENA high-Ti group with which it shares similarities (REE, Ti, Rb, Sr, Zr, Co) but from which it is different in having a lower Ni content and hence a lower Ni/Co ratio. The corehole basalts are closer in composition to the high Fe-type than to the high-Ti type. A close similarity exists between the corehole basalts and the high-Fe type in abundances of stable minor and trace elements (Ti, Zr, Hf, Nb) and of mobile elements (K, Rb), as well as in the unusually low Ni/Co ratios. This similarity can be extended to include Cu which, as noted previously (table 2), is unusually low in the corehole basalts (~25 ppm). In high-Fe types, Cu decreases as the Ni/Co ratio decreases to values as low as 37–44 ppm (Weigand and Ragland, 1970).

A comparison of the REE pattern of the corehole basalts (from fig. 2) with average REE patterns for the ENA high-Ti quartz-normative diabase (an average which includes the high-Fe type), ENA olivine-normative diabase, and oceanic-ridge tholeiitic basalts is shown in figure 5. The abundances and REE pattern for the corehole basalts and for the ENA high-Ti type are virtually the same. The REE pattern for the ENA olivine-normative type is similar to that for the high-Ti type but is distinctly lower in absolute abundance. Light-REE enriched patterns intermediate between those of the

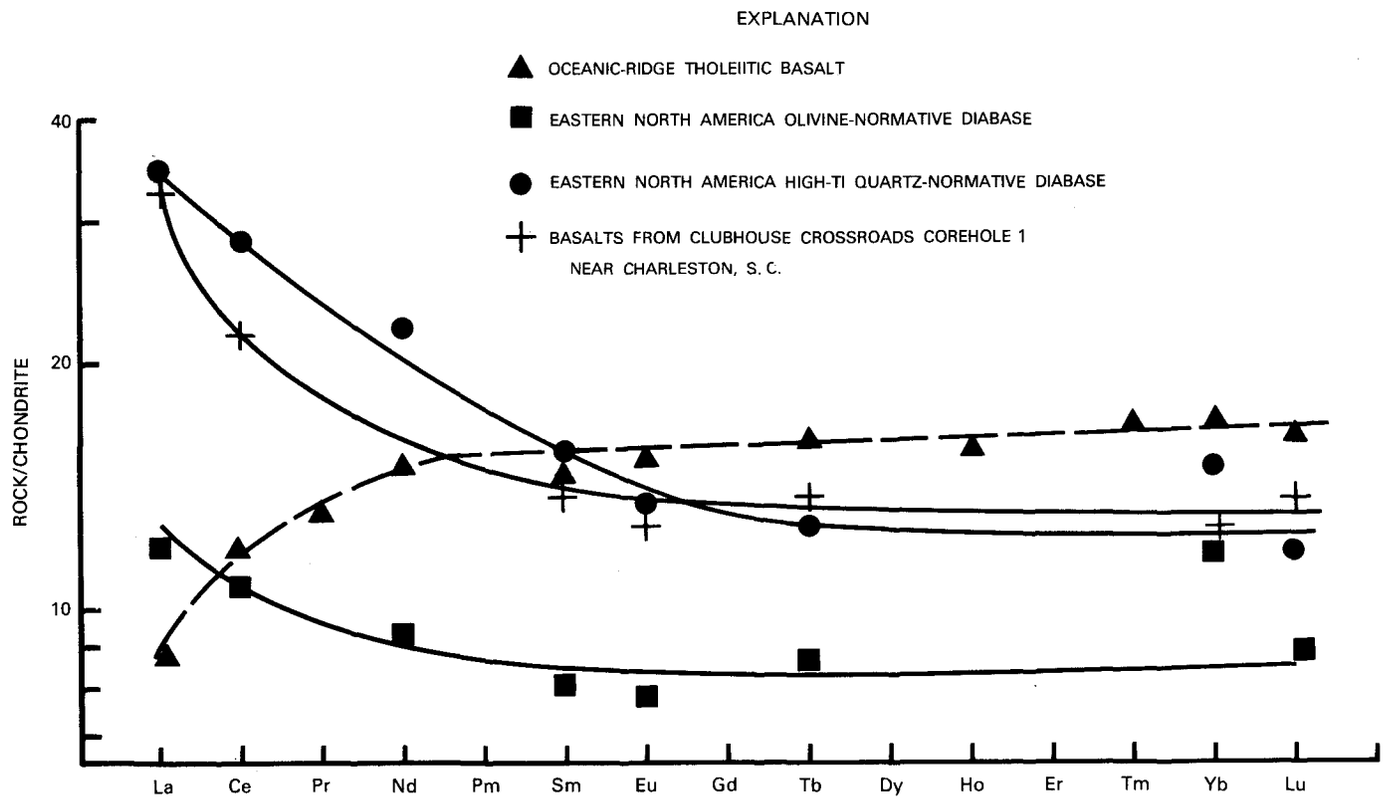

FIGURE 5.—Average abundances of rare-earth elements (REE) in tholeiitic diabases and basalts normalized to average REE abundances in 20 chondrites (Haskins and others, 1966). Data sources: oceanic-ridge tholeiitic basalt (Schilling, 1971); eastern North America olivine-normative diabase and eastern North America high-Ti quartz-normative diabase (Ragland, Brunfelt, and Weigand, 1971); and basalts from Clubhouse Crossroads corehole 1 near Charleston, S.C., table 2 (this paper).

high-Ti and olivine-normative types characterize the low-Ti type (fig. 4 in Ragland, Brunfelt, and Weigand, 1971; Ragland, Weigand, and Brunfelt, 1971). The light-REE depleted patterns of oceanic-ridge tholeiitic basalt (fig. 5) are in sharp contrast to the light-REE enriched patterns of the corehole basalts and ENA high-Ti and olivine-normative tholeiitic types. Other trace-element contents and interelement ratios that clearly distinguish the corehole basalts and the ENA tholeiitic diabases from oceanic-ridge tholeiitic basalts are higher Rb, Ba, and Th contents, higher Nb/Ti ratios, and lower K/Rb ratios. However, the abundance levels for Nb, Zr, and heavy REE (Sm-Lu) are either similar or even lower in the ENA low-Ti type, ENA olivine-normative type, and Tasmanian tholeiitic diabase than in the average oceanic- ridge tholeiitic basalt. Depletion of trace elements of large ionic radii such as Cs, Rb, Ba, Th, and U and the high K/Rb, K/Ba, and K/Cs ratios have led to the interpretation that the oceanic-ridge tholeiitic basalt was derived from a source in the mantle that had previously undergone one or more periods of partial melting (Tatsumoto and others, 1965; Gast, 1968; Hart, 1969, 1971; Hart and others, 1970). These geochemical features once considered unique to the worldwide oceanic-ridge system have also been recognized in volcanic suites, designated by Jakeš and Gill (1970) as the island arc tholeiitic series. The REE patterns of these rocks are indistinguishable from those of the oceanic-ridge tholeiitic basalt (Jakeš and Gill, 1970), as are several other geochemical features shown in table 4.

Thus far, it can clearly be shown that the corehole basalt is neither an ocean-floor basalt that originated from the mid-Atlantic ridge system nor a basaltic rock with affinities to the island arc tholeiite series. The corehole basalt, and for that matter, the ENA quartz-normative types, have many features in common with basalt, or basaltic andesite, of the calc-alkalic series of island arcs. These include the low Ti, Ni, Co, and Cr contents, which, as previously mentioned, are considered distinctive of the calc-alkalic basalts (table 4) and andesites. They

also have similar K/Rb ratios (Jakeš and White, 1970) and light-REE enrichment patterns (Jakeš and Gill, 1970). However, important differences that can be observed are the generally higher K_2O, Al_2O_3, and Sr abundances in the calc-alkalic basaltic rocks, than in the ENA high-Ti and high-Fe quartz-normative diabases. These differences may be related to differences in water pressure and oxygen fugacity of the magmas from which they formed. The higher water content in calc-alkalic magmas favors crystallization of large amounts of plagioclase (Yoder, 1969) which results in the higher Al and Sr contents. The presence of low Ni, Co, Cr, and Cu in the continental ENA high-Ti quartz-normative diabase cannot be explained by the two-stage model of Taylor (1969) which involves partial melting of oceanic crust carried down the Benioff Zone in an island arc environment. The geochemical data indicate that the ENA and corehole basalt magmas were derived from a mantle undepleted with regard to the lithophilic elements. We suggest that prior to extrusion, olivine and copper-bearing minerals may have crystallized and depleted the Ni, Co, Cr, and Cu of the magma. Studies of immiscible sulfide melts and polymineralic sulfide minerals from Hawaiian tholeiitic basalts (Skinner and Peck, 1969; Desborough and others, 1968) indicate that crystallization of chalcopyrite and Cu- and Ni-rich pyrrhotite solid solutions has taken place. These studies, and those referred to earlier, show that these features are the result of late-stage fractionation processes of basaltic magma.

The (Nb×100)/Ti ratio (0.05) in high-Al basalts (from data in Pearce and Cann, 1973) is lower than that in the corehole basalts (0.12) and continental tholeiites (0.11 to 0.14). This ratio may serve as a useful discriminant because it remains relatively constant during the early and middle stages of differentiation of tholeiitic magmas (Gottfried and others, 1968). Variation of Zr/Hf in the comparison suites, with the exception of suites of the Tasmanian province, has not yet been adequately documented and at this stage provides no more information than Zr alone.

The preceding discussions of the implications of the geochemical data with regard to magma type can be summarized as follows: (1) the corehole basalts can be classified as quartz-normative tholeiites and were derived from an undepleted source area, presumably the upper mantle; (2) striking similarities between major-element, trace-element, and REE compositions of the corehole basalts and those from the Mesozoic ENA tholeiitic province indicate that the corehole basalts are continental tholeiitic basalts.

TECTONIC SETTING

In recent years, extensive geochemical studies have shown that young mafic volcanic rocks in a given geographic or geologic setting have consistent or characteristic geochemical features that characterize their tectonic setting. These studies have led to the recognition of several trace elements that were shown to be relatively insensitive to alteration processes and that were characteristic of magma type and tectonic setting. Subsequently, the abundance patterns of these trace elements were used to construct binary or ternary discrimination diagrams which allowed comparisons to be made between trace-element abundances in an unknown rock and those in volcanic rocks of known tectonic setting. The volcanic rocks are generally classified according to a scheme that combines tectonic setting and chemical characteristics (Pearce and Cann, 1973). Tectonic setting is based on the relative motions of lithospheric plates. Thus mafic volcanic rocks are designated as (1) ocean-floor basalts (diverging plate margins), (2) low-K tholeiites and calc-alkalic basalt of the island arc series (converging plate margins), and (3) oceanic island and continental basalts (intraplate oceanic crust and intraplate continental crust). Elements generally used are Ti, Zr, Y, Nb, P and, also, K and Sr in situations where the rocks are considered unaltered (Pearce and Cann, 1973; Floyd and Winchester, 1975; Winchester and Floyd, 1976; Pearce and others, 1975). The most widely applied discrimination diagrams are the Ti-Zr, Ti-Zr-Y, and Ti-Zr-Sr diagrams of Pearce and Cann (1973).

The results of plotting the abundances of these elements in the corehole basalts and in some comparison continental basalt samples on these three diagrams are presented in figure 6. The comparison samples include basalts or chilled diabases from the eastern North America, Tasmania, Antarctica, and Karroo tholeiitic provinces. The Ti and Zr values for the corehole basalts and ENA high-Ti types plot in fields B and C on the Ti-Zr diagram (fig. 6*A*) which would indicate the samples are calc-alkalic basalts of the island-arc series. The other continental tholeiitic diabases show affinities to island arc tholeiitic basalt or ocean-floor basalt. Figure 6*B* (Ti-Zr-Y) shows that the corehole basalts are in the field of ocean-floor basalts; the diabase from

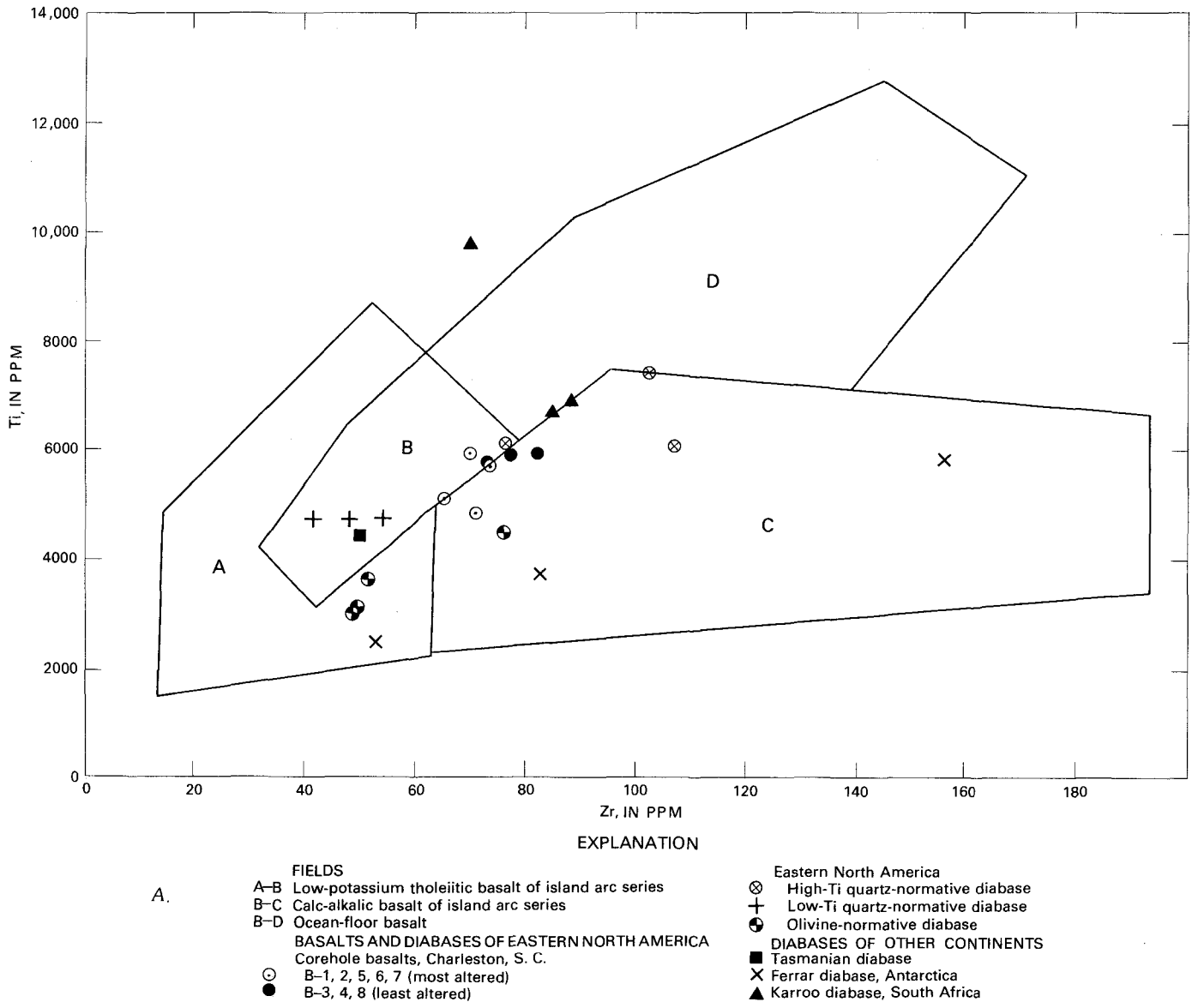

FIGURE 6.—Samples of corehole basalts and some tholeiitic basalts and diabases from continental provinces plotted on discrimination diagrams of Pearce and Cann (1973). *A*, Samples plotted on the Ti-Zr discrimination diagram. Data sources: basalts from Clubhouse Crossroads corehole 1 near Charleston, S.C., tables 1 and 2 (this paper); eastern North America (ENA), table 3 of Ragland, Brunfelt, and Weigand (1971); Great Lake sheet, Tasmania, McDougall (1964), Gottfried ond others (1968); Ferrar diabase, Gunn (1966); Karroo basalts of southern province, South Africa, table 3 of Cox and others (1967). *B*, Plot of corehole basalts and chilled diabase of Palisades sill on Zr-Ti-Y discrimination diagram. Note that the corehole basalts and chilled margin of the Palisades sill (Walker, 1969) plot in fields B and C, respectively. *C*, Samples of corehole basalts and diabases from eastern North America plotted on Zr-Ti-Sr diagram.

the Palisades sill is in the field of calc-alkalic basalts. In figure 6*C* (Ti-Zr-Sr), the samples cluster at or near the junctions of the fields: ocean-floor basalt, island arc tholeiitic basalt, and calc-alkalic basalts of the island-arc series. It is thus clear that these diagrams are inappropriate for identification of tectonic setting and magma type of these types of continental tholeiites.

Each of the continental tholeiitic magma types that we used for comparison occurs on Atlantic-type passive continental margins and represents the early cycles of magmatism that preceded or coincided with rifting, continental drift, and sea-floor spreading. A comparison between the chondrite-normalized REE abundance pattern for the corehole basalts and the chondrite-normalized REE

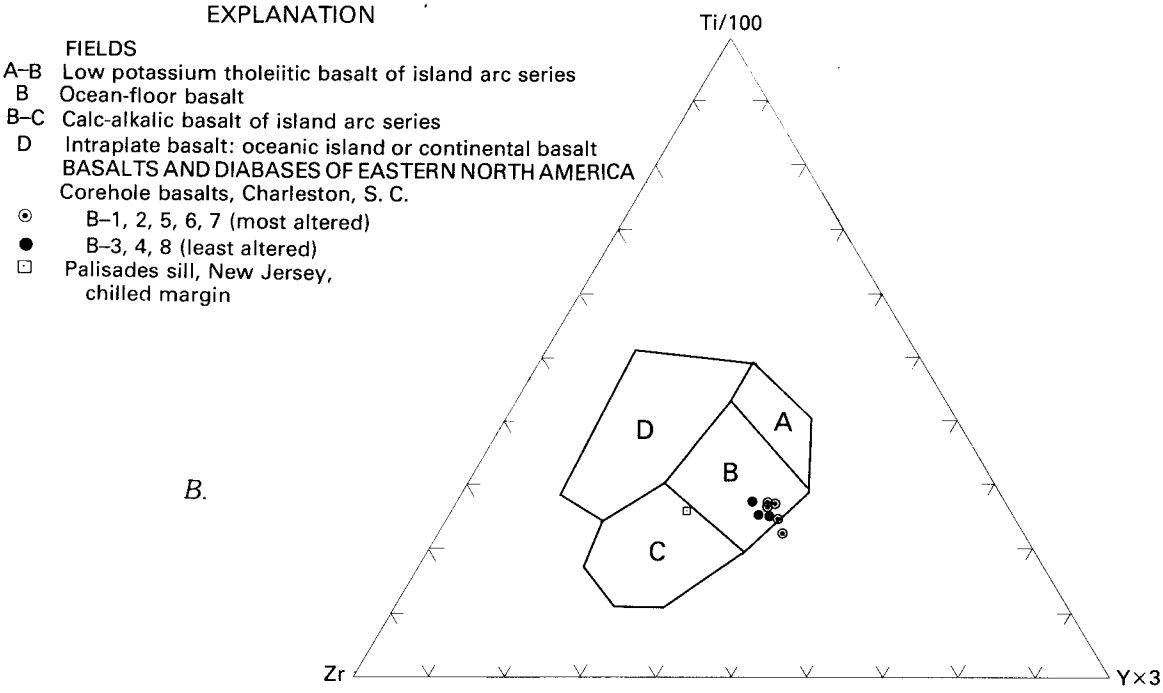

B.

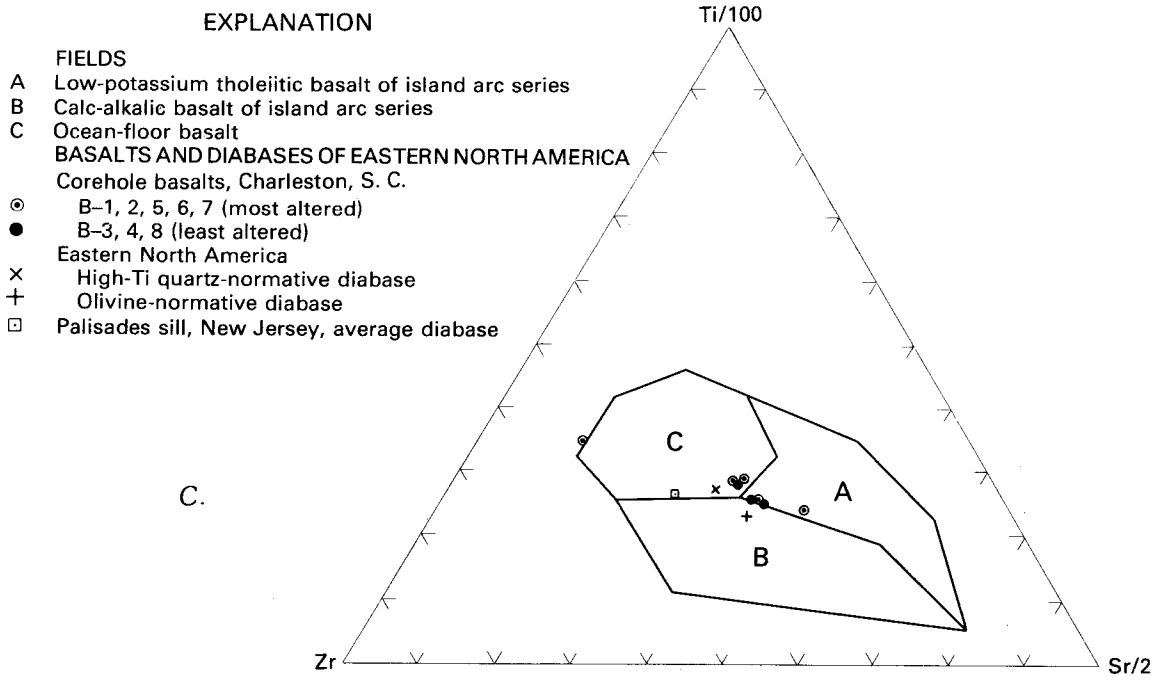

C.

abundances for the Karroo, Ferrar, and Red Hill diabases (Philpotts and Schnetzler, 1968) is shown in figure 7. Plots of the REE data for each of these suites are on a single variation curve and show that the suites are indistinguishable from each other on the basis of their REE variation patterns.

Other important geochemical features shared by the corehole basalts, rocks of the ENA tholeiitic

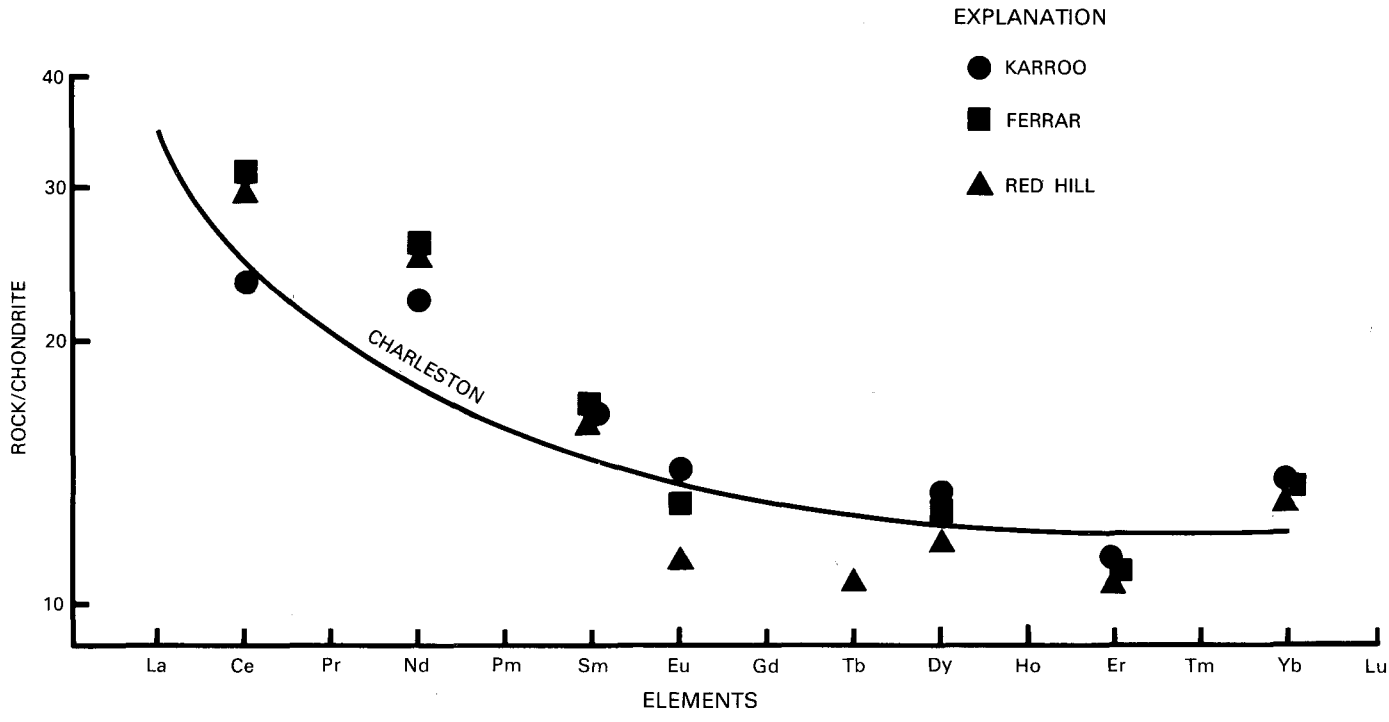

FIGURE 7.—Comparison of chondrite-normalized rare-earth element (REE) abundance patterns in basalts from Clubhouse Crossroads corehole 1 near Charleston, S.C. (see fig. 2, this paper), with average REE abundances of chilled margins of Karroo diabase, South Africa; Ferrar diabase, Antarctica; and Red Hill diabase, Tasmania (Philpotts and Schnetzler, 1968).

province, and the Tasmanian-Antarctic and Karroo tholeiitic rocks are their unusually low abundances of Ti, Nb, and Zr. Schilling (1971) suggested that the relatively low abundances of REE in the chilled diabases of these provinces might be related to differences between extrusive and intrusive crystallization regimes. This difference in regime appears not to be the reason for different REE patterns because the REE patterns and absolute abundances are essentially the same in the Palisades diabase (Philpotts and Schnetzler, 1968) and in the Watchung Basalt flow (Donnelly and others, 1973). Furthermore, Smith, Rose, and Lanning (1975) found that flows, sills, and dikes of the high-Ti quartz-normative magma type in Pennsylvania are nearly identical in chemical composition. For comparisons with the corehole basalts, we selected samples or suites of continental rocks of similar composition to minimize effects of fractional crystallization or other differentiation processes on the abundance variations. The petrogenetic implications of the similar or lower abundance levels of lithophilic elements of small ionic radii (Ti, Zr, Hf, Nb, Ta) in a Tasmanian diabase-granophyre suite as compared to those in oceanic-ridge tholeiitic basalt were discussed previously (Gottfried and others, 1968). Ragland, Brunfelt, and Weigand (1971) showed that the olivine-normative tholeiitic dikes from North Carolina have half the absolute REE concentrations of oceanic-ridge tholeiitic basalt. Smith and others (1975) pointed out similarities between the low-Ti quartz-normative diabase and island arc tholeiitic basalt.

The rocks selected by Pearce and Cann (1973) for establishing the field of continental basalts on their discrimination diagrams are from the African Rift Valley, Karroo, and Deccan provinces. Their mean contents in parts per million for Ti (15,150); Zr (215), and Nb (20) are at least twice those of the abundances found in the corehole basalts, in the chilled margins of the sills and dikes of the ENA province, and in the Tasmanian province. In the Red Sea region, which is considered the modern analog of early Mesozoic rifting and continental drift, magma associated with rifting and crustal extension was dominantly of the alkalic basalt type, and magma in the median trough of the Red Sea was tholeiitic (Gass, 1970; Mohr, 1972). The REE patterns of the tholeiites from the Red Sea trough are similar to those of basalts from the oceanic-ridge system (Schilling, 1969; 1973). Both the

Karroo and Deccan provinces contain a wide range of tholeiitic basalts as well as intermediate, felsic, and undersaturated alkalic rocks (Ghose, 1976; Cox, 1970). Clearly, the basalts (containing 328 ppm Zr and 27 ppm Nb) of the Karroo province selected by Pearce and Cann (1973) are more strongly fractionated than the Karroo samples we selected for comparison. A similar situation may exist with regard to REE abundances in the Deccan basalts. The REE pattern for the Deccan basalt given by Frey and others (1968) was considered "typical" of continental basalts but shows light REE absolute abundances two to three times those shown by the comparison suites shown in figure 7 and is more similar to that of alkalic basalts. The REE pattern of the average Deccan plateau basalt given by Nakamura and Masuda (1971) is believed to be more representative of the province and shows REE abundances similar to those of our comparison quartz-normative tholeiites. The examples noted above indicate that part of the data used for characterizing continental basalt provinces seems to have given misleading impressions about the representative geochemical features for some continental tholeiitic provinces.

The preceding discussion noted that most of the suites of samples selected for construction of the discrimination diagrams discussed previously represented magmas of alkalic affinity or highly evolved tholeiitic magmas. By way of contrast, the tholeiitic magmas of Mesozoic age in eastern North America represent perhaps the most primitive end of the spectrum of tholeiitic magma types erupted into continental crust. This is particularly true for the olivine-normative type (Ragland and others, 1972; Ragland, Weigand, and Brunfelt, 1971; Gottfried and Greenland, 1972). By virtue of the striking similarities of geochemical features of the corehole basalts with those of the quartz-normative tholeiitic magmas of this province, it is reasonable to assume a similar mode of origin and tectonic environment at the time of extrusion. The similarity of K-Ar ages of the corehole basalt and the age of the overlying sediments presents a knotty problem. Although we considered the K-Ar age (~100 m.y.) as a minimum age because of posteruption alteration effects, it could be argued that alteration occurred shortly after extrusion and that the basalt is of Cretaceous age. However, on the basis of their characteristic geochemical features, we suggest that the corehole basalts are related to the tholeiitic province of eastern North America in time as well as space. The age of the quartz-normative tholeiites in the northern part of the province is Late Triassic or Early Jurassic on the basis of geologic and paleontologic evidence (Johnson and McLaughlin, 1957; Cornet and others, 1973). In general, it is believed that the magmas representing these tholeiitic flows, sills, and dikes were intruded at the onset of rifting and separation of North America from North Africa (Faust, 1975). Evidence from deep drilling and magnetic anomaly patterns indicate that continental drift began 180 m.y. ago (Pitman and Talwani, 1972; Vogt, 1973). Magmatism, rifting, and an extensional tectonic regime were associated with upwelling of the mantle and a steep geothermal gradient. A rather high degree of partial melting of the upper mantle in this area of high heat flow could account for the "primitive" nature of the ENA tholeiitic magmas and their intrinsic geochemical features. If the corehole basalt is approximately 100 m.y. old, then volcanism took place after the continental margin moved progressively further from the spreading axis. It is reasonable to assume that the petrochemical features of later formed magma types would be different because of differences in the thermal regimes that prevailed at the time of their formation.

SUMMARY AND CONCLUSIONS

The results of our geochemical study of 11 corehole samples can be summarized as follows:

1. Major- and minor-element and petrographic data indicate that the basalts have undergone slight to extreme oxidation, hydration, and hydrothermal alteration. Effects of these processes are strongest on the marginal zones of the flows and are reflected mineralogically by the presence of zeolites, calcite, and chlorite, and chemically by high abundances of H_2O, Fe_2O_3, and CO_2 and by remobilization of K, Ba, Rb, and Sr. Rubidium is the most sensitive indicator of alteration and is useful for assessing the degree and extent of alteration in the flows. The minor elements P and Ti and the trace elements Zr, Nb, Hf, Th, and REE are essentially uniform in the two flows and indicate the absence of any in situ differentiation trends. Normative compositions of the least altered samples indicate that the basalts are of the quartz-normative tholeiitic magma type.
2. The major-element and trace-element composition of the corehole basalts is compared with available data on rocks of theoleiitic composition from Atlantic-type, passive continental

margins (eastern North America, Tasmania, Antarctica, South Africa) and on basalts from island arc (calc-alkalic basalt, low-potassium tholeiitic basalt) and mid-oceanic ridge settings. The light REE enrichment pattern and low K/Rb ratio (~300) of the corehole basalts contrast markedly with corresponding data on island arc tholeiitic basalt and oceanic-ridge basalt which characteristically are depleted in light REE and have high K/Rb ratios (~950–1050). These data indicate that the corehole tholeiitic magma was derived from an undepleted source area in the upper mantle. Some geochemical features believed to be characteristic of orogenic high-Al basalts and andesites are shared by both the corehole basalts and the high-Fe quartz-normative tholeiitic diabase of the eastern North America province. These include low Ti, Cr, Cu, Ni, and Co contents and low Ni/Co ratios. We attribute some of these features to low-pressure fractional crystallization processes involving separation of olivine and Cu- and Ni-bearing sulfides during magmatic ascent. On the basis of the REE pattern, as well as absolute abundances, the corehole basalts are virtually indistinguishable from the quartz-normative tholeiitic rocks from eastern North America, Karroo (South Africa), Ferrar (Antarctica), and Red Hill (Tasmania).

3. The low abundances of ions of relatively small ionic radii, (Ti, Zr, Hf, Nb, and Ta) in the corehole basalts and in our comparison suites of continental tholeiites are more similar to those found in island arc and oceanic-ridge basalts than to "average" abundances in continental basalts. As a result of these primitive features, Mesozoic continental tholeiitic diabases from eastern North America, Tasmania, and Antarctica would be erroneously classified as oceanic-ridge and (or) island arc tholeiites on the basis of their Ti-Zr-Nb abundance relations. In the present study, no single group or pair of geochemically associated elements could be used alone for distinguishing magma type and tectonic setting of the corehole basalts from basalts of all of the contrasting tectonic environments considered. This emphasizes the importance of using trace elements of widely different chemical properties and sizes for discrimination purposes.
4. K-Ar analyses of two whole-rock samples yield ages of 94.8 m.y. for the least altered sample, and 109 m.y. for an altered K-rich sample. These dates are considered minimum ages which may be significantly younger than the time of volcanism.

Geochemical data on the corehole basalts constitute a substantial body of information which has placed certain constraints on proposed models of the regional tectonic setting. The geochemical features of the basalts suggest to us that they are related in space and time to the tholeiitic province of eastern North America and have features in common with quartz-normative tholeiitic suites found on other rifted continental margins. The tectonic regime associated with magmatic activity during early rifting is dominated by extensional tectonics. Flows, dikes, and sills of the eastern North America province are closely associated with Triassic-Early Jurassic rift valleys and deep-seated grabens. Geophysical studies and limited chemical and radiometric age data indicate that mafic flows and dikes are found in similar structural settings which underlie the Coastal Plain of the southeastern United States (Barnett, 1975; Milton and Hurst, 1965; Milton, 1972; Marine and Siple, 1974) and the Gulf of Maine (Ballard and Uchupi, 1975). The primary geochemical features of the corehole basalts may be taken as an indication of the presence of a buried Triassic-Jurassic basin beneath the Charleston area. The secondary features (hydrothermal alteration effects and minimum ages) may reflect postmagmatic processes associated with later tectonic activity.

REFERENCES CITED

Anderson, A. T., and Gottfried, David, 1971, Contrasting behavior of P, Ti, and Nb in a differentiated high-alumina olivine tholeiite and a calc-alkaline andesitic suite: Geol. Soc. America Bull., v. 82, no. 7, p. 1929–1942.

Anderson, A. T., and Greenland, L. P., 1969, Phosphorus fractionation diagram as a quantitative indicator of crystallization differentiation of basaltic liquids: Geochim. et Cosmochim. Acta, v. 33, no. 4, p. 493–505.

Annell, C. S., 1964, A spectrographic method for the determination of cesium, rubidium, and lithium in tektites, *in* Geological Survey research 1964: U.S. Geol. Survey Prof. Paper 501–B, p. B148–B151.

——— 1967, Spectrographic determination of volatile elements in silicates and carbonates of geologic interest, using an argon d-c arc, *in* Geological Survey research 1967: U.S. Geol. Survey Prof. Paper 575–C, p. C132–C136.

Armstrong, R. L., and Besancon, James, 1970, A Triassic time scale dilemma; K-Ar dating of Upper Triassic mafic igneous rocks, Eastern U.S.A. and Canada and post-Upper Triassic plutons, western Idaho, U.S.A.: Eclogae Geol. Helvetiae, v. 63, no. 1, p. 15–28.

Baedecker, P. A., 1976, SPECTRA: Computer reduction of gamma-ray spectroscopic data for neutron activation analysis, *in* Taylor, R. E., ed., Advances in obsidian glass studies: Park Ridge, N. J., Noyes Press, p. 334–349.

Ballard, R. D., and Uchupi, Elazar, 1975, Triassic rift structure in Gulf of Maine: Am. Assoc. Petroleum Geologists Bull., v. 59, no. 7, p. 1041–1072.

Barnett, R. S., 1975, Basement structure of Florida and its tectonic implications: Gulf Coast Assoc. Geol. Socs. Trans., v. 25, p. 122–142.

Bastron, Harry, Barnett, P. R., and Murata, K. J., 1960, Method for the quantitative spectrochemical analysis of rocks, minerals, ores, and other materials by a powder d-c arc technique: U.S. Geol. Survey Bull. 1084–G, p. 165–182.

Bickel, M. J., and Nisbet, Euan, 1972, The oceanic affinities of some alpine mafic rocks based on their Ti-Zr-Y contents: Geol. Soc. London Quart. Jour., v. 128 pt. 3, p. 267–271.

Bloxam, T. W., and Lewis, A. D., 1972, Ti, Zr, and Cr in some British pillow lavas and their petrogenic affinities: Nature: Physical Sci., v. 237, no. 78, p. 134–136.

Cann, J. R., 1970, Rb, Sr, Y, Zr and Nb in some ocean-floor basaltic rocks: Earth and Planetary Sci. Letters, v. 10, no. 1, p. 7–11.

Compston, W., McDougall, Ian, and Heier, K. S., 1968, Geochemical comparison of the Mesozoic basaltic rocks of Antarctica, South Africa, South America, and Tasmania: Geochim. et Cosmochim. Acta, v. 32, no. 2, p. 129–149.

Cornet, Bruce, Traverse, Alfred, and McDonald, N. G., 1973, Fossil spores, pollen, and fishes from Connecticut indicate Early Jurassic age for part of the Newark Group: Science, v. 182, no. 4118, p. 1243–1247.

Cox, K. G., 1970, Tectonics and vulcanism of the Karroo Period and their bearing on the postulated fragmentation of Gondwanaland, *in* Clifford, T. N., and Gass, I. G., eds., African magmatism and tectonics: Darien, Conn., Hafner Pub. Co., p. 211–235.

Cox, K. G., Macdonald, R., and Hornung, G., 1967, Geochemical and petrographic provinces in the Karroo basalts of southern Africa: Am. Mineralogist, v. 52, no. 9–10, 1451–1474.

Desborough, G. A., Anderson, A. T., and Wright, T. L., 1968, Mineralogy of sulfides from certain Hawaiian basalts: Econ. Geology, v. 63, no. 6, p. 636–644.

Donnelly, T. W., Melson, William, Kay, Robert, and Rogers, J. J. W., 1973, Basalts and dolerites of Late Cretaceous age from the central Caribbean, *in* California Univ., Scripps Institution of Oceanography, La Jolla, Initial reports of the Deep Sea Drilling Project, Volume XV: Washington, D.C., Natl. Sci. Foundation, p. 989–1013.

Eales, H. V., and Robey, J. van A., 1976, Differentiation of tholeiitic Karroo magma at Birds River, South Africa: Contr. Mineralogy and Petrology, v. 56, no. 1, p. 101–117.

Edwards, A. B., 1942, Differentiation of the dolerites of Tasmania, I.; Jour. Geology, v. 50, no. 5, p. 451–480.

Engel, A. E. J., Engel, C. G., and Havens, R. G., 1965, Chemical characteristics of oceanic basalts and the upper mantle: Geol. Soc. America Bull., v. 76, no. 7, p. 719–734.

Faure, G., Bowman, J. R., Elliot, D. H., and Jones, L. M., 1974, Strontium isotope composition and petrogenesis of the Kirkpatrick Basalt, Queen Alexandra Range, Antarctica: Contr. Mineralogy and Petrology, v. 48, no. 3, p. 153–169.

Faust, G. T., 1975, A review and interpretation of the geologic setting of the Watchung Basalts flows, New Jersey: U.S. Geol. Survey Prof. Paper 864–A, p. A1–A42.

Flanagan, F. J., 1973, 1972 values for international geochemical reference samples: Geochim. et Cosmochim. Acta, v. 37, no. 5, p. 1189–1200.

Fleck, R. J., Sutter, J. F., and Elliott, D. H., 1977, Interpretation of discordant $^{40}Ar/^{39}Ar$ age-spectra of Mesozoic tholeiites from Antarctica: Geochim. et Cosmochim. Acta, v. 41, no. 1, p. 15–32.

Fleischer, Michael, 1968, Variation of the ratio Ni/Co in igneous rock series: Washington Acad. Sci. Jour., v. 58, no. 5, p. 108–117.

Floyd, P. A., and Winchester, J. A., 1975, Magma type and tectonic setting discrimination using immobile elements: Earth and Planetary Sci. Letters, v. 27, no. 2, p. 211–218.

Frey, F. A., Haskin, M. A., Poetz, J. A., and Haskin, L. A., 1968, Rare earth abundances in some basic rocks: Jour. Geophys. Research, v. 73, no. 18, p. 6085–6098.

Gass, I. G., 1970, Tectonic and magmatic evolution of the Afro-Arabian dome, *in* Clifford, T. N., and Gass, I. G., eds., African magmatism and tectonics: Darien, Conn., Hafner Pub. Co., p. 285–300.

Gast, P. W., 1968, Trace element fractionation and the origin of tholeiitic and alkaline magma types: Geochim. et Cosmochim. Acta, v. 32, no. 10, p. 1057–1086.

Ghose, N. C., 1976, Composition and origin of Deccan basalts: Lithos, v. 9, no. 1, p. 65–73.

Gill, J. B., 1970, Geochemistry of Viti Levu, Fiji, and its evolution as an island arc: Contr. Mineralogy and Petrology, v. 27, no. 3, p. 179–203.

Gottfried, David, and Greenland, L. P., 1972, Variation of iridium and gold in oceanic and continental basalts: Internat. Geol. Cong. 24th, Montreal, 1972, Proc., sec. 10, p. 135–144.

Gottfried, David, Greenland, L. P., and Campbell, E. Y., 1968, Variation of Nb-Ta, Zr-Hf, Th-U and K-Cs in two diabase-granophyre suites: Geochim. et Cosmochim. Acta, v. 32, no. 9, p. 925–947.

Green, D. H., and Ringwood, A. E., 1967, The genesis of basaltic magmas: Contr. Mineralogy and Petrology, v. 15, no. 2, p. 103–190.

Greenland, L. P., and Campbell, E. Y., 1974, Spectrophotometric determination of niobium in rocks: U.S. Geol. Survey Jour. Research, v. 2, no. 3, p. 353–355.

Greenland, L. P., and Lovering, J. F., 1966, Fractionation of fluorine, chlorine and other trace elements during differentiation of a tholeiitic magma: Geochim. et Cosmochim. Acta, v. 30, no. 9, p. 963–982.

Gunn, B. M., 1966, Modal and element variation in Antarctic tholeiites: Geochim. et Cosmochim. Acta, v. 30, no. 9, p. 881–920.

Hart, S. R., 1969, K, Rb, Cs contents and K/Rb, K/Cs ratios of fresh and altered submarine basalts: Earth and Planetary Sci. Letters, v. 6, no. 4, p. 295–303.

——— 1971, K, Rb, Cs, Sr and Ba contents and Sr isotope ratios of ocean floor basalts: Royal Soc. London Philos. Trans., Ser. A, v. 268, p. 573–587.

Hart, S. R., Brooks, C., Krogh, T. E., Davis, G. L., and Nava, D., 1970, Ancient and modern volcanic rocks; A trace element model: Earth and Planetary Sci. Letters, v. 10, no. 1, p. 17–28.

Hart, S. R., Erlank, A. J., and Kable, E. J. D., 1974, Sea floor basalt alteration; Some chemical and Sr isotopic effects: Contr. Mineralogy and Petrology, v. 44, no. 3, p. 219–230.

Haskin, L. A., Frey, F. A., Schmitt, R. A., and Smith, R. H., 1966, Meteoritic, solar and terrestrial rare-earth distributions, *in* Ahrens, L. H., Press, Frank, Runcorn, S. K., and Urey, H. C., eds., Physics and chemistry of the earth, v. 7: New York, Pergamon Press, p. 167–321.

Hedge, C. E., 1971, Nickel in high-alumina basalts: Geochim. et Cosmochim. Acta, v. 35, no. 5, p. 522–524.

Heier, K. S., Compston, W., and McDougall, Ian, 1965, Thorium and uranium concentrations, and the isotopic composition of strontium in the differentiated Tasmanian dolerites: Geochim. et Cosmochim. Acta, v. 29, no. 6, p. 643–659.

Herrmann, A. G., Potts, M. J., and Knake, Doris, 1974, Geochemistry of the rare earth elements in spilites from the oceanic and continental crust: Contr. Mineralogy and Petrology, v. 44, no. 1, p. 1–16.

Jakeš, Petr, and Gill, J., 1970, Rare earth elements and the island arc tholeiitic series: Earth and Planetary Sci. Letters, v. 9, no. 1, p. 17–28.

Jakeš, Petr, and White, A. J. R., 1970, K/Rb ratios of rocks from island arcs: Geochim. et Cosmochim. Acta, v. 34, no. 8, p. 849–856.

——— 1972a, Hornblendes from calc-alkaline volcanic rocks of island arcs and continental margins: Am. Mineralogist, v. 57, no. 5–6, p. 887–902.

——— 1972b, Major and trace element abundances in volcanic rocks of orogenic areas: Geol. Soc. America Bull., v. 83, no. 1, p. 29–40.

Johnson, M. E., and McLaughlin, D. B., 1957, Triassic formations in the Delaware Valley, field trip no. 2, *in* Geol. Soc. America, Guidebook for field trips, Atlantic City meeting 1957: p. 31–68.

Kaneoka, Ichiro, 1972, The effect of hydration on the K/Ar ages of volcanic rocks: Earth and Planetary Sci. Letters, v. 14, no. 2, p. 216–220.

Kay, R. W., Hubbard, N. J., and Gast, P. W., 1970, Chemical characteristics and origin of oceanic ridge volcanic rocks: Jour. Geophys. Research, v. 75, no. 8, p. 1585–1613.

Kay, R. W., and Senechal, R. G., 1976, The rare earth geochemistry of the Troodos ophiolite complex: Jour. Geophys. Research, v. 81, no. 5, p. 964–970.

Mankinen, E. A., and Dalrymple, G. B., 1972, Electron microprobe evaluation of terrestrial basalts for whole-rock K-Ar dating: Earth and Planetary Sci. Letters, v. 17, no. 1, p. 89–94.

Marine, I. W., and Siple, G. E., 1974, Buried Triassic basin in the Central Savannah River area, South Carolina and Georgia: Geol. Soc. America Bull., v. 85, no. 2, p. 311–320.

Marsh, B. D., 1976, Some Aleutian andesites; Their nature and source: Jour. Geology, v. 84, no. 1, p. 27–45.

Martin, R. F. and Piwinskii, A. J., 1972, Magmatism and tectonic settings: Jour. Geophys. Research, v. 77, no. 26, p. 4966–4975.

McDougall, Ian, 1964, Differentiation of the Great Lake dolerite sheet, Tasmania: Geol. Soc. Australia Jour., v. 11, pt. 1, p. 107–132.

McDougall, Ian, and Lovering, J. F., 1963, Fractionation of chromium, nickel, cobalt, and copper in a differentiated dolerite-granophyre sequence at Red Hill, Tasmania: Geol. Soc. Australia Jour., v. 10, pt. 2, p. 325–338.

Milton, Charles, 1972, Igneous and metamorphic basement rocks of Florida: Florida Bur. Geology Geol. Bull. 55, 125 p.

Milton, Charles, and Hurst, V. J., 1965, Subsurface "basement" rocks of Georgia: Georgia Dept. Mines, Mining and Geology, Bull. 76, 56 p.

Miyashiro, Akiho, 1974, Volcanic rock series in island arcs and active continental margins: Am. Jour. Sci., v. 274, no. 4, p. 321–355.

Miyashiro, Akiho, and Shido, Fumiko, 1975, Tholeiitic and calc-alkalic series in relation to the behaviors of titanium, vanadium, chromium, and nickel: Am. Jour. Sci., v. 275, no. 3, p. 265–277.

Mohr, P. A., 1972, Regional significance of volcanic geochemistry in the Afar Triple Junction, Ethiopia: Geol. Soc. America Bull., v. 83, no. 1, p. 213–222.

Nakamura, Norboru, and Masuda, Akimasa, 1971, Rare earth elements in abyssal basalts and plateau basalts: Nature: Physical Sci., v. 233, no. 42, p. 130–131.

Nichols, R. L., 1936, Flow-units in basalt: Jour. Geology, v. 44, no. 5, p. 617–630.

Obradovich, J. D., and Cobban, W. A., 1975, A time-scale for the late Cretaceous of the Western Interior of North America, *in* Caldwell, W. G. E., ed., The Cretaceous System in the Western Interior of North America: Geol. Assoc. Canada Spec. Paper 13, p. 31–54.

Pearce, J. A., 1975, Basalt geochemistry used to investigate past tectonic environments on Cyprus: Tectonophysics, v. 25, no. 1-2, p. 41–67.

Pearce, J. A., and Cann, J. R., 1971, Ophiolite origin investigated by discriminant analysis using Ti, Zr and Y: Earth and Planetary Sci. Letters, v. 12, no. 3, p. 339–349.

Pearce, J. A., and Cann, J. R., 1973, Tectonic setting of basic volcanic rocks determined using trace element analyses: Earth and Planetary Sci. Letters, v. 19, no. 2, p. 290–300.

Pearce, T. H., Gorman, B. E., and Birkett, T. C., 1975, The TiO_2-K_2O-P_2O_5 diagram; A method of discriminating between oceanic and non-oceanic basalts: Earth and Planetary Sci. Letters, v. 24, no. 3, p. 419–426.

Perfit, M. R., 1977, Petrology and geochemistry of mafic rocks from the Cayman Trench—Evidence for spreading: Geology, v. 5, no. 2, p. 105–110.

Philpotts, J. A., and Schnetzler, C. C., 1968, Genesis of continental diabases and oceanic tholeiites considered in light of rare-earth and barium abundances and partition coefficients, *in* Ahrens, L. H., ed., Origin and distribution of the elements: New York, Pergamon Press, p. 939–947.

Philpotts, J. A., Schnetzler, C. C., and Hart, S. R., 1969, Submarine basalts—Some K, Rb, Sr, Ba, rare-earth, H_2O, and CO_2 data bearing on their alteration, modification by plagioclase, and possible source materials: Earth and Planetary Sci. Letters, v. 7, no. 3, p. 293–299.

Pitman, W. C., III, and Talwani, Manik, 1972, Sea-floor spreading in the North Atlantic: Geol. Soc. America Bull., v. 83, no. 3, p. 619–646.

Prinz, Martin, 1967, Geochemistry of basaltic rocks—Trace elements, *in* Hess, H. H., and Poldervaart, Arie, eds., Basalts; The Poldervaart treatise on rocks of basaltic composition, v. 1: New York, Interscience Publishers, p. 271–323.

Ragland, P. C., Brunfelt, A. O., and Weigand, P. W., 1971, Rare-earth abundances in Mesozoic dolerite dikes from eastern United States, *in* Brunfelt, A. O., and Steinnes, Eiliv, eds., Activation analysis in geochemistry and cosmochemistry: Oslo, Universitetsfarlaget, p. 227–235.

Ragland, P. C., Fullagar, P. D., Wiegand, P. W., and Brunfelt, A. O., 1972, 'Primitive' nature of Mesozoic dolerites from the southeastern U.S. [abs.]: Internat. Geol. Cong., 24th, Montreal, 1972, Abstracts [Volume], p. 53.

Ragland, P. C., Rogers, J. J. W., and Justus, P. S., 1968, Origin and differentiation of Triassic dolerite magmas, North Carolina, U.S.A.: Contr. Mineralogy and Petrology, v. 20, no. 1, p. 57–80.

Ragland, P. C., Weigand, P. W., and Brunfelt, A. O., 1971, Rare-earth element abundance patterns in Mesozoic dolerites from eastern United States [abs.]: Geol. Soc. America, Abs. with Programs, v. 3, no. 5, p. 342–343.

Schilling, J.-G., 1969, Red Sea floor origin; rare-earth evidence: Science, v. 165, no. 3900, p. 1357–1360.

——— 1971, Sea-floor evolution; rare-earth evidence: Royal Soc. London Philos. Trans., ser. A, v. 268, no. 1192, p. 663–706.

——— 1973, Afar mantle plume; rare earth evidence: Nature: Physical Sci., v. 242, no. 114, p. 2–5.

Schilling, J.-G., and Winchester, J. W., 1967, Rare-earth fractionation and magmatic processes, *in* Runcorn, S. K., ed., Mantles of the earth and terrestrial planets; New York, Interscience Publishers, p. 267–283.

Seidel, Eberhard, 1974, Zr contents of glaucophane-bearing meta-basalts of Western Crete, Greece: Contr. Mineralogy and Petrology, v. 44, no. 3, p. 231–236.

Shapiro, Leonard, 1975, Rapid analysis of silicate, carbonate, and phosphate rocks—revised edition: U.S. Geol. Survey Bull. 1401, 76 p.

Skinner, B. J. and Peck, D. L., 1969, An immiscible sulfide melt from Hawaii *in* Wilson, H. D. B., and Bateman, A. M., eds., Magmatic ore deposits—a symposium: Econ. Geol. Mon. 4, p. 310–322.

Smewing, J. D., Simonian, K. O., and Gass, I. G., 1975, Metabasalts from the Troodos Massif, Cyprus; Genetic implication deduced from petrography and trace element geochemistry: Contr. Mineralogy and Petrology, v. 51, no. 1, p. 49–64.

Smith, R. C. II, Rose, A. W., and Lanning, R. M., 1975, Geology and geochemistry of Triassic diabase in Pennsylvania: Geol. Soc. America Bull., v. 86, no. 7, p. 943–955.

Tatsumoto, M., Hedge, C. E., and Engel, A. E. J., 1965, Potassium, rubidium, strontium, thorium, uranium, and the ratio of strontium-87 to strontium-86 in oceanic tholeiitic basalt: Science, v. 150, no. 3698, p. 886–888.

Taylor, S. R., 1965, Geochemical analysis by spark source mass spectrography: Geochim. et Cosmochim. Acta, v. 29, no. 12, p. 1243–1261.

——— 1969, Trace element chemistry of andesites and associated calc-alkaline rocks, *in* McBirney, A. R., ed., Proceedings of the Andesite Conference, Eugene and Bend, Oreg., July 1–6, 1968: Oregon Dept. Geology and Mineral Industries Bull. 65, p. 43–63.

Taylor, S. R., Kaye, Maureen, White, A. J. R., Duncan, A. R., and Ewart, A., 1969, Genetic significance of Co, Cr, Ni, Sc and V content of andesites: Geochim. et Cosmochim. Acta, v. 33, no. 2, p. 275–286.

Taylor, S. R., and White, A. J. R., 1966, Trace element abundances in andesites: Bull. Volcanol., v. 29, p. 177–194.

Taylor, S. R., White, A. J. R., Ewart, A., and Duncan, A. R., 1971, Nickel in high-alumina basalts; A reply: Geochim. et Cosmochim. Acta, v. 35, no. 5, p. 525–528.

Vogt, P. R., 1973, Early events in the opening of the North Atlantic, *in* Tarling, D. H., and Runcorn, S. K., eds., Implications of continental drift to the earth sciences New York, Academic Press, v. 2, p. 693–712.

Walker, K. R., 1969, The Palisades sill, New Jersey; a reinvestigation: Geol. Soc. America Spec. Paper 111, 178 p.

Weigand, P. W., and Ragland, P. C., 1970, Geochemistry of Mesozoic dolerite dikes from eastern North America: Contr. Mineralogy and Petrology, v. 29, no. 3, p. 195–214.

Winchester, J. A., and Floyd, P. A., 1976, Geochemical magma type discrimination; Application to altered and metamorphosed basic igneous rocks: Earth and Planetary Sci. Letters, v. 28, no. 3, p. 459–469.

Yoder, H. S., Jr., 1969, Calcalkalic andesites—experimental data bearing on the origin of their assumed characteristics, *in* McBirney, A. R., ed., Proceedings of the Andesite Conference, Eugene and Bend, Oreg., July 1–6, 1968: Oregon Dept. Geology and Mineral Industries Bull. 65, p. 77–89.

Yoder, H. S., Jr., and Tilley, C. E., 1962, Origin of basalt magmas; an experimental study of natural and synthetic rock systems: Jour. Petrology, v. 3, no. 3, p. 342–529.

Zietz, Isidore, Popenoe, Peter, and Higgins, B. B., 1976, Regional structure of the southeastern United States as interpreted from new aeromagnetic maps of part of the Coastal Plain of North Carolina, South Carolina, Georgia, and Alabama [abs.]: Geol. Soc. America, Abs. with Programs, v. 8, no. 2, p. 307.

Heat Flow From a Corehole Near Charleston, South Carolina,

By J. H. SASS and JOHN P. ZIAGOS

STUDIES RELATED TO THE CHARLESTON, SOUTH CAROLINA, EARTHQUAKE OF 1886—A PRELIMINARY REPORT

GEOLOGICAL SURVEY PROFESSIONAL PAPER 1028-H

CONTENTS

ILLUSTRATIONS

TABLE

STUDIES RELATED TO THE CHARLESTON, SOUTH CAROLINA, EARTHQUAKE OF 1886—
A PRELIMINARY REPORT

HEAT FLOW FROM A COREHOLE NEAR CHARLESTON, SOUTH CAROLINA

By J. H. Sass and John P. Ziagos

ABSTRACT

Temperature measurements were made at 3-m intervals from the surface to total depth (790 m) in Clubhouse Crossroads corehole 1 located near the epicenter of the 1886 Charleston earthquake. The temperature profile is irregular, reflecting the observed variability of thermal conductivity with depth. With the exception of one 150-m-thick interval within the Middendorf Formation (Upper Cretaceous), temperature gradient varies inversely with thermal conductivity over individual stratigraphic units, resulting in internally consistent component values of heat flow averaging 1.3±0.12 hfu (1 heat flow unit, hfu,$=10^{-6}$ cal cm^{-2} $s^{-1}=41.8$ mW m^{-2}). This value is within the range of other values measured in the region; thus, no thermal anomaly is associated with the observed seismicity in the area.

INTRODUCTION

As an adjunct to the geological, geophysical, and seismological investigations related to the 1886 Charleston earthquake, thermal studies were made in the Clubhouse Crossroads corehole 1 (CCC 1), located about 40 km west-northwest of Charleston (fig. 2, Rankin, this volume). The thermal studies were undertaken primarily to obtain a well-documented value of regional heat flux but incidentally to discover if any thermal anomalies were associated with the observed seismicity (Bollinger and Visvanathan, this volume; Tarr, this volume) of the area. In general, thermal anomalies would be expected only in regions of strong and recent tectonic strain, such as plate margins (Lachenbruch and Sass, 1973) or where igneous activity has occurred during the last few million years over areas having horizontal dimensions on the order of a crustal thickness (Lachenbruch and others, 1976; Lachenbruch and Sass, 1977).. Thermal anomalies might also be expected in regions of large-scale convective water movement (see, for example, Lachenbruch and Sass, 1977). This report summarizes the thermal studies in CCC 1 and their relation to regional heat flux and the tectonic setting. The thermal measurements are discussed in detail by Ziagos, Sass, and Munroe (1976).

HEAT-FLOW DATA

Temperatures were measured at 3-m intervals over the entire length of the hole (fig. 1). Irregularities in the temperature profile, which indicate abrupt changes in thermal conductivity, reflect the stratification of the sedimentary section.

Ninety measurements of thermal conductivity on water-saturated sections of core showed a stratification that corresponded closely to the variations in thermal gradient with depth. The lowest thermal conductivities (2–4 cal cm^{-1} s^{-1} $°C^{-1}$ were measured in the Cooper Formation in the uppermost 60 m of the hole and in shale and clay-rich units. Basalt had a small range of conductivities (4.2–4.6 cal cm^{-1} s^{-1} $°C^{-1}$), and gravelly and sandy sections and well-indurated sandy and silty limestone and sandstone had the highest conductivities (5–8 cal cm^{-1} s^{-1} $°C^{-1}$).

With the exception of the depth interval 555–698 m (mostly within the Middendorf Formation (Upper Cretaceous); Gohn and others, this volume), component heat flows range from 1.1 to 1.5 hfu (1 hfu, heat flow unit, $=10^{-6}$ cal cm^{-2} $s^{-1}=41.8$ mW m^{-2}) (table 1). The mean of these seven values, weighted according to the thickness of the intervals, is 1.30±0.12 hfu. The value of 0.71 hfu within the Middendorf Formation is significantly lower than the mean for the other intervals. This formation contains layers of coarse sand and pebbles, and we attribute the low heat flow mainly to the convective transfer of heat across the formation by moving ground water.

Ziagos, Sass, and Munroe (1976) used a number of methods for reducing the data, and, in all in-

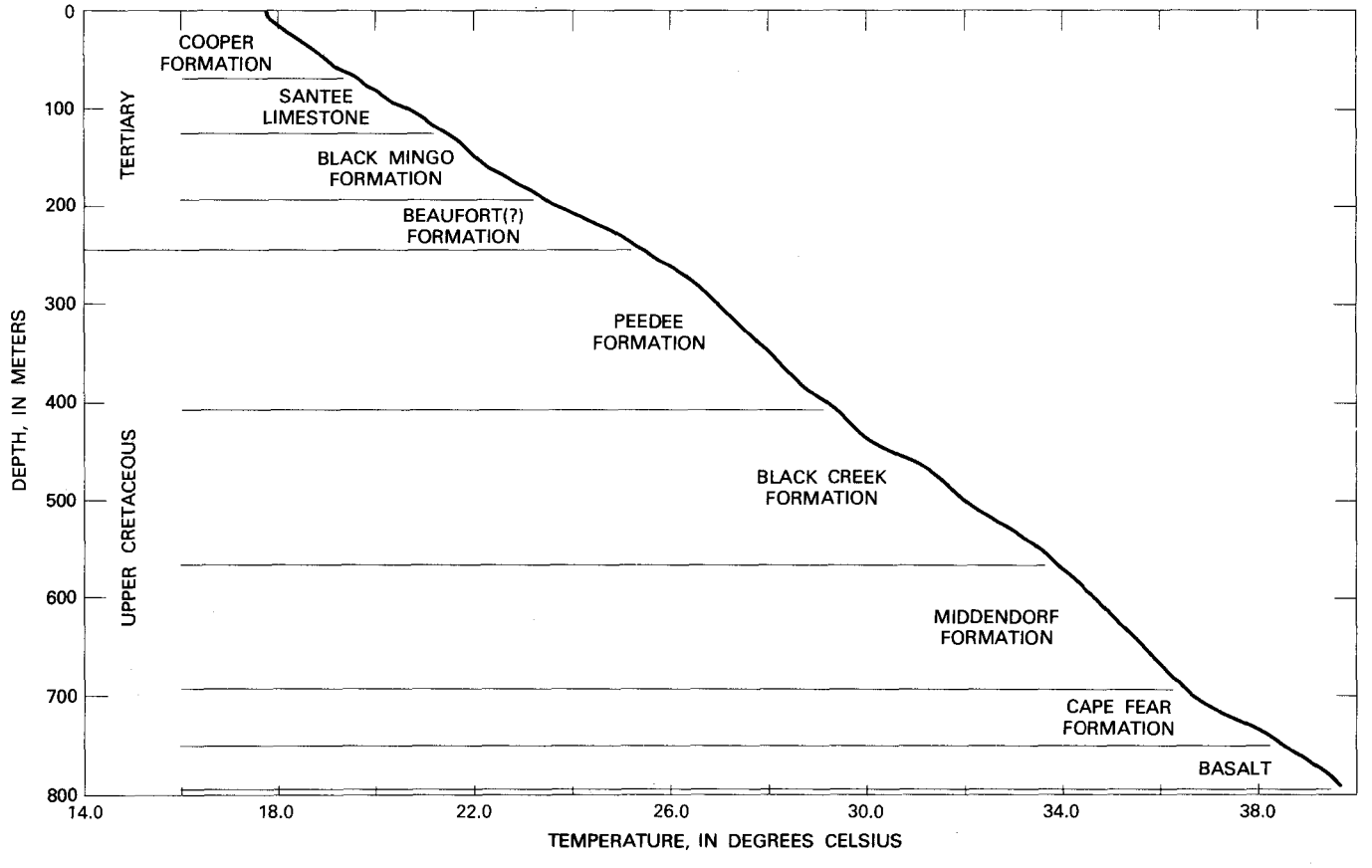

FIGURE 1.—Temperature versus depth in Clubhouse Crossroads corehole 1. Temperatures were measured at 3-m intervals. Lithologic column based on figure 2 of Gohn and others, this volume.

TABLE 1.—*Temperature gradient, harmonic mean thermal conductivity, and heat flow for nearly linear segments of the temperature profile (fig. 1) in Clubhouse Crossroads corehole 1*

Depth interval (m)	Temperature gradient, (°C km^{-1})	Number of samples	Thermal conductivity (10^{-3} cal cm^{-1} s^{-1} °C^{-1})	Heat flow (10^{-6} cal cm^{-2} s^{-1})
274–399	21.0	11	5.99±0.29	1.26
405–442	23.0	5	6.38± .83	1.47
442–469	40.1	5	3.39± .16	1.36
469–515	25.3	6	5.28± .55	1.34
509–555	30.1	4	3.76± .82	1.13
555–698	18.4	15	3.88± .32	0.71
713–738	42.2	5	3.43± .11	1.45
754–789	30.4	16	4.23± .13	1.28

stances, the heat flow calculated was within the limits of 1.3 ± 0.2 hfu.

REGIONAL SIGNIFICANCE

The heat flow of 1.3 hfu is within the range of values commonly found in the Coastal Plains physiographic province and adjoining parts of the Appalachian province of Fenneman (1946) (see fig. 1 of Ziagos and others, 1976, fig. 2 of Sass and others, 1976, or fig. 1 of Lachenbruch and Sass, 1977, for the most recent maps). From a thermal standpoint, the Charleston area seems to be indistinguishable from the rest of the United States east of the Great Plains. It thus appears that steady-state frictional heating within the upper crust does not contribute significantly to the observed heat flux in this region of relatively high seismicity. In contrast, in the San Andreas fault zone north of the Transverse Ranges in California, Lachenbruch and Sass (1973) estimated that as much as 0.8 hfu might be produced by shear-strain heating associated with relative movement between the Pacific and American plates (Atwater, 1970) over a band about 100 km wide, roughly coincident with the fault zone.

REFERENCES CITED

Atwater, Tanya, 1970, Implications of plate tectonics for the Cenozoic tectonic evolution of western North America: Geol. Soc. America Bull., v. 81, no. 12, p. 3513–3535.

Fenneman, N. M., 1946, Physical divisions of the United States: Map prepared in cooperation with the Physiographic Committee, U.S. Geological Survey, U.S. De-

partment of the Interior, Washington, D. C. scale 1:7,500,000.

Lachenbruch, A. H., and Sass, J. H., 1973, Thermo-mechanical aspects of the San Andreas Fault system, *in* Proceedings of the conference on tectonic problems of the San Andreas fault system: Standford Univ. Pubs. Geol. Sci., v. 13, p. 192–205.

Lachenbruch, A. H., and Sass, J. H., 1977, Heat flow in the United States and the thermal regime of the crust: Am. Geophys. Union Geophys. Mon. 20, in press.

Lachenbruch, A. H., Sass, J. H., Munroe, R. J., and Moses, T. H., Jr., 1976, Geothermal setting and simple heat conduction models for the Long Valley caldera: Jour. Geophys. Research, v. 81, no. 5, p. 769–784.

Sass, J. H., Diment, W. H., Lachenbruch, A. H., Marshall, B. V., Munroe, R. J., Moses, T. H., Jr., and Urban, T. C., 1976, A new heat-flow contour map of the conterminous United States: U.S. Geol. Survey open-file rept. 76–756, 24 p.

Ziagos, J. P., Sass, J. H., and Munroe, R. J., 1976, Heat flow near Charleston, South Carolina: U.S. Geol. Survey open-file rept. 76–148, 21 p.

The Nature of the Geophysical Basement Beneath the Coastal Plain of South Carolina and Northeastern Georgia

By PETER POPENOE and ISIDORE ZIETZ

STUDIES RELATED TO THE CHARLESTON, SOUTH CAROLINA, EARTHQUAKE OF 1886—A PRELIMINARY REPORT

GEOLOGICAL SURVEY PROFESSIONAL PAPER 1028-I

CONTENTS

ILLUSTRATIONS

TABLE

THE NATURE OF THE GEOPHYSICAL BASEMENT BENEATH THE COASTAL PLAIN OF SOUTH CAROLINA AND NORTHEASTERN GEORGIA

By PETER POPENOE and ISIDORE ZIETZ

ABSTRACT

Geophysical data delineate two distinctive crustal provinces beneath the Coastal Plain of Georgia and South Carolina. The province adjacent to and east of the Fall Line is a continuation of the Piedmont, composed chiefly of schist and gneiss units, which geologically and geophysically reflect the fabric of the Appalachian orogen. In structure and composition, the basement rocks are similar to those of the Carolina slate belt and the Charlotte belt immediately west of the Fall Line. At least two small Triassic basins are present within the province and are clearly delineated by the magnetic data.

The second basement provice that underlies southeastern South Carolina and east-central Georgia has no counterpart in the exposed southern Appalachians. This basement is composed of undeformed tuffaceous clastic rocks intermixed with basaltic and rhyolitic flows and ash-fall deposits, which are associated with a relatively smooth, low-amplitude magnetic and gravity field. Emplaced within and directly adjacent to this sequence of rocks are a number of mafic plutons, which produce high-amplitude, steep-gradient, circular aeromagnetic and gravity positives. These positives occur within broad areas of higher magnetic level, which may reflect extensive basaltic flows, but also appear to be related to deeper mafic crustal sources. The association of the mafic plutons with basaltic flows at the basement surface suggests that the two are genetically related.

The boundary between the region of northeast-trending aeromagnetic anomalies and the smooth magnetic field consists of a number of long, straight segments. This boundary probably reflects a series of major faults, which juxtapose a metamorphic and nonmetamorphic terrane. The association of mafic plutons with the boundary suggests a deep crustal break.

The smooth gravity and magnetic fields associated with basement in southeastern South Carolina and east-central Georgia are similar to those associated with Triassic basins, suggesting that a large area of the basement is underlain by a deep structural basin filled with Triassic(?) clastic and volcanic material, and intruded by a number of Triassic(?) or later mafic plutons.

INTRODUCTION

Although the area of the 1886 earthquake and that of present earthquake activity near Charleston, S. C., geographically belongs to the Coastal Plain physiographic province, analyses of the depth of focus of present seismicity (Tarr, this volume; Bollinger, 1972) and the depth estimation of the 1886 earthquake (Dutton, 1889) indicate that these earthquakes occurred within the basement underlying the Coastal Plain sedimentary section. This "basement" is traditionally believed to be the buried eastward extension of the Appalachian Piedmont province which, where exposed, consists of highly to moderately deformed metamorphic rocks and intrusive igneous rocks of Precambrian and Paleozoic age, overprinted in places by a system of downfaulted basins containing clastic rocks and a system of northwest-trending mafic dikes, both of Triassic(?) age. Because the crystalline rocks in eastern South Carolina and eastern Georgia are covered by up to 2 km of Coastal Plain sedimentary rocks and cannot be mapped directly, geophysical methods must be employed to aid in understanding the composition and structure of these rocks, the so-called geophysical basement.

The geophysical basement is defined as the top of a moderate-to high-velocity layer identified by seismic refraction surveys. Velocities of this layer range generally from 4.3 to 6.8 km/s, and are characteristic of well-indurated sedimentary rocks, volcanic flows or sills, or crystalline basement. The surface of this layer is the lower limit of the poorly-indurated Coastal Plain sedimentary rocks, with velocities typically less than 3.0 km/s.

Within the last several years, detailed gravity and magnetic surveys covering the Coastal Plain area of southeastern South Carolina and eastern Georgia have been obtained. These data document that two very different basement provinces are present beneath the Coastal Plain of South Carolina and Georgia, one with a geophysical expression that is typical of rocks of the Appalachian orogen and one

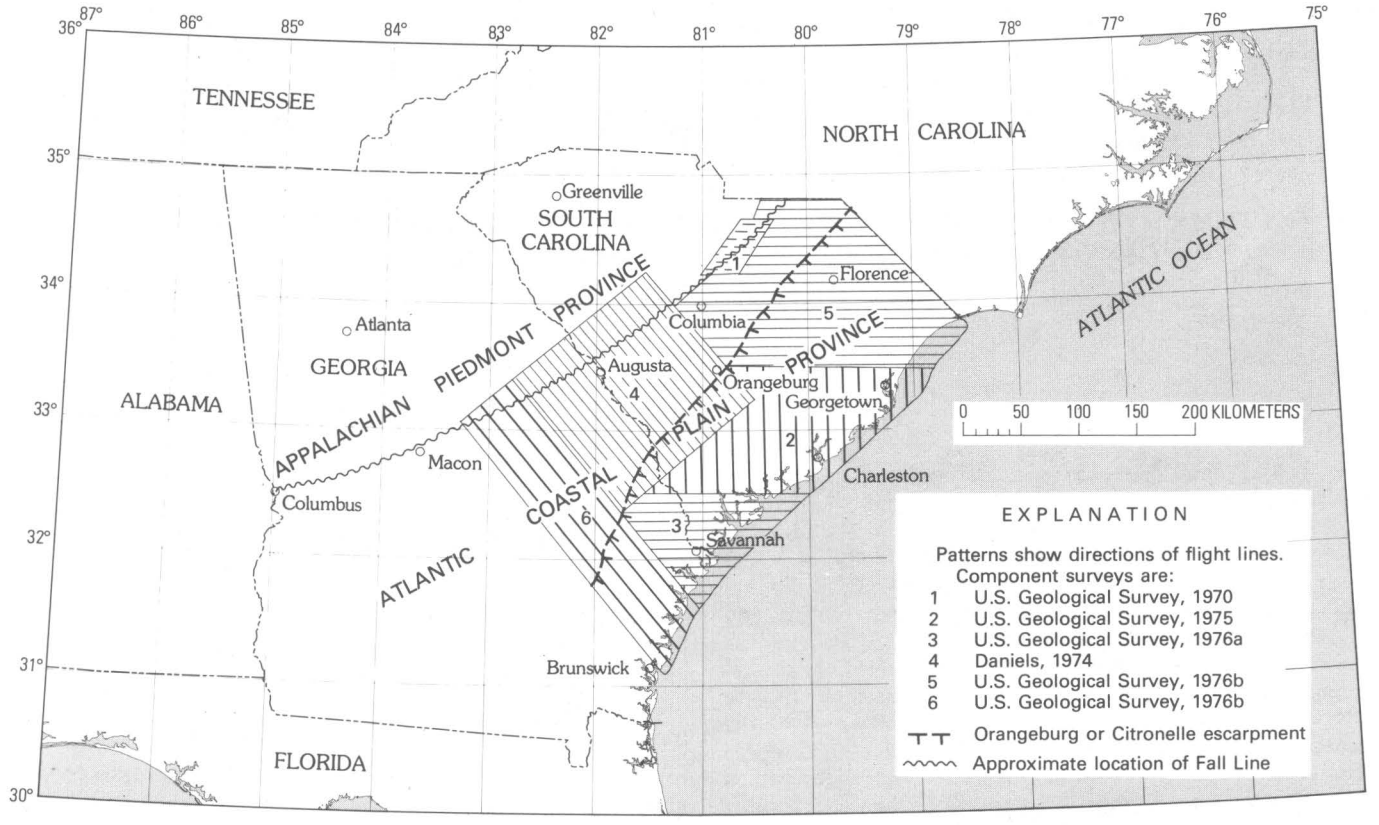

FIGURE 1.—Index map showing the location of the area discussed in this report and boundaries of the individual aeromagnetic surveys.

that appears to have no counterpart in the exposed Appalachian system. Geophysical differences between these two provinces and probable sources are discussed.

REGIONAL SETTING

The area of aeromagnetic data coverage (fig. 1) lies in parts of two physiographic provinces: the Appalachian Piedmont province underlain chiefly by highly deformed and metamorphosed sedimentary and igneous rocks of Precambrian and Paleozoic age, and the Atlantic Coastal Plain physiographic province underlain chiefly by consolidated and unconsolidated younger sedimentary rocks of Cretaceous to Holocene age. The line dividing the two provinces is known as the Fall Line. At this line, the ancient crystalline rock surface, which slopes gently toward the coast, becomes covered by the younger sedimentary rocks of the Atlantic Coastal Plain.

For a general discussion and summary of the geology of the exposed Piedmont within the area covered by the aeromagnetic survey, see Overstreet and Bell (1965a, b); Bell and others (1974); Georgia Geological Survey (1976a, b); Crickmay (1952); Hurst (1970); and Snoke, Secor, and Metzgar (1977). The rocks of the Piedmont are generally discussed in terms of geologic "belts" that have distinctive lthologies or metamorphic grades. In many places, these belts are distinct tectonic units bounded by faults. The northwest edge of the Survey area is within the Carolina slate belt of South Carolina and the similar Bel Air belt of Georgia, which consist of low-grade, mildly deformed metasedimentary and metavolcanic rocks. Locally, adjacent to the Fall Line is the Kiokee belt, which consists of various granitoid gneisses, biotite muscovite gneiss, and hornblende gneiss. The major difference between the two belts has been interpreted to be not their original composition, but metamorphic grade and type of deformation. The Carolina slate belt-Bel Air belt rocks are low-grade greenschist facies/rocks, which have been only mildly deformed and folded along northeast-trending, subhorizontal axes, whereas the Kiokee belt rocks are highly deformed and injected albite-epidote-amphibolite to amphibolite facies/rocks.

The relationship of the two metamorphic and tectonic styles exhibited by these two belts is poorly

understood. In places, the contact between the belts is clearly along major fault systems.

The rocks of both the Carolina slate belt-Bel Air belt and the Kiokee belt are cut by granodioritic to quartz-monzonitic plutons whose crosscutting relationships and lack of strong foliation clearly show that these plutons were emplaced after the main metamorphic event of the Appalachian orogen. The two main bodies of these porphyritic granites exposed in the survey area are the Liberty Hill and Pageland plutons of South Carolina (Bell and Popenoe, 1976), which intrude Carolina slate belt rocks. On the basis of their unmetamorphosed character and because they are intruded by mafic dikes believed to be of Triassic age, these intrusive bodies have been considered late Paleozoic or Carboniferous in age. Rubidium-strontium whole rock isochron ages of the granites range from 249 to 332 m.y. (Fullagar, 1971; Butler and Fullager, 1975).

Although no large structural basins containing Triassic age rocks are exposed in the area covered by the survey, the area is just south of the Wadesboro-Deep River Triassic basin of North Carolina, and structural basins of similar-appearing clastic rocks of presumed Triassic age are known to exist beneath the Coastal Plain of both South Carolina and Georgia (Marine and Siple, 1974). The Triassic basins of the east coast characteristically are northeast-trending, deep trough-shaped grabens, filled with coarse- to fine-grained continental clastic rocks, representing both high and lower energy deposits. The structures probably formed during the initial stages of continental rifting that accompanied the formation of the present Atlantic Ocean. Basaltic volcanism and intrusion of mafic rock accompanied or closely followed this rifting. Massive diabase stocks, dikes, and sills were emplaced both within the Triassic and in the surrounding older rocks. The dikes were emplaced in a remarkably systematic regional pattern, trending consistently northwest in the southern Appalachians, north-northeast in the central Appalachians, and northeast in the northern Appalachians (King, 1971).

The structure and composition of the basement rocks underlying the Coastal Plain of South Carolina and Georgia are not well known. Some drill holes have penetrated basement in widely scattered areas of the Coastal Plain. Published descriptions of basement samples within the survey area are listed in table 1.

TABLE 1.—*Data on wells penetrating basement rocks in South Carolina and northeastern Georgia*

Well No.	Name and location	Type of basement rock	Altitude of basement (meters)	Source
1	Town of Hartsville water well, Darlington County, S.C.	Pre-Cretaceous schist (granite).	−80	Maher, 1971 (granite) Woollard, Bonini, and Meyer, 1957 (pre-Cretaceous schist).
2	Town of Dillon water well, Dillon County, S.C.	Rhyolite breccia	−147	Maher, 1971.
3	Town of Florence water well, Florence County, S.C.	Triassic olivine diabase	−173	Maher, 1971.
4	Town of Marion water well, Marion County, S.C.	Pre-Cretaceous schist	−193	Maher, 1971.
5	Palmetto Drilling Allsbrook No. 1, 1.6 km N of Allsbrook, Horry County, S.C.	"Pre-Cretaceous"	−318	Maher, 1971.
6	Pioneer Oil, Smart No. 1, 19 km SW of Conway, Horry County, S.C.	"Pre-Cretaceous"	−417	Maher, 1971.
7	Myrtle Beach, Horry County, S.C.	Chlorite schist	−433	Zupan and Abbot, 1976.
8	Calabash, Brunswick County, N.C.	Chlorite schist	−395	Zupan and Abbot, 1976.
9	Town of Sumter water well, Sumter County, S.C.	Pre-Cretaceous granite	−189	Maher, 1971.
10	Oil test between Perry and Wagner, Aiken County, S.C.	Pre-Cretaceous granite	−59	Maher, 1971.
11	Town of Aiken water well, 226, 1.6 km S of center of Aiken, Aiken County, S.C.	Pre-Cretaceous granite	−12	Maher, 1971; Daniels, 1974.
12	Survey Drilling oil test, 8 km SW of Aiken County, S.C.	Pre-Cretaceous granite	−41	Maher, 1971.

TABLE 1.—*Data on wells penetrating basement rocks in South Carolina and northeastern Georgia*—Continued

Well No.	Name and location	Type of basement rock	Altitude of basement (meters)	Source
13	Aiken County, S.C.	Chlorite schist	−108	Daniels, 1974.
14	Aiken County, S.C.	Hornblende chlorite	−210	Daniels, 1974.
15	Aiken County, S.C.	Epidote chlorite schist	−196	Daniels, 1974.
16	Aiken County, S.C.	Hornblende chlorite schist	−198	Daniels, 1974.
17	Aiken County, S.C.	Chlorite schist	−178	Daniels, 1974.
18	Aiken County, S.C.	Quartz-feldspar gneiss	−187	Daniels, 1974.
19	Aiken County, S.C.	Hornblende chloride schist	−192	Daniels, 1974.
20	Aiken County, S.C.	Mica quartzite and chlorite-biotite schist.	−205	Daniels, 1974.
21	Barnwell County, S.C.	Triassic(?) fanglomerate	------	Daniels, 1974.
22	Barnwell County, S.C.	Triassic(?) siltstone	−309	Daniels, 1974.
23	Sumerville	Diabase	−740	Cooke, 1936.
24	USGS Clubhouse Crossroads corehole 1, Dorchester County, S.C.	Amygdaloidal basalt	−744	Gottfried, this volume.
25	Seabrook Island, Charleston County, S.C.	Fine-grained quartzitic sandstone (basement?).	−814	Charles Speier, drillers log.
26	Richmond County, Ga.	Talcose schist	−58	Daniels, 1974.
27	Allens Station, 14.5 km S of Augusta, Richmond County, Ga.	Talcose schist	−6	Milton and Hurst, 1965; Daniels, 1974.
28	Burke County, Ga.	Chlorite-sericite schist	−144	Daniels, 1974.
29	Middle Georgia Oil and Gas, 19 km NW of Sandersville, Washington County, Ga.	Crystalline rock	+27	Milton and Hurst, 1965.
30	Town of Sandersville, Washington County, Ga.	Quartzite, biotite gneiss and schist.	------	Maher, 1971.
31	Layne-Atlantic NSC water well, 3.2 km SW of Tennile, Washington County, Ga.	Granite	------	Milton and Hurst, 1965.
32	A. F. Lucas and Georgia Petroleum oil well, 5.6 km SW of Louisville, Jefferson County, Ga.	Crystalline rock	------	Milton and Hurst, 1965.
33	Grace McCain No. 1, 0.8 km S of Minter, Laurens County, Ga.	Diabase	−691	Milton and Hurst, 1965.
34	Barnwell No. 1, Jim Gillis, 4.8 km S of Soperton, Treutlen County, Ga.	"Paleo" (metaquartzite)	−879	Milton and Hurst, 1965.
35	McCain and Nicholson H. Gillis No. 1, 11 km E of Soperton, Treutlen County, Ga.	"Basement" (biotite gneiss)	−865	Milton and Hurst, 1965.
36	Pryor No. 1, 6.5 km NE of Newington, Screven County, Ga.	"Granite" (no bedrock sample recovered).	−777	Milton and Hurst, 1965; Pickering (oral commun.) 1976.
37	J. E. Weatherford-Lonnie Wilkes No. 1, .8 km S of Higgston, Montgomery County, Ga.	Diabase	−943	Milton and Hurst, 1965.
38	Tropic Oil Co., Gibson No. 1, 11 km SE of Vidalia, Toombs County, Ga.	Conglomeratic arkose	−1062	Milton and Hurst, 1965.
39	S. J. Felsenthal No. 1, 11 km W of Baxley, Appling County, Ga.	"Quartzite" (sandstone probably indurated by intrusive diabase).	−1180 (appr.)	Milton and Hurst, 1965.
40	J. E. Weatherford, S. J. Felsenthal, W. E. Bradley, No. 1, 1.6 km W of Baxley, Appling County, Ga.	Amygdaloidal basalt	−1182	Milton and Hurst, 1965.
41	Jelks-Rogers No. 1, LaRue and others. S of Retreat, Liberty County, Ga.	Quartz rhyolite porphyry	−1289	Milton and Hurst, 1965.
42	Union Bag & Paper Co. No. 1, 11 km N of Gardi, Wayne County, Ga.	Volcanic ash	−1372	Milton and Hurst, 1965.

TABLE 1.—*Data on wells penetrating basement rocks in South Carolina and northeastern Georgia*—Continued

Well No.	Name and location	Type of basement rock	Altitude of basement (meters)	Source
43	Brunswick Peninsular No. 1, 2.9 km E of McKinnon, Wayne County, Ga.	Tuffaceous arkose	−1386	Milton and Hurst, 1965.
44	California Co., Brunswick Peninsula Corp. No. 1, Wayne County, Ga.	Gray and pink arkosic quartzite and diabase.	−1375	Applin and Applin, 1964.
45	Humble Oil Co., W. C. McDonald No. 1, Ga. Military District 1499, SW of Brunswick, Glynn County, Ga.	Granite	−1436	Maher, 1971.

The basement descriptions (Milton and Hurst, 1965; Maher, 1971; Siple, 1967; Cooke, 1936; Daniels, 1974) show that a heterogeneous basement underlies the Coastal Plain. Many of the basement rocks appear similar in composition to rocks of the Piedmont, particularly near the Fall Line; however, in other areas, only fine-grained igneous rocks, such as basalt and diabase, have been found. A few holes have bottomed in clastic rocks resembling those in exposed Triassic basins.

Of particular interest to this study are a series of fine-grained igneous rocks and clastic rocks (Milton and Hurst, 1965) known to underlie a large area of the Coastal Plain of Georgia. These rocks show little or no deformation, and include volcanic flows of both basaltic and rhyolitic composition, ashfall deposits, and tuffaceous arkose (Milton and Hurst, 1965).

The surface of the basement is an erosional surface, which slopes gently eastward beneath the Coastal Plain sediments. During the Early Cretaceous, this surface apparently occupied a regional topographic high, which was not fully inundated until late in the Cretaceous Period. Figure 2 is a regional structure-contour map of the surface of the geophysical basement which is in part this erosion surface. The map is based chiefly on published depths of drill holes that have reached basement or near basement, and the seismic refraction studies of Ackerman (this volume); Bonini (1957); Bonini and Woollard (1960); Meyer (1956); Pooley (1960); Hersey and others (1959); and unpublished seismic reflection data of the U.S. Geological Survey.

Only broad, regional structures are shown on the map because of the wide data spacing. The most prominent of these structures in northeastern South Carolina is the Cape Fear arch, which trends northwest and brings the basement to within 400 m of the surface near the coast at the North Carolina-South Carolina State boundary. A thick section of Lower Cretaceous rocks are present north of the arch, but these rocks are absent over the arch and to the south. This, plus a vertical displacement of strand lines at the surface attest to a long tectonic history. The second most prominent feature is the southeast Georgia embayment, which is recessed into the coast roughly between the Georgia-South Carolina and the Georgia-Florida State boundaries. The embayment is believed to be primarily a tectonically passive feature (Maher, 1971), and the uplift probably occurred on the Peninsular arch of Florida and Cape Fear arch, rather than downwarp in the embayment.

In addition to the broader regional structures, a basement feature known as the Yamacraw Ridge lies parallel to the coast in eastern Georgia. The Yamacraw Ridge, a ridge of about 350 m relief, was defined on the basement surface by seismic refraction studies (Meyer, 1956; Pooley, 1960). Drilling in Georgia in the area of the ridge indicates that it apparently is not reflected in the overlying beds (Maher, 1971). Basement contours and the apparent lack of deformation of the overlying sediments suggest that the ridge may be topography on the basement erosional surface.

In South Carolina, the Beaufort or Burton High are along the strike of the Yamacraw Ridge. These features and a trough to the west named "Ridgeland trough" were defined by structure contours on different elevations of Tertiary horizons (Siple, 1969; Heron and Johnson, 1966). The expression of these features within the Tertiary rocks suggests a basement structural control, but our structure-contour map indicates that these are only minor features on the basement in the area in which they were defined. We have used the name Ridgeland trough for the basement depression west of the Yamacraw Ridge in Georgia.

The refraction work of Ackerman (this volume) and the electrical work of Campbell (this volume)

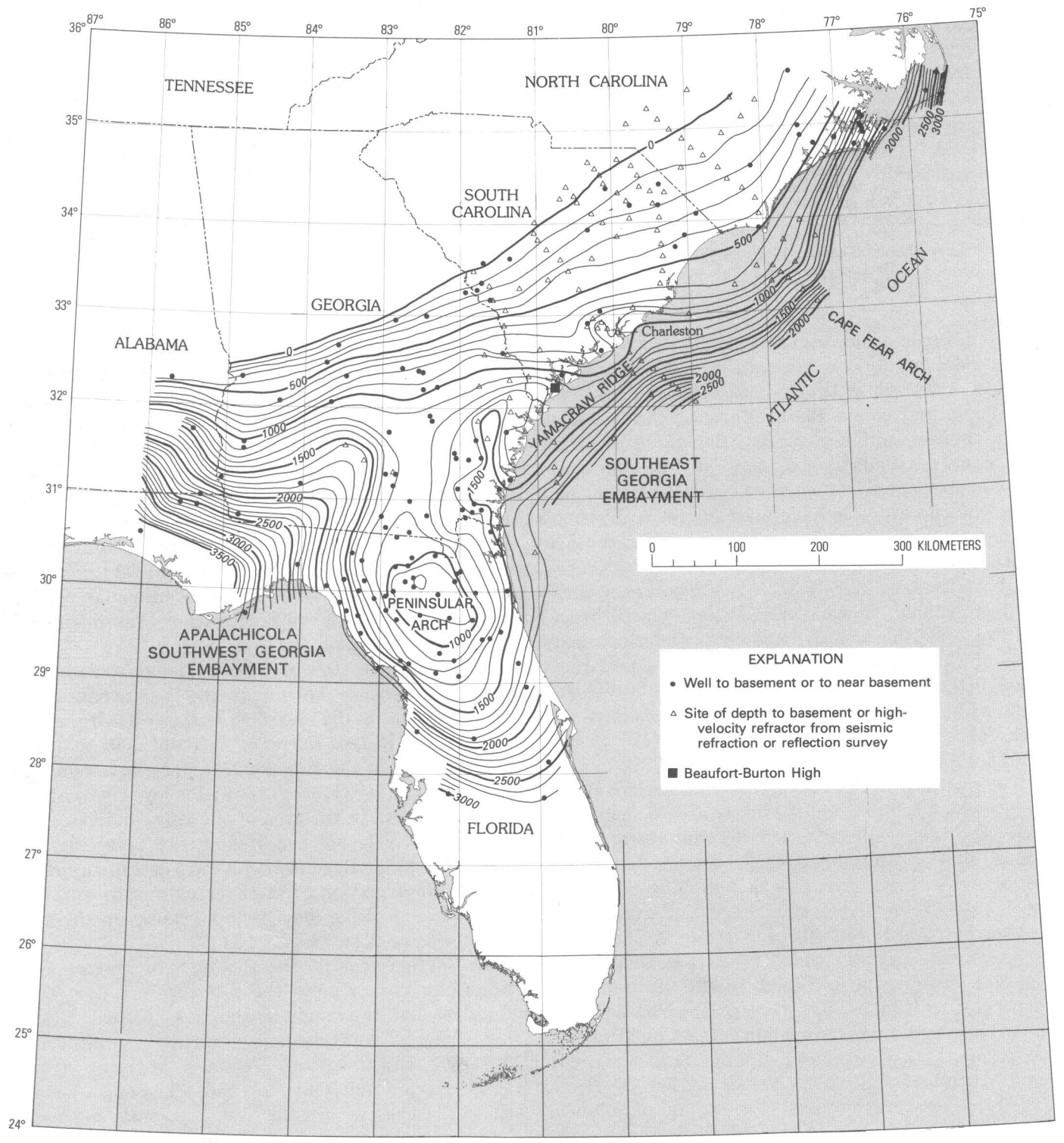

FIGURE 2.—Structure-contour map of the surface of the geophysical basement in parts of North Carolina, South Carolina, Georgia, Florida, and Alabama. Elevations are in meters below sea level. Basement is defined as the top of the crystalline rocks, top of the Triassic rocks or Jurassic volcanic rocks, or top of the high-velocity refractor in South Carolina and Georgia.

have defined a trough-shaped depression on the surface of the amygdaloidal basalt horizon (basement?) in the seismically active area west of Charleston, S. C. The significance of this feature is still under study.

A discussion of the geology of the Coastal Plain rocks is given by Gohn and others (this volume) and Rankin (this volume), and will not be repeated here. The only important physiographic feature relating to this study is the Orangeburg or Citronelle escarpment (see fig. 1). This escarpment produces a 15 to 60 m change in the general topographic level along a 965-km line, extending from Florida to Washington, D. C. (Doering, 1960), and its maximum development is in South Carolina. At its northern end, it follows the Fall Line, but in South Carolina, it divides the upper from the middle Coastal Plain with its toe at about 60 m and its crest at about 110 m elevation. The Orangeburg scarp in South Carolina is believed to be composite in origin (Colquhoun, 1965), formed by a late Miocene and perhaps Oligocene sea level transgression.

AEROMAGNETIC AND GRAVITY SURVEYS

Figure 3 presents a composite aeromagnetic map of southeastern South Carolina and eastern Georgia, compiled from the six smaller surveys shown in figure 1. These surveys were conducted by the U.S. Geological Survey in cooperation with the U.S. Nuclear Regulatory Commission, the Coastal Plains Regional Commission of the U.S. Department of Commerce, and the former U.S. Atomic Energy Commission. The map has a contour interval of 100 gammas and is a simplification of the more detailed individual maps, which have contour intervals of 10 to 50 gammas. Data in all areas were obtained at a nominal flight elevation of 152.4 m above mean terrain, and have been reduced to remove the international geomagnetic reference field (Fabiano and Peddie, 1969), which permits a comparison of magnetic levels over widely separated areas. Flight line spacing was 1.6 km for all data but area 1, where it was 0.8 km.

The patterns shown on the magnetic map reflect structure and lithology in crystalline and metamorphic rocks. The crystalline and metamorphic rocks are the basement rocks or in thin intrusive rocks or volcanic flows within the sedimentary section. The magnetic contribution of sedimentary rocks, such as those of the Coastal Plain, is negligible. The only significant effect of the sedimentary rocks is to increase the distance between the anomaly-producing rocks of the basement and the airborne magnetometer. The effect of this increased distance causes both a smoothing and merging of anomalies from deeper sources and a lowering in their amplitude and gradient.

The magnetic properties of crystalline and metamorphic rocks are generally related to magnetite content, but similar rocks may vary widely in magnetization because of such factors as magnetic size domain and remanent and induced components. Generally, mafic rocks are more magnetic than felsic varieties, but this is not always true. Daniels (1974) measured the magnetic susceptibility of exposed rocks in the central Savannah River area and found that only a small fraction of Carolina slate belt rocks are significantly magnetic (10^{-4} to 10^{-2} cgs/cm^3), whereas a large fraction of felsic gneisses from a small area of the Kiokee belt fall in this magnetic range. Amphibolitic schists (chlorite-epidote-hornblende schist) from basement cores in the Savannah River Plant area are also fairly high in susceptibility ($\cong 2.1 \times 10^{-3}$ cgs/cm^3). The difference in this measured susceptibility appears to be related to metamorphic grade rather than to composition. The concept that metamorphic grade affects magnetic susceptibility was outlined by Reed, Owens, and Stockard (1968), who suggested that medium-grade metamorphic rocks (epidote-amphibolite facies) are enhanced in magnetite relative to those of either higher or lower grade.

Figure 4 is a simple Bouguer gravity map of the area of the magnetic survey. The map is based on the simple Bouguer anomaly map of South Carolina and Georgia by Long, Bridges, and Dorman (1972) and Long, Talwani, and Bridges (1976), as well as on unpublished data from H. L. Krivoy. Contour intervals are 5 and 10 mGals based on a station spacing of 4 to 6 km.

The patterns on gravity maps reflect density variations associated with lithologic changes in the Earth's crust. These changes are of both regional and local extent and derive from both near-surface and deep sources. In figure 4, most of the anomalies are believed to be produced by intra-basement sources because of the limited thickness and lateral homogeneity of the Coastal Plain rocks in this area.

An established practice in interpreting gravity and magnetic maps is to observe the anomaly-lithology relations in areas of exposed or known geology and to use these observations as principal guidelines in interpreting anomalies in covered areas. This is the method that we have used in the following interpretation. Insight into the anomaly source is provided by shape, amplitude, and the cor-

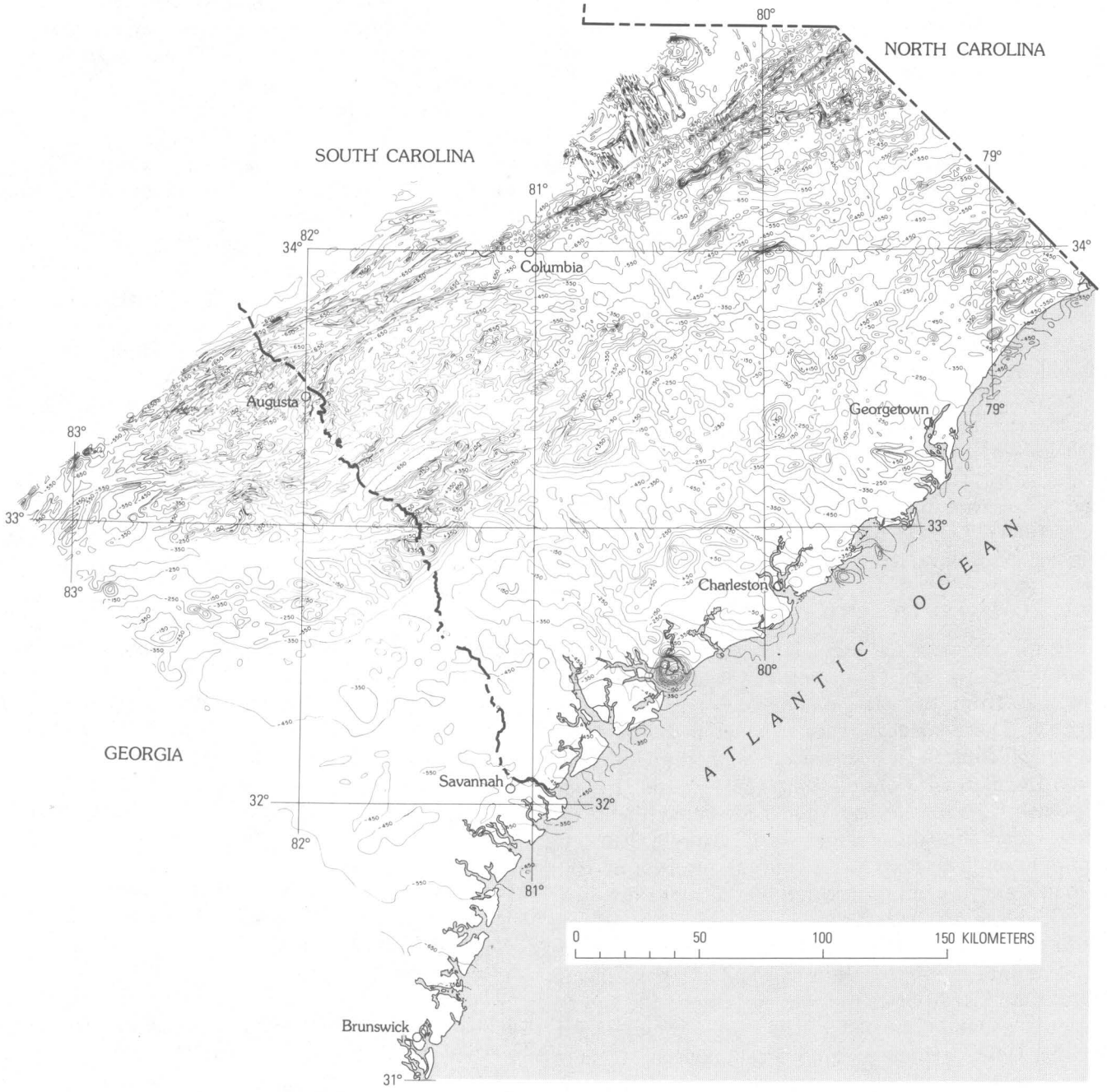

FIGURE 3.—Generalized aeromagnetic map of southeastern South Carolina and eastern Georgia. See figure 1 for location of area and sources of data. Contour interval is 100 gammas, and values are relative to a datum of 53,715.02 gammas. The data have been reduced to remove the international geomagnetic reference field (Fabiano and Peddie, 1969).

relation or lack of correlation of the gravity and magnetic fields. As examples, granitic plutons of the Piedmont generally produce gravity lows, and mafic plutons produce gravity highs. Usually felsic plutons produce aeromagnetic lows, but many produce aeromagnetic highs. Magnetic aureoles in the country

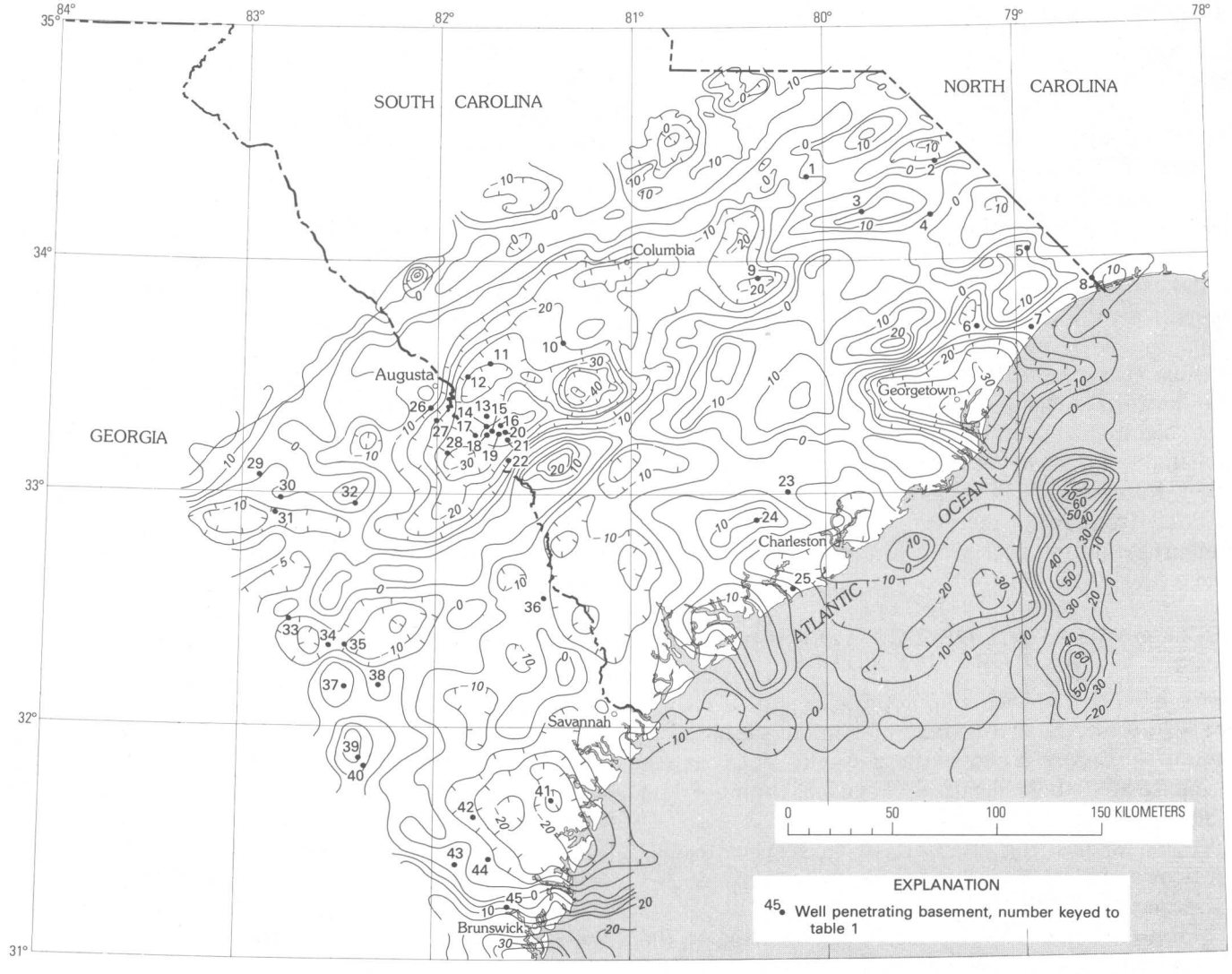

FIGURE 4.—Simple Bouguer anomaly map of the South Carolina and Georgia Coastal Plain in the area of aeromagnetic coverage. Contour intervals are 5 and 10 milligals; hachures indicate areas of lower gravity. See text for sources of data.

rock and magnetic border phases or compositional layering of the younger plutons are reflected in the magnetics. Linear aeromagnetic high anomalies, particularly those associated with corresponding gravity high anomalies, are often caused by bedded sources. Other linear high magnetic anomalies may reflect cataclastic zones or compositional layering in plutonic rocks. The least ambiguous of all geophysical fields is the association of steep gradient, high amplitude, circular or elongate gravity and aeromagnetic highs with mafic or ultramafic plutons.

Aeromagnetic and gravity maps also provide information not only on lithology, but also on the structural deformation of the rocks of an area. For example, when rocks are subjected to a horizontal compressive stress exceeding their elastic limit, they fold, elongate, buckle, and shear, and at sufficiently high temperatures become injected along axes perpendicular to the direction of applied force. Even large bodies of solid granite, if subjected to sufficient stress and heat, flow through plastic deformation to reflect the direction of applied stress.

The stress direction is imprinted in their geologic fabric, which, in turn, is reflected in the magnetic grain.

Such a grain is strongly developed in the geologic and aeromagnetic patterns of rocks of the Appalachian system. The rocks involved in the Appalachian orogen have a common geologic fabric and a corresponding geomagnetic pattern of anomalies that are elongated in the northeast direction. Regardless of the causative rocks or structures, this pattern of anomalies may be observed on aeromagnetic maps from diverse parts of the Appalachian system, including rocks beneath the Atlantic Coastal Plain. The pattern reflects lithologic changes associated with bedding repeated through folding, tilting, or faulting, and shear structures along the geologic grain. Later intrusive rocks can generally be differentiated from rocks involved in the orogen because they crosscut this geologic grain or do not show the above fabric.

INTERPRETATION OF THE AEROMAGNETIC AND GRAVITY FIELDS

We have divided the magnetic map shown on figure 3 into a number of areas of similar geophysical signature. Figure 5 shows these subdivisions, in addition to drill hole locations keyed to numbers on table 1.

To aid in locating the units with respect to cultural or political boundaries, we have also plotted these major units on a location map (fig. 6).

Magnetic zones 1n, 1s, and 2a all lie west of the Fall Line (fig. 1) where sources are generally exposed. Areas 1n and 1s are underlain by bedded, tuffaceous metavolcanic rocks of the Carolina slate belt and area 2a by the higher grade gneissic granite, granitic gneiss, hornblende gneiss, and quartz-microcline gneiss of the Kiokee belt. The most prominent trend in the magnetics over both belts is northeast, reflecting the geologic grain of the Appalachian orogen.

In the Carolina slate belt, the magnetic anomalies are sharp, and wavelengths are about 1 km, and amplitudes generally less than 200 gammas. Many are continuous for distances up to 50 km, suggesting a continuity of the causative units. Most of the field, however, is smooth. The anomaly pattern is known to reflect dipping bedding within the volcanic and depositional units of the belt. The tectonic style of the belt is one of broad regional folding along subhorizontal axes. The beds are tilted gently to the east in area 1n (Bell and Popenoe, 1976), and gently folded in area 1s.

The Kiokee belt in area 2a is characterized by a more complex flat to moderately convoluted magnetic field of slightly higher amplitude and generally more discontinuous sharp linear northeast-trending anomalies. These linear anomalies occur over both granitic gneiss and gneissic granite units.

The linear zone dividing magnetic zone 1 from magnetic zone 2 is labeled F_1 and reflects a major fault system that can be traced from North Carolina into Georgia by its magnetic pattern (Hatcher and others, 1977; Daniels, 1974; Bell and others, 1974; Bell and Popenoe, 1976). The fault system not only separates areas of differing geophysical character, but is marked by short wavelength, linear magnetic highs characteristic of cataclastic zones of major faults of the Piedmont. Similar aeromagnetic highs have been noted associated with the Alexander City, Brevard, Towaliga, Bartletts Ferry, and Goat Rock fault systems (Neathery and others, 1976).

The general gravity field of the Carolina slate belt is flat, and has an average Bouguer value of +5 mGals (fig. 4). This is high, relative to the more felsic rocks of the Kiokee belt.

Magnetic highs and deep gravity lows of 10 to 15 mGals amplitude are associated with granitic to quartz-monzonitic plutons underlying areas 1a (Pageland pluton) and 1b (Liberty Hill pluton) (fig. 6). These plutons exhibit a strong discontinuous magnetic aureole. Both plutons exhibit some internal compositional differences evident in the aeromagnetic signature. Their crosscutting relationships identify that the plutons were emplaced after the last regional metamorphic event (Bell and Popenoe, 1976). This is evident from their magnetic signature.

A second prominent magnetic trend is evident in area 1n and in extensive areas over the Coastal Plain. These are northwest-trending linear aeromagnetic highs which correlate with diabase dikes of assumed Triassic or Jurassic age (King, 1961, 1971; Bell and Popenoe, 1976). Figure 7 shows our interpretation of the distribution of these dikes in the survey area. Where deeply buried, only the largest are traceable, and no doubt other dikes exist that are not shown on figure 7. The dikes can be recognized most easily where they cut low-susceptibility material, or in areas of aeromagnetic lows, but some are evident in areas of aeromagnetic highs.

In addition to the northwest-trending set of dikes, a north-trending dike set is evident over the Coastal Plain near long 79°30′ W. Dikes of this trend and longitudinal position are exposed in the Deep River

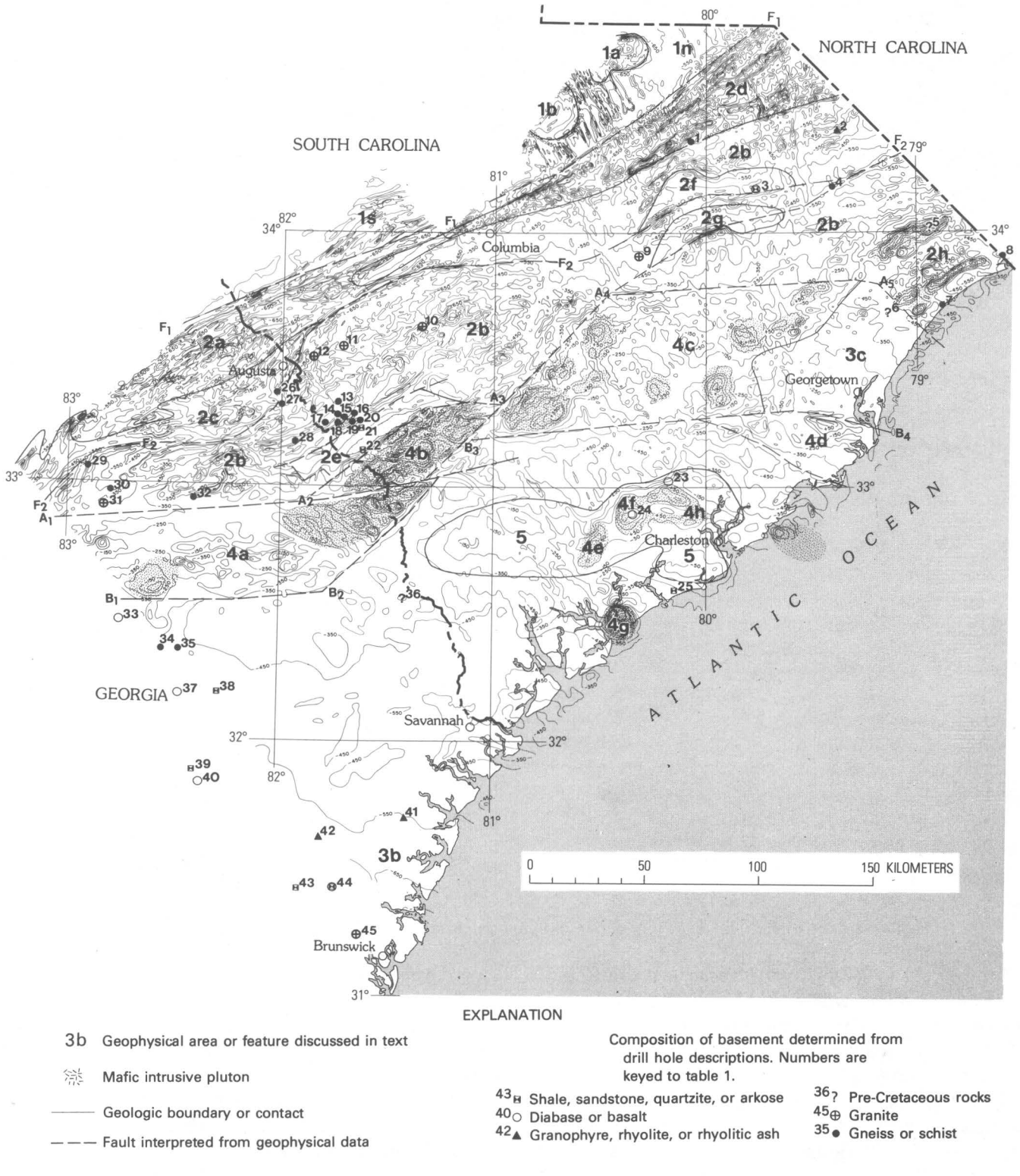

FIGURE 5.—Interpretive map showing the major geophysical and geologic basement units underlying the Coastal Plain of South Carolina and eastern Georgia.

Triassic basin of North Carolina, where they were mapped discontinuously by Reinemund (1955). Although Reinemund did not recognize the north-trending dikes as continuous at the surface, new magnetic data (U.S. Geol. Survey, 1974) indicate that this dike set is continuous at depth in that area.

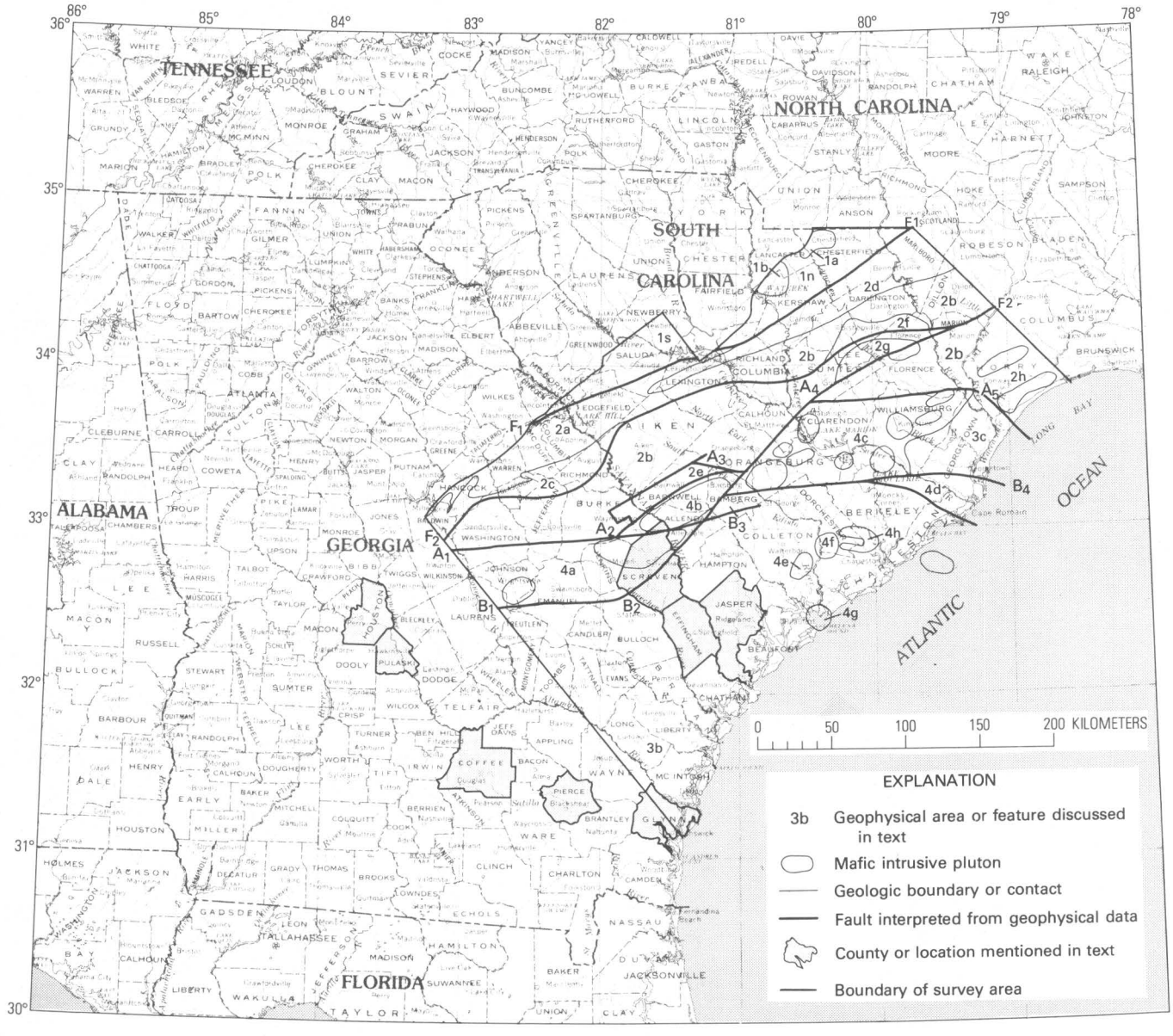

FIGURE 6.—Location map showing major geophysical basement units and localities discussed in text.

If the two widely separated areas are connected by continuous dikes, which they appear to be, the length of this swarm is thus greater than 275 km.

Anomalies characteristic of the Kiokee belt and Carolina slate belt are extensive in a broad area under the Coastal Plain, and drill data confirm that similar sources cause the anomalies. We have labeled this area 2b on figure 5. In addition, several subareas labeled 2c and 2d have been delineated. The magnetic signature of area 2c was correlated by Daniels (1974) with exposures of low-grade rocks near Augusta, Ga. (Bel Air belt of Crickmay, 1952), and we have extended Daniels' correlation to the south. The highly convoluted and distinctive magnetic unit 2d appears to correlate with low-grade rocks exposed in river valleys north of Columbia, S. C. (lower metasiltstone unit of Daniels). We have extended this unit to the northeast of Columbia on the magnetic signature.

The central area of zone 2b is characterized by a large, closed gravity low with a minimum value of −45 mGals and an average Bouguer value on the

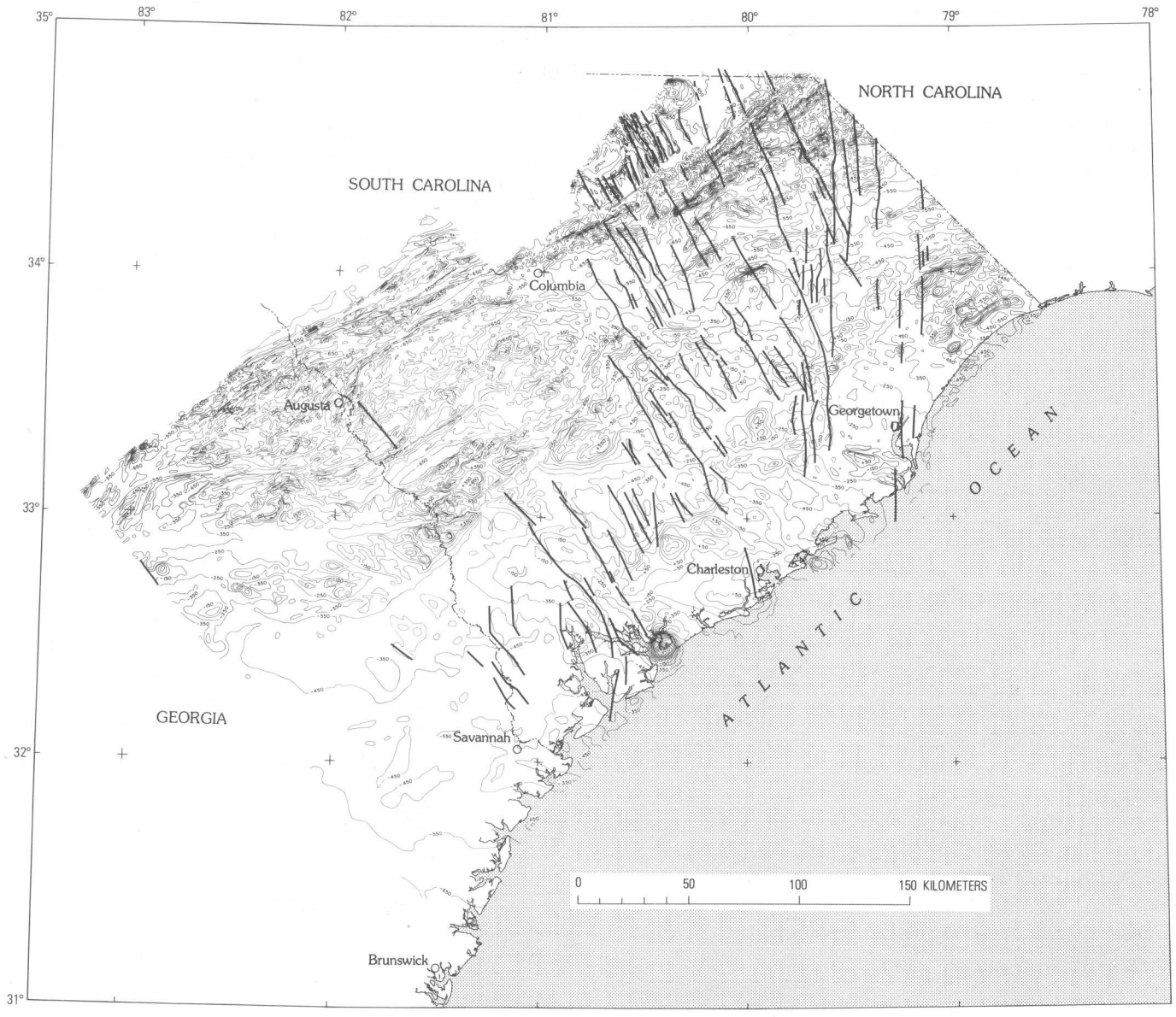

FIGURE 7.—Interpretive map showing the larger diabase dikes of assumed Triassic or Jurassic age present beneath the Coastal Plain of South Carolina and eastern Georgia.

order of −25 mGals. Basement samples (holes 9–12, fig. 5) and magnetic and gravity data indicate that a large proportion of this area is underlain by low-density gneissic granite. The proportion of granite to the rock it intrudes seems to be directly related to the Bouguer value. The granite appears to be the predominant basement lithology south and east of Columbia, S. C., but is probably subordinate to metavolcanic rocks near the North Carolina State boundary, where longer, more continuous linear magnetic and gravity highs and lows predominate, indicating probable bedded sources. Areas underlain by this foliated granite have a northeast-trending linear magnetic grain similar to areas underlain by bedded sources. This grain probably reflects compositional layering.

We could find no aeromagnetic anomalies characteristic of the large bodies of nonfoliated porphyritic granites such as the Pageland and Liberty Hill plutons in the area of 2b beneath the Coastal

Plain. Gravity anomalies that suggest circular plutons are present south of drill hole 10 and at drill hole 9; however, the magnetic highs characteristic of the exposed plutons are not associated with these gravity lows. The linear aeromagnetic highs over the gravity minima indicate that the source of these gravity lows is probably foliated granite.

A number of long, moderate amplitude aeromagnetic highs crossing areas 2a, 2b, and 2c are not associated with gravity highs. Their anastomosing pattern suggests that they may reflect cataclastic zones associated with Piedmont faults. We have labeled one particularly prominent break, which is probably, a fault, F_2. Daniels (1974) showed that amphibolitic rocks (hornblende-chlorite schist) are probably the cause of the long, linear highs north of area 2e.

Area 2h has two pronounced 10+ mGal gravity highs associated with aeromagnetic highs and area 2f lies on a 15 mGal high. If the source of these anomalies derive from the contrast of amphibolitic gneiss (2.8–2.9 gs/cm^3) with more felsic rocks (2.7–2.8 gs/cm^3), the source would have a minimum depth extent of 1.2 and 1.8 km, respectively. If they derive from the contrast of diabase or gabbro (2.9–3.0 gs/cm^3) with felsic volcanic rocks, their minimum depth extent would be 0.8 and 1.2 km. In both areas we favor intrusive gabbros as the source of the gravity highs.

The Dunbarton Triassic(?) basin, described by Marine and Siple (1974), underlies area 2e. This basin is the cause of a deep, smooth, northeast-trending aeromagnetic low due to a considerable depth of nonmagnetic rock. Marine and Siple (1974) have shown from drill data and geophysical analysis that the basin is 50 km long, 10 km wide, and contains more than 900 m of fanglomerate, mudstone, and sandstone. No volcanic flows or sills are present in the sequence.

Areas 2f and 2g are underlain by smooth, northeast-trending aeromagnetic lows, although the lows are not well developed, as in area 2e. Area 2f is also underlain at basement depth by a Triassic(?) structural basin, as a deep well at Florence, S. C., penetrated 221.6 m of Triassic-appearing sediment below basement depth before bottoming in "trap rock" (Darton, 1896, p. 218), and seismic refraction velocities (Bonini and Woollard, 1960, station 43) are compatible with Triassic sediments at the basement (3.9 km/s). The identification of "trap rock" suggests that some of the linear aeromagnetic highs surrounding area 2f could reflect diabase sills or flows of Triassic age, as suggested by Bonini and Woollard (1960) from seismic velocity data; however, the 15 mGal gravity anomaly is more compatible with a body of greater depth extent than a sill (previously discussed) and suggests that either an intrusive body or a dense lithologic unit underlies the basin. The seismic refraction velocity in area 2g (Bonini and Woollard, 1960, station 44) of 6.8 km indicates that this magnetic low probably does not reflect a sediment-filled Triassic basin unless it is overlain by a diabase sill or flow.

The geophysical fields discussed thus far are all typical of those produced by rocks of the Appalachian orogen. The anomalies of the older crystalline rocks have a northeast grain; the Triassic(?) basins cause smoth, northeast-trending aeromagnetic lows of limited width and length. The geophysical fields of the southern part of the area discussed in the subsequent section are quite different in character, suggesting profound differences in the crustal composition, structure, and (or) metamorphic history of these areas.

The straight boundaries in segments between B_1–B_2, B_2–B_3, B_3–B_4 and the profound change in basement character across the boundaries strongly suggest a series of faults juxtaposing high density magnetic rocks on the northwest and lower density nonmagnetic to mildly magnetic rocks on the southeast. The abruptness of the gravity and magnetic breaks also suggests faulting. The postulated fault between B_2 and B_3 is continuous with B_3–A_4, which together closely follow the base of the Orangeburg or Citronelle escarpment at the surface of the Coastal Plain for a distance of more than 150 km. The coincidence almost certainly reflects a structural control for the scarp, a conclusion reached on geologic evidence by Doering (1960), who believed the scarp marked a hinge line, but refuted by Colquhoun (1965) on the basis of heavy-mineral assemblages in the upper beds of the Coastal Plain.

South of line A_1–A_2–A_3–A_4–A_5 (fig. 5) and north of B_1–B_2–B_3–B_4 (fig. 5), the crust is highly mafic, causing high-amplitude gravity and magnetic anomalies, except for area 3c, the large gravity low centered around Georgetown, S.C. The magnetic field south of B_1–B_2–B_3–B_4 does not have the grain of the Appalachian orogen and is composed of a smooth southward decreasing field of low amplitude, random to east-trending anomalies, and several areas of higher magnetic level that enclose sharp, steep-gradient, high-amplitude circular anomalies. The Bouguer gravity field of this southern area is smooth and can be viewed as a broad regional low, averaging

−10 mGals, on which are superimposed sharp, steep-gradient gravity positives.

Part of the smoothing of the regional field south of line B_1–B_4 can be accounted for by an increased section of Coastal Plain rocks in the southeast Georgia embayment. Figure 2 indicates that this thickening is not rapid, however, but gradual, and magnetic anomalies from northwest-trending dike sources are not significantly diminished. Therefore, the low-amplitude field south of the line indicates weakly magnetic rocks beneath the Coastal Plain sediments, caused by a major change in basement composition, metamorphic grade, tectonic style, or a combination of all three. The smooth field contains many low-amplitude, moderately sharp-gradient anomalies that can be shown to originate from sources at or near the depth of known or seismic basement; however, only linear anomalies reflecting dikes and a few circular anomalies, perhaps reflecting small plutons, have amplitudes of over 100 gammas. This suggests that many of these anomalies, particularly areas of low-amplitude button-like anomaly fields seem in the detailed 10-gamma contour aeromagnetic data, may originate from thin sources.

Several possible lithologies could reasonably account for the smooth magnetic and gravity field south of line B_1–B_4. From observations of the geophysical fields of exposed Piedmont rocks, these would include high-grade schist or gneiss, granitic rocks, or a deep basin of flat-lying or unmetamorphosed sedimentary rocks. Our interpretation is that most of the smooth field reflects a thick section of unmetamorphosed flat-lying clastic and volcanic rocks within a structural basin for the following reasons:

1. The straight boundaries B_1–B_2, B_2–B_3, and B_3–B_4 suggest faults.

2. The general geophysical character of the entire southern province resembles that seen over some Triassic basins where a flat magnetic field is associated with stratified continental deposits, and anomalies are associated with exposures of mafic intrusive or extrusive rocks (see Kane and others, 1972) and, in some cases, secondary horst structures juxtaposing older rocks with the younger rocks.

3. No high-grade schist or gneiss is known from drill holes in the smooth field, with the exception of drill holes 34 and 35, which are discussed later. Instead, all drill holes within the area have bottomed in unmetamorphosed flat-lying volcanic flows, volcaniclastic rocks, and tuffaceous clastic rocks (wells 23–25, 37–55, table 1). These lithologies within the survey area include quartz-rhyolite porphyry, amygdaloidal basalt and diabase, volcanic ash, and arkosic to fine-grained sandstone. No felsic intrusive rocks, such as granites, are known from basement samples south of the boundary B_1–B_4 and north of Glynn, Pierce, and Coffee Counties, Ga. (fig. 6).

In South Carolina, granitic basement has been suggested as the cause of the smooth magnetic field (Taylor and others, 1968, p. 776; Daniels, 1974), on the basis of reported granite at the basement recovered from a well that was drilled in Screven County, Ga. (well 36, table 1); however, new information reveals that no basement sample was recovered from the Screven County well (Sam Pickering, Jr., oral commun., 1976) and the identification of basement material as granite was based on the resistance to the drill. Seismic and magnetic evidence suggests that the "basement" in Screven County, Ga., is composed of stratified rocks. Two sub-horizontal seismic refractors were recorded by Pooley (1960) (refraction line 4) only 3 km from the Screven County well, one at 0.7 km (the surface contoured in fig. 2) and a second at 2.1 km. No gravity or magnetic break is evident between the well location and seismic refraction line location. If the resistive rock penetrated in the Screven County well was a volcanic flow, it would explain the high basement velocity of 5.3 km/s recorded by Pooley and the deeper subbasement refractor.

4. The shoreward extension of the Brunswick, Ga., branch of the East Coast magnetic high, discussed by Taylor, Zietz, and Dennis (1968), Emory and others (1970), and Rabinowitz (1974) touches the southern corner of our study area in area 3b. Along the shelf edge, the magnetic high, continuous with the Brunswick anomaly, has been interpreted as related to Mesozoic continental extension.

5. Seismic, electrical, and magnetic analysis show that subhorizontal layers are present at several depths beneath the basalt (geophysical basement) in the Summerville, S.C., area (Ackermann, this volume; Campbell, this volume; Phillips, this volume). Subhorizontal refractors were also recorded below the geophysical basement in the area of smooth magnetic field in Jasper County, S.C., and Effingham County, Ga. (Pooley, 1960, refraction lines 10, 2). The most probable explanation for the high velocity, high-resistivity layers beneath the geophysical basement depth (fig. 2) is deeper volcanic flows or sills, or the true crystalline basement.

We favor a Triassic(?) age rather than a Paleozoic age for the unmetamorphosed sedimentary and

volcanic rocks within the structural basin for the following reasons:

1. The abruptness of the boundary dividing the smooth field from the northeast-trending Piedmont anomalies suggests structure rather than a metamorphic gradient.

2. All of the rock penetrated in the area of the smooth field suggest Triassic lithologies, except for the rhyolites and ignimbrites. The rhyolitic lithologies do not preclude a Triassic age, as rhyolites and ignimbrites of Triassic age are extensive in the southern Florida volcanic province (Barnett, 1975, p. 127).

3. The area lies on the predictable continuation to the east-northeast of the deep Triassic graben system that underlies the region of the Apalachicola–southwest Georgia embayment in southwestern and south-central Georgia (Barnett, 1975; Marine and Siple, 1974) (fig. 2). In Florida and western Georgia, the graben system is more than 200 km wide (Barnett, 1975; Neathery and Thomas, 1975; Marine and Siple, 1974) and contains a number of secondary horst blocks of older Paleozoic sedimentary rocks and Precambrian(?) or lower Paleozoic(?) crystalline rocks. The various basins of the graben system are filled with coarse red feldspathic and arkosic clastics, and tabular, sometimes amygdular, diabases believed to be intrusive sills (Barnett, 1975).

The northern boundary of this graben system is structural, as a well in Pulaski County, Ga. (R. O. Leighton-Dana No. 1, Milton and Hurst, 1965), penetrated 1,176 m of coarse- to fine-grained sandstones and diabase layers of Triassic(?) age below the Upper Cretaceous Coastal Plain sedimentary rocks only 30 km southeast of wells in Houston County, Ga., that bottomed at basement depth in Piedmont rocks (Tricon Minerals-Gilbert No. 1, Milton and Hurst, 1965). There is a distinct gravity break between the Houston County, Ga., and the Pulaski County, Ga., wells (see Long and others, 1972). This break is similar to and along the strike of our magnetic break and corresponding gravity break B_1–B_2 (fig. 5), suggesting a similar cause.

4. Northwest-trending anomalies probably reflecting mafic dikes cut the smooth field in South Carolina (fig. 7). These dikes are along the same trend and are assumed to be continuous with dike swarms of Triassic(?) or Jurassic(?) age that cut the exposed Piedmont rocks. Depth analyses on these dikes indicate that they have tops at basement depth (basalt) (0.7 to 1 km) in South Carolina. This would put a minimum probable age of Jurassic(?) on the basement material in the area of the smooth field in South Carolina.

5. There are no obvious structural breaks within the smooth field. Instead, magnetic data suggest that flow units are extensive in the basement and form zones of more or less localized, discontinuous bodies, which cause low-amplitude magnetic anomalies. The flows appear to be mixed with and separated by intervening zones or layers of clastic materials, causing areas of smoother aeromagnetic and gravity lows.

Basement compressional velocities in the area of smooth magnetic field (Pooley, 1960, Bonini and Woollard, 1960) of 4.5–5.6 km/s are not compatible with velocities of Triassic sedimentary rocks (2.3–4.5 km/s) but could be explained by the extensive volcanic flows or sills known to be present at the basement.

Wells 34 and 35 are within the area of smooth magnetic field. These wells were reported to have bottomed in metamorphosed rocks (Milton and Hurst, 1965, p. 17). If the identification of basement in this area is correct, these rocks may occupy a small secondary horst structure within the proposed structural basin. Clearly, metamorphism is nil to low grade in all other wells that have pentrated basement within the smooth magnetic field.

The shape and amplitudes of the aeromagnetic and gravity highs in areas 4a, 4b, 4c, 4d, 4e, 4f, 4g, and 4h (figs. 4 and 5) clearly indicate that these areas are underlain by mafic intrusive masses. Mafic intrusive masses of this abundance, shape, and size are not known elsewhere in the south Appalachian Piedmont. A similar, but less pronounced, occurrence of mafic plutons along the coast of Maine and Massachusetts was interpreted by Kane and others (1972) as marking a major crustal break resulting from adjustments between distinctive crustal blocks offshore and onshore. The association of the aeromagnetic and gravity highs in areas 4a, 4b, and 4c with the boundary between Piedmont-type metamorphic rocks and undeformed rocks, and the arrangement of the plutons within the ridgelike zone along an eastwest and northeast trend, suggest that the zone also marks a major crustal break.

Anomalies 4e, 4f, and 4g have the classic gravity and magnetic forms of unmetamorphosed, stocklike mafic plutons, and may be feeders for basalt flows known to underlie the area (wells 23 and 24, table 1). Anomalies 4e and 4f are deep or may be produced by plutons with outward-dipping contacts, whereas 4g is typical of an anomaly from a steep-sided, cylindrical, compositionally zoned pluton.

Depth analyses on anomalies 4e, 4f, and 4h by the technique of Vaquier and others (1951) and by Phillips (this volume) show that the tops of the main plutonic masses lie at about 1.5-km depth or below basement (basalt) depth. If the three small circular anomalies associated with the top of anomaly 4f are treated as separate sources, these anomalies originate at about 0.8 km below ground level, or the known depth to the basalt flows drilled in this area (drill hole 24, table 1). The small anomaly centered between drill hole 23 and 24 similarly originates from the basalt depth. Depth analyses by the same technique on anomaly 4g indicates a depth to the top of this pluton of about 1 km, or near the depth to the high velocity refractor (0.925 km) in this area (Bonini and Woollard, 1960; Pooley, 1960).

Areas 4a, 4b, 4c, and 4d outline zones composed of a complex of mafic plutons which appear to intrude a mafic crust, perhaps similar to the Bays of Maine igneous complex (Chapman, 1968; Kane and others, 1972). Individual plutons in the zone are not isolated, as are anomalies 4e–4h, but discrete plutonic masses can be identified from both the gravity and the magnetic data. On figure 5 we have patterned the most prominent of these plutons within the zones. The plutons appear to be arranged reticularly along apparent north-northeast and east trends.

The zones surrounding individual plutons in areas 4a, 4b, and 4c, and zone 5 near plutons 4e, 4f, and 4h have an unusually high magnetic level. Our modeling and that of Phillips (this volume) in area 5 suggest that in this area much of the magnetic buildup (broad wavelength anomalies) originates from a deep source; however, there is a strong possibility that at least some of the high magnetic level originates from the cumulative effect of many shallower, thin magnetic sources. Depth analyses show that many individual anomalies within this zone of high magnetic level originate near basement (basalt) depth. Our interpretation in area 5 and area 4c is that these areas of high level may, in part, outline areas of extensive mafic flows, although we were unable to model the broader sources as flows.

There is a deep gravity low underlying Georgetown, S. C., and a corresponding high magnetic level in area 3c of the magnetic map. This gravity low has been interpreted by Talwani and others (1975) to be caused by a deep structural basin of low-density rock capped by a mafic sill or flow. The sill would explain high seismic velocities (6.7 km/s) (Bonini, 1957) and high magnetic level associated with the gravity low. A second interpretation, which would also fit the data, is that the gravity anomaly reflects a low-density basement rock, such as a granite body, coincidentally overlain by diabase or basalt (Talwani and others, 1975). On the basis of the amplitude of the gravity low (35 mGals), the magnetic expression, which suggests a prismatic source, and the drill hole 7, which bottomed in chlorite schist, we favor the second interpretation, whereas Talwani favored the first.

CONCLUSIONS

The major point in our analysis is that the basement beneath southeastern South Carolina and east-central Georgia is not simply an extension of the Appalachian Piedmont, as generally believed, but differs strikingly from the Piedmont. The area near the Charleston earthquake zone is particularly anomalous, as it is underlain by a number of large mafic plutons and an extensive volcanic field. These plutons intrude nonmagnetic and undeformed layered rocks that could be as old as Paleozoic, although some evidence in the Charleston, S. C., area suggests that here they may be Triassic(?) and perhaps as young as Cretaceous. The presence of mafic plutons of this size and abundance suggest that they mark deep structural breaks interpreted to be of Mesozoic age.

The boundary between the deformed rocks of the Piedmont and the undeformed rocks beneath the Coastal Plain is abrupt, marked along most of its length by a ridgelike zone of mafic plutons. The straight segments along much of the zone suggests a series of faults, rather than a metamorphic gradient.

If the smooth magnetic field in South Carolina and south-central Georgia does reflect a complex structural basin of Triassic(?) age rocks, this basin is an order of magnitude larger than any exposed Triassic(?) basin in the Eastern United States, and is a major geologic feature requiring explanation. The apparent overlap of Florida has long been noted in most continental reconstructions (Bullard and others, 1965; Dietz and Holden, 1970). The proposed graben system could furnish a zone along which the overlap could be accommodated. Also, it is possible that Florida, during the initial stages of continental separation, occupied a separate crustal fragment attached to the trailing edge of the African-South American blocks and later became stranded with the North American plate. There are

any number of interesting speculations; in fact, the extension of the graben system into South Carolina and eastern Georgia at this time is a speculation based on geophysics yet to be proved by drilling.

REFERENCES CITED

Applin, E. R., and Applin, P. L., 1964, Logs of selected wells in the Coastal Plains of Georgia: Georgia Geol. Survey Bull. 74, 229 p.

Barnett, R. S., 1975, Basement structure of Florida and its tectonic implications: Gulf Coast Assoc. Geol. Socs. Trans., v. 25, p. 122–142.

Bell, Henry, III, Butler, R. J., Howell, D. E., and Wheeler, W. H., 1974, Geology of the Piedmont and Coastal Plain near Pageland, South Carolina and Wadesboro, North Carolina: South Carolina Devel. Board, Div. Geology [Carolina Geol. Soc. Field Trip Guidebook], 23 p.

Bell, Henry, III, and Popenoe, Peter, 1976, Gravity studies in the Carolina Slate belt near the Haile and Brewer mines, north-central South Carolina: U.S. Geol. Survey Jour. Res., v. 4, no. 6, p. 667–682.

Bollinger, G. A., 1972, Historical and recent seismic activity in South Carolina: Seismol. Soc. America Bull., v. 62, no. 3, p. 851–864.

Bonini, W. E., 1957, Subsurface geology in the area of the Cape Fear Arch as determined by seismic-refraction measurements: Madison, Wisconsin Univ. Ph.D. thesis, 180 p.

Bonini, W. E., and Woollard, G. P., 1960, Subsurface geology of North Carolina-South Carolina Coastal Plain from seismic data: Am. Assoc. Petroleum Geologists Bull., v. 44, no. 3, p. 298–315.

Bullard, E. C., Everett, J. E., and Smith, A. G., 1965, The fit of continents around the Atlantic, *in* A symposium on continental drift: Royal Soc. London Philos. Trans., ser. A, v. 285, no. 1088, p. 41–51.

Butler, J. R., and Fullagar, P. D., 1975, Lilesville and Pageland plutons and the associated meta-rhyolites, eastern Carolina slate belt: Geol. Soc. America Abs. with Programs, v. 7, no. 4, p. 475.

Chapman, C. A., 1968, A comparison of the Maine coastal plutons and the magmatic central complexes of New Hampshire, *in* Zen, E-an and others, eds., Studies of Appalachian geology—northern and maritime: New York, Interscience Publishers, p. 385–396.

Colquhoun, D. J., 1965, Terrace sediment complexes in central South Carolina—Atlantic Coastal Plain Geol. Assoc., Field Conf. 1965: Columbia, S.C., Univ. South Carolina, 62 p.

Cooke, C. W., 1936, Geology of the Coastal Plain of South Carolina: U.S. Geol. Survey Bull. 867, p. 176–177.

Crickmay, G. W., 1952, Geology of the crystalline rocks of Georgia: Georgia Geol. Survey Bull. 58, 54 p.

Daniels, D. L., 1974, Geologic interpretation of geophysical maps, central Savannah River area, South Carolina and Georgia: U.S. Geol. Survey Map GP–893, 9 p. text.

Darton, N. H., 1896, Artesian-well prospects in the Atlantic Coastal Plain region: U.S. Geol. Survey Bull. 138, 232 p.

Dietz, R. S., and Holden, J. C., 1970, Reconstruction of Pangaea: Breakup and dispersion of continents, Permian to present: Jour. Geophys. Research, v. 75, no. 26, p. 4939–4956.

Doering, J. A., 1960, Quaternary surface formations of southern part of the Atlantic Coastal Plain: Jour. Geology, v. 68, no. 2, p. 182–202.

Dutton, C. E., 1889, The Charleston earthquake of August 31, 1886: U.S. Geol. Survey Ann. Rept. 9, p. 203–528.

Emery, K. O., Uchupi, Elazar, Phillips, J. D., Bowin, C. O., Bunce, E. T., and Knott, S. T., 1970, Continental rise off eastern North America: Am. Assoc. Petroleum Geologists Bull., v. 54, no. 1, p. 44–108.

Fabiano, E. G., and Peddie, N. W., 1969, Grid values of total magnetic intensity, EGRF–1965: U.S. ESSA tech. Rept. CGS–38, 55 p.

Fullagar, P. D., 1971, Age and origin of plutonic intrusions in the Piedmont of the southeastern Appalachians: Geol. Soc. America Bull. v. 82, no. 10, p. 2845–2862.

Georgia Geological Survey, 1976a, Geologic map of Georgia: Georgia Geol. Survey, scale 1:500,000.

———1976b, Preliminary data on age dates in Georgia: Georgia Geol. Survey Open-file Rept. 9 p.

Hatcher, R. D., Jr., Howell, D. E., and Talwani, Pradeep, 1977, Eastern Piedmont fault system: Speculations on its extent: Geology, v. 5, no. 10, p. 636–640.

Heron, S. D., Jr., and Johnson, H. S., Jr., 1966, Clay mineralogy, stratigraphy, and structural setting of the Hawthorn Formation, Coosawhatchie district, South Carolina: Southeastern Geology, v. 7, no. 2, p. 51–63.

Hersey, J. B., Bunce, E. T., Wyrick, R. F., and Dietz, F. T., 1959, Geophysical investigations of the continental margins between Cape Henry, Virginia, and Jacksonville, Florida: Geol. Soc. America Bull., v. 70, no. 4, p. 437–465.

Hurst, V. J., 1970, The Piedmont in Georgia, *in* Fisher, G. W., and others, eds., Studies of Appalachian geology—central and southern: New York, Interscience Publishers, p. 383–396.

Kane, M. F., Yellin, M. J., Bell, K. G., and Zietz, I., 1972, Gravity and magnetic evidence of lithology and structure in the Gulf of Maine region: U.S. Geol. Survey Prof. Paper 726–B, 22 p.

King, P. B., 1961, Systematic pattern of Triassic dikes in the Appalachian region: U.S. Geol. Survey Prof. Paper 424–B, p. B93–B95.

King, P. B., 1971, Systematic pattern of Triassic dikes in the Appalachian region, Second report: U.S. Geol. Survey Prof. Paper 750–D, p. D84–D88.

Long, L. T., Bridges, S. R., and Dorman, L. M., 1972, Simple Bouguer gravity map of Georgia: Georgia Inst. Technology, scale 1:500,000.

Long, L. T., Talwani, P., and Bridges, S. R., 1976, Simple Bouguer gravity map of South Carolina: South Carolina Devel. Board, Div. Geology, scale 1:500,000.

Maher, J. C., 1971, Geologic framework and petroleum potential of the Atlantic Coastal Plain and Continental Shelf: U.S. Geol. Survey Prof. Paper 659, 98 p.

Marine, I. W., and Siple, G. E., 1974, Buried Triassic basin in the central Savannah River area, South Carolina and Georgia: Geol. Soc. America Bull., v. 85, no. 2, p. 311–320.

Meyer, R. P., 1956, The geologic structure of the Cape Fear axis as revealed by refraction seismic measurements: Madison, Wisconsin Univ., Ph.D. thesis, 85 p.

Milton, Charles, and Hurst, V. J., 1965, Subsurface basement rocks of Georgia: Georgia Geol. Survey Bull. 76, 56 p.

Neathery, T. L., and Thomas, W. A., 1975, Pre-Mesozoic basement rocks of the Alabama Coastal Plain: Gulf Coast Assoc. Geol. Soc. Trans., v. 25, p. 86-99.

Neathery, T. L., Bentley, R. D., Higgins, M. W., and Zietz, I., 1976, Preliminary interpretation of aeromagnetic and aeroradioactivity maps of the Alabama Piedmont: Geology (Boulder), v. 4, no. 6, p. 375–381.

Overstreet, W. C., and Bell, Henry, III, 1965a, The crystalline rocks of South Carolina: U.S. Geol. Survey Bull. 1183, 126 p.

——— 1965b, Geologic map of the crystalline rocks of South Carolina: U.S. Geol. Survey Misc. Geol. Inv. Map I–413, scale 1:250,000.

Pooley, R. N., 1960, Basement configuration of subsurface geology of eastern Georgia and southern South Carolina as determined by seismic refraction measurements: Madison, Wisconsin Univ., Masters Thesis, 47 p.

Rabinowitz, P. D., 1974, The boundary between oceanic and continental crust in the western North Atlantic, *in* Burk, C. A., and Drake, C. L., eds., The geology of continental margins: New York, Springler-Verlag, Inc., p. 67–84.

Reed, J. C., Jr., Owens, J. P., and Stockard, H. P., 1968, Interpretation of basement rocks beneath the Atlantic Coastal Plain from reconnaissance aeromagnetic data (abs.): Geol. Soc. America Spec. Paper 115, p. 182–183.

Reinemund, J. A., 1955, Geology of the Deep River coal field, North Carolina: U.S. Geol. Survey Prof. Paper 246, 159 p.

Siple, G. E., 1967, Geology and ground water of the Savannah River Plant and vicinity, South Carolina: U.S. Geol. Survey Water-Supply Paper 1841, 113 p.

——— 1969, Salt-water encroachment of Tertiary limestones along coastal South Carolina: South Carolina Div. Geology Geol. Notes, v. 13, no. 2, p. 51–65.

Snoke, A. W., Secor, D. T., Jr., and Metzgar, C. R., 1977, Batesburg-Edgefield catalastic zone—a fundamental tectonic boundary in the South Carolina Piedmont: Geol. Soc. America Abs. with Programs, v. 9, no. 2, p. 185–186.

Talwani, Pradeep, Ressetar, Robert, McAleer, Jacqueline, Holmes, Tom, Grothaus, Train, Findlay, Marsh, Cable, Mark, and Amick, David, 1975, Gravity and magnetic profile across the Georgetown gravity low: South Carolina Div. Geology Geol. Notes, v. 19, no. 2, p. 24–32.

Taylor, P. T., Zietz, Isidore, and Dennis, L. S., 1968, Geologic implications of aeromagnetic data for the eastern continental margin of the United States: Geophysics, v. 33, no. 5, p. 755–780.

U. S. Geological Survey, 1970, Aeromagnetic map of the Camden-Kershaw area, north-central South Carolina: U.S. Geol. Survey open-file map, scale 1:62,500.

——— 1974, Aeromagnetic map of parts of the Greensboro and Raleigh 1° by 2° quadrangles, North Carolina: U.S. Geol. Survey open-file map 74–29, scale 1:250,000.

——— 1975, Aeromagnetic map of Charleston and vicinity, South Carolina: U.S. Geol. Survey open-file map 75–590, scale 1:250,000.

——— 1976a, Aeromagnetic map of parts of the Brunswick and Savannah 1°×2° quadrangles, Georgia and South Carolina: U.S. Geol. Survey open-file map 76–155, scale 1:250,000.

——— 1976b, Aeromagnetic map of parts of Georgia, South Carolina, and North Carolina: U.S. Geol. Survey open-file map 76–181, scale 1:250,000.

Vacquier, V., Steenland, N. C., Henderson, R. G., and Zietz, Isidore, 1951, Interpretation of aeromagnetic maps: Geol. Soc. America Mem. 47, 151 p. (Reprinted 1963.)

Woollard, G. P.; Bonini, W. E., and Meyer, R. P., 1957, A seismic refraction study of the subsurface geology of the Atlantic Coastal Plain and Continental Shelf between Virginia and Florida: Madison, Wisconsin Univ. Dept. Geol. Geophys. Sec., 128 p.

Zupan, Alan-Jon, and Abbott, W. H., 1976, Appendix B—Comparative geology of onshore and offshore South Carolina, *in* Preliminary summary of the 1976 Atlantic margin coring project of the U.S. Geological Survey: U.S. Geol. Survey open-file rept. 76–844 p. 206–214.

Magnetic Basement Near Charleston, South Carolina—A Preliminary Report

By JEFFREY D. PHILLIPS

STUDIES RELATED TO THE CHARLESTON, SOUTH CAROLINA, EARTHQUAKE OF 1886—A PRELIMINARY REPORT

GEOLOGICAL SURVEY PROFESSIONAL PAPER 1028-J

CONTENTS

ILLUSTRATIONS

MAGNETIC BASEMENT NEAR CHARLESTON, SOUTH CAROLINA—A PRELIMINARY REPORT

By JEFFREY D. PHILLIPS

ABSTRACT

Automated depth analysis has been performed on aeromagnetic profiles collected in an area of current and historical seismicity near Charleston, S. C. Model studies, based on the computer-generated depth estimates, have been used to construct basement cross sections along two north-south lines. These cross sections reveal that extensive surfaces of magnetization contrast are present at two different depths, with the deeper surface having the stronger contrast. The shallower surface corresponds to the seismically determined crystalline basement. The deeper surface is interpreted to be the top of a mafic intrusive complex. Linear zones of anomalously low magnetization within the crystalline rocks appear to be responsible for linear lows in the magnetic anomaly. Reversely magnetized volcanic flows are an alternative interpretation. Contour maps of the computer-generated depth estimates are used to study depths and trends of subsurface structures in the epicentral area.

INTRODUCTION

The aeromagnetic map of Charleston and vicinity, S.C. (U.S. Geol. Survey, 1975) is characterized by localized strong magnetic highs superimposed upon broad, but sharply defined regional highs. The overall pattern suggests that interesting structures and lithologies exist within the crystalline rocks underlying the South Carolina Coastal Plain. The definition of these structural and lithologic features is of particular interest because of the historical seismicity of the Charleston area (Bollinger, this volume; Bollinger and Visvanathan, this volume; Tarr, this volume).

The magnetization contrasts responsible for magnetic anomalies usually are found at the boundaries of relatively homogeneous zones of magnetization. Such magnetization boundaries may be found at the crystalline basement surface (the contact between buried crystalline rock and the overlying sedimentary rock), at lithologic boundaries within the crystalline rock, and at the surfaces of dikes, sills, and volcanic flows within the sedimentary column. In the Charleston region, there is evidence for all three forms of magnetization boundaries.

To locate magnetization boundaries, an automated depth-analysis technique has been used on selected aeromagnetic profiles taken from the Charleston survey (U.S. Geol. Survey, 1975). Two complementary sets of depths have been calculated for each profile. Model studies, based on both sets of solutions, have been used to obtain basement cross sections along two north-south lines. These cross sections indicate the presence of at least two extensive surfaces of magnetization contrast, the deeper surface having the stronger contrast.

The shallower of these two surfaces is interpreted to be crystalline basement on the basis of seismic-refraction studies (Ackermann, this volume). The deeper surface is interpreted to be the top of a mafic intrusive complex. In addition to defining these magnetic-basement surfaces, the depth estimates and model studies suggest that linear zones of anomalously low magnetization are present within the crystalline basement rocks. Contour maps of the computer-generated depth estimates are used to examine these linear features, as well as other apparent structures, in a 40 × 55 km area west of Charleston.

This study was funded by the U.S. Nuclear Regulatory Commission, Office of Nuclear Regulatory Research, Agreement AT (49–25)–1000.

AEROMAGNETIC DATA

A total-field aeromagnetic survey was flown over the South Carolina Coastal Plain between lat

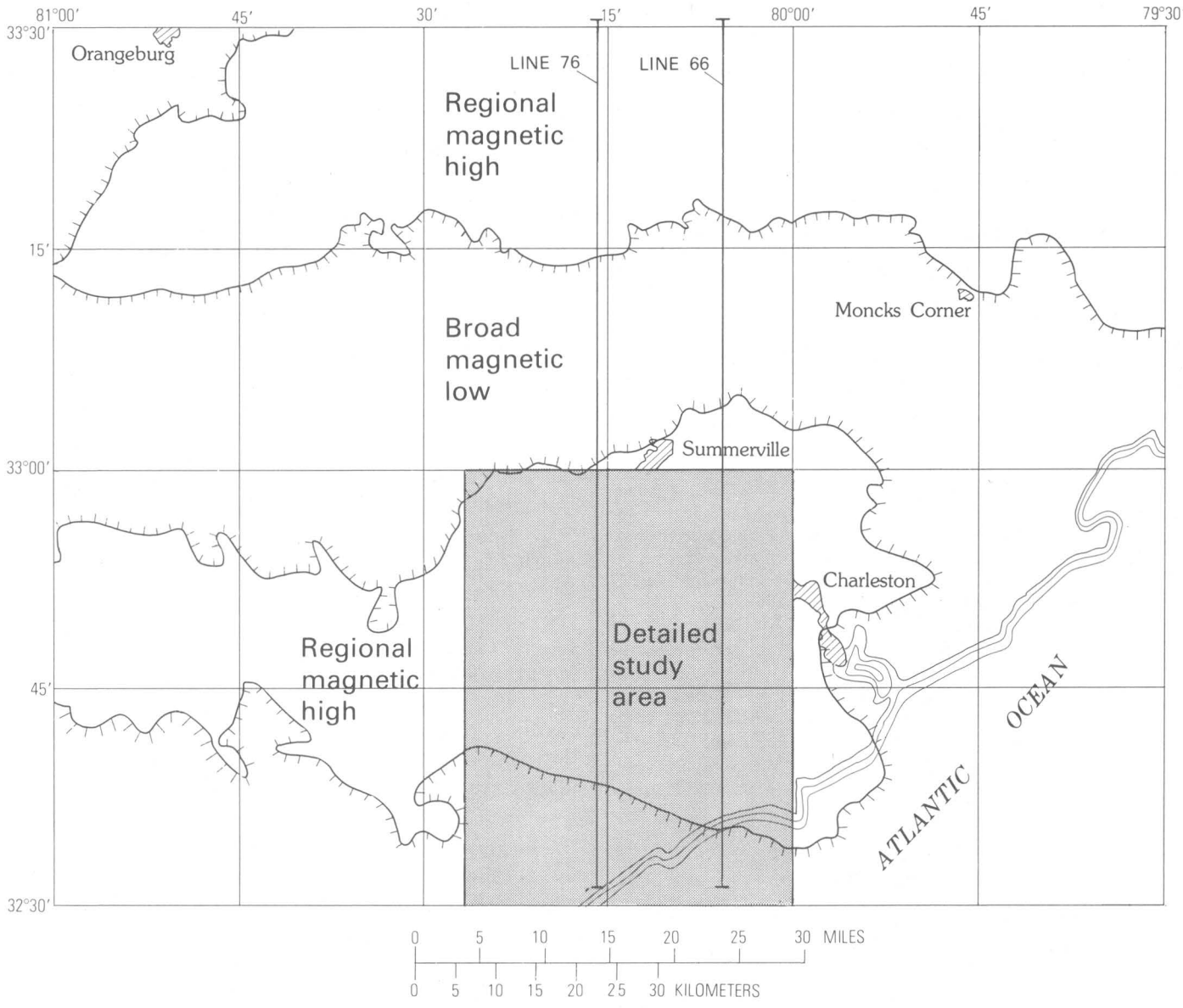

FIGURE 1.—Map showing location of the study area. Magnetic profiles 66 and 76 are indicated. The line with tick marks is the zero contour of the aeromagnetic map (U.S. Geological Survey, 1975).

33°30′ N. and 32°30′ N. in 1973. The flight lines were north-south at 1 mile (1.6 km) spacing. The flight elevation was 500 ft (152 m). The resulting total field anomaly map was released as an open-file report (U.S. Geol. Survey, 1975).

The regional magnetic pattern consists of broad regional highs separated by broad belts of low magnetic intensity. Superimposed upon the regional highs are stronger, more localized highs. In figure 1 the regional magnetic highs and lows are outlined, and the location of the detailed study area is indicated. The part of the aeromagnetic map covering this detailed study area is reproduced in figure 2. Indicated on this figure are the locations of Middleton Place, the Charleston Air Force Base, and the USGS corehole site (Clubhouse Crossroads corehole 1). Strong magnetic highs are found over the corehole site, north and southeast of Middleton Place, and along the coast in the southeast quadrant and the southwest corner of the mapped area. Middleton Place itself sits on an east-west linear magnetic low, bounded on three sides by strong closed magnetic highs and on the south by an east-west linear magnetic high. Both this linear high and the strong triple-peaked magnetic high over the USGS corehole site correspond to similar highs in the gravity anomaly (Long and Champion, this volume). In addition, the regional magnetic highs correspond, for

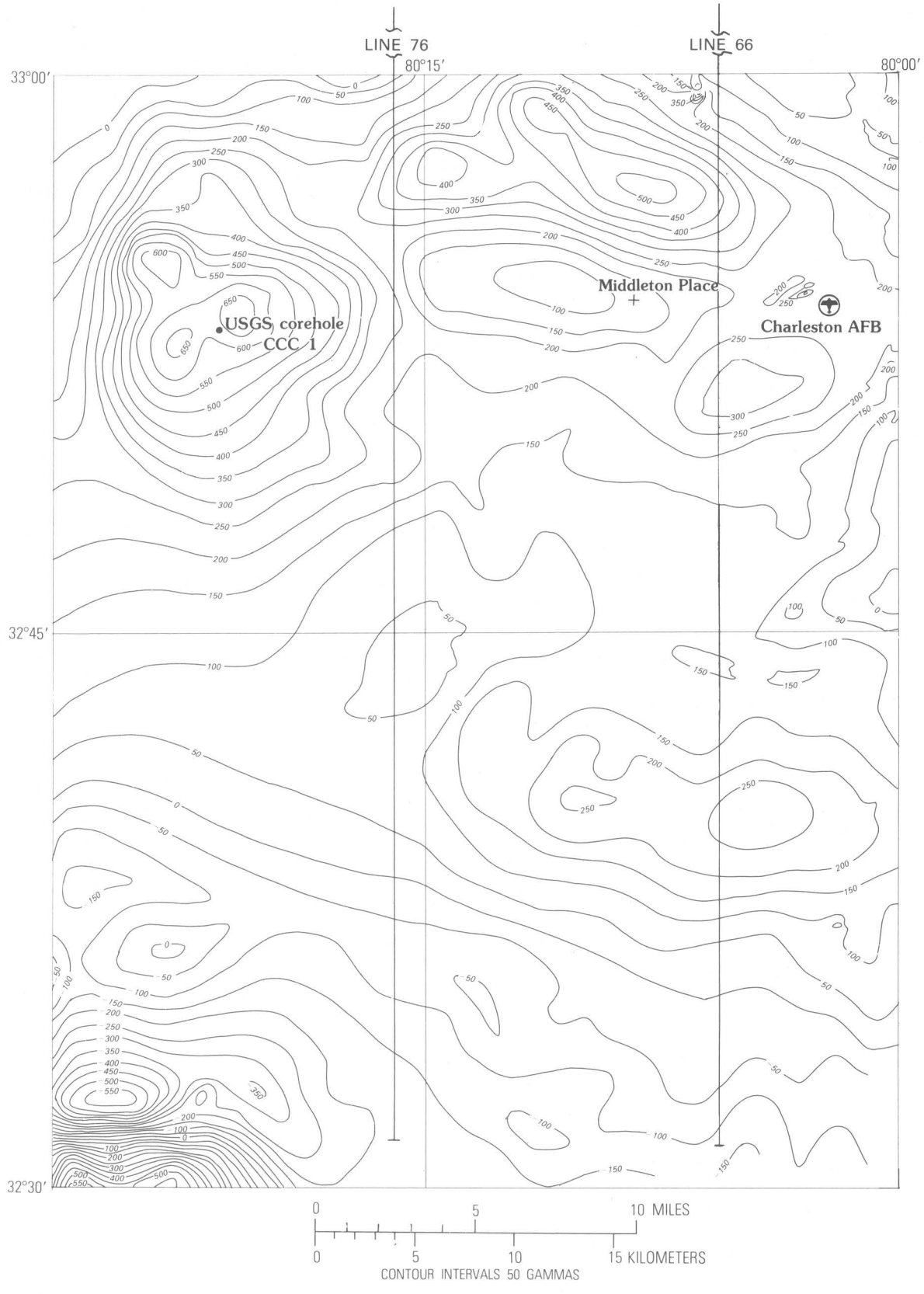

FIGURE 2.—Aeromagnetic map of the study area (modified from U.S. Geological Survey, 1975). The southern ends of magnetic profiles 66 and 76 are indicated.

the most part, to similar regional gravity highs. This correspondence suggests that both the strong magnetic highs and the regional highs are produced by mafic intrusive bodies at depth.

DEPTH ANALYSIS

In order to obtain magnetic-basement depth estimates, digital aeromagnetic data, as recorded along the flight lines, were first interpolated to a rectangular grid. The resulting interpolated profiles were oriented north-south, spaced at 1-mile (1.6 km) intervals, and sampled at quarter-mile (0.4 km) intervals. Selected profiles were analyzed for source depth using the automated high-resolution technique of Phillips (1975). In this technique a statistical source model is used to estimate depth from the autocorrelation function of the magnetic profile. The autocorrelation function is calculated within short windows about each observation point, and compared with a theoretical autocorrelation function that would be produced by a two-dimensional basement having uncorrelated magnetization. This means that the magnetization contrast at the basement surface is assumed to be statistically independent from point to point. Where the fit between the observed and theoretical autocorrelation functions is good, a depth can be estimated. Where the fit is poor, it means the data violate the assumptions of the model, and no reliable depth estimate is possible. In practice then, the computer only locates the segments of the basement where the assumptions of two dimensionality and uncorrelated magnetization appear to be satisfied. When two slightly different statistical models (assuming zero-mean and nonzero-mean source magnetization) are used, two complementary solutions can be obtained—one emphasizing shallow sources and one emphasizing deep sources. The two solutions are combined in cross section form prior to structural or geologic interpretation.

Because the depth-analysis technique uses a sliding data window to search for a continuous basement surface, its response to a sudden vertical change in the basement is often delayed, resulting in hyperbolic tails on the depth estimates. These computer artifacts are generally ignored in the subsequent interpretation. Horizontal shifts of the depth estimates due to phase effects of the magnetic anomaly are reduced in the technique, through use of the analytic signal (Nabigihian, 1972), which has its power centered directly over the sources. However, some horizontal shifts will always remain as a result of the technique's slow response to sudden vertical changes.

One possible source of error in the estimated depths is the assumption that two-dimensional trends in the magnetic anomaly are perpendicular to the flight lines. Where this assumption is not satisfied, the depths will be somewhat overestimated. Fortunately, the major two-dimensional features of the aeromagnetic map do trend at right angles to the flight lines.

Although the required assumptions of two-dimensionality and uncorrelated source magnetization may seem unreasonable, this technique has been successfully tested, both on synthetic data (generated assuming uniformly magnetized bodies) and on real data collected in areas of known source depth. For this reason, we can have some confidence in the estimated depths.

MODEL STUDIES

Two-dimensional modeling techniques were used to obtain cross sections along profiles 66 and 76 (fig. 1). Where possible, computer-generated depths were used to define the models. In areas where no computer-generated depths were available, simple models were used to match the general character of the anomaly and thus complete the cross section. Uniform-induced magnetization in a small number of bodies was assumed in all models. It should be emphasized that model studies of this sort yield nonunique solutions, and commonly alternative solutions are reasonable. However, in areas where computer-generated depths are available, the present solutions fit both the amplitude and the correlation statistics of the observed magnetic profiles, thereby restricting the alternatives.

Line 66 is near the eastern edge of the detailed study area, and extends beyond it to the north (see fig. 1). The magnetic profile shown at the top of figure 3 is characterized by broad magnetic highs in the north and south separated by a broad low. The northern high and the low are outside the detailed study area. The southern high contains three strong peaks, two of which flank the Middleton Place magnetic low (lat 32°54′ N.). An interpreted basement cross section is shown at the bottom of the figure. The heavy lines on the cross section indicate depths obtained from the computer, and the lighter connecting lines define the model used to fit the magnetic anomaly.

In the northern part of the cross section, a well-defined southward-dipping magnetic basement is seen at depths of 600–1,500 m below the ground

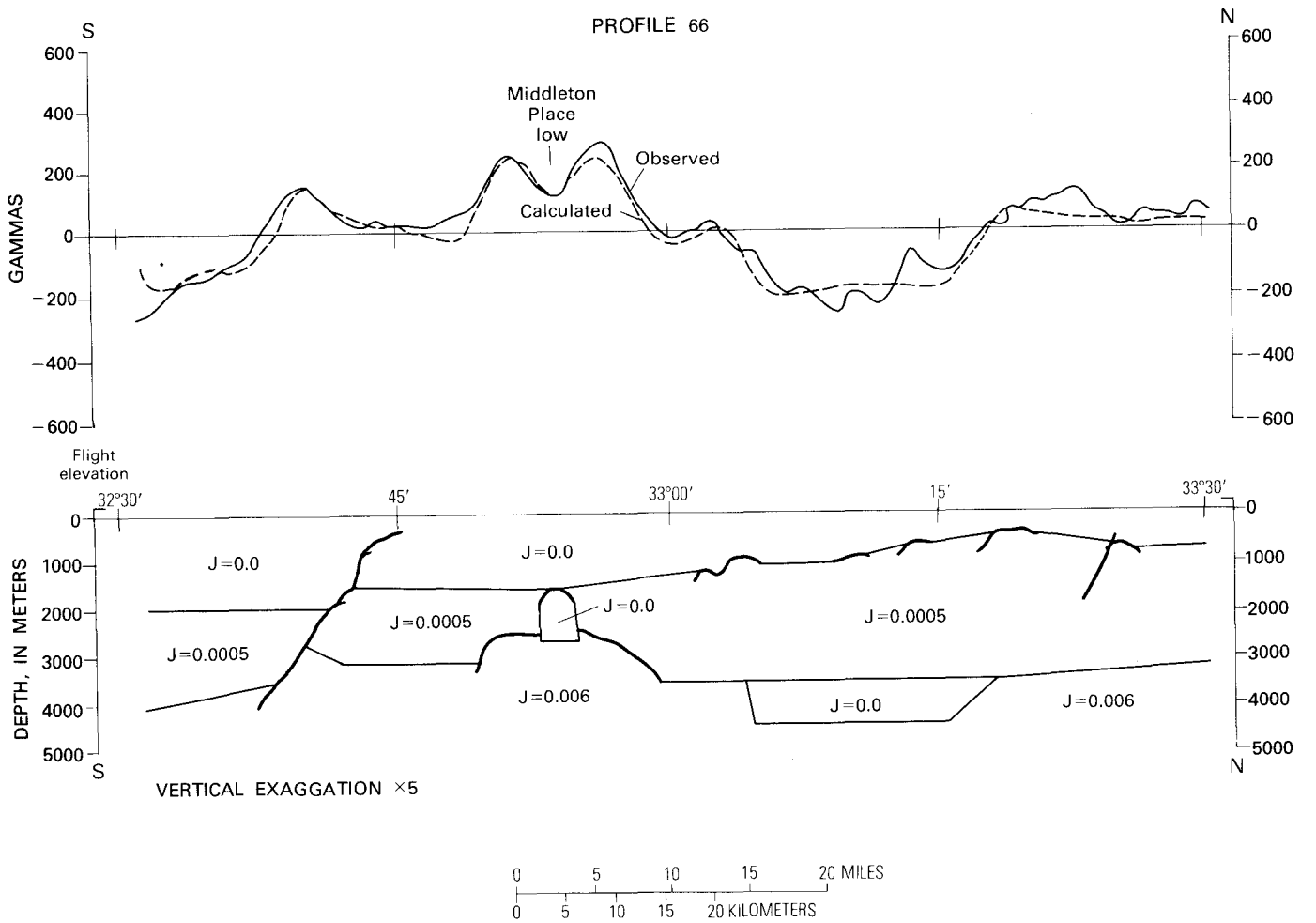

FIGURE 3.—Magnetic profile 66 and interpreted basement cross section. The observed magnetic profile is given by the solid curve at the top of the figure. The computed magnetic profile is given by the dashed curve. Heavy lines on the cross section represent computer-generated depths. Lighter lines have been added to form the model. Magnetizations (J) are given in gauss. Depths are relative to ground level.

surface. Because these depths correspond to the seismically determined crystalline basement depths south of Middleton Place (Ackermann, this volume), this surface has been interpreted to be crystalline basement. The underlying material has been assigned a weak magnetization of 5×10^{-4} gauss, which corresponds to a susceptibility of 10^{-3}, a reasonable value for granitic or metamorphic rocks.

Because of the low magnetization contrast and low relief of this basement surface, it contributes very little to the calculated magnetic anomaly. Consequently it could just as easily be modeled as an unconformity in a thick nonmagnetic sedimentary sequence. in either interpretation, the surface is defined magnetically by the dikes or volcanic flows that contribute to the short wavelength part of the magnetic anomaly. No attempt has been made to include these features in the model.

The computer-generated depths provide no information on intrabasement sources in the northern part of this line, but deep sources have been added to the model, based on results from nearby lines. These sources consist of a strongly magnetized body at 3.6 km depth in the north and a weakly magnetized or nonmagnetic body at similar depth under the broad magnetic low. The northern source has been interpreted to be a mafic intrusive body on the basis of the regional gravity map (Long and Champion, this volume), which shows a relative high over this feature. The modeled nonmagnetic body under the broad magnetic low does not make any significant contribution to the calculated magnetic anomaly, and it could easily be replaced by a thickened section of the overlying material.

The three magnetic highs and the regional high in the southern part of the line appear to be pro-

duced at depths of between 2.4 km and 3.6 km by a strongly magnetized source, which is again interpreted to be a mafic intrusive body on the basis of a corresponding regional gravity high.

The Middleton Place magnetic low (lat 32°54′ N.) corresponds to a topographic high in the estimated magnetic basement. Depth analysis of adjacent magnetic profiles reveals that this apparent topographic high is a linear feature, extending to the west under the magnetic low. On the cross section the topographic high is interpreted to be the upper boundary of a nonmagnetic zone within the crystalline rock. The width of this hypothetical zone may be exaggerated by the depth-estimation technique. This nonmagnetic zone is shown extending down into the top of the mafic intrusive body, and in fact, this relief at the top of the mafic body can account for nearly all of the observed decrease in magnetic intensity. Although this suggests that the source of the magnetic low is at great depth, the correlation between the low and the shallower depth estimates is an argument for a source nearer the crystalline basement surface. The nonmagnetic zone is included in the model mainly on the basis of this correlation.

This modeled nonmagnetic zone could represent a zone of alteration around a fault. Three types of evidence support this interpretation: (1) The linearity of the feature, (2) the close association with Middleton Place, an area of active seismicity (Tarr, this volume), and (3) the negative sign of the anomaly, which is what one would expect from a mechanically or hydrothermally altered zone within granitic rock. Although none of the other geophysical studies indicate a west-trending fault in the Middleton Place area, there is a pronounced east-west linear high in the gravity anomaly immediately to the south, along lat 32°52′ N. (Long and Champion, this volume).

An alternative explanation for the Middleton Place magnetic low requires reversely magnetized material at or above the crystalline basement. The presence of such material is a distinct possibility, as basalt flows were encountered in the USGS corehole at a depth of 750 m (Gohn and others, this volume), and similar flows could be present at greater depths. In order to produce a magnetic low, basalt flows that have reversed remanent magnetization would be required. Topographic relief on the tops or bottoms of the flows would result in a magnetic anomaly. The presence of reversely magnetized flows of limited extent would help explain some of the differences between the magnetic and gravity anomalies. In the gravity anomaly linear lows are absent, and the gravity high is not broken up into separate peaks north and west of Middleton Place. Reversely magnetized basalt flows could be the source of the linear magnetic lows that break up this feature on the aeromagnetic map.

The computer-generated surface at the southern end of the section (south of lat 32°45′ N.) has been modeled as a low-angle fault. Although this surface is almost certainly a boundary of the mafic intrusive body at depth, displacement of the crystalline basement along this surface is hypothetical. At its northern end this apparent surface extends up into the sedimentary column and may level off at the top of the basalt horizon seen in the USGS corehole to the northwest. Computer artifacts (hyperbolic tails) may be responsible for the apparent continuity of this surface.

Line 76 passes through the western end of the Middleton Place magnetic low (figs. 1 and 2). The magnetic profile, shown in figure 4, is similar to profile 66. The interpreted basement cross section differs from the previous one in several ways. Deep sources have been detected in the northern part of the section by using the technique of Phillips (1975). As before, these are modeled as a mafic intrusive body in the north and as a nonmagnetic body under the broad magnetic low. The magnetization of the northern mafic body has decreased to 5×10^{-3} gauss, whereas the magnetization of the southern mafic body has increased to 9×10^{-3} gauss. The latter value is unusually large, even for mafic rock. Because of the oblique trends of the anomalies relative to the flight line (fig. 2), the depth of the southern mafic body is likely to be overestimated. A shallower body would not require as strong a magnetization to fit the observed anomaly.

Another difference is the growth of the nonmagnetic zone overlying the southern mafic body. There are now two peaks in the upper boundary of this zone, which correlate with relative lows in the magnetic anomaly at lat 32°51′ N. and 32°54′ N. On the aeromagnetic map (fig. 2) the two magnetic lows appear to be separate features, but contour maps of the computer-generated depth estimates, to be covered later, suggest the lows can be connected along a north-northwest-trending line. Consequently, the section of figure 4 may be presenting a nearly longitudinal view of an altered zone about a north-northwest-trending fault. An alternative interpretation, presented earlier, would explain the magnetic lows as the result of reversely magnetized

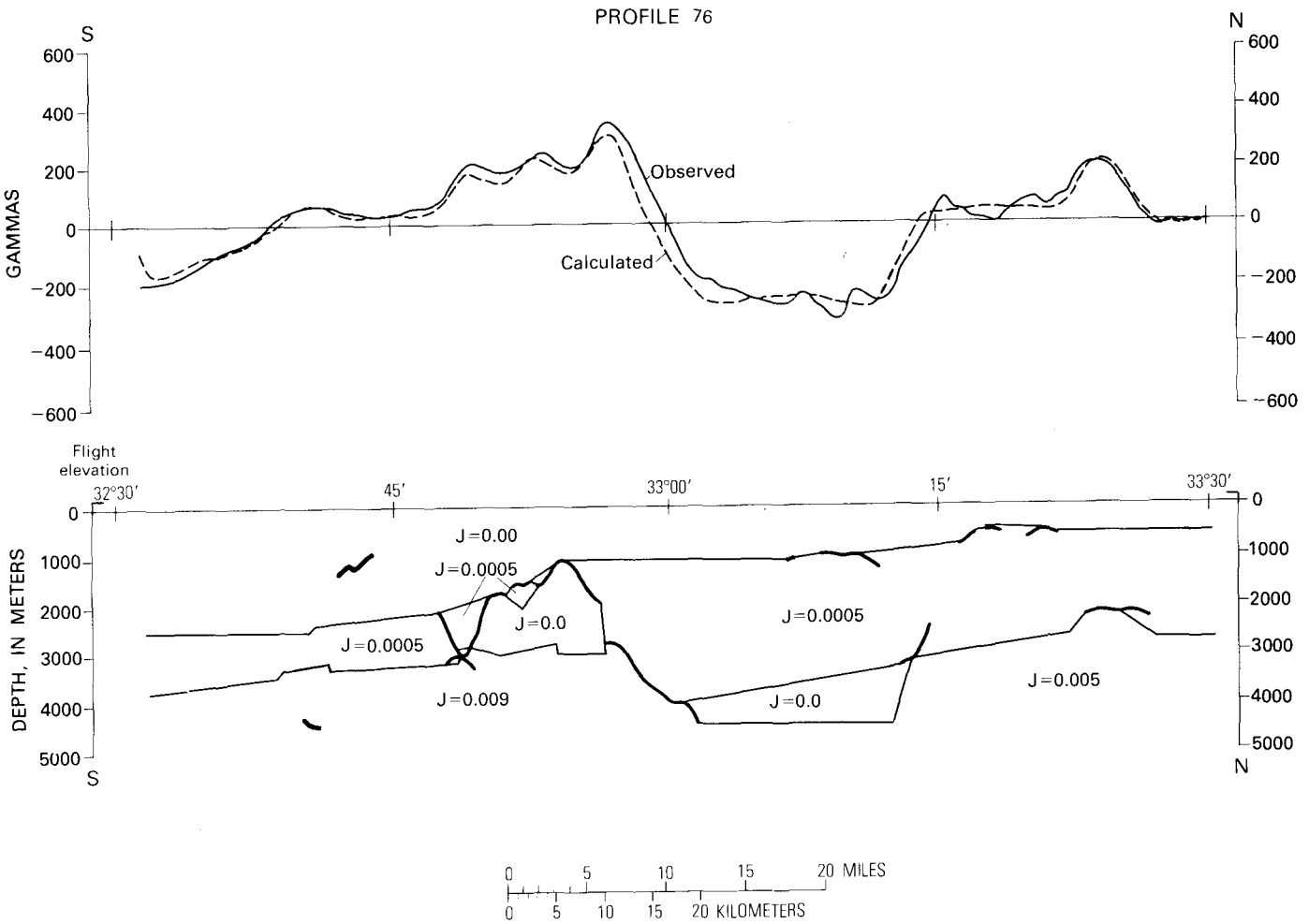

FIGURE 4.—Magnetic profile 76 and interpreted basement cross section. Symbols are as in figure 3.

basalt flows. In this interpretation no nonmagnetic intrabasement zones would be required.

In a final difference, crystalline basement is shown deepening to the south above the southern mafic body. This brings the model into agreement with the gravity interpretation of Long and Champion (this volume) which places a fault with a similar sense of motion in this location. The shallow (~1 km) depth estimates at lat 32°43′ N. would have to result from intrasediment volcanics in this interpretation. An alternative model more in agreement with the seismic refraction data (Ackermann, this volume) would have crystalline basement remaining flat and shallow at about 1,200 m depth, passing through the shallow depth estimates. This modification would not significantly affect the calculated anomaly.

DISCUSSION OF RESULTS

Both the depth estimates and the model studies suggest that several different crystalline materials are present beneath the Coastal Plain sediments. The shallowest of these is the basalt unit encountered in the corehole. Below is the weakly magnetic granitic or metamorphic material which forms the crystalline basement. Because of the weak magnetization, depths to this basement can only be estimated where dikes or volcanic flows are present. South of Middleton Place this surface is known to be crystalline basement from the seismic refraction results (Ackermann, this volume). If further geophysical studies should prove that a shallow crystalline basement is absent in the northern part of the section, then the shallow magnetic sources there could be reinterpreted as dikes or volcanic flows at a surface of unconformity within a thick sedimentary column.

The model studies have shown that most of the power in the magnetic anomalies is produced by strongly magnetized sources at depth. On the basis of the strong magnetization and the associated

gravity highs (Long and Champion, this volume), these sources have been interpreted to be mafic intrusive bodies. Although some mafic material may extend up to the crystalline basement in parts of the study area, the mafic bodies seen in the cross sections generally appear to be covered by a kilometer or more of weakly magnetic crystalline material. Mafic intrusive bodies are absent beneath the broad magnetic and gravity low to the north of Summerville.

Recent earthquake hypocenters under Middleton Place cluster at depths of 1–8 km (Tarr, this volume). According to our models, the top of the mafic intrusive complex in this area is located at depths of 2.5–3.5 km; thus, the shallower seismic events could be occurring within the crystalline rock near the surface of the mafic intrusive bodies, as proposed by Kane (this volume). On both cross sections crustal magnetization appears to be homogeneous below about 4.5 km, so nothing can be said about structures associated with the deeper seismic events.

DEPTH CONTOURS

In order to examine more fully the relation between the computer-generated depth estimates and the aeromagnetic anomalies, contour maps of the depth estimates have been prepared. There are difficulties in interpreting such maps. The contours do not represent geologic surfaces such as the crystalline basement or the tops of the mafic bodies. Instead, they indicate spots or patches on these surfaces where the correlation statistics of the magnetic profiles could be used to estimate depth. These patches are often surrounded by deeper contours, which represent the fictitious surfaces of the hyperbolic tails. It follows that topographic highs in the contoured depth estimates are more reliable indicators of geologic surfaces than are gradients. However, our model studies have shown that some gradients can have a geologic interpretation. The depth-estimation technique introduces distortion by exaggerating the widths of vertical bodies, and by overestimating depths when anomaly trends are not perpendicular to the flight lines. In addition, in many areas depth estimates are unavailable because of unacceptable behavior of the correlation statistics. Despite these difficulties depth estimates often show remarkable consistency from line to line, and, when contoured, show good correlation with features of the aeromagnetic map.

In figures 5 and 6 the "deep" and "shallow" computer-generated depth solutions have been contoured. These figures only contain information of the type shown by the heavy lines in figures 3 and 4. Blank areas indicate regions where no reliable depth estimates could be obtained.

The shallower features of these contour maps will be compared with the seismic interpretation of Ackermann (this volume). The deeper features will be analyzed using the gravity data of Long and Champion (this volume).

BASALT HORIZON

The seismic interpretation places the basalt horizon above 900 m depth east of Middleton Place and west of long 80°15′ W. Magnetic-basement depth estimates above 900 m are found on the "deep" solution (fig. 5) at the center right and on the "shallow" solution (fig. 6), both northeast of the corehole and within an east-west belt around lat 32°45′ N. These depth estimates, which are shallower than 600 m in places, probably represent the basalt horizon. The seismic interpretation shows a north-south trough in the basalt horizon west of Middleton Place. Maximum depth to the horizon within the trough is 1 km. Closed highs in the magnetic basement contours at depths above 1.2 km just west and south of Middleton Place (figs. 5 and 6) may indicate the depressed region of the basalt horizon, or they may indicate crystalline basement.

CRYSTALLINE BASEMENT

The seismic interpretation has crystalline basement dipping southeast, increasing in depth from 900 m near the corehole to 1,300 m under Middleton Place, and flexing to 2,000 m further southeast. Magnetic-basement depth estimates in the range 1.2–1.5 km are found throughout the detailed study area, not just to the southeast of Middleton Place. This depth range includes the apparent east-west linear topographic high passing through Middleton Place, and the apparent north-northwest linear topographic high halfway between Middleton Place and the corehole (fig. 6). If the tops of these linear topographic highs are located at the crystalline basement, then the basement appears to be at a fairly constant depth of 1.2 km. There is no evidence of a southeast dip or flexure.

The linear topographic highs in the basement have been modeled as nonmagnetic zones within the crystalline rocks. These topographic highs are associated with relative lows in the magnetic anomaly (fig. 2) and can be interpreted either as altered zones about faults within the crystalline rocks or as

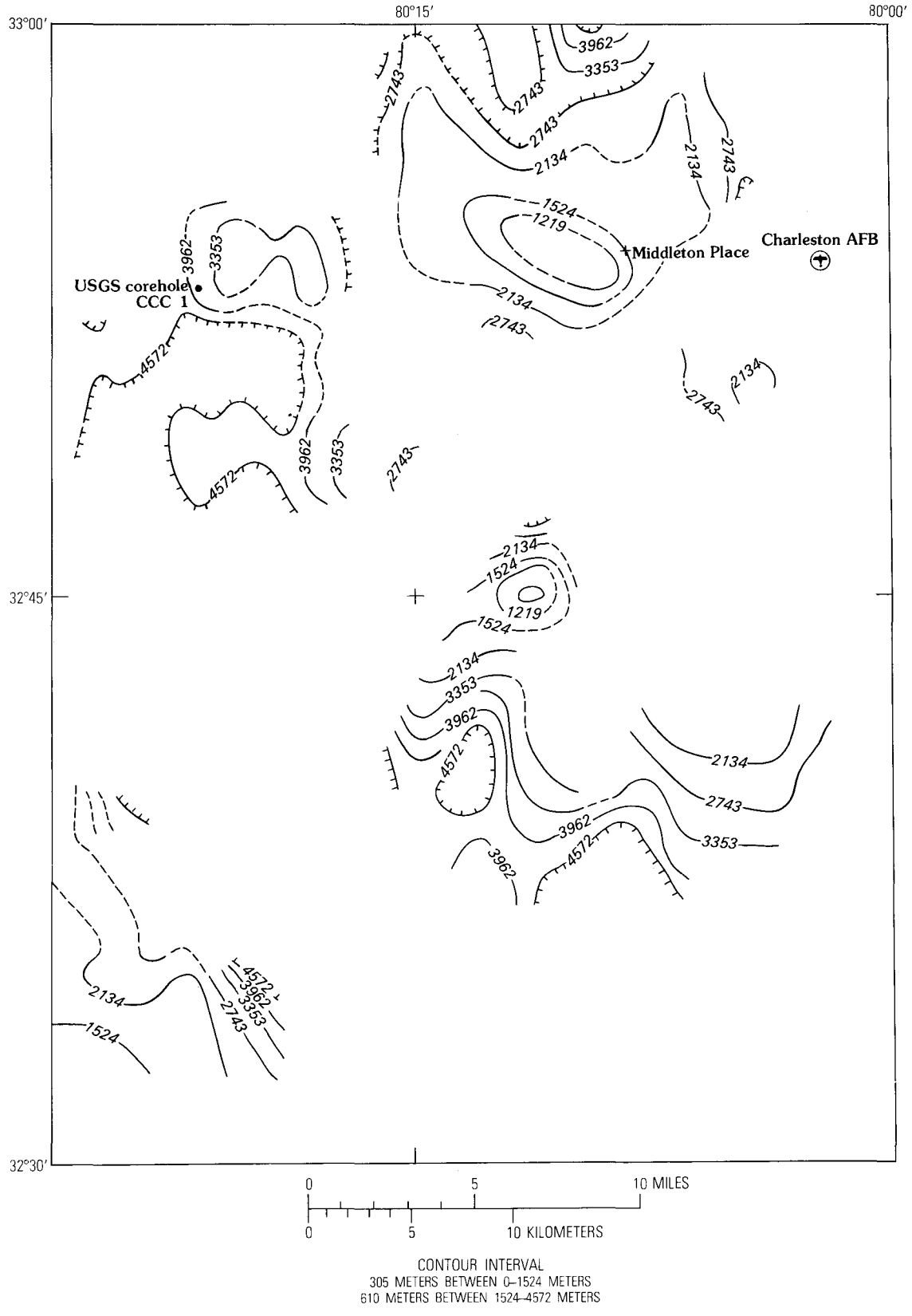

FIGURE 5.—Contour map of depths to magnetic basement corresponding to the computer-generated "deep" solution within the study area. Contours are dashed where inferred. Blank areas represent regions where no depth estimates were generated.

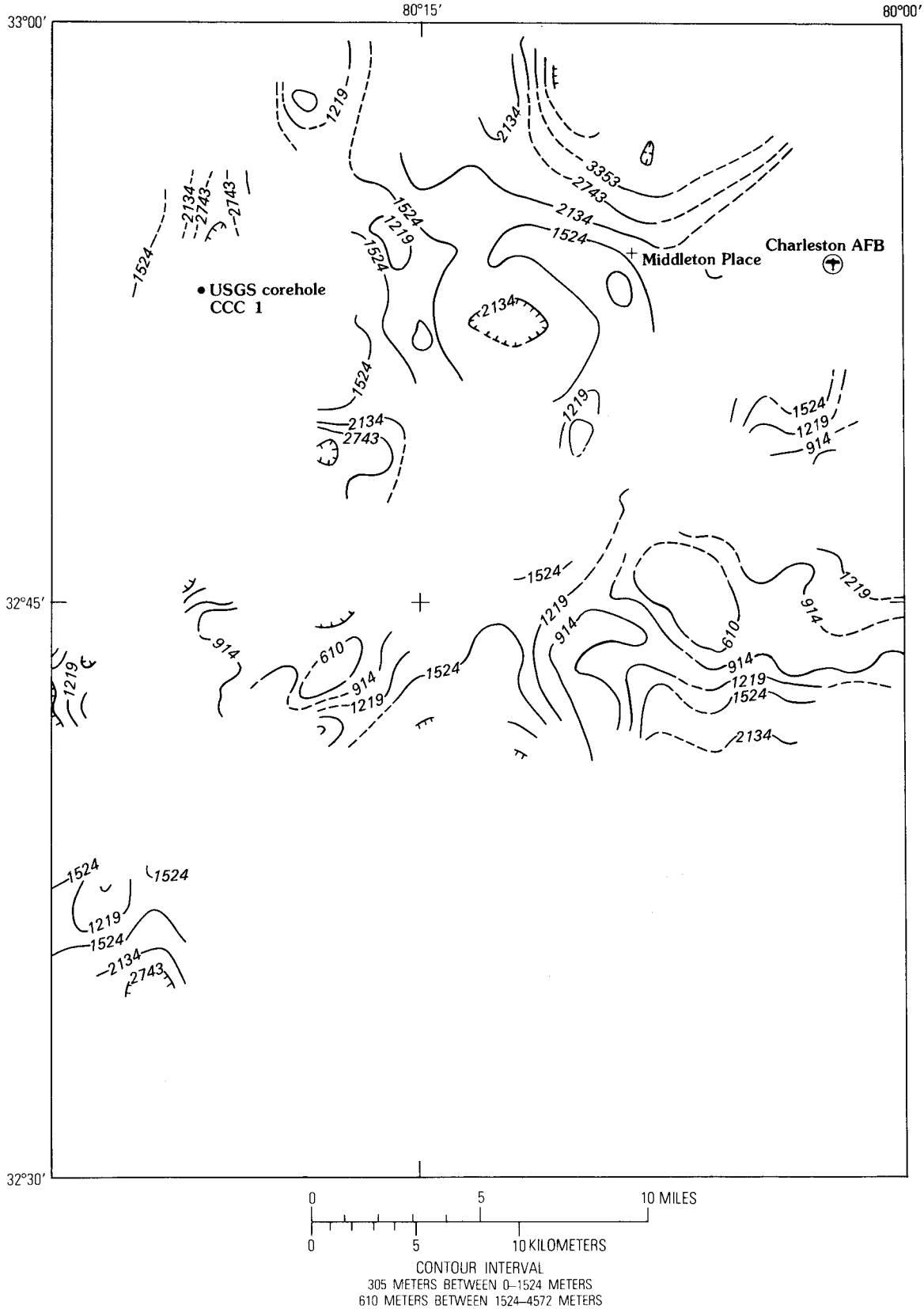

FIGURE 6.—Contour map of depths to magnetic basement corresponding to the computer-generated "shallow" solution. Contours are dashed where inferred. Blank areas represent regions where no depth estimates were generated.

reversely magnetized volcanic flows on top of the crystalline basement.

A third interpretation may be advanced for the north-northwest-trending linear topographic high. The feature is located along the eastern boundary of the strong magnetic high over the USGS corehole site. If the top of the mafic body responsible for this magnetic high is at the crystalline basement as the gravity interpretation of Long and Champion (this volume) suggests, then the linear topographic high in the magnetic-basement depth estimates may represent a vertical contact between crystalline basement material to the east and mafic material to the west. Similar contacts may exist on other sides of the mafic body as well, as indicated by the 1.5-km depth estimates northwest and southeast of the corehole site in figure 6.

MAFIC BODIES

The estimated depths to magnetic basement contoured in figure 5 reflect what are interpreted to be mafic intrusive bodies at depths of 2–4.5 km. These sources are responsible for the strong magnetic highs and the regional magnetic high in the aeromagnetic map (fig. 2). The mafic bodies are shallowest in the northern part of the study area, where the magnetic anomalies are the strongest. They deepen to the south, most rapidly along the southward-dipping surface appearing in the southeast quadrant of figure 5. Mafic bodies are absent under the broad magnetic low immediately north of the study area (fig. 1).

In discussing the mafic bodies, we will ignore contours above a depth of 2 km in figure 5, such as those near Middleton Place and those near the center of the figure. These contours represent the shallow magnetic sources discussed earlier.

Shallow mafic sources, indicated by the magnetic highs north of the Middleton Place magnetic low in figure 2, are found in figure 5 to have estimated depths of between 2.0 and 2.7 km. Similar depths are indicated under the magnetic high to the southeast of Middleton Place (figs. 2, 5).

Apparent small-scale relief on the magnetic basement, such as the V-shaped trough northwest of Middleton Place in figure 5, is most likely a computer artifact resulting from nonperpendicularity of the magnetic contours to the flight lines. It is interesting, however, that one leg of the trough trends northwest along the trace of a nodal plane of the 22 November 1974 earthquake (Tarr, this volume), and the other leg trends northeast along a lineation defined by the gravity anomaly (Long and Champion, this volume). Both legs of the trough correspond to saddles in the magnetic anomaly (fig. 2).

The positive magnetic anomaly over the USGS corehole site (fig. 2) is the strongest magnetic high in the area, and it is coincident with the strongest positive gravity anomaly (Long and Champion, this volume). The strength of the magnetic anomaly and the results of the gravity modeling suggest that the 3.2–4.5 km depths indicated under this feature in figure 5 are unlikely to represent the top of the source body. It is more likely that the top is at the crystalline basement and that the contours of figure 5 represent either the bottom of the source body or a mineralization boundary within the source body. This is probably the shallowest mafic body in the study area. None of the other mafic sources appear to extend up to the crystalline basement.

The large elongate magnetic high in the southeast quadrant of the study area (fig. 2) corresponds to a gravity low (Long and Champion, this volume). This suggests that the material responsible for this magnetic high differs from the mafic material to the north. In our model studies, the magnetic source has been placed at depths of 2.7–3 km.

A final strong magnetic high is found in the southwest corner of the study area (fig. 2). A corresponding gravity high (Long and Champion, this volume) indicates a mafic source body. According to figure 5 the body is at a depth of 1.5 km.

REFERENCES CITED

Nabigihian, M. N., 1972, The analytic signal of two-dimensional magnetic bodies with polygonal cross-section: Its properties and use for automated anomaly interpretation: Geophysics, v. 37, no. 4, p. 507–517.

Phillips, J. D., 1975, Statistical analysis of magnetic profiles and geomagnetic reversal sequences: Stanford, Calif., Stanford Univ., Ph.D. dissert. p. 81–134.

U. S. Geological Survey, 1975, Aeromagnetic map of Charleston and vicinity, South Carolina: U.S. Geol. Survey open-file rept. 75–590.

Bouguer Gravity Map of the Summerville-Charleston, South Carolina, Epicentral Zone and Tectonic Implications

By LELAND TIMOTHY LONG *and* J. W. CHAMPION, JR.

STUDIES RELATED TO THE CHARLESTON, SOUTH CAROLINA, EARTHQUAKE OF 1886—A PRELIMINARY REPORT

GEOLOGICAL SURVEY PROFESSIONAL PAPER 1028-K

CONTENTS

ILLUSTRATIONS

STUDIES RELATED TO THE CHARLESTON, SOUTH CAROLINA, EARTHQUAKE OF 1886—
A PRELIMINARY REPORT

BOUGUER GRAVITY MAP OF THE SUMMERVILLE–CHARLESTON, SOUTH CAROLINA, EPICENTRAL ZONE AND TECTONIC IMPLICATIONS

By LELAND TIMOTHY LONG[1] and J. W. CHAMPION, JR.[2]

ABSTRACT

A new Bouguer anomaly map of the Summerville–Charleston, S.C., epicentral zone is interpreted to reveal a mafic intrusive body and associated flows and a northeast-trending Triassic(?) basin. Two shallow structures interpreted from the gravity data and associated with the Triassic(?) basin may be significant in determining the mechanism for the 1886 Charleston earthquake. The first is a border fault on the northwest side of the basin striking N. 45° E., and the second is a linear positive anomaly striking east. The first structure suggests the more conventional earthquake mechanism of reactivation of a basement fault. The second structure suggests a newly proposed mechanism of stress amplification in the anomalously rigid structure responsible for the linear positive anomaly. Intensity data from the August 31, 1886, Charleston earthquake and epicenters of recent events favor stress amplification as the more likely explanation for earthquake activity in the Summerville–Charleston epicentral zone.

INTRODUCTION

The lack of a confirmed tectonic mechanism for the Charleston, S.C., earthquake of August 31, 1886, and for its foreshocks and aftershocks has been a major obstacle in the development of a realistic evaluation of seismic hazard in the Eastern United States. Although more than 400 events (Taber, 1914; Bollinger, 1972) have been felt in the region since 1886, no fault to which the activity can be definitely attributed has been observed at the surface. The probable reason that no tectonic mechanism has yet been agreed upon is that the basement structures responsible are not only unknown but also hidden by more than 0.79 km of post-Paleozoic sedimentary and extrusive rocks.

The Summerville–Charleston epicentral zone does not lie near an active plate boundary. Hence, the association of the Summerville–Charleston events with plate tectonics would have to be indirect. Intraplate movements near the epicentral zone, if present, are obscured by a lack of appropriate data except, perhaps, recent releveling data. Within the context of the theories of plate tectonics, the Charleston earthquake is one manifestation of intraplate tectonics that as yet has not been satisfactorily explained.

Taber (1914), in one of the earliest attempted explanations of the seismic activity near Charleston, hypothesized a fault in the crystalline basement. On the basis of intensity data only, he suggested that the unobserved fault trended in a general northeast-southwest direction and was near Woodstock, S.C., 8 km southeast of Summerville. A deep well near Summerville bottomed in basaltic rocks (diabase) (Cooke, 1936). The 0.26 km of sedimentary rocks directly above the diabase was interpreted to be Triassic (Cooke, 1936). Mansfield (1936) placed this section in the Cretaceous. Woollard, Bonini, and Meyer (1957) and Pooley, Meyer, and Woollard (1960), assuming that Mansfield was correct, suggested that the tectonics of the Charleston epicentral area might be related to a topographic feature of the basement surface, the Yamacraw Ridge, and the associated basement valley to the north, rather than to a Triassic basin perhaps related to the Florence Triassic basin. Bollinger (1973) conjectured that a general relation existed among seismicity, regional uplift, and old Appalachian structures. Oliver and Isacks (1972) and Fletcher, Sbar, and Sykes (1974) suggested that the Charleston activity and other earthquakes of the South Carolina belt are related to the landward extension of a major transform fault

[1] School of Geophysical Sciences, Georgia Institute of Technology, Atlanta, Ga.
[2] Chevron Oil Co., Houston, Tex.

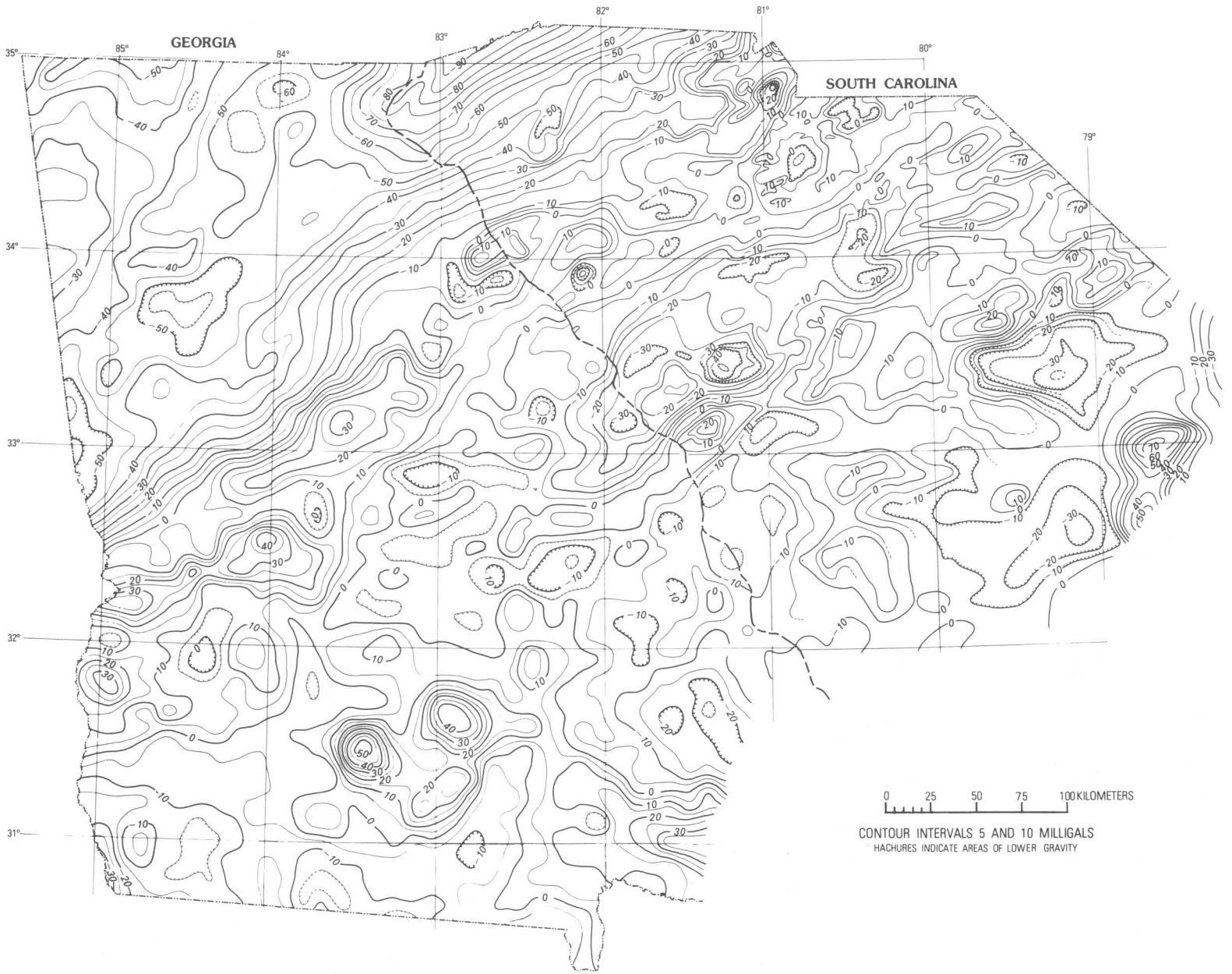

FIGURE 1.—Simple Bouguer anomaly map of Georgia and South Carolina (taken from Long, Bridges, and Dorman, 1972, and Long, Talwani, and Bridges, 1975).

and structures associated with the early opening of the Atlantic Ocean.

The first objective of this paper is to present an analysis and structural interpretation of gravity data covering the Summerville–Charleston epicentral zone. The gravity data consist of approximately 1,000 regional observations at a mean separation of 1.0 km and an additional 1,000 observations at a mean separation of 0.3 km along selected lines. The gravity analysis presented herein is largely a condensation of the master's thesis of the second author (Champion, 1975). A listing of the gravity data and details concerning its reduction are given in Champion (1975). Standard reduction techniques were used, and the theoretical gravity was computed using the 1931 international gravity formula.

The second objective of this paper is to discuss the interpretation of the structure in terms of possible mechanisms for the Charleston earthquake of August 31, 1886. In particular, we propose that stress amplification within an anomalously rigid crustal structure could have been responsible for the 1886 Charleston earthquake. The hypothesis of stress amplification should be given serious consideration as new data become available.

The gravity data were obtained by the second author during the summer of 1974. His fieldwork, the data reduction, and the analysis were supported by the U.S. Geological Survey (grant 14–08–0001–G–127). Studies on the stress amplification mechanism were supported by the National Science Foundation under grant DES75–15756.

REGIONAL GRAVITY

The regional Bouguer gravity pattern of the South Carolina and Georgia Coastal Plain is characterized by numerous sharp positive anomalies and smoother, less pronounced negative anomalies (fig. 1). The sharp positive anomalies range in magnitude from +15.0 to +70.0 mGal. Those that were studied in detail have the size and character of mafic volcanic plugs and associated basaltic flows and dikes (Long, 1974). The negative anomalies could be explained by shallow basins, perhaps of Triassic age, or by blocks of less dense or thicker continental crust. In general, the gravity data imply a highly inhomogeneous upper crust beneath the Coastal Plain.

The area of detailed gravity coverage (fig. 2) includes one of the sharp positive anomalies and a major part of the suspected epicentral zone of the 1886 earthquake, as well as the epicenters of more recent seismic events. The borders of the area investigated are defined by the coordinates 32°37′30″ N., 80° W., and 33°07′30″ N., 80°22′30″ W. The gravity map (fig. 3) is contoured at 1.0 mGal from individual gravity observations and has an estimated precision of 0.2 mGal.

The gravity isogals in figure 3 indicate that the Summerville–Charleston epicentral zone is near the contact between a sharp positive anomaly, here interpreted as a volcanic plug, and a negative anomaly, here interpreted as a Triassic basin. In the western part of the study area (fig. 3), a positive anomaly having a peak value of 15.0 mGal exhibits a steep gravity gradient of 2.0–3.0 mGal/km on both its northern and its southern sides. To the east of this feature, the gravity gradient becomes less steep, and the isogals spread to form a noselike feature. To the south and to the northeast, negative anomalies appear to form an arc around the noselike feature. The northwestern part of the study area is characterized by a reasonably constant negative anomaly of approximately −3.0 mGal.

Three prominent zones of alinement in the contour lines and anomalies can be observed. The trend of the strongest alinement of contour lines is approximately east-west and is formed by the steep gradient south of the central positive anomaly. Another alinement of contour lines is defined by the trend of the isogals north of the central positive anomaly and bears approximately N. 50° W. These two contour alinements appear to be a consequence of the shape of the central positive anomaly. A third alinement is defined by the western termination of the northeastern and southern negative anomalies. The northwestern edges of these negative regions define an alinement of isogals trending N. 40°–50° E. (labeled NE linear anomaly on fig. 3) that intersects the central positive anomaly in the region where the isogals begin spreading to form the noselike positive anomaly.

ANALYSIS OF LINE DATA

Approximately one-half of the new data were obtained along lines at an average separation of 0.3 km. However, many of these lines (see fig. 4) were restricted to major rights- of-way or were obtained prior to knowledge of the strike of the crustal structures. The lines that proved to be normal to the strike of the crustal structures could be used for interpretation of depths and structures using simple two-dimensional models. Lines *G–G′*, the north part of *A–A′*, and a profile *L–L′*, which all cross the positive anomalies in the north part of the map, give information on the depths to these structures. Lines *A–A′*

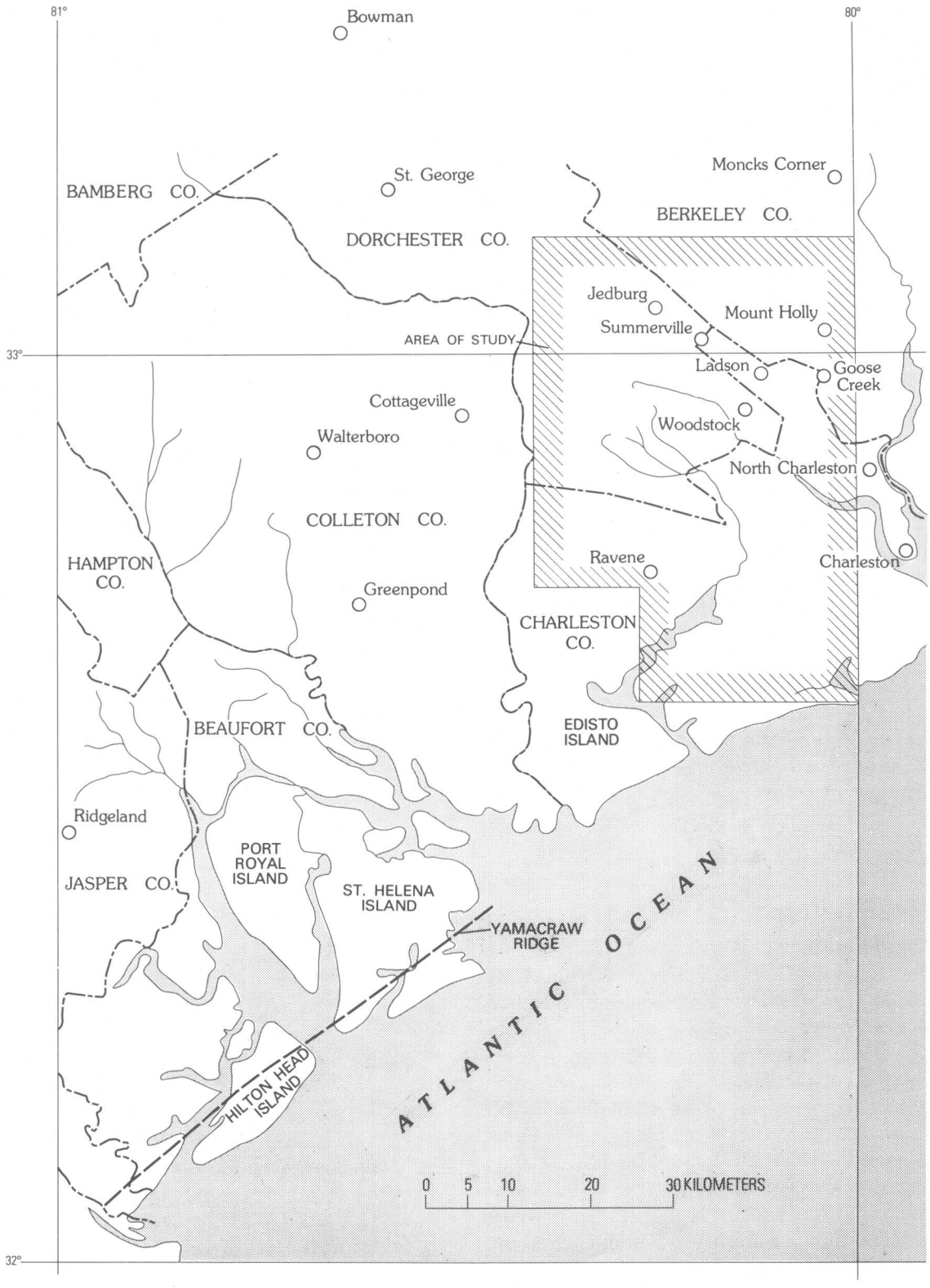

FIGURE 2.—Index map of southern South Carolina showing the location of the area of study.

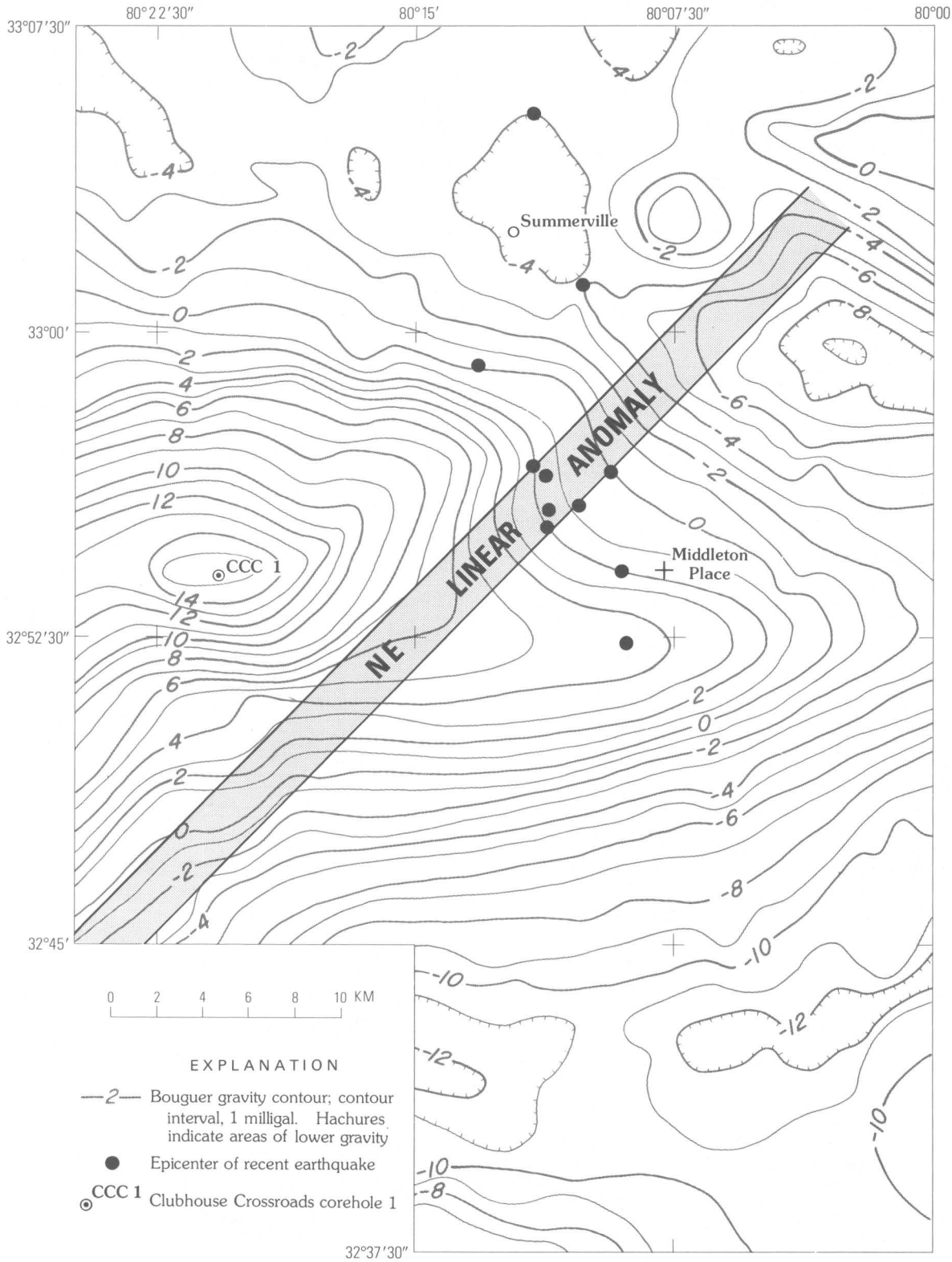

FIGURE 3.—Simple Bouguer gravity map of the Summerville–Charleston, S.C., epicentral zone (taken from Champion, 1975). Epicenters of recent earthquakes are from Tarr (this volume).

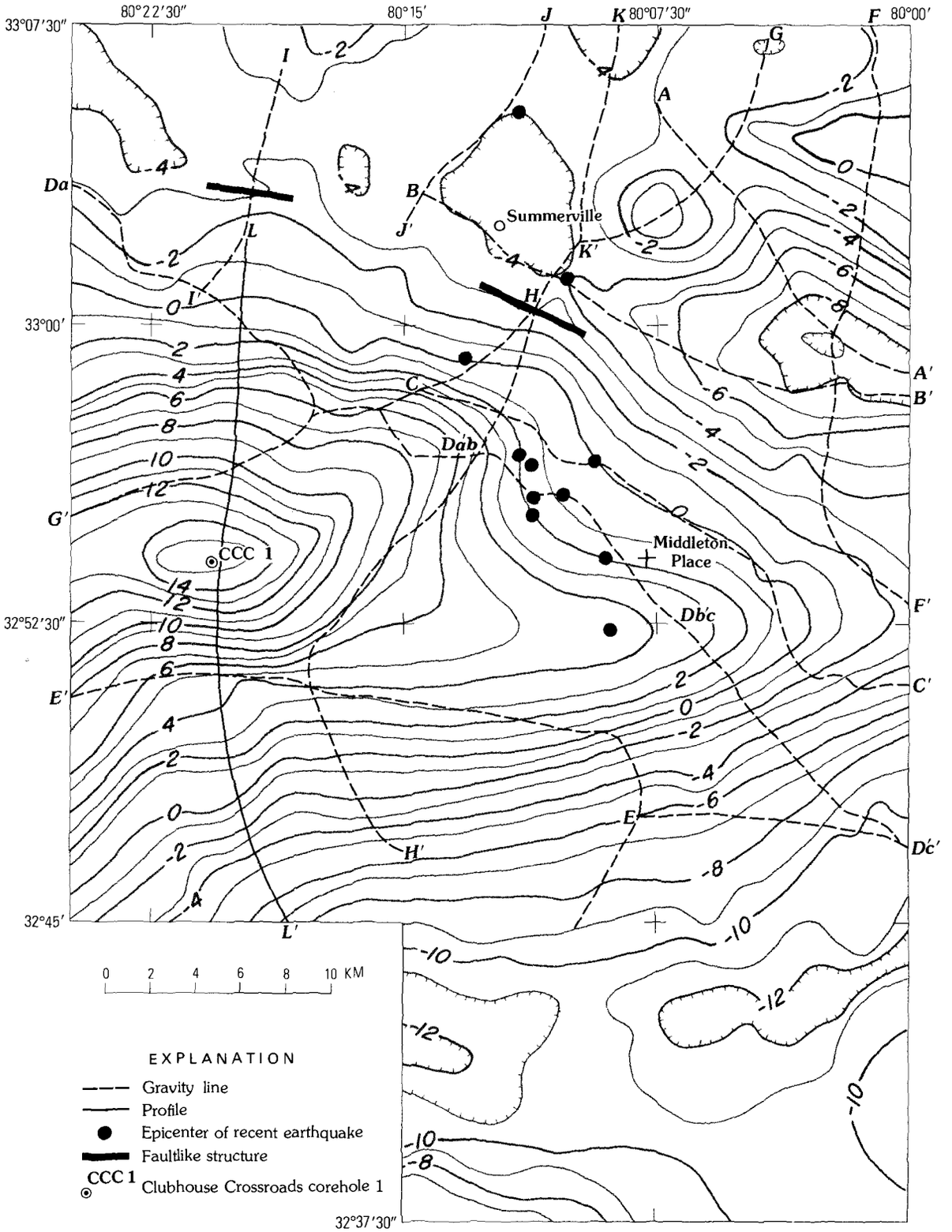

FIGURE 4.—Index map showing the locations of the detailed gravity lines and the profile. Epicenters of recent earthquakes (Tarr, this volume) are plotted on the gravity map of figure 3.

and *F–F′* are used to model the negative anomaly in the northeast. Line *D–D′* provides information on the depth and size of the eastward protruding positive anomaly. Lines *I–I′*, *G–G′* and *F–F′* give information on a possible northwest-trending structure. Simple two- or three-dimensional models (Nettleton, 1976) are used in the analysis. Corrections for end effects in two-dimensional models would not significantly affect the results. Similarly, more detailed models that remove the deviations of the observed gravity from the modeled gravity would not change any of the conclusions. Most of the irregularities that have magnitudes less than 1.0 mGal are inversely proportional to the elevation. However, the implied Bouguer reduction densities are often unreasonably low, or even negative. The explanation probably relates to a fundamental difference between near-surface materials in the dry elevated areas and those in the river bottoms.

The northern part of line *G–G′* crosses two positive anomalies. The anomaly at 4.0 km on line *G–G′* (see fig. 5) can be modeled with a horizontal cylinder that has a 1.3-km depth to its center and a radius of 0.45 km at a density contrast of 0.3 g/cm^3. The anomaly at 9.0 km can be modeled by a sphere that has a depth to its center of 1.7 km and a radius of 0.9 km at a density contrast of 0.3 g/cm^3. Both of these anomalies are consistent with a depth of 0.8 km to the tops of these structures.

Profile *L–L′*, which was interpolated from the contours because of the lack of appropriate rights-of-way for a detailed profile, crosses the largest positive anomaly (fig. 6). Examination of this anomaly indicated that the steepest gradient lies on the north side and has a half-width of about 2.0 km. The central peak was modeled as a 4.0-km-wide two-dimensional structure that has its top at a depth of 1.5 km and its bottom at 4.0 km (fig. 6). The interpretation of a structure at depths less than 1.5 km along line *L–L′* is difficult because of the smoothing that is inherent in the interpolation from contours. The sides of the anomaly can be modeled with a thinner or less dense structure that also has its top at 1.5 km and its bottom at 4.0 km. The depth to the top of the largest positive anomaly is consistent with depths to basement structures toward the northeast. The negative gravity values to the south are modeled by a less dense basin.

Line *A–A′* intersects the prominent negative anomaly in the northeastern part of the study area. The structure under line *A–A′* (fig. 7) can be modeled as a nearly vertical fault that offsets a block 0.3 g/cm^3 denser than the overlying material. The fault is interpreted as striking N. 40° E. (labeled NE linear anomaly in fig. 3) and intersects line *A–A′* at 6.0 km (fig. 4). The throw of the fault is 0.65 km, and the upper boundary of the upthrown block on the northwest is at a depth of 0.8 km. The positive residual at 5.0 km is derived in part from the posi-

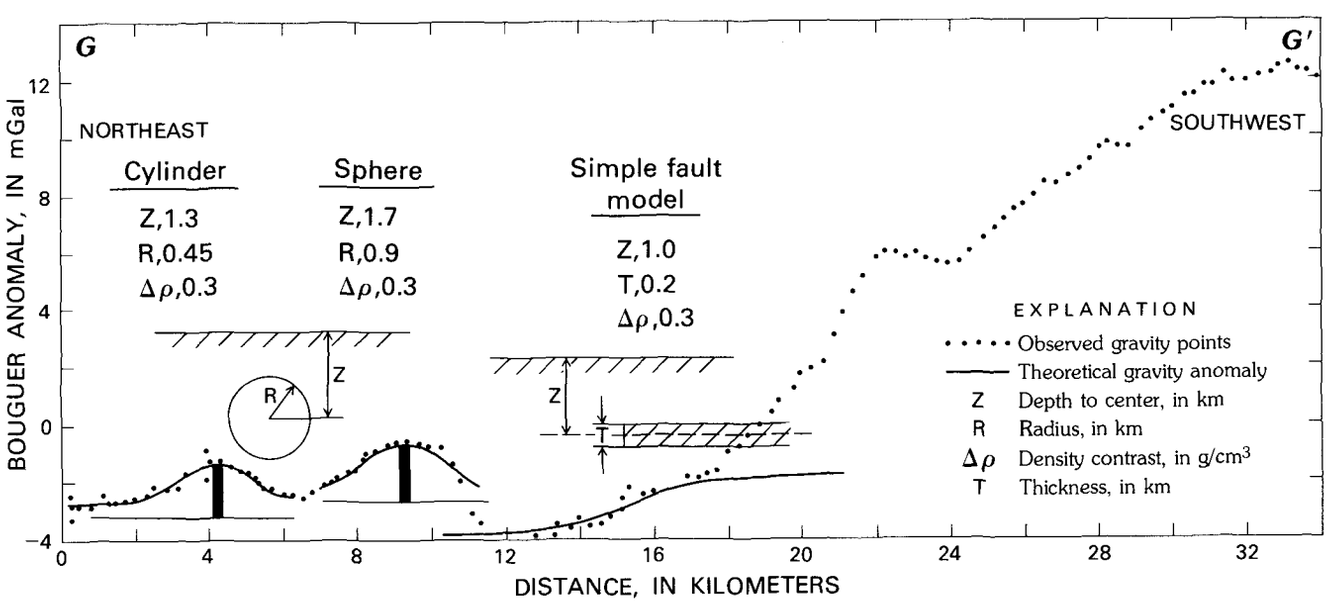

FIGURE 5.—Detailed gravity line *G–G′* showing the horizontal cylinder (at 4.0 km) and sphere (at 9.0 km) interpretations for the two northern positive anomalies and the simple fault model interpretation for the anomaly at 16.0 km. The location of *G–G′* is shown in figure 4.

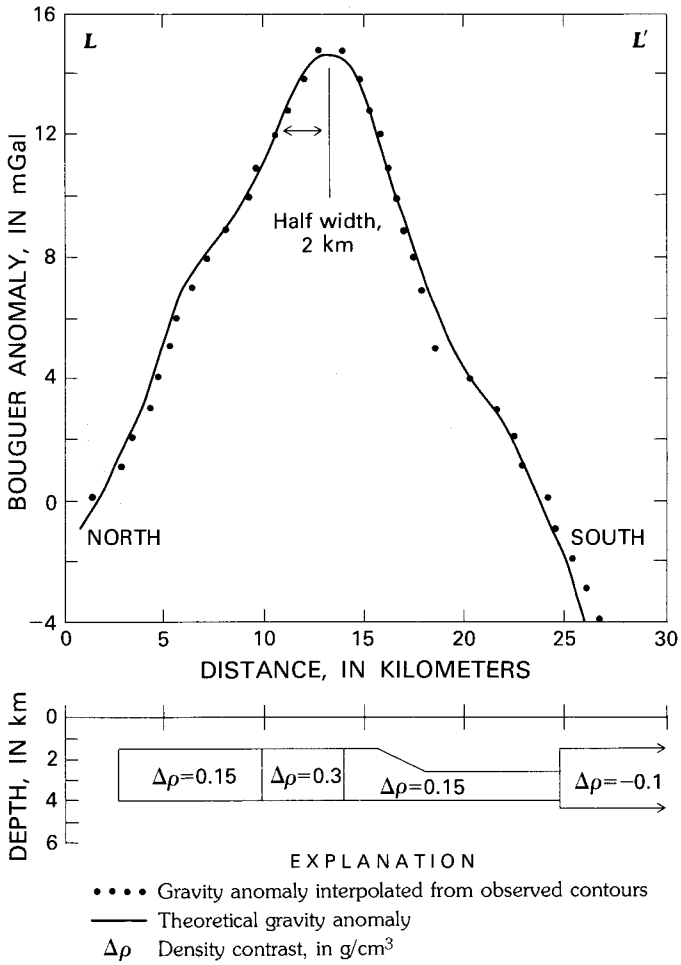

FIGURE 6.—Profile *L–L'* showing a model for the central positive anomaly. This profile was interpreted from the contour lines.

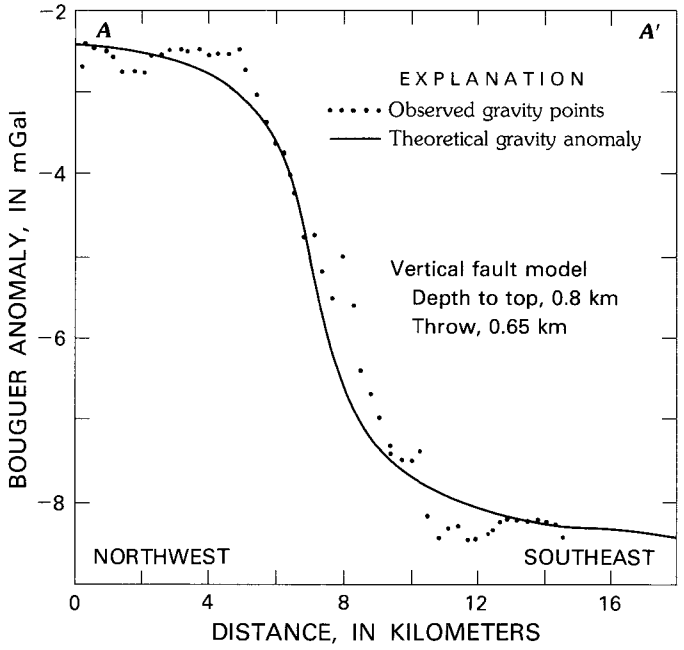

FIGURE 7.—Line *A–A'* compared with the theoretical anomaly from a fault model having a density contrast of 0.3 g/cm³.

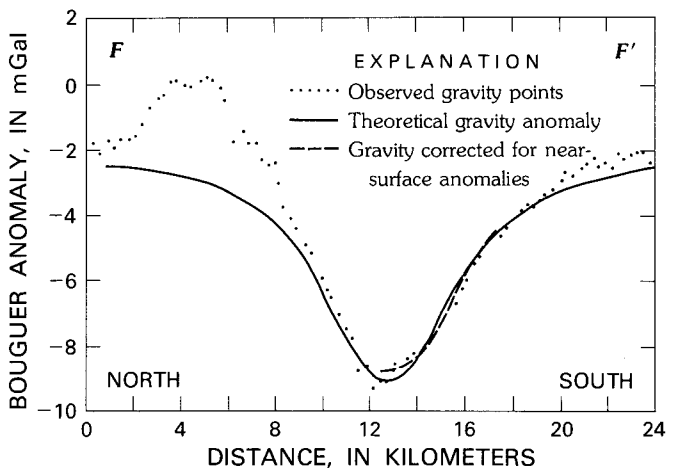

FIGURE 8.—Line *F–F'* compared with the theoretical anomaly from a horizontal cylinder that has a depth of 3.7 km to its center and a radius of 1.8 km at a density contrast of −0.2 g/cm³.

tive density anomalies on the upthrown block related to the two positive anomalies of line *G–G'*, previously noted. It may also be derived in part from the inverse relation of gravity to elevation caused by applying a Bouguer reduction density of 2.67 to Coastal Plain consolidated sedimentary rocks. Line *B–B'* gives similar results (Champion, 1975).

Line *F–F'* (see fig. 8) was used to estimate the extent of the feature responsible for the negative anomaly—a possible basin—corresponding to the downthrown side of the fault interpreted under lines *A–A'* (fig. 7) and *B–B'*. A horizontal cylinder was used for the model and indicated a depth to its center of 3.7 km and a radius of 1.8 km at a density contrast of −0.2 g/cm³. Maximum depths to the tops of two-dimensional structures can be computed using 0.65 times the ratio of the maximum anomaly to the maximum gradient. The positive anomalies on the north end of line *F–F'* are an extension of the positive anomaly at 4.0 km in line *G–G'*. Its northern gradient and its maximum anomaly (respectively, 1.1 mGal/km and 3 mGal) indicate a maximum depth of 1.8 km, which is consistent with, or slightly deeper than, the structures along line *G–G'*. However, the northern and southern edges of the basin have respective gradients of 2.0 and 1.2 mGal/km for a maximum anomaly of −8.0 mGal. The respective maximum depths to the tops of the northern and southern edge of the basin would be 2.6 and 4.3 km.

Furthermore, the scatter in the gravity data on the southern edge of the basin can be almost completely removed by using a correction factor proportional to the elevation. Consequently, the negative anomaly is interpreted as a basin in the depth range of 0.8 (from line *G–G′*) to perhaps 5.5 km. The westward extension of the basin is interpreted as being truncated by a fault. The northern edge could also be interpreted to be a fault. The southern edge is deeper and probably represents a density contrast within or below the basin. The maximum depth of the basin cannot be estimated without better control on the density contrast.

The southeastern part of line *D–D′* crosses the eastward protruding positive anomaly. This structure is modeled (fig. 9) as a rectangular bar whose width is 8.0 km, depth to top is 1.5 km, and depth to bottom is 4.0 km on the basis of a density contrast of 0.2 g/cm^3. The actual depth to the bottom may be greater since density contrasts become more difficult to discriminate at greater depths. The residuals are

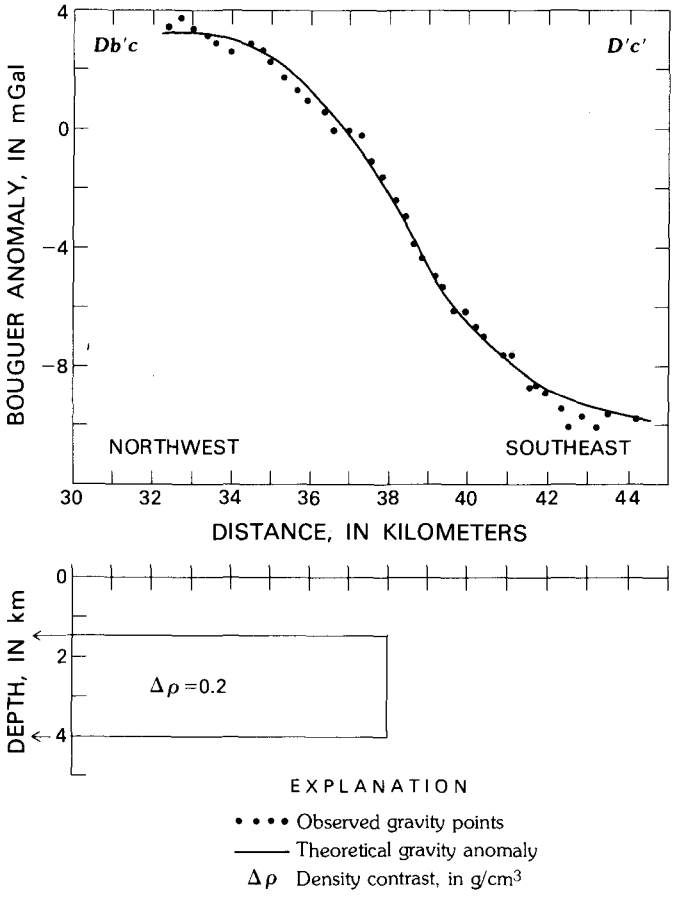

FIGURE 9.—Eastern part of line *D–D′* compared with the theoretical anomaly for a two-dimensional rectangular structure.

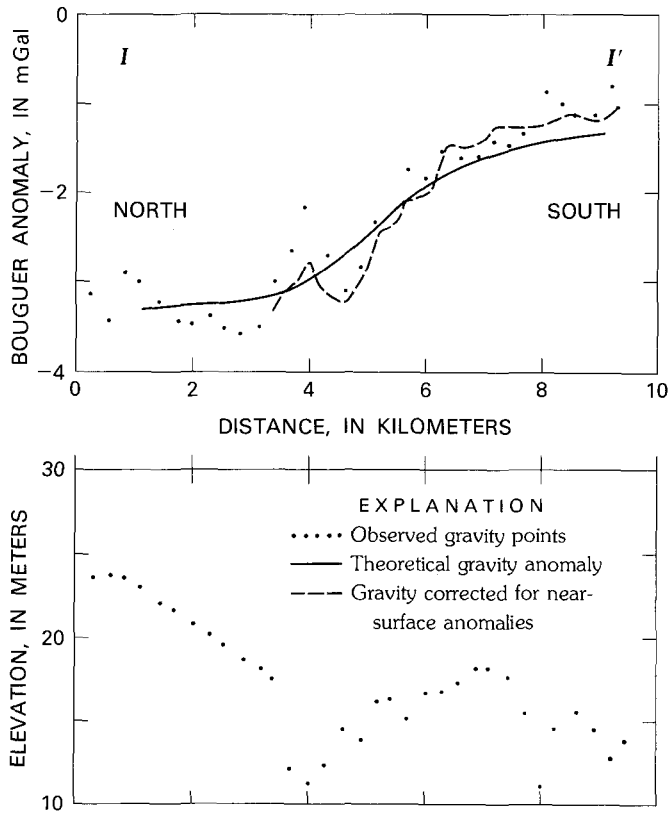

FIGURE 10.—Line *I–I′* compared with a simple fault model that has a depth of 0.8 km to its center and a throw of 0.2 km at a density contrast of 0.3 g/cm^3.

within the precision of the data. The maximum gradient of 2.4 mGal/km and maximum anomaly of 12 mGal imply a maximum depth of 3.25 km to the top of the structure. On the basis of this computation and the depth computations for line *F–F′*, the top of the eastward-protruding positive anomaly may be deeper than the tops of the other structures to the northwest. The difference in depths to the tops of the structures is consistent with the fault interpretation for line *A–A′*.

In an analysis of earthquakes and structures near Bowman, S.C., McKee (1974) noted an alinement of epicenters N. 40° W. parallel to Bollinger's (1973) transverse South Carolina–Georgia seismic belt. Tarr (this volume) also noted the N. 40° W. alinement of epicenters. Lines *I–I′*, *G–G′*, and *F–F′* are normal to this trend (fig. 4) and have been examined for evidence of a faultlike structure. Line *I–I′* and part of line *G–G′* are consistent with the model for a thin faulted slab with the downthrown side assumed to be infinitely deep (see Nettleton, 1976, p. 195). The depth to its center is 0.8 km, and its thickness is 0.2 km at a density contrast of 0.3 g/cm^3. The thin faulted slab model is mathematically identical to a

semi-infinite horizontal sheet and does not necessarily require interpretation as a fault. Line *I–I′* indicates a possible thin slab truncated at 5.5 km from the south end (fig. 10; see fig. 4 also). Line *G–G′* shows a possible thin slab truncated at 16.0 km from the northeast end (fig. 5). The scatter in the data about the theoretical anomaly for the thin faulted slab in line *I–I′* correlates inversely with the elevation (see fig. 10). The scatter is related to the near-surface density variations which correlate with the topography, and, hence, the scatter can be reduced prior to computation of the model parameters. However, the proportionality constant is often too large to be explained completely by an improper Bouguer reduction density and implies that near-surface structures are controlled in part by their elevation. Line *F–F′* has a negative deviation from the theoretical anomaly (fig. 8) at 15.0–16.0 km and again at 12 km from the north end. However, the interpretation that these deviations result from a thin faulted slab is inappropriate because they can be virtually eliminated by a correction factor proportional to the elevation and, hence, are related to near-surface structures. The two thin faulted slab models line up along a strike of N. 70° W. This strike is not consistent with the N. 40° W. alinement of regional epicenters noted by Bollinger (1973), McKee (1974), and Tarr (this volume). The gravity data do not indicate the existence of a continuous fault that has vertical displacements greater than 200 m oriented N. 40° W. The N. 70° W. alinement is consistent with, but displaced from, some recent shallow epicenters plotted in figure 4 (Tarr, this volume). However, the interpretation that the alinement of the thin faulted models is a single fault is not unique. An alternate interpretation that these features are the edges of basalt flows is preferred by the authors since this would be consistent with the interpretation that the positive anomalies are volcanic plugs and associated flows; also the regional data and lack of a fau'tlike structure along line *F–F′* do not support a continuous linear structure.

RESIDUAL GRAVITY ANOMALIES

In order to facilitate further analysis, gravity values were computed at a regular grid interval of 1.0 km using a distance-weighted mean-value interpolation algorithm. The area of the interpolated gravity data encompassed the area defined by the simple Bouguer gravity map. A regional field was obtained by convolving the gravity data with a smoothing operator which has an effective half-width of 2.5 km. The residual gravity map (fig. 11) is the

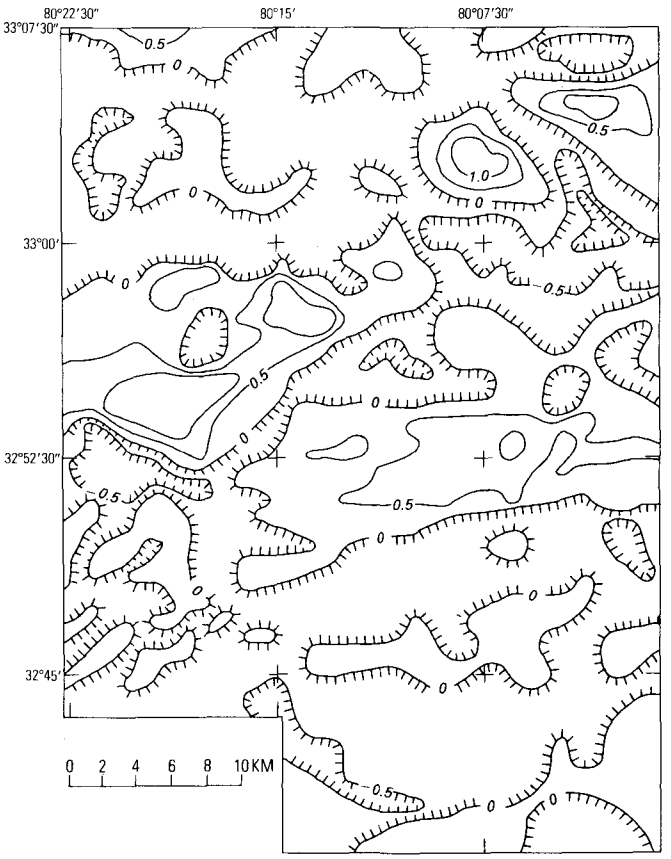

FIGURE 11.—Residual gravity map of the Summerville-Charleston, S.C., epicentral zone. Contour interval, 0.5 mGal. Hachures are used to indicate the negative side of the zero and all negative contour lines.

difference between the simple Bouguer gravity map and the regional field already described. Positive residual anomalies are shown in the central part of figure 11 and are located in the same positions as the positive anomalies in the original map (fig. 3), implying that parts of the source of these anomalies are less than 2.5 km deep (the radius of the smoothing operator). The westernmost large positive anomaly is resolved by the residual anomalies into two peaks. These two peaks are in a line with the two positive anomalies to the northeast. The line strikes N. 45° E. A long, narrow negative residual anomaly that also strikes N. 45° E. occurs approximately 4.0 km southeast of the line of positive anomalies. This negative residual anomaly connects the northwest edge of the basin (where a fault, shaded on fig. 3, was interpreted along line *A–A′*) and the northwest edge of a negative simple Bouguer anomaly (fig. 3) in the southwest part of the area shown on the map. This long, narrow negative residual anomaly is interpreted as evidence of the southwest continuation of the edge fault for the basin interpretation of the

negative Bouguer anomaly near 80° W., 33° N. The negative residual anomaly occurs on the downthrown block of a fault. The positive anomaly protruding to the east (fig. 11) is smoother than the peaks to the northwest and supports the hypothesis of a deeper source for this anomaly.

The northeastern and southwestern negative Bouguer anomalies may be part of one continuous basin (see fig. 1). The total depth of the basin is unknown but could be as deep as 5.5 km on the basis of the horizontal cylinder model applied to line *F–F′* (fig. 83. Mann and Zablocki (1961) noted very similar anomalies associated with the Jonesboro fault, a border fault on the southeast edge of the Deep River Triassic basin in North Carolina. However, they interpreted the density contrast to be -0.1 g/cm^3. If a density contrast of 0.1 g/cm^3 applies to the basin near Charleston, its depth may exceed the 5.5-km estimate from the cylinder model applied to line *F–F′*. The displacement of shallow or more recent flows near the fault could be significantly less or even nonexistent, since some of the volcanic activity and the faulting could have been contemporaneous.

THREE-DIMENSIONAL MODELS

Although gravity data generally do not allow a unique structural interpretation, the addition of constraints on the acceptable structures will often allow a direct inversion that provides insight into the distribution of the anomalous masses. One simple constraint is to assume that the anomalies are derived from a variation in the thickness of less dense rocks near the surface. In this model, the sedimentary rocks or less dense volcanic rocks were assumed to provide a density contrast of 0.3 g/cm^3 above more dense basic volcanic rocks or intrusive rocks. A lower density contrast or greater depth would lead to numerical instability for the shallow anomalies in the northwest part of the study area. Coastal Plain sediments were neglected in this model. An iterative process was used to effect a perfect fit of the theoretical anomaly to the data interpolated at a grid interval of 1.0 km. In this type of reduction, shallow anomalies are made more sharp, while the deeper sources remain smooth. The effect is similar to a downward continuation of the gravity field.

The elevation contours of the interpreted subbasement (fig. 12) are similar to those of the gravity anomalies, except that they show steeper gradients and tend to emphasize some of the structural contacts. In this model, the sharp peaks in the northwest part of the study area are at depths equivalent to 0.7–2.1 km. The eastward-protruding positive anomaly now appears as a ridge and has an average gradient significantly less than those on the edges of the large positive anomaly to the northwest. The smooth gradient provides additional support for the hypothesis of a possible deeper structure as the cause of this anomaly.

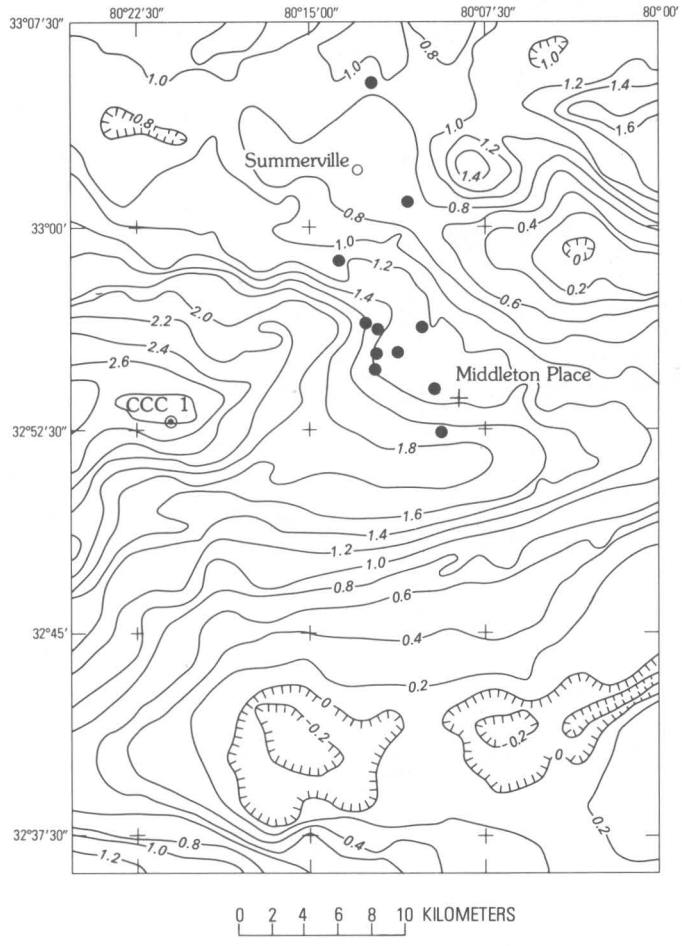

FIGURE 12.—Elevation contours of a surface derived by modeling Bouguer gravity anomalies assuming a density contrast of 0.3 g/cm^3. The contours are in kilometers above an arbitrary surface at a depth of 3.5 km. Hachures indicate areas below 3.5 km. Epicenters of recent earthquakes (solid circles) are from Tarr (this volume). CCC 1, Clubhouse Crossroads corehole 1.

Figure 13 shows two results of three-dimensional modeling of the gravity anomalies using the method of Talwani and Ewing (1960). Regional gravity data to the west of the area were included in this modeling to minimize the edge effects related to the positive anomaly. The models were obtained by assuming a structure compatible with the line data and perturbing the model until the computed gravity anomaly varied no more than ±2 mGal from the observed data. Regional data, interpolated onto a grid

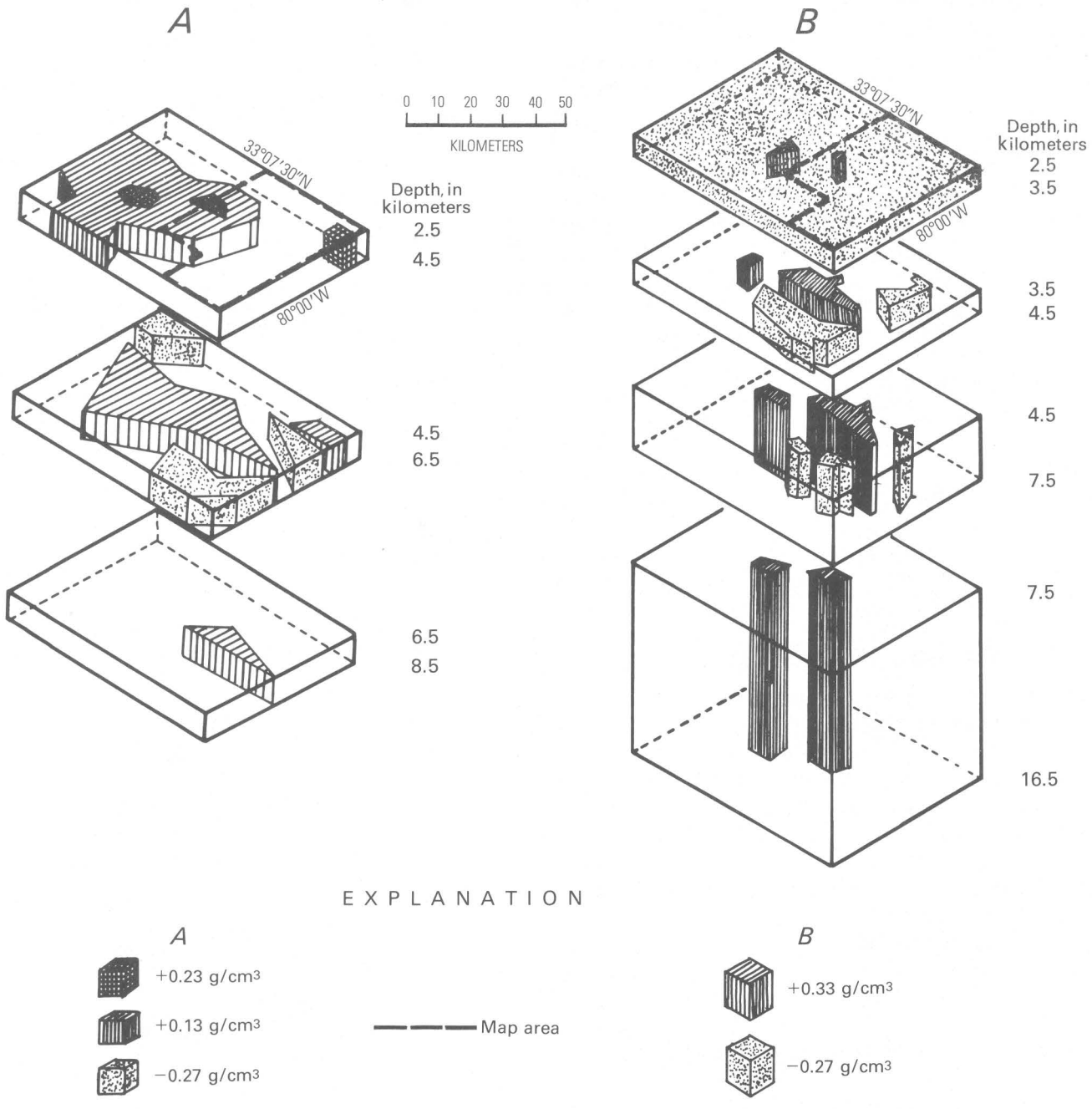

FIGURE 13.—Diagrams showing three-dimensional modeling of the gravity anomalies following the method of Talwani and Ewing (1960). This method uses polygons of anomalous density in stacked vertical sheets at intermediate-depths (*A*) and at maximum depths (*B*). The dashed lines on the top blocks outline the area of the gravity map in figure 3. The vertical dimension is exaggerated by a factor of five, and the sheets are separated for clarity. The maximum error for either model is 10 percent.

with a 5.0-km separation, were used to the west of the study area for the comparison. In the study area, the data interpolated to a 1.0-km grid were used for the comparison, and the maximum error allowed was 1.0 mGal. Resolution of models or structures at depths less than 2.5 km was not practical for data interpolated to a 1.0-km grid interval.

Figure 13*A* shows a model based on the depths and structures interpreted from the line data. The top sheet contains most of the sources for the positive anomalies. These extend over parts of the second and third sheet where no anomalous masses are shown. Hence, some of these may be interpreted as near-surface flows or sills. The second sheet contains the

sources for the negative anomalies and the eastward extension of the positive anomalies. The third sheet contains only a source for part of the eastward protruding anomaly.

Figure 13*B* shows the result of extending the modeled structures as deep as possible. However, in both models, shallow structures (2.5–4.5 km) are required to maintain a satisfactory fit to the observed data; only the core of the large positive anomalies can be extended to significantly greater depths. Both models suggest that a vertical offset of the structure responsible for the eastward-protruding positive anomaly is compatible with the gravity data.

POSSIBLE EARTHQUAKE MECHANISMS

Two large-scale features of the interpreted structures are considered significant to the mechanism of the 1886 Charleston earthquake. The first is a fault in the basement interpreted as the northwest edge of a basin. The fault strikes generally N. 45° E., but is displaced to the northwest by more than 6.0 km from the hypothesized Woodstock fault described by Taber (1914). The offset on the fault is estimated to be at least 0.6 km on the basis of the interpretation of the gravity data for the zones that cross this feature. The 0.6-km vertical displacement is reasonable for basins associated with rift zones and is comparable to the displacement of the Deep River basin in North Carolina (Reinemund, 1955). The second significant large-scale feature is the linear positive anomaly extending east from the positive high. This is interpreted to be a ridge or barlike structure of high-density material in the depth range of 1.0–6.0 km or greater in the crust. High density rocks typically have high seismic velocities. Higher velocities would imply that this protrusion has a higher modulus of rigidity than would be expected for the surrounding basin materials.

These two large-scale features of the interpreted crustal structure pose two independent explanations for the occurrence of earthquakes near Charleston. The first explanation, and perhaps the more conventional, is that the earthquakes are the result of the reactivation of the northeast-striking basement fault. This mechanism is essentially that proposed by Taber (1914), except that the fault interpreted from gravity data is farther to the northwest than the proposed Woodstock fault. In this first explanation, earthquake epicenters and intensities should be closely associated with the fault trace.

The second explanation is that the earthquakes are the result of fracture of the structure responsible for the eastward protruding positive anomaly. The contrast between the rigidity of this structure and the rigidity of the surrounding sedimentary or igneous rocks would allow the concentration of stress through the mechanism of "stress amplification." In stress amplification, the geometry of the structure is such that regional shear stress is concentrated in an anomalously rigid crustal unit, and the stress within the anomalously rigid unit is amplified at geometrically appropriate locations. Consequently, stress amplification could lead to stress levels significantly higher than expected for an homogeneous medium. During a steady change in regional ambient stress, fracture will occur first at geometrically appropriate locations in the more rigid structures. The existence of contemporary stress changes related to a flexure of the crust is implied by differential vertical movement (Meade, 1971; Brown and Oliver, 1976) measured along the South Carolina coast. However, appropriate data prior to the 1886 Charleston earthquake are not available. Nevertheless, bending of the east-west axis of the structure could account for the concentration of stress necessary for the occurrence of earthquakes in or near the structure.

Earthquakes in this model would be expected to occur at points of weakness or stress concentration, such as where the structure thins or joins a larger structure. For the mass of rigid material identified near Charleston, one possible point of weakness or stress concentration would be near lat 32° 52′ 20″ N. between long 80° 7′ 30″ W. and 80° 12′ W. Near this point, the structure in the inversion model (fig. 12) shows a slight thinning and is near its junction with the larger structure. The east-west strike of the structure would imply a higher susceptibility to stress amplification from regional shear stress oriented normal to the strike. These stresses would be conducive to a generally north-south strike to a plane of rupture caused by stress amplification.

EARTHQUAKE LOCATIONS AND SLOAN'S INTENSITY MAP

Sufficiently precise epicenters and intensity maps might now allow identification of one of the two above-described mechanisms as the more likely mechanism of the Charleston earthquake. Unfortunately, the reported epicenters for the historic activity near Charleston are based largely on intensity reports or seismograms written at distant stations. The precision of such data is insufficient for a resolution of mechanism of the Charleston earthquakes. The November 22, 1974, earthquake, however, was recorded by the U.S. Geological Survey's recently installed seismic net as well as by more distant sta-

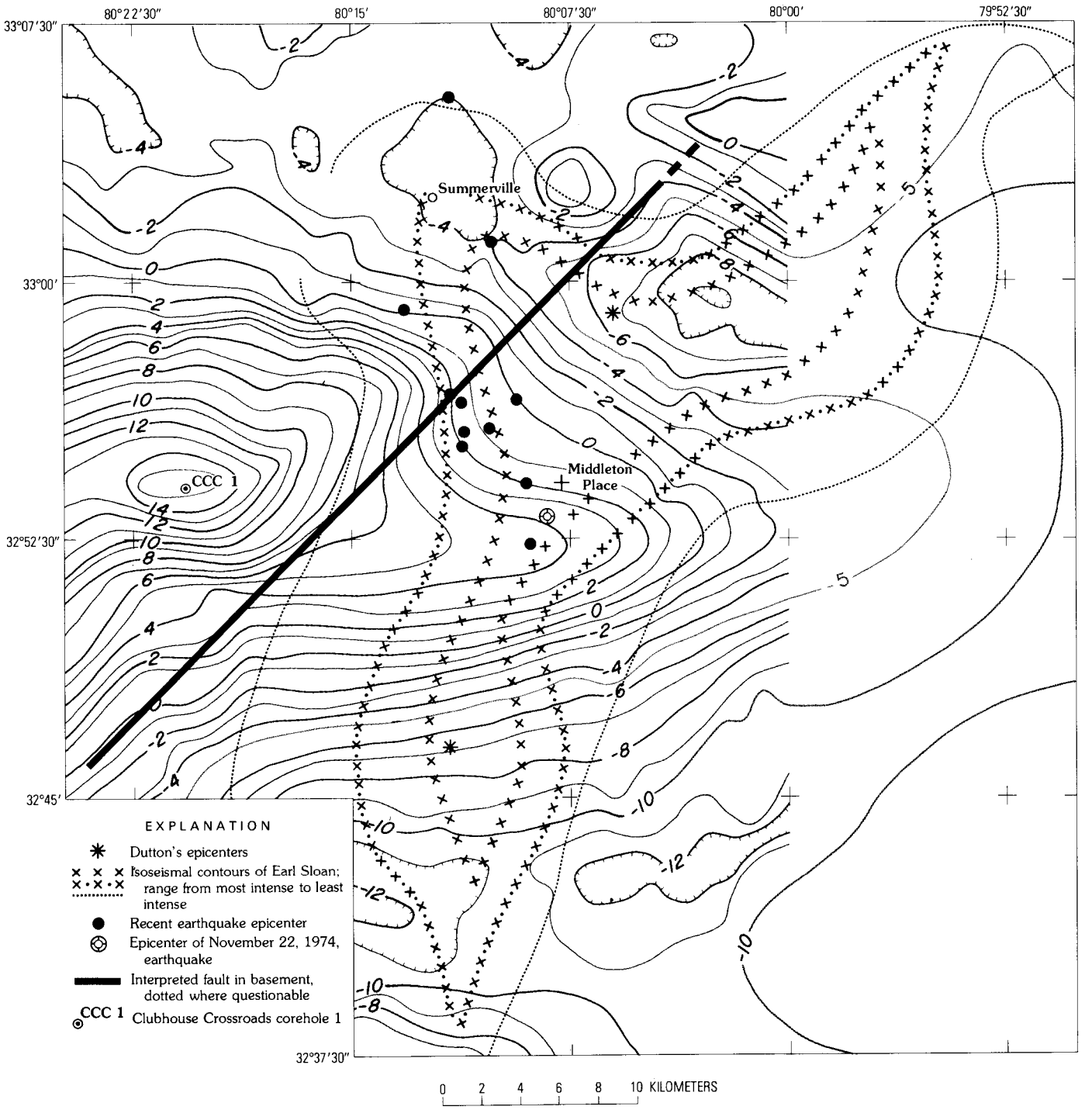

FIGURE 14.—Superposition of isoseismal contours of Earl Sloan (Dutton, 1889) on Bouguer gravity anomalies of figure 3. The solid line indicates the near-surface position of the interpreted basement fault. Epicenters of recent earthquakes are from Tarr (this volume).

tions, and consequently its hypocenter should be more precise (see fig. 14). The hypocenter (Tarr, this volume) falls 7.0 km southeast of the proposed basement fault, but less than 2.0 km north of the center of the eastward-protruding ridge. The hypocenter of an aftershock of the November 22, 1974, earthquake was near the center of the protruding ridge. These hypocenters are compatible with the hypothesized hypocenters for the stress amplification mechanism. Their depths of 4.1 km and 2.2 km, respectively, are

close to or within the structures modeled. Unfortunately, both the precision of the hypocenter depth computations and the maximum depth of the structure are unknown and difficult to compute with existing data. Many of the other events occur where the gravity model indicates dense, shallow, and hence more rigid structures, such as near-surface flows. If these events are shallow they could be attributed to stress amplification in the shallow structures. This could explain part of the apparent scatter in the epicenters. Unfortunately, the gravity data are not sufficient to resolve the details of these shallow structures.

The isoseismal contours according to Earl Sloan (Dutton, 1889) are shown in figure 14 for comparison to the epicenters, gravity contours, and crustal structure. Unfortunately, Sloan's map was not completely true to scale, and the contours have been adjusted to fit the known locations of still-existing towns or stable physiographic features shown on his map. The intensity data are distributed so as to form two apparent "maximum intensity areas" at the ends of a linear zone of maximum intensity striking N. 20° E. This distribution prompted Taber (1914) to propose the Woodstock fault. The isoseismal contours do not correspond to an intensity distribution that would be expected from reactivation of the basement fault interpreted from the gravity data. While the intensity contours may be partially controlled by the near-surface soils and the distribution of intensity observations, the predominance of the higher intensities to the southeast of the fault would be difficult to explain completely by variations in near-surface soils. The distribution of the intensities given by Sloan does, however, correspond remarkably well to the intensity that one would expect from an earthquake resulting from fracture in the eastward protruding structure because of stress amplification. Consequently, the epicentral zone of the 1886 earthquake may be presumed to be midway between the dual epicenters of Dutton (1889) and subsequently near the epicenter of the November 22, 1974, earthquake. However, this immediate epicentral zone was sparsely populated, and remains so today. Although the completeness of the data and the effects of soil response to intensities in the immediate epicentral zone are questionable, the distributions of intensities near the two macroseismic epicenters were well documented. Remarkably, the crustal structure interpreted from the gravity data is consistent with the intensity pattern. In the stress amplification mechanism, the seimic waves would originate largely in the more rigid, higher velocity structure and would propagate into the lower velocity adjacent basins. Because of a possible combination of focusing of the seismic waves and a change in acoustical impedance near the edge of the structure, the seismic waves could undergo dynamic amplification near the observed dual epicenters. In general, Sloan's intensities are lower where the gravity data imply denser and, consequently, higher velocity crustal structures. As a tribute to Sloan's evaluation of the intensities about 5.0 km north-northwest of Dutton's northern epicenter (see fig. 14), we note that even the apparent reduction in the intensities—which was discounted by Dutton (1889)—is supported by the crustal structures interpreted from the gravity data and the supposition that the intensities over the more rigid crustal rock were subdued.

The intensity data for the historic and recent Summerville–Charleston earthquakes show that audible sounds are associated with these earthquakes (Louderback, 1941). Louderback (1941) also suggested that these unusual sounds imply the fracturing of fresh rock under high stress rather than movement along established faults. These sounds may imply anomalously high corner frequencies and, hence, the existence of a greater proportion of energy at frequencies higher than generally observed for earthquakes of equivalent magnitudes occurring in the other seismic zones. By consideration of the spectral theory of earthquakes (Randall, 1973), these conditions imply relatively high stress drops for the Summerville–Charleston earthquakes. Furthermore, the width of the eastward protruding ridge would allow an effective fault radius of about 6 km if the entire structure ruptures according to the stress amplification mechanism. A magnitude (m_b) range of 6.8–7.1 (Bollinger, this volume) is implied by intensity data. Since m_b is equivalent to M_L in the 6.0–7.0 magnitude range, these magnitudes and a fault radius of 6 km would theoretically allow stress drops of 40–200 bars (Randall, 1973). According to Gibowicz (1973), a magnitude-7.0 event would normally have a stress drop of about 22 bars and (after Randall, 1973) a fault radius of 25 km. A 50-km-long fault is not reasonable for the Charleston event. If correct, the maximum intensity and a reasonable fault radius imply an abnormally high stress drop for the 1886 Charleston earthquake. These observations are consistent with the stress amplification mechanism for the Summerville–Charleston earthquakes.

CONCLUSION

Of the two mechanisms—reactivation of a basement fault and stress amplification—suggested by the structures interpreted from the gravity data, the stress amplification mechanism better satisfies the historic intensity data and recent-event epicenters. Stress amplification should be considered carefully as a probable mechanism for the great Charleston earthquake of 1886 as more data become available.

REFERENCES CITED

Bollinger, G. A., 1972, Historical and recent seismic activity in South Carolina: Seismol. Soc. America Bull., v. 62, no. 3, p. 851–864

——— 1973, Seismicity and crustal uplift in the southeastern United States: Am. Jour. Sci., *in* The Byron N. Cooper Volume 273–A. p. 396–408.

Brown, L. D., and Oliver, J. E., 1976, Vertical crustal movements from leveling data and their relation to geologic structure in the Eastern United States: Rev. Geophysics and Space Physics, v. 14, no. 1, p. 13–35.

Champion, J. W., Jr., 1975, A detailed gravity study of the Charleston, South Carolina, epicentral zone: Atlanta, Georgia Inst. of Tech., Master's thesis, 97 p.

Cooke, C. W., 1936, Geology of the Coastal Plain of South Carolina. U.S. Geol. Survey Bull. 867, 196 p.

Dutton, C. E., 1889, The Charleston earthquake of August 31, 1886: U.S. Geol. Survey Ann. Rept. 9, 1887–88, p. 203–528.

Fletcher, J. P., Sbar, M. L., and Sykes, L. R., 1974, Seismic zones and travel time anomalies in eastern North America related to fracture zones active in the early opening of the Atlantic [abs.]: in EOS (Am. Geophys. Union Trans.), v. 55, no. 4, p. 447.

Gibowicz, S. J., 1973, Stress drop and aftershocks: Seismol. Soc. America Bull., v. 63, no. 4, p. 1433–1446.

Long, L. T., 1974, Bouguer gravity anomalies of Georgia, *in* Symposium on the petroleum geology of the Georgia Coastal Plain: Georgia Geol. Survey Bull. 87, p. 141–166.

Long, L. T., Bridges, S. R., and Dorman, L. M., 1972, Simple Bouguer gravity map of Georgia: Georgia Geol. Survey.

Long, L. T., Talwani, P., and Bridges, S. R., 1975, Simple Bouguer gravity map of South Carolina: South Carolina Div. Geology. Map. Ser. 21, 27 p.

Louderback, G. D., 1941, The personal record of Ada M. Trotter of certain aftershocks of the Charleston earthquake of 1886: Seismol. Soc. America Bull., v. 31, no. 4, p. 199–206.

Mann, V. I., and Zablocki, F. S., 1961, Gravity features of the Deep River–Wadesboro Triassic basin of North Carolina: Southeastern Geology, v. 2, no. 4, p. 191–215.

Mansfield, W. C., 1936, Some deep wells near the Atlantic Coast in Virginia and the Carolinas: U.S. Geol. Survey Prof. Paper 186–I, p. 159–161.

McKee, J. H., 1974, A geophysical study of microearthquake activity near Bowman, South Carolina: Atlanta, Georgia Inst. of Tech., Master's thesis, 65 p.

Meade, B. K., 1971, Report of the sub-commission on recent crustal movements in North American: Internat. Assoc. Geodesy, 15th General Assembly, Moscow, USSR.

Nettleton, L. L., 1976, Gravity and Magnetics in oil prospecting: New York, McGraw-Hill Inc., 464 p.

Oliver, Jack, and Isacks, Bryan, 1972, Seismicity and tectonics of the eastern United States [abs.] Earthquake Notes, v. 43, no. 1, p. 30.

Pooley, R. N., Meyer, R. P., Woollard, G. P., 1960, Yamacraw Ridge, pre-Cretaceous structure beneath South Carolina-Georgia Coastal Plain [abs.]: Am. Assoc. Petroleum Geologists Bull., v. 44, no. 7, p. 1254–1255.

Randall, M. J., 1973, The spectral theory of seismic sources: Seismol. Soc. America Bull., v. 63, no. 3, p. 1133–1144.

Reinemund, J. A., 1955, Geology of the Deep River coal field, North Carolina: U.S. Geol. Survey Prof. Paper 246, 159 p.

Taber, Stephen, 1914, Seismic activity in the Atlantic Coastal Plain near Charleston, S.C.: Seismol. Soc. America Bull., v. 4, no. 3, p. 108–160.

Talwani, Manik, and Ewing, W. M., 1960, Rapid computation of gravitational attraction of three-dimensional bodies of arbitrary shape: Geophysics, v. 25, no. 1, p. 203–225.

Woollard, G. P., Bonini, W. E., and Meyer, R. P., 1957, A seismic refraction study of the subsurface geology of the Atlantic Coastal Plain and continental shelf between Virginia and Florida: Wisconsin Univ., Dept. Geology Geophysics Sec., 128 p.

Exploring the Charleston, South Carolina, Earthquake Area with Seismic Refraction—A Preliminary Study

By HANS D. ACKERMANN

STUDIES RELATED TO THE CHARLESTON, SOUTH CAROLINA, EARTHQUAKE OF 1886–A PRELIMINARY REPORT

GEOLOGICAL SURVEY PROFESSIONAL PAPER 1028-L

CONTENTS

ILLUSTRATIONS

STUDIES RELATED TO THE CHARLESTON, SOUTH CAROLINA, EARTHQUAKE OF 1886—
A PRELIMINARY REPORT

EXPLORING THE CHARLESTON, SOUTH CAROLINA, EARTHQUAKE AREA WITH SEISMIC REFRACTION—A PRELIMINARY STUDY

By HANS D. ACKERMANN

ABSTRACT

Seismic refraction soundings northwest of Charleston, S.C., show:

1. A marked decrease in the velocity of an approximately 800-m-deep basalt layer (of Cretaceous or older age).
2. A possible small downwarp in this basalt layer and the shallower sedimentary section.
3. A flexure or fault in the 1,000- to 2,000-m-deep crystalline basement.

The spatial near coincidence of these three features with the high-intensity zone of the 1886 earthquake and recent earthquake epicenters may strengthen the argument that the Charleston seismic trend is an area of high stress along a preexisting fault zone.

INTRODUCTION

During the spring of 1975, 12 seismic-refraction spreads, each approximately 2,600 m long, were recorded near Charleston, S. C. The purpose of this work was to investigate deformations that may be related to the historical earthquakes of the area. The problem is twofold—(1) to find deformations, and (2) to determine whether they are recent.

One possible approach to this problem is to identify deformations that involve recent geologic features. On the Atlantic Coastal Plain, this approach would mean locating basement faults that extend into the shallow sedimentary section. The seismic-reflection method is well suited for this purpose. This approach presents two problems, however. First of all, an earthquake-generating fault need not disrupt shallow rocks. Second, although seismic reflection is very sensitive for delineating vertical displacements, it cannot detect strike-slip displacements. Nevertheless, a high-resolution seismic-reflection survey was seriously considered in the early stages of this project. We felt that in order to investigate recent earthquakes, the survey should focus to depths between at least 200 and 1,000 m, the latter having been the assumed depth to the crystalline basement. In addition, resolution must be sufficient to detect vertical displacements as small as 15 m, and the survey should be sufficiently extensive to cross the Charleston structure if one exists. The cost of contracting a survey to meet these minimum requirements was prohibitive.

A seismic-refraction survey, on the other hand, also permits the study of recent tectonism, but from a different point of view. In refraction, the path traveled by the recorded signal is largely horizontal instead of vertical. Hence, although the refraction method is considerably less accurate than the reflection method for delineating vertical displacements, the long horizontal travel path permits the accurate calculation of lateral velocity variations in the layers recorded. One important cause for lateral velocity changes in a layer is inhomogeneity resulting from changes in fracture porosity (Wyllie and others, 1956; Ackermann and others, 1975). One may certainly expect large variations in fracture porosity in a zone of recent earthquakes because fractures caused by the large stresses have not had the opportunity to close. Hence, we chose to use seismic refraction to search for lateral velocity variations in the deep rocks of the Charleston area. Furthermore, refraction is a powerful reconnaissance tool, and the results are extremely valuable for possible later high-resolution reflection studies.

This work was supported by the U.S. Nuclear Regulatory Commission, Office of Nuclear Regulatory Research, Agreement no. AT (49–25)—1000.

THE SURVEY

Locations of the 12 seismic spreads are shown in figure 1. Also shown are the centers of highest in-

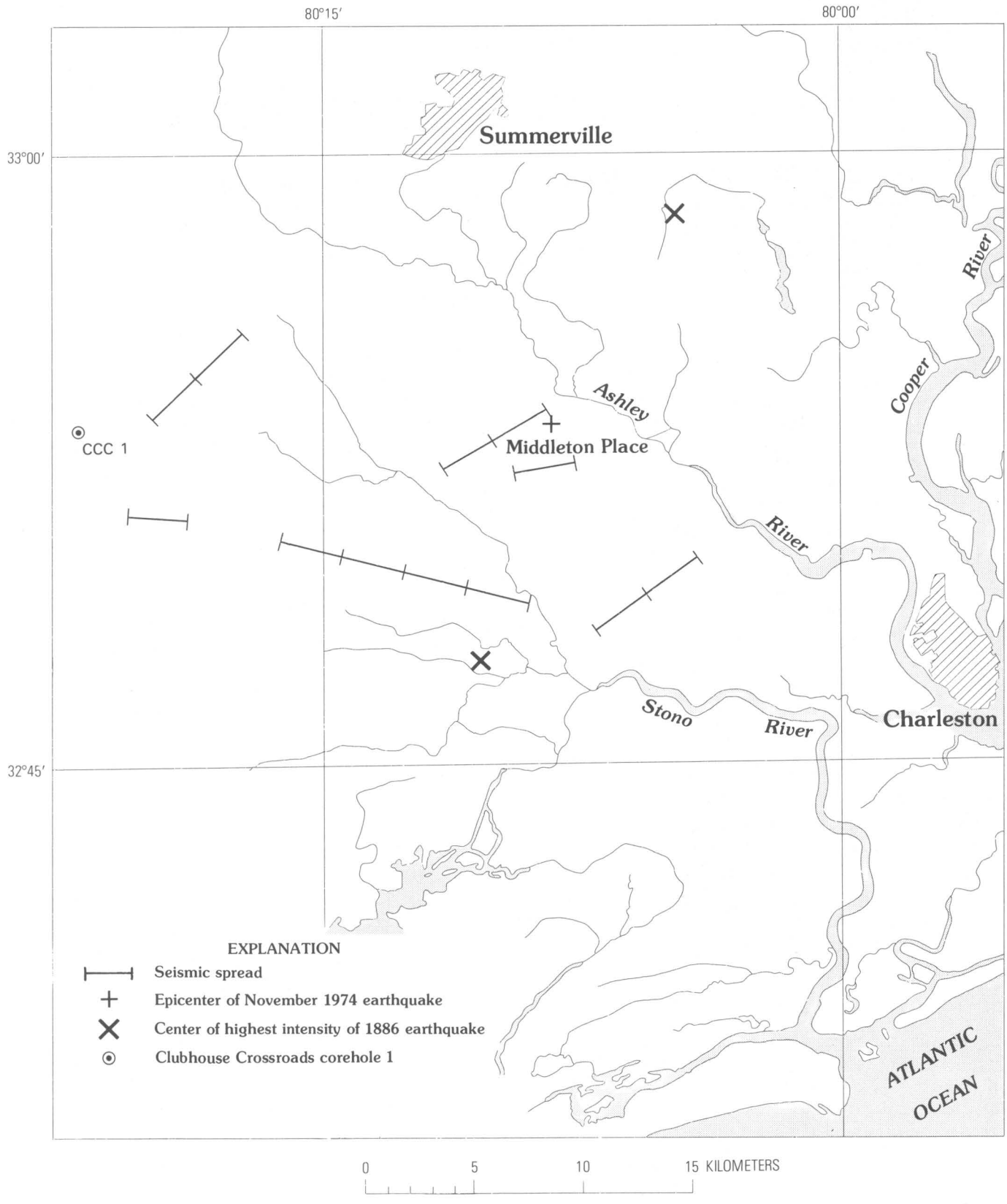

FIGURE 1.—Location map showing area of study near Charleston, S. C.

tensity (Dutton, 1889) for the 1886 MM intensity X earthquake; the location of the 792-m-deep Clubhouse Crossroads corehole 1 (CCC 1); and the epicenter, near the historic Middleton Place plantation, of the Nov. 22, 1974, magnitude-3.8 earthquake (Tarr, this volume). The plan was to tie the CCC 1 to the refraction profiles and to extend coverage towards the most southern of Dutton's centers and also to the Middleton Place epicenter. The seismic spreads were recorded with sufficient shot points to obtain full reverse coverage from a basement horizon 600–1,000 m deep, and partial reverse coverage from shallower horizons within the sedimentary sequence.

RESULTS

The refraction interpretations revealed three distinct seismic marker horizons that were continuous throughout the area surveyed. The shallowest and intermediate refracting horizons were penetrated by CCC 1 and are evident on both the geologic and sonic well logs. The deepest horizon is below the total depth of the hole (792 m).

The shallowest refractor correlates with a thin, well-indurated crossbedded calcarenite at the base of the Santee Limestone (Eocene), which is about 100 m deep at the well site. The velocity of this calcarenite member of the Santee is 2.5–2.7 km/s. Its higher velocity is a result of cementation by carbonate rocks dissolved from the overlying section.

The intermediate horizon corresponds to the top of the Cretaceous(?) basalt lava flows, intersected by CCC 1 at a depth of 750 m. (See Gottfried and other geophysical data to obtain a preliminary crust-basalt.) Its velocity near the well site is 5.8 km/s. Drilling was terminated after 42 m of basalt had been cored.

The deepest horizon recorded has a velocity of about 6.3–6.5 km/s. This undoubtedly represents the crystalline basement.

We note, once again, that shot locations were planned to provide complete reverse coverage for a single high-velocity basement horizon 600–1,000 m deep. The recordings revealed two high-velocity layers; one, the basalt, which was within the expected interval, and the other, the deeper crystalline basement. Full coverage was not obtained from the crystalline basement. Consequently, velocity and depth control are incomplete for this layer.

The sonic well log showed several layers between the shallow Santee Limestone (Eocene) and the Cretaceous(?) basalt that have velocities slightly more than 2.7 km/s. However, the position of these layers in the sedimentary section did not permit them to appear as conspicuous events on a refraction record. Thus, for all practical purposes, the refraction data revealed only the three above-mentioned layers.

CHARACTER OF REFRACTED ARRIVALS

The arrivals recorded from the marker horizon in the Santee attenuate rapidly and cannot be identified on the recordings beyond 700 to 1,100 m from any shot point. Apparently, the high-velocity-sandstone part of the Santee is too thin to transmit a seismic wave efficiently.

Similarly, arrivals from the basalt layer also attenuate rapidly and are generally shingled. A shingle is a form of multiple arrival (Spencer, 1965; Cassinis and Borgonovi, 1966) associated with a high-velocity layer imbedded in a lower velocity medium. Therefore, we infer that the basalt is again underlain by lower velocity rocks, possibly a pre-Upper Cretaceous sedimentary sequence.

VARIATIONS IN VELOCITY

Interpretations for the intermediate horizon, which correlates with the basalt at CCC 1, are that its velocity ranges from 4.3 to 5.8 km/s. Significant velocity variations for the shallow marker horizon in the Santee Limestone, on the other hand, were not identified. Furthermore, data from the deep crystalline basement rocks were insufficient to calculate velocity changes for this layer.

Figure 2 shows the lateral variations in compressional velocity of the intermediate (basalt) horizon. We see a general eastward decrease in velocity. The focus of the November 22, 1974, magnitude-3.8 earthquake (Tarr, this volume) was at a depth of 4.1 km, directly under the area of lowest velocity.

STRUCTURAL INTERPRETATIONS

Figures 3 and 4 are contour maps of interpreted depths to the marker horizon within the Santee Limestone and to the intermediate (basalt) marker horizon, respectively. Depths were calculated using a vertical velocity function obtained from the sonic log of CCC 1. By so doing, the countoured depths for these two horizons agree with their actual measured depths at the well site. We point out, however, that because of the shingling of the basalt arrivals, depth calculations for this horizon are based, in part, on subjectively shifting recorded data. Thus, to some extent, the interpreted depths and structure for the basalt horizon are uncertain.

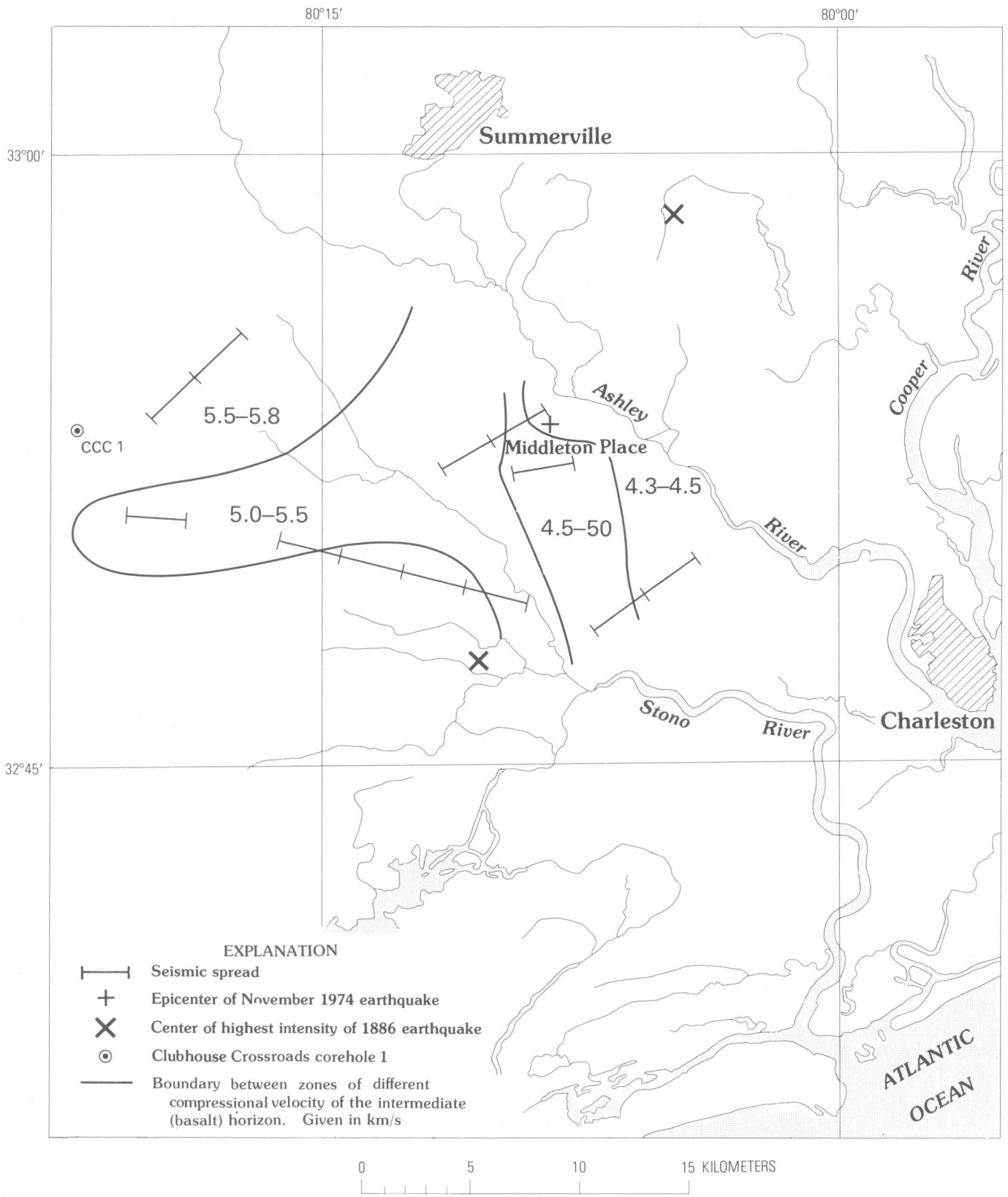

FIGURE 2.—Lateral variations in compressional velocity of the intermediate (basalt) horizon.

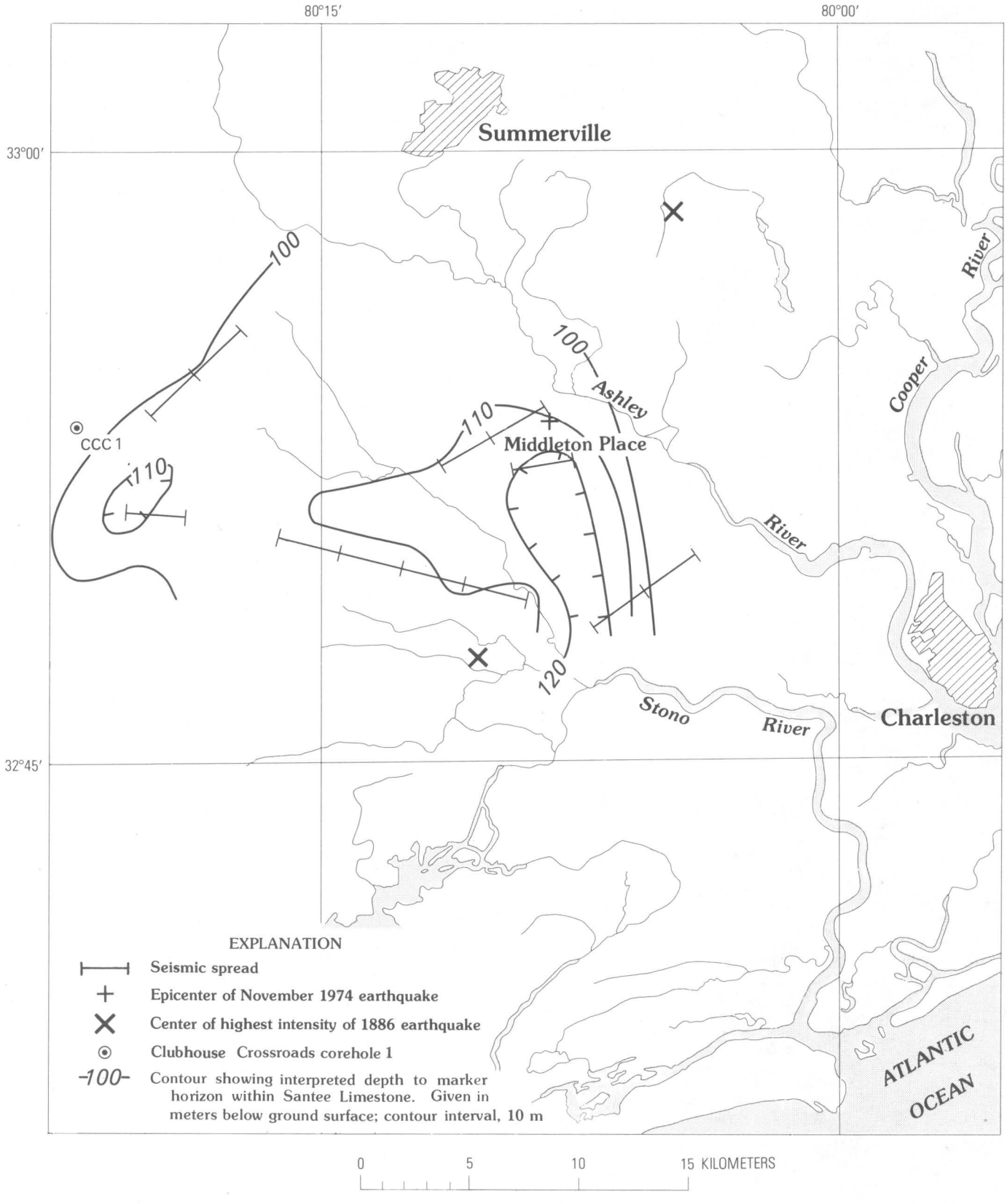

FIGURE 3.—Contour map of interpreted depths to the marker horizon within the Santee Limestone. Ground-surface elevation approximately 7.5 m.

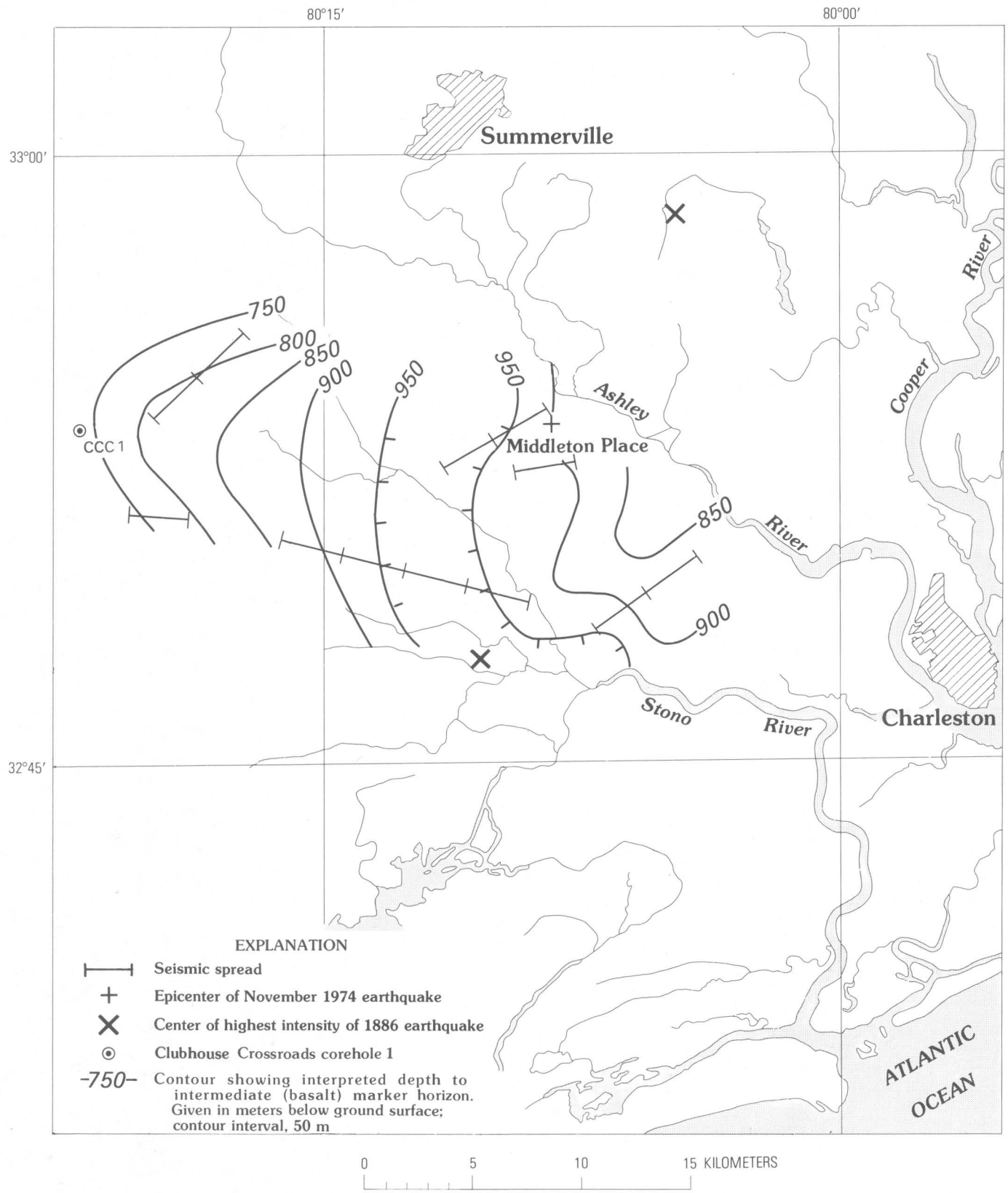

FIGURE 4.—Contour map of interpreted depths to the intermediate (basalt) marker horizon.

Figure 3 shows that the Santee is nearly horizontal throughout the area surveyed. The data suggest, however, that the Santee contains an approximately 20-m-deep north-trending troughlike depression near the eastern edge of surveyed area.

The most striking feature of the basalt-horizon contours (fig. 4) is also a north-trending broad troughlike depression which is offset slightly westward from the axis of the overlying Santee trough. The size of this depression may exceed 50 m, though it is difficult to determine because it modulates the regional dip which is to the southeast. The axis of this trough also parallels the trend of the basalt-velocity variations noted above, though offset several kilometers westward from the velocity minimum.

Figure 5 is a contour map of interpreted depths to the deep crystalline basement. Because data from this horizon are incomplete, structural details could not be determined. In particular, the downward continuation of the troughlike feature from the Santee and basalt horizons could not be calculated. Crystalline basement depths were calculated, assuming a constant 4.2-km/s velocity between basement and the overlying basalt. If a sedimentary section underlies the basalt, its average velocity may be less than 4.2 km/s. If so, the calculated crystalline basement depths are too large. In any case, the basalt and basement horizons diverge southeastward. Near CCC 1, the distance between the two may be less than 200 m. In the southeastern part of the area surveyed, it may be 1,000 m. The more tightly spaced depth contours in the southeastern part of the area indicate either a flexure or a fault in the crystalline basement. Unfortunately, data for this horizon are insufficient to make a definitive judgment.

DISCUSSION

The seismic-refraction data allow one to map three horizons, the upper two of which were identified in CCC 1. The intermediate horizon correlates with a Cretaceous(?) basalt at the depth of 750 m in the corehole. The velocity of this horizon is definitely variable, decreasing from a high value of about 5.8 km/s at the well to about 4.5 km/s along the eastern edge of the area surveyed, which includes the epicenter of the November 22, 1974, earthquake. Furthermore, a north-trending troughlike feature, which parallels the velocity trend, has been tentatively identified in the intermediate horizon. The axis of this trough is offset a few kilometers west of the velocity minimum. The data also suggest a similar but smaller depression in the shallowest horizon, which is within the 100-m-deep Santee Limestone.

Shingling in the refracted arrivals for the intermediate (basalt) horizon indicates that this horizon is underlain by lower velocity materials, possibly a pre-Upper Cretaceous sedimentary section, which thickens southeastward.

The deepest of the three mappable horizons is the true crystalline basement. Because data from this horizon are incomplete, details of its structure and velocity cannot be calculated. However, the data do indicate either a flexure or a fault of the crystalline basement in the southeastern part of the area surveyed. Neither the intermediate (basalt) nor the shallow Santee horizons show evidence of this structure. Furthermore, the velocity of the intermediate (basalt) layer attains a minimum value in the immediate area of this basement flexure or fault. In addition, the troughlike depression in the basalt and one of the two centers of highest intensity (Dutton, 1889) are just a few kilometers westward.

Thus we see the near coincidence of four events or features: (1) a line of earthquake activity defined by the Dutton high-intensity points and the recent epicenter at Middleton Place; (2) a compressional velocity minimum of a Cretaceous(?) basalt layer; (3) possible downwarping of this basalt layer and a shallower Eocene horizon; and (4) a flexure or fault in the crystalline basement. The spatial proximity of these four suggests a genetic relationship.

Sbar and Sykes (1973) delineated a region of high horizontal compressive stress in eastern North America. They proposed that the Charleston seismic trend is due to these high stresses acting along a zone of weakness, such as an unhealed fault or the continental extension of a major oceanic fracture zone. Our interpretation of the Charleston seismic data then suggests the possibility that the flexure or fault found in the crystalline basement may actually be a manifestation of such a zone of crustal weakness. Additional data are necessary to define this structure clearly and to determine its trend. The small downwarp tentatively identified in the two shallower horizons may then be the product of more recent earthquake activity. We further note the decrease in compressional velocity of the intermediate (basalt) layer and suggest that this may be due to increased fracture porosity also resulting from earthquake activity over an extended period of time. Another possible explanation for the low-

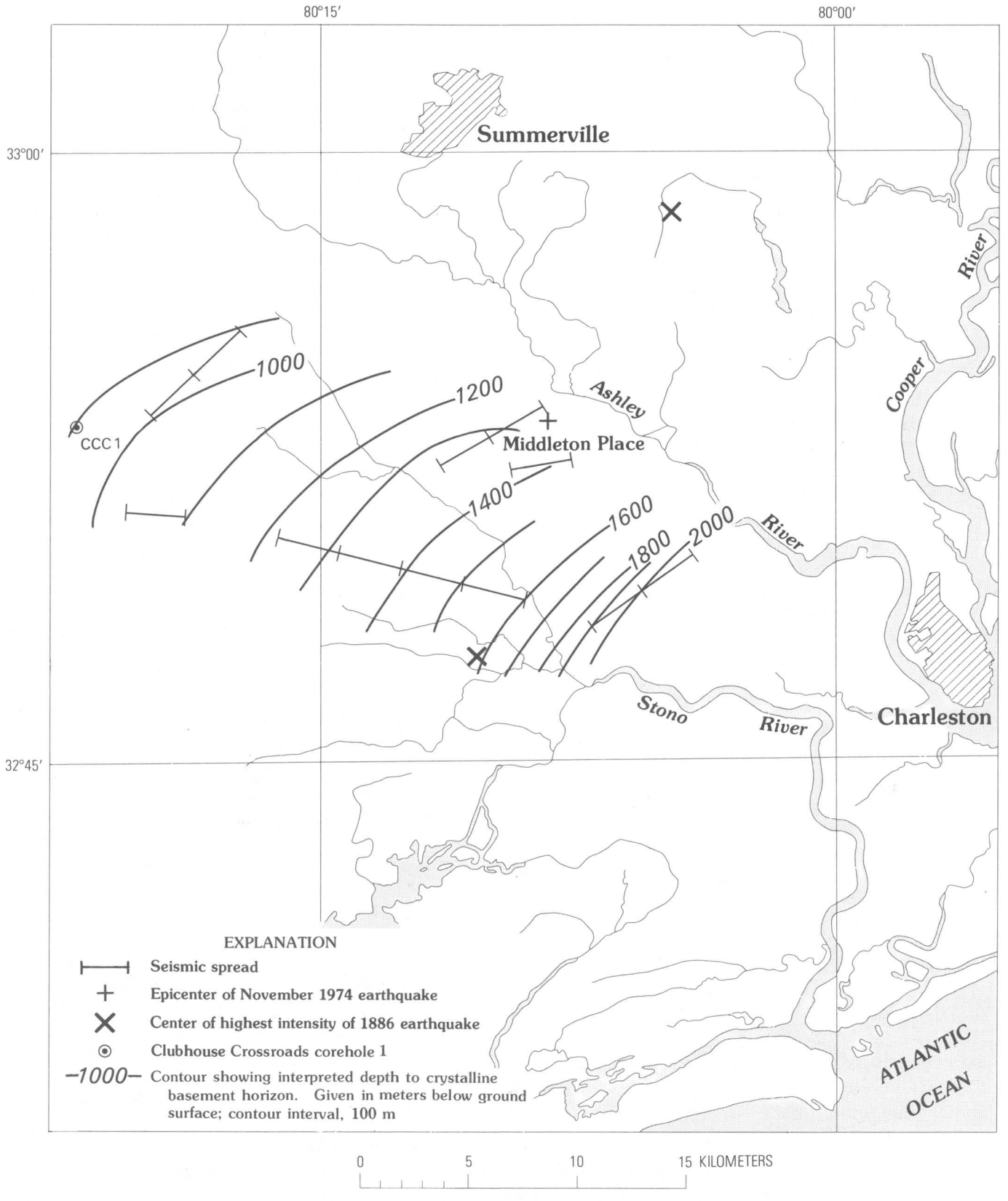

FIGURE 5.—Contour map of interpreted depths to the crystalline basement horizon.

ered compressional velocity is that it simply represents the termination of the basalt layer and that the arrivals recorded there are from the rocks that elsewhere underlie the basalt. The velocity of 4.5 km/s, for example, is an acceptable value (Stewart and others, 1973) for Triassic sedimentary rocks.

REFERENCES CITED

Ackermann, H. D., Godson, R. H., and Watkins, J. S., 1975, A seismic refraction technique used for subsurface investigations at Meteor Crater, Arizona: Jour. Geophys. Research, v. 80, no. 5, p. 765–775.

Cassinis, R. and Morgonovi, L., 1966, Significance and implications of shingling in refraction records: Geophys. Prospecting, v. 14, no. 4, p. 547–565.

Dutton, C. E., 1889, The Charleston earthquake of August 31, 1886: U.S. Geol. Survey, Ann. Rept. 9, 1887–1888, p. 203–528.

Sbar, M. L., and Sykes, L. R., 1973, Contemporary compressive stress and seismicity in eastern North America; an example of intraplate tectonics: Geol. Soc. America Bull., v. 84, no. 6, p. 1861–1881.

Spencer, T. W., 1965, Refraction along a layer: Geophysics, v. 30, no. 3, p. 369–388.

Stewart, D. M., Ballard, J. A., and Black, W. W., 1973, A seismic estimate of depth of Triassic Durham basin, North Carolina: Southeastern Geology, v. 15, no. 2, p. 93–103.

Wyllie, M. R. J., Gregory, A. R., and Gardner, L. W., 1956, Elastic wave velocities in heterogeneous and porous media: Geophysics, v. 21, no. 1, p. 41–70.

A Preliminary Shallow Crustal Model Between Columbia and Charleston, South Carolina, Determined from Quarry Blast Monitoring and Other Geophysical Data

By PRADEEP TALWANI

STUDIES RELATED TO THE CHARLESTON, SOUTH CAROLINA, EARTHQUAKE OF 1886—A PRELIMINARY REPORT

GEOLOGICAL SURVEY PROFESSIONAL PAPER 1028-M

CONTENTS

ILLUSTRATIONS

STUDIES RELATED TO THE CHARLESTON, SOUTH CAROLINA, EARTHQUAKE OF 1886—A PRELIMINARY REPORT

A PRELIMINARY SHALLOW CRUSTAL MODEL BETWEEN COLUMBIA AND CHARLESTON, SOUTH CAROINA, DETERMINED FROM QUARRY BLAST MONITORING AND OTHER GEOPHYSICAL DATA

By PRADEEP TALWANI [1]

ABSTRACT

To obtain the velocity model under the Coastal Plain of South Carolina, blasts at five quarries were monitored. The data, incorporated with other refraction and gravity data, suggest that the crustal model is extremely complicated. A Triassic(?) graben is inferred near Summerville, and its border faults may be associated with the seismicity observed in the Summerville-Charleston area.

INTRODUCTION

The 10-station South Carolina seismographic network went into operation in May 1974 (Tarr, this volume). To best use the data accumulated by this network for the location of hypocenters, we must first determine the subcrustal velocity structure. Data pertinent to the velocity structure of the Coastal Plain of South Carolina were obtained at five quarries. These data have been incorporated with other geophyhical data to obtain a preliminary crustal model between Columbia and Summerville.

This study was supported by U.S. Geological Survey Contract No. 14–08–0001–14553. I am grateful to my students, Donald Stevenson, David Amick, and Robert Van Nieuwenhuise, for their help in carrying out the fieldwork, and to the various quarry superintendents for their cooperation. I thank Hans Ackermann for allowing me to use some of his unpublished seismic refraction data. I also benefited from the discussions with A. C. Tarr of the U.S. Geological Survey and Prof. Donald T. Secor of the University of South Carolina. I also thank Dr. John Sumner of Lehigh University, who reviewed the manuscript and offered valuable comments.

[1] Dept. of Geol., University of South Carolina, Columbia, S.C. 29208.

DATA COLLECTION

Locations.—Most of the blast data were collected in the summers of 1975 and 1976. Of the five quarries monitored, two are in the crystalline rocks near the Fall Line, and the others are in the Coastal Plain (fig. 1). The Columbia quarry (COQ) and the Cayce quarry (CAQ) produce granite and are in the northwest quadrant of the study area. Berkeley quarry (BEQ) produces fine-grained clastic limestone of the Santee Limestone, and the Georgetown (GTQ) and Bass (BAQ) quarries produce indurated recrystallized limestone of the lower part of the Santee Limestone. BEQ, GTQ, and BAQ provided data from the southeast quadrant of the study area. Locations of various shots at BEQ and GTQ were determined from quarry maps (1 inch =200 feet). The location of each shot was determined to ±0.01′ (about 20 m) by tieing the shot point to a Coast and Geodetic Survey triangulation station. The blasts were monitored at remote station sites lying along the various refraction lines (fig. 1). The locations of stations within 6 km of the blast site were determined from the quarry map or from aerial photographs of the area surrounding the quarry (1 inch=800 feet). Thus, the accuracy of locating stations close to the blast site was ±0.02′ (±40 m). The locations of more distant stations were determined from 7.5′ topographic quadrangle maps or county maps, and the accuracy was ±100 m.

All remote stations were within 45 km of the blast site, as beyond that distance the blast could not be detected on portable seismographs.

Traveltime.—The origin times of all quarry blasts were obtained by recording the shot at the quarry

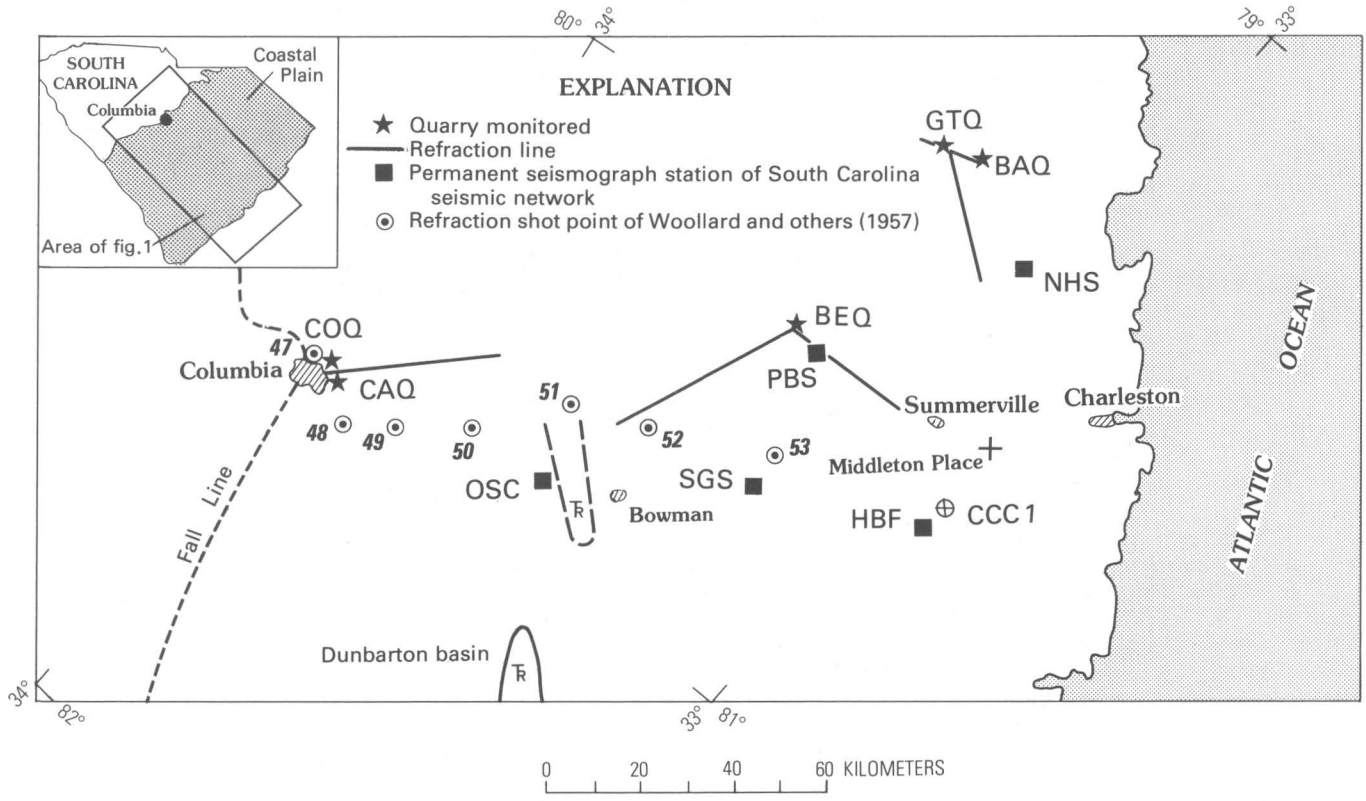

FIGURE 1.—Location map around Charleston, S.C., showing study area, quarries monitored, refraction lines, permanent seismograph stations of the South Carolina seismographic network, refraction shot points of Woollard and others (1957), and interpreted Triassic (Tr). The locations of the center of seismic activity, Middleton Place, and of the wells to the basalt at the Clubhouse Crossroads core hole 1 (CCC 1) are also shown. The town of Orangeburg is 6 km west of OSC. Abbreviations: COQ, Columbia quarry; CAQ, Cayce quarry; BEQ, Berkeley quarry; GTQ, Georgetown quarry; BAQ, Bass quarry. Seismograph station abbreviations, coordinates, and instrumentation are discussed by Carver, Turner, and Tarr (1977).

on a portable seismograph equipped with a paper speed of 300 mm/min. Origin times at quarry sites and the *P*- and *S*-wave arrival times on seismographs at remote stations were read to an accuracy of at least ± 0.02 s by using a low-power microscope. A WWVB time signal was recorded on all seismograms to obtain a uniform absolute time. Traveltimes from various blasts to stations of the seismographic network were also incorporated wherever they were available.

RESULTS

Velocity values from most traveltime data presented below were obtained by drawing an eyeball fit curve through the data. Local geology and the quality of the first arrivals were incorporated where a single line did not pass through all the data points. The velocity was also calculated by a method of least squares. The standard deviation and the coefficient of determination, r^2, were also determined by linear regression. The velocity values obtained by the two methods agree well, and the values obtained by eyeball fit were used in computing depths. The least square values are given in figure captions 2*C*–*F*.

The two quarries, located on either side of the Congaree River to the south of Columbia (COQ and CAQ), are about 1 km apart. The traveltime data for the Columbia blasts recorded in a southeast direction were plotted, and those for COQ and CAQ were grouped together (fig. 2*A*). The data suggest a *P*-wave velocity (v_P) of 6.0 km/s. This velocity is reasonable for crystalline basement, which outcrops near Columbia.

Figure 2*B* shows two possible interpretations of traveltime data for blasts at BEQ and recorded within 8 km in a northwest direction. In the first interpretation (*a*), the traveltimes for the near stations (within 1 km) and for the distant stations (near 5

km and 8 km) lie on a 3.65 km/s line. Both near stations lie in the Berkeley quarry, and 3.65 km/s probably represents the velocity of Santee Limestone. From borehole data north of Santee River (Alan-Jon Zupan, oral commun., 1977), Santee Limestone is known to be less than 100 m thick. Traveltime data from BEQ, in a northwest direction beyond 7 km, lie on 5.70 km/s curve (fig. 2*C*). A simple two-layer example of a 3.65-km/s overlying a 5.70-km/s layer would imply that the 3.65-km/s layer is 1.8 km thick. North of BEQ, Santee Limestone is known to overlie Black Mingo and Peedee Formations, which are a few hundred meters thick. Thus, a 3.65-km/s layer, if it exists, has to be younger than the Black Mingo Formation. In interpretation *a* (fig. 2*B*), data from a station 1.74 km distant were not incorporated. These data indicate a 2.2-km/s layer (interpretation *b*). In this latter interpretation, data from the two nearer stations have been neglected on the assumption that they represent the thin Santee Limestone, which has a higher *P*-wave velocity because of its greater induration. The sedimentary rocks, which have a *P*-wave velocity of 2.2 km/s, in turn overlie a 0.56-km-deep layer with a 5.70-km/s *P*-wave velocity. This depth, 0.56 km, appears to be more reasonable in view of a 5.5 km/s layer 0.5 km deep at Woollard's (1957) station 53 (fig. 1).

Figure 2*C* shows the preferred traveltime data for blasts at BEQ recorded in a northwest direction out to a distance of about 31 km. This profile lies almost completely on the mapped Santee Limestone (see, for example, the Coastal Plain geology taken from Cooke (1936) and incorporated on the gravity map on South Carolina (Talwani and others, 1975). If interpretation *b* from figure 2*B* is accepted, the 5.70-km/s layer is offset by 0.7 km, 5 km from BEQ. The postulation of a fault is based on data from a single station. If data from that station are neglected, the depth to the 5.70-km/s layer is 0.90 km. The *P*-wave velocity of 5.70 km/s suggests a basalt flow, and the implications thereof will be discussed later.

In recording blasts at BEQ to the south (fig. 2*D*) there are no data within 3 km. Assuming that the velocity of the near-surface material is 2.2 km/s, the calculated depth to the 5.2-km/s layer is 0.8 km. If we assume that the true *P*-wave velocity of this layer (basalt flow) is 5.70 km/s, then an apparent velocity of 5.2 km/s suggests a southerly dip of 2.3°.

Figure 2*E* shows the reversed profile between GTQ to the north of Santee River and BAQ to the south. Sedimentary rocks that have a *P*-wave velocity of 2.05 km/s overlie a 6.0 km/s layer (crystalline basement), which dips from a depth of 0.48 km below BEQ to 0.63 km below GTQ.

In figure 2*F*, two interpretations are presented for travel-time data for blasts at GTQ and BAQ recorded to the southwest. The data from the two quarries are grouped together in figure 2*F*. Two interpretations were made owing to the uncertainty resulting from a lack of data between 11 and 24 km. In interpretation *a*, a layer with an apparent velocity of 5.70 km/s. underlies a 2.0 km/s. sedimentary layer. The underlying layer is 0.57 km deep and dips 1° to the southwest. Alternatively, if we assume that a 6.0-km/s. layer underlies the sedimentary rocks (interpretation *b*), it is 0.57 km deep, and somewhere between 11 and 24 km from BAQ, it is downthrown by 0.64 km.

DISCUSSION

The quarry blast data presented above are sparse and somewhat inconclusive. However, by incorporating gravity, magnetic, and other seismic refraction data, some constraints can be applied and a preliminary interpretation made.

Figure 3*A* shows seismic refraction data of Woollard and others (1957). Only profiles at locations 48, 49, and 53 were reversed. A low velocity of 4.82 km/s. at location 51 together with an aeromagnetic low has been inferred by Daniels (1974) to indicate a possible Triassic basin. This basin lies to the northeast of the Dunbarton basin, where red beds of assumed Triassic age are known to occur in the subsurface (fig. 1) (Marine and Siple, 1974).

Data from Figures 2*A* and 2*C* were combined with those from figure 3*A* to obtain a schematic model along a line southeast from Columbia (fig. 3*B*).

Seismic refraction data obtained at BEQ (and recorded to the south) were insufficient to obtain a velocity model in the Summerville area. However, other refraction data are available in the area (Ackermann, this volume, and written commun.). These were combined with drill-hole data at Clubhouse Crossroads and the gravity map of the area to obtain a velocity model.

Figure 4 shows a part of the Bouguer anomaly map of South Carolina (Talwani and others, 1975). The location of the seismic refraction profiles from quarries, and those of Ackermann (unpub. data, and this volume) are also shown. BEQ and the Clubhouse Crossroads corehole 1 both lie on broad gravity highs, which are separated by an east-west gravity low. This gravity low coincides with a broad low seen on the aeromagnetic map of the area (Phillips, this volume). Unpublished refraction data from

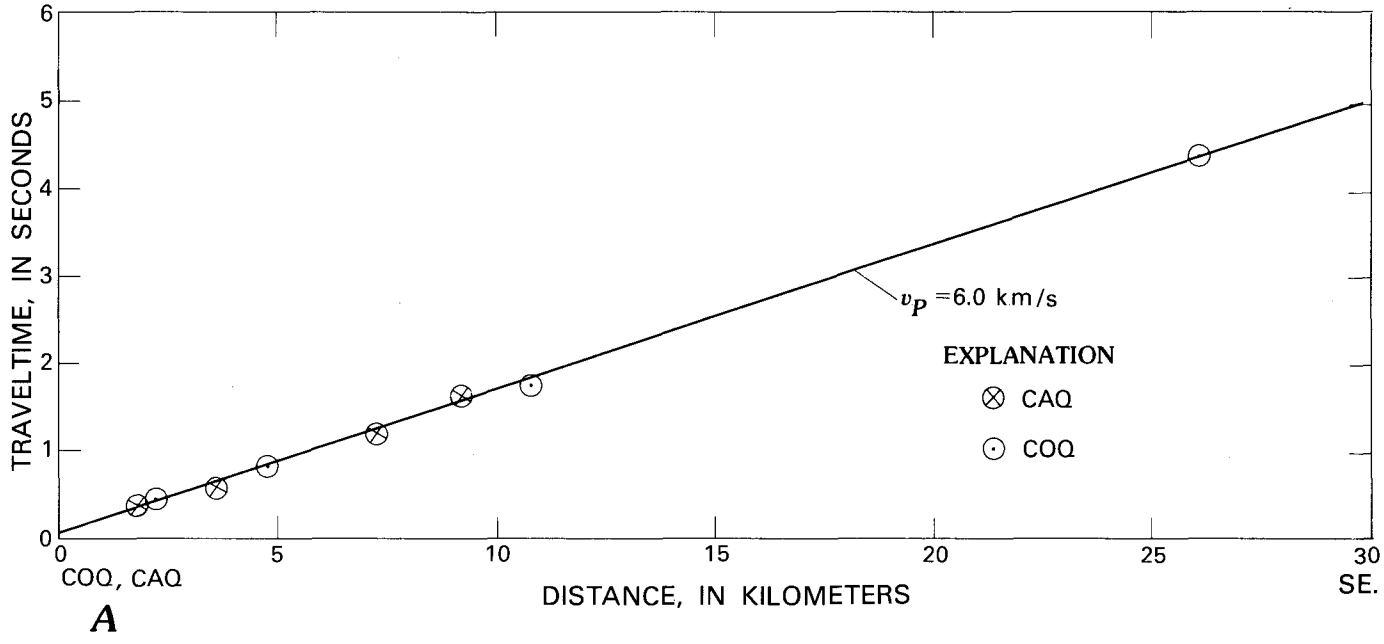

FIGURE 2.—Traveltime curves for quarry blasts in the Coastal Plain of South Carolina. *A*, Shots at Columbia (COQ and CAQ) recorded in a southeast direction.

Interstate (I), Knightsville (K) profiles (Ackermann, written commun.) and those at Middleton Place (MP), Clubhouse Crossroads (CC), County Line East (CLE) and Bees Ferry (BF) (Ackermann, this volume) were extrapolated to a north-south profile from BEQ (fig. 4). The direction of extrapolation was along strike of the structures suggested by the gravity contours. This profile passes through BEQ in the north, and through the eastern end of a gravity high to the south of Summerville.

Ackermann (this volume) noted that some seismic refractions were shingled. These were interpreted as being caused by a thin basalt flow, and the *P*-wave velocity was found to vary between 4.5 and 5.8 km/s.

Figure 5 shows the observed gravity profile and three proposed shallow crustal models. In making the gravity models, the density values used were those obtained at the Clubhouse Crossroads corehole 1: 2.1 g/cm^3 and 2.9 g/cm^3 for Tertiary and Upper Cretaceous sedimentary rocks and the basalt, respectively (Brenda Higgins, written commun.).

Below the sedimentary rocks that have v_P=2.0 −2.2 km/s., seismic data at BF and I indicated an absence of the 5.8 km/s. horizon, which had been observed at BEQ and CC. At CLE and K, a velocity of 5.0–5.4 km/s was obtained, and the refractions were associated with shingling. At Middleton Place (MP), the velocity decreased from 5.5 to 4.5 km/s. eastward. This is interpreted as the edge of the basalt flow. A 6.2 km/s. horizon (crystalline basement) was observed at BF, CLE, and MP.

The low-velocity, low-density sediments of the Coastal Plain are 600–950 m thick. If the standard Bouguer density of 2.67 g/cm^3 is used in reduction of gravity data, the contribution of these sediments is −20 mGal for a −0.6-g/cm^3 density contrast and an 800-m thickness. Since the Coastal Plain is only a few tens of meters above sea level, a normally compensated crust would have a slightly negative Bouguer anomaly associated with it. However, the Simple Bouguer gravity values in the area are positive, ranging from 0 to 10 mGal and indicating a thinned continental crust in this part of the Coastal Plain. To model the near-surface geology (to a depth of 2.5-3 km), a datum density value of 2.5 g/cm^3 rather than the standard 2.67 g/cm^3 was used. This has the effect of removing the regional gravity gradient due to a deep basement structure.

The gravity models were constrained by the depths obtained from refraction data (short thick lines, fig. 5). In the first model, a 500-m-thick basalt flow is assumed below CC, a sedimentary basin below I, and a basalt flow below BEQ. The basalt flow below CC is at least 100 million years old, and possibly as old as Triassic (Gottfried and others, this volume), which suggests that the sedimentary horizon (v_P =4.4 km/s) is older—possibly of Triassic age. A density of 2.4 g/cm^3 was used to model this horizon.

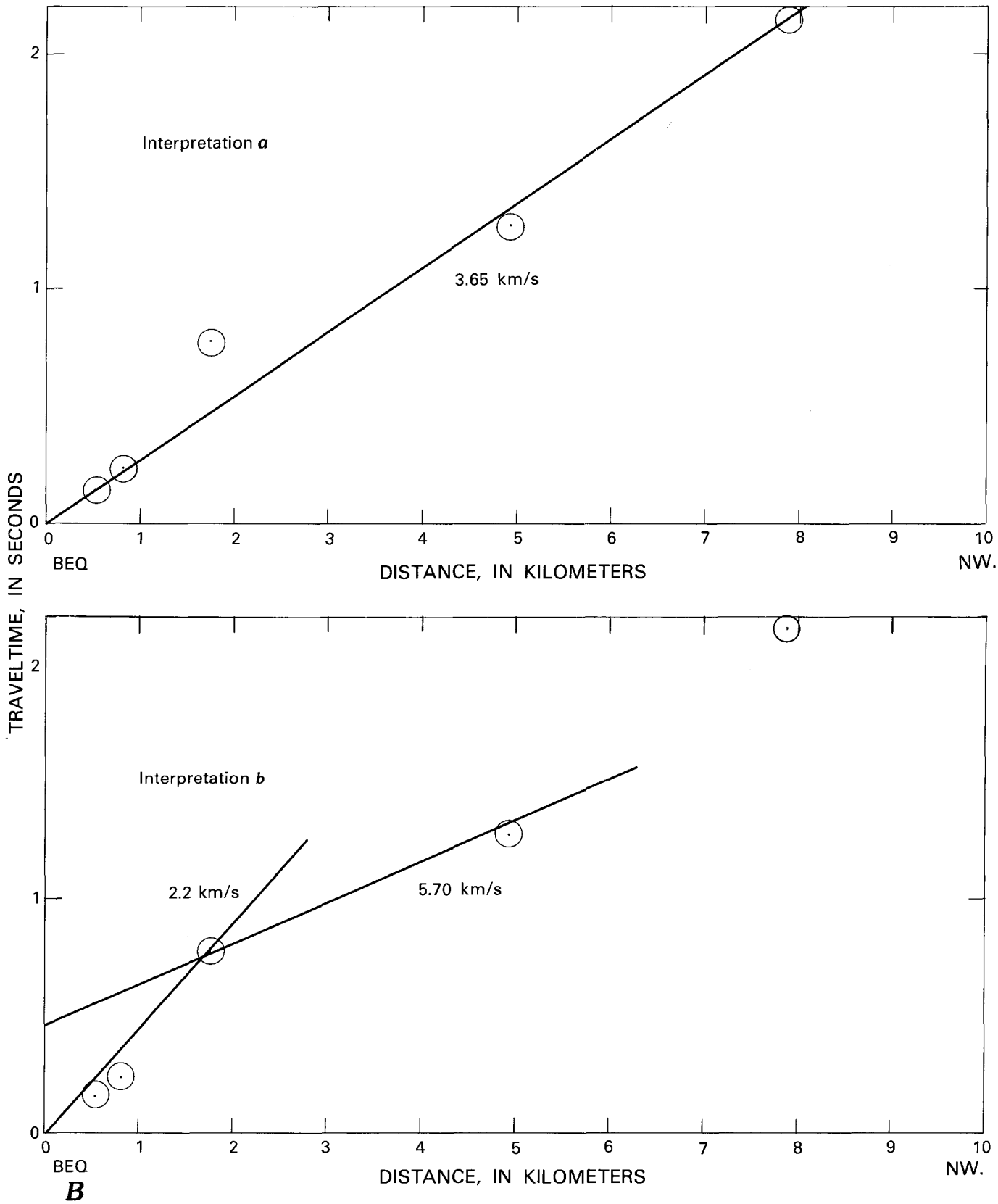

FIGURE 2.—Continued. *B*, Shots at BEQ recorded in a northwest direction within 8 km of the site—two possible interpretations (see text for discussion).

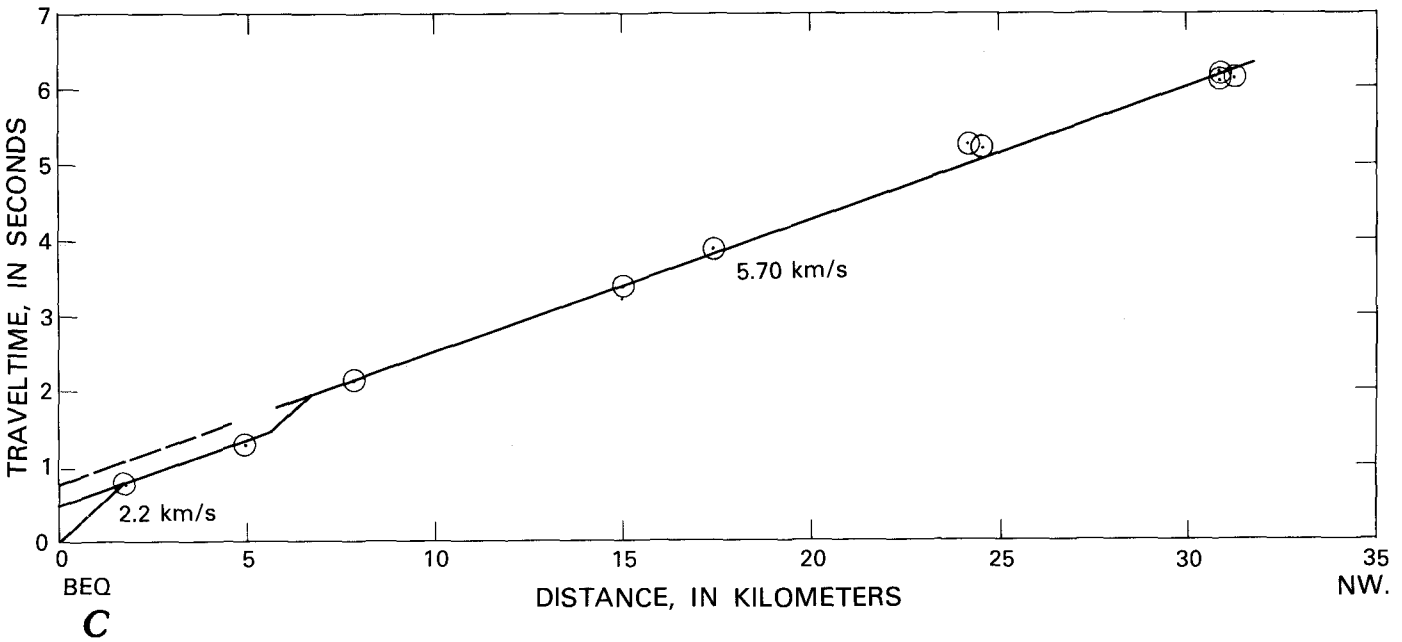

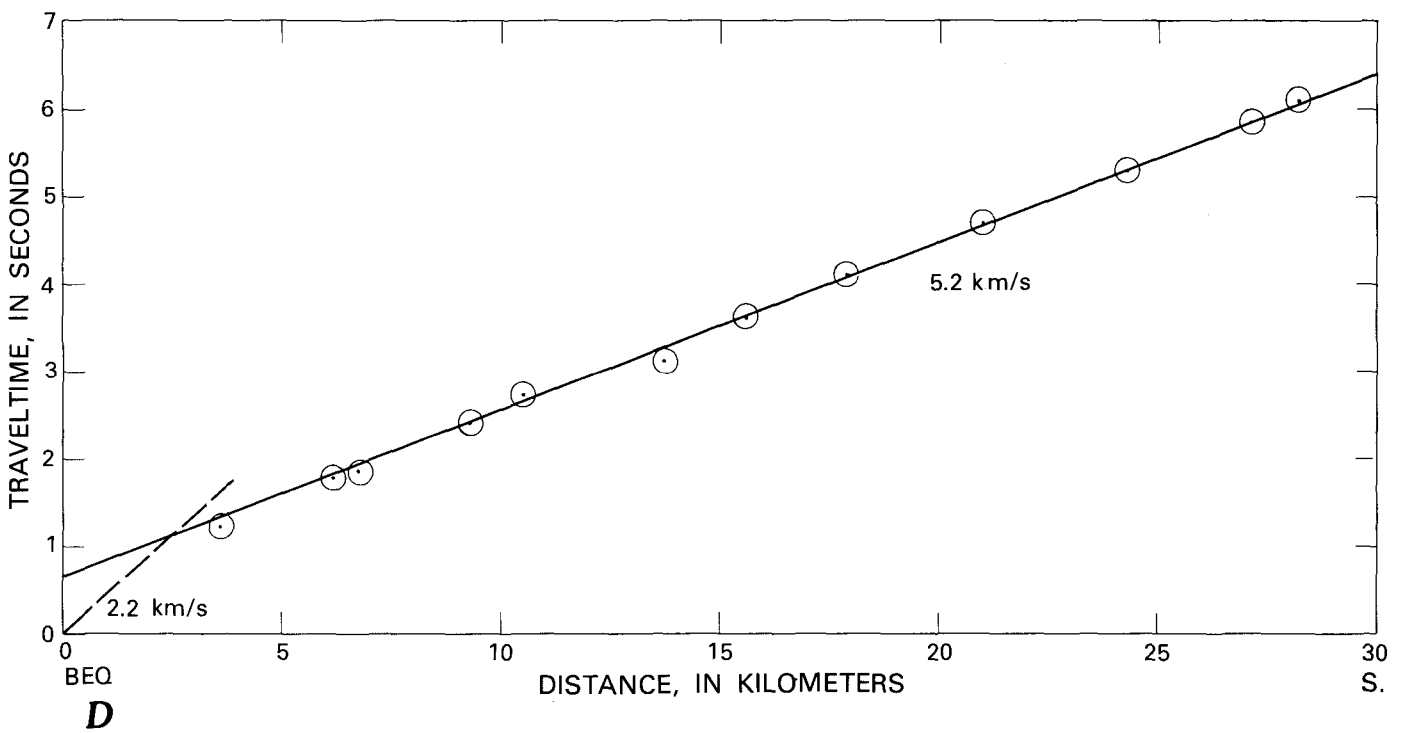

FIGURE 2.—Continued. *C*, Shots at BEQ recorded in a northwest direction for distances greater than 7 km from the site. Curve is projected to zero time at distances shorter than 7 km and shows that if interpretation *b* (fig. 2*B*) is accepted, faulting is suggested close to BEQ. Velocity obtained by eyeball fit (5.70 km/s) agrees well with that obtained by the method of least squares (5.68 km/s, standard deviation 0.18, and r^2=0.994). *D*, Shots at BEQ recorded to the south. Dashed line represents the assumed velocity of near-surface material. Velocity by eyeball fit (5.2 km/s) agrees with that obtained by method of least squares (5.07 km/s, standard deviation 0.06, and r^2=0.9985).

This value was used by Marine (1974) to model postulated Triassic rocks at Dunbarton basin. A graben is required to model the gravity low. The Bouguer anomaly due to a basalt flow (~500 m thick) below CC is insufficient to match the observed gravity anomaly.

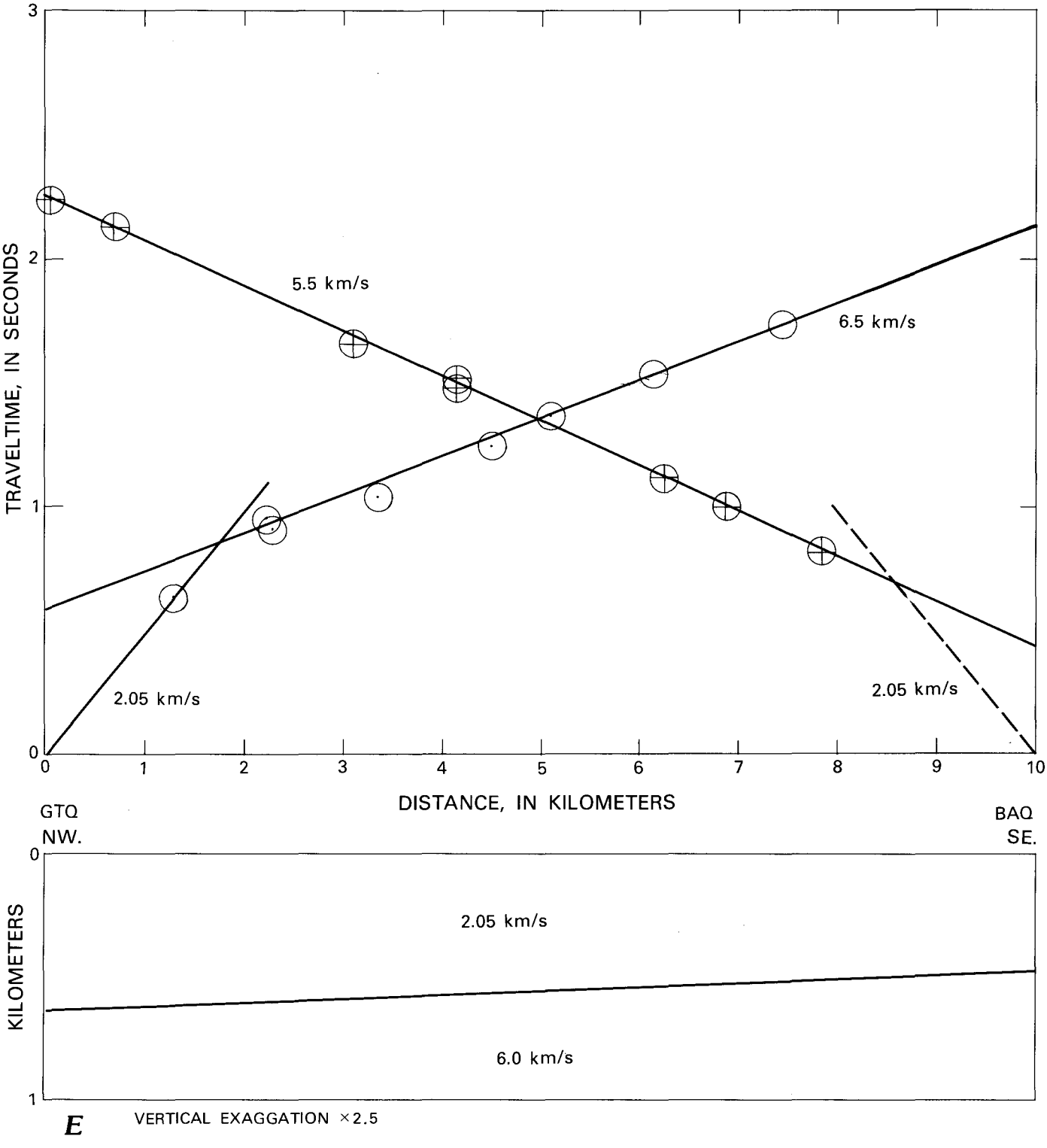

FIGURE 2.—Continued. *E*, Reversed refraction profile between blasts at GTQ and BAQ, as well as an interpretative model. Velocities by eyeball fit (6.5 km/s and 5.5 km/s) agree well with those obtained by method of least squares (6.29) km/s, standard deviation 0.26, r^2=0.992; and 5.49 km/s, standard deviation 0.07, r^2=0.999, respectively). The near-surface velocity of 2.05 km/s obtained at GTQ was also used at BAQ.

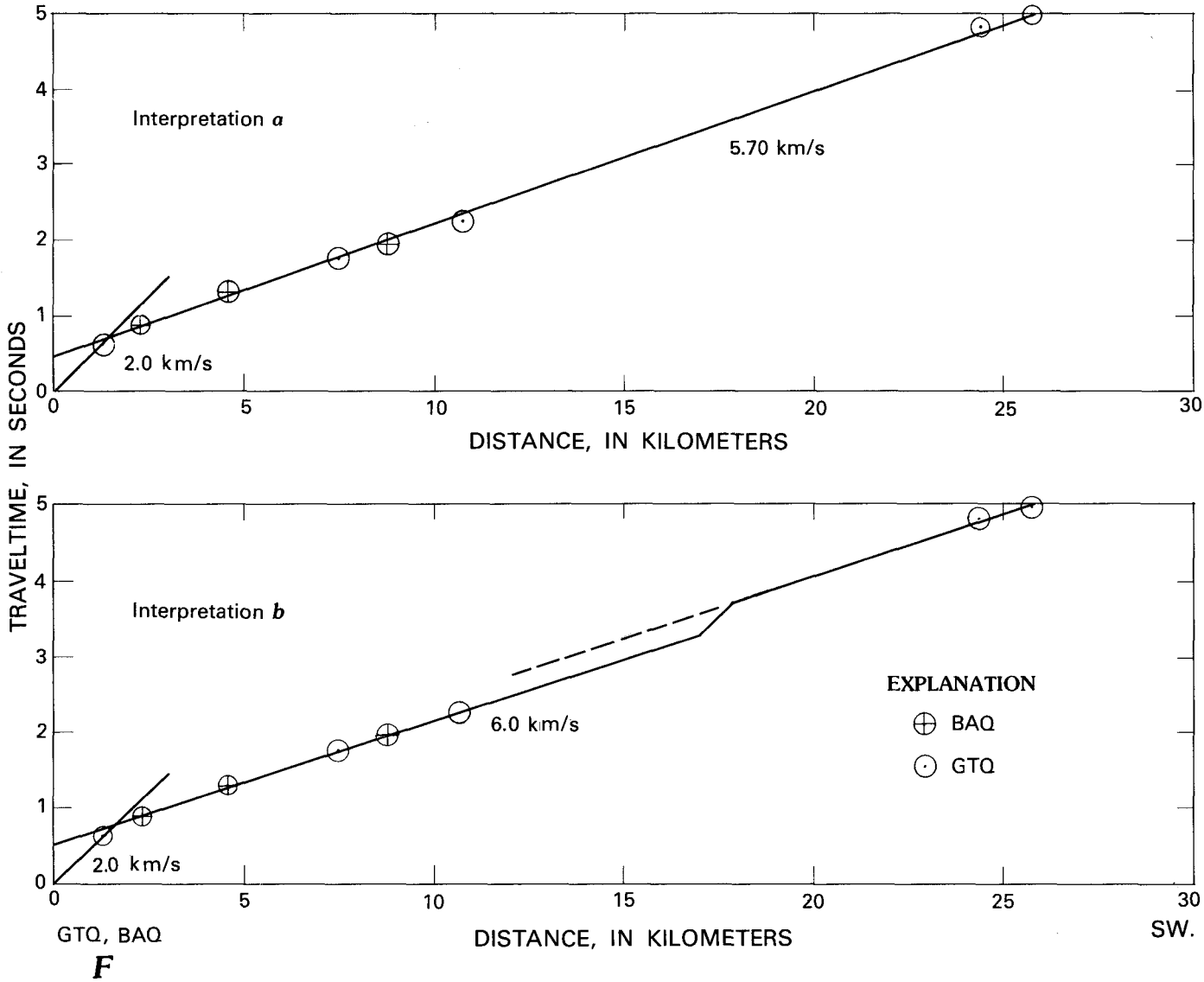

FIGURE 2.—Continued. *F*, Shots at GTQ and BAQ recorded in a southwest direction. Two interpretations are given. Velocity values obtained by eyeball fit (5.70 and 6.0 km/s agree with those obtained by the method of least squares (5.65 km/s, standard deviation 0.09, r^2=0.9988; and 6.12 km/s, standard deviation 0.12, r^2=0.9988, respectively).

In the second model, the basalt flow below CC is replaced by a broad volcanic plus having an umbrellalike flow at the top. The shingling of refractions and v_P<5.8 km/s observed at CLE, MP and K is interpreted to be due to thin basalt flows around the plug, whose stem, lying below CC, is associated with no shingling and a velocity of 5.8 km/s. BF and I lie outside the plug where the post-Cretaceous sedimentary rocks (v_P=2.0−2.2 km/s and underlain by Triassic sedimentary rocks (v_P=4.4 km/s). The crystalline basement (v_P=6.2 km/s) dips gently to the south and extends from BEQ to the south of BF, being interrupted by a volcanic plug at CC. The Bouguer anomaly associated with this model fits the observed data over the gravity highs on the ends of the profile but does not match the gravity low. To match the gravty low, a buried graben is required below I (model 3).

Thus, model 3 represents the preferred interpretation of the observed gravity data using constraints supplied by seismic refraction data and drilling. Some of the features of this model are:

a. A broad volcanic plug was punched into a broad Triassic basin.
b. The seismic velocity is 5.8 km/s in the stem of this plug, while on the flanks (associated with basalt flows) it decreases to 5.0 km/s and causes shingling of refractions.

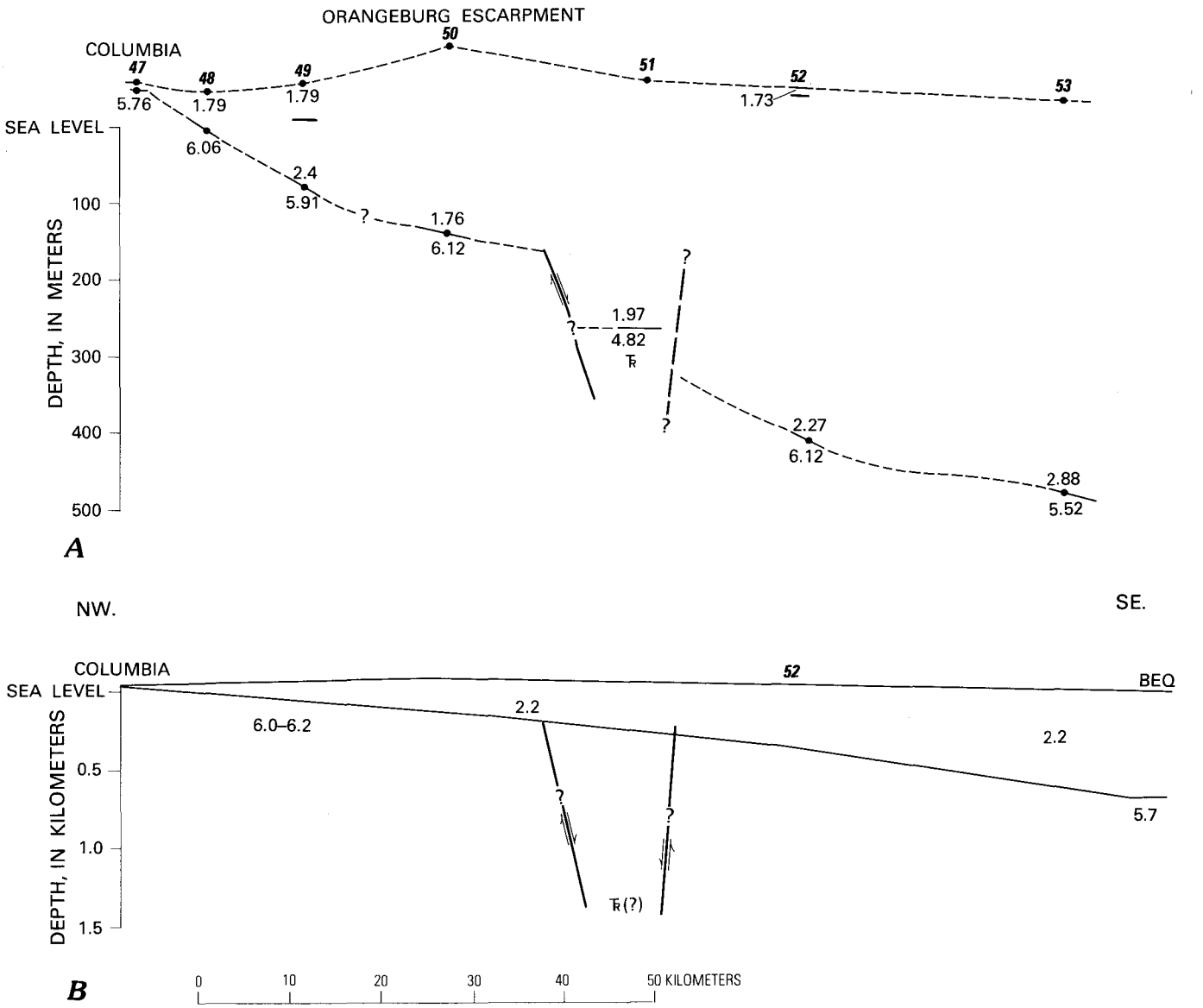

FIGURE 3.—Velocity models southeast of Columbia. *A*, Model between Columbia and location 53 of Woollard and others (1957). The numbers 47–53 are the refraction locations (see fig. 1), and the others are the observed seismic velocities (km/s). *B*, Interpreted model along a line southeast from Columbia through location 52 to the Berkeley quarry. Seismic velocity values in km/s are incorporated.

c. The broad lows on the aeromagnetic and gravity maps are due to a broad Triassic basin below Summerville.

d. Middleton Place lies on top of the southern flank of the graben, and the observed seismicity there may be associated with the border faults of this graben.

e. The gravity high at BEQ is associated with a shallow crystalline basement having a thin basalt cap. (This is suggested by an absence of the basalt on the southwest profile from GTQ fig. 4).

These results are preliminary, and this summer (1977) H. D. Ackermann and I will collect more data to test the model.

REFERENCES CITED

Carver, David, Turner, L. M., and Tarr, A. C., 1977, South Carolina seismological data report, May 1974-June 1975: U.S. Geo. Survey open-file report 77–429, 66 p.

Cooke, C. W., 1936, Geology of the Coastal Plain of South Carolina: U.S. Geol. Survey Bull. 867, 196 p.

Daniels, D. L., 1974, Geologic interpretation of geophysical maps, central Savannah River area, South Carolina and Georgia: U.S. Geol. Survey Geophys. Inv. Map GP–893 [1975].

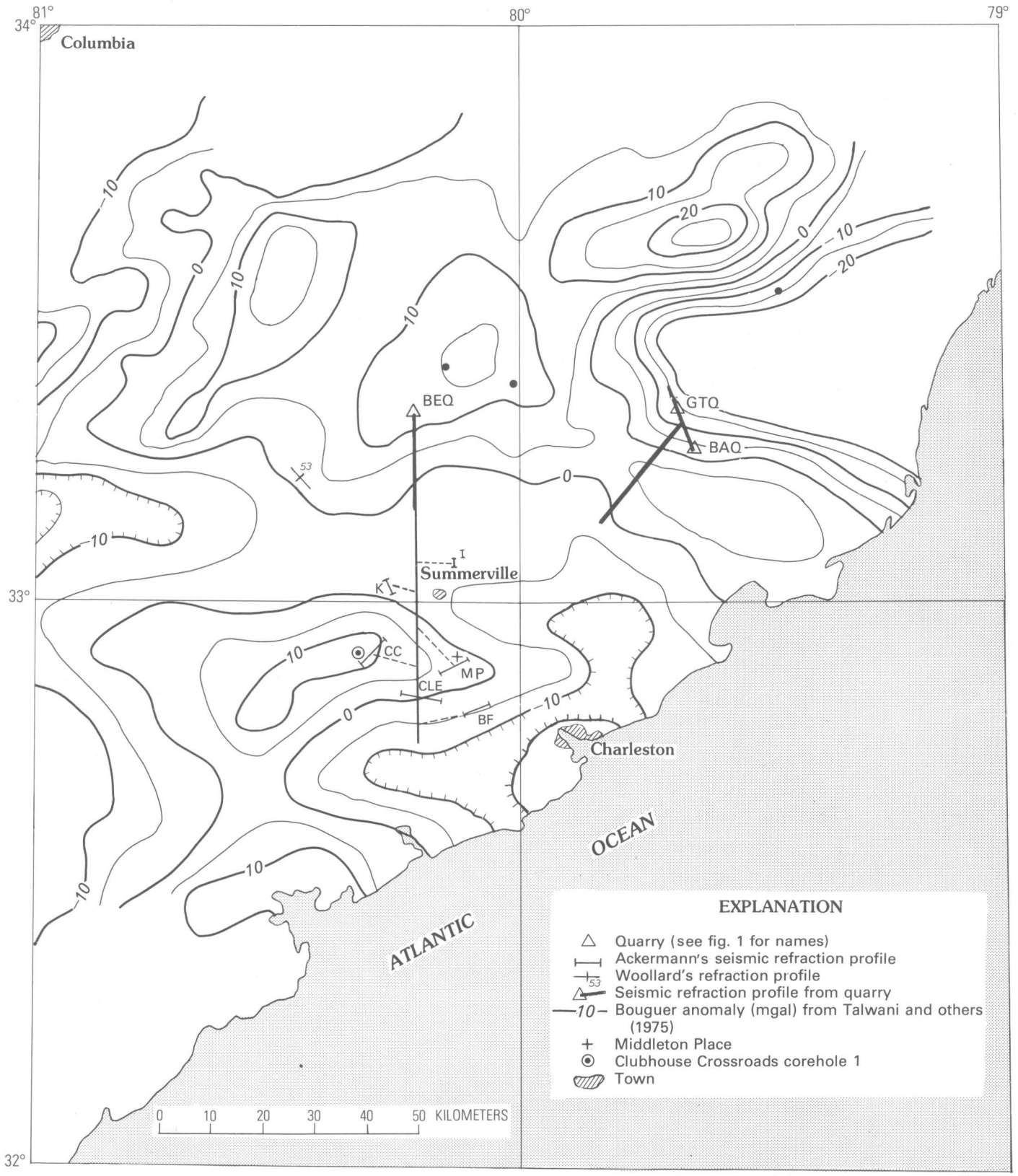

FIGURE 4.—Simple Bouguer anomaly map (modified from Talwani and others, 1975) of the area around Charleston, S.C., showing the location of refraction data from Ackermann (this volume and written commun.). Location of a north-south profile from BEQ is also shown. This profile was extrapolated from unpublished refraction data from Interstate (I) and Knightsville (K) profiles (Ackermann, written commun.), as well as profiles at Middleton Place (MP), Clubhouse Crossroads (CC), County Line East (CLE), and Bees Ferry (BF) (Ackermann, this volume). The direction of extrap-

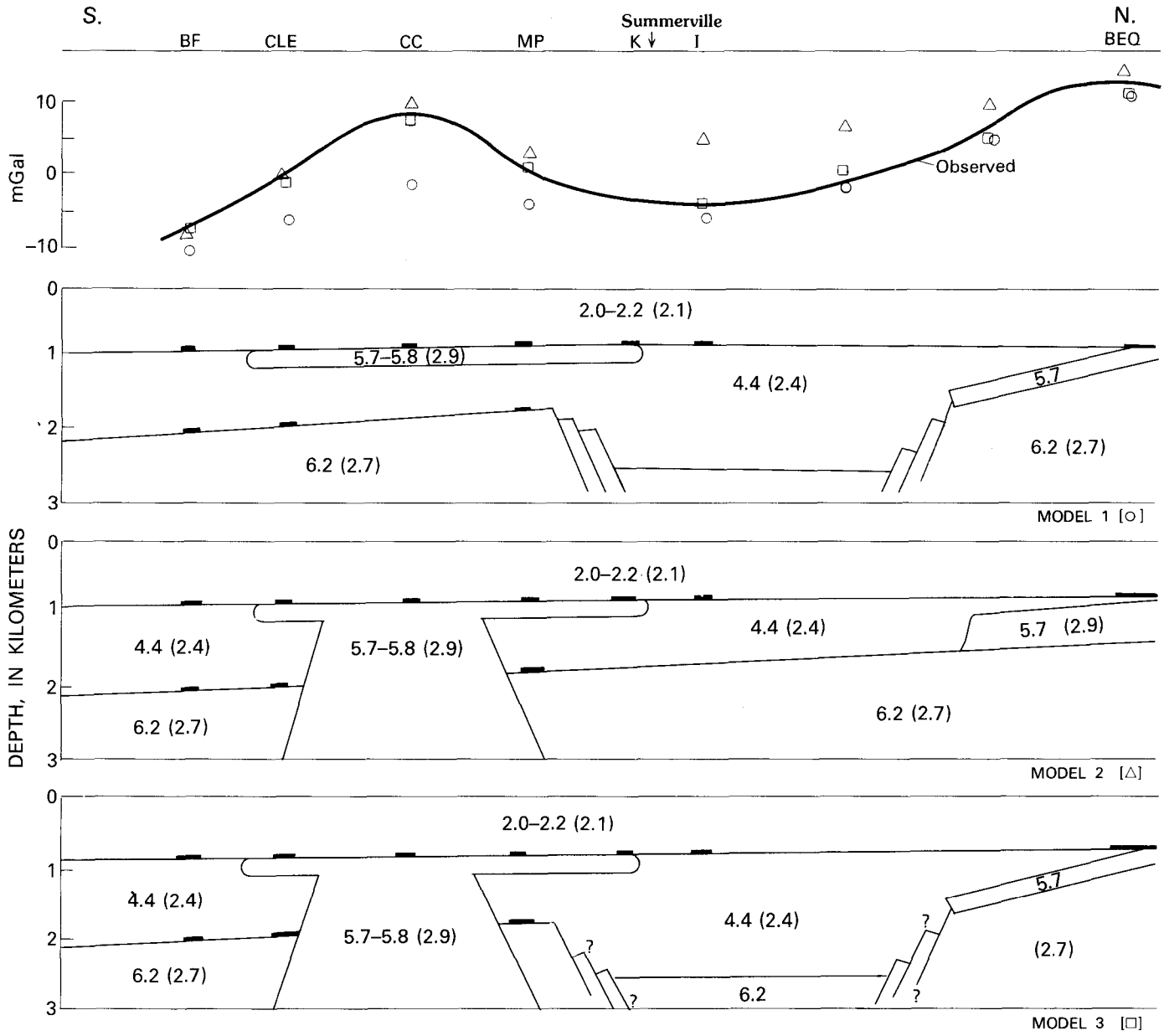

FIGURE 5.—Observed gravity profile and three interpretative shallow crustal models. The *P*-wave velocities in km/s of the Tertiary and Upper Cretaceous sedimentary rocks, Triassic(?) sedimentary rocks, basalt, and crystalline basement are, respectively: 2.0–2.2, 4.4, 5.7–5.8, and 6.2. The corresponding density values (in parentheses) are 2.1, 2.4, 2.9 and 2.7 g/cm^3. Computed gravity due to model 1 (circles), model 2 (triangles), and model 3 (squares) is also shown along with the observed gravity profile. Locations such as BF and, CLE, extrapolated to the north-south profile, are shown in figure 4. The short thick lines at velocity boundaries show depths obtained from refraction data.

Marine, I. W., 1974, Geohydrology of buried Triassic basin at Savannah River plant, South Carolina: Am. Assoc. Petroleum Geologists Bull., v. 58, no. 9, p. 1825–1837.

Marine, I. W., and Siple, G. E., 1974, Buried Triassic basin in the central Savannah River area, South Carolina and Georgia: Geol. Soc. America Bull., v. 85, no. 2, p. 311–320.

Talwani, P., Long, L. T., and Bridges, S. R., 1975, Simple Bouguer anomaly map of South Carolina: South Carolina Div. Geology Map Ser. MS–21.

Woollard, G. P., Bonini, W. E., and Meyer, R. P., 1957, A seismic refraction study of the subsurface geology of the Atlantic Coastal Plain and Continental Shelf between Virginia and Florida: Wisconsin Univ., Dept. Geology Geophys. Sec., 128 p.

Electric and Electromagnetic Soundings Near Charleston, South Carolina— A Preliminary Report

By DAVID L. CAMPBELL

STUDIES RELATED TO THE CHARLESTON, SOUTH CAROLINA, EARTHQUAKE OF 1886—A PRELIMINARY REPORT

GEOLOGICAL SURVEY PROFESSIONAL PAPER 1028-N

CONTENTS

ILLUSTRATIONS

TABLE

ELECTRIC AND ELECTROMAGNETIC SOUNDINGS NEAR CHARLESTON, SOUTH CAROLINA—A PRELIMINARY REPORT

By DAVID L. CAMPBELL

ABSTRACT

In an attempt to outline structural features which may bear on earthquake activity near Charleston, S. C., the U.S. Geological Survey has completed 9 Schlumberger d.c. resistivity soundings and 18 audio-frequency magnetotelluric (AMT) soundings in the region. Typical soundings show up to 60 m of surface sediments of variable resistivity, underlain by 100–250 m of 15–25 ohm-m material and 500–1,000 m of 4–10 ohm-m material.

The resistivity soundings failed to detect a basalt (Cretaceous or older) encountered at 750 m depth in U.S. Geological Survey Clubhouse Crossroads corehole 1. Drilling had been stopped after penetrating 42 m into this basalt. We now estimate this flow to be less than 75 m thick; it is underlain by low-resistivity material. Interpretation of the soundings indicates that the depth to high-resistivity electric basement near the corehole is approximately 1,300 m.

The AMT data outline a higher resistivity zone approximately 11 km wide, trending northeast-southwest, roughly corresponding to the higher isoseismal region of the 1886 earthquake. This zone seems to be bordered on the northwest by a lineament interpreted by Long and Champion in 1975, on the basis of gravity, to represent a steeply dipping fault with the southeast side downthrown. Three d.c. soundings over this zone, however, show shallower electric basement (around 900 m) than those outside it. If this basement represents a thickened version of the Cretaceous(?) basalt encountered in the corehole, some 150 m of vertical displacement would be indicated along this fault since Cretaceous time.

BACKGROUND

On August 31, 1886, Charleston, S.C., was shaken by a large earthquake which was felt throughout the eastern United States. Dutton (1889) studied this earthquake, finding maximum isoseismals along an elongated northeast-trending region between Charleston and the town of Summerville, which is about 35 km inland. The seismicity of South Carolina has been studied by Bollinger (1972), who finds historical earthquakes occurring in a northwest-trending band across South Carolina through Charleston and Summerville, roughly perpendicular to the coast and the Appalachian Mountains. Tarr (this volume) reports that a magnitude 3.8 earthquake occurred November 22, 1974, and 15 km west of Charleston, at a depth of 4.1 km. The focal mechanism of this earthquake was well determined and involved either a reverse fault or a thrust that strikes N. 42° W. Thus the scene is set: earthquakes seem to occur at shallow depths in a northwest-trending belt which passes under Charleston, but a northeast-trending feature, perhaps only in the shallow subsurface between Charleston and Summerville, transmitted and focused the shaking of the 1886 quake.

In the winter of 1975, the U.S. Geological Survey drilled a deep corehole near Clubhouse Crossroads, 24 km southwest of Summerville. This corehole (Clubhouse Crossroads corehole 1) was located on an aeromagnetic and gravity high; geophysical analysis predicted a mafic basement at about 1,300 m depth. Instead, at least two successive basalt flows were encountered, beginning at 750 m depth. The core had penetrated 42 m into these basalts before the core barrel became wedged in the hole and the hole was abandoned. Gottfried and others (this volume) reports that K–Ar ages of 94.8±4.2 m.y. and 109±4 m.y. for the basalt must be considered minimum ages because geochemical studies indicate that all samples are altered somewhat. The K–Ar ages are consistent, however, with a Late Cretaceous age for the overlying Cape Fear Formation (Hazel and others, this volume).

Figure 1 shows an electric log (microlaterolog) of Clubhouse Crossroads corehole 1, with a tentative stratigraphic description by Gohn and others (this

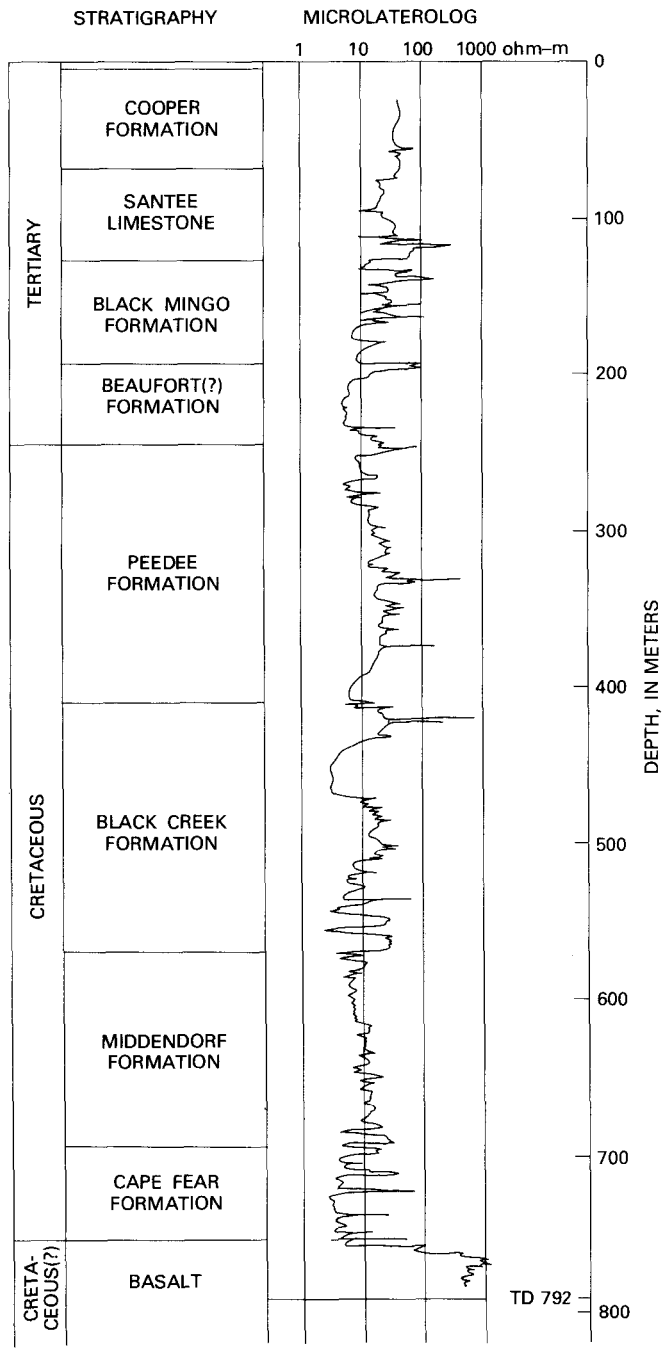

FIGURE 1.—Sketch of electric microlaterolog of Clubhouse Crossroads corehole 1 near Clubhouse Crossroads, S. C. Also shown is a tentative stratigraphic identification by Gohn and others (this volume). TD, total depth.

volume). In general, the logged resistivities do not seem particularly indicative of lithologic or stratigraphic boundaries. An exception is the thin 80 ohm-m zone between 116 and 126 m in depth, which corresponds to the tight calcareous sands at the base of the Santee Limestone. Below this zone, resistivities vary between 2 and 20 ohm-m throughout the sedimentary section. The interface between freshwater and saltwater should be no deeper than 220 m at this location, but no specific resistivity drop on the log is identified as due to this cause. The microlaterolog shows a resistivity of 600 ohm-m for the basalt at the bottom of the corehole.

In June 1975, the U.S. Geological Survey completed further geophysical work in the Charleston area, including 6 refraction seismic spreads, 18 audio-frequency magnetotelluric (AMT) resistivity soundings, and 9 Schlumberger d.c. vertical electric soundings (VES). The results of the refraction seismic work are reported by Ackerman (this volume), and this paper discusses the resistivity results. The locations of the VES and AMT soundings are shown on figure 2.

This study has been funded by the U.S. Nuclear Regulatory Commission, Office of Nuclear Regulatory Research, Agreement No. AT(49–25)–1000. Charles Tippens and Harold Kaufmann made the AMT soundings.

The material in this report was presented orally March 26, 1976, at the Combined Meeting of the Northeastern–Southeastern Sections of the Geological Society of America, at Arlington, Va.

AUDIO-FREQUENCY MAGNETOTELLURIC SOUNDINGS

A general description of audio-frequency magnetotelluric (AMT) techniques and theory may be found in Chapter IV of Keller and Frischknecht (1966). Each AMT measurement described here yielded 11 apparent resistivity values for a given site, each value corresponding to one of 11 different frequencies in the band from 7.5 Hz to 18.6 Hz. Schematically, one may regard each apparent resistivity value as a weighted average of true resistivities in the earth below that site, with successively lower frequencies weighting successively deeper resistivities more heavily. In the Charleston area, near-surface resistivities were too low for very deep penetration of audio-frequency electromagnetic waves, so that negligible weights resulted at even the lowest AMT frequency for depths greater than about 700 m.

The equipment used in the Charleston area received electromagnetic waves broadcast by the lightning strokes in thunderstorms. Ideally, the equipment should be oriented to measure the maximum

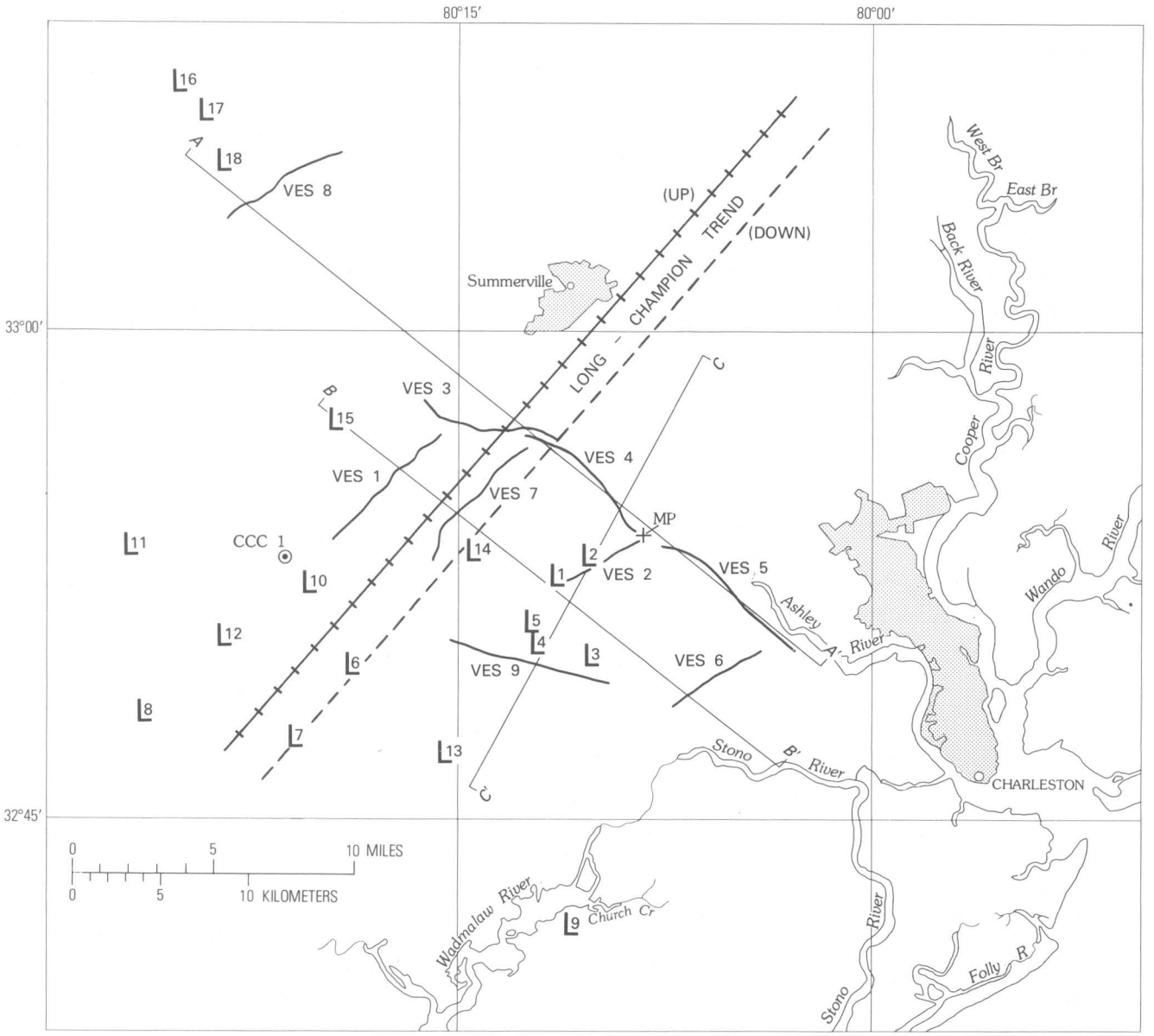

FIGURE 2.—Map showing locations of vertical electric soundings (VES) (heavy lines) and audio-frequency magnetotelluric (AMT) resistivity soundings (heavy L's) described in this report. Also shown are the locations of Clubhouse Crossroads corehole 1 (CCC 1), the historical plantation Middleton Place (MP), and section lines *A–A′*, *B–B′*, and *C–C′* (figs. 5, 6, and 7). The broken line indicates a trend which Long and Champion (this volume) picked on the basis of gravity to represent a basement fault with the southeast side dropped 0.65 km. In the present study we prefer that Long and Champion's line be shifted somewhat to the position indicated by heavy railroad bars.

horizontal electric field [1] at each frequency; in practice, however, the direction to the particular storm(s) in progress is unknown, and therefore the direction of maximum field is unknown. Therefore, two electric fields are measured, in north-south and east-west directions, and later combined in a way which varies with the interpreter. According to Stodt (oral commun., 1975), this azimuthal uncertainty can give rise to a scatter of as much as an order of magnitude in the derived apparent resistivity values. Other problems with AMT data involve changes in relative calibrations from frequency to frequency due to drift in the electronic gear, contamination by cultural noise, and near field effects due to very local storms (in Charleston

[1] Magnetotelluric technique actually involves simultaneous measurement of horizontal magnetic field, too, in a direction perpendicular to that of the electric field. In practice, however the electrical field is of chief concern to us, as it is found to vary in magnitude much more than the magnetic field.

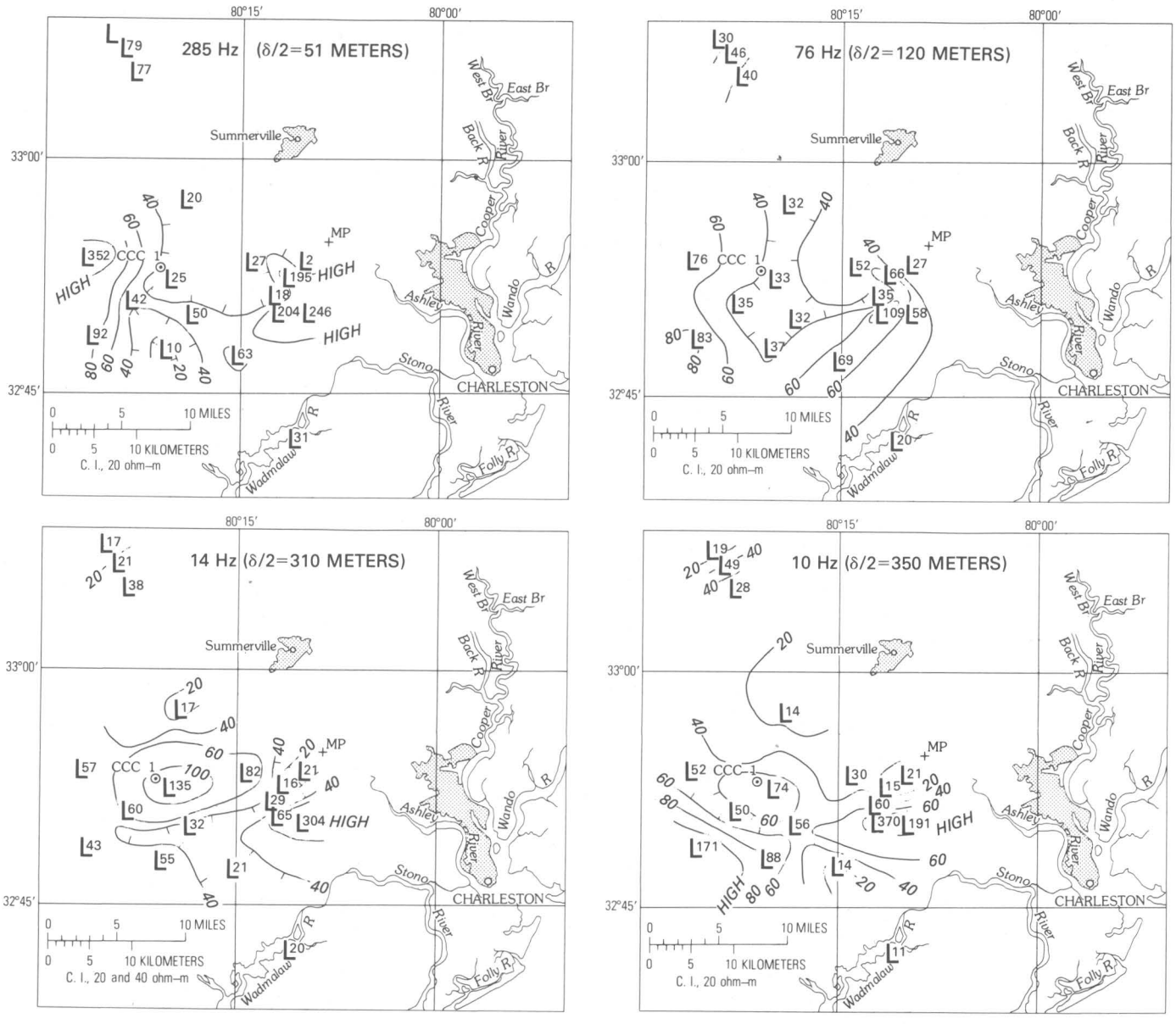

FIGURE 3.—Hand-contoured maps of AMT apparent resistivities at six frequencies for north-south oriented E (electrical)-field. Each L represents a station, and the number in the L gives observed apparent resistivity in ohm-meters at that frequency and location. Here δ equals skin depth in 20 ohm-m material; $\delta/2$ values are given to indicate roughly the depth to which each map applies. Contours are schematic; note that the contour interval (C.I.) varies from map to map. MP is Middleton Place, and CCC 1 is Clubhouse Crossroads corehole 1.

in June, such storms were often visible on the horizon).

Figures 3 and 4 are contour maps of apparent resistivities at the six lowest AMT frequencies for north-south and east-west measurements respectively. For the reasons given above, the exact apparent resistivity values shown are not considered significant, though general magnitudes and trends may be of interest. A representative depth is given on each map, equal to half the skin depth δ for a uniform halfspace of resistivity 20 ohm-m, a fair average for the Charleston area near-surface. Such values are meant to be only approximate, given to show roughly the depth to which each map applies; they have no rigorous meaning.

We make the following generalizations about figures 3 and 4:

1. On any given map the north-south values are usually higher than the east-west ones. This is probably an artifact of geometrical direc-

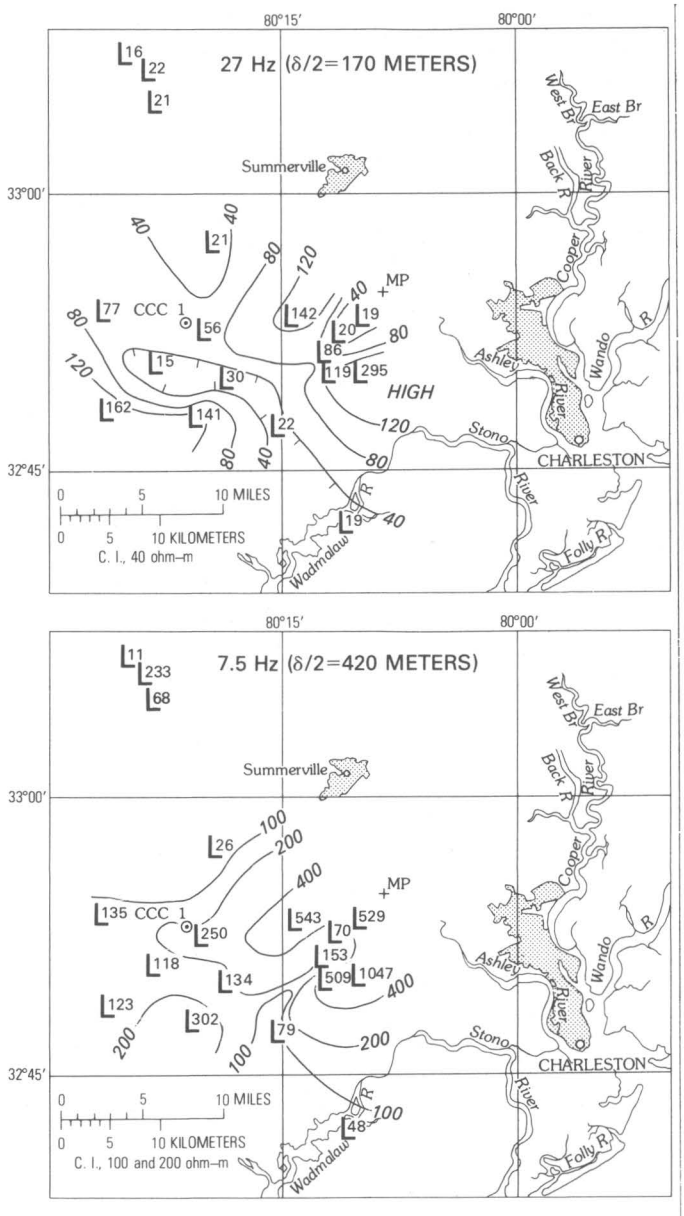

FIGURE 3.—Continued.

tion to dominant nearby storm activity (See Goldstein and Strangway, 1975), but conceivably could indicate east-west trends in near-surface lithologies. (Electric current usually flows more readily along layers than across them, so that the lower resistivity direction is along the layers.)

2. The contours on the two shallower maps (285 and 76 Hz) appear to trend generally north-south. The contours on the four deeper maps (27, 14, 10, and 7.5 Hz) appear to trend generally northeast, especially in the vicinity of Middleton Place. A change in orientation of geologic grain of the area below about 150 m depth therefore may be indicated. We may expect to find northeast trends in the deep structure near Middleton Place.
3. The dominantly northeast-trending pattern seems to be crossed in the southwestern part of the map by a single, constant low-resistivity zone. The uniformly high apparent resistivity values found on AMT soundings 3 and 8 (locations shown on fig. 2) may be due to cultural and (or) instrumental difficulties at those two sites.

There are various reasons for focusing on the northeast-trending feature indicated in figures 3 and 4. First, Dutton's isoseismals were elongated to the northeast in precisely this area, so that we may be picking up the geological structure responsible for this effect. Second, this feature is roughly parallel to and bounded on the northwest by a line picked by Long and Champion (this volume) on the basis of gravity to represent a steeply dipping vertical fault. Third, certain characteristics of the interpreted VES (discussed next), as well as the refraction seismic interpretations (Ackerman, this volume), may be explained by postulating such a northeast-trending feature.

VERTICAL ELECTRIC SOUNDINGS

A general description of Schlumberger vertical electric sounding (VES) technique and theory may be found in Zohdy, Eaton, and Mabey (1974). Near Charleston we worked along existing roads, placing as much as 10 km of wire on the ground in order to get the necessary 1½ km depth penetration. The field data were processed according to standard U.S. Geological Survey procedure—curve segments from different potential-electrode spacings were shifted to form a single continuous curve, this curve was smoothed by splining and sampled at uniform intervals, and the sampled points then inverted by automatic computer to give resistivity layering versus depth (Zohdy and others, 1973; Zohdy, 1974a; and Zohdy, 1975). This layer model was then simplified using the Dar Zarrouk technique (Zohdy, 1974b) to give the most conservative solution (that with fewest layers) which would still fit the (smoothed) field data. In this way, spurious apparent layers due to noise in the field data were suppressed. At the same time, however, certain thin but probably real layers such as the 80 ohm-m base of the Santee Limestone were also suppressed. To the extent allowed by the field data, the solutions for adjacent soundings used similar resistivities at similar depths, and all these values were made to correspond

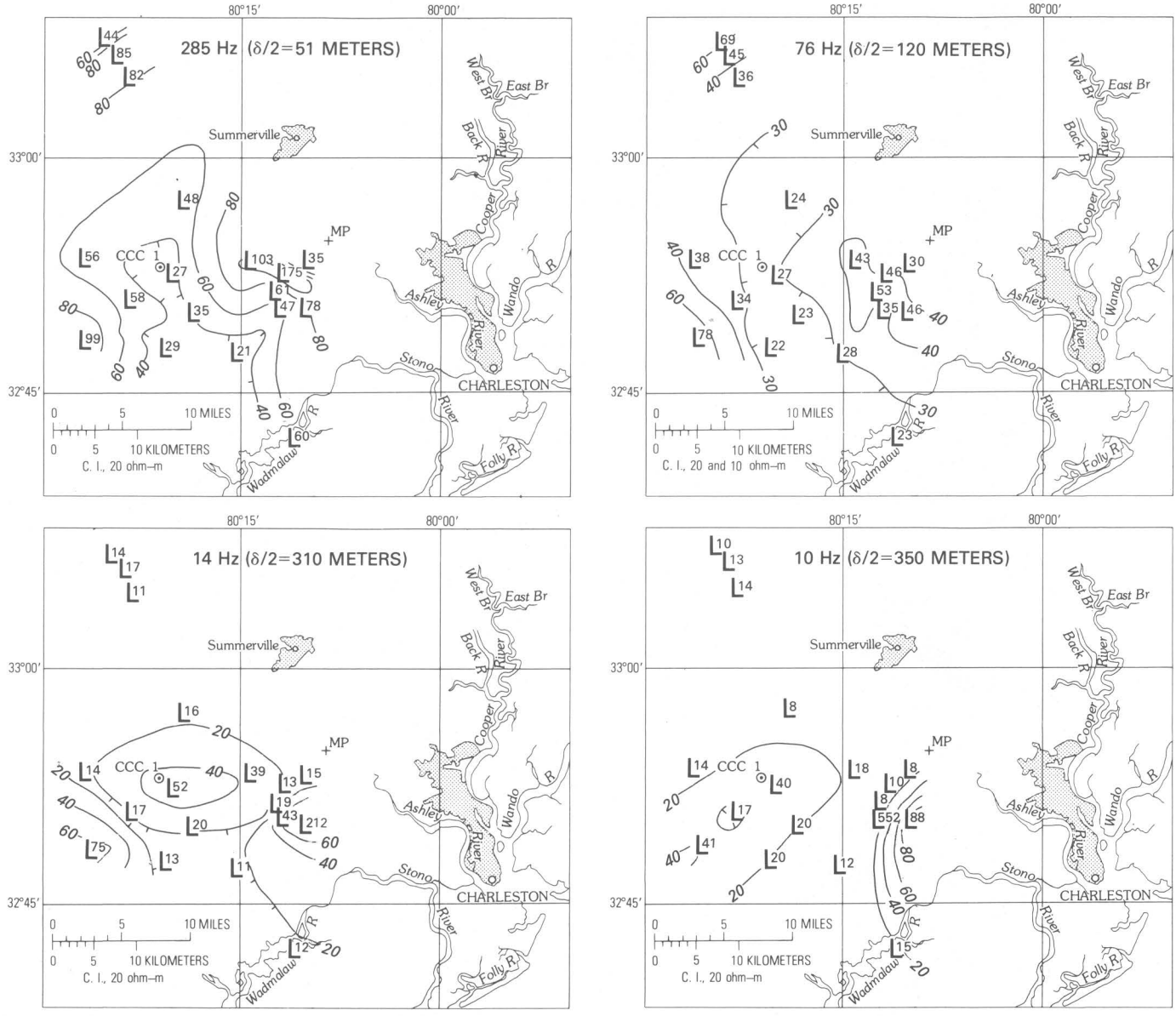

FIGURE 4.—Hand-contoured maps of AMT apparent resistivities at six frequencies for east-west oriented E-field. Each L represents a station, and the number in the L gives observed apparent resistivity in ohm-meters at that frequency and location. Here δ equals skin depth in 20 ohm-m material; δ/2 values are given to indicate roughly the depth to which each map applies. Contours are schematic, and the contour interval (C.I.) varies from map to map. MP is Middleton Place, and CCC 1 is Clubhouse Crossroads corehole 1.

in a general way with the resistivities seen on Clubhouse Crossroads corehole 1 well log. Depths were not specified in any way, however; all were determined solely by the interpretation scheme. Electric basement was assumed to have a resistivity of 200 ohm-m everywhere. This value is arbitrary. The field data indicate only that basement resistivity is high with respect to that of the overlying sediments (more than 100 ohm-m) but do not give its exact value. The poor resolution of this parameter is not serious, giving a probable uncertainty in depth to basement of the order of 10 percent.

Interpreted solutions for the nine VES are given in table 1. With the exceptions of VES 4 and VES 6, all depths are thought to have an uncertainty of 10 percent or less. Owing to severe contamination of the raw data by cultural noise, the entire solution for VES 6 and the depth to electric basement at VES 4 are thought to be good to only 20 percent. Resistivities shown are averages in the Dar

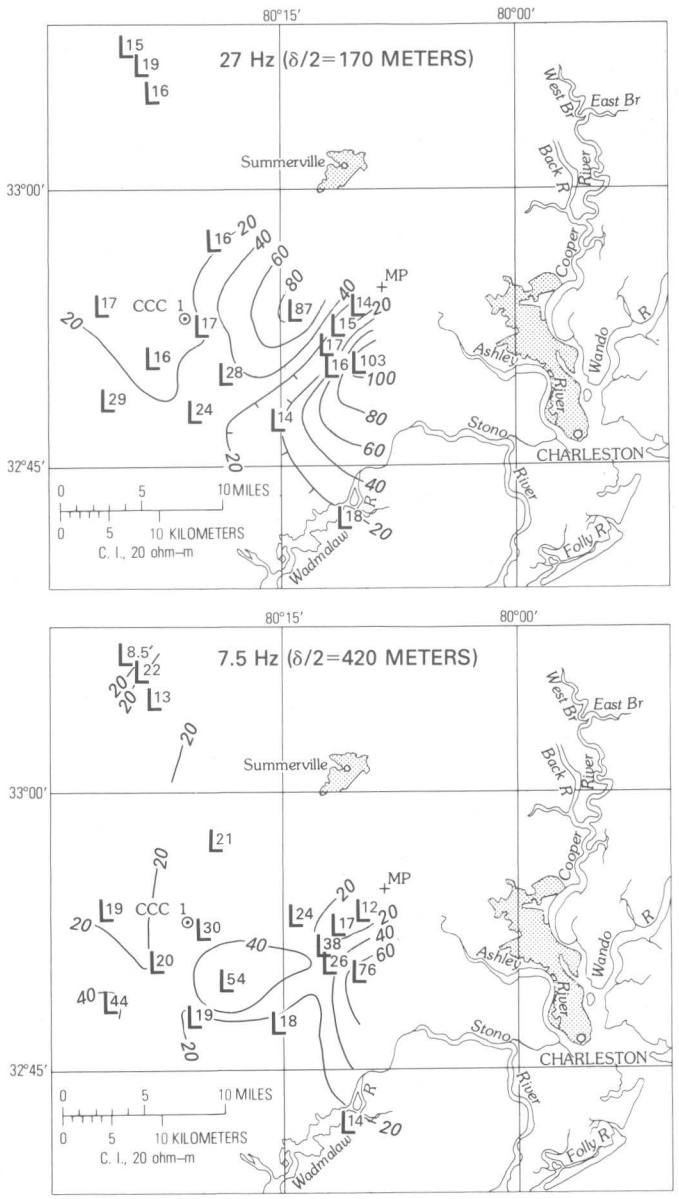

FIGURE 4.—Continued.

Zarrouk sense (Zohdy, 1974b) of the true resistivity versus depth function below each sounding.

Not one of the nine VES showed a high-resistivity layer near 750 m depth which would correspond to the basalt encountered at the bottom of Clubhouse Crossroads corehole 1. We infer that this basalt is either absent or quite thin below the VES locations. A useful rule of thumb for VES interpretations is that a layer of sufficient (more than 20 times) resistivity contrast will be indicated on d.c. soundings whenever its thickness to depth ratio exceeds 1/20. Clubhouse Crossroads corehole 1 penetrated 42 m into this basalt, a sufficient minimum thickness under the 1/20 rule that a basalt layer maintaining this thickness everywhere should have been indicated on all soundings. As it was not, we conclude that the basalt flow, if present at all, was (a) deeper, (b) thinner, and (or) (c) of lower resistivity at the VES locations than at the corehole location near Clubhouse Crossroads. Computer modeling indicates that such a basalt layer, 750 m deep, could be up to a maximum of 75 m thick and still be missed, providing its resistivity were only 50 ohm-m, one twelfth the logged value. I consider this the extreme possible thickness-resistivity estimate.[1]

Because electric basement was indicated at about 1,300 m on several soundings near the corehole site (VES 1, 3, 8, and 9), I infer that about one-half kilometer of sediment lies below the basalt flow but above electric basement. Interpreted resistivities at these depths are all in the range 1–10 ohm-m, values appropriate for water-saturated sediments. A series of alternating very low resistivity sediments and thin basalt flows would, however, also fit the data. If, for example, 90 percent of the section consists of 1 ohm-m sediments, and the remaining 10 percent is thin 100 ohm-m basalt flows, a net apparent resistivity of 3.4 ohm-m would be seen at the surface VES (Campbell, 1977). In that case, the one-half kilometer of sediments could be replaced by only 160 m of interleaved sediments and basalts and still give the observed VES curves. Then, however, depth to true electric basement (910 m) would no longer agree with magnetic basement depth estimates of more than 1,000 m (Phillips, this volume). The most likely interpretation is that there are few, if any, additional basalt flows in the sedimentary section below the flow encountered in Clubhouse Crossroads corehole 1.

CROSS SECTIONS

Under VES 2, 4, and 7, electric basement is near 900 m depth; elsewhere it is at depths greater than 1,000 m. These three shallow basement locations are on, or immediately east of, the Long-Champion trend (fig. 2), which may represent a steeply dipping fault. Sections *A–A′* and *B–B′* on figures 5 and 6 show interpreted VES 1–8, including the Long–Champion conjectured fault. Near VES 7, the fault is shown shifted 2 km to the northwest from its originally inferred position in order to include VES 7 with the other shallow-basement soundings to the east (both original and shifted positions are also

[1] Additional information was received on May 10, 1977. Another U.S. Geological Survey corehole, 2.6 km southwest of the center of VES 1, encountered basalt between 774 m and 1,031 m depth, and passed into well-indurated sediments below 1,031 m depth. The total basalt thickness at this location is 257 m compared with 75-m maximum thickness I have interpreted from data at the VES 1 site.

TABLE 1.—*Interpreted VES solutions*

[ρ, resistivity of layer in ohm-m; d, depth to bottom of layer in meters]

VES 1									
ρ=	810	90	313	39	23	71	10.8	1.63	200
d=	1.5	4.9	6.6	30	125	166	689	1319	∞
VES 2									
ρ=	1200	256	75	14	4.5	200			
d=	2.6	10.1	64	310	190	∞			
VES 3									
ρ=	80	146	63	7	25	8	200		
d=	2.3	4.9	27	59	194	1186	∞		
VES 4									
ρ=	120	25	60	16	50	4	200		
d=	1.5	8	26	110	150	900	∞		
VES 5									
ρ=	1200	300	15	40	7	200			
d=	1.5	14	64	96	1350	∞			
VES 6									
ρ=	45	91	21	40	10.6	4.2	200		
d=	1.65	5	14.5	47	409	1113	∞		
VES 7									
ρ=	320	64	302	20.6	52.1	4.8	200		
d=	1.7	4.4	11.3	182	320	965	∞		
VES 8									
ρ=	1000	74.5	38.4	124	23	7.6	200		
d=	2.3	25	68.4	139.2	889	1475	∞		
VES 9									
ρ=	700	72	15	6	200				
d=	10.6	70.5	226	1300	∞				

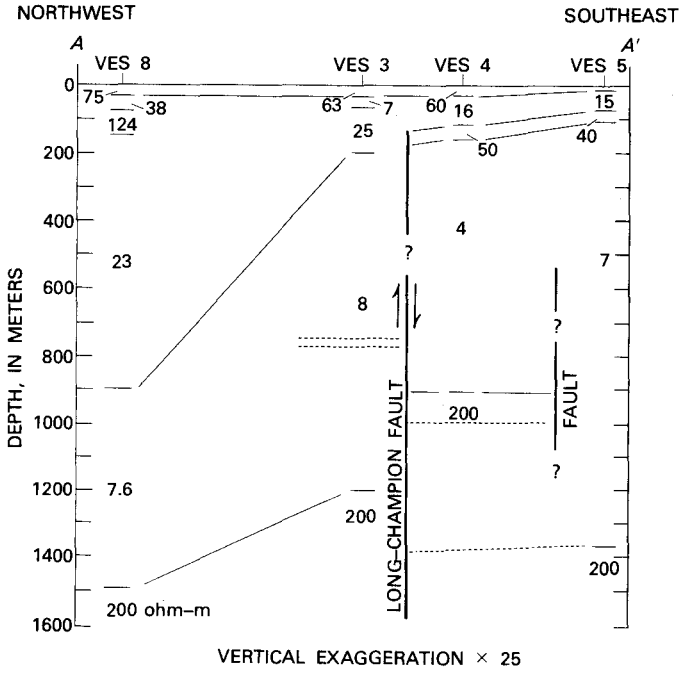

FIGURE 5.—Interpreted VES projected onto section *A–A'*. Thin lines indicate divisions between different electrical layers. Numbers are resistivities in ohm-meters. Dotted horizons indicate features inferred from other evidence, but not seen in the VES data.

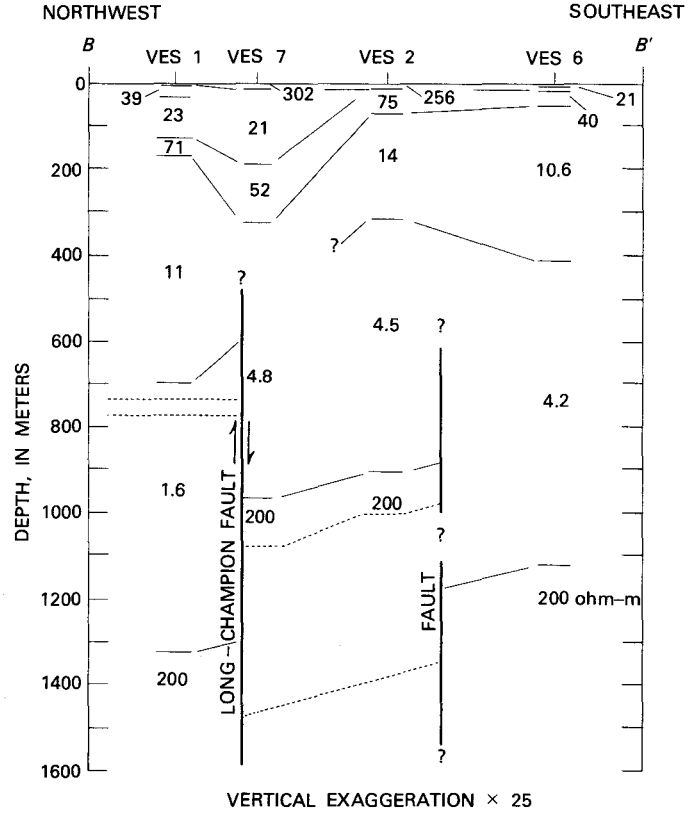

FIGURE 6.—Interpreted VES projected onto section *B–B'*. Thin lines indicate divisions between different electrical layers. Numbers are resistivities in ohm-meters. Dotted horizons indicate features inferred from other evidence, but not seen in the VES data.

shown on fig. 2). A second fault in the subsurface is shown parallel to the Long–Champion trend and 11 km southeast of it in order to separate the different resistivity structures of VES 4 and 5. The position

of this fault has been chosen to coincide with some linear segments on the aeromagnetic contour map. Both faults are conjectural and interpreted as faults mainly to separate soundings of differing layer thicknesses and resistivities. Though the conjectured faults also separate regions of shallow and deep electric basement, any two adjacent basement depths may be connected with slopes not exceeding 5°. A rather gentle anticline would therefore fit the basement depth data as well as the faulted structure shown on sections *A–A′* and *B–B′*.

Section *C–C′* (fig. 7) trends northeast between the two conjectured faults. We see that the shallow electric basement of VES 2 and 4 has been lost to the southwest under VES 9.

INTERPRETATION AND SOME SPECULATIONS

The original gravity interpretation of Long and Champion (this volume) involved downdrop of the block to the southeast of the Long–Champion line. The VES interpretations shown on sections *A–A′* and *B–B′*, however, show shallower basements southeast of this line. I would reconcile these two interpretations by postulating that the "basement" seen on VES 2, 4, and 7 is, in fact, a thickened interval of the Cretaceous(?) basalt encountered in Clubhouse Crossroads corehole 1. If the Long-Champion fault were already active in the Late Cretaceous, some surface relief may have been expressed along it at that time. The basalt floods which inundated the area at that time would have filled the valley southeast of the fault resulting in greater basalt thicknesses there. Computer models indicate that a 100-m thickness of 200 ohm-m basalt, even when underlain by one-half kilometer of low-resistivity sediments, would be sufficient to give an "electric basement" signature equal within experimental error to those obtained from VES 2, 4, and 7.

The hypothesis of a thickened basalt interval under VES 2, 4, and 7 may explain the apparent change in basement depth seen along section *C–C′*. The deep basement seen at VES 9 would represent crystalline basement some one-half kilometer below the basalt flow. The flow itself presumably is too thin to be seen at the VES 9 location. The basalt is present at 750 m Clubhouse Crossroads corehole 1 to the west of the fault, but (according to the thickened basalt hypothesis) at around 900 m under VES 2, 4, and 7 east of it. Thus, some 150 m of post-Cretaceous vertical offset could be indicated across the Long-Champion line in the vicinity of these particular soundings. Long and Champion's (this

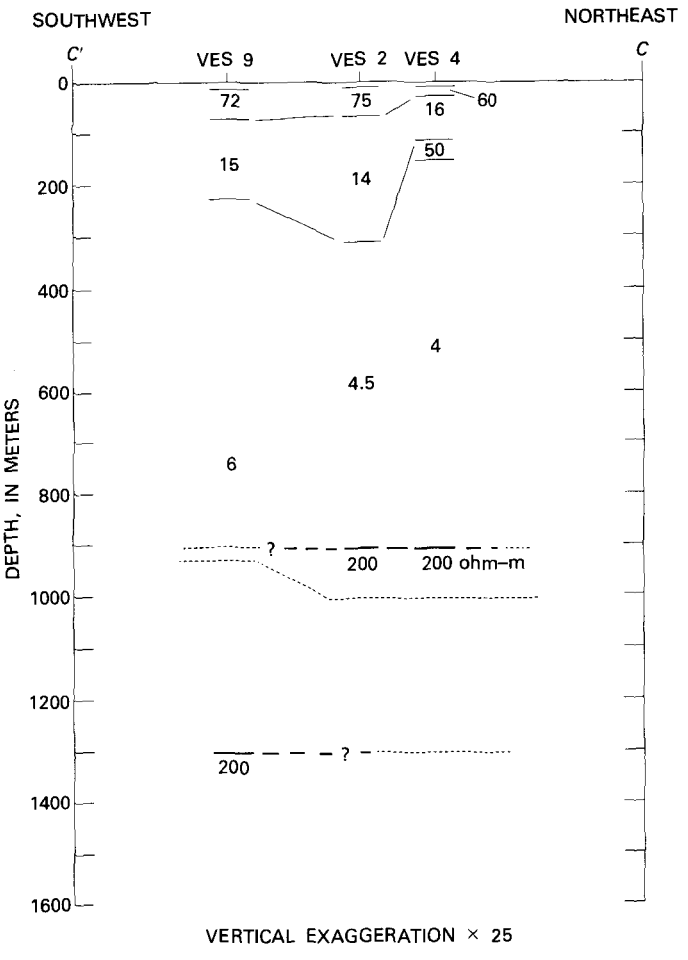

FIGURE 7.—Interpreted VES projected onto section *C–C′*. Thin lines indicate divisions between different electrical layers. Numbers are resistivities in ohm-meters. Dotted horizons indicate features inferred from other evidence, but not seen in the VES data.

volume) gravity interpretation involved a 600-m vertical offset in the basement across this line at a location 12 km further northeast, indicating either that displacement increases northeasterly, or that substantial vertical displacement was already there before the basalt flow came. I tend to favor the first interpretation, on the grounds that the interpreted basement offset in the southeast is small, with no significant difference between VES 1 and VES 9.

The structure east of the Long-Champion line may be a Cretaceous(?) analog of the Atlantic coast Triassic and Jurassic basins farther to the north. The Long-Champion fault would be the western border fault of this basin with the postulated thickened basalt and west-dipping flow within its sedimentary pile. (Some west dip seems likely between VES 2 and 7 as shown on section *B–B′*.) The lower resistivity seen above basement within the

structure (4 ohm-m as opposed to 10 ohm-m outside it) could be indicative of ground water pooled in such a basin.

Though the question is not closed, indications are that present-day earthquake activity has little to do with the postulated Long–Champion fault. The one well-determined earthquake focal mechanism (Tarr, this volume) and general seismicity trends (Bollinger, 1972) are at nearly right angles to it. There is no longer any surface expression of the Long–Champion fault. Its only significance for present-day earthquake planners may be the transmission and concentration of shaking along its associated shallow basin in response to large earthquakes which take place deeper in the section.

A second U.S. Geological Survey corehole, 2.6 km southwest of the center of VES 1, encountered basalt between 774 m and 1,031 m depth, and passed into well-indurated sediments below 1,031 m depth. The total basalt thickness at this location is 257 m compared with 75-m maximum thickness I have interpreted from data at the VES 1 site.

REFERENCES CITED

Bollinger, G. A., 1972, Historical and recent seismic activity in South Carolina: Seismol. Soc. America Bull., v. 62, no. 3, p. 851–864.

Campbell, D. C., 1977, A model for estimating electric macroanisotropy coefficient of fractured aquifers: Geophysics, v. 42, no. 1, p. 114–117.

Dutton, C. E., 1889, The Charleston earthquake of August 31, 1886: U.S. Geol. Survey Ann. Rept. 9, 1887–88, p. 203–528.

Goldstein, M. A., and Strangway, D. W., 1975, Audio-frequency magnetotellurics with a grounded electric dipole source: Geophysics, v. 40, no. 4, p. 669–70.

Keller, George, and Frischknecht, Frank, 1966, Electrical methods in geophysical prospecting: New York, Pergamon Press, 519 p.

Zohdy, Adel A. R., 1974a, A computer program for the automatic interpretation of Schlumberger sounding curves over horizontally stratified media: U.S. Natl. Tech. Inf. Service PB–232703/AS, 25 p.

——— 1974b, Use of Dar Zarrouk curves in the interpretation of vertical electrical sounding data: U.S. Geol. Survey Bull. 1313–D, 41 p.

——— 1975, Automatic interpretation of Schlumberger sounding curves, using modified Dar Zarrouk functions: U.S. Geol. Survey Bull. 1313–E, 39 p.

Zohdy, Adel A. R., Anderson, L. A., and Muffler, L. J. P., 1973, Resistivity, self-potential and induced polarization surveys of a vapor-dominated geothermal system: Geophysics, v. 38, no. 6, p. 1130–1144.

Zohdy, Adel A. R., Eaton, G. P., and Mabey, D. R., 1974, Application of surface geophysics to ground-water investigations, Chapter D1, *of* Book 2 *of* Techniques of water-resources investigations of the U.S. Geol. Survey: Washington, D. C., U.S. Govt. Printing Office, p. 10–22.

Correlation of Major Eastern Earthquake Centers With Mafic/Ultramafic Basement Masses

By M. F. KANE

STUDIES RELATED TO THE CHARLESTON, SOUTH CAROLINA, EARTHQUAKE OF 1886—A PRELIMINARY REPORT

GEOLOGICAL SURVEY PROFESSIONAL PAPER 1028-O

CONTENTS

ILLUSTRATIONS

STUDIES RELATED TO THE CHARLESTON, SOUTH CAROLINA, EARTHQUAKE OF 1886—
A PRELIMINARY REPORT

CORRELATION OF MAJOR EASTERN EARTHQUAKE CENTERS WITH MAFIC/ULTRAMAFIC BASEMENT MASSES

By M. F. KANE

ABSTRACT

Extensive gravity highs and associated magnetic anomalies are present in or near seven major eastern North American earthquake areas. The seven include the five largest of these centers. The immediate localities of the gravity anomalies are, however, relatively free of seismicity, particularly of the largest seismic events. The anomalies are presumably caused by extensive mafic or ultramafic masses embedded in the crystalline basement. Laboratory experiments show that serpentinized gabbro and dunite fail under stress in a creep mode rather than in a stick-slip mode. A possible explanation of the correlation between the earthquake patterns and the anomalies is that the mafic/ultramafic masses are serpentinized and can sustain only low-stress fields, thereby acting to concentrate regional stress outside their boundaries. The proposed model is analogous to the hole-in-plate problem of mechanics whereby stresses around a hole in a stressed plate may reach values several times the average.

INTRODUCTION

Earthquakes of the Eastern United States are markedly lower in frequency and magnitude than those of the western regions, particularly when compared with those occuring along the San Andreas fault of California. Because of the low damping of earthquake energy in the Eastern United States, however, relatively high intensities are anticipated when compared with the intensities resulting from corresponding magnitudes of the western earthquakes (Nuttli, 1973). A second aspect of the eastern earthquake region that contrasts with that of western regions is the sparsity of readily identifiable major faults. To some extent, this lack may be attributed to a thick cover of incompetent sedimentary strata, but it seems surprising that ongoing studies have not uncovered direct evidence of major fault systems in the major eastern earthquake regions.

As part of the earthquake investigation program of the U.S. Geological Survey, aeromagnetic and gravity studies of the New Madrid, Mo., and Charleston, S.C., earthquake areas began in 1972. Coverage of much of these regions was completed by 1975, although surveys in the New Madrid area are still underway. The initial efforts were directed towards discernment of linear magnetic or gravity features that could be attributed to major faults in the crystalline, presumably magnetic, basement rocks, but evidence of such features was not detected, at least not in the sense of readily apparent lineaments or discontinuities. Major magnetic and gravity highs were recognized in the near-epicentral regions of both the New Madrid and Charleston areas, but coincidence seemed to be the most plausible explanation. Positive magnetic and gravity anomalies have now been identified, however, for the seven major Eastern United States earthquake areas as defined by Hadley and Devine (1974), so that implications other than coincidence must be considered.

COMPARISON OF GRAVITY ANOMALIES AND EARTHQUAKE AREAS

Figure 1 illustrates the comparison of earthquake epicenter areas with gravity anomalies for seven well-identified eastern North American earthquake regions. The dashed line shown on each map of the figure is the maximum frequency contour line showing the total number of earthquakes per 10^4 km^2 from 1800 to 1972 that have had an intensity of Modified Mercali III or larger (Hadley and Devine, 1974). As explained by Hadley and Devine, the contours are "only * * * a guide for estimating regional seismicity." Also shown on figure 1 is the

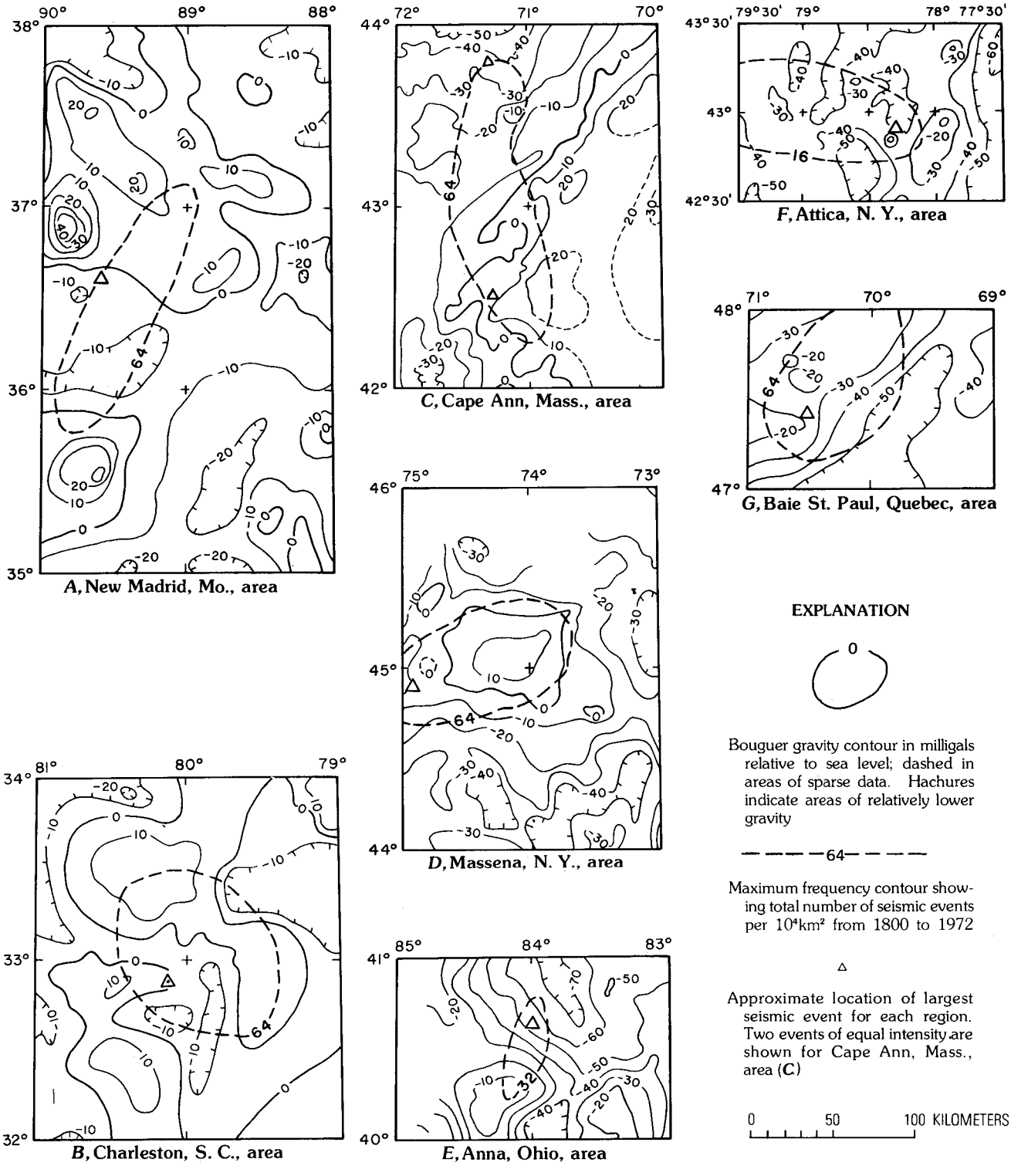

FIGURE 1.—Sketch maps showing gravity and seismicity data for seven major earthquake regions in eastern North America. Seismicity data were modified from Hadley and Devine (1974). Gravity data in *A* and *B* are from American Geophysical Union (1964); gravity data in *C* and *D* from Kane and others (1972); gravity data in *E* from Heiskanen and Uotila (1956); gravity data in *F* from Revetta and Diment (1971); and gravity data in *G* from Thompson and Garland (1957).

earthquake of maximum intensity within each region. The fact that these largest earthquakes are all within the maximum contour lines gives assurance that the contour lines also locate the areas of maximum energy release.

An examination of the small-scale maps of figure 1 shows that positive gravity anomalies of 10 milligals or greater and horizontal extents of more than 30 km are present in each of the earthquake regions. The New Madrid, Mo., area (fig. 1*A*) is notable for two large circular anomalies northwest and south of the zone of maximum epicenter frequency. The largest seismic event is also located between the gravity highs. In the Charleston, S.C., area (fig. 1*B*), the largest event and the center of maximum epicenter frequency are both just east of a gravity high that has an easterly elongation. In the Cape Ann, Mass. (fig. 1*C*), Anna, Ohio (fig. 1*E*), and Attica N. Y. (fig. 1*F*), areas the zones enclosed by the contour of maximum epicenter frequency are elongated, one end of the zone overlapping the gravity high in each area. In each of these last three areas, the event of maximum intensity is near but outside the locus of the gravity high. In the Cape Ann area (fig. 1*C*) two events of approximately equal intensity are indicated; the second event is north of the seismicity zone, well removed from any notable gravity high. The strongest known earthquakes of this area, however, took place in the early and mid-18th century and are approximately located in the region east of the gravity high (Richard Holt written commun., 1976). In the Massena, N.Y. (fig. 1*D*), and Baie St. Paul, Quebec (fig. 1*G*), areas, the gravity highs are quite broad and have local highs superimposed. The maximum frequency contour is within the broad high; the events of maximum intensity are near but outside the superimposed gravity highs.

In general the gravity anomalies, and hence their sources, tend to be peripheral to the earthquake maximum frequency contour. As this contour encloses, for the most part, the earthquake of maximum intensity this relation also indicates that the sources of the gravity highs are outside the region of maximum strain energy release.

Figure 2 illustrates a more precise comparison of earthquake incidence and gravity anomalies for the New Madrid, Mo., and Charleston, S.C., areas. The earthquake plot for the New Madrid area (fig. 2*A*) (Stauder and others, 1976) represents cumulative seismic events from June 29, 1974, to March 31, 1976. Events in the patterned zones are too close to be shown individually. In figure 2*A*, the earthquake epicenters are shown, for the most part, between the two prominent gravity highs north and south of the earthquake zone. A suggestion of an arcuate zone is seen southeast of the northern gravity high. Earthquakes are sparse or lacking in the immediate vicinity of the gravity highs. In the Charleston area (fig. 2*B*), the earthquakes (A. C. Tarr, this volume; C. E. Dutton, 1889) are east of the gravity high, which in detail has the shape of a sharp nose (Long and Champion, this volume). In both areas, depths to the earthquakes generally are less than 15 km (A. C. Tarr, this volume, William Stauder, oral commun., 1976).

A POSSIBLE SOURCE MECHANISM

In reviewing possible causal relationships between the gravity anomalies and the earthquakes, we have considered isostatic effects, intrusive activity, and anomalies in the distribution of regional stress. Isostatic effects would appear to be negligible as the loads represented by the gravity highs are small compared with surface loads imposed by topography. Intrusive activity might be a factor, but the anomaly in the Baie St. Paul area is associated with mafic masses of Precambrian age, seeming to rule out this possibility for at least one of the areas. Of the three factors, the most plausible one would seem to be a relationship between the distribution of the regional stress field and crustal lithology. Long (this volume), in reporting on the gravity high in the Charleston, S.C., earthquake area, suggested that stress amplification caused by lithologic contrast may be related to the occurrence of the earthquakes.

In a study of the relations between rock type, stress, and mechanical failure, Byerlee and Brace (1968) concluded that serpentinized gabbro and dunite, limestone, and porous tuff failed by creep rather than by stick slip, a small-scale analog to earthquakelike failure. When one considers the gravity anomalies in the region of the earthquakes shown in figure 1, plausible sources of the anomalies are large masses of mafic and (or) ultramafic rock imbedded in a crust of generally more silicic rock. If these masses are serpentinized, they may, as suggested by Byerlee and Brace's results, deform continuously by creep rather than intermittently by stick slip as regional stress changes. The behavior of the stress in the host rock enclosing these masses might, therefore, be similar to that which takes place in a rigid plate near a hole or plastic plug. Timoshenko and Goodier (1951, p. 78–82) showed

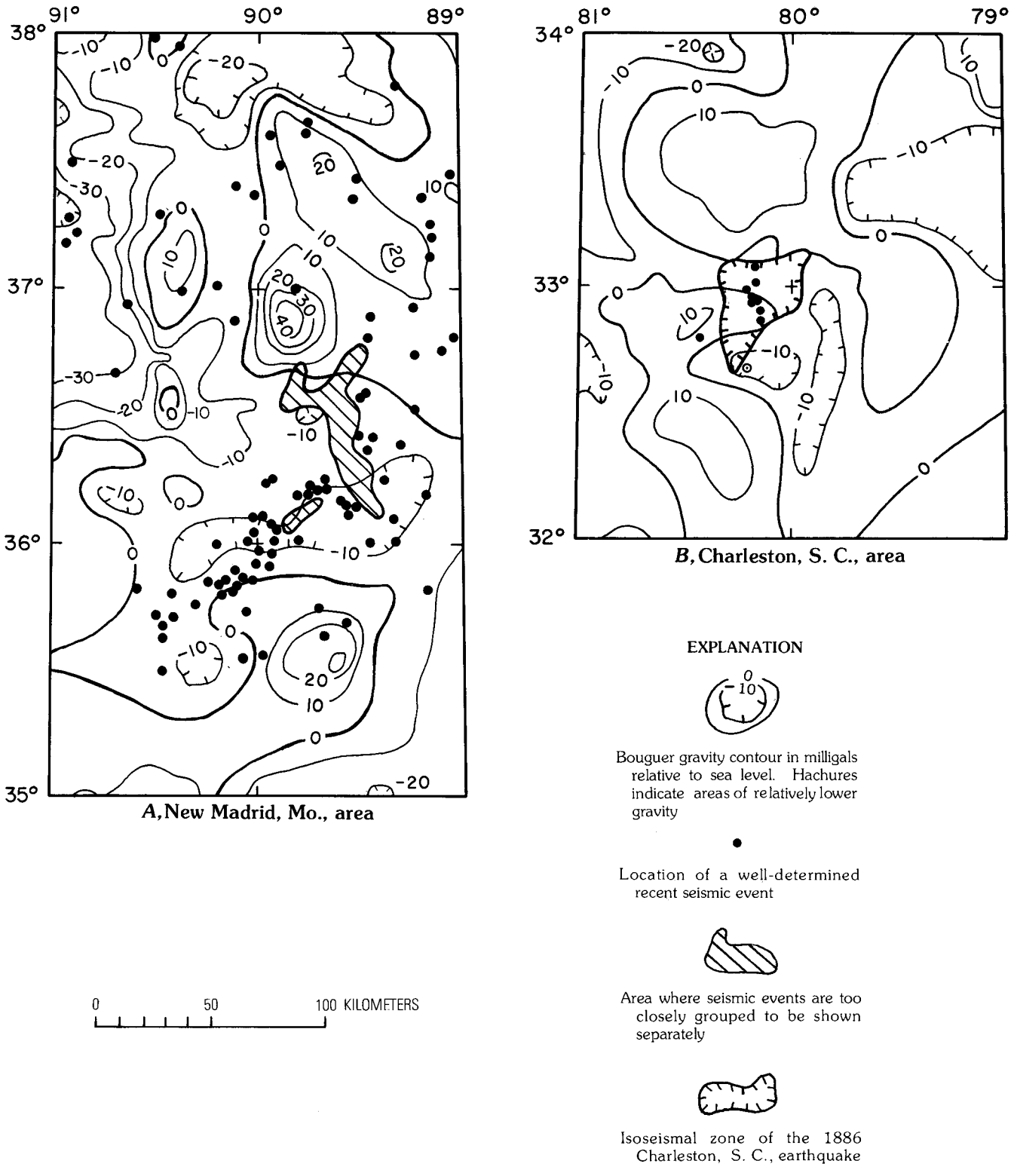

FIGURE 2.—Sketch maps showing gravity and contemporary epicenter data for the New Madrid, Mo., and Charleston, S. C., earthquake areas. Sources of gravity data are given in figure 1. Epicenter data in the New Madrid, Mo., area are from Stauder and others (1976). Epicenter data in the Charleston, S. C., area are from Tarr (this volume). Isoseismal boundary is from Dutton (1889).

that stresses are localized at the margin of a hole in a plate and attain values several times those of the applied stresses. The thrust of this model is that large rock masses that have distinctive deformation contrasts may distort regional stress fields in much the same way that distinctive magnetization and density contrasts distort the magnetic and gravity fields.

The role of serpentine in the mode of deformation of the San Andreas fault has been commented on by Allen (1968). He noted the "great abundance" of serpentine in the part of the fault zone characterized by creep and suggested that the creep may be related to the presence of serpentine. Although th geometry of the model described above and that of the San Andreas fault zone are greatly different, the two situations may be linked by the unusual deformation properties of serpentine.

The stress concentration near holes in plates is dependent, among other things, on the direction and type of stresses, shapes of the holes, and on the relative location of plate boundaries. The arcuate zone (fig. 2*A*), for example, might be analogous to the high-stress zone that exists between a hole-in-a-plate and a nearby boundary. In the New Madrid, Mo., area, a boundary may be indicated by the southwest-trending zone for earthquakes that is southwest of the arcuate zone (fig. 2*A*). As such the zone would represent a fault influenced by the location of serpentinized mafic/ultramafic masses near either end. Similarly, the earthquakes near the eastern nose of the gravity anomaly in the Charleston region (fig. 2*B*) might be analogous to high-stress zones associated with the ends of narrow cracks in plates when tension is applied normal to the crack.

Undoubtedly, the model of the hole-in-a-plate, if valid, is greatly oversimplified, as the masses are more analogous to plastic plugs, and geologic bodies are three dimensional. Uncertainties are also present in other aspects of the data including the precise cause of the gravity anomalies, the directions and types of stress, the shapes and orientations of the anomalous masses, and the dimensions and boundaries of the host rock in which the anamalous masses are embedded. The only densities, however, that could reasonably explain the high positive gravity amplitudes, are those associated with mafic or ultramafic rocks. At present, no direct evidence of serpentinization exists.

Perhaps the major question that arises about a relationship between mafic basement masses and stress-field distribution is why other regions in eastern North America underlain by large positive gravity anomalies do not have associated earthquake activity. Lack of serpentinization would be the most obvious answer. Other possible answers include the lack of a sufficiently large or changing regional stress field, or inappropriate geometric relations between the causative masses and stress-field directions.

The present evidence indicates, for example, that most, if not all the masses so far considered are at depths where they would be enclosed in highly competent basement. Mafic masses in softer, less competent sedimentary strata that yield more easily would presumably not give rise to the same stress concentrations. Possibly, also, the continental stress field, probably imparted by plate-tectonic conditions, is strongly zoned in a regional sense. The southwest alinement of earthquake areas from the Gulf of St. Lawrence to the New Madrid region and the similar trend in the broad earthquake region of the Appalachians indicated by the seismotectonic map of Hadley and Devine (1974) may be expressions of regional zoning of the continental stress field.

In summary, a correlation has been shown to exist between major eastern North American earthquake areas and the presence of mafic-ultramafic masses as evidenced by gravity anomalies. It is not true, however, that all mafic-ultramafic masses are associated with earthquake areas. A model has been proposed whereby stress is concentrated near the margin of these masses in much the same manner as stress concentrations take place near the margins of defects or holes in plates under stress. This model has major implications in the consideration of eastern North America seismicity, as it suggests that larger earthquakes are restricted to relatively local areas. The model may also explain why major through-going faults of continental or subcontinental dimensions are not evident in eastern North America. Presumably the faults associated with the localized stress zones would be similarly localized and of relatively small dimensions, perhaps 10 km long or less.

REFERENCES CITED

Allen, C. R., 1968, The tectonic environments of seismically active and inactive areas along the San Andreas fault system, *in* Dickinson, W. R., and Grantz, Arthur, eds., Proceedings of Conference on geologic problems of San Andreas fault system: Stanford Univ. Pub. Geol. Sci., v. 11, p. 70–80.

American Geophysical Union, Special Committee for the Geophysical and Geological Study of the Continents, 1964, Bouguer gravity anomaly map of the United

States (exclusive of Alaska and Hawaii): Washington, D.C., U.S. Geol. Survey, 2 sheets, scale 1:2,500,000.

Byerlee, J. D., and Brace, W. F., 1968, Stick slip, stable sliding, and earthquakes—Effect of rock type, pressure, strain rate, and stiffness: Jour. Geophys. Research, v. 73, no. 18, p. 6031–6037.

Dutton, C. E., 1889, The Charleston earthquake of August 31, 1886: U.S. Geol. Survey Ninth Ann. Rept., p. 203–528.

Hadley, J. B., and Devine, J. F., 1974, Seismotectonic map of the Eastern United States: U.S. Geol. Survey Misc. Field Studies Map MF–620.

Heiskanen, W. A., and Uotila, U. A. K., 1956, Gravity survey of the State of Ohio: Ohio Div. Geol. Survey, Rept. Inv. 30, 34 p.

Kane, M. F., Simmons, Gene, Diment, W. H., Fitzpatrick, M. M., Joyner, W. B., and Bromery, R. W., 1972, Bouguer gravity and generalized geologic map of New England and adjoining areas: U.S. Geol. Survey Geophys. Inv. Map GP–839.

Nuttli, Otto, W., 1973, The Mississippi Valley earthquakes of 1811 and 1812: intensities, ground motion, and magnitudes, Seismol. Soc. America Bull., v. 63, no. 1, p. 227–248.

Revetta, F. A., and Diment, W. H., 1971, Simple Bouguer gravity anomaly map of western New York: New York State Mus. Sci. Service, Geol. Survey, Map and Chart Series 17.

Stauder, William, Schaefer, Stephen, Best, John, and Morrisey, S. T., 1976, 1 January–31 March 1976: St. Louis Univ. Southeast Missouri Regional Seismic Network Quart. Bull. 7, 25 p.

Thompson, L. G. D., and Garland, G. D., 1957, Gravity measurements in Quebec (south of latitude 52° N): Ottawa Dominion Observatory Pub., v. 19, no. 4, p. 111–167.

Timoshenko, S., Goodier, J. N., 1951, Theory of elasticity: New York, McGraw-Hill, 506 p.


U. S. DEPARTMENT OF THE INTERIOR
March 3, 1849